Image-Guided Interventions in Oncology

An Interdisciplinary Approach

Christos Georgiades
Hyun S. Kim
Editors

Springer

Image-Guided Interventions in Oncology

Christos Georgiades • Hyun S. Kim
Editors

Image-Guided Interventions in Oncology

An Interdisciplinary Approach

Springer

Editors

Christos Georgiades, MD, PhD
Professor of Radiology, Oncology & Surgery
Vascular and Interventional Radiology
Johns Hopkins Hospital
Baltimore, MD
USA

Hyun S. Kim, MD, MHS
Professor of Radiology and Medicine (Oncology)
Yale Cancer Center
Yale School of Medicine
New Haven, CT
USA

ISBN 978-3-030-48766-9 ISBN 978-3-030-48767-6 (eBook)
https://doi.org/10.1007/978-3-030-48767-6

This Springer imprint is published by the registered company Springer Nature Switzerland AG
The registered company address is: Gewerbestrasse 11, 6330 Cham, Switzerland

To Marianna, still….and Marilena
and Savvas.

– Christos Georgiades

To love of my life, Angelica and Hanna

– Hyun S. Kim

Preface

Interventional Oncology is a specialty that conjointly with Surgical, Medical, and Radiation Oncology provides contemporary, comprehensive care to the cancer patient. It does so by availing targeted, loco-regional therapies to tumors. As the treatment of the cancer patient gravitates towards individualized, tailored care, treatment coordination between these different specialties becomes increasingly important.

Bearing the above in mind, the aim of this book is

1. To highlight the potential contributions of Interventional Oncology to the care of the cancer patient
2. To do so in a disease-specific manner
3. To include updates from not just Interventional Oncologists but also Surgeons as well as Medical and Radiation Oncologists as needed
4. To provide insight to multimodality combination treatments and future directions

In doing so we hope to stimulate further cross-collaboration between the different cancer care specialties in both the clinical and research setting and enhance the care of cancer patients. As a reference and updated primer, we hope this textbook will serve members of any multidisciplinary cancer care group well.

Baltimore, MD, USA — Christos Georgiades
New Haven, CT, USA — Hyun S. Kim

Contents

Contributors

Nadine Abi-Jaoudeh, MD, FSIR, CCRP Department of Radiological Sciences, University of California Irvine Medical Center, Orange, CA, USA

Moishir Anwar, MD Department of Radiation Oncology, University of California San Francisco, San Francisco, CA, USA

Ronald S. Arellano, MD, FACR, FSIR, FCIRSE Department of Radiology, Massachusetts General Hospital, Harvard Medical School, Boston, MA, USA

Thomas D. Atwell, MD Department of Radiology, Mayo Clinic, Rochester, MN, USA

Ivan Babin, MD Department of Radiology, SUNY Upstate Medical University, Syracuse, NY, USA

Emily K. Bergsland, MD Department of Medicine – Gastrointestinal Oncology, University of California San Francisco, San Francisco, CA, USA

Yolanda C. D. Bryce, MD Department of Radiology, Memorial Sloan Kettering Cancer Center, New York, NY, USA

Matthew R. Callstrom, MD, PhD Department of Radiology, Mayo Clinic, Rochester, MN, USA

Juan C. Camacho, MD Interventional Radiology, Memorial Sloan Kettering Cancer Center, New York, NY, USA

Michael Cecchini, MD Section of Medical Oncology, Department of Internal Medicine, Yale School of Medicine, New Haven, CT, USA

Yale Cancer Center, Yale School of Medicine, New Haven, CT, USA

Jin Woo Choi, MD Department of Radiology, Seoul National University Hospital, Seoul, Republic of Korea

Jin Wook Chung, MD Department of Radiology, Seoul National University Hospital, Seoul, Republic of Korea

Jeeban Paul Das, MD Department of Radiology, Memorial Sloan Kettering Cancer Center, New York, NY, USA

Farshid Dayyani, MD, PhD Division of Hematology and Oncology, Department of Medicine, University of California Irvine Medical Center, Orange, CA, USA

Thierry de Baere, MD Department of Interventional Radiology, Gustave Roussy Cancer Center, Villejuif, France

Amy R. Deipolyi, MD, PhD Department of Radiology, Memorial Sloan Kettering Cancer Center, New York, NY, USA

Joseph P. Erinjeri, MD, PhD Interventional Radiology Service, Memorial Sloan Kettering Cancer Center, New York, NY, USA

Louis Fanucci, MD Department of Radiological Sciences, University of California Irvine Medical Center, Orange, CA, USA

Nicholas Fidelman, MD Department of Interventional Radiology, University of California San Francisco, San Francisco, CA, USA

Dimitrios K. Filippiadis, MD, PhD, MSc, EBIR 2nd Department of Radiology, University General Hospital "ATTIKON", Medical School, National and Kapodistrian University of Athens, Athens, Greece

Christos Georgiades, MD, PhD Vascular and Interventional Radiology, Johns Hopkins University, Baltimore, MD, USA

Darragh F. Halpenny, MD Department of Radiology, Memorial Sloan Kettering Cancer Center, New York, NY, USA

Alan Ho, MD Medical Oncology, Memorial Sloan Kettering Cancer Center, New York, NY, USA

Thomas A. Hope, MD Department of Nuclear Medicine, University of California San Francisco, San Francisco, CA, USA

Maha Jarmakani, DO Interventional Radiology, Department of Radiological Sciences, OU Medical Center, Oklahoma City, OK, USA

Zeljka Jutric, MD Division of Hepatobiliary and Pancreas Surgery, University of California Irvine Medical Center, Orange, CA, USA

Alexios Kelekis, MD, PhD, EBIR 2nd Department of Radiology, University General Hospital "ATTIKON", Medical School, National and Kapodistrian University of Athens, Athens, Greece

DaeHee Kim, MD Interventional Radiology Service, Memorial Sloan Kettering Cancer Center, New York, NY, USA

Hyo-Cheol Kim, MD Department of Radiology, Seoul National University Hospital, Seoul, Republic of Korea

Hyun S. Kim, MD, MHS Section of Interventional Radiology and Section of Medical Oncology, Yale Cancer Center, Yale School of Medicine, New Haven, CT, USA

Maureen P. Kohi, MD Department of Interventional Radiology, University of California San Francisco, San Francisco, CA, USA

Eduardo A. Lacayo, MD Interventional Radiology, Memorial Sloan Kettering Cancer Center, New York, NY, USA

Aaron Lisberg, MD Department of Hematology Oncology, David Geffen School of Medicine at University of California, Los Angeles, Los Angeles, CA, USA

Johannes Maximilian Ludwig, MD Section of Interventional Radiology, Department of Radiology and Biomedical Imaging, Yale School of Medicine, New Haven, CT, USA

Department of Diagnostic and Interventional Radiology and Neuroradiology, University Hospital Essen, University of Duisburg-Essen, Essen, Germany

Dilip Maddirela, PhD Department of Radiology, Medical College of Wisconsin, Wauwatosa, WI, USA

Thaddeus J. Maguire, MD Early Specialization in Interventional Radiology, Department of Radiology, Medical College of Wisconsin, Froedtert Memorial Lutheran Hospital, Milwaukee, WI, USA

Amgad M. Moussa, MD Interventional Radiology Service, Memorial Sloan Kettering Cancer Center, New York, NY, USA

Eric K. Nakakura, MD Department of Surgery, University of California San Francisco, San Francisco, CA, USA

Kari Nelson, MD Vascular and Interventional Radiology, University of California Irvine Medical Center, Orange, CA, USA

Ines Nikolovski, MD Department of Radiology, Memorial Sloan Kettering Cancer Center, New York, NY, USA

Ryan Nipp, MD, MPH Department of Hematology/Oncology, Massachusetts General Hosptial, Harvard Medical School, Boston, MA, USA

Andrew C. Picel, MD Division of Interventional Radiology, Department of Radiology, Stanford University, Stanford, CA, USA

William S. Rilling, MD, FSIR Department of Radiology, Division of Vascular & Interventional Radiology, Medical College of Wisconsin, Froedtert Memorial Lutheran Hospital, Milwaukee, WI, USA

Rene Roberts, MD Interventional Radiology, MD Anderson Cancer Center, Houston, TX, USA

Adam Schwertner, MD Department of Interventional Radiology, University of California San Francisco, San Francisco, CA, USA

Rahul A. Sheth, MD Interventional Radiology, MD Anderson Cancer Center, Houston, TX, USA

Aditya Shreenivas, MD, MS Division of Hematology and Medical Oncology, Medical College of Wisconsin, Froedtert Memorial Lutheran Hospital, Milwaukee, WI, USA

Bilal A. Siddiqui, MD Genitourinary Medical Oncology, MD Anderson Cancer Center, Houston, TX, USA

Brittany L. Siontis, MD Division of Medical Oncology, Mayo Clinic, Rochester, MN, USA

Stephen Solomon, MD Interventional Radiology, Memorial Sloan Kettering Cancer Center, New York, NY, USA

Michael C. Soulen, MD Department of Radiology, Abramson Cancer Center, University of Pennsylvania, Philadelphia, PA, USA

Sumit K. Subudhi, MD, PhD Genitourinary Medical Oncology, MD Anderson Cancer Center, Houston, TX, USA

Robert D. Suh, MD Department of Radiological Sciences, David Geffen School of Medicine at University of California, Los Angeles, Los Angeles, CA, USA

Daniel Y. Sze, MD, PhD Division of Interventional Radiology, Department of Radiology, Stanford University, Stanford, CA, USA

Scott M. Thompson, MD, PhD Department of Radiology, Mayo Clinic, Rochester, MN, USA

Maria Tsitskari, MD, PhD 2nd Department of Radiology, University General Hospital "ATTIKON", Athens, Greece

R. Michael Tuttle, MD Endocrinology, Memorial Sloan Kettering Cancer Center, New York, NY, USA

Maria A. Velez, MD Department of Internal Medicine, University of Pittsburgh Medical Center, Pittsburgh, PA, USA

Sarah B. White, MD, MS, FSIR Department of Radiology, Division of Vascular and Interventional Radiology, Medical College of Wisconsin, Froedtert Memorial Lutheran Hospital, Milwaukee, WI, USA

Etay Ziv, MD, PhD Department of Radiology, Memorial Sloan Kettering Cancer Center, New York, NY, USA

Chapter 1
Physics and Physiology of Thermal Ablations

Kari Nelson, Zeljka Jutric, and Christos Georgiades

Thermal Ablation

Thermal ablation of tumor occurs with either extreme high or low temperatures. The desired result, irreversible cellular injury, results in coagulative necrosis. Coagulative necrosis may result from many conditions including extreme temperatures, ischemia, or hypoxia, and is characterized by short-term preservation of the architecture of the necrotic tissue, as the injury which results in necrosis also destroys intrinsic mechanisms for breakdown of cellular material. Coagulative necrosis is seen throughout the body and contrasts with liquefactive necrosis, which is characteristic in the central nervous system. Hypothermic injury leading to coagulative necrosis occurs with cryoablation (CA). Hyperthermic injury leading to coagulative necrosis occurs with radiofrequency ablation (RFA), microwave ablation (MWA), high-intensity focused ultrasound, and laser ablation (Fig. 1.1 and Table 1.1).

Heat-ablated lesions have been characterized as having three zones: the central zone in which ablation-induced coagulative necrosis occurs; a peripheral zone of sub-lethal hyperthermia in which cells may undergo apoptosis or may recover; and a surrounding zone of unaffected tissue [1]. Direct cellular damage depends upon the thermal energy applied, the rate of energy application, and the sensitivity of the target tissue. Mitochondrial dysfunction and inhibition of DNA replication are

K. Nelson (✉)
Vascular and Interventional Radiology, University of California Irvine Medical Center, Orange, CA, USA
e-mail: k2nelson@hs.uci.edu

Z. Jutric
Division of Hepatobiliary and Pancreas Surgery, University of California Irvine Medical Center, Orange, CA, USA
e-mail: zjutric@hs.uci.edu

C. Georgiades
Vascular and Interventional Radiology, Johns Hopkins University, Baltimore, MD, USA

C. Georgiades, H. S. Kim (eds.), *Image-Guided Interventions in Oncology*,
https://doi.org/10.1007/978-3-030-48767-6_1

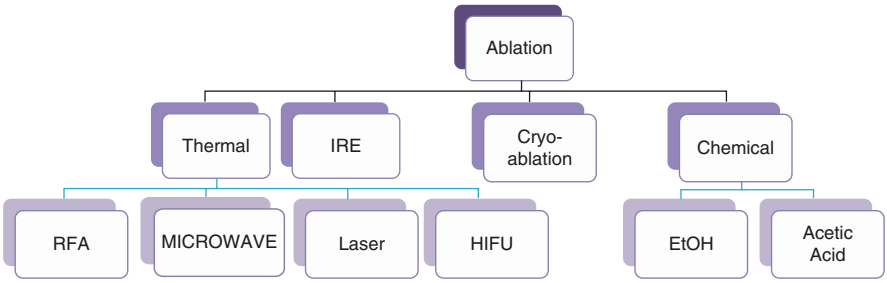

Fig. 1.1 Ablation modalities. In general, ablation modalities can be subdivided into thermal and non-thermal. Thermal modalities depend on increasing temperature to effect tissue necrosis and they include RFA, microwave ablation, laser ablation and high-frequency ultrasound ablation (HIFU). Non-thermal ablation modalities include: cryoablation, chemical ablation, and irreversible electroporation (IRE). Chemical ablation (acetic acid and alcohol ablation) has fallen out of favor in the USA. Despite being inexpensive, its efficacy is unpredictable and requires repeated procedures to approach the efficacy of other ablative modalities. HIFU and IRE are still in an investigational stage and their applicability is limited. Cryoablation and microwave ablation are becoming the most commonly utilized tumor ablative modalities in the USA

Table 1.1 Comparison of ablative modalities

	Cost	Experience	Ease of use	Outcomes
RFA	+	++++	++++	++
MWA	++	++++	++++	++++
Cryoablation	+++	+++	+++	++++
IRE	++++	+	+	++

Even though most published experience is with RFA, it has fallen out of favor because MWA and cryoablation have been shown to have superior outcomes. Cryoablation, though costlier than thermal ablative modalities, has shown better outcomes for renal cell carcinoma and for pain palliation. Cryoablation's advantages include visibility and uniformity of ablation zone (Fig. 1.7). IRE data are lacking, which coupled with its cumbersome technique and high cost has limited its applicability.

well-correlated with hyperthermic injury, ultimately resulting in changes to cell membrane integrity and cell death [1].

Complete destruction by thermal ablation requires that the entire tumor and an ablative margin be subjected to cytotoxic temperatures [2]. The ability to heat or cool large volumes of tissue in different environments is dependent upon the energy deposited, local tissue interactions, and energy lost before inducing thermal damage [2].

Radiofrequency Ablation

Physics

Radiofrequency ablation is based upon the application of alternating electric current which is delivered to the target tissue between electrode(s) resulting in frictional tissue heating and ultimately coagulative necrosis.

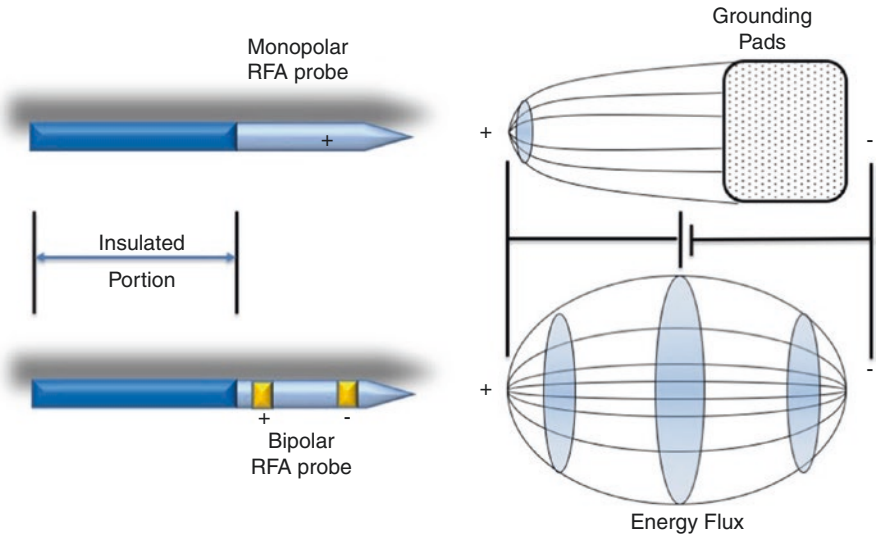

Fig. 1.2 RFA system design: In a monopolar (upper) RFA system, the alternating electric current travels within the patient between the RFA electrode (cathode) and the grounding pad (anode). At the probe tip energy flux is very high as the cross sectional area it traverses is small, resulting in energy deposition. The same amount of energy is dispersed over a larger area reducing the energy flux, on the pad side. In a bipolar (lower) RFA system, the electric current travels within the patient between two or more electrodes which function as both anode and cathode. No grounding pads are necessary

Radiofrequency (RF) energy is part of the electromagnetic spectrum, spanning frequencies from 3 Hz to 300 GHz. The RF ablation electrodes are part of an electrical circuit which when closed results in energy deposition in the form of heat (ablation) in the target tissue. RFA systems may be monopolar or bipolar in design (Fig. 1.2). Within the electrical circuit of a monopolar system, the RFA electrode acts as the cathode. Dispersing/grounding pads, which are typically applied to the patient's thighs, close the circuit and function as the anode. In the monopolar system, the RF current travels from the system generator to the ablation electrode in the tumor, through body tissues to the grounding pads on the skin, and then back to the generator. The area of the RFA electrode is quite small and creates high energy flux. Conversely, the large area of the dispersing/grounding pads minimizes energy flux. Therefore, within this circuit, tissue damage is limited to the area with high energy flux surrounding the ablation electrode, and tissue damage is avoided at the grounding pads when properly applied.

Bipolar RFA systems, which are less common in clinical RFA, utilize two or more bipolar ablation electrodes which are placed into the tumor. The applied RF current runs between the ablation electrodes without the need for grounding pads. Each electrode in bipolar systems contains high energy flux. By eliminating dispersing pads, bipolar RF systems minimize energy loss and more efficiently create greater ablation volumes without risking skin burns.

The mechanism of heating with RF ablation occurs through rapid realignment of molecules adjacent to the RF electrode as an alternating current is applied to the circuit. Dipolar molecules within the target tissue, which are predominantly water

molecules, attempt to align with the current. As the direction of the current rapidly alternates, the dipolar molecules rapidly realign with the current resulting in vibration and frictional heating. The frictional heating resulting from dipolar molecule realignment causes high temperatures within the tissues immediately adjacent to the electrode. These high temperatures, resulting from frictional heating, are then thermally conducted to the adjacent tissue.

Ohm's law, *current* = *voltage*/*resistance*, assists with understanding RFA. RFA is dependent upon the flow of current within the circuit. However, RFA is adversely impacted by increased resistance to flow within the circuit, known as impedance. The significance of impedance is further understood when assessing the power of a system, *Power* = *voltage* × *current*. When substituting into this equation using Ohm's law, $Power = voltage^2/resistance$, the inverse relationship of power and resistance is noted. Several methods to decrease impedance have been employed in RFA systems: these include the expansion of electrode surface area, such as with multi-tine electrodes, which increases heat distribution within the target tissue and decreases the occurrence of charring; pulsing the power input of a system which allows brief termination of power input to an electrode when a rapid increase in impedance is detected, allowing the tissue to cool, thereby decreasing charring; internal cooling of the electrode to eliminate charring at the electrode-tissue interface; and injection of saline into the ablation zone to increase conduction of electricity into the target tissues. Any source of impedance, or resistance to flow, within the circuit limits the efficacy of RFA. Tissue desiccation occurs when too much energy is deposited in a target tissue too rapidly. The water vapor and tissue charring associated with desiccation insulate the electrode, limiting current flow, which limits further tissue ablation (Fig. 1.3).

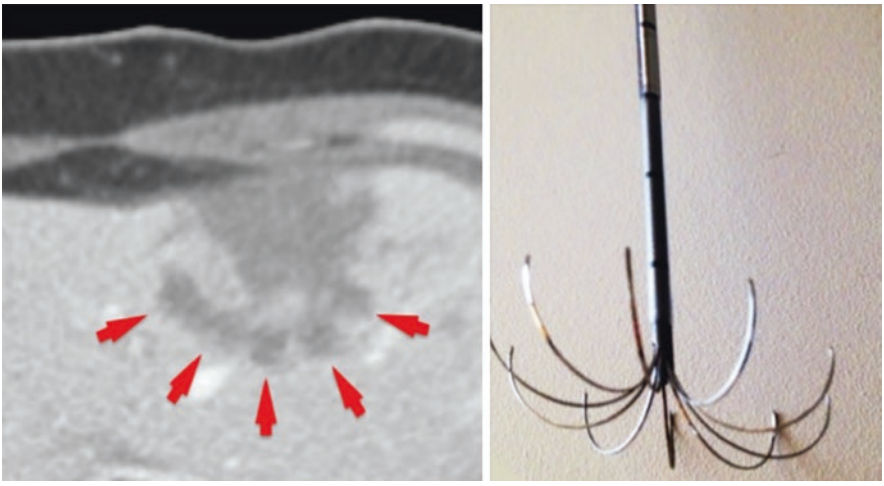

Fig. 1.3 Effect of time on ablation efficacy. Contrary to MWA, RFA relies on a closed electrical circuit and a continuously flowing electrical current to deposit energy in the tissue. If the initial power is set too high (as in this example using an umbrella probe – right), the resulting initial high energy deposition chares the tissue surrounding the RFA tines (red arrows). The dehydrated tissue ceases to be a conductor and the circuit opens. This prevents further deposition of energy and limits the efficacy of RFA and the size of the ablation zone

Physiology

Body tissues are sensitive to temperature change. Tissue death occurs within 2 seconds at 55 °C and is instantaneous at 100 °C [3]. Ideal RFA occurs when target tissues are heated to the range of 60–70 °C for several minutes in a controlled manner, resulting in coagulative necrosis without charring or vaporization. When temperatures exceed 100 °C, undesirable tissue changes occur, including boiling, vaporization, and charring, all of which result in increased impedance, directly decreasing energy transmission through the circuit and limiting the ablation zone. To maximize the RF ablation zone, energy deposition in RFA should be slow and controlled.

Inhomogeneity within tissues results in variable energy conduction. This variable energy conduction results in significant inhomogeneity in heating within the RFA zone. The energy conducted through the local tissues is also adversely affected by temperature losses that occur with flowing blood in the ablation zone, known as "heat sink". Temperature losses are encountered when a blood vessel 3 mm or greater in diameter is in the region of the target lesion. Flowing blood leads to relative cooling of tissues along a vessel in the ablation zone, counteracting the thermal conduction of heat from the tissues surrounding RF ablation device. The "heat sink" effect increases the likelihood of residual viable tumor near the vessel wall and increases the likelihood of local tumor progression.

Within the peripheral RFA zone of sub-lethal hyperthermia, inflammatory infiltrates specific to the ablated tissue have been reported [1]. Following RFA, immune activation has been demonstrated within the ablation zone as well as within untreated tumors and in the peripheral bloodstream [1]. The release of intracellular material as well as components from the disrupted extracellular tissues results in activation of immune response and pro-inflammatory cytokines within hours to days after RFA [1].

Microwave Ablation

Physics

Microwave ablation is based upon the generation of an oscillating electromagnetic field resulting in continuous realignment of polar water molecules in the ablation zone which causes frictional tissue heating and ultimately coagulative necrosis.

Microwave electromagnetic energy ranges from 300 MHz to 300 GHz. Clinically used microwave ablation devices typically operate between 915 MHz and 2.5 GHz [1, 2]. Following placement and activation of a microwave ablation antenna, molecules which possess an intrinsic dipole moment (primarily water) begin to continuously realign in response to the oscillating electromagnetic field (Fig. 1.4). The phenomenon of energy loss as rotating dipoles cannot keep up with the alternating magnetic field is known as dielectric hysteresis. The increased kinetic energy generated by the rotation of these molecules leads to tissue heating. The ablation zone

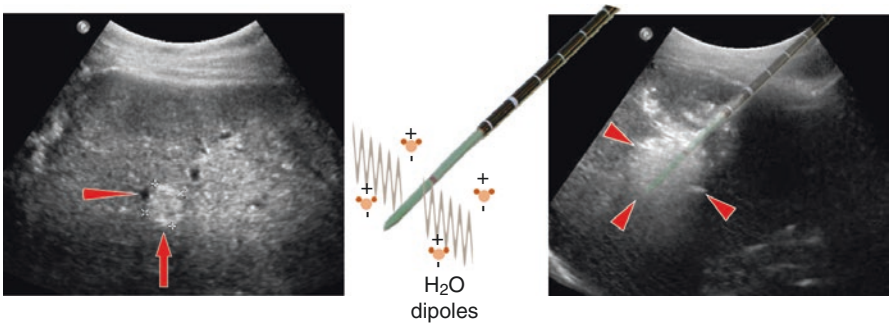

Fig. 1.4 Microwave ablation. The image on the left shows a 1.5 cm colon metastasis to the liver (red arrow) abutting a blood vessel (red arrowhead). The microwave antenna generates an oscillating electromagnetic field resulting in oscillation of dipole molecules (predominantly water). The phenomenon known as dielectric hysteresis leads to energy deposition and tissue heating. The electromagnetic field penetrates all biological tissues and can generate heat rapidly, with the potential to overcome heat sink and charred tissue. The image on the right is during ablation and shows the target lesion obscured by a large gas containing ablation zone (red arrowheads). The heat sink from the vessel (no longer seen) noted in the first image failed to limit the ablation zone

generated with MWA is not dependent upon electrical conductivity nor subject to impedance, but rather permeates all biological tissues. Without concern for tissue desiccation or charring, MWA is capable of producing larger and hotter ablation zones at a more rapid rate when compared to RFA. As MWA utilizes an electromagnetic field and not a circuit, grounding pads are not required.

Microwave ablation zones are dependent upon the number, design, and orientation of antenna, upon the power applied and upon the microwave frequency. The antennae provide energy transfer from the system into the target tissue. There are many MWA antenna designs, and designs often involve trade-offs in efficiency, size, and heating pattern [2]. At certain microwave frequencies, tissues may be actively heated up to 2 cm away from the antenna, which contrasts with the active zone of heating with RFA which is limited to a few millimeters around the ablation electrode [1]. Multiple antennae may be used simultaneously with MWA. With constructive phasing of the electromagnetic fields, the generated heat is proportional to the square of the number of antennae, working synergistically to increase the size of the ablation zone [1].

Physiology

Coagulative necrosis characterizes cell death in MWA, as in the other thermal ablation modalities. Temperatures with MWA can exceed 150 °C. Such temperatures are instantly lethal to biological tissues. The rapid and high temperatures that occur with MWA result in extensive vaporization and charring of ablated tissues, which in contrast to RFA do not adversely impact ablation and yield more consistent ablation

results across all tissue types [4]. The large volume of MWA zones, coupled with rapid generation of high temperatures, makes MWA less susceptible to heat sink effect and results in shorter ablation times when compared to RFA.

MWA is considered a weak stimulator of local inflammation and immunogenicity when compared to other ablation modalities, with minimal induction of pro-inflammatory cytokines [1]. Despite this, a statistically significant correlation between survival outcomes and extent of immunocyte infiltration has been demonstrated with MWA [5].

Cryoablation

Physics

Cryoablation is based upon the circulation of a cryogen, a gas that cools as it expands, into a cryoprobe resulting in creation of ice, with resultant coagulative necrosis of the target tissue. The phenomenon is called the Joule-Thomson effect.

As the cryogen gas passes from a region of high pressure to low pressure within the device (no gas is released in the patient), whether through a valve or into an expansion chamber, rapid cooling of the cryoprobe to −160 °C or colder occurs [4]. This rapid cooling results in freezing and creation of an ice ball surrounding the cryoprobe (Fig. 1.5). After the initial formation of ice within the tissue along the cryoprobe, passive thermal diffusion results in growth of the ice ball.

Cryogenic liquids have boiling points less than −150 °C. Liquid nitrogen has the greatest freezing capacity of liquid cryogens but cannot be used in devices with a diameter less than 3 mm [6]. In contrast, Argon is safely used in small diameter percutaneous devices and therefore is the cryogen mostly used for clinical cryoablation.

The surface area of a cryoprobe is proportional to its cooling capacity, with larger cryoprobe diameters resulting in greater size of ablation zones. Multiple cryoprobes are generally required to treat a target tumor percutaneously. In addition to creation of a larger ice ball and cryoablation zone, the use of multiple cryoprobes creates a more uniform zone of lethal ablation and lower ablative temperatures in the targeted tissue [6].

Inhomogeneity within target tissues may result in variable expansion of the ablation zone and growth of the ice ball. Cryoablation is challenged by loss of intended freezing temperature changes in the presence of nearby large blood vessels. Flowing blood leads to relative warming of tissues along vessels in the cryoablation zone, counteracting the removal of energy from the tissues by the cryoprobe. As with the “heat sink” effect seen with RFA, this increases the likelihood of residual viable tumor near the vessel wall and increases the likelihood of local tumor progression. Being the opposite of a heat sink effect, this is properly termed the heat-pump effect.

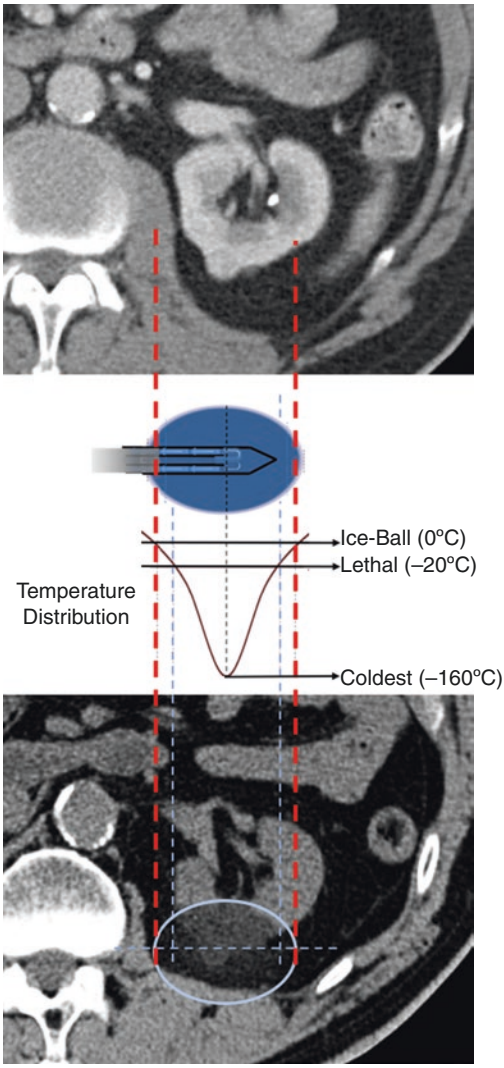

Fig. 1.5 Cryoablation. The top image shows a small exophytic RCC in the posterior aspect of the left kidney. As Argon (a cryogen) passes from a region of high pressure to low pressure within the device (middle image), whether through a valve or into an expansion chamber, rapid cooling of the cryoprobe to −160 °C or colder occurs via the Joule-Thomson effect. This results in the creation of an ice ball surrounding the cryoprobe. The only visible isotherm is the ice ball itself at 0 °C (dashed red lines). The lethal isotherm (~ −20 °C) is 2–5 mm deep to the visible ice ball (dashed blue lines)

Physiology

Tissue response to cryoablation depends upon the severity of freezing within the tissue. Various biological responses have been described with cryoablation and are dependent upon the temperature within that portion of the ablation zone. Severe freezing injury, as occurs with "lethal ice", is the objective of cryoablation. Direct cellular injury occurs when extracellular water freezes before intracellular water, resulting in an osmotic gradient with fluid flux from the cell to the extracellular space, causing cell dehydration. This dehydration results in distortion of the plasma

membrane [1]. Intracellular freezing results in direct cell membrane and organelle injury, leading to loss of homeostasis and further cell desiccation. Ice crystals from cellular freezing cause mechanical injury via shearing forces [6]. With thaw of the ice ball, the hypertonic intracellular compartment experiences an exaggerated fluid shift which results in cell membrane rupture [1]. In the central zone near the cryoprobe, uniform cell death is characteristic.

A zone of non-lethal ice is present toward the periphery of the ice ball, where the tissue temperatures are 0 to −20 °C. In this region, some cells are killed while others survive. Apoptosis may be seen within this portion of the cryoablation zone, where temperatures are insufficient to uniformly kill all cells. Tissue injury related to non-lethal ice may trigger apoptosis up to several days after ablation [6].

Cryoablation is dependent upon implementation of sequential freeze-thaw cycles, and each component of the freeze-thaw cycle (such as the cooling rate, the warming rate, and the temperature produced) contributes to injury to the target tissues [6]. The fastest cooling rate is desired, as faster freezing to lower temperatures results in the formation of lethal intracellular ice crystals. Cells die in progressively greater numbers as the temperature falls from −5 °C to −50 °C. With the treatment of cancer, the goal is to obtain the coldest lethal ice possible throughout the target area and within a volume of tissue around the tumor to ensure death of all cancer cells. While extensive tissue damage occurs at −20 °C to −30 °C, cancer cell destruction may be incomplete [6]. Duration of freezing with cryoablation varies and is partially determined by growth of the ice ball. Ideally, tissues should be kept in the frozen state for 5 minutes or longer to produce solute effects, ice-crystal formation, and recrystallization effects [6].

Slow, passive thawing of the frozen tissue is a major destructive factor. With a longer duration of thaw, greater damage to cells occurs, including increased solute effects, ice-crystal restructuring, prolonged oxidative stress, and growth of ice crystals [6]. Vasoconstriction and vascular injury which occur in response to cryoablation are prolonged with a longer, passive thaw. This allows further destructive changes to occur within the ablation zone. Providing a delay after thawing, before initiating the second freeze cycle, results in ongoing tissue hypothermia and oxidative stress [6]. Rapid thawing increases the chance of cell survival and should be avoided.

Repeating the freeze-thaw cycle produces faster and more extensive tissue cooling, resulting in an increased volume of frozen tissue which is seen as a larger ice ball. By repeating the freeze-thaw cycle, the margin of lethal ablation is moved closer to the outer limit of the frozen volume [6]. The use of temperature sensors, mounted in needles, enables accurate assessment of temperatures within the ice ball. This specific temperature information is useful both for ensuring adequacy of lethal ice covering target tissues and for protecting adjacent non-target tissues.

In contrast to RFA and MWA, cryoablation does not result in denaturation of proteins. These tumor antigens are preserved and released upon tumor thawing and reperfusion, resulting in a robust inflammatory response and the potential to stimulate an immune response. Cryoablation has been shown to produce antibodies to

ablated tumor antigens in both animals and humans [7]. After cryoablation, pro-inflammatory cytokines are released in higher quantities than after RFA or MWA. The systemic response to the release of recognizable intracellular contents following cryoablation of hepatocytes may lead to the rare phenomenon of cryoshock. Kupffer cells are stimulated to release pro-inflammatory mediators that may result in systemic inflammatory response syndrome, disseminated intravascular coagulopathy, multi-system organ failure, and death [1]. Cryoshock is most severe when at least 35% of the liver has been cryoablated. In addition to a robust stimulatory effect on the immune system, cryoablation may also result in an immunosuppressive effect which has been attributed to the balance between necrosis and apoptosis [1]. Apoptosis does not result in release of intracellular contents as seen with necrosis, and may result in immunosuppression toward apoptotic cell antigens [1]. Whether necrosis or apoptosis will exert more effect on the inflammatory and immune responses following cryoablation is not readily predicted, and may be influenced by factors related to ablation, tumor type, and the individual [1].

Non-thermal Ablation

Irreversible Electroporation (IRE)

Non-thermal ablation occurs with electroporation, in which electrical pulses applied induce permeabilization of the cell membrane. Irreversible electroporation (IRE) is a non-thermal ablation technique that permanently creates nanoscale defects in the cell membrane by exposing cells to short and intense electric fields [8]. The altered intracellular environment ultimately induces cell death via both apoptosis and coagulative necrosis [9]. Electroporation can ablate significant volumes of tissue without producing a thermal effect, thereby preventing damage to surrounding structures. IRE planning uses mathematical modeling to precisely predict the treated area and allows for accurately delineated ablation zones [8]. In contrast to thermal ablation (RFA and MWA), the nonthermal nature of IRE makes it forgiving to extracellular matrix and organ architecture, thereby allowing for treatment of complex lesions that are unapproachable with thermal techniques.

Physics

Electroporation generates a destabilizing electric potential across cell membranes that leads to the creation of nanoscale defects in the lipid bilayer [10]. In IRE, these defects are non-transient and lead to cell death. Contact electrodes are used to apply short (microsecond to millisecond) high voltage pulses to cells or tissues, permeabilizing the cell membrane (Fig. 1.6) [10].

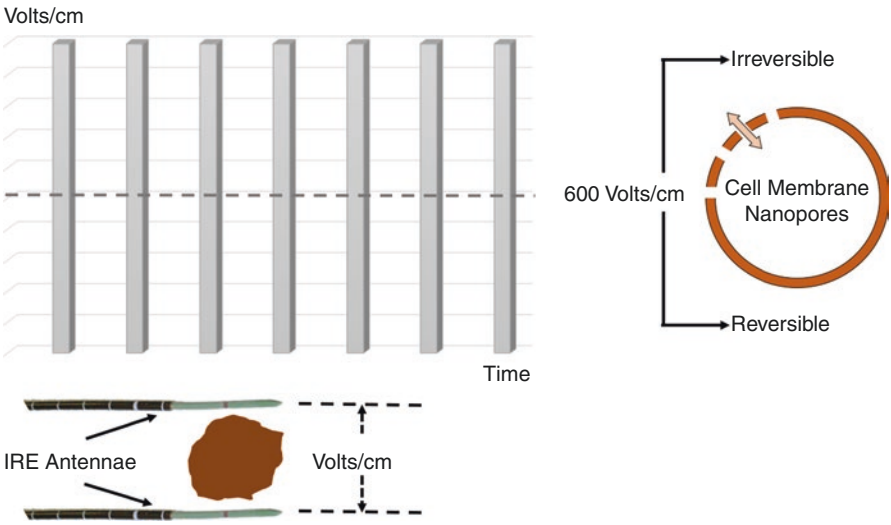

Fig. 1.6 Irreversible electroporation. IRE probes are placed parallel within or spanning the target tissue to ensure a uniform ablation zone. A series of high-voltage, microsecond electrical pulses are delivered through the probes to the target tissue. The physiological effect is the creation of small membrane pores in the affected cells. When the voltage gradient between the IRE antennae is below 600 Volts/cm, the nanopores heal spontaneously after cessation of the voltage and transmembrane homeostasis is re-established. When the voltage gradient between the IRE antennae is above 600 Volts/cm, these nanopores are generally irreversible. The subsequent permanent loss of cell homeostasis results in cell death

An IRE device has three components: the generator, monopolar probes, and a cardiac syncing device. The generator is interfaced with a computer system with treatment planning software [11]. The generator delivers low-voltage, high-energy current through monopolar probes connected to the generator. The system can connect up to six monopolar needle electrodes and the electrical pulse is delivered between two probes at a time. The treatment planning software helps determine the number of probes required to create the desired ablation zone.

Voltage, pulse frequency, pulse duration, electrode number, and electrode spacing are parameters that are entered into the IRE console, which then generates a two-dimensional representation of the ablation shape, perpendicular to the direction of the needle electrode insertion [11]. Ongoing research in this area is underway, but the most important parameters affecting the ablation zone are impedance distribution, pulse characteristics, and electrode configuration (size, spacing, and number) [12]. Currently, the most common practiced settings for tumor ablation are voltage 1500 V/cm, 70–90 pulses of 70–90 μs, electrode spacing of 1.5–2 cm, and active electrode tip length of 1–1.5 cm [11].

The monopolar probes are 15–20 cm length, 19-gauge needles with 1 cm depth markings along the shaft of the probe. The active tip can be exposed between 1 and 4 cm, depending on the desired size of the ablation zone and the depth of the lesion.

The needles are placed under ultrasound guidance, and therefore the exposed electrode surface is echogenic. Parallel insertion of the probes is important, as is avoiding convergence or divergence of the probes, which can result in a nonuniform ablation zone. The ideal spacing between probes is 1.5 and 2 cm. Inaccurate spacing increases the chances of high current errors.

Early experiences resulted in transient arrhythmia in human subjects undergoing IRE and therefore the generator also incorporates a five-lead system which synchronizes pulse delivery with the patient's electrocardiogram (ECG). When an electrical energy pulse is delivered, this system detects the rising slope of the R-wave and sends a signal to the generator [11].

Physiology

Electroporation increases the permeability of the cell membrane as it exposes the cell to an electrical pulse [13]. This produces disruption of the lipid bilayers of the cell membrane on which nano-pores are formed allowing normally impermeant matter to diffuse freely through the membrane [10, 13]. A combination of studies showed that as electric potential across the cell membrane increases due to the pulse delivered, the cell membrane can either be permeabilized reversibly (does not induce cell death) or irreversibly (which would lead to necrosis and death). This mechanism of permeabilization of the cell membrane with electrical pulses is not fully understood. However, the outcome depends on the pulse amplitude and duration of number of pulses [10]. Unlike thermal ablation, the cell membrane's permeabilizing electric filed is unaffected by local blood flow and thus allows for control over the extent of the affected tissue.

The external electric field delivered is the main parameter that affects the transmembrane potential——the potential difference across the plasma membrane [13]. Intra- and extracellular solute transport is highly regulated by the lipid bilayer membrane. This creates a density difference between the intra- and extracellular space, resulting in a voltage potential difference across the membrane. The electric field provides a local driving force that propels larger or polar molecules and ions, which the membrane would normally be impermeable to, into the cell [13]. When this transmembrane potential reaches a specific threshold, electroporation occurs and the plasma membrane undergoes structural rearrangement. Once the nanoscale pores are created in the membrane, the cell requires increasing energy to preserve its transmembrane ionic differences. If the adenosine triphosphate-dependent protein pumps are unable to compensate for the diffusion differences, this altered intracellular environment that IRE has created will induce cell death via apoptosis and coagulative necrosis [13] (Fig. 1.7).

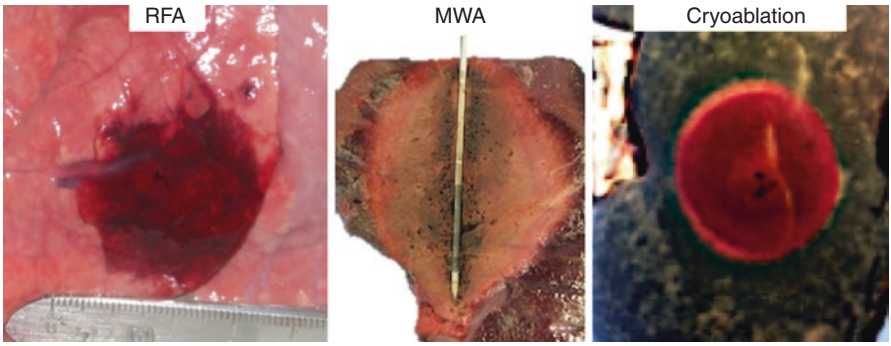

Fig. 1.7 Ablation zone comparison between ablation modalities. RFA ablation zone shows the highest border irregularity which contributes to lower response rates. Consequently, a wider ablation margin is recommended for RFA, up to 10 mm. MWA shows a relatively smoother ablation boundary whereas cryoablation is characterized by a near-spherical and uniform ablation zone

References

1. Chu KF, Dupuy DE. Thermal ablation of tumours: biological mechanisms and advances in therapy. Nat Rev Cancer. 2014;14(3):199–208.
2. Ahmed M, Brace CL, Lee FT Jr, Goldberg SN. Principles of and advances in percutaneous ablation. Radiology. 2011;258(2):351–69.
3. Hong K, Georgiades C. Radiofrequency ablation: mechanism of action and devices. J Vasc Interv Radiol. 2010;21(8):S179–86.
4. Hinshaw JL, Lubner MG, Ziemlewicz TJ, Lee FT Jr, Brace CL. Percutaneous tumor ablation tools: microwave, radiofrequency, or cryoablation--what should you use and why? Radiographics. 2014;34(5):1344–62.
5. Dong BW, Zhang J, Liang P, Yu XL, Su L, Yu DJ, et al. Sequential pathological and immunologic analysis of percutaneous microwave coagulation therapy of hepatocellular carcinoma. Int J Hyperth. 2003;19(2):119–33.
6. Baust JG, Gage AA. The molecular basis of cryosurgery. BJU Int. 2005;95(9):1187–91.
7. Erinjeri JP, Clark TW. Cryoablation: mechanism of action and devices. J Vasc Interv Radiol. 2010;21(8):S187–91.
8. Al-Sakere B, Andre F, Bernat C, Connault E, Opolon P, Davalos RV, et al. Tumor ablation with irreversible electroporation. PLoS One. 2007;2(11):e1135.
9. Davalos RV, Bhonsle S, Neal RE. Implications and considerations of thermal effects when applying irreversible electroporation tissue ablation therapy. Prostate. 2015;75(10):1114–8.
10. Edd JF, Horowitz L, Davalos RV, Mir LM, Rubinsky B. In vivo results of a new focal tissue ablation technique: irreversible electroporation. IEEE Trans Biomed Eng. 2006;53(7):1409–15.
11. Wagstaff PG, Buijs M, van den Bos W, de Bruin DM, Zondervan PJ, de la Rosette JJ, et al. Irreversible electroporation: state of the art. Onco Targets Ther. 2016;9:2437–46.
12. Edd JF, Davalos RV. Mathematical modeling of irreversible electroporation for treatment planning. Technol Cancer Res Treat. 2007;6(4):275–86.
13. Davalos RV, Mir IL, Rubinsky B. Tissue ablation with irreversible electroporation. Ann Biomed Eng. 2005;33(2):223–31.

Chapter 2
Physics and Physiology of 90Y Radioembolization for Liver Tumors

Andrew C. Picel and Daniel Y. Sze

Introduction

Transarterial radioembolization (TARE) is a type of intra-arterial brachytherapy during which yttrium-90 (^{90}Y) attached or incorporated into microspheres is selectively delivered to destroy tumor cells while attempting to spare the healthy liver parenchyma. A wide variety of tumor cells are sensitive to radiotherapy, but the procedure is most frequently performed for hepatocellular carcinoma (HCC) and metastatic colorectal cancer (mCRC) following the FDA indications. Successful treatment relies on understanding patient and tumor physiology and radionuclide physics to administer a tumoricidal dose safely.

Two different devices are available for radioembolization. TheraSphere (glass microspheres; Nordion/BTG/Boston Scientific, Marlborough, Massachusetts) was approved by the FDA in 1999 under a Humanitarian Device Exemption (HDE) to treat unresectable HCC. SIR-Spheres (resin microspheres; Sirtex Medical, Boston, MA, USA) gained FDA Premarket Approval (PMA) in 2002 for the treatment of mCRC in conjunction with intra-arterial infusion of floxuridine.

A. C. Picel (✉) · D. Y. Sze
Division of Interventional Radiology, Department of Radiology, Stanford University, Stanford, CA, USA
e-mail: apicel@stanford.edu

C. Georgiades, H. S. Kim (eds.), *Image-Guided Interventions in Oncology*,
https://doi.org/10.1007/978-3-030-48767-6_2

Hepatic Anatomy and Physiology

The liver receives up to 25% of the cardiac output. Approximately 20–30% of the blood supplied to the liver is from the hepatic artery; the remaining 70–80% is from the portal vein [1]. The hepatic arteries supply oxygen-rich blood and the portal vein supplies nutrient-rich blood to the hepatic sinusoids. The hepatic lobule is comprised of a polygonal structure with a central hepatic venule and peripheral portal triads comprised of portal venules, bile ducts, and hepatic arterioles. The hepatic sinusoids extend between the portal triads and central hepatic veins and are comprised of endothelial cells with fenestrations to facilitate exchange with hepatocytes. The terminal portal venules range in size from 15 to 50 μm in diameter and the sinusoids from 5 to 8 μm.

The majority of hepatocellular carcinoma arises in patients with cirrhosis. Severe liver damage results in a chronic inflammatory state leading to dysfunctional parenchymal regeneration. In cirrhosis, hepatocytes demonstrate shortened telomeres and reduced regenerative capacity. Persistent inflammation results in reactive oxygen species and lack of DNA checkpoint inhibition that may lead to progression to dysplastic nodules and neoplasms. This process of malignant transformation is characterized by an ischemic microenvironment that leads to upregulation of angiogenic and growth factors [2].

Intra-arterial tumor therapies rely on the dual blood supply to the liver to protect healthy liver tissue and to target malignant cells, since primary and metastatic hepatic tumors are predominantly supplied by the hepatic artery [1]. As a neoplasm becomes larger and dedifferentiated, arterial angiogenesis progresses and portal venous flow decreases [3]. The hepatic arterial blood supply becomes hypertrophied and parasitized with preferential flow to the tumor relative to normal hepatic tissue. Arterial flow shunting to the tumor along the margins of the mass may create a high pressure system that impedes portal venous inflow. A dense network of abnormal tumor vessels develops as tumors grow in size.

Tumors larger than 0.5 cm in diameter typically derive >90% of their blood supply from the hepatic arteries, as compared to 30% in normal liver parenchyma. Tumor neovascularity is disorganized with larger and irregular capillary diameters, endothelial proliferation, and arteriovenous shunting. Tumor vessel diameters usually range in size from 25 to 75 μm along the periphery of tumors, but particles smaller than 100 μm have the potential to pass through hepatic sinusoids and dysplastic vascular shunts and may result in nontarget embolization to the lungs. Studies in rats showed that 40 μm particles have the most favorable tumor to normal liver distribution ratio [4]. The dual blood supply to the liver and the proliferation of hepatic arterial neovascularity within tumors permits hepatic arterial treatments with microspheres to concentrate deposition within the tumor arterioles while minimizing exposure to the surrounding normal tissue.

Although hepatic parenchyma is predominantly supplied by portal veins, intrahepatic bile ducts are primarily supplied by hepatic arteries. The peribiliary arterial plexus measures approximately 30 μm in vessel diameter and is of similar size to

^{90}Y microspheres. Injury to the biliary tree is uncommon but can result in biliary stricture, biloma, and cholangitis [5]. Patients with metastatic disease may be more likely to incur biliary injury than those with HCC.

^{90}Y Microsphere Products

^{90}Y is typically produced in a nuclear reactor from the neutron bombardment of ^{89}Y. It decays into stable zirconium-90 [6]. ^{90}Y is a pure beta emitter with a 64.1 hour physical half-life. Ninety-four percent of the radiation dose results from decay during the first 11 days after treatment. The average beta particle energy is 0.927 MeV, with a maximum energy of 2.27 MeV. Mean tissue penetration is 2.5 mm with a maximum of 11 mm. ^{90}Y also produces internal pair positrons at a very low branching ratio of 32×10^{-6} but enough to be imaged with a PET scan.

Two different types of radioembolization microspheres are commercially available for treatment (Table 2.1) [7, 8]. TheraSphere are silicon and aluminum oxide glass microspheres 20–30 μm in size with integrated ^{90}Y. Calibrated at a specific activity of 2500 Bq/sphere, one 3 GBq vial contains 1.2 million microspheres, while the largest 20 GBq vial contains 8 million microspheres. Treatment has minimal embolic effect due to the relatively small numbers of microspheres needed to achieve high radiation doses. TheraSphere is supplied in 0.6 mL of sterile water in a 1 mL V-bottom vial within a clear acrylic shield. Therasphere is available in 6 different standard activities, 3, 5, 7, 10, 15, and 20 GBq, calibrated for Sunday at 12 pm Eastern Standard Time. Custom doses may also be ordered at 0.5 GBq increments between 3 and 20 GBq [9]. The desired activity is prescribed based on the original activity, elapsed time, and decay between calibration and administration. The entire vial is administered at the time of treatment. A fraction of the vial cannot be infused.

SIR-Spheres are cation-exchange resin microspheres 20–60 μm in size (mean 32 μm) with bound ^{90}Y immobilized by phosphate precipitation. According to specifications, SIR-Spheres are 30% larger than TheraSphere. SIR-Spheres are provided in a 5 mL vial of water, calibrated at 3 GBq ± 10% at 6 pm on the specified day of calibration, and shipped five days a week in a 6.4 mm minimum thickness lead pot. The specific activity of SIR-Spheres is 50 Bq/sphere at the time of calibration, so one 3 GBq vial contains 40–80 million microspheres [9]. Shelf-life is 24 hours after calibration. The desired activity is aliquoted from the supplied vial. The entire vial

Table 2.1 Comparison of microsphere products

	TheraSphere	SIR-Spheres
Particle size (μm)	20–30	20–60
Particles per 3 GBq vial	1.2 million	40–80 million
Specific gravity (g/dL)	3.6	1.6
Specific activity per sphere at the time of calibration (Bq)	2500	50
Activities available (GBq)	3–20	3–7.2

is not typically infused. Treatment with SIR-Spheres may have a moderate embolic effect in addition to the brachytherapy and may cause a post-embolization syndrome. Operators must be cautious to avoid stasis and reflux during administration, which can limit the activity administered and result in nontarget deposition-related complications. SIR-Spheres are now available as early as 3 days before calibration via the FLEXdose program, resulting in a specific activity as high as 120 Bq/sphere, with correspondingly decreased embolic effect and risk.

Radiation Dosimetry

Dosimetry refers to the process of simulating microsphere distribution, prescribing the activity of ^{90}Y to be administered to result in specified absorbed doses to the target tumors and to background tissues, and measuring and calculating the actual absorbed dose distribution. Activity is the amount of ^{90}Y radioactivity in the microspheres and is measured in gigabecquerels (GBq), and absorbed dose is the amount of radiation deposited in tissue and is measured in Grays (Gy). The Medical Internal Radiation Dose (MIRD) Committee of the Society of Nuclear Medicine reports that 1 GBq of ^{90}Y uniformly distributed throughout 1 kg of tissue results in an absorbed dose of approximately 50 Gy. Absorbed dose is determined by the volume of the vascular bed supplied by the artery catheterized during treatment, the activity of ^{90}Y injected, and the differential distribution of microspheres within the vascular bed.

Optimal results are expected from a tumor dose above a tumoricidal threshold and a functional liver dose below a toxic threshold [10]. Dose-response curves are difficult to establish because microspheres may form clumps of spheres resulting in a heterogenous distribution on a microscopic level, and the specific activity and number of microspheres injected differs widely between glass and resin products. In general, the higher the specific activity of the microspheres, the fewer microspheres are injected, but a higher absorbed dose is needed to compensate for heterogeneity and to be tumoricidal. For standard resin microspheres, the tumoricidal threshold appears to be in the range of 100 Gy, and for glass microspheres decayed 2–3 half-lives, the threshold appears to be around 200 Gy for HCC. The toxicity threshold for normal liver treated with standard resin microspheres is around 30–40 Gy, but for glass microspheres the threshold is about 70 Gy. The thresholds for cirrhotic or otherwise compromised liver are about half that of normal liver.

Dose distribution simulation is performed during the planning mesenteric angiography procedure by injection of 2–5 mCi ^{99m}Tc-macroaggregated albumin (^{99m}Tc-MAA) at the intended catheter site for treatment. Planar and SPECT imaging is then performed to evaluate microsphere distribution within the liver and tumors, and to calculate the proportion of activity that traversed hepatic and tumoral arteriovenous shunts to become lodged in the pulmonary vasculature, known as the lung shunt fraction (LSF) or hepatopulmonary shunt fraction (HPSF) (Figs. 2.1 and 2.2). Due to the range of particle sizes of ^{99m}Tc-MAA, that includes particles smaller than 10 μm, and volume averaging of the hepatic dome and right lower lobe of lung, the

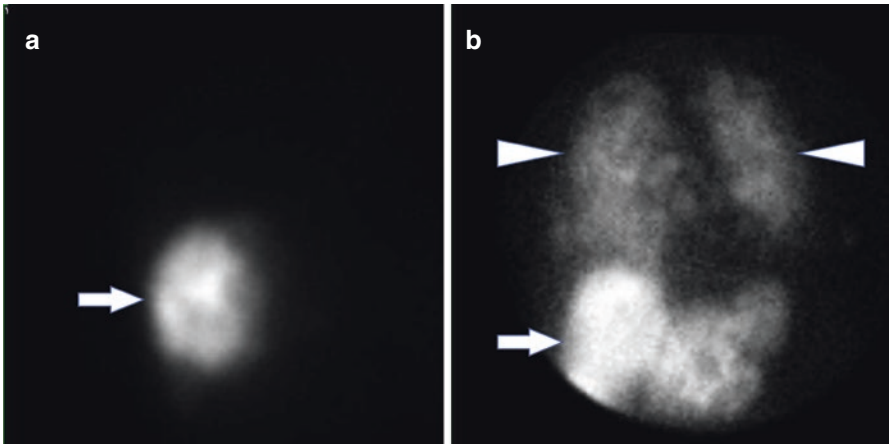

Fig. 2.1 Planar images after hepatic arterial infusion of ^{99m}Tc-MAA to calculate the lung shunt fraction prior to definitive treatment. The first patient (**a**) had a calculated lung shunt less than 1.5%. Note activity within the hepatic masses and no significant activity over the lung fields. The second patient (**b**) showed activity in the liver (white arrow) and a large amount of activity in the lungs (white arrowheads). A lung shunt fracture of 50% in this case was a contraindication to treatment

calculated LSF is frequently an overestimate compared with calibrated therapeutic Therasphere and SIR-Spheres [9].

The following formulae are used to calculate the LSF and lung absorbed dose from the ^{99m}Tc-MAA imaging:

1. LSF = total lung counts/(total lung counts + total liver counts)
2. Lung dose (Gy) = 50 * prescribed activity (GBq) * LSF/lung mass (kg)

From anterior and posterior planar images, LSF is usually reported as the geometric mean. Potentially more accurately, LSF can also be calculated from SPECT using voxel-based partitioning. Lung mass is difficult to measure, but is often approximated to be 1 kg in an average patient. The radiation pneumonitis toxicity limits are 30 Gy per treatment and 50 Gy cumulative over a lifetime [9, 11]. Although some guidelines suggest dose reduction if the LSF is greater than 10%, this could also compromise tumor dose and efficacy, so activity prescription based on lung dose may be preferable to that based solely on LSF [12, 13]. Adjunctive procedures may be performed to fractionate or reduce LSF, but if an adequate dose cannot be delivered to the tumor because of a high LSF, radioembolization is contraindicated.

Further tailoring of dose distribution may be achieved by administering more selectively in multiple arteries. In addition, coil embolization of intrahepatic

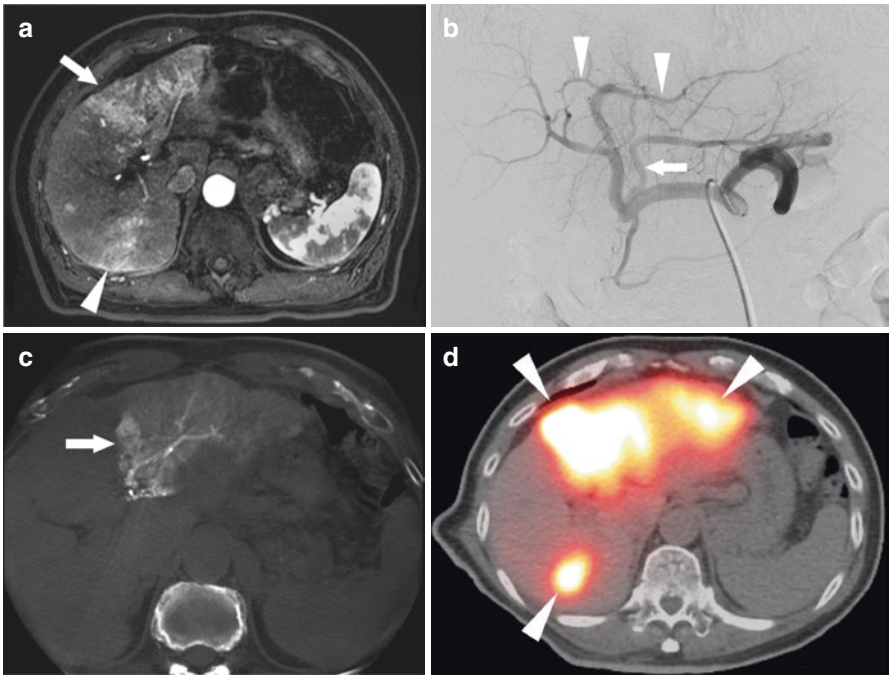

Fig. 2.2 A 64-year-old male with cirrhosis and infiltrative HCC presented for palliative radioembolization. (**a**) Arterial phase contrast-enhanced MRI showed multifocal infiltrative HCC replacing segments 2 and 3 (white arrow) and part of segments 6 and 7 (white arrowhead). (**b**) Celiac arteriogram showed segment II and segment III hepatic arteries supplying the region of confluent disease in the left hepatic lobe. This patient had variant anatomy with separate origins of the segment III hepatic artery (white arrow) and the segment II and IV hepatic arteries (white arrowheads). (**c**) Cone-beam CT angiogram performed after selection of the segment III hepatic artery showed perfusion to the majority of the left hepatic lobe (white arrow) without evidence of extrahepatic supply. (**d**) SPECT-CT after administration of 4 mCi ^{99m}Tc-MAA to the proper hepatic artery showed radiotracer activity within the tumors (white arrowheads). The lung shunt fraction (LSF) was 9.3%. Treatment was staged with the left hepatic lobe treated in one session and the patient returning a month later for segment 6 and 7 treatment

feeding arteries or accessory arteries, or particle and coil embolization of parasitized extrahepatic arteries may be performed to allow for flow redistribution [9]. Flow redistribution may reduce the number of injection sites and improve safety by reducing the risk of reflux into hepatico-enteric anastomotic arteries near the hilum and ligamentum venosum.

Patients on systemic therapy may require radioembolization dose reduction and/or may be asked to hold the therapy 2–6 weeks before and after radioembolization, since some chemotherapeutic agents such as gemcitabine are radiation sensitizing and increase the risk of radioembolization-induced liver disease (REILD). Other risk factors include prior radiation exposure from external beam radiotherapy,

prior radioembolization, and hepatic fibrosis or congestion from systemic therapy. Patients with REILD present with jaundice and ascites 1–4 months after radioembolization. REILD causes pathologic changes of hepatic sinusoidal obstruction, which is distinguished from external beam radiation-induced liver disease (RILD), which is characterized by veno-occlusive obstruction and anicteric hepatomegaly, ascites, and elevated alkaline phosphatase. Although patients differ in tolerance to radiation, avoidance of REILD requires accurate dosimetry [11, 14].

Therasphere Dosimetry

The Therasphere package insert recommends the use of MIRD dosimetry, which assumes uniform distribution of microspheres in the single compartment volume of liver treated. Tumor burden and hypervascularity are not taken into account [9]. The treated volume is estimated from cross-sectional images, and converted to mass by a conversion factor of 1.05 g/cm^3. Estimating treatment volumes requires either accurate Couinaud segmentation on noninvasive imaging or selective arterial enhancement on cone-beam CT. The MIRD formula is used to calculate the necessary activity to deliver a recommended dose of 80–150 Gy:

$$\text{Activity administered}(\text{GBq}) = (\text{target dose}(\text{Gy})) * (\text{mass of tissue treated}(\text{kg})) / 50 * (1 - \text{LSF})$$

TheraSphere at calibration has an average specific activity of 2500 Bq/sphere, which is felt to be too high for immediate clinical use. Treatment is planned with consideration of the 64.1 hour decay half-life, and typically spheres are administered 3–9 days after calibration, at a reduced specific activity of 1200–275 Bq/sphere. The appropriate activity to order is back-calculated from the treatment day and time and the activity needed after decay to achieve the desired target dose. Spreadsheet and online calculators are available to display treatment options.

Microsphere vials can be administered during the first or second week after calibration, with greater number of microspheres administered to achieve the same tissue dose using decayed second week vials. Many operators use decayed Therasphere microspheres to improve distribution and coverage of larger tumors. For target volumes that have only a small amount of functional liver that is considered expendable, higher activities may be delivered to guarantee an ablative tumoricidal dose. Use of first week microspheres with higher specific activity allows prescription of target doses of 200–500 Gy, a technique referred to as radiation segmentectomy. Use of more decayed spheres less selectively, and at a lower dose of about 120 Gy, with the intention of causing hypertrophy of the contralateral lobe may be referred to as radiation lobectomy [15].

SIR-Spheres Dosimetry

Dosimetery for SIR-Spheres can be performed by the empiric method, body surface area (BSA) method, or partition method. The empiric method prescribes the activity to be administered based on the tumor burden as a fraction of the total liver mass. Although the package insert still describes the empiric method, it is inadequately personalized, obsolete, and should not be used [16].

The BSA method also described in the package insert is the most commonly used method for resin microsphere dosimetry and relies on the assumption that liver volume is correlated to body surface area. The prescribed activity is then adjusted for percentage tumor burden, according to the following calculations:

1. $BSA(m^2) = 0.20247 \times height(m)^{0.725} \times weight(kg)^{0.425}$
2. Activity administered (GBq) = BSA – 0.2 + (%tumor involvement/100)

The above formula calculates activity for whole liver treatment; if less than the whole liver is to be treated, the prescribed activity is based on the fraction of the total liver treated. The BSA technique is simple but subject to many inaccuracies. Like the MIRD method, it does not take into account the hypervascularity of the tumors. Large tumor burdens and large livers, particularly in smaller patients, are often underdosed to below the tumoricidal threshold, and larger patients with small livers may be overdosed. The package insert further advises accommodating for high LSF by decreasing activity administered, by 20% for LSF 10–15%, 40% for LSF 15–20%, and foregoing treatment for LSF > 20% [9]. Although this guideline helps to maintain pulmonary safety, many of these patients will receive subtherapeutic dose to the tumor.

The partition method estimates the dose partitioned into the liver, lung, and tumor compartments [8]. The partition method is based on an assessment of tumor burden and the tumor to normal (T/N) ratio of uptake and results in more personalized patient-specific dosing. The activity is increased approximately 0.5 GBq for each 25% increase in tumor burden [9], calculated based on the following formulae:

1. T:N ratio = (activity in tumor/mass of tumor)/(activity in liver/mass of normal liver)
2. Activity (GBq) = target dose to tumor (Gy) * [(tumor mass (kg) * T:N) + normal liver mass kg)]/50 * (1-LSF)

The partition model may provide the most tailored dose and activity calculations but also has limitations. The model uses mean activity in each compartment, assuming uniform distribution throughout each compartment. Indistinct compartments such as tumor necrosis and hypervascular rims composed of functional liver confound the calculations. ^{99m}Tc-MAA scintigraphy is the main source used to estimate the T:N ratio but may not exactly simulate ^{90}Y microsphere distribution due to differences in microparticle size and number, specific gravity, embolic effect,

microcatheter position, and blood flow dynamics. The model is also difficult to apply to diffuse liver disease, infiltrative disease, and small lesions [16].

Emerging technologies of voxel-based dosimetry based on pre-treatment ^{99m}Tc-MAA SPECT/CT and/or post-treatment ^{90}Y PET/CT, some translated from external beam radiotherapy technology, may eventually allow for more accurate determination of dosimetric parameters [8]. Dose-volume histograms (DVH) for tumors can better predict efficacy, and DVH of functional liver can better predict toxicity. Commercial software is becoming available from multiple vendors.

Microsphere Administration

In the United States, ^{90}Y radioembolization is regulated by the Nuclear Regulatory Commission Code of Federal Regulations (NRC: 10 CFR Part 35). ^{90}Y administration is performed by an Authorized User (AU) who has completed brachytherapy training as well as vendor-specific training. Before administration, the microsphere activity is verified with a standard dose calibrator and portable ionization chamber. For SIR-Spheres, the desired activity is transferred by a radionuclide technologist from the shipment vial into the treatment vial. For TheraSphere, the microspheres are not transferred and are administered in their entirety, which reduces the risk of dosing error and radiation exposure to the technologist [9]. The administered activity must be within 20% of the prescribed activity to avoid a technical misadministration.

The IR procedure room floor and the pathway from the delivery system to the patient's arterial access site should be covered with absorbent liner to protect from contamination and to aid in cleaning any possible radiation spill. All potentially radioactive components of the delivery system (including biohazards such as the used microcatheter) are disposed of in a Nalgene container within an acrylic cylinder shield. The residual activity in the waste container is measured with an ionization chamber, and the delivered activity is calculated by subtraction of the residual from the original activity, corrected for decay. The personnel, tables, floor, and equipment are checked for spilled radioactivity after the procedure using a Geiger-Müller detector. A portable ionization chamber is used to measure maximum bremsstrahlung radiation emitted from the patient's liver, measured at skin level and at 1 meter distance. Any major spill must be cleaned under the supervision of the NRC and could require quarantine of the procedure room for weeks to allow for decay of spilled but irretrievable microspheres.

The delivery sets and administration techniques are different for TheraSphere and SIR-Spheres (Fig. 2.3). Step-by-step instructions for assembly and disassembly of the administration sets can be found in the manufacturer package inserts. An incorrectly set-up delivery box system may lead to misadministration and/or

Fig. 2.3 (**a**) The TheraSphere administration box. The dose vial within the lead pig is positioned within the box, and the needle assembly has been snapped in place. Saline flushed through the "B" line suspends the microspheres which then flow from the dose vial into the exit tubing and microcatheter. (**b**) Close up image of the TheraSphere administration box shows the radiation dosimeter near the dose vial. The reading should drop to zero during administration. The overflow vial is seen below "A". This serves to limit the rate of injection. If there is excess pressure during administration, excess saline will flow into this vial rather than over-pressurize the needle assembly. (**c**) The SIR-Spheres administration box. Dextrose solution injected in line and needle "D" agitates and suspends the microspheres, which then exit the vial through the outlet needle toward the three-way stopcock mounted on the interior of the box, connected to the external black knob. The distal outlet line "A" is connected to the microcatheter, and can be cleared by turning the black knob toward "Flush/Contrast" and injecting into line "B". The external stopcock attached to line "B" allows injection of contrast medium to perform interval angiography between aliquots of microspheres to assess arte-

rial flow for stasis. A radiation dosimeter has been placed inside the administration box to monitor completeness of administration (not recommended by manufacturer). (**d**) Interior of the SIR-Spheres administration box showing the administration needles positioned within the v-bottom dose vial. The inlet needle is positioned just above the microsphere pellet and is used to suspend the particles, and the outlet needle is positioned near the top of the meniscus where dilute suspended microspheres exit the proximal outlet line toward the three-way stopcock mounted on the interior of the box. The stopcock can be turned remotely by the external knob and allows alternating between microsphere aliquot administration and distal outlet line flushing or contrast medium injection

contamination. Connections must be fastened tightly and the systems thoroughly flushed to avoid air bubbles in the delivery lines. The microcatheter should not be occlusive in the artery, since forward flow is required for administration. Small bore microcatheters (<0.027″ lumen diameter) are not recommended due to the risk of clogging and the increased pressure needed for delivery potentially resulting in leaks in the infusion system. Treatment directly through a 4 or 5 Fr catheter is also not recommended since rapid low-resistance injection increases the risk of reflux and may alter flow dynamics and particle distribution [9].

The TheraSphere delivery box incorporates sites to attach two Rados radiation detectors near the dose vial and microcatheter connection. The dose vial within layered acrylic and lead pig shielding is accessed within the acrylic delivery box with a snap-on two-needle inlet/outlet flush system. Saline is infused into the dose vial to agitate and expel the microspheres into the microcatheter. The large majority (>90%) of the microspheres is flushed out by the first 20 mL of saline [9]. A total of 60 mL of flushing is recommended for complete evacuation, usually with >98% efficiency. The lines, and especially the microcatheter connection, may be gently tapped and tilted during administration to avoid microspheres lodging or accumulating in dependent areas, especially at the microcatheter hub. To reduce the risk of nontarget deposition, the rate of infusion should mimic the hepatic artery flow, and excessive injection pressure is diverted into a waste vial.

The SIR-Spheres administration set consists of an acrylic shield box, inlet and outlet needles and lines, and injection syringes. Recommendations have changed from using sterile water flush to using 5% dextrose solution (D5W) to reduce vasospasm and hemolysis. The use of saline or contrast medium to flush is not recommended, because the presence of cations may cause some 90Y to elute from the resin microspheres. D5W is injected into the inlet line and needle, whose tip is positioned just above the microsphere pellet, to agitate and suspend the microspheres. Microspheres exit the vial via the outlet needle and line, which is connected to the microcatheter. The distal outlet line and microcatheter may be cleared by turning a three-way stopcock mounted on the inner wall of the acrylic box. The progress of the infusion can thus be monitored under fluoroscopy by injecting contrast medium through the three-way stopcock into the distal outlet line to assess embolic effect and stasis. A minimum flush of 60 mL is recommended. The infusion is completed by injection of air into the inlet line, which expels the remaining D5W and microspheres from the vial. Tapping and tilting the lines and the three-way stopcock may also reduce the amount of residual microspheres deposited in drifts at the stopcock and the microcatheter hub. The treatment is complete when the entire dose is administered or stasis has been reached.

Conclusion

^{90}Y radioembolization has become a standard of care for patients with unresectable HCC and mCRC, as well as other primary and metastatic hepatic malignancies. The commercially available radioembolization devices, TheraSphere and SIR-Spheres, different in several important characteristics, dosimetry techniques, and delivery methods. Meticulous dosimetry and technique are mandatory to ensure safe delivery of microspheres and to achieve tumoricidal absorbed doses without incurring toxic hepatic, gastrointestinal, or pulmonary parenchymal doses.

Conflicts of Interest and Financial disclosures DYS is a consultant for Boston Scientific/BTG/Nordion, SIR-Tex, and Terumo/Quirem, and has received institutional research support from Boston Scientific/BTG/Nordion and SIR-Tex.

References

1. Kan Z, Madoff DC. Liver anatomy: microcirculation of the liver. Semin Interv Radiol. 2008;25(2):77–85.
2. O'Rourke JM, Sagar VM, Shah T, Shetty S. Carcinogenesis on the background of liver fibrosis: implications for the management of hepatocellular carcinoma. World J Gastroenterol. 2018;24(39):4436–47.
3. Tajima T, Honda H, Taguchi K, et al. Sequential hemodynamic change in hepatocellular carcinoma and dysplastic nodules: CT angiography and pathologic correlation. AJR Am J Roentgenol. 2002;178(4):885–97.
4. Anderson JH, Angerson WJ, Willmott N, Kerr DJ, McArdle CS, Cooke TG. Regional delivery of microspheres to liver metastases: the effects of particle size and concentration on intrahepatic distribution. Br J Cancer. 1991;64(6):1031–4.
5. Atassi B, Bangash AK, Lewandowski RJ, et al. Biliary sequela following radioembolization with yttrium-90 microspheres. J Vasc Interv Radiol. 2008;19:691–7.
6. Murthy R, Kamat P, Nunez R, Salem R. Radioembolization of yttrium-90 microspheres for hepatic malignancy. Semin Interv Radiol. 2008;25(1):48–57.
7. Lee EW, Alanis L, Cho SK, Saab S. Yttrium-90 selective internal radiation therapy with glass microspheres for hepatocellular carcinoma: current and updated literature review. Korean J Radiol. 2016;17(4):472–88.
8. Tong AK, Kao YH, Too CW, Chin KF, Ng DC, Chow PK. Yttrium-90 hepatic radioembolization: clinical review and current techniques in interventional radiology and personalized dosimetry. Br J Radiol. 2016;89(1062):20150943.
9. Salem R, Thurston KG. Radioembolization with 90Yttrium microspheres: a state-of-the-art brachytherapy treatment for primary and secondary liver malignancies. Part 1: technical and methodologic considerations. J Vasc Interv Radiol. 2006;17(8):1251–78.
10. Salem R, Padia SA, Lam M, et al. Clinical and dosimetric considerations for Y90: recommendations from an international multidisciplinary working group. Eur J Nuc Med Mol Imag. 2019;46(8):1695–704.
11. Riaz A, Lewandowski RJ, Kulik LM, et al. Complications following radioembolization with yttrium-90 microspheres: a comprehensive literature review. J Vasc Interv Radiol. 2009;20(9):1121–30.

12. Salem R, Thurston KG. Radioembolization with 90yttrium microspheres: a state-of-the-art brachytherapy treatment for primary and secondary liver malignancies. Part 2: special topics. J Vasc Interv Radiol. 2006;17(9):1425–39.
13. Kao YH, Magsombol BM, Toh Y, et al. Personalized predictive lung dosimetry by technetium-99m macroaggregated albumin SPECT/CT for yttrium-90 radioembolization. EJNMMI Res. 2014;4(33):1–12.
14. Braat MN, van Erpecum KJ, Zonnenberg BA, van den Bosch MA, Lam MG. Radioembolization-induced liver disease: a systematic review. Eur J Gastroenterol Hepatol. 2017;29(2):144–52.
15. Saini A, Wallace A, Alzubaidi S, et al. History and evolution of yttrium-90 radioembolization for hepatocellular carcinoma. J Clin Med. 2019;8(1):E55.
16. Doherty JO. A review of 3D image-based dosimetry, technical considerations and emerging perspectives in 90Y microsphere therapy. J Diagn Imag Thr. 2015;2(2):1–34.

Chapter 3
Physics and Physiology of Transarterial Chemoembolization and Drug-Eluting Beads for Liver Tumors

Michael C. Soulen and Thierry de Baere

Transarterial chemoembolization (TACE) developed circa 1980 in Japan using an emulsion of Lipiodol with an anthracycline chemotherapeutic drug [1–5]. Lipiodol is an ethyl ester of iodized fatty acids of poppy seed oil (Guerbet, Aulnay, France). TACE using a Lipiodol drug emulsion followed by a solid embolic material became the standard treatment for intermediate stage hepatocellular carcinoma (HCC) without portal vein thrombosis as a result of two randomized studies which used either doxorubicin [6] or cis-platinum [7] mixed with Lipiodol, followed by administration of an embolic agent. To date these studies represent the only controlled trials for intra-arterial therapies for HCC demonstrating the superiority of Lipiodol TACE to best supportive care.

TACE is also employed in patients with more advanced HCC, such as macrovascular invasion or limited extrahepatic disease in the setting of adequately preserved hepatic function, but survival benefit in this population has not been evaluated in a randomized trial. In a prospective nonrandomized study, 164 HCC patients with segmental or subsegmental portal vein thrombosis were treated with TACE or conservative care according to the patient's preference after counseling from a tumor board. The 12- and 24-month overall survival rates for the TACE and conservative groups were 30.9% and 9.2%, vs. 3.8% and 0% ($p < 0.001$) [8]. TACE is also used in patients with early-stage HCC as a bridge to liver transplantation or when liver transplantation, hepatic resection, and image-guided ablation are not possible [9]. Combination treatment with TACE and thermal ablation has been demonstrated of

M. C. Soulen (✉)
Department of Radiology, Abramson Cancer Center, University of Pennsylvania, Philadelphia, PA, USA
e-mail: michael.soulen@pennmedicine.upenn.edu

T. de Baere
Department of Interventional Radiology, Gustave Roussy Cancer Center, Villejuif, France
e-mail: Thierry.DEBAERE@gustaveroussy.fr

C. Georgiades, H. S. Kim (eds.), *Image-Guided Interventions in Oncology*,
https://doi.org/10.1007/978-3-030-48767-6_3

benefit over ablation alone in a randomized controlled trial for HCC smaller than 7 cm [10].

In addition to HCC, liver-directed therapy has a significant role in the management of liver-dominant neuroendocrine tumors (NETs). Current guidelines from the National Comprehensive Cancer Network (NCCN), European Neuroendocrine Tumor Society (ENETS), and North American (NANETS) Neuroendocrine Tumor Society all include TACE as part of the treatment algorithm for progressive or symptomatic liver metastases [11, 12].

Mechanism of TACE

When injected in the hepatic artery, Lipiodol is selectively taken up and retained in hepatocellular carcinoma and in hypervascular liver metastases [13–15]. Ethiodized oil circulates from the tumor-feeding arteries through the peribiliary capillary plexus into the terminal portal sinusoids and the drainage route from the tumor [16, 17]. Lipiodol exerts a temporary embolic effect on both the arterial and portal branches which persists for less than an hour. Because the embolic effect of Lipiodol is temporary, it is followed by a solid embolic material in order to maintain ischemia and retain the emulsion within the tumor vasculature [18]. When used as a vehicle for chemotherapeutic drug delivery, Lipiodol drug emulsion followed by particles embolization demonstrates a better pharmacokinetic benefit over Lipiodol drug emulsion alone or drug alone [19] and induces substantially greater tumor necrosis compared to injection of Lipiodol alone or as a drug emulsion without particles [20]. The addition of particulate embolic increases the rate of necrosis of main tumor from 13% to 83% and the rate of necrosis of satellite nodules from 6% to 53% [20]. In HCC the combination of Lipiodol drug emulsion with particles demonstrates better long-term survival than injection of Lipiodol drug emulsion without particles [21]. The liver cancer study group of Japan reported significantly better overall survival when particulate embolization material is used in the largest study to date on the efficacy of TACE (11,030 patients including 8057 TACE and 2523 chemotherapy-Lipiodol injections without embolization) [21] .

In addition to arterial ischemia, TACE induces a transient 70%–100% increase in portal venous pressure that peaks around 20 minutes after Lipiodol injection and subsides over 1 hour [22]. Patients with esophageal varices must be monitored as they can rupture immediately after treatment.

There are no controlled trials demonstrating superiority of TACE over transarterial embolization without drug. The theoretical basis for TACE is a synergy between ischemia and deposition of chemotherapeutic drugs at several times their lethal concentration. Hepatic malignancies express the multi-drug resistance gene (MDR1) which promotes expression of metabolically active cell membrane pumps that remove chemotherapeutic drugs from the cell. The hypoxia induced by embolization causes these cell membrane pumps to fail, leading to increased intracellular drug uptake under conditions of ischemia [23].

Chemotherapeutic Drugs and Embolics

For HCC, the most common single anticancer drugs used during TACE are the anthracycline group including doxorubicin or epirubicin [24]. The use of cisplatin has decreased due to shortage of cisplatin powder, which has only recently come back on the market in the USA. Several combination drug regimens have been reported, the most popular being cisplatin, doxorubicin, and mitomycin C [25]. Although some cohort studies have demonstrated a superiority of cisplatin over doxorubicin [26, 27], a randomized study showed no difference between single-drug regimens of cisplatin and epirubicin [28]. A more recent study reported significantly higher response rate and a lower incidence of tumor progression, with fewer required treatment sessions with combined regimens versus a single-drug treatment [29], also confirmed by investigators in a randomized study including 365 patients [30]. The dosing regimen reported varies among centers; however, doxorubicin is most often used in the range of 30–100 mg and cisplatin between 50 and 100 mg [31]. The drugs recommended by EASL-EORTC clinical practice guidelines include doxorubicin or cisplatin [32] .

For GEP-NET, the vast majority of interventional radiology centers are using doxorubicin adjusted to body weight doses in the range of 1 mg/kg. Streptozotocin demonstrates a better tumor response than doxorubicin in multivariate analysis, while it was not demonstrated on univariate analysis, with no difference in TTP [33] while requiring general anesthesia due to significant pain during hepatic intra-arterial injection induced by acid pH [34].

Creating a TACE Emulsion

The drug(s) selected for TACE are mixed with Lipiodol to form an emulsion. Water-in-oil emulsion (droplets of the internal phase containing drug in aqueous solution and continuous external phase of oily Lipiodol) was demonstrated to be more selectively retained within the tumors than the alternative oil-in-water emulsion [15]. In order to favor a water-in-oil emulsion, the volume of drug aqueous solution should be lower than the volume of Lipiodol [2]. Contrast medium can be used for preparation of doxorubicin aqueous solution; the use of nonionic contrast medium will increase the density of the drug solution and thus will favor stability of the drug/Lipiodol emulsion by lowering the sedimentation process induced by gravity [35]. The emulsion is prepared by using the 3-way stopcock method with glass or polycarbonate syringes and metal stopcocks that resist degradation by the emulsion. The content of the syringe loaded with the drug should be first pushed toward the syringe containing Lipiodol, in order to favor a water-in-oil emulsion by inducing large drops of drug within Lipiodol. Vigorous mixing of the chemotherapy aqueous solution and Lipiodol via the 3-way stopcock generates sufficient energy to decrease the size of the internal phase droplets. At least 20 pumping exchanges through the

stopcock are needed to obtain an internal phase size of droplet in the range of 70–100 microns [14]. Gradual addition of the chemotherapy solution to the Lipiodol in several small aliquots with interval pumping improves the stability of the resulting emulsion [36]. The mixture must be prepared at the time of administration and used promptly after preparation. If necessary during the treatment session, the mixture can be re-homogenized. The volume of Lipiodol that can be injected is directly related to volume and vascularity of the tumor. A dose of up to 10 ml is most often reported in clinical studies. It is recommended to use no more than 15 ml of Lipiodol per session. Injection in excess of 20 mL poses a risk of potentially life-threatening adverse events, including liver failure and pulmonary toxicity from hepatic venous shunting to the lungs.

Gelfoam particles are the most commonly used particulate materials. Gelfoam demonstrates complete recanalization in 1–2 weeks [37], therefore allowing for subsequent TACE treatment through the same tumor feeders. Hand cutting of Gelfoam particles measuring 1–1.5 mm is recommended over "pumping" large pieces of Gelfoam between two syringes because the "cutting method" provides more homogeneous distribution of particle size [38]. The use of non-resorbable calibrated microspheres is reported without added benefit. The size of calibrated microspheres, if used, should be 100–300 microns in order to ensure distal occlusion with preservation of feeding segmental arteries. Smaller diameters increase the risk of adverse events due to shunting through the hypervascular tumors [39] and bile duct injuries.

Catheter Positioning, Embolization Technique, and Endpoint

Superselective embolization is recommended when a single tumor or low number of tumors are treated, because it has demonstrated better results than lobar or whole liver TACE. Selective embolization demonstrated improved survival (hazard ratio 0.68; 95% CI 0.48–0.97; $p = 0.033$) in a multivariate analysis of 815 patients receiving TACE for HCC [40]. The use of microcatheter (2.8–2.0 French) is highly recommended in order to place the tip of the catheter in the segmental or subsegmental tumor-feeding or more distal tumor-feeding vessel(s) while ensuring that there is sufficient flow around the catheter to carry the drug/Lipiodol mixture and embolic without reflux (Fig. 3.1). A balloon occlusion microcatheter is an option to obtain dense accumulation of Lipiodol emulsion, reported in 91% of HCC nodules treated, mainly when the saturation of the tumor with Lipiodol cannot be obtained with a regular microcatheter [41].

Intra-arterial lidocaine, up to 150 mg divided into 30 mg boluses given before and between aliquots of the chemoembolic emulsion, is useful to reduce intra- and post-procedure pain [42]. A prospective trial of 113 patients receiving no lidocaine, a bolus of lidocaine prior to TACE, or a bolus of lidocaine immediately after TACE showed a significant reduction in narcotic requirements when lidocaine was given

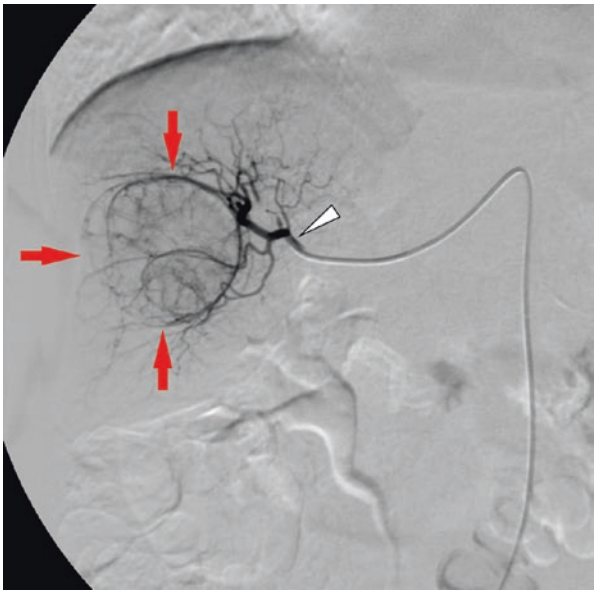

Fig. 3.1 Digital subtraction angiogram during transarterial chemoembolization for hepatocellular carcinoma (Red arrows). The catheter is positioned into a branch of the right hepatic artery (White arrowhead). Ideal location is one that treats the entire target lesion while minimizing exposure of normal hepatic parenchyma to chemoembolization

before chemoembolization. The bolus was made of 5 ml of 2% lidocaine delivered into the feeding vessel used for TACE [43].

A major advantage of Lipiodol TACE is the ability to control the delivery of the treatment by continuous visualization of the therapeutic agents due to radio-opacity of Lipiodol. Lipiodol drug emulsion is actively monitored until stasis is obtained in the very peripheral branches. Opacification of small peripheral portal branches around the tumor with Lipiodol is a common finding and has been demonstrated as a predictive factor for a lower rate of local recurrence [44], more complete necrosis [45] including necrosis of satellite nodules, and achieving safety margins in a manner similar to radiofrequency ablation [44].

Gelfoam embolization performed after drug/Lipiodol emulsion delivery should provide complete stasis up to the catheter tip when placed superselectively. When performing chemoembolization less selectively to treat large or multifocal tumors (lobar or major segments), the endpoint is a "tree-in-winter" appearance with occlusion of small tumor-feeding radicals but preservation of flow in the major lobar and segmental arteries in order to permit subsequent embolizations. In most cases, once slowing of the blood flow is observed after Lipiodol emulsion administration, only a small amount of embolics (1–2 ml of microspheres or gelatin sponge suspension) is needed to reach the embolization endpoint. However, the occlusion by gelatin sponge is often temporary, and flow recovers within a few minutes; therefore, it is recommended to wait 5 or more minutes prior to last embolization to obtain a stronger embolic effect.

Due to radio-opacity of Lipiodol, there is a real-time visualization of targeting and distribution of the chemotherapy, including visualization of nontarget

deposition, which is currently not possible with other liver-directed therapies. If arterioportal or arteriovenous shunts are detected, this may result in nontarget embolization as well as ineffective concentration of therapy in the tumor itself. Not surprisingly, patients with such arterial-portal shunting demonstrate a lower efficacy of the treatment [46]. Arterioportal or arteriovenous shunts, when present, must be occluded prior to TACE in order to avoid passage of Lipiodol, drug, and embolic through to the portal vein or to the hepatic vein.

Treatment Schedule

A set of two sequential TACEs is usually performed. In case of localized disease, the second session will target the same location of disease if triple-phase imaging does not show a complete response by necrosis criteria. In case of bilobar disease, each lobe of the liver will be targeted, one after another. At least two TACE procedures should be performed before treatment is abandoned due to lack of response. Indeed, 44–65% of patients who were not initial responders to the first cycle of TACE demonstrated a significant response after the second session of treatment [47, 48]. The size of the largest and second largest tumor are independent predictive factors determining the number of TACE sessions needed to achieve best response, with one session for tumors 4.7 cm +/− 2.1 cm and two sessions for tumors 5.1 cm +/− 2.5 cm [47].

TACE sessions are performed 2–8 weeks apart according to treatment tolerance, treatment efficacy, and the need for a subsequent treatment, until complete response is obtained. New progression after response to treatment, including either progression of a treated tumor or new tumor foci in a non-treated part of the liver, is an indication for additional treatment with TACE.

Treatment with TACE should be discontinued in patients presenting with untreatable progression [49] that is defined by the absence of tumor response in the treated territories after two embolizations or the impossibility to reach tumor feeders of some territories. Untreatable progression can also be linked to clinical or functional deterioration including ECOG performance status ≥2 or hepatic decompensation. A combined score including increase in AST, Child-Pugh score, and absence of tumor response has been recently reported useful for determining patients that will not benefit from TACE [50, 51]; however, further validation is necessary.

Lipiodol as a Biomarker

The retention of Lipiodol serves as an imaging biomarker for tumor response with necrosis proportional to the fraction of tumor volume opacified by oil [52]. Lipiodol can also be used as an imaging biomarker for survival, with European and Asian studies demonstrating improved survival in patients with more complete oil

retention [53, 54]. Cone-beam CT imaging obtained without contrast injection immediately after TACE allows quantification of Lipiodol deposition within the targeted HCC, which is an important predictive factor of local recurrence [52]. Technical success of TACE requires verifying that the entire tumor burden has been adequately treated by assessing the Lipiodol saturation of the targeted tumors. If Lipiodol saturation of the tumor volume is incomplete, cone-beam CT angiography can help identify additional tumor feeders that can be catheterized either during the same session or during a subsequent TACE session [55].

Drug-Eluting Embolics

An alternative platform to Lipiodol emulsion for delivery of chemotherapeutics to tumors is polymeric microspheres capable of carrying a drug payload. Several now exist commercially, mostly based on formulations of polyvinyl alcohol. Because microspheres cannot cross the peribiliary capillary plexus, they lodge in the distal arterioles where the payload elutes from the polymer and distributes locally via diffusion.

Most of the clinical data with drug-eluting embolics involves doxorubicin-loaded microspheres used to treat HCC. Three randomized trials have shown no oncologic benefit of the drug-eluting embolic platform over Lipiodol TACE or bland embolization with unloaded microspheres, with nearly identical PFS and OS in the bland trials [56–58]. Therefore, Lipiodol TACE remains the current standard of care in international guidelines for large or multinodular tumor isolated to the liver with preserved liver function and absence of portal vein invasion [32]. Tumor invasion of the portal (Fig. 3.2) or hepatic vein (Fig. 3.3) in patients with preserved liver function can still be treated with transarterial chemoembolization as the tumor is supplied in its entirety by branches of the hepatic artery.

Of greater concern are toxicity and safety issues. The most concentrated drug release is adjacent to the microspheres at the level of the peribiliary capillary plexus, where the doxorubicin causes local coagulation necrosis of the surrounding hepatic parenchyma, a phenomenon not seen with bland embolics [59]. The consequence of this off-target drug delivery is an increased incidence of hepatobiliary injury with doxorubicin-loaded embolics that has been reported following chemoembolization of HCC and NET metastases [60–62]. Furthermore, the lack of radiographic conspicuity of drug-eluting embolics results in a higher incidence of nontarget embolization than with Lipiodol TACE. A series of 237 cases reported a rate of injury to the gallbladder, stomach, pancreas, and other extrahepatic sites between 5% and 10%, in excess of the Society of Interventional Radiology Quality Assurance Guidelines for TACE [63].

The lack of efficacy and unacceptable toxicity of doxorubicin-loaded microspheres is sufficiently well evidenced to preclude their use in clinical practice. This does not negate the concept of using embolics as delivery platforms for therapeutics. This technology allows use of different drugs for different tumor types,

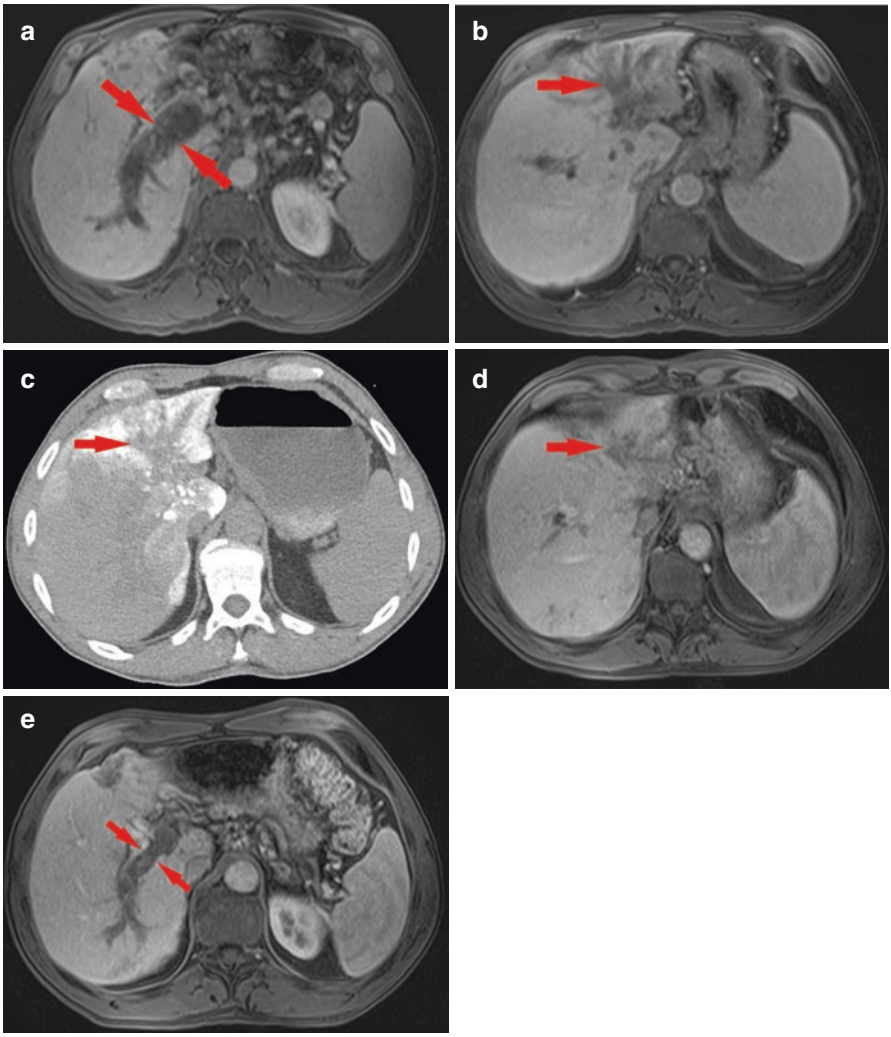

Fig. 3.2 Magnetic resonance imaging (**a**) shows a hepatocellular carcinoma filling the right (Red arrow) portal vein. The lesion originates from the left lobe (**b**) where it fills the entire left portal vein (Red arrow). Non-contrast CT after a single session of chemoembolization (**c**) shows Lipiodol deposited in the left lobe (Red arrow). MRI 6 weeks post-chemoembolization (**d**) shows near complete response of the lesion in the left lobe (Red arrow). The tumor in the right portal vein (**e**, red arrow) showed partial response, even though the right hepatic artery was not treated. The tumor originates from the left lobe; thus it is supplied by the left hepatic artery in its entirety, even the portion filling the right portal vein

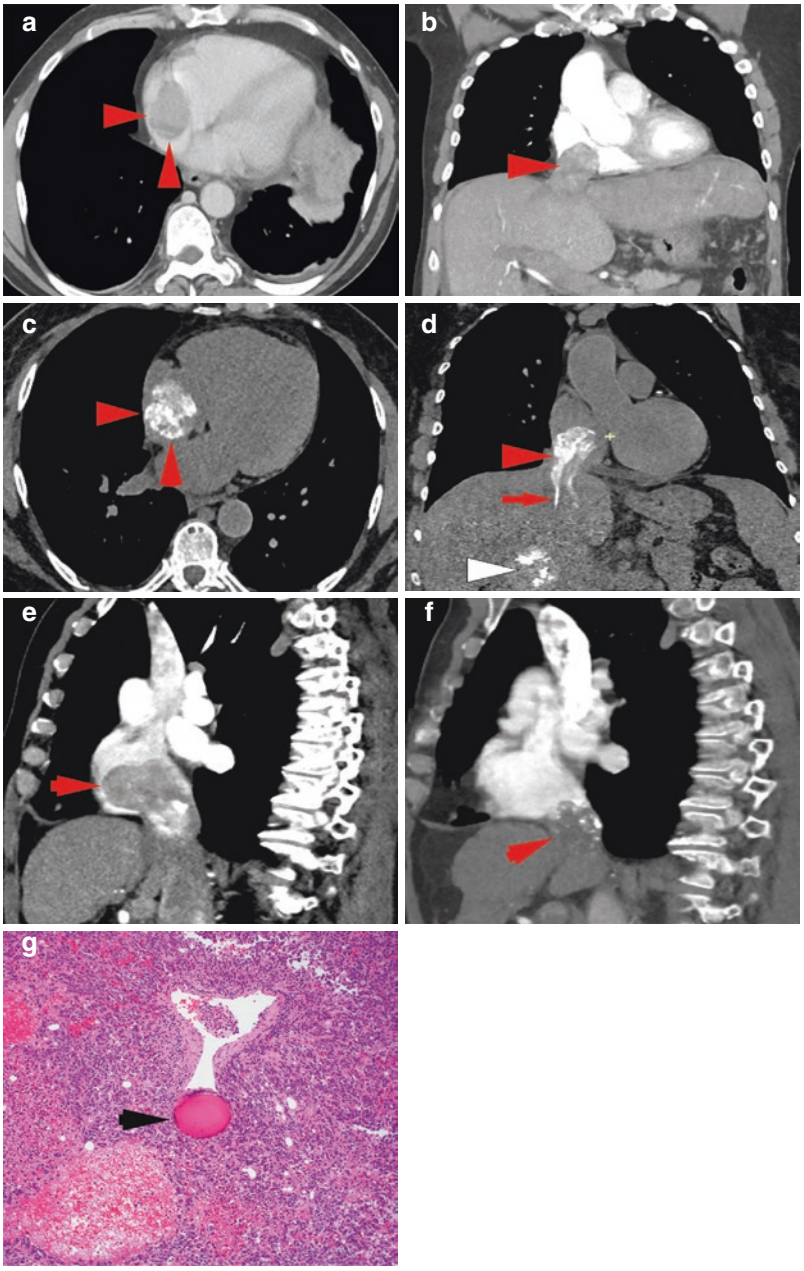

Fig. 3.3 Axial (**a**) and coronal (**b**) contrast-enhanced CT images show a hepatocellular carcinoma extending from the right hepatic vein into the right atrium (Red arrows). Axial (**c**) and coronal (**d**) non-contrast CT images post-chemoembolization show Lipiodol deposition into the intra-atrial portion of the tumor (Red arrowheads). The tumor is fed by neovascular feeders (Red arrow) from the primary intrahepatic mass (White arrowhead). Sagittal, contrast-enhanced CT images before (**e**) and 2 months after (**f**) treatment show significant response and retraction of the mass from the right atrium (Red arrows). Eosin and hematoxylin stained pathology slide after resection (**g**) of the mass shows a particle embolized in a hepatic arteriole

expanding the range of liver-directed therapies. For example, microspheres loaded with irinotecan have been used to treat metastatic colon cancer with promising early results [64].

Limitations of TACE

Despite the imaging appearance of complete tumor response and deposition of lethal concentrations of chemotherapeutic drugs, liver tumors often survive TACE. Local recurrences arise from latent tumor cells that survive therapy and are not detectable by conventional clinical imaging techniques ([65]. Tumor cells enter a quiescent state and activate multiple pathways in response to metabolic stress including autophagy, the unfolded protein response, and HIF upregulation [66]. These pathways permit cell survival until nutrient supply is restored. Cells surviving severe ischemia also have increased resistance to doxorubicin. Blockade of these pathways, such as by hydroxychloroquine for autophagy, results in less cell survival in preclinical models. This has led to clinical trials combining TACE with agents that target the metabolic stress response. Understanding the molecular mechanisms of TACE action and resistance will lead to a new generation of TACE cocktails employing drugs that work synergistically with ischemia.

Another limitation of current TACE technology is the stability of the Lipiodol emulsion and its ability to deliver and retain emulsified drug into the tumor. Novel formulations created by adding biodegradable polylactic-co-glycolic acid (PLGA) nanoparticles to the aqueous phase result in a more stable Pickering emulsion with a slower drug release profile and higher therapeutic index for retention of drug in tumor relative to a normal liver or systemic release [67, 68].

References

1. Konno T, Maeda H, Iwai K, et al. Effect of arterial administration of high-molecular-weight anticancer agent SMANCS with lipid lymphographic agent on hepatoma: a preliminary report. Eur J Cancer Clin Oncol. 1983;19:1053–65.
2. Nakamura H, Hashimoto T, Oi H, Sawada S. Transcatheter oily chemoembolization of hepatocellular carcinoma. Radiology. 1989;170:783–6.
3. Uchida H, Ohishi H, Matsuo N, et al. Transcatheter hepatic segmental arterial embolization using lipiodol mixed with an anticancer drug and Gelfoam particles for hepatocellular carcinoma. Cardiovasc Intervent Radiol. 1990;13:140–5.
4. Yamada R, Sato M, Kawabata M, Nakatsuka H, Nakamura K, Takashima S. Hepatic artery embolization in 120 patients with unresectable hepatoma. Radiology. 1983;148:397–401.
5. Matsui O, Kadoya M, Yoshikawa J, et al. Small hepatocellular carcinoma : treatment with subsegmental transcatheter arterial embolization. Radiology. 1993;188:79–83.
6. Llovet JM, Real MI, Montana X, et al. Arterial embolisation or chemoembolisation versus symptomatic treatment in patients with unresectable hepatocellular carcinoma: a randomised controlled trial. Lancet. 2002;359:1734–9.

7. Lo CM, Ngan H, Tso WK, et al. Randomized controlled trial of transarterial lipiodol chemoembolization for unresectable hepatocellular carcinoma. Hepatology. 2002;ik35:1164–71.
8. Luo J, Guo RP, Lai EC, et al. Transarterial chemoembolization for unresectable hepatocellular carcinoma with portal vein tumor thrombosis: a prospective comparative study. Ann Surg Oncol. 2011;18:413–20.
9. Pomfret EA, Washburn K, Wald C, et al. Report of a national conference on liver allocation in patients with hepatocellular carcinoma in the United States. Liver Transpl. 2010;16:262–78.
10. Peng ZW, Zhang YJ, Chen MS, et al. Radiofrequency ablation with or without transcatheter arterial chemoembolization in the treatment of hepatocellular carcinoma: a prospective randomized trial. J Clin Oncol. 2013;31:426–32.
11. Frilling A, Modlin IM, Kidd M, et al. Recommendations for management of patients with neuroendocrine liver metastases. Lancet Oncol. 2014;15:e8–21.
12. Pavel M, Baudin E, Couvelard A, et al. ENETS consensus guidelines for the management of patients with liver and other distant metastases from neuroendocrine neoplasms of foregut, midgut, hindgut, and unknown primary. Neuroendocrinology. 2012;95:157–76.
13. Laval-Jeantet M, Tristant H, Guerbet M, et al. A new method of lipiodol hepatography using an intraarterial approach. J Radiol Electrol Med Nucl. 1972;53:29–34.
14. de Baere T, Dufaux J, Roche A, et al. Circulatory alterations induced by intra-arterial injection of iodized oil and emulsions of iodized oil and doxorubicin : experimental study. Radiology. 1995;194:165–70.
15. de Baere T, Zhang X, Aubert B, et al. Quantification of tumor uptake of iodized oils and emulsions of iodized oils : experimental study. Radiology. 1996;201(3):731–5.
16. Kan Z, Ivancev K, Lunderquist A. Peribiliary plexa – important pathways for shunting of iodized oil and silicon rubber solution from the hepatic artery to the portal vein. An experimental study in rat. Investig Radiol. 1994;29:671–6.
17. Terayama N, Matsui O, Gabata T, et al. Accumulation of iodized oil within the nonneoplastic liver adjacent to hepatocellular carcinoma via the drainage routes of the tumor after transcatheter arterial embolization. Cardiovasc Intervent Radiol. 2001;24:383–7.
18. de Baere T, Dromain C, Lapeyre M, et al. Artificially induced pneumothorax for percutaneous transthoracic radiofrequency ablation of tumors in the hepatic dome: initial experience. Radiology. 2005;236:666–70.
19. Raoul JL, Heresbach D, Bretagne JF, et al. Chemoembolization of hepatocellular carcinomas. A study of the biodistribution and pharmacokinetics of doxorubicin. Cancer. 1992;70:585–90.
20. Takayasu K, Shima Y, Muramatsu Y, et al. Hepatocellular carcinoma : treatment with intra arterial iodized oil with and without chemotherapeutic agents. Radiology. 1987;162:345–51.
21. Takayasu K, Arii S, Ikai I, et al. Overall survival after transarterial lipiodol infusion chemotherapy with or without embolization for unresectable hepatocellular carcinoma: propensity score analysis. AJR Am J Roentgenol. 2010;194:830–7.
22. de Baere T, Denys A, Briquet R, Chevalier P, Laurent A, Roche A. Modification of arterial and portal hemodynamic after injection of iodized oil in the hepatic artery : experimental study. J Vasc Interv Radiol. 1998;9:305–10.
23. Kruskal JB, Hlatky L, Hahnfeldt P, Teramoto K, Stokes KR, Clouse ME. In vivo and in vitro analysis of the effectiveness of doxorubicin combined with temporary arterial occlusion in liver tumors. J Vasc Interv Radiol. 1993;4(6):741–7.
24. Marelli L, Stigliano R, Triantos C, et al. Transarterial therapy for hepatocellular carcinoma: which technique is more effective? A systematic review of cohort and randomized studies. Cardiovasc Intervent Radiol. 2007;30:6–25.
25. Gaba RC. Chemoembolization practice patterns and technical methods among interventional radiologists: results of an online survey. AJR Am J Roentgenol. 2012;198:692–9.
26. Ono Y, Yoshimasu T, Ashikaga R, et al. Long-term results of lipiodol-transcatheter arterial embolization with cisplatin or doxorubicin for unresectable hepatocellular carcinoma. Am J Clin Oncol. 2000;23:564–8.

27. Yamanaka K, Hatano E, Narita M, et al. Comparative study of cisplatin and epirubicin in transcatheter arterial chemoembolization for hepatocellular carcinoma. Hepatol Res. 2011;41:303–9.
28. Sahara S, Kawai N, Sato M, et al. Prospective comparison of transcatheter arterial chemoembolization with Lipiodol-epirubicin and Lipiodol-cisplatin for treatment of recurrent hepatocellular carcinoma. Jpn J Radiol. 2010;28:362–8.
29. Petruzzi NJ, Frangos AJ, Fenkel JM, et al. Single-center comparison of three chemoembolization regimens for hepatocellular carcinoma. J Vasc Interv Radiol. 2013;24:266–73.
30. Shi M, Lu LG, Fang WQ, et al. Roles played by chemolipiodolization and embolization in chemoembolization for hepatocellular carcinoma: single-blind, randomized trial. J Natl Cancer Inst. 2013;105:59–68.
31. Ikeda M, Arai Y, Park SJ, et al. Prospective study of transcatheter arterial chemoembolization for unresectable hepatocellular carcinoma: an Asian cooperative study between Japan and Korea. J Vasc Interv Radiol. 2013;24:490–500.
32. Llovet J, Ducreux M, Lencioni R, et al. EASL-EORTC clinical practice guidelines: management of hepatocellular carcinoma. Eur J Cancer. 2012;48:599–641.
33. Marrache F, Vullierme MP, Roy C, et al. Arterial phase enhancement and body mass index are predictors of response to chemoembolisation for liver metastases of endocrine tumours. Br J Cancer. 2007;96:49–55.
34. Dominguez S, Denys A, Madeira I, et al. Hepatic arterial chemoembolization with streptozotocin in patients with metastatic digestive endocrine tumours. Eur J Gastroenterol Hepatol. 2000;12:151–7.
35. Tzeng WS, Wu RH, Chang SC, et al. Ionic versus nonionic contrast media solvents used with an epirubicin-based agent for transarterial chemoembolization of hepatocellular carcinoma. J Vasc Interv Radiol. 2008;19:342–50é.
36. Deschamps F, Moine L, Isoardo T, Tselikas L, Paci A, Mir LM, Huang N, Fatal E, de Baere T. Parameters for stable water-in-oil lipiodol emulsion for liver trans-arterial chemoembolization. Cardiovasc Intervent Radiol. 2017;40:1927–32.
37. Louail B, Sapoval M, Bonneau M, Wasseff M, Senechal Q, Gaux JC. A new porcine sponge material for temporary embolization: an experimental short-term pilot study in swine. Cardiovasc Intervent Radiol. 2006;29:826–31.
38. Katsumori T, Kasahara T. The size of gelatin sponge particles: differences with preparation method. Cardiovasc Intervent Radiol. 2006;29:1077–83.
39. Brown KT. Fatal pulmonary complications after arterial embolization with 40-120- micro m tris-acryl gelatin microspheres. J Vasc Interv Radiol. 2004;15:197–200.
40. Yamakado K, Miyayama S, Hirota S, et al. Hepatic arterial embolization for unresectable hepatocellular carcinomas: do technical factors affect prognosis? Jpn J Radiol. 2012;30:560–6.
41. Irie T, Kuramochi M, Takahashi N. Dense accumulation of lipiodol emulsion in hepatocellular carcinoma nodule during selective balloon-occluded transarterial chemoembolization: measurement of balloon-occluded arterial stump pressure. Cardiovasc Intervent Radiol. 2013;36:706–13.
42. Molgaard CP, Teitelbaum GP, Pentecost MJ, et al. Intraarterial administration of lidocaine for analgesia in hepatic chemoembolization. J Vasc Interv Radiol. 1990;1:81–5.
43. Lee SH, Hahn ST, Park SH. Intraarterial lidocaine administration for relief of pain resulting from transarterial chemoembolization of hepatocellular carcinoma: its effectiveness and optimal timing of administration. Cardiovasc Intervent Radiol. 2001;24:368–71.
44. Miyayama S, Mitsui T, Zen Y, et al. Histopathological findings after ultraselective transcatheter arterial chemoembolization for hepatocellular carcinoma. Hepatol Res. 2009;39:374–81.
45. Miyayama S, Matsui O, Yamashiro M, et al. Ultraselective transcatheter arterial chemoembolization with a 2-f tip microcatheter for small hepatocellular carcinomas: relationship between local tumor recurrence and visualization of the portal vein with iodized oil. J Vasc Interv Radiol. 2007;18:365–76.

46. Vogl TJ, Nour-Eldin NE, Emad-Eldin S, et al. Portal vein thrombosis and arterioportal shunts: effects on tumor response after chemoembolization of hepatocellular carcinoma. World J Gastroenterol. 2011;17:1267–75.
47. Choi J, Shim JH, Shin YM, Kim KM, Lim YS, Lee HC. Clinical significance of the best response during repeated transarterial chemoembolization in the treatment of hepatocellular carcinoma. J Hepatol. 2014;60:1212–8.
48. Georgiades C, Geschwind JF, Harrison N, et al. Lack of response after initial chemoembolization for hepatocellular carcinoma: does it predict failure of subsequent treatment? Radiology. 2012;265:115–23.
49. Raoul JL, Gilabert M, Piana G. How to define transarterial chemoembolization failure or refractoriness: a European perspective. Liver Cancer. 2014;3:119–24.
50. Hucke F, Sieghart W, Pinter M, et al. The ART-strategy: sequential assessment of the ART score predicts outcome of patients with hepatocellular carcinoma re-treated with TACE. J Hepatol. 2014;60:118–26.
51. Sieghart W, Hucke F, Pinter M, et al. The ART of decision making: retreatment with transarterial chemoembolization in patients with hepatocellular carcinoma. Hepatology. 2013;57:2261–73.
52. Takayasu K, Arii S, Matsuo N, et al. Comparison of CT findings with resected specimens after chemoembolization with iodized oil for hepatocellular carcinoma. AJR Am J Roentgenol. 2000;175:699–704.
53. El Khaddari S, Gaudin JL, Abidi H, Picaud G, Rode A, Souquet JC. Chemoembolization in hepatocellular carcinoma: multivariate analysis of survival prognostic factors after the first session. Gastroenterol Clin Biol. 2002;26:728–34.
54. Kim DY, Ryu HJ, Choi JY, et al. Radiological response predicts survival following transarterial chemoembolisation in patients with unresectable hepatocellular carcinoma. Aliment Pharmacol Ther. 2012;35:1343–50.
55. Takayasu K, Muramatsu Y, Maeda T, et al. Targeted transarterial oily chemoembolization for small foci of hepatocellular carcinoma using a unified helical CT and angiography system: analysis of factors affecting local recurrence and survival rates. AJR Am J Roentgenol. 2001;176:681–8.
56. Lammer J, Malgari K, Vogo T, et al. Prospective randomized study of doxorubicin-eluting -bead embolization in the treatment of hepatocellular carcinoma: results of the PRECISION V study. Cardiavasc Intervent Radiol. 2010;33:41–52.
57. Malagari K, Pomoni M, Kelekis A, Pomoni A, Dourakis S, Spyridopoulos T, Moschouris H, Emmanouil E, Rizos S, Kelekis D. Prospective randomized comparison of chemoembolization with doxorubicin-eluting beads and bland embolization with BeadBlock for hepatocellular carcinoma. Cardiovasc Intervent Radiol. 2010;33(3):541–5.
58. Brown KT, Do RK, Gonen M, Covey AM, Getrajdman GI, Sofocleous CT, Jarnagin WR, D'Angelica MI, Allen PJ, Erinjeri JP, Brody LA, O'Neill GP, Johnson KN, Garcia AR, Beattie C, Zhao B, Solomon SB, Schwartz LH, DeMatteo R, Abou-Alfa GK. Randomized trial of hepatic artery embolization for hepatocellular carcinoma using doxorubicin-eluting microspheres compared with embolization with microspheres alone. J Clin Oncol. 2016;34(17):2046–53.
59. Namur J, Wassef M, Mollot J-M, et al. Drug-eluting beards for liver embolization: concentration of doxorubicin in tissue and in beads in a pig model. J Vasc Intervent Radiol. 2010;21:259–67.
60. Monier A, Guiu B, Duran R, Aho S, Bize P, Deltenre P, Dunet V, Denys A. Liver and biliary damages following trans arterial chemoembolization of hepatocellular carcinoma: comparison between drug-eluting beads and lipiodol emulsion. Our Radiol. 2016;27:1431–9.
61. Bhagat N, Reyes DK, Lin M, et al. Phase II study of chemoembolization with drug-eluting beads in patients with hepatic neuroendocrine metastases: high incidence of biliary injury. Cardiovasc Intervent Radiol. 2013;36:449–59.
62. Guiu B, Deschamps F, Aho S, et al. Liver/biliary injuries following chemoembolisation of endocrine tumours and hepatocellular carcinoma: lipiodol vs. drug-eluting beads. J Hepatol. 2012;56:609–17.

63. Malagari K, Pomoni M, Spyridopoulos TN, Moschouris H, Kelekis A, Dourakis S, Alexopoulou E, Koskinas J, Angelopoulos M, Kornezos J, Pomoni A, Tandeles S, Marinis A, Rizos S, Kelekis D. Safety profile of sequential transcatheter chemoembolization with DC Bead™: results of 237 hepatocellular carcinoma (HCC) patients. Cardiovasc Intervent Radiol. 2011;34:774–85.
64. Fiorentini G, Aliberti C, Tilli M, Mulazzani L, Graziano F, Giordani P, Mambrini A, Montagnani F, Alessandroni P, Catalano V, Coschiera P. Intra-arterial infusion of irinotecan-loaded drug-eluting beads (DEBIRI) versus intravenous therapy (FOLFIRI) for hepatic metastases from colorectal cancer: final results of a phase III study. Anticancer Res. 2012;32(4):1387–95.
65. Perkons NR, Kiefer RM, Noji MC, Pourfathi M, Ackerman D, Siddiqui S, Tischfield D, Profka E, Johnson O, Pickup S, Mancuso A, Pantel A, Denburg MR, Nadolski GJ, Hunt SJ, Furth EE, Kadlecek S, Gade TPF. Hyperpolarized metabolic imaging detects latent hepatocellular carcinoma domains surviving locoregional therapy. Hepatology. 2019; https://doi.org/10.1002/hep.30970. [Epub ahead of print]
66. Gade TPF, Tucker E, Nakazawa MS, Hunt SJ, Wong W, Krock B, Weber CN, Nadolski GJ, Clark TWI, Soulen MC, Furth EE, Winkler JD, Amaravadi RK, Simon MC. Ischemia induces quiescence and autophagy dependence in hepatocellular carcinoma. Radiology. 2017;283(3):702–10.
67. Deschamps F, Harris KR, Moine L, et al. Pickering-emulsion for liver trans-arterial chemoembolization with oxaliplatin. Cardiovasc Intervent Radiol. 2018;41:781–8.
68. Deschamps F, Isoardo T, Denis S, Tsapis N, Tselikas L, Nicolas V, Paci A, Fattal E, de Baere T, Huang N, Moine L. Biodegradable Pickering emulsions of Lipiodol for liver trans-arterial chemo-embolization. Acta Biomater. 2019;87:177–86.

Chapter 4
Primary Lung Cancer

Maria A. Velez, Aaron Lisberg, and Robert D. Suh

Epidemiology and Pathophysiology of Lung Cancer

Lung cancer is the most second most common type of cancer and the leading cause of cancer-related deaths in the United States and worldwide. The estimated incidence of lung cancer in the United States is around 200,000 new cases diagnosed per year, with around 100,000 estimated deaths yearly. While the overall incidence of lung cancer diagnosis has decreased in the past few decades, the total number of cases has increased. Even though lung cancer has one of the lowest survival rates with a 5-year survival rate of about 12%, there has been a marked decline in lung cancer-related deaths in the past two decades, which reflects the decrease in tobacco consumption [1].

Non-Hispanic black men have the highest incidence of lung cancer in the United States, followed by non-Hispanic white men and American Indian/Alaskan Native men. In the female population, the highest incidence of lung cancer is in non-Hispanic white women followed by non-Hispanic black women and then by

The authors Maria A. Velez and Aaron Lisberg are equally contributed to this work.

M. A. Velez (✉)
Department of Internal Medicine, University of Pittsburgh Medical Center, Pittsburgh, PA, USA
e-mail: velezma@upmc.edu

A. Lisberg
Department of Hematology Oncology, David Geffen School of Medicine at University of California, Los Angeles, Los Angeles, CA, USA
e-mail: alisberg@mednet.ucla.edu

R. D. Suh
Department of Radiological Sciences, David Geffen School of Medicine at University of California, Los Angeles, Los Angeles, CA, USA
e-mail: rsuh@mednet.ucla.edu

C. Georgiades, H. S. Kim (eds.), *Image-Guided Interventions in Oncology*,
https://doi.org/10.1007/978-3-030-48767-6_4

American Indian/Alaskan Native and Hispanic women. Additionally, other demographic factors such as age greater than 55 years old and lower educational levels are more commonly seen in patients with lung cancer [1].

Lung cancer originates from the epithelial cells of the respiratory system and is classified in two main categories: non-small cell lung cancer (NSCLC) which accounts for about 85% of cases of lung cancer and small-cell lung cancer (SCLC) which accounts for about 15% of lung cancer cases [2]. Identifying the type of lung cancer is important since the staging, treatment, and prognosis varies greatly between NSCLC and SCLC. NSCLC is further divided into three major histopathologic subtypes, which include adenocarcinoma (AC), squamous cell carcinoma (SCC), and large-cell carcinoma [2].

The main risk factors for the development of lung cancer include environmental and genetic risk factors. The greatest environmental risk factor for the development of lung cancer is the use of tobacco cigarettes, with up to 90% of lung cancer attributed to tobacco consumption [1]. Other less common environmental factors include exposure to radon, asbestos, and particulate matter in the air. However, lung cancer can occur in the absence of these risk factors in patients with genetic susceptibility to it, for instance, mutations in certain chromosome regions such as at the 15q25-26 chromosome and 6p21 increase the risk of developing lung cancer in never smokers. Furthermore, some intrinsic genetic mutations in the EGFR gene and EML4-ALK gene are associated with the development of AC in nonsmokers [1]. The understanding of the pathophysiology, epidemiology, and specific histology are essential in the development of treatment strategies for lung cancer including targeted therapies, immunotherapy, and ablation [3].

Role of Surgery for Lung Cancer

Surgery plays an important role in the diagnosis, staging, and treatment of NSCLC. However, this is not the case for SCLC, as SCLC rarely presents at a stage that is amenable to resection [4]. Surgical resection is the treatment modality of choice in stage I and II NSCLC defined by the AJCC eighth edition as a tumor that is equal to or less than 5 cm in size with no lymph node involvement in and less than 7 cm with ipsilateral lymph node involvement, respectively [5]. The role of surgery for stage III NSCLC is less well-defined and remains controversial [5].

A variety of surgical techniques are used for lymph node sampling, which is important for staging in NSCLC, as the stage is one of the factors that helps dictate the treatment plan [5]. Lymph node evaluation can be done through different surgical techniques, but the most common ones include cervical mediastinoscopy and less invasive approaches such as endobronchial ultrasound (EBUS). These procedures are used to evaluate mediastinal lymph nodes (N2), which help stage NSCLC. The indications for mediastinal lymph node evaluation include FDG positive lymph nodes on a PET CT or mediastinal lymph nodes that are >1 cm in size on the short axis [5].

There are different surgical techniques used to perform a lobectomy, which is the standard of care for lung cancer resection. Open lobectomy improves disease-free survival at 5 years when done in the early-stage setting. Similarly, video-assisted thoracoscopic surgery (VATS) is a safe technique for lobar resection. Published data suggests that there are reduced rates of perioperative complications with VATS when compared to open lobectomy [4]. Most recently, robotic lobectomy has become more common as it can result in less perioperative trauma, and data shows similar survival outcomes between robotic approaches and VATS [5].

Sublobar resection for stage I NSCLC has lower mortality rates as compared to lobectomy, with the caveat of higher risk of developing local recurrence [5]. Thus, this type of procedure is most often performed in patients whose comorbidities deem them unsuitable for lobectomy since there may be better preservation of pulmonary function [4].

Oligometastatic disease in NSCLC is defined as metastatic disease to five or fewer sites. The strongest evidence for surgical resection in the oligometastatic disease setting is in patients with limited brain metastases, as studies have shown that it improves overall survival [6]. Similarly, other studies have explored the role of resection in oligometastatic disease to other sites such as the liver, adrenal glands, and vertebrae. Results from these studies show encouraging results with 5-year overall survival rates up to 24% and suggest that there is a subset of patients who may greatly benefit from aggressive local and systemic therapy for oligometastatic disease control. Thus, further studies are needed to identify this subset of patients who may benefit from aggressive therapy for oligometastatic disease [7].

Systemic Therapy for NSCLC

Systemic therapy for NSCLC depends on the stage, histology, and molecular characteristics of the tumor. Thus, tissue sampling by biopsy is imperative in the development of a treatment plan for patients with NSCLC. Molecular testing helps to identify therapeutically targetable gene mutations. These molecular alterations include anaplastic lymphoma kinase (*ALK*) gene rearrangements, epidermal growth factor receptor (*EGFR*) mutations, ROS proto-oncogene receptor tyrosine kinase 1 (*ROS1*) rearrangements, and *BRAFV600E* mutations [8].

Immune checkpoint inhibitors (ICIs) are now the standard of care in all eligible patients with NSCLC. Programmed death ligand 1 (PD-L1) proportion score measured by immunohistochemistry (IHC) helps to identify patients that are more likely to benefit from ICI [8]. Thus, obtaining a tissue biopsy is important when selecting the appropriate treatment regimen for these patients. Currently, image-guided transthoracic core needle biopsy has been proven to be efficient in obtaining tissue for PD-L1 expression analysis [9].

The goal of treatment for metastatic NSCLC is to improve the quality of life and survival by decreasing the tumor burden [8]. A combination of platinum-based chemotherapy improves survival. However, in the presence of an *EGFR* mutation, the

standard of care is treatment with the EGFR tyrosine kinase inhibitor (EGFR-TKI) osimertinib [10]. Similarly, in patients whose tumors harbor *ALK* rearrangements or *ROS1* mutations, the current standard of care is treatment with ALK tyrosine kinase inhibitors (TKIs) [8]. While *BRAF*V600E mutations are only present in about 1 to 2% of patients with adenocarcinoma, these patients respond well to a combination a BRAF and MEK inhibitor.

ICIs have revolutionized the treatment of metastatic NSCLC pembrolizumab, an antibody against PD-1, is currently the standard of care for all immunotherapy eligible patients in combination with platinum-doublet chemotherapy. In patients with PD-L1 ≥50%, pembrolizumab monotherapy is also a reasonable treatment option [8]. Similarly, atezolizumab, a PD-L1 inhibitor, is also approved in combination with platinum-doublet chemotherapy and bevacizumab, a vascular endothelial growth factor (VEGF) inhibitor. It is important to note that ICIs have been shown to have limited activity and increased toxicity in patient with *EGFR* and *ALK* mutations [8].

Radiation Therapy

Radiation therapy plays an important role in the curative and palliative treatment of NSCLC. There are multiple different techniques used to deliver radiation to the thorax, each with different indications based on disease site in the chest, proximity to vital organs such as the heart as well as extent of the disease.

Stereotactic body radiation therapy (SBRT) has been approved for the treatment of stage I and II NSCLC. SBRT is the current standard of care in early-stage NSCLC for patients who are not deemed surgical candidates and have peripheral tumors [11]. The role of SBRT in patients who are fit to undergo surgery is still controversial, as trials to evaluate this were prematurely closed due to slow accrual [11]. Local recurrence rates in patients treated with SBRT range from 9 to 20% at 5 years. Similar to patients treated with lobectomy, about 20% of patients who undergo SBRT experience distant recurrence. Centrally located tumors, defined as tumors within 2 cm of any critical mediastinal structure, are difficult to treat with SBRT, as increased toxicity has been observed in this setting. Other treatment modalities, such as proton beam therapy and MR-guided radiation therapy, are being evaluated for the treatment of centrally located tumors [11].

Stereotactic radiosurgery (SRS) is also used for the treatment of stage IV disease in combination with systemic therapies, mainly in the treatment of oligometastatic disease to the brain. However, the size of the tumor and the number of lesions are limiting factors in the use of this treatment modality [12]. In patients with high tumor burden, like those with large tumors or multiple tumors, whole-brain radiotherapy (WBRT) remains the standard of care [13]. The use of SBRT has also been described in the setting of adrenal and hepatic metastases, as well as in the palliative treatment of spinal metastases [14].

Multimodality Treatment

Stage III NSCLC comprises a heterogeneous group of patients, and the treatment for it is not well standardized and continues to be controversial. Thus, multimodality therapy is important in the treatment of stage III disease, which often includes surgery, radiation, and systemic chemotherapy, as well as immunotherapy. In patients with resectable stage III NSCLC, treatment options include definitive surgery with neoadjuvant or adjuvant chemotherapy with or without postoperative radiation (PORT). Cisplatin is usually given for four cycles after surgical resection of stage III disease.

Similarly, the PD-L1 inhibitor durvalumab plays an important role in the treatment of stage III disease as maintenance therapy after definitive chemoradiation [15]. In contrast to resectable disease, the standard of care for unresectable stage III NSCLC is well established. In this patient population definitive concurrent chemoradiation followed by durvalumab is standard of care [15].

Ablation

Treatment with thermal ablation involves the percutaneous application of heat or cold energy to lung and tumor tissue by strategic insertion of an applicator(s), under image guidance, to create a region of cell death that encompasses the targeted tumor and provides an ablative margin. Since the first description of thermal ablation for lung tumors almost two decades ago, techniques, which were at one time novel, have been refined and developed that have improved the safety and efficacy of the procedure. Today, image-guided thermal ablation (IGTA) is inclusive of radiofrequency ablation (RFA), microwave ablation (MWA), and cryoablation (CA) and is a form of "local therapy" or "local ablative therapy" and generally, is considered a potential alternative to other local therapies.

Indications/Patient Selection

The treatment of primary and secondary pulmonary malignancies are simply the two main indications for thermal ablation in the lung, this chapter focusing on the role of ablation in the setting of early and advanced stage lung cancer than metastatic disease to the lung from extrathoracic malignancy. Most of the medical literature has focused on the treatment of early-stage lung cancer in a patient cohort that has become defined as "high risk"; those that are for the most part surgically resectable but rendered medically inoperable due to comorbidities. The ACOSOG Z4033 trial, a phase II study of radiofrequency ablation of stage IA NSCLC in medically inoperable patients, objectively defined "high risk" with a single major and/or two

or more minor criteria. Major criteria included an FEV1 or DCLO ≤50%, and minor criteria, a less depressed FEV1 or DLCO between 51 and 60%, advanced age ≥75 years, pulmonary hypertension, LVEF ≤40%, resting or exercise PaO2 <55 mmHg, and pCO2 >45 mmHg. For the most part, ablation provides only local control for early-stage lung cancers. When comparing patient demographics in three completed NCI trials on stage I NSCLC, Crabtree et al. found that those patients who underwent RFA in the ACOSOG Z4033 trial were significantly older and had lower diffusion capacities, compared to those treated in the ACOSOG Z4032 with surgical wedge and brachytherapy and RTOG 0236 with SBRT trials. When comparing those patients receiving sublobar resection versus RFA, other authors have also found that RFA patients are significantly older with poorer lung function than their surgical counterparts.

For stage I NSCLC, ablation alone may be used with curative intent, most often in this high-risk patient population, but for stages II-IV, ablation should be combined with other therapies. Increasingly, ablation has been utilized to treat synchronous and metachronous lung cancers, locally recurrent lung cancer (oligo-recurrent) after failure of local therapy, specifically surgical resection, radiotherapy or ablation, or even systemic therapy, limited or low-volume metastases to the lung (oligo-metastatic) and as a form of salvage therapy in advanced disease or palliation.

As early as the RAPTURE trial, published in Lancet Oncology in 2008, many studies regardless of the thermal energy used for ablation have demonstrated consistent preservation of lung function without permanent decline after treatment compared to baseline. Although ablation can show a transient decline in VC at 1 month and VC and FEV1 at 1 and 3 months largely associated with pleuritis and larger ablation volumes ≥20 cm^3 after RFA, lung function consistently returns to baseline shown in both RAPTURE and ACOSOG Z4033 RFA trials with preserved quality of life seen in ECLIPSE trial utilizing cryoablation for pulmonary oligometastatic disease. Other forms of local control, specifically surgical resection and SBRT, consistently reduce lung function after treatment although to variable extent. In general, wedge resections (up to three) can result in a cumulative decline in postoperative FEV1 of 5%, segmentectomy 3–11%, and lobectomy 9–16%. Although associated with less decline than surgical resection, Horner-Rieber and colleagues demonstrated a relative decline of 9.8% (−33.9 to +33.3) occurring approximately 9 months after radiation delivery. At 12 months following SBRT, Stone et al. demonstrated decline in FEV1 of 4.1%, corrected diffusion capacity for carbon monoxide 5.2%, forced vital capacity 5.7%, and total lung capacity 3.6%, and these declines persisted at 24 months. The ability to preserve lung function benefits those patients with comorbid pulmonary insufficiency, synchronous, and metachronous primary lung malignancies and premalignant lung nodules undergoing continuous imaging surveillance that may require local control in the future. In addition, 10–32% of patients, surviving surgical resection for lung cancer will develop a second lung cancer with a continuing 3% risk of lung cancer diagnosis each year.

Techniques

In contrast to surgical resection, thermal ablation can be performed safely and comfortably with intravenous moderate sedation and analgesia as an outpatient procedure especially when there is no anticipated need for cardiopulmonary support or unusual pain control requirements. General anesthesia is favored in those patients with severe medical comorbidities and/or anticipated complications, which may necessitate an inpatient admission, usually brief in duration. Epidural and/or regional anesthesia can be useful.

Similar to percutaneous CT-guided lung biopsy, site of entry, adequate pleural anesthesia, and awareness of important anatomy, such as bronchovascular planes, fissures, and mediastinal structures, maximize the success of any ablation while minimizing the risk for complications, significant or otherwise. Given that the parietal pleura is the first or second most sensitive structure along the path of the ablation applicator, adequate pleural anesthesia ensures patient comfort and cooperation which form the cornerstone of successful ablation. Effective anesthesia of the parietal pleura requires the precise and careful placement of the anesthesia needle tip, usually a styleted introducer needle, immediately deep to the endothoracic fascia into the extrapleural space adjacent to and superficial to the parietal pleura, while avoiding traversal of the underlying parietal and visceral pleura, the latter which if violated increases the risk of pneumothorax.

An understanding of the pulmonary bronchovascular computed tomographic anatomy provides a safe transthoracic route to a central lesion. The pulmonary hila are composed of the major bronchi with accompanying pulmonary arteries and pulmonary veins that extend radially into the lobes, segments, and subsegments of the lungs. Although it is often difficult to avoid blood vessels and airways within the periphery of the lung, such disturbances result in minimal to no significant complications. The radial orientation of the bronchovascular structures emanating from the hila to the periphery of the lung typically provides a safe abronchovascular route to the central portions of the lung, allowing safe access to a centrally located tumor. For peripheral or subpleural tumors, a long, or tangential, approach offers a more consistent applicator-target relationship that withstands the natural fluctuations of respiration and helps limit problematic overlap of the ablation zone along the applicator with the visceral pleura, a known mechanism of bronchopleural fistula with microwave energy. Avoidance of interlobar and accessory fissures reduces the risk of pneumothorax, which may result in a problematic or persistent air leak due to the multiplicity of visceral pleural breaches.

Tumor size is arguably the most important factor in determining the success of ablation. The best oncologic outcomes in the setting of NSCLC have been reported for T1 tumors, less than 3 cm. Although complete ablation of larger tumors is attainable, efficacy is more operator-dependent, and rates of incomplete ablation are greater. Most manufacturer's strategy for creation of larger ablation volumes occurs through placement of multiple applicators, which often behave synergistically, within and/or around the margins of the targeted tumor. Obtaining adequate ablation

margins around larger tumors, between 3 and 5 cm, usually requires multiple ablation applicators and applicator repositioning and adds to the complexity of the procedure. Nevertheless, experienced centers have reported good outcomes even for these larger tumors. For tumors larger than 5 cm, the likelihood of complete ablation decreases significantly, and the risk of complications increases. Regardless of energy employed, understanding of the anticipated ablation zone geometry with repositioning and/or placement of adequate number of applicators to power the ablation relative to tumor size correctly and recognition of the realized ablation zone determine the technical success and local control from ablation. The ablation zone for each specific device and applicator currently available on the market varies based on the type of energy and power and duration of ablation and is directly available from the respective vendors; this information is also readily available in the applicator packaging.

Location of the tumor within the lung and chest plays an important role in treatment planning. Although there are few locations that preclude successful thermal ablation, local anatomic factors may influence choice of ablation modality and applicator or probe placement. For example, tumors in peripheral or subpleural locations may be better suited to cryoablation over heat-based ablation modalities such as microwave energy, due to the greater tendency of the latter to result in indiscriminate tissue destruction in and around somatically innervated parietal pleura causing sometimes excessive procedural and recovery pain and complications such as bronchopleural fistula. Similarly, tumors in close proximity to central airways are often best treated with cryoablation, particularly since the ice created during the ablation can be visualized by CT. Proximity to large pulmonary airways and blood vessels does not preclude thermal ablation provided the ablation probes are positioned carefully, and direct puncture of either is avoided. However, flowing blood within large vessels, and to a lesser extent, airways will dissipate thermal energy, a phenomenon known as heat- or cold sink, and therefore greater energy may be required to overcome this effect and achieve successful ablation. Extrapulmonary structures at risk for damage must always be considered when planning the ablation procedure, particularly for tumors in peripheral locations within the lung lobe but central within the chest, including the esophagus, pericardium, heart, and diaphragm, as well as nerves such as the brachial plexus, phrenic, and recurrent laryngeal nerves. Damage to intercostal nerves can occur, but clinical sequelae are generally not as severe.

Each of the three most commonly available energies, specifically RF, MWA, or CA, has relative advantages and disadvantages both inherently and comparatively (Table 4.1). Unfortunately, no one thermal energy is a clear choice for all ablation applications within the lung and chest. For tumors $\leq$3 cm within the center of the lobe parenchyma, any modality is a great choice provided the operator has knowledge, familiarity, expectation, and comfort regarding the device and its usage. For tumors >3 cm, newer generation microwave and cryoablation are favored given ability to efficiently delivery ablation volume and/or employ simultaneous applicators. Cryoablation may be a better choice to ablate tumors residing $\leq$1.5 cm from the somatically innervated parietal pleura, since cold is a natural anesthetic and better

Table 4.1 Comparative ablative technologies

Parameter(s)	Radiofrequency	Microwave	Cryoablation
≤3 cm	+++	+++	+++
>3 cm	+ (up to 3)[a]	+++ (up to 3)[a]	++ (up to 25)[a]
≤1.5 cm pleura	+ (pain)	+ (air leak)	+++
Chest wall	+	++	+++
Mediastinum	+	+	++
Sinks	+	+++ (least)	++(+)
Pacer/AICD	+	++	+++
Coagulopathy	+++	+++	+
Maneuverability	(+)	(+)	++
Time	+(+)	+++ (shortest)	++

[a]Number of applicators

tolerated during ablation and recovery. However, RF and MWA can be successful. Situations in which intraprocedural visualization of the ablation zone is necessary within or adjacent to the chest wall and mediastinum, the ice produced by cryoablation zone is easily seen on CT. Thermal sinks can degrade optimal delivery of all three energies, but MW appears to be somewhat less affected than RF and CA. To help overcome sink effects imparted by large airways and blood vessels, ice is generally safer to use in proximity to these structures with cryoprobes placed very adjacent and/or packed closely together to the anticipated sink than the heat energies. Although coagulopathies are corrected prior to ablation, heat-based energies are generally preferred because of the inclination to bleed with CA during the thaw cycles. With electrical current passing through, the patients receiving RF, MW, and CA offer better alternatives in those patients with cardiac devices. Although some RF electrodes and MW antennas can engage the targeted tumor, CA with its advantage to freeze/stick can push/pull and/or lever the targeted tumor into a more favorable location to administer ablation energy. Time of setup and ablation is slowest with CA, the latter from the number of freeze-thaw cycles associated with cumulative tumor cell death.

Irrespective of the energy used, successful ablation is determined by two factors: First, adequate positioning, repositioning, and/or adequate number and placement of applicators to create effective energy delivery for cell death to the targeted tumor and its margin, accounting for structures and variables, they pose particularly limitation of collateral damage during energy delivery and sink (Fig. 4.1a). Second, recognition of end points associated with ablation, which can be technical, such as thermocouple temperature, impedance and reflective power, and imaging, specifically ground glass produced during heat-based ablation and proper tumor and ice-related isotherm coverage (Fig. 4.2a). Ground glass opacity on visualized on CT must encompass the treated tumor in its entirety and extend at least 5 mm, or a more confidence-inspiring >10 mm, beyond the periphery of the lesion. Larger ground glass margins have been associated with better local control rates and indirectly overall survival. Multiplanar reformatted (MPR) display of images both parallel to (long axis views) and perpendicular to (short axis views) the axis of the applicator(s)

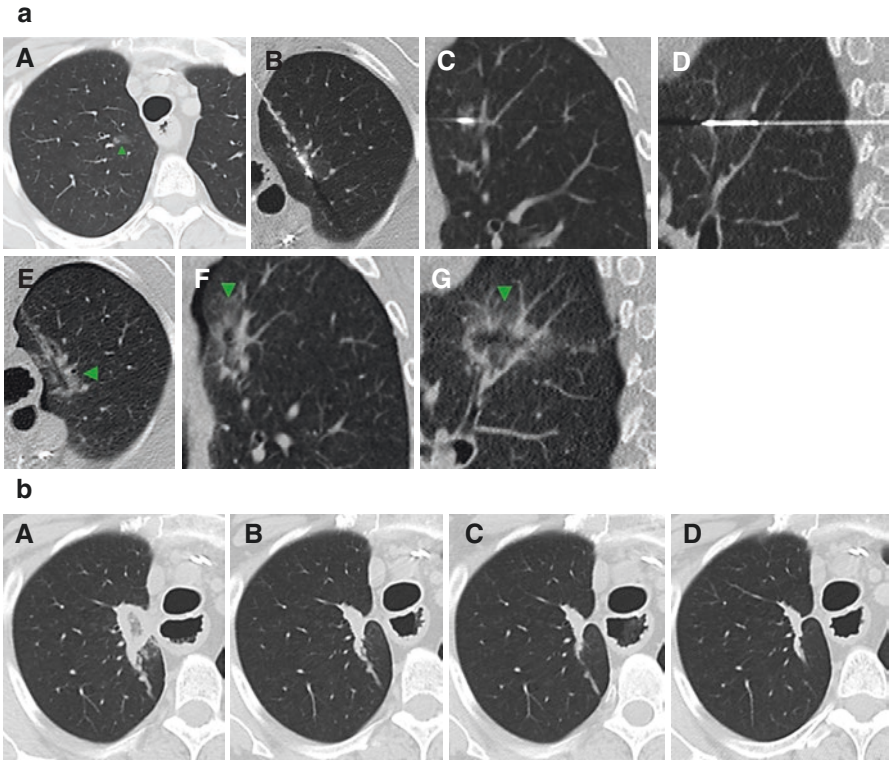

Fig. 4.1 (**a**) Microwave ablation. Image A demonstrates part-solid nodule within the right upper lobe (arrowhead), consistent with early invasive non-small cell lung adenocarcinoma, confirmed by percutaneous core needle biopsy. Images B–D with patient in prone oblique position show final position of microwave antenna on axial (B) and confirmed on corresponding coronal (C) and sagittal (D) reformatted images. Images E–G following 10 minute ablation at 65 watts after removal of antenna document ablation-related ground glass attenuation encompassing the entire targeted tumor on images in all three planes. (**b**) Post-ablation chest CT follow-up. Image A at 1 month after microwave ablation of patient depicted in Fig. 4.1a shows ground glass surrounded by airspace attenuation corresponding to ablation zone completely replacing initial part-solid adenocarcinoma. Image B at 6 months after ablation demonstrates involution of now homogenous ablation zone. The ablation zone continues to involute on image C at 1 year and image D at 3 years, consistent with long-term local control

should always be employed and can provide valuable information regarding depth of device penetration; the exact position of the applicators relative to the target tumor and its margins, especially along the z-axis where most local failures result; the configuration of multiple applicators; and the relationship to essential and nontargeted structures. The principal limitation of CT is the lack of real-time imaging feedback for advancement of devices into the targeted tumor, although some operators have found CT fluoroscopy and cone beam CT to be useful adjuncts for device placement.

Prescriptive strategies for ablation differ among experienced operators and certainly are different with regard to the type of energy utilized and the size and location of the target tumor. In general, a subcentimeter tumor will be impossible to

penetrate with current applicator needle design accentuated by the inherent compliance of the lung and requires advancing the applicator and aligning its active site immediately adjacent to the intended tumor so that its anticipated ablation geometry provides coverage. If microwave energy is used, time and power can be selected to

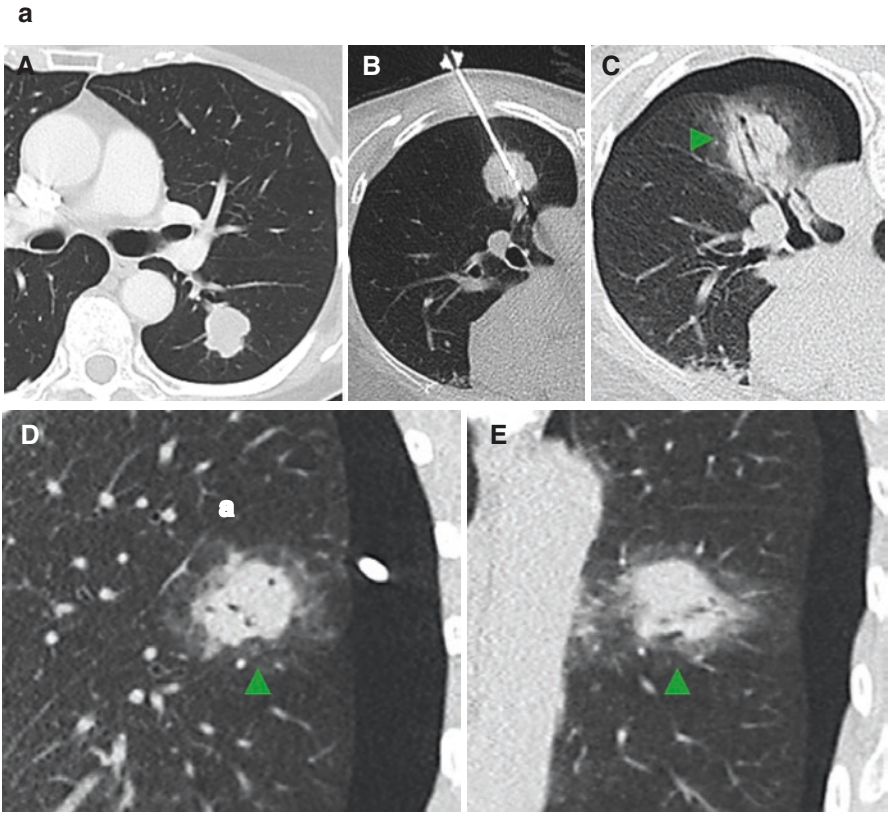

Fig. 4.2 (**a**) Microwave ablation. Image A demonstrates 2.7 × 2.3 cm non-small cell lung adenocarcinoma, confirmed by percutaneous core needle biopsy. After endobronchial ultrasound (EBUS) staging confirmed the absence of pathological lymph nodes, image B with patient in prone position shows initial microwave antenna position. Completion axial image C following a total time 18 minutes at 5 different antenna positions all at 65 watts within the targeted tumor show encapsulating ground glass attenuation (arrowheads), confirmed on corresponding coronal (D) and sagittal (E) reformatted images. A small postprocedural pneumothorax is evident. (**b**) Incomplete ablation. Axial (A), coronal (B), and sagittal (C) images at 1 month following microwave ablation in patient shown in Fig. 4.2a demonstrate conspicuous nodular bulge at superior aspect of recently ablated tumor (arrowheads) not encased by postablation margin, consistent with incomplete ablation. (**c**) Repeat cryoablation. Initial position depicted in image A of single cryoprobe placed through superior aspect of incompletely ablated tumor in patient in Fig. 4.2a and b. Image B after 3 minutes freeze shows very little change since in most cases, initial ice is difficult to visualize within aerated lung. Image C after 7 minutes freeze and image D after 12 minutes freeze show new (C) and increased (D) airspace attenuation (arrowheads), consistent with localized edema and hemorrhage associated with cryoablation. Immediate completion image E after cryoprobe removal demonstrates fully realized edema and hemorrhage surrounding targeted site of incomplete ablation (arrowheads)

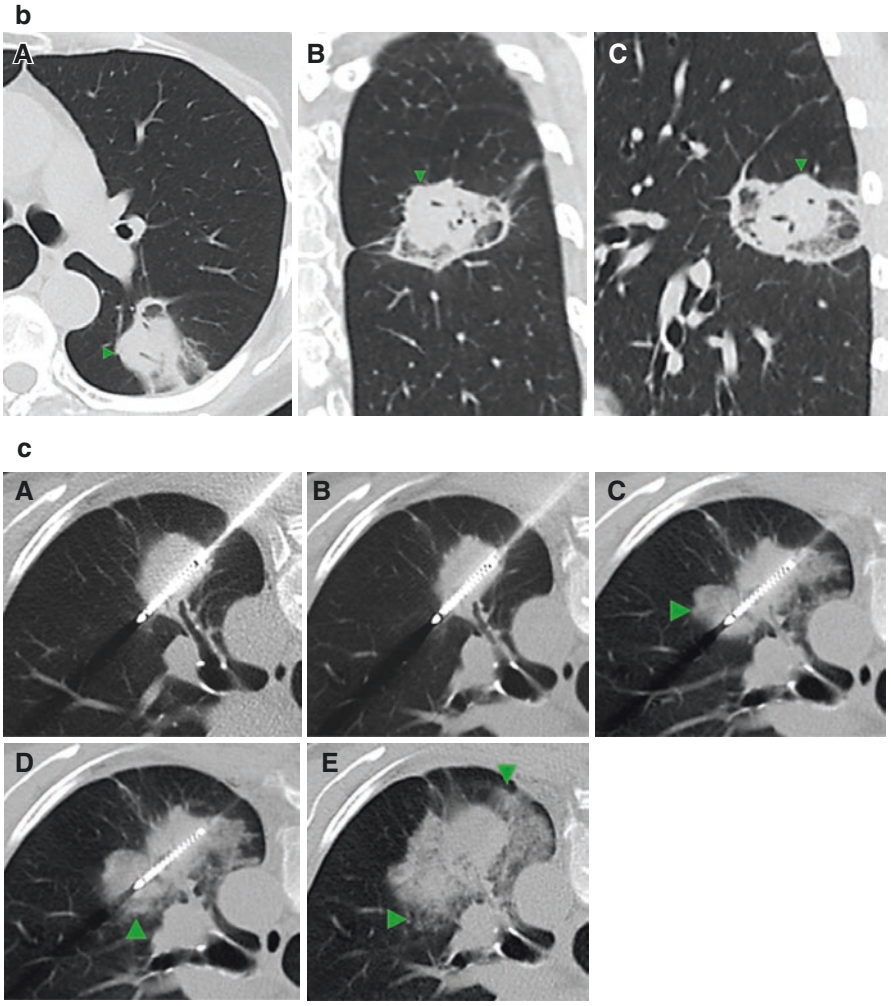

Fig. 4.2 (continued)

provide half of an ablation zone to adequately treat the tumor and provide its ablation margin since the tumor was not directly punctured. For larger tumors, this approach would produce potentially significant collateral damage on the opposite nontumor side of the applicator unnecessary to fulfill successful ablation. Regardless of the manner or intent in which the ablation was planned and started, the microwave antenna should be readily repositioned to gain any margin that appears inadequate. Cryoablation, on the other hand, is fundamentally different in its approach to applicator placement since the tissue is ultimately frozen and susceptible to fracture with excessive applicator torque. All cryoprobes are generally placed up front, and in the case of a pericentimeter tumor, two cryoprobes are placed on each side to bracket the tumor, the ensuing ablation zones ultimately coalescent. Although

dependent on manufacturer, most applicators should be placed no more than 1.5–2.0 cm apart and no more than 1 cm from a tumor margin. In general, the effective isotherms generated by cryoprobes that ensure cell death are smaller relative to potential ablation zones afforded by their similar gauge microwave antenna counterparts. Regardless of energy chosen, ablation margins require confirmation by imaging to the operator's best ability, and a judiciously low threshold should yield more time and/or power, repositioning or addition of applicators as necessary to complete a satisfactory ablation.

Postprocedural Recovery Care

Following thermal ablation, patients require observation for potential complications from anesthesia and ablation effects. Patients should be observed and monitored in the postanesthesia care unit with regular vital signs and continuous pulse oximetry. An upright chest radiograph should be obtained within 2 hours of the procedure, and a second expiratory chest radiograph should be obtained at 3–4 hours postprocedure. Chest radiographs can exclude immediate complications, such as a pneumothorax, pleural effusion, hemothorax, and unexpected or excessive pulmonary infiltrates. Postprocedure pain control can include either oral analgesics or patient-controlled analgesia pumps for parenteral administration of narcotics. Use of anti-inflammatory agents, such as ibuprofen, is recommended to suppress postablation inflammation, particularly with RFA, and to a lesser extent MWA and prescribed for at least 3–5 days postprocedure; these agents may decrease the degree of pain, pleural effusion, and systemic inflammatory response. Postprocedural low-grade fever for 2–3 days is not uncommon especially with larger ablation volumes. Depending on the patient's clinical course and assessment, the operator determines whether limited or overnight admission for observation is required. Many operators, however, routinely discharge patients on the same day, with strict postprocedure instructions and close follow-up.

Postablation Imaging

A follow-up clinic visit with a chest radiograph should be conducted within a week postprocedure, to assess for complications such as delayed pneumothorax and reactive pleural effusion as well as overall patient recovery and well-being. Apart from the fleeting celebration of technical success, diligent, thorough, and regular postablation imaging documents true ablation success (Fig. 4.1b). The ablation zone should be assessed with chest CT or PET/CT at regular intervals post ablation. Baseline PET/CT is recommended as part of clinical staging and should be reasonably contemporary to the anticipated ablation. 1-month chest CT, then chest CT ± abdomen and pelvis CT at 3–4 months are obtained thereafter to complete first year, then

4–6 months intervals during second year. PET/CT can be substituted, if necessary, at any time point, particularly if diagnostic uncertainty arises. Apart from the 1-month chest CT, which establishes a baseline appearance and relationship of the ablation zone to the index tumor (Fig. 4.2b) after the acute changes have resolved from which the ablation zone should continually involute and eventually stabilize, imaging timeline after lung ablation is very similar to most clinical oncology timelines.

Although some variation exists between the ablation zones generated by different energies, more commonalities exist than not. In general, all have consolidation and ground glass ± cavitation, and all technically successful ablation zones will demonstrate a combination of ground glass and/or airspace attenuation notably larger than the index tumor. Cavitation has been associated with better prognosis, perhaps because cavitation is a sign of over-ablation, but can be an expected feature of ablation especially if performed near a larger airway. All ablation zones are bigger than the initial tumor, the size being maximal usually during first 2 weeks, and all ablation zones improve in margination and decay over time. Most ablation zones should be smaller than initial tumor after 6 months. Cryoablation zones involute more quickly than RF and MWA and involute accordingly respective to their initial size, roughly 60% decrease in size from largest at 12 months. All zones lose enhancement within early (1 month) and intermediate (1–3 months) phases with exception of benign periablational enhancement, which is a benign physiological response to thermal injury and characterized by a smooth thin rim of contrast enhancement at the outer ablation margin representing reactive hyperemia and early reparative fibrosis. On occasion, cryoablation zones may demonstrate central enhancement during the first month after ablation, and over time, all zones recover enhancement to some degree during chronic (>3 months) phase but should not be nodular, excessive or above initial tumor enhancement. FDG activity mirrors contrast enhancement and has specific patterns for local failure, specifically diffuse or central activity and rim + focal uptake corresponding to original tumor at 1 and 4 months postablation. In up to 62.5% cases of RFA, transient or reactive lymphadenopathy can occur within the early and intermediate phases but generally resolve at 3- and 6 months. On occasion, it is reasonably common to image the fading residuals of complications in immediate (<24 hours), early and intermediate phases, particularly pneumothorax or contained pneumothorax which most likely represents a contained bronchopleural fistula and pleural effusion.

For the most part, local failure, incomplete ablation, tumor progression, or residual disease is characterized by the following:

1. Growth at ablation site (WHO criteria) after 3- and certainly after 6 months. For cryoablation, significant enlargement ≥1 month
2. ↑ contrast enhancement (> 15 HU) at ablation site after 3- and certainly after 6 months. Nodular and/or central enhancement >15 mm (10 mm)
3. FDG activity at 1(4) months: focal and rim + focal corresponding
4. Continuous regional or distant lymph node enlargement
5. New sites of intrathoracic disease outside ablation site or treated lobe or extrathoracic locations

Early identification of local failure is critical, since it can be retreated with repeat thermal ablation, stereotactic radiotherapy, and possibly, surgery, if feasible (Fig. 4.2c). In cases of regional nodal or distant failure, systemic therapy would be appropriate.

Complications

Pneumothorax is the most common complication and is seen to some degree in almost all treated patients. Only a small portion of this group requires intervention, with most requiring conservative management, and by some operators, this occurrence is not considered a complication but rather an expected part of the procedure, similar to a chest tube being placed after lung resection. Reported rates of pneumothorax in series of thermal ablation range between 1.3 and 60%, likely partly due to difference in technique and differences in definition. The incidence of a pneumothorax requiring chest tube placement or aspiration is approximately 10 to 20%. The largest series of lung ablation procedures focusing on complications reported a rate of CTCAE grade 1 or 2 pneumothorax of 45% and a rate of grade 3 pneumothorax, requiring pleurodesis, of 1.6%. Other reported major complications in the series included aseptic pleuritic (2.3%), pneumonia (1.8%), lung abscess (1.6%), bleeding requiring blood transfusion (1.6%), bronchopleural fistula (0.4%), nerve injury (0.3%), tumor seeding (0.1%), and diaphragmatic injury (0.1%). Procedure-related death is a rare occurrence. In the above series, 4 deaths occurred in 1000 procedures (0.4%), 3 related to exacerbation of interstitial pneumonia, and 1 related to hemothorax.

In a study examining complications after MWA of lung cancer, major complications occurred in 21% of ablations. Published rates of pneumothoraces requiring chest tubes are comparable with RFA at 13–16%. In the MWA cohorts, patients with emphysema or other underlying respiratory dysfunction, subpleural tumors, and large tumors had higher likelihood of complications. Patients with longer ablations times and with multiple probes may also benefit from antibiotic prophylaxis to prevent pneumonia. Despite initial public anxiety surrounding microwave ablation and the incidence of bronchopleural fistula, true occurrence of bronchopleural fistula rates is remains low at 2.8% and 0.5%.

Comparatively, one study examining cryoablation for lung tumors found that pleural effusion was the most common postprocedural complication (71%). The use of greater number of probes and no history of ipsilateral surgery were statistical predictors of pleural effusion. In that cohort, 62% of patients had pneumothoraces. Despite this relatively high rate, only 18% required chest tube insertion, similar to ranges reported for MWA and RFA. Delayed and recurrent pneumothorax was frequent, and a majority of these patients required chest tubes. Although high rates of hemoptysis (37%) occurred, all cases were self-limited and correlated with a greater number of cryoprobes. Other complications rarely observed after cryoablation included phrenic nerve palsy, frostbite, empyema, and tumor implantation.

Outcomes

Overall Survival

Numerous series of thermal ablation have been published with overall survival (OS) data now out to 5 years and even 10 years. Five-year OS in these series ranges from 16 to 68 percent (Table 4.2). This wide range is likely due to different patient characteristics, as well as differences in procedure technique. A review of 14 studies by Hiraki et al. found 1-, 2-, 3-, and 5-year OS rates after RFA of stage I NSCLC were 78–100%, 53–86%, 36–88%, and 25–61%, respectively, with median survival time ranging from 29 to 67 months. In contrast, the median survival of untreated stage I/II lung cancer is approximately 14.2 months. Relatively less data are available on MWA and cryoablation compared to RFA, with most from combined reports of primary lung cancer and metastases. However, one of the highest 5-year survival rates was reported by Moore et al., who achieved a 68% 5-year OS and 88% progression-free survival following cryoablation in medically inoperable patients. In this series, all patients underwent staging PET/CT within 6 weeks prior to the ablation procedure, with any suspicious adenopathy then investigated by bronchoscopic biopsy. This insistence on adequate staging may have contributed to their excellent results. Three large single-institution studies of MWA, each with >50 patients treated, yielded survival rates ranging from 47.6 to 83% at 1 year, 23.8 to 73% at 2 years, and 14.3 to 61% at 3 years.

Results of ablation are even more favorable for ground glass nodules or opacities, which often represent atypical adenomatous hyperplasia evolving into in situ or

Table 4.2 Overall survival and local control of stage I NSCLC with ablative therapies

	Trials	*N* (total = 610)	1 year	2 year	3 year	4 year	5 year	Local control
RFA	Simon 2007 [16]	71	78%	57%	36%	27%	27%	47%
	Huang 2011 [17]	33	80%	46%			24%	76%
	Ambrogi 2011 [18]	57	83%	62%	40%	32%	25%	41%
	Hiraki 2011 [19]	50	94%	86%	74%	67%	61%	69%
	Kodama 2012 [20]	44	98%		73%		55%	89%
	Palussiere 2014 [21]	87	92%	78%	66%	63%	58%	79%
	Huang 2018 [22]	50	96%	87%	67%		36%	74%
	RAPTURE [23]	33	70%	48%				88%
	ACOSOG Z4033 [24]	51	86%	70%				60%
	Palussiere 2018 [25]	42	92%	64%	58%			81%
MWA	Yang 2014 [26]	47	89%	63%	43%	37%	16%	48%
CA	Moore 2015 [27]	45	89%		78%		68%	89%

RFA radiofrequency ablation, *MWA* microwave ablation, *CA* cryoablation

minimally invasive adenocarcinomas. Five-year OS after ablation of these lesions has been reported at 96.4% by Kodama et al. and 93.3% by Iguchi et al., with local progression rates of 14% and 17.6%, respectively. Yang et al. showed safety and efficacy in treating peripheral ground glass nodules with MWA. Technical success rate was 100%, and the reported rates of 3-year local progression-free survival, cancer-specific survival, and OS were 98%, 100%, and 96%, respectively. More recently, in a pilot study, Liu et al. treated 14 patients with 19 ground glass opacities and demonstrated successful ablation in all patients at follow-up periods between 18 and 34 months (average of 24 months).

Clinical Trials

Several clinical trials of thermal ablation for lung cancer have been reported (Table 4.2). The Radiofrequency Ablation of Pulmonary Tumors Response Evaluation (RAPTURE) trial was published in 2008 and prospectively examined a series of 106 patients treated with RFA for 183 unresectable lung tumors. Patients had contraindications to chemotherapy and radiotherapy. Tumor types included NSCLC ($n = 33$), colorectal metastasis ($n = 53$), and metastases from other primary tumors ($n = 20$). The study results demonstrated nearly universal technical success. The primary major complication was pneumothorax ($n = 27$) with no posttreatment effects on PFTs. For NSCLC patients, OS was 70% at 1 year (CI 51–83) and 48% at 2 years (30–65). Cancer-specific survival for NSCLC was 92% (78–98) at 1 year and 73% (54–86) at 2 years. Thirteen patients treated for stage I NSCLC demonstrated OS of 75% (45–92%) at 1 year and cancer-specific survival of 92% (66–99) at 2 years. In patients with colorectal metastases, 1 year survival was 89% (76–95) and 66% (53–79) at 2 years. Metastases from various other primary cancers had a 1 year survival of 92% (65–99) and 2 year survival of 64% (43–82). A major conclusion of the trial was the high rate of and sustained complete response observed in 88% of assessable tumors 1 year after treatment.

The ACOSOG Z4033 was a prospective trial published in 2015 that studied inoperable stage IA NSCLC treated with RFA. Fifty-one patients were studied. PFTs were performed prior to RFA and repeated 3 months and 2 years after treatment. The OS was 86% (77–96) at 1 year and 70% (58–84) at 2 years. Tumor size <2 cm and performance status of 0 or 1 were associated with improved survival. In 19 patients with local failure, a majority were retreated with RFA. Compared to baseline, no detectable decreases in FEV1, TLC, and DLCO were observed. In fact, a sustained increase in FVC was observed, possibly due to reduced air trapping after the procedure rendered by the thermoplasty effect of heat-based ablation. In addition to demonstrating a 2 years OS comparable to SBRT, the study provided compelling longitudinal evidence that RFA does not negatively impact pulmonary function.

A recent phase II prospective trial by Palussiere et al. published in 2018 examined survival outcomes of patients with unresectable stage IA NSCLC treated with RFA. A total of 42 patients were enrolled in the study, though only 32 were fully

assessable. The local control rate at 1 year was 84% (67–96), and at 3 years was 81% (54–96). Of note, local failure was defined tumor growth within the RFA treatment zone, whereas in the aforementioned Z4033 trial, local failure was defined as any tumor growth within the RFA site, primary tumor lobe, or hilar lymph node. The OS at 1 year was 92% (78–98), and at 3 years was 58% (41–74). Quality of life and global health was not affected by treatment. The study supports previously reported findings that no substantial functional pulmonary decline occurs after treatment and that survival rates after RFA are comparable to reported outcomes after SBRT.

Local Failure

Rates of local control in major series of thermal ablation for NSCLC with long-term follow-up range from 41% to 89% within 5 years (Table 4.2). A majority of local failure occurs within 2 years following ablation. The primary factor associated with local failure of lung cancer after thermal ablation is initial lesion size greater than 3 cm. Simon et al. demonstrated that in 153 patients treated with RFA for pulmonary malignancies, tumor size >3 cm was a statistically significant predictor of local tumor progression post-RFA. Another study showed that RFA of stage I NSCLC lesions >3 cm had local tumor progression rates as high as 50%. Similarly, in MWA and cryoablation, lung tumor size >3 cm increases the risk of local failure and likely requires usage of multiple probes at once.

In ascending order, local control improves when comparing radiofrequency, microwave ablation, cryoablation, stereotactic body radiotherapy, and surgical lobectomy; however, despite enhanced local control, the rate of distant disease remains highly variable between studies whether comparing like or unlike therapies. Simply and most plausibly, this variability is the direct result of already microscopic disease at the time of treatment in some surgical series reported as high as 16% in 1 cm apical cancers. In other words, even complete, or 100%, local control will have already microscopic locoregional and distant disease. This is further exacerbated in the high-risk population which may be ineligible for formal nodal staging through mediastinoscopy, left to complete reliance on medical imaging, specifically CT-PET. Ultimately, the rate of local and locoregional progression may not negatively impact overall survival. Specifically in 2012, Lanuti et al. looked at locoregional recurrence in patients with stage I lung cancer initially treated with radiofrequency ablation, and despite retreatment with radiofrequency ablation, radiotherapy, chemoradiotherapy, and chemotherapy, the authors found no significant difference in 5-year overall and disease-free survival in radiofrequency ablation patients without recurrence vs. those patients with treated recurrences. Similarly, reported in the ACOSOG Z4033, 31 patients treated with RFA had no local recurrence, and 13 patients had local recurrence within the first year of follow-up, all of which were retreated with repeat RFA or SBRT. At 1-year, local recurrence did not affect overall survival.

Cost Differential

In an analysis of the SEER-Medicare-linked database with a final matched cohort of 128 patients with comparable baseline characteristics and OS, Kwan et al. found a significant cost advantage favoring ablation over sublobar resection, with a median treatment-related cost difference of $16,105 and significant decrease in cumulative costs in the 1-month, 3-month, and 12-month posttreatment periods, with median cumulative costs of $12,329. The difference in cumulative costs echoes the findings of Alexander et al., who reported a significant decrease in costs among a similar cohort of patients undergoing RFA compared with sublobar resection; the monthly posttreatment cost differed between the two groups by a factor of 1.93, or $620.71 versus $1195.92, respectively. When compared with other modalities in the setting of oligometastatic non-small cell lung cancer, cryoablation appeared the most cost-effective, even when added to the cost of best supportive care or systemic regimens with an adjunctive cost-effectiveness ratio of US$49,008–87,074. In their study, cryoablation was associated with very low morbidity and local tumor recurrence rates for all anatomic sites and possibly increased overall survival.

Although prospective cost-efficacy studies comparing image-guided tumor ablation and stereotactic body radiotherapy are nonexistent with the exception of a single study utilizing Markov modeling and older radiofrequency ablation data, Dupuy reported in 2013 that global Medicare reimbursement in Rhode Island for radiotherapy was 4.25 times that of radiofrequency ablation at US$17,000 vs.US$4000. Whether or not the higher cost of radiotherapy for better local control and arguably better overall survival is justified remains to be seen in the high-risk population, particularly given similar microscopic locoregional and distant disease rates reported in radiotherapy and radiofrequency ablation studies.

Combination Therapy

Few studies report outcomes following combination of both radiation therapy and IGTA. Combination therapy has been utilized in large and/or central tumors, which are difficult to treat with either modality alone. In 2006, Dupuy et al. reported outcomes at a minimum 2 years for 24 medically inoperable patients with stage I NSCLC undergoing RFA, followed by conventional radiotherapy to a dose of 66 Gy. At a mean follow-up period of 26.7 months (range, 6 to 65 months), 14 patients (58.3%) died with cumulative 2-year and 5-year survival rates of 50% and 39%, respectively. Ten deaths were cancer-related. Two patients had local recurrence (8.3%), while nine patients had systemic metastatic disease. Three patients died of respiratory failure with no evidence of active disease. Chan and colleagues reported 17 medically inoperable patients with biopsy-proven stage I NSCLC treated with RFA, followed by single-fraction high-dose-rate brachytherapy on the same day. Although limited to 22 months follow-up, local control was reported in four of seven cases with stage T2N0 and in all nine patients with T1 disease. In a

recent study by Sandler et al., SBRT and heat-based ablation, either RFA or MWA, targeted 17 tumors in 16 patients with 1-year and 2-year actuarial local control rates of 93% and 81%, respectively. Three patients had grade ≥3 toxicity including bronchial stenosis, pain, and pulmonary hemorrhage. The percent predicted FEV1 and FVC decreased by 8% and 8.5%, respectively, at 3 months after treatment ($P < 0.001$ for both).

Future Trends

Over almost 3 decades, there have been a handful of papers focused on intra-arterial delivery of chemotherapy, some nanoformulated, and most are and share a number of similarities, specifically in treatment of advanced NSCLC. In 2012, Nakanishi and colleagues prospectively enrolled 25 patients with stage III or IV or recurrent NSCLC without distant metastasis (M1b), ECOG 2+ who were not candidates for either standard chemotherapy or chemoradiotherapy. Feeding arteries were identified and tumor staining graded on a scale of I-IV. Docetaxel and cisplatin (25 mg/m^2 and 25 mg/m^2, respectively) were administered by arterial infusion. The total dose of each was divided among feeding arteries according to the degree of tumor staining. Overall response was 52% with 1 patient with complete response and 12 patients with partial response. Median progression-free survival was 6.5 months, median overall survival at 17.4 months and 1- and 2-year overall survival at 81% and 32%, respectively. Survival was significantly better for patients with good PS (0 or 1) than poor PS (≥2) and those with grade 4 tumor staining than without grade 4 tumor staining. Grade 3 general fatigue or appetite loss developed in patients with performance status (PS) ≥3. No grade 4 hematological or non-hematological toxicity or treatment-related death occurred. Yuan et al. retrospectively studied 40 patients with stage III NSCLC, each receiving intra-arterial infusion chemotherapy with gemcitabine and cisplatin. Overall survival rates at 1, 6, 12, and 24 months were 97.5%, 82.3%, 28.4%, and 10.7%, respectively. The most frequent drug-related adverse events were cough in 17 patients (42.5%), anorexia in 14 patients (35%), and pain in 9 patients (22.5%).

Strategies to enhance the already established doublet chemotherapy regimen for lung cancer have been investigated for more than 20 years. Initially, the concept was to administer chemotherapy drugs locally to the tumor site for efficient diffusion through passive transport within the tumor. Recent advances have enhanced the diffusion of pharmaceuticals through active transport by using pharmaceuticals designed to target the genome of tumors whether by interarterial and/or intratumoral delivery. In 2013 in five patients with EGFR-negative stage IIIa–IV NSCLC, Hohenforst-Schmidt et al. administered platinum-based doublet chemotherapy using combined intratumoral-regional and intravenous route of administration. Cisplatin analogues were injected at 0.5–1% concentration within the tumor lesion and proven malignant lymph nodes according to pretreatment histological/cytological results, and the concentration of systemic infusion was decreased to 70% of a

standard protocol. Patients experienced greater than 50% reduction after five injections and two cycles systemic infusion.

A phase I study by Lee and colleagues was conducted to determine safety, clinical efficacy, and antitumor immune responses in patients with advanced non-small cell lung carcinoma (NSCLC) following intratumoral administration of autologous dendritic cells (DC) transduced with an adenoviral (Ad) vector expressing the CCL21 gene (Ad-CCL21-DC). Sixteen stage IIIB/IV NSCLC subjects received two vaccinations by CT- or bronchoscopic-guided intratumoral injections at days 0 and 7. Twenty-five percent (4/16) of patients had stable disease at day 56. Median survival was 3.9 months. ELISPOT assays revealed 6 of 16 patients had systemic responses against tumor-associated antigens (TAA). Tumor CD8þ T-cell infiltration was induced in 54% of subjects (7/13; 3.4-fold average increase in the number of CD8þ T cells per mm^2). Patients with increased CD8þ T cells following vaccination showed significantly increased PD-L1 mRNA expression. Future studies will evaluate the role of combination therapies with PD-1/PD-L1 checkpoint inhibition combined with DC-CCL21 in situ vaccination.

Key Points

Although certainly not meant as a comprehensive review of the topic, the following provide insight into the best practices in lung ablation:

1. Initial size of the targeted tumor is the best predictor for local control by thermal ablation.
2. Mindful patient selection for both primary and secondary lung malignancies, ideally within the setting of a multidisciplinary tumor board(s). Restage patients prior to ablation. Consider PET-CT for PET-avid tumors.
3. Maintain active participation and presence at multidisciplinary care meetings focused on thoracic tumor treatments. Be engaged and become versed in the advantages and disadvantages, results, and outcomes of IGTA for lung malignancies and competing and complementary treatments and therapies.
4. Firmly understand the ablation energies and technologies and their relative strengths and limitations specific to the device(s) utilized. Ablate wisely to optimize local control while resisting the temptation to aggressive over-ablation.
5. Appreciation of potential heat- or cold sinks affecting ablation site and local tumor control and safe strategies to mitigate their influence.
6. When possible, utilize techniques to avoid collateral damage of normal adjacent structures, specifically the intrathoracic and intercostal nerves, esophagus, trachea, and skin. Techniques include insufflation of air or CO2, instillation or injection of D5W, normal saline or short- or long-acting local anesthetic, and mechanical manipulation (lever, push, pull) of target tumors to simply produce a more favorable location for ablation

and provide protective offset. (1) Be very familiar with regional nerve anatomy. (2) Nerves of particular interest in thoracic ablation include phrenic, vagus, recurrent laryngeal, brachial plexus, and sympathetic nerves.

7. Develop familiarity with complication profile associated with lung ablation in order to prevent and effectively manage complications. Develop effective pneumothorax management skills; become extremely comfortable with the management of pneumothorax during and after thermal ablation and bronchopleural fistulas. Appreciate the differences in recognition and management of hemorrhagic complications related to lung ablation, specifically hemoptysis, hemothorax, and extrapleural hematoma.
8. Develop and practice comprehensive and diligent patient follow-up. Organize, order, and review relevant imaging. Of particular importance, minimize potential to lose track of patients after ablation. Collaborate and communicate with referring physicians and diagnostic radiology colleagues on imaging follow-up protocol and assessment.
9. Understand expected and unexpected appearances of ablation site(s) on intraprocedural imaging and follow-up chest CT and PET-CT. Confirm ablation margins with liberal use of coronal and sagittal reformations. Consider repeat biopsy and/or ablation for suspected tumor progression, or incomplete ablation. Incorporate 1-month follow-up chest CT to establish a baseline post-ablation, from which time the ablation zone should gradually involute and stabilize.
10. Assemble a dedicated program for lung ablation, including knowledgeable and skillful operating interventional radiologist(s) including yourself, nurses, technologists, anesthesiologists, and support staff.

References

1. de Groot PM, Wu CC, Carter BW, Munden RF. The epidemiology of lung cancer. Transl Lung Cancer Res. 2018;7(3):220–33.
2. Dela Cruz CS, Tanoue LT, Matthay RA. Lung cancer: epidemiology, etiology, and prevention. Clin Chest Med. 2011;32(4):605–44.
3. Abtin F, De Baere T, Dupuy DE, Genshaft S, Healey T, Khan S, et al. Updates on current role and practice of lung ablation. J Thorac Imaging. 2019;34(4):266–77.
4. Raman V, Yang CJ, Deng JZ, D'Amico TA. Surgical treatment for early stage non-small cell lung cancer. J Thorac Dis. 2018;10(Suppl 7):S898–904.
5. Lackey A, Donington JS. Surgical management of lung cancer. Semin Intervent Radiol. 2013;30(2):133–40.
6. Tumati V, Iyengar P. The current state of oligometastatic and oligoprogressive non-small cell lung cancer. J Thorac Dis. 2018;10(Suppl 21):S2537–S44.
7. Stephens SJ, Moravan MJ, Salama JK. Managing patients with oligometastatic non-small-cell lung cancer. J Oncol Pract. 2018;14(1):23–31.
8. Arbour KC, Riely GJ. Systemic therapy for locally advanced and metastatic non-small cell lung cancer: a review. JAMA. 2019;322(8):764–74.

9. Tsai EB, Pomykala K, Ruchalski K, Genshaft S, Abtin F, Gutierrez A, et al. Feasibility and safety of intrathoracic biopsy and repeat biopsy for evaluation of programmed cell death ligand-1 expression for immunotherapy in non-small cell lung cancer. Radiology. 2018;287(1):326–32.
10. Soria JC, Ohe Y, Vansteenkiste J, Reungwetwattana T, Chewaskulyong B, Lee KH, et al. Osimertinib in untreated EGFR-mutated advanced non-small-cell lung cancer. N Engl J Med. 2018;378(2):113–25.
11. Baker S, Dahele M, Lagerwaard FJ, Senan S. A critical review of recent developments in radiotherapy for non-small cell lung cancer. Radiat Oncol. 2016;11(1):115.
12. Aoyama H, Shirato H, Tago M, Nakagawa K, Toyoda T, Hatano K, et al. Stereotactic radiosurgery plus whole-brain radiation therapy vs stereotactic radiosurgery alone for treatment of brain metastases: a randomized controlled trial. JAMA. 2006;295(21):2483–91.
13. Mehta MP, Rodrigus P, Terhaard CH, Rao A, Suh J, Roa W, et al. Survival and neurologic outcomes in a randomized trial of motexafin gadolinium and whole-brain radiation therapy in brain metastases. J Clin Oncol. 2003;21(13):2529–36.
14. Faria SL. Role of radiotherapy in metastatic non-small cell lung cancer. Front Oncol. 2014;4:229.
15. Jones CM, Brunelli A, Callister ME, Franks KN. Multimodality treatment of advanced non-small cell lung cancer: where are we with the evidence? Curr Surg Rep. 2018;6(2):5.
16. Simon CJ, Dupuy DE, DiPetrillo TA, Safran HP, Grieco CA, Ng T, et al. Pulmonary radiofrequency ablation: long-term safety and efficacy in 153 patients. Radiology. 2007;243:268–75.
17. Huang L, Yan Y, Zhao J, Wang X, Cheng Q, Li X, et al. Is radiofrequency thermal ablation a safe and effective procedure in the treatment of pulmonary malignancies? Eur J Cardiothorac Surg. 2011;39(3):348–51.
18. Ambrogi MC, Fanucchi O, Cioni R, Dini P, De Liperi A, Cappelli C, et al. Long-term results of radiofrequency ablation treatment of stage I non-small cell lung cancer: a prospective intention-to-treat study. J Thorac Oncol. 2011;6:2044–51.
19. Hiraki T, Gobara H, Mimura H, Matsui Y, Toyooka S, Kanazawa S. Percutaneous radiofrequency ablation of clinical stage I non-small cell lung cancer. J Thorac Cardiovasc Surg. 2011;142:24–30.
20. Kodama H, Yamakado K, Takaki H, Kashima M, Uraki J, Nakatsuka A, et al. Lung radiofrequency ablation for the treatment of unresectable recurrent non-small-cell lung cancer after surgical intervention. Cardiovasc Intervent Radiol. 2012;35:563–9.
21. Palussiere J, Lagarde P, Auperin A, Deschamps F, Chomy F, de Baere T. Percutaneous lung thermal ablation of non-surgical clinical N0 non-small cell lung cancer: results of eight years' experience in 87 patients from two centers. Cardiovasc Intervent Radiol. 2015;38:160–6.
22. Huang BY, Li XM, Song XY, Zhou JJ, Shao Z, Yu ZQ, et al. Long-term results of CT-guided percutaneous radiofrequency ablation of inoperable patients with stage IA non-small cell lung cancer: a retrospective cohort study. Int J Surg. 2018;53:143–50.
23. Lencioni R, Crocetti L, Cioni R, Suh R, Glenn D, Regge D, et al. Response to radiofrequency ablation of pulmonary tumours: a prospective, intention-to-treat, multicentre clinical trial (the RAPTURE study). Lancet Oncol. 2008;9:621–8.
24. Dupuy DE, Fernando HC, Hillman S, Ng T, Tan AD, Sharma A, et al. Radiofrequency ablation of stage IA non-small cell lung cancer in medically inoperable patients: results from the American College of Surgeons Oncology Group Z4033 (Alliance) trial. Cancer. 2015;121:3491–8.
25. Palussiere J, Chomy F, Savina M, Deschamps F, Gaubert JY, Renault A, et al. Radiofrequency ablation of stage IA non-small cell lung cancer in patients ineligible for surgery: results of a prospective multicenter phase II trial. J Cardiothorac Surg. 2018;13:91.
26. Yang X, Ye X, Zheng A, Huang G, Ni X, Wang J, et al. Percutaneous microwave ablation of stage I medically inoperable non-small cell lung cancer: clinical evaluation of 47 cases. J Surg Oncol. 2014;110:758–63.
27. Moore W, Talati R, Bhattacharji P, Bilfinger T. Five-year survival after cryoablation of stage I non-small cell lung cancer in medically inoperable patients. J Vasc Interv Radiol. 2015;26:312–9.

Chapter 5
Secondary Lung Cancer

Eduardo A. Lacayo, Stephen Solomon, and Alan Ho

Abbreviations

CIRSE	Cardiovascular and Interventional Radiology Society of Europe
CRC	Colorectal cancer
EGFR-TKI	Epidermal growth factor receptor tyrosine kinase inhibitors
GGO	Ground-glass opacity
LCT	Local consolidative therapy
MWA	Microwave ablation
OS	Overall survival
PET/CT	Positron-emission tomography/computed tomography
PFS	Progression-free survival
RFA	Radiofrequency ablation
SBRT	Stereotactic body radiotherapy
SCC	Squamous cell carcinoma

Introduction

Lung metastases are identified in 30–55% of all cancer patients, though prevalence varies according to the type of primary cancer. Among the most common extrathoracic malignancies to metastasize to the lung are colorectal (CRC), breast, and head and neck. The lung is the second most frequent site of metastatic spread for CRC

E. A. Lacayo (✉) · S. Solomon
Interventional Radiology, Memorial Sloan Kettering Cancer Center, New York, NY, USA
e-mail: lacayoe@mskcc.org; solomons@mskcc.org

A. Ho
Medical Oncology, Memorial Sloan Kettering Cancer Center, New York, NY, USA
e-mail: hoa@mskcc.org

C. Georgiades, H. S. Kim (eds.), *Image-Guided Interventions in Oncology*,
https://doi.org/10.1007/978-3-030-48767-6_5

and breast cancer, following liver and bone, respectively [1, 2]. In patients with CRC, lung metastases develop in approximately 10–15% of patients [3].

Pulmonary metastases are usually considered signs of advanced disease, and treatment options for these patients are rarely curative. However, in a subset of patients, metastasis can occur as an isolated and early event. In these circumstances, treatment with curative intent can be performed, a state known as oligometastasis. Oligometastasis is defined as metastases that are limited in number and location, with the aim of long-term survival or even cure [4, 5]. Curative local therapy, either by surgical resection, stereotactic body radiotherapy (SBRT), or thermal ablation, can be applied to oligometastases [4].

Thermal ablation such as radiofrequency ablation (RFA), microwave ablation (MWA), and cryoablation of lung metastases is a viable substitute for surgery or radiation in appropriately selected patients. It has developed into a treatment option and shown good rates of local control for those patients with oligometastatic and oligoprogressive disease, as well as patient that are undergoing chemotherapy holiday. Additionally, thermal ablation may also be a local treatment option in those patients with cancers that demonstrate resistance to chemotherapy.

Surgery as the Foundation for Local Lung Therapies

In patients with oligometastatic disease, surgical resection of all metastatic sites has been practiced the longest for lung oligometastases. In 1990, Pastorino et al. created the International Registry of Lung Metastases with clear objectives: to set up a common database through the major centers of thoracic surgery in Europe and the United States in order to facilitate the exchange of information, perform a more homogeneous evaluation of the results for the various primary tumors, define prognostic factors, propose a novel system of stage grouping, and define areas of uncertainty concerning surgery and other therapeutic modalities to be explored by prospective randomized trials [6]. The registry reported survival rates after complete surgical metastasectomy of 36%, 26%, and 22%, at 5-year, 10-year, and 15-year, respectively. This registry set the foundation for treating lung oligometastases.

The following 5-year overall survival rates after resection of single pulmonary metastasis have been reported: adenoid cystic carcinoma and squamous cell carcinoma (SCC) of the head and neck 63%, 40–50%, respectively, colon cancer 40%, and breast cancer 30–50%. The 5- and 10-year OS rates for H&N, CRC, and breast cancer are summarized in (Table 5.1) [7].

Table 5.1 Rates of overall survival

Overall survival	CRC	Breast Ca	SCCa	ACCa
5 year	35–45%	50%	34%	84%
10 year	20–30%	–	–	–

Selection Criteria/Indications for Surgery

Surgical candidacy for pulmonary metastasectomy has evolved since its original description. Patients should meet the following criteria: (1) Complete control of the primary tumor, (2) no evidence of extrapulmonary metastases; or if present, it can be controlled by surgery or another treatment modality, (3) the patient must be a good risk for surgical intervention, and (4) pulmonary metastases are thought to be completely resectable [6–8]. Additional indications include good respiratory function compatible with the proposed lung resection procedure, existence of effective systemic chemotherapy as a combined modality, and symptomatic pulmonary metastasis (i.e., pneumothorax, hemoptysis) [7].

Oligoprogression

There is data supporting the use of local therapy as a treatment option for chemotherapy resistant cancers with pulmonary oligometastatic disease (known as oligoprogression). For example, it has been used in oligoprogressive epidermal growth factor receptor (EGFR) mutant lung cancer patients with acquired resistance to EGFR tyrosine kinase inhibitors (EGFR TKI). A retrospective study by Yu et al. found the median time to progression with the addition of local therapies such as surgical resection, radiotherapy, and RFA is 10 months and a median overall survival of 41 months. The authors conclude that local therapy followed by continued treatment with an EGFR TKI is well tolerated and associated with long progression-free survival (PFS) and overall survival (OS). It should be noted that these data are derived from a small retrospective study of 18 patients. However, it does suggest the potential therapeutic benefits combination therapy provides for the treatment of resistant clones [9].

Radiation Therapy

In patients that are not surgical candidates, another therapeutic option has been radiation therapy. With the advent of stereotactic body radiotherapy (SBRT) and proton therapy, radiation therapy has become much more prec2ise, and has shown favorable results when treating extracranial oligometastases. A retrospective study of 637 patients with 858 SBRT treatments for multiple different histological cancer primaries (most common were breast, non-small cell lung cancer and colorectal), with a median follow-up of 13.0 months (range 0.2–131.9 months), demonstrates a median OS of 23.5 months [10].

Recently, a multi-institutional, phase II randomized trial for patients with oligometastatic non-small cell lung cancer compared local consolidative therapy (LCT) with

surgery or radiation to maintenance therapy and/or observation. They found no progression after initial therapy for 3 months in patients with <3 metastases, a median progression-free survival of 14.2 months for LCT group and 4.4 months for the maintenance therapy group. Median overall survival benefit in this study was found to be 41.2 months in the LCT arm vs 17.0 months for those in the maintenence therapy/observation arm [11].

Despite the positive results in the literature, the safety and toxicity profile of radiation are still inferior when compared to thermal ablation. Salama et al. reported 11.7% grade 3 toxicity in patients undergoing SBRT for extracranial oligometastases. McCammon et al. published a grade 3 toxicity in approximately 5% of patients in his study, with eight patients requiring steroids for pneumonitis. Dunlap et al. reported 28.3% chest wall pain (grade 3) and 9% rib fractures when treating peripheral lung cancers [12–14].

Thermal Ablation

Percutaneous thermal ablation has been found to be another useful treatment option for patients with pulmonary oligometastatic disease. Significant medical comorbidities and compromised cardiopulmonary function limit surgical candidacy and often impede surgical intervention. Additionally, recurrence in patients after lung metastasectomy are common, ranging from 20 to 68%, and subsequent surgery is challenging due to limited pulmonary reserve [3].

Thermal ablation is a minimally invasive image-guided technique that produces irreversible tumor tissue destruction through the application of either hot or cold thermal energy [15]. Image guidance is utilized to percutaneously advance and guide the ablation probe within the lesion to deliver the thermal energy [15, 16]. The treatment should aim for a 0.5–1.0 cm zone of surrounding normal tissue to achieve a surrogate for a "surgical" clear margin [16]. The thermal ablation modalities that are currently used are RFA, MWA, and cryoablation. The most commonly used modality has been RFA, with MWA becoming more popular in the recent years.

Basic Concepts of Thermal Ablation

RFA is a technique utilizing an electric current to heat tissue by fractioning electrons at a frequency of 400 KHz. This is achieved by rapid alternating electrical currents that are transmitted through the probe, into the target lesion and back to the generator through a grounding electrode. The current causes ionic molecule agitation to the surrounding tissue; this generates the heat necessary for tissue destruction. In order to treat sufficient volume, there needs to be adequate conduction of heat, which may be limited in the lungs due to its air-filled spaces insulating the heated volume [17]. Additionally, performing RFA in close proximity to large blood vessels increases the possibility of an incomplete ablation secondary to the "heat-sink effect," caused by the cooling effect of blood flow.

MWA applies an electromagnetic field created around the ablation probe; the field varies from 915 MHz to 2450 MHz. This heats the tissue by forcing water molecules to continuously realign with the oscillating field resulting in heat generation. In MWA, temperatures rise faster and much higher due to the friction of the water molecules. This in turn will allow MWA to rely less on conduction into tissues, decreasing the "heat-sink effect," yielding a more uniform ablation zone [17].

MWA has several advantages over RFA; it can generate much higher temperatures in a shorter period of time. MWA is capable of heating tissues with low electrical conductivity, resulting in a larger ablation zone. Furthermore, due to its low tissue conduction of heat, it decreases the chances of "heat-sink effect."

Cryoablation damages and destroys tumor cells by alternating between tissue freezing and thawing. At −20 °C, cells are killed by protein denaturation and membrane disruption. The continuous repetition of the freeze-thaw cycle induces the formation of intra- and extracellular ice crystals, increasing cellular injury. Additionally, cryoablation has certain indirect actions that facilitate tissue destruction, such as vasoconstriction and occlusion of blood vessels, osmotic changes, and local tissue edema, which results in hypoxic tissue damage and coagulative necrosis. The air-filled lung and alveolar structures may interfere with the ice ball creation, limiting its freezing potential. Cryoablation preserves collagenous architecture of the area of ablation, which may show some advantage when treating central tumors, or tumors adjacent to bronchi [17].

Indications

Indications for thermal ablation in patients with pulmonary oligometastatic disease are: (1) patients with a limited number of metastases (up to 6) in each hemithorax, preferably <3 tumors per hemithorax, (2) small tumor size (up to 2.5 cm), (3) tumors should demonstrate biologic stability over several scans without evidence of new tumors; this allows additional metastases which may be present, but undetected, to be identified ("test of time" approach), and (4) limited or controlled extrathoracic disease [3, 18, 19].

The CIRSE (Cardiovascular and Interventional Radiology Society of Europe) standards of practice guidelines 2012 state that there is no specifically defined number of lesions that may be ablated; however, most centers treat patients with five or fewer metastases [15].

Contraindications

Percutaneous thermal ablation is generally well tolerated by patients, making absolute contraindications difficult to identify. Untreatable coagulopathies are the only clear exception. Anticoagulation and/or antiplatelet drugs should be discontinued 5–10 days prior to the procedure, based on your institution's standards of practice.

Patients with an Eastern Cooperative Oncology Group performance status of >2 or with a life expectancy of less than 1 year are not good candidates for lung ablation. Patients with lesions of <1 cm from the hilum, esophagus, or trachea should generally be avoided or moved with artificial pneumothorax creation. Direct contact with a vessel >3 mm or with the myocardium has been already reported as a negative predictive factor for complete coagulation of lung lesions [15].

Technique Selection

Criteria for patient selection between thermal ablative modalities are similar, with the exception that MWA is theoretically able to ablate larger tumors. MWA is less affected by the "heat-sink effect" in lesions adjacent to vessels, when compared to RFA. This is secondary to the technologies ability to generate higher temperatures, improving the possibility of obtaining a complete ablation in lesions close to blood vessels [20]. However, MWA can potentially cause more injury to its surrounding vessels. RFA may interfere with the function of implantable cardiac devices [21].

Technique

Based on patient or radiologist preference, the procedure is performed via sterile technique with the patient under monitored sedation or general anesthesia. The procedure is most commonly performed with CT guidance. Patient positioning, tumor location, and proximity to fissures and bronchovascular structures should be considered before the procedure [21]. Prior to initiation of the procedure, the probe trajectory and number of applicators that will be used are planned. The size of the lesion and its location will determine the number of applicators used. While planning the trajectory, the aim is to traverse the least number of pleural surfaces possible, to decrease the risk of pneumothorax. Peripheral lesions are difficult to target via a direct puncture, perpendicular to the pleural surface, as the probe may not be appropriately anchored in the lung and can potentially be displaced with breathing [21]. These nodules are best approached tangentially to secure the needle in a larger volume of lung, for more optimal anchorage. Additionally, when using MWA, this tangential approach helps avoid the "back burn" to the pleura, decreasing the risk of a bronchopleural fistula. When using cryoablation, this tangential approach will help contain lung hemorrhage and prevent blood from tracking back into the pleura [21]. In patients with central lesions, adjacent to bronchovascular structures, the ablation probe should be positioned parallel to the anatomic structure, avoiding injury [21].

Ablation of lesions close to the lung surface increases the risk of chest wall and nerve injury. A technique that has been described to prevent this by separating the tumor from the chest wall includes creation of an artificial pneumothorax [22]. This allows for a safer ablation with increased distance from the chest wall.

Table 5.2 Most common complications after thermal lung ablation

Complication	RFA (%)	MWA (%)
Pneumothorax		
With chest tube	~22	4–22
Without chest tube	~22	28–39
Major complications – (pleuritis, pneumonia, lung abscess, hemorrhage)	9.8	7
Mortality	0.4	0.5

The ablation applicator (or applicators) is advanced under CT guidance. According to operator preference, real-time or CT fluoroscopy can be utilized. The applicator position is confirmed using CT with multiplanar reformats once the desired location is achieved. Following this, energy should be applied following the recommended algorithm for lung tissue ablation. Post-treatment CT is performed and should show a halo of ground-glass opacity (GGO) in patients post RFA or MWA. If the GGO encompasses the lesion with a satisfactory margin, this has been found to correlate with cell death and successful treatment [23].

Bilateral lung tumors should not be treated in the same session for safety reasons, particularly the increased risk of delayed pneumothorax.

Complications

Pneumothorax is the most common complication after thermal ablation, with a reported incidence of 22% after RFA and as high as 38% after MWA (Kashima et al. 2010, Kurilova et al. 2018). Pneumothorax requiring thoracostomy tube placement had a similar incidence of 22.1% for RFA and 15.6% for MWA [24, 25]. Incidence for major complications has been reported as 9.8% and 7% for RFA and MWA, respectively and includes pleuritis, pneumonia, lung abscess, and hemorrhage. Rare complications such as bronchopleural fistula, nerve injury, and tumor seeding have been reported to have an incidence of <0.5%. The reported mortality rate after RFA and MWA are 0.4% and 0.5%, respectively [24, 25] (Table 5.2).

Follow-Up

Surveillance

In the follow-up period, contrast-enhanced CT is typically performed at 1 month to set a new baseline size, 3 months, 6 months, and then yearly following thermal ablation. Positron-emission tomography/computed tomography (PET/CT) can be used as a problem-solving study when findings on CT are suspicious for recurrence.

Radiofrequency and Microwave Ablation Imaging Findings

The ablation zone following RFA and MWA are similar given they are both heat-based modalities. The appearance of the ablation zone is divided into three phases: (1) immediate and early phase (<24 hours to 1 week), (2) intermediate phase (1 week to 2 months), and (3) late phase (>2 months) [26] (Fig. 5.1).

In the immediate post ablation phase, usually a non-contrast-enhanced CT scan is performed to depict the ablation zone as an area of concentric ground GGO covering the target tumor with a minimal ablation margin of at least 10 mm uniformly around target metastasis. This should be the minimal margin required to ensure complete tumor ablation [26, 27]. Once in the recovery area, at our institution we routinely obtain chest radiographs immediately and at 2 hours to determine need for chest tube.

In the intermediate phase, there should be a noticeable decrease in size of the GGO surrounding the tumor with filling in of the GGO. This involution may last 1 to 3 months and is due to regression of parenchymal edema, inflammation, and hemorrhage [26]. Cavitation of the ablation zone can occur during this intermediate phase, usually within the first 2 months post ablation [26, 27]. These findings are considered a positive response to thermal ablation.

In the late phase, there should be a progressive decrease in size of the ablation zone with near complete resolution of the GGO. The ablation zone may completely disappear with only parenchymal scar visualized on cross-sectionally imaging in its

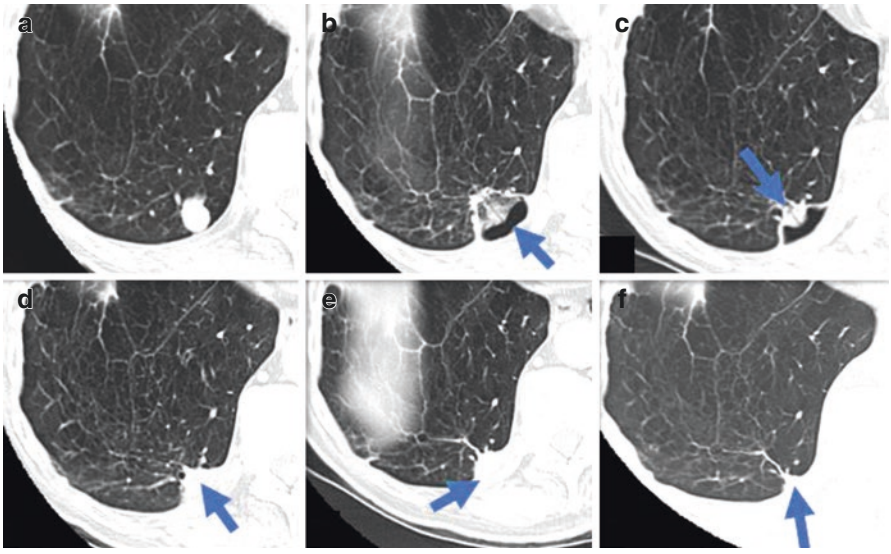

Fig. 5.1 Axial computed tomography of the right lower lobe (RLL). (**a**) Metastatic colorectal cancer to the RLL, pre-RFA. (**b**) 1-month post-RFA. (**c**) 5 months post-RFA. (**d**) 8 months post-RFA. (**e**) 15 months post-RFA. (**f**) 30 months post-RFA

place, especially in tumors that were <2 cm in size [26]. For tumors that measured >2 cm in size, they may have a more nodular pattern making their evaluation more unpredictable, which makes differentiation between post-treatment changes and incomplete treatment response difficult. This is where contrast-enhanced CT proves to be most valuable, and it will help differentiate nonenhancing scars from enhancing residual tumor [27]. At 3 months the ablation zone should be equal or slightly larger than the size of the baseline tumor, followed by continued size reduction by 6 months. A continuously enlarging ablation zone at 3 months and 6 months is suspicious for recurrence, especially if a nodular growth pattern is identified. After 6 months it is reasonable to expect the ablation zone will be smaller than the size of the baseline tumor [26, 27].

After 6 months, the CT should show a residual elongated linear nodule which is stable or decreasing in size, atelectasis or cavitation. Complete disappearance of the initial nodule is rarely observed [28].

Cryoablation Imaging Findings

In the immediate and early phase, non-contrast CT scan post ablation can delineate a low-density ovoid ice ball within the background of higher attenuated hemorrhage. Once the ablation is complete, the ice ball will begin to melt, forming GGO and consolidation around the ablation zone. During the first week, most of the GGO and consolidation will slowly resolve. Occasionally, cavitation may occur during this time [26].

In the intermediate phase, the previously visualized GGO surrounding the ablation zone should resolve at the end of the first month. Cavitation of the ablation is common during the intermediate phase. During this phase, the ablation zone becomes more discrete and rounded with well-delineated margins [26].

In the late phase, the ablation zone continues to shrink in size; it maintains its rounded, well-demarcated appearance. It slowly involutes into a linear parenchymal scar. By 3 months, most of the cavitation will have resolved. Occasionally, the cavitation may continue as long as 9 months [26].

Outcomes

Favorable outcomes have been demonstrated with thermal ablation achieving good control of tumor and tumor progression, comparable to those found in the surgical literature, while avoiding the morbidity associated with surgery. The most studied modality in the literature is RFA.

Lencioni et al. published a prospective, multicenter clinical trial where 106 patients with different primary tumor histology were enrolled for RFA. A total of 183 metastatic lung tumors were treated. Fifty-three of these patients had colorectal metastases with a mean tumor size of 1.4 cm (range 0.5–3.4 cm). One lesion per

patient had a confirmed histopathologic diagnosis. Cancer-specific survival was found to be 91% at 1 year and 68% at 2 years in patients with colorectal metastases. This study showed a 99% technical success rate and a 1-year and 2-year overall survival rate of 89% and 66%, respectively, in patients with pulmonary metastases from a colorectal primary [1].

A large series published by De Baere et al. compared his results of RFA for lung metastases from various tumor types with those of the surgical literature. The study evaluated 566 patients treated for 1037 lung metastases from different primary extrathoracic malignancies, most frequently CRC (34%). Most patients had one (53%) or two (25%) lung metastases, while other patients had up to eight lesions. He found that the median OS was 62 months, and the 5-year OS rate was 51%, this is within the range of the best results obtained by surgical metastasectomy. They describe that size >2 cm and number of metastases >3 were poor prognostic factors for OS. They concluded that RFA is an option for treatment of metastatic tumors <2–3 cm in size and with <3 metastases [29].

Petre et al. reported their data from a series of 45 patients with 69 lung metastases whom underwent RFA for metastatic colorectal lung metastases. Median overall survival from ablation was 46 months, with a 1-, 2-, and 3-year progression-free survival of 92%, 77%, and 77%, respectively. Thirty-six of the patients underwent chemotherapy prior to RFA. Nineteen of the 36 patients received a chemotherapy "holiday" for 1–20 months after ablation [30]. If lung metastases are cleared after thermal ablation, patients can then potentially come off chemotherapy, followed by repeat imaging to evaluate for new disease.

Vogl et al. published a series of 80 patients with 130 lung lesions whom underwent MWA for unresectable pulmonary metastases from different extrathoracic malignancies. Fifty percent of these patients (40/80, 58 lesions) had colorectal metastases, and 25% of patients (20/80, 32 lesions) had breast carcinoma. Complete ablation was achieved in 73.1% (95/130) lesions, with preablation tumor size of <3 cm the most significant predictor of successful ablation. Survival rates were 91.3% and 75% at 12 and 24 months, respectively [31].

A prospective multicenter trial performing cryoablation on 40 patients with 60 metastatic lung lesions, with a mean tumor size of 1.4 cm. Local tumor control was achieved in 96.6% (56/58) and 94.2% (49/52) of lesions at 6 and 12 months, respectively. One-year overall survival rate was 97.5% [32].

Multimodality Treatment

Combined multimodality treatments may result in improved survival when using thermal ablation, surgery, and radiation therapy or chemotherapy, when compared to these modalities alone. Inoue et al. published a retrospective study of 21 patients

analyzing the long-term results of multimodality therapy. The study reported a median survival of 38.6 months, a cumulative 3-year survival of 87.5% after multimodality treatment including RFA, radiotherapy, and chemotherapy compared with 33.3% using chemotherapy alone [33].

Advantages of Thermal Ablation

Thermal ablation will preserve the lung parenchyma with minimal collateral damage. Surgical resection may take too much tissue, with the risk of other metastatic lesions appearing and limiting future resections. Radiation therapy cannot be repeated if necessary. Using thermal ablation for small metastatic nodules amenable to treatment is beneficial initially to avoid damage to the surrounding lung and preserve function. Given its minimally invasive and can be performed multiple times, it may be a good first line tool while reserving surgery and radiation therapy for patients that we cannot ablate.

Future Trends

In situ tumor cell death caused by thermal ablation is known to upregulate the immune system causing tumor suppression of metastatic sites [34]. It has been shown that tumors can serve as their own antigenic vaccine after thermal ablation, as long as immunotherapy can provide additional pro-inflammatory stimuli to activate immune-mediated tumor rejection signals. Thermal ablation alone is unlikely to cause a system-wide and sustained regression of metastases. Therefore, a combination approach where thermal ablation is paired with immunotherapy may provide a synergistic effect, increasing the antitumor response and maintaining tumor suppression of distant metastases. To date, the ablative technique that optimally primes the immune system and should be tested in combination with immunotherapy remains unclear. Limited evidence suggests that cryoablation may have a better post-procedure immune response on tumor cells when compared to other modalities. A study by McArthur et al. shows potentially favorable intratumoral and systemic immunologic effects combining cryoablation with the cytotoxic T-lymphocyte-associated protein 4 (CTLA-4) targeted antibody ipilimumab (ipi) in patients with early-stage breast cancer. These data may suggest the possibility of synergistic antitumor immunity stimulated by cryoablation in the context of immunotherapy [35]. However, further study is needed to better identify which ablative modality may work best in synergy with immunotherapy to optimally treat lung metastases.

References

1. Lencioni R, Crocetti L, Cioni R, Suh R, Glenn D, Regge D, et al. Response to radiofrequency ablation of pulmonary tumours: a prospective, intention-to-treat, multicentre clinical trial (the RAPTURE study). Lancet Oncol. 2008;9(7):621–8.
2. Clark GM, Sledge GW, Osborne CK, McGuire WL. Survival from first recurrence: relative importance of prognostic factors in 1,015 breast cancer patients. J Clin Oncol. 1987;5(1):55–61.
3. Kurilova I, Gonzalez-Aguirre A, Beets-Tan RG, Erinjeri J, Petre EN, Gonen M, et al. Microwave ablation in the management of colorectal cancer pulmonary metastases. Cardiovasc Intervent Radiol [Internet]. 2018;41(10):1530–44.. Available from: https://doi.org/10.1007/s00270-018-2000-6.
4. Kaneda H, Saito Y. Oligometastases: defined by prognosis and evaluated by cure. Cancer Treat Commun. 2015;3:1–6.
5. Hellman S, Weichselbaum RR. Oligometastases. J Clin Oncol [Internet]. 1995;13(1):8–10.. Available from: https://doi.org/10.1200/JCO.1995.13.1.8.
6. Pastorino U, Buyse M, Friedel G, Ginsberg RJ, Girard P, Goldstraw P, et al. Long-term results of lung metastasectomy: prognostic analyses based on 5206 cases. J Thorac Cardiovasc Surg. 1997;113(1):37–49.
7. Kondo H, Okumura T, Ohde Y, Nakagawa K. Surgical treatment for metastatic malignancies. Pulmonary metastasis: indications and outcomes. Int J Clin Oncol. 2005;10(2):81–5.
8. Casiraghi M, De Pas T, Maisonneuve P, Brambilla D, Ciprandi B, Galetta D, et al. A 10-year single-center experience on 708 lung metastasectomies: the evidence of the "international registry of lung metastases". J Thorac Oncol [Internet]. 2011;6(8):1373–8.. Available from: https://doi.org/10.1097/JTO.0b013e3182208e58.
9. Yu HA, Sima CS, Huang J, Solomon SB, Rimner A, Paik P, et al. Local therapy with continued EGFR tyrosine kinase inhibitor therapy as a treatment strategy in EGFR-mutant advanced lung cancers that have developed acquired resistance to EGFR tyrosine kinase inhibitors. J Thorac Oncol [Internet]. 2013;8(3):346–51.. Available from: https://doi.org/10.1097/JTO.0b013e31827e1f83.
10. Klement RJ, Hoerner-Rieber J, Adebahr S, Andratschke N, Blanck O, Boda-Heggemann J, et al. Stereotactic body radiotherapy (SBRT) for multiple pulmonary oligometastases: analysis of number and timing of repeat SBRT as impact factors on treatment safety and efficacy. Radiother Oncol [Internet]. 2018;127(2):246–52.. Available from: https://doi.org/10.1016/j.radonc.2018.02.016.
11. Gomez DR, Tang C, Zhang J, Blumenschein GR, Hernandez M, Jack Lee J, et al. Local consolidative therapy vs. maintenance therapy or observation for patients with oligometastatic non–small-cell lung cancer: long-term results of a multi-institutional, phase II, randomized study. J Clin Oncol. 2019;37(18):1558–65.
12. McCammon R, Schefter TE, Gaspar LE, Zaemisch R, Gravdahl D, Kavanagh B. Observation of a dose-control relationship for lung and liver tumors after stereotactic body radiation therapy. Int J Radiat Oncol Biol Phys. 2009;73(1):112–8.
13. Salama JK, Hasselle MD, Chmura SJ, Malik R, Mehta N, Yenice KM, et al. Stereotactic body radiotherapy for multisite extracranial oligometastases: final report of a dose escalation trial in patients with 1 to 5 sites of metastatic disease. Cancer. 2012;118(11):2962–70.
14. Dunlap NE, Cai J, Biedermann GB, Yang W, Benedict SH, Sheng K, et al. Chest wall volume receiving >30 Gy predicts risk of severe pain and/or rib fracture after lung stereotactic body radiotherapy. Int J Radiat Oncol Biol Phys. 2010;76(3):796–801.
15. Pereira PL, Salvatore M. Standards of practice: guidelines for thermal ablation of primary and secondary lung tumors. Cardiovasc Intervent Radiol. 2012;35(2):247–54.
16. Dempsey PJ, Ridge CA, Solomon SB. Advances in interventional oncology: lung cancer. Cancer J (United States). 2016;22(6):393–400.
17. Palussière J, Catena V, Buy X. Percutaneous thermal ablation of lung tumors – radiofrequency, microwave and cryotherapy: where are we going? Diagn Interv Imaging [Internet]. 2017;98(9):619–25.. Available from: https://doi.org/10.1016/j.diii.2017.07.003.

18. Livraghi T, Solbiati L, Meloni F, Ierace T, Goldberg SN, Gazelle GS. Percutaneous radiofrequency ablation of liver metastases in potential candidates for resection: the "test-of-time" approach. Cancer. 2003;97(12):3027–35.
19. Fong Y, Fortner J, Sun RL, Brennan MF, Blumgart LH. Clinical score for predicting recurrence after hepatic resection for metastatic colorectal cancer: analysis of 1001 consecutive cases. Ann Surg. 1999;230(3):309-321. https://doi.org/10.1097/00000658-199909000-00004.
20. De Baere T, Tselikas L, Catena V, Buy X, Deschamps F, Palussière J. Percutaneous thermal ablation of primary lung cancer. Diagn Interv Imaging [Internet]. 2016;97(10):1019–24.. Available from: https://doi.org/10.1016/j.diii.2016.08.016.
21. Abtin F, De Baere T, Dupuy DE, Genshaft S, Healey T, Khan S, et al. Updates on current role and practice of lung ablation. J Thorac Imaging. 2019;34(4):266–77.
22. Hiraki T, Gobara H, Fujiwara H, Ishii H, Tomita K, Uka M, et al. Lung cancer ablation: complications. Semin Intervent Radiol. 2013;30(2):169–75.
23. Smith SL, Jennings PE. Lung radiofrequency and microwave ablation: a review of indications, techniques and post-procedural imaging appearances. Br J Radiol. February 2015; 88(1046): 20140598. Published online 2015 Jan 12. https://doi.org/10.1259/bjr.20140598PMCID: PMC4614249.
24. Kashima M, Yamakado K, Takaki H, Kodama H, Yamada T, Uraki J, et al. Complications after 1000 lung radiofrequency ablation sessions in 420 patients: a single center's experiences. Am J Roentgenol. 2011;197(4):576–80.
25. Zheng A, Wang X, Yang X, Wang W, Huang G, Gai Y, et al. Major complications after lung microwave ablation: a single-center experience on 204 sessions. Ann Thorac Surg [Internet]. 2014;98(1):243–8.. Available from: https://doi.org/10.1016/j.athoracsur.2014.03.008.
26. Chheang S, Abtin F, Guteirrez A, Genshaft S, Suh R. Imaging features following thermal ablation of lung malignancies. Semin Intervent Radiol. 2013;30(2):157–68.
27. Palussière J, Marcet B, Descat E, Deschamps F, Rao P, Ravaud A, et al. Lung tumors treated with percutaneous radiofrequency ablation: computed tomography imaging follow-up. Cardiovasc Intervent Radiol. 2011;34(5):989–97.
28. Ridge CA, Solomon SB. Percutaneous ablation of colorectal lung metastases. J Gastrointest Oncol. 2015;6(6):685–92.
29. De Baère T, Aupérin A, Deschamps F, Chevallier P, Gaubert Y, Boige V, et al. Radiofrequency ablation is a valid treatment option for lung metastases: experience in 566 patients with 1037 metastases. Ann Oncol. 2015;26(5):987–91.
30. Petre EN, Jia X, Thornton RH, Sofocleous CT, Alago W, Kemeny NE, et al. Treatment of pulmonary colorectal metastases by radiofrequency ablation. Clin Colorectal Cancer [Internet]. 2013;12(1):37–44.. Available from: https://doi.org/10.1016/j.clcc.2012.07.003.
31. Vogl TJ, Naguib NNN, Gruber-Rouh T, Koitka K, Lehnert T, Nour-Eldin NEA. Microwave ablation therapy: clinical utility in treatment of pulmonary metastases. Radiology. 2011;261(2):643–51.
32. De Baere T, Tselikas L, Woodrum D, Abtin F, Littrup P, Deschamps F, et al. Evaluating cryoablation of metastatic lung tumors in patients-safety and efficacy the ECLIPSE trial-interim analysis at 1 year. J Thorac Oncol [Internet]. 2015;10(10):1468–74.. Available from: https://doi.org/10.1097/JTO.0000000000000632.
33. Inoue Y, Miki C, Hiro J, Ojima E, Yamakado K, Takeda K, et al. Improved survival using multi-modality therapy in patients with lung metastases from colorectal cancer: a preliminary study. Oncol Rep. 2005;14(6):1571–6.
34. Rao P, Escudier B, De Baere T. Spontaneous regression of multiple pulmonary metastases after radiofrequency ablation of a single metastasis. Cardiovasc Intervent Radiol. 2011;34(2):424–30.
35. McArthur HL, Diab A, Page DB, Yuan J, Solomon SB, Sacchini V, et al. A pilot study of preoperative single-dose ipilimumab and/or cryoablation in women with early-stage breast cancer with comprehensive immune profiling. Clin Cancer Res. 2016;22(23):5729–37.

Chapter 6
Hepatocellular Carcinoma: Western Experience

Thaddeus J. Maguire, Aditya Shreenivas, and William S. Rilling

Epidemiology

Hepatocellular carcinoma is the most common primary hepatic malignancy. With an estimated 850,000 new diagnoses annually, hepatocellular carcinoma is the fifth most common type of cancer worldwide. Each year it is also associated with up to 810,000 deaths, and it is commonly ranked the second or third leading overall cause of cancer-related mortality [1–4].

It is well-established that the risk of developing hepatocellular carcinoma is closely associated with both the presence and severity of underlying chronic liver disease. A reported 80–90% of hepatocellular carcinoma arises in patients with cirrhosis, irrespective of etiology [3, 5]. The annual incidence of hepatocellular carcinoma among all patients with cirrhosis ranges from approximately 1–8% [2, 4, 6].

The vast majority (80–85%) of patients with hepatocellular carcinoma are found in Eastern Asia and sub-Saharan Africa. Infection is the most common predisposing factor in this population, due to the endemic rates of hepatitis B (HBV) and *Aspergillus* aflatoxin exposure [1–3].

T. J. Maguire (✉)
Early Specialization in Interventional Radiology, Department of Radiology, Medical College of Wisconsin, Froedtert Memorial Lutheran Hospital, Milwaukee, WI, USA
e-mail: tmaguire@mcw.edu

A. Shreenivas
Division of Hematology and Medical Oncology, Medical College of Wisconsin, Froedtert Memorial Lutheran Hospital, Milwaukee, WI, USA
e-mail: ashreenivas@mcw.edu

W. S. Rilling
Department of Radiology, Division of Vascular & Interventional Radiology, Medical College of Wisconsin, Froedtert Memorial Lutheran Hospital, Milwaukee, WI, USA
e-mail: wrilling@mcw.edu

C. Georgiades, H. S. Kim (eds.), *Image-Guided Interventions in Oncology*,
https://doi.org/10.1007/978-3-030-48767-6_6

In the United States, the incidence of hepatocellular carcinoma has steadily risen for several decades. Nearly 40,000 new diagnoses of hepatocellular carcinoma were made in the United States in 2014 alone [3, 7]. The majority of cirrhosis and by extension hepatocellular carcinoma in the American populace have historically been related to alcohol and hepatitis C (HCV) infection. There is a recognized dose-dependent relationship between alcohol consumption and the risk of hepatocellular carcinoma. The proportion of hepatocellular carcinoma related to alcohol use in the West has remained fairly constant at 20–25% [6, 7]. Peak estimates ascribed 30–50% of hepatocellular carcinoma in the United States to HCV infection, though this has begun to decline following the development of effective anti-viral therapy [4]. In some patients, it can take decades for the cumulative hepatocellular damage caused by HCV infection to progress to cirrhosis. Consequently, the annual incidence of hepatocellular carcinoma in those infected by HCV is less than 1% but climbs to 8% among those with HCV-related cirrhosis [6].

In recent years, the prevalence of nonalcoholic fatty liver disease (NALFD) has risen considerably. NAFLD broadly refers to a spectrum of disorders in which lipids accumulate in the hepatic parenchyma. There is a strong association of NALFD with metabolic syndrome, with which it shares several interrelated risk factors including obesity, hyperlipidemia, and diabetes mellitus type 2.

Studies estimate the prevalence of NAFLD to be 25% worldwide and as high as 34% in the United States. NAFLD is now a leading cause of chronic liver disease in Americans and the second leading cause of liver transplantation. The most severe manifestation, nonalcoholic steatohepatitis (NASH), is defined by the presence of steatosis and associated hepatocyte injury. NASH has an estimated prevalence of 1–6% in the general population and confers a significantly increased risk of liver-related mortality. Approximately one-half of patients with otherwise uncomplicated fatty liver will progress to NASH within 7 years [6, 8–10].

It is important for patients and medical practitioners to recognize that metabolic disorders, including type 2 diabetes and NAFLD, each pose an independent risk for developing both cirrhosis and hepatocellular carcinoma. The impact of these disorders on clinical practice is set to escalate in conjunction with the ongoing obesity epidemic. The incidence of hepatocellular carcinoma related to NAFLD is reportedly growing at a rate of 9% annually [8]. In 2018, the American Association for the Study of Liver Diseases (AASLD) reported that the relative contribution of obesity and metabolic disorders to the burden of hepatocellular carcinoma in the United States had overtaken that of HCV [3]. This is presumably due to more effective therapies for viral hepatitis, as well as the mounting prevalence and relatively indolent natural history of most metabolic disorders. This is supported by the work of Welzel et al., who calculated the population attributable fraction for each of the common causes of hepatocellular carcinoma by weighting the relative risk of each factor with its prevalence in Americans. By their analysis, eliminating diabetes and obesity could potentially decrease the incidence of hepatocellular carcinoma by upward of 35%, more than any other common factor including alcohol (24%), HCV (22%) and HBV (6%) [6, 7].

Patients with comparatively rare conditions, including autoimmune hepatitis, Wilson's disease, hereditary hemochromatosis, and primary biliary cirrhosis,

together comprise a far smaller proportion of Americans at risk for developing hepatocellular carcinoma.

In clinical practice, patients may have multiple concurrent risk factors for chronic liver disease. When present in combination, these further potentiate hepatic damage, thereby hastening progression to cirrhosis and by extension hepatocellular carcinoma. Metabolic syndrome, excessive alcohol consumption, and co-infection with either HIV or a second hepatitis strain confer additive risk when coexistent with hepatitis B or C [2, 5, 6, 11].

In addition to the etiology and severity of underlying liver disease, an individual patient's risk of developing hepatocellular carcinoma is modulated by several minor factors including age, race, and geographic region. Likely as a consequence of lifestyle differences, hepatocellular carcinoma is more commonly found in males and tobacco users [2, 4].

Of note, through mechanisms which are still being elucidated, a growing body of evidence indicates that coffee consumption offers a hepatoprotective benefit, decreasing the risk of hepatocellular carcinoma as well as overall liver-related mortality [2, 12].

Pathophysiology

Hepatocellular carcinoma is a heterogeneous family of tumors. Research into their complex genetics is ongoing as part of an international effort to expand therapeutic opportunities. The development and progression of hepatocellular carcinoma is a multifaceted biomolecular process, the details of which are beyond the scope of this publication. Briefly, damage to the hepatic parenchyma incites a local inflammatory cascade. Sustained insults, such as frequent alcohol use or persistent infection, can perpetuate the cycle of inflammation. Hepatocytes undergo necrosis, engendering further inflammation and eventually the fibrotic interstitial scarring pathognomonic of cirrhosis. As damaged hepatocytes regenerate, they accrue genetic mutations resulting in clonal lines which are uncoupled from critical regulatory functions, including cell death. Though early results are encouraging, investigators are working to validate a panel of genetic tests which could stratify patients' risk for developing hepatocellular carcinoma [6, 13, 14].

Clinical Surveillance

Despite their modest quality, multiple studies from across the globe agree that clinical surveillance for hepatocellular carcinoma in patients with cirrhosis is cost-effective and improves survival by identifying early-stage patients while still candidates for curative therapy [1–3, 6].

Regular screening evaluations with hepatic ultrasound, with or without an alpha-fetoprotein (AFP) level, are the present standards of care in the United States and

Table 6.1 Child-Pugh score

Factor	1 point	2 points	3 points
Total Bilirubin (mg/dL)	2	2–3	>3
Serum Albumin (g/dL)	>3.5	2.8–3.5	<2.8
INR	<1.7	1.7–2.2	>2.2
Ascites	None	Mild	Moderate to Severe
Hepatic Encephalopathy	None	Grade 1–2 (medically controlled)	Grade 3-4 (Refractory)
	Class A	Class B	Class C
Total	5–6	7–9	10–15

Europe. In practice, ultrasound screening for HCC has significant limitations in obese patients and in steatotic livers. The AASLD recommends screening evaluations every 6 months for all patients Child-Pugh class A or B cirrhosis, given they are more often candidates for aggressive treatment (Table 6.1). Due to the poor prognosis, screening is not routinely recommended for those with Child-Pugh C disease. However, even patients with advanced cirrhosis should remain in surveillance when under consideration for liver transplant. The European Association for the Study of the Liver (EASL) endorses similar practice guidelines. Both organizations also report a benefit of screening high-risk patients with chronic HBV which have not yet advanced to cirrhosis. Continued surveillance is appropriate in patients with HCV cirrhosis even after having achieved serologic viral remission [1, 6].

To date, screening all patients with HCV and NAFLD in the absence of cirrhosis has not been found cost-effective and is of uncertain benefit [2, 6]. It is plausible that shifting patient demographics, as well as our developing understanding of tumor genetics and the risk profiles of metabolic disorders, may alter these recommendations in the future.

Diagnosis

Per the AASLD, cirrhotic patients with a hepatic nodule detected on ultrasound measuring ≥1 cm should proceed to a diagnostic multi-phase CT or MRI. Hepatocellular carcinoma is unique among common malignancies in that characteristic imaging may obviate the need for a tissue sample diagnosis.

Reporting criteria for cross-sectional imaging have been developed by the American College of Radiology (ACR) and the Organ Procurement and Transplant Network (OPTN). Both the ACR's LI-RADS and the OPTN criteria are validated for assessing the likelihood of imaging findings to represent hepatocellular carcinoma. As of 2018 the ACR LI-RADS have been integrated into the AASLD practice guidance algorithm (Fig. 6.2). Prior to full integration, modifications to the 2017 version simplified and broadened the definition of the highest suspicion category, LI-RADS 5 (LR-5 = definite hepatocellular carcinoma). While this effectively increased the sensitivity of LR-5 for malignancy, a small retrospective review also found slightly improved accuracy of LI-RADS 2018 over 2017 [15]. In a lesion

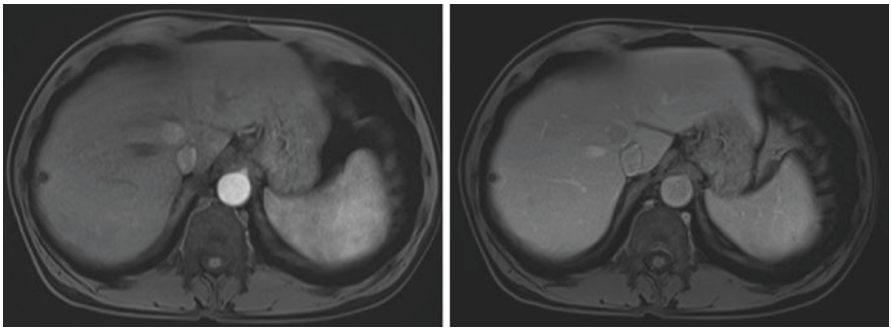

Fig. 6.1 Axial T1 fat-suppressed multi-phase contrast-enhanced MRI. There is a 1.5 cm lesion at the border of hepatic segment IV and the caudate lobe which exhibits relatively homogenous central arterial enhancement (*left*) and subsequent venous phase central washout with a peripheral pseudo-capsule (*right*). This meets both LI-RADS and OPTN 5 criteria, diagnostic of hepatocellular carcinoma. *(All case images in this chapter courtesy of William S. Rilling, MD, FSIR. Medical College of Wisconsin Department of Radiology)*

measuring greater than 2 cm, the presence of central ("non-rim") hyper-enhancement in the arterial phase combined with either subsequent venous phase "washout," a "pseudo-capsule" appearance, or significant interval growth is considered under both criteria to be diagnostic of hepatocellular carcinoma (Fig. 6.1). Together these findings have a reported sensitivity of 80%, while the specificity and positive predictive value approaches 100%. The ACR also assigns LR-5 designation to hepatic lesions measuring greater than 1 cm with characteristic enhancement and the presence of either washout or threshold growth. The OPTN criteria are nearly identical to LI-RADS. However, OPTN 5, the highest risk category, is stricter in its assessment of lesions less than 2 cm, requiring both enhancement and washout as well as either growth or a pseudo-capsule. It may be argued that certain patients are either over-staged with LI-RADS or under-staged with OPTN. The OPTN is approved for use in all transplant candidates and is the reporting standard at the authors' institution. Further large-scale studies will be required to fully reconcile LI-RADS and OPTN staging into a unified American diagnostic schema.

At American tertiary care centers, including the authors' institution, patients with a potential hepatocellular carcinoma diagnosis will be discussed at a multidisciplinary care board. These boards are comprised at a minimum of surgical oncology, transplant surgery, hepatologists, oncologists, and interventional radiologists. Depending on the degree of clinical and imaging suspicion, patients with indeterminant hepatic lesions may proceed to treatment, undergo additional cross-sectional imaging, or return to routine clinical surveillance. The AASLD recommends against routine biopsy of lesions highly suspected to represent hepatocellular carcinoma by validated imaging criteria, citing an undue risk for tumor seeding and hemorrhage. Targeted percutaneous biopsies of liver nodules may be falsely negative in up to 30% of cases [1]. However, a biopsy may be required in cases where the diagnosis remains uncertain. Although not currently standard practice, obtaining a tissue biopsy through established percutaneous access prior to performing ablation has been

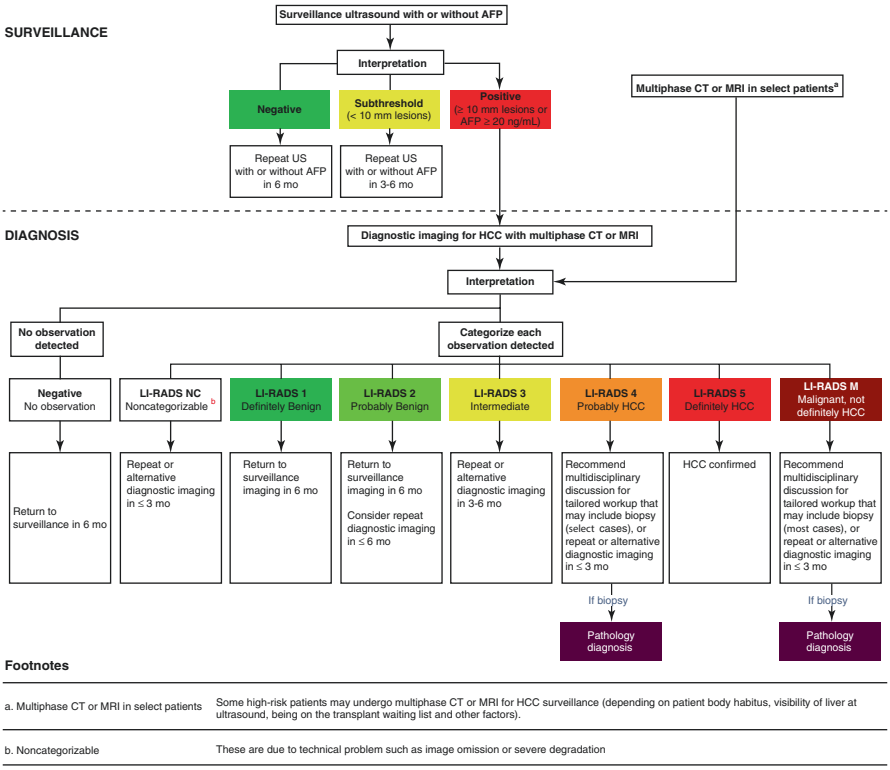

Fig. 6.2 AASLD Hepatocellular Carcinoma Diagnostic Algorithm. (Copyright of the American Association for the Study of Liver Disease and reproduced with permission from Marrero et al. [6]. Originally published by Wiley & Sons.)

proposed as a means for refining LI-RADS and OPTN imaging criteria by correlating each with histopathologic analysis. As new biomarkers are discovered that may inform therapeutic decisions, biopsy of HCC may become increasingly important.

Of note, indeterminant liver nodules measuring less than 1 cm on ultrasound pose a diagnostic dilemma as they often cannot be reliably differentiated even on advanced imaging. These patients may be closely monitored on an accelerated schedule [6] (Fig. 6.2).

Clinical Staging

There are many systems available for the staging of hepatocellular carcinoma. Several societies, including the AASLD, utilize a form of the Barcelona Clinic Liver Cancer (BCLC) criteria, the prognostic ability of which has been widely validated (Fig. 6.3) [6].

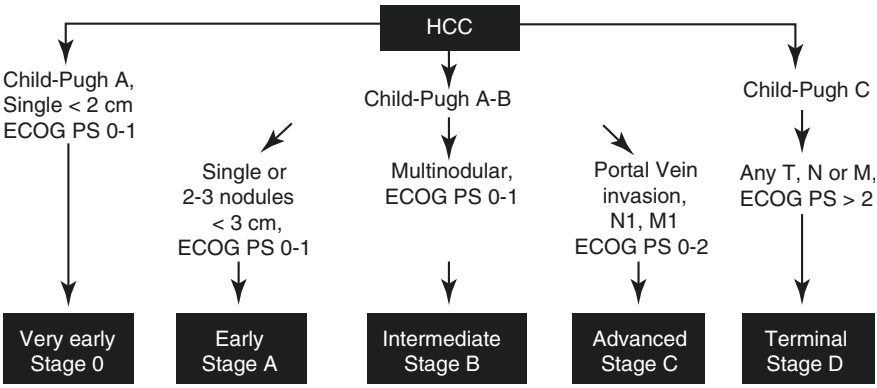

Fig. 6.3 BCLC hepatocellular carcinoma staging system. Abbreviations: N, nodal metastasis; M, extra-hepatic metastasis. (Copyright of the American Association for the Study of Liver Disease and reproduced with permission from Marrero et al. [6]. Originally published by Wiley & Sons.)

This contemporary staging method is a composite which takes into account the condition of the background liver using the Child-Pugh score (Table 6.1) and the overall functional capacity of the patient with the Eastern Cooperative Oncology Group (ECOG) score. These two clinical assessments predict survival in patients with liver disease and malignancy, respectively, and by extension their ability to tolerate cytotoxic therapies. Anatomic tumor characteristics are the third component of staging which have technical implications on treatment planning.

Treatment

The body of published literature regarding the treatment of hepatocellular spans continents and decades, across which there remains wide variation in both clinical practice and the quality of technical reporting. Inconsistency makes it difficult to equitably compare the safety and efficacy of available therapies. The problem is further compounded by the frequent introduction of investigational techniques, tools, and medications. As such, the majority of treatment guidance for hepatocellular carcinoma is not based on primary, high-level evidence.

While the AASLD provides recommendations adapted from the BCLC (Fig. 6.4), the treatment of patients with hepatocellular carcinoma in the United States is ultimately determined by a multitude of factors including clinical status, transplant candidacy, social support, local expertise, and resource availability. At large tertiary treatment centers, integrating this information and designing a therapeutic strategy is also the purview of the multidisciplinary treatment board. Typical treatment considerations at the authors' institution are outlined in Fig. 6.5.

Treatment strategies for hepatocellular carcinoma can be broadly split into two main categories: those with a curative intent and those with a palliative intent.

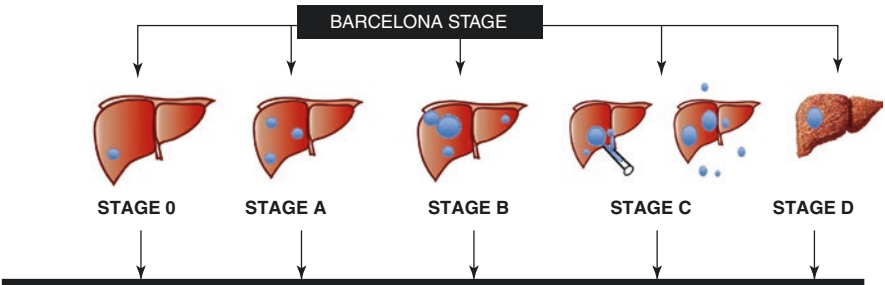

Level of Evidence					
1	Resection		TACE	Sorafenib (1L) Lenvatinib (1L) Regorafenib (2L) Cabozantinib (2L)	
2	RFA MWA	Resection OLT RFA MWA TARE TACE SBRT	TARE Downsize OLT	Nivolumab (2L)	OLT BSC
3				TARE	

Fig. 6.4 AASLD recommended treatments by BCLC Stage. Abbreviations: MWA microwave ablation, BSC best supportive care, 1L first-line therapy, 2L second-line therapy. (Copyright of the American Association for the Study of Liver Disease and reproduced with permission from Marrero et al. [6]. Originally published by Wiley & Sons.)

Curative-intent therapies aim to eradicate all malignant cells. Liver transplantation, percutaneous ablation, and surgical resection are commonly considered curative. Unfortunately, fewer than 30% of patients with hepatocellular carcinoma will ultimately qualify for a curative-intent therapy [16].

Palliative therapies are directed at prolonging survival and minimizing symptoms in more advanced stages of disease. Transarterial chemoembolization (TACE), transarterial radioembolization (TARE), systemic therapy, and external beam radiation (SBRT) are conventionally considered palliative.

The natural history of cirrhosis is a progression between a compensated, or largely asymptomatic, and a decompensated state. Decompensated cirrhosis is characterized by successive degrees of portal hypertension and failure of the liver's intrinsic synthetic and metabolic functions. The reported median survival is approximately 12 years for patient with compensated cirrhosis but only 2 years following decompensation [17]. As the vast majority of hepatocellular carcinoma occurs in the setting of cirrhosis, treatments other than liver transplantation must balance the predicted benefit of tumor response against the potential harm to the background liver in order to minimize the risk of iatrogenic decompensation.

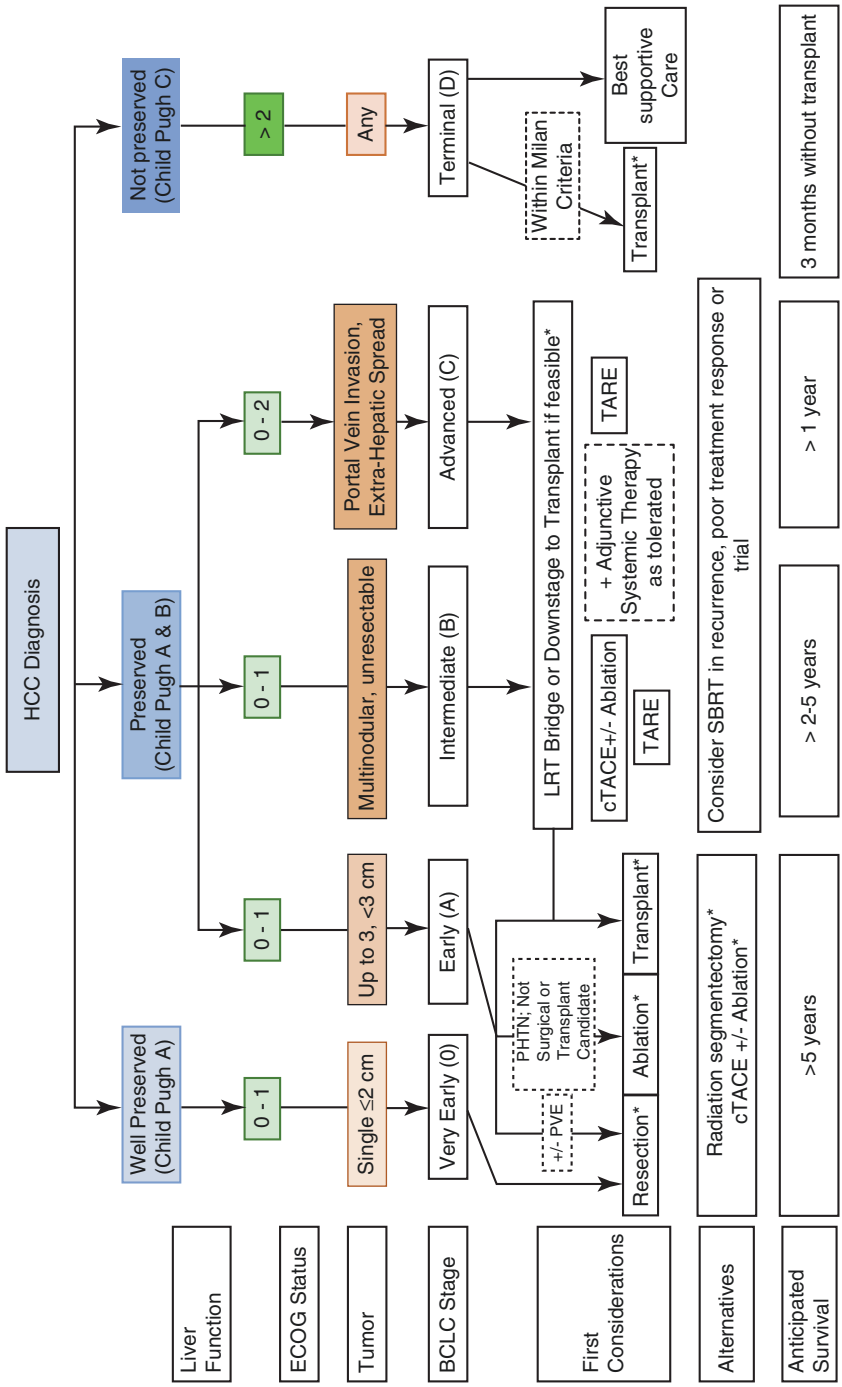

Fig. 6.5 Medical College of Wisconsin Current Treatment Algorithm. (*) designates curative intent. Abbreviations: PVE, portal vein embolization; PHTN, portal hypertension; LRT, locoregional therapy; cTACE, conventional transarterial chemoembolization; TARE, transarterial radioembolization

BCLC Stage 0 (Very Early) and Stage A (Early)

BCLC 0 or very early-stage hepatocellular carcinoma is defined as a single lesion measuring less than 2 cm in a patient with well-preserved liver function (Child-Pugh A). BCLC A or early-stage patients may have a single lesion of any size or up to 3 lesions all less than 3 cm in diameter. BCLC A have well or reasonably preserved liver function (Child-Pugh A or B) and good functional status (ECOG 0–1).

One study of American patients with BCLC 0-A hepatocellular carcinoma reported the median survival be approximately 14 months when left untreated [18].

Given the relatively small anatomic disease burden, it is often possible to ablate or resect lesion(s) while leaving an adequate volume of functional liver undisturbed. Resection and transplantation have reported 5-year survival rates as high as 60–80% for appropriately selected patients. Percutaneous radiofrequency ablation (RFA) has also demonstrated similar survival outcomes for patients with lesions 3 cm or less in diameter [19]. BCLC 0-A patients may safely undergo more than one resection or ablation in their lifetime if necessary.

Liver Transplantation

Orthotopic transplantation is the gold-standard curative therapy for hepatocellular carcinoma, as it addresses both the malignancy and underlying liver disease.

The Milan criteria have been developed to ensure the best possible outcomes following liver transplant. Patients within Milan criteria have a solitary lesion measuring no more 5 cm or up to 3 lesions all under 3 cm, no extra-hepatic disease, and no evidence of malignant hepatic vascular invasion. This essentially encompasses all BCLC 0-A patients with some larger solitary lesions technically meeting BCLC B. For patients within Milan criteria, transplantation has a commonly reported 5-year survival rate exceeding 70% and a 1-year morbidity and mortality of approximately 10%. There is a low reported risk (approximately 10–15%) of hepatocellular carcinoma recurrence following liver transplant [1, 3, 19].

In general, liver transplant is the preferred treatment for early-stage patients with decompensating cirrhosis, significant portal hypertension, or other complicating factors which make primary curative resection or ablation unfeasible.

Deceased whole-organ donation accounts for the vast majority of transplanted livers in America [20]. Unfortunately, the need for donor organs has always outpaced availability. Together, the Organ Procurement and Transplant Network (OPTN) and United Network for Organ Sharing (UNOS) share the onerous responsibility of regulating organ transplantation in the United States. The rules governing liver transplantation are complex, a matter of intense scientific and medicolegal scrutiny and thus continually subject to change. Current guidelines and updates are made available by the OPTN freely on their website.

As a brief review, patients are listed as candidates for transplant when determined appropriate by the specialty board at a local transplant center. A successful

donor-recipient match depends on tissue antigens as well as prognostic and geographic factors. For several decades, American adult liver transplant candidates have been ranked based on the Model for End-Stage Liver Disease (MELD), a predictor of short-term (3-month) mortality without transplant. A candidate's MELD score is recalculated at regular intervals. A higher MELD score indicates degrees of cirrhotic decompensation and for most patients reflects the urgency of transplantation. Candidates with certain conditions, including hepatocellular carcinoma, have also been eligible to receive MELD exception points to account for their additional disease-specific mortality risk. Introduced in 2013, the "Share 35" rule states that patients with a MELD score exceeding 35 are to be considered a shared priority of all transplant centers within a defined geographic territory. This widens the field of potential donors from a local to a regional territory for high-risk patients, including those with MELD scores inflated by exception points. Initially, this resulted in a national shift toward preferential transplantation of patients with hepatocellular carcinoma. OPTN/UNOS policies have been repeatedly revised in an effort to rebalance organ allocation among patients with all manner of liver disease. As of 2019, a national review board has replaced regional oversight in order to standardize the distribution of MELD exception points. The previously established regional transplant territories, which had been criticized as arbitrary, have been replaced with firmer rules to prioritize potential donor-recipient matches based on the objective distance between their respective transplant centers.

As of 2017, there is a 6-month mandatory wait time from hepatocellular carcinoma diagnosis to transplant listing. This allows the transplant team to monitor how biologically aggressive the tumor behaves, which can influence transplant outcomes, particularly the risk of post-transplant recurrence. Once listed, the average wait for transplant is variable at transplant centers throughout the United States, typically ranging from 6 to 18 months.

Surgical Resection

Surgical resection is the recommended curative treatment for anatomically appropriate hepatocellular carcinoma in patients without underlying cirrhosis. Unfortunately, this accounts for less than 10% of American cases [6].

Resection is still considered a first-line therapy by the AASLD for patients who are effectively within Milan criteria but have well-compensated cirrhosis and no urgent need for transplant. The AASLD acknowledges that the definition of "resectable" hepatic malignancy has not been uniformly reported. Regional variations in practice and resources have historically ushered even high-risk patients to surgery with variable results. Currently, macroscopic portal vein invasion is generally a contraindication to primary resection in the United States regardless of the overall tumor burden [1]. Patients with portal hypertension are likewise often not surgical candidates. A meta-analysis performed by Berzigotti et al. found that the presence of clinically evident portal hypertension in those undergoing primary resection

effectively doubled the risk of mortality at 3 and 5 years and tripled the risk of post-operative cirrhotic decompensation [21].

Portal Vein Embolization

The decision to pursue resection remains largely subject to local expertise. The Milan criteria encompass a large spectrum of tumor distribution, and resection may not be feasible for lesions of a certain size or location. Local wedge resection, segmentectomy or lobectomy may all be considered, though at the expense of a diminishing liver remnant. The risk of post-hepatectomy liver failure and other complications are inversely related to the predicted volume and function of the future liver remnant. If an extensive resection is anticipated, an interventional radiologist may perform a preoperative embolization of a portal vein (PVE) to redirect portal blood flow away from the diseased segments prior to removal. The unique hemodynamic and regenerative abilities of the liver result in compensatory hypertrophy of the intended remnant while the tumor-bearing segment atrophies. Preoperative portal vein embolization is a well-established technique which reduces the risk of postoperative hepatic failure and can potentially make curative therapy available to patients who were otherwise ineligible [22].

Percutaneous Ablation

Tumor ablation is broadly defined as the attempt to destroy all cells in a specified lesion with the direct application of chemical or thermal therapies. Many patients with early hepatocellular carcinoma are considered poor surgical candidates by virtue of anatomic disease burden, liver function, or any number of comorbidities. Image-guided, percutaneous ablative techniques have emerged as viable option for this challenging patient population. On average, lower morbidity, recovery time, and hospital length of stay are recognized advantages of percutaneous interventions over surgery [23].

Radiofrequency Ablation

In the United States, percutaneous thermal ablation is favored over chemical ablation for the treatment of hepatocellular carcinoma. Radiofrequency ablation (RFA) is the most extensively studied thermal ablation technique in the liver [6]. RFA is performed by inserting probes into the target lesion, where a defined heat field is generated around the probe tip to induce coagulative necrosis in the target tissues.

As with resection, the success of a curative percutaneous ablation depends on ensuring complete tumor coverage along with an adequate margin. Including a circumferential 5–10 mm rim of healthy tissue in the treatment field is considered acceptable to address any local, occult microscopic spread which could potentially contribute to recurrence. Most available ablation probes create a thermal treatment field which nominally measures up to 5 cm in maximum diameter, though at the periphery of the field, the temperatures are less uniform and often sublethal. Hence, traditionally lesions 3 cm or less are candidates for ablation if anatomy is favorable. Lesions near the hepatic dome, the liver capsule, the heart, or in close association

with major vascular and biliary structures may not be amenable given the elevated risk of non-target damage. There are advanced techniques which can allow for ablation to be performed safely even in challenging anatomy (Fig. 6.11).

Ablation has the potential to address multiple solitary lesions while sparing more healthy parenchyma than resection. Multiple tumors may be treated in a single session, and it can be performed safely following a previous surgery or other locoregional therapies.

The AASLD currently recommends RFA for BCLC 0 and A patients who are not otherwise candidates for resection.

Unfortunately, the quality of primary evidence comparing resection to percutaneous ablation remains suboptimal, particularly in Western populations [3]. A recent retrospective review by Huang et al. evaluated over 800 American patients with hepatocellular carcinoma. No significant difference in overall survival was found between those patients with small lesions (≤2 cm) treated only with either RFA or resection [24]. Another retrospective analysis of the 2014 SEER database, which tracks cancer statistics in the United States, found similar overall and disease-specific survival in patients with a solitary lesion measuring 4 cm or less addressed with either surgical resection or thermal ablation [25].

The literature comparing RFA to resection in Asian populations is more extensive but often contradictory. Some authors have reported better outcomes following surgical resection, though in many cases the ablations were not necessarily performed percutaneously or by physicians trained in image-guided intervention. Nonetheless, several prospective randomized trials and a subsequent meta-analysis performed in Asia comparing surgical resection and percutaneous ablation techniques have found similar overall survival at 1 and 3 years. Data regarding survival are less conclusive at 5 years. Some authors have found higher rates of local recurrence following RFA, while others report no significant difference [23, 24, 26, 27].

Microwave Ablation

The tissues closest to a thermal ablation probe experience the highest temperatures, while the ability to transmit energy away from the probe is determined by the conductive properties of the surrounding parenchyma. During RFA, as the tissues immediately around the probe vaporize, the developing char can limit heat radiance and effectively shrink the anticipated lethal ablation zone.

Microwave ablation (MWA) is a newer technology which has largely supplanted RFA for the treatment of hepatocellular carcinoma at many American centers, including the authors' interventional radiology department (Fig. 6.6). Microwave probes can generally achieve higher temperatures more rapidly than radiofrequency probes. These probes are less affected by heat sink phenomena which limit RFA, and thermal conductance through the charred, desiccated tissue around the probe tip is not dampened to the same degree. No direct randomized trials have compared RFA and MWA in the treatment of hepatocellular carcinoma, though it is generally assumed that any established benefits of RFA extend to MWA. There are data to suggest MWA is safe and effective monotherapy in tumors even measuring up to 5 cm [28].

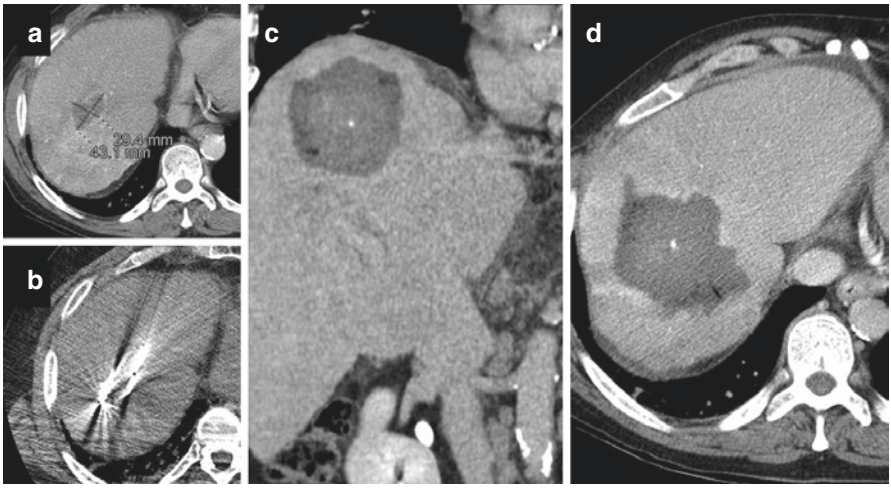

Fig. 6.6 Microwave ablation. (**a**) Enlarging solidary segment VIII hepatocellular carcinoma. (**b**) Microwave ablation using multiple overlapping probes. (**c, d**) Short-term interval follow-up CT demonstrates a wide margin of necrosis enveloping the treated lesion. There is a small calcification within the lesion and no residual enhancement

Cryoablation

Cryoablation is another thermal ablation technique which utilizes volatile gases to generate a zone of freezing temperatures around the probe tip (Figs. 6.10l and 6.11c). Alternating cycles of freezing and thawing result in the formation of ice crystals within cells and interstitial spaces which are ultimately lethal. Unlike RFA and MWA, the cryoablation zone can be monitored actively under CT or ultrasound guidance. This is a significant advantage, as the ablation zone size achieved with RFA and MWA is influenced by local tissue factors and not entirely predictable. Cryoablation may be better tolerated by patients, and there is data to suggest it is safer than other thermal ablation techniques when used near large vascular and biliary structures. Early comparative data has suggested similar efficacy of cryoablation to RFA in the treatment of hepatocellular carcinoma [29]. A retrospective, propensity-matched analysis of the SEER database from 2004–2013 found no significant difference in overall and liver cancer-related survival between patients with hepatocellular carcinoma treated with cryoablation or RFA [30]. While this data is promising, the SEER database lacks some information, including other therapies received by patients as well as certain components of BCLC staging, which would be useful for patient selection.

Recurrent Early Stage

Retrospective studies performed in Asia have suggested outcomes are largely similar when using TACE or RFA to address early recurrent disease in patients who have previously undergone resection. Overall reported 5-year survival rates for each strategy were approximately 25%. One study found RFA may be better specifically for BCLC 0. Interestingly, authors noted significantly improved

survival when treatment was crossed over, either from RFA to TACE or vice versa, rather than repeating the original therapy for patients with a second recurrence [31, 32].

BCLC Stage B (Intermediate) and Stage C (Advanced)

BCLC stage B includes patients who, similar to stage A, have reasonably preserved liver function and good functional status. However, their disease is considered intermediate due to a more substantial, multifocal tumor burden, with greater than three nodules with diameters exceeding 3 cm. These patients do not have evident hepatic vascular invasion by tumor nor extra-hepatic spread.

BCLC stage C are considered to have advanced disease. These patients can have any anatomic tumor burden which is accompanied by the presence of either portal vein invasion or extra-hepatic metastatic spread, both of which confer a worse prognosis and response to locoregional therapy. These patients have reasonably preserved liver (Child-Pugh A or B) but may have mildly compromised overall functioning (ECOG <2).

When untreated, the median survival of BCLC B disease in a cohort of American patients was approximately 9–10 months. In the untreated BCLC C patients, median survival was approximately 4 months [18].

Bridging and Downstaging

Given the worse prognosis, the AASLD currently recommends palliative therapy with conventional TACE for BCLC B patients and systemic therapy with sorafenib for BCLC C patients. However, at specialty transplant centers including the authors' institution, these patients are frequently considered for more aggressive treatment regimens. When feasible, these patients will be treated with the intention of maximizing transplant eligibility.

As patients await transplant, hepatocellular carcinoma may progress beyond Milan criteria. Employing locoregional therapies to delay the progression of early-stage disease and prevent a patient from losing transplant eligibility is known as "bridging" to transplant. From 2004 to 2014, the number of patients in the United States listed for transplant remained relatively stable. In this same study period, the number of patients who either died on the transplant list or "fell off" the list due disease progression rose by 30% [20]. While the AASLD recommends bridging qualified patients to transplant, no specific treatment strategy is recommended over any other.

In addition, American patients with BCLC intermediate and advanced-stage disease beyond Milan criteria may be treated with the intention of downstaging their disease. As studies have shown reasonable outcomes, the AASLD suggests patients be considered for transplant if successfully downstaged to Milan criteria with locoregional therapy [6].

If not otherwise suitable for transplant, a multimodality palliative intent approach to BCLC B and C patients is the standard consideration at the author's institution

(Fig. 6.10). Regardless of treatment intent, these patients frequently receive at least one locoregional treatment and a systemic agent as tolerated with the intention of optimizing symptoms and survival.

Locoregional Therapy

Embolization

Embolization refers to the delivery an occlusive agent (embolic) into a blood vessel via a catheter under image guidance. It is a fundamental Interventional Radiology procedure with a broad range of clinical applications. In the case of hepatocellular carcinoma, transarterial embolization takes advantage of the fact that mature tumors are supplied primarily by the hepatic arteries, while the hepatic parenchyma remains perfused chiefly by the portal venous system. Following embolization, the affected vascular bed and its dependent tissue become ischemic, which may be temporary or permanent depending on the material used.

When embolization is performed from a mainstem left or right hepatic artery, it is considered lobar or non-selective. Dispersing embolic, as well as any admixed pharmaceutical agents, throughout the hepatic lobe results in a lower proportion delivered to the target lesion(s) and exposes a larger portion of the background parenchyma to therapy. Alternatively, in contemporary practice, microcatheters can be used to select successively smaller hepatic arterial branches supplying a tumor, in order to embolize in a segmental or selective, sub-selective, or super-selective fashion. With greater selectivity, an escalating proportion of embolic is delivered to the tumor relative to the hepatic parenchyma. This is of particular importance in patients who cannot tolerate further degradation of hepatic function.

Transarterial Chemoembolization (TACE)

The goal of transarterial chemoembolization is to saturate the tumor with chemotherapy while arresting tumor perfusion. The tandem cytotoxic effects of chemotherapy and ischemia are thought synergistic in producing tumor necrosis. In conventional TACE (cTACE), the chemotherapy is combined with ethiodized oil: a viscous, radiopaque substance which allows for angiographic visualization as the drug-oil emulsion permeates the tumor vasculature (Fig. 6.7). Common chemotherapeutic agents include doxorubicin, cisplatin, and mitomycin [33]. This is typically followed by embolization with Gelfoam or polyvinyl alcohol (PVA) particles.

TACE was first performed in Japan in 1977. Catheter techniques and drug-embolic preparations varied, along with results, as the procedure was adopted across the world. Following the introduction of microcatheters, selective TACE became more widely adopted, and seminal randomized trials published in 2002, by Llovet et al. in the West and Lo in the East, first demonstrated a clear survival advantage over traditional conservative management [34–36].

Procedural technique plays a large role in treatment response. This was demonstrated elegantly in 2011 by Golfieri et al. who performed histopathologic analysis of liver explants from patients bridged to transplant exclusively with TACE. Lobar

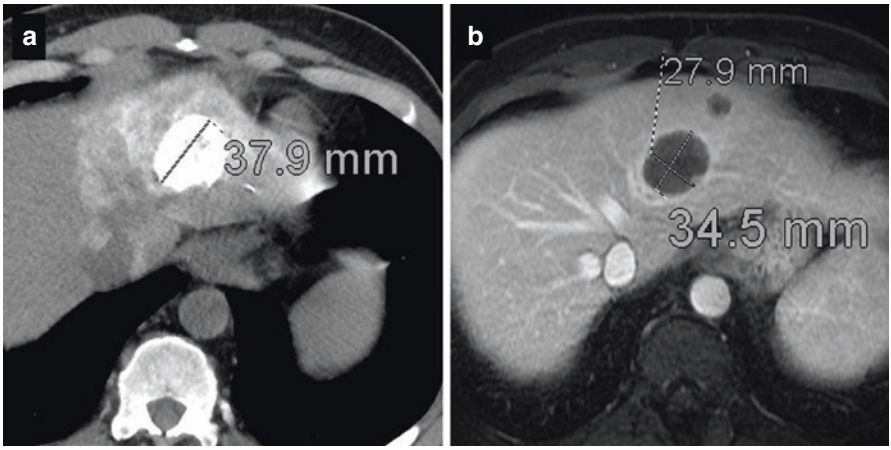

Fig. 6.7 Conventional TACE. (**a**) CT obtained 1-day post-cTACE demonstrates dense near-uniform saturation of ethiodized oil in the left lobe hepatocellular carcinoma. (**b**) Follow-up MRI demonstrates complete radiologic treatment response in the index lesion as well as in a small satellite nodule

TACE resulted in complete necrosis in approximately 30% of treated lesions, compared to 54% of lesions treated more selectively. Histologic necrosis was maximal in selectively treated lesions measuring 3–5 cm [37]. Kwan et al. also noted higher rates of histopathologic necrosis were achieved with selective as opposed to lobar TACE. Their analysis also found that the extent of necrosis correlated to the degree of complete, uniform deposition of drug-oil emulsion within the tumor following TACE [38]. Other authors have confirmed that dense saturation of tumor and the surrounding tissues with drug-oil emulsion is not only highly predictive of complete tumor necrosis but also resulted to improved 1 and 2 year survival (67% and 50%, respectively) compared to full saturation of only the lesion (49% and 29%) and only partial deposition in the lesion (29% and 15%) [39].

Underscoring the importance of these technical advances, in a large 2016 systematic review, Lencioni et al. noted that long-term survival rates tended to improve in trials published after 2002 which largely made use of selective TACE techniques [33]. Their review aggregated over 10,000 patients treated with conventional TACE over 30 years. Techniques and embolic preparation understandably varied. The authors found a median overall survival of 19.4 months. Overall survival rates were 70%, 52%, 40%, and 32% at 1, 2, 3, and 5 years, respectively. The most common adverse events were self-limited hepatic enzyme abnormalities and features of post-embolization syndrome, which may include fever, abdominal pain, and nausea. A total of 214 deaths were reported following 50,953 TACE procedures, for a mortality rate of 0.6%, which is considered generally safe. Though not all deaths were directly attributable to the procedure, the most common cause was hepatic insufficiency, which also illustrates the importance of selecting patients with appropriate tumor anatomy and adequate hepatic reserve [33].

A good response to TACE is generally considered to reflect favorable tumor biology, which confers a higher likelihood of successful bridging and/or downstaging to transplant [34]. A complete response to the first attempted chemoembolization is further predictive of a favorable long-term outcome. In an analysis of over 300 patients, Kim et al. found the overall survival of patients with a complete response to the initial TACE to be nearly double that of those who achieved complete response with multiple sessions and quadruple that of patients who achieved partial response at best [40].

Drug-Eluting Bead Transarterial Chemoembolization (DEB-TACE)

Drug-eluting beads are a class of bio-compatible, hydrogel microspheres which can be loaded with chemotherapeutic agents, commonly doxorubicin (Fig. 6.8). The proposed advantage of beads is that smaller calibrated particles penetrate deeper into the microvasculature of tumors. Trials have shown increased intra-tumoral retention of drug with a lower systemic dose using beads. This should bolster recognized advantages of selective TACE techniques by enhancing tumor drug delivery while minimizing parenchymal exposure [41]. Embolization of the microvasculature also tends to result in a lower frequency and severity of post-embolization syndrome. However, these technical benefits have failed to consistently translate to a meaningful survival advantage [36, 42, 43].

The PRECISION V trial published by Lammer et al. in 2009 was a large, international multicenter, single-blind, phase II randomized trial. The trial was performed in Europe, with patients having predominantly alcohol-related cirrhosis and hepatocellular carcinoma. Patients received doxorubicin via DEB-TACE or cTACE [41]. Patients were BCLC A-B. Those with advanced liver failure, or diffuse HCC

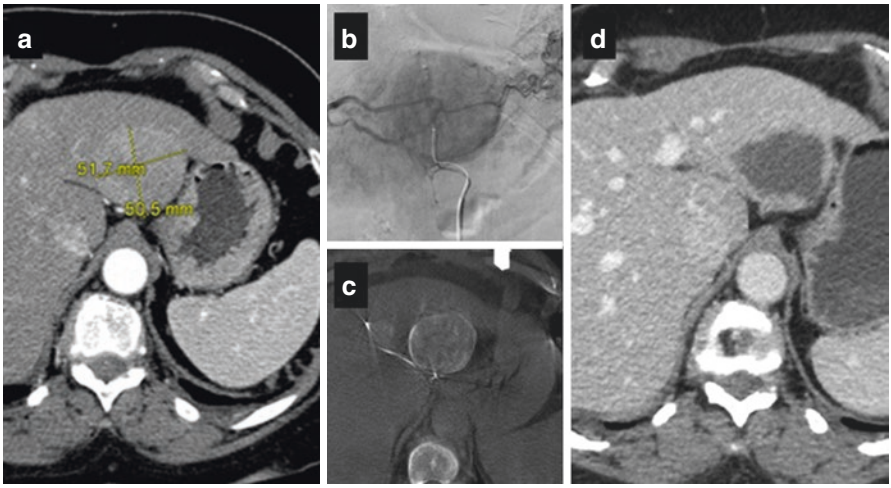

Fig. 6.8 HCV (treated) cirrhosis. BCLC B. Drug-eluting bead TACE. (**a**) Large left lobe hepatocellular carcinoma. (**b**) Digital subtraction angiography demonstrates left hepatic arterial supply to tumor. (**c**) Saturation of tumor with beads confirmed by intra-procedural cone beam CT. (**d**) Follow-up CT demonstrates extensive central necrosis compatible with complete treatment response. No residual viable tumor

>50% of the liver, among other standard criteria, were excluded. Patients in both groups received up to three treatments over 6 months. Endpoints were safety and tumor response. A trend toward improved overall response rates for DEB-TACE was noted but not statistically significant, due to a better response to cTACE than was predicted. The authors noted a higher delivered dose and lower rate of doxorubicin toxicity with DEB compared to cTACE. However, the principal toxicity difference was alopecia, which was temporary. Subgroup analysis suggested that overall tumor response rates were relatively improved following DEB-TACE for those patients with more severe background liver disease. However, this has not been confirmed in subsequent studies.

Transarterial Embolization (TAE)

Alternatively known as "bland" or hepatic arterial embolization, transarterial embolization of the liver is felt by some interventionalists to be comparable to TACE in the treatment of hepatocellular carcinoma. Proponents suggest that the dominant therapeutic mechanism underlying conventional TACE is the local ischemia.

In 2002, Camma et al. published a retrospective meta-analysis which included over 400 patients hepatocellular carcinoma patients treated over several decades. This found a significant reduction in mortality at 2 years in patients who underwent TACE compared to conservative management. However, their analysis found no statistically significant difference in overall survival between patients treated with TAE and TACE [44]. Unfortunately, there was significant variability in TACE technique noted among the included trials, from the chemotherapy and embolic agents to the vessel selectivity, and many studies lacked clinical data necessary to classify patients by tumor burden or Child-Pugh score. Subsequently, a systematic analysis by Llovet and Bruix followed in 2003 found significantly improved 2-year survival following TACE but not TAE [16].

Though conventional TACE has been found beneficial by most authors, there is data to suggest that TAE is of similar efficacy to DEB-TACE. In 2016, Brown et al. conducted a single-blinded, randomized controlled trial which was published in the Journal of Oncology [45]. Patients were largely BCLC A-B and were randomized to treatment with either DEB-TACE or bland TAE utilizing embolic beads of a similar size. The authors found no significant benefit in overall or progression-free survival using DEB-TACE over TAE. At approximately 20 months, the overall survival was similar to other DEB-TACE trials; however, the mean progression-free survival for this cohort DEB-TACE was relatively low at 2.8 months.

Transarterial Radioembolization (TARE)

Transarterial radioembolization with Yttrium-90 (^{90}Y) is a type of brachytherapy. Embolic microspheres are pre-loaded with ^{90}Y, a beta-emitter with a tissue penetration of roughly 2–11 mm. With a half-life just under 65 hours, the radiation dose of ^{90}Y is delivered in less than 2 weeks as it decays into inert zirconium [46]. The individual microspheres are small enough travel through the microvasculature of the tumor but will eventually accumulate and congest these small vessels when delivered in high volume. Patients must be evaluated in advance for evidence of arteriolovenous shunting through the tumor, and TARE is contraindicated if a

significant portion of the intended dose will instead migrate through the tumoral vasculature to the lungs or gastrointestinal tract.

TARE is considered second-line therapy by the AASLD though it has become a primary consideration at many American transplant centers. Early experience with TARE was with lobar administration for the treatment of diffuse and invasive tumors. When performed in appropriate patients, with adequate hepatic reserve and minimal shunting, TARE has a limited toxicity profile. Treatment efficacy and side effects are predominantly related to the effects of localized radiation necrosis. The ischemia related to microspheres is minimal, as are the incidence and severity of the classic post-embolic syndrome.

Tumor-associated portal vein thrombosis and infiltrative tumor subtypes have had historically poor response to TACE [47]. TARE is safe and likely to be more effective than TACE in BCLC C patients with macroscopic vascular invasion (Fig. 6.9c) [48, 49]. In a study of patients with BCLC intermediate and advanced-stage disease, Mazzeferro et al. observed a median overall survival of 13 months following a lobar TARE in the presence of portal vein thrombosis and 18 months in patients without [50].

Just as TACE has evolved from a lobar administration to a more selective therapy, so has TARE. Radiation lobectomy and radiation segmentectomy are emerging concepts with promising early results. A radiation segmentectomy refers to the administration of a lobar ^{90}Y dose (>190 Gy) concentrated into one or two hepatic segments. This is a potentially ablative radiation dose delivered to the index tumor as well as any potentially undetected microsatellite lesions which contribute to disease progression and recurrence (Fig. 6.9).

A study from 2013 demonstrated that increasing the radiation dose delivered to the index tumor may lead to superior outcomes [51]. This study included primarily BCLC B and C patients with inoperable hepatocellular carcinoma, who were also thought poor candidates for palliative chemoembolization due to tumor burden or progression on prior therapy. If deemed safe by pre-procedural imaging and clinical evaluation, a subset of patients received an intensified TARE dose compared to the standard. Patients with a tumor dose exceeding 205 Gy, as would be the goal of a radiation segmentectomy, experienced a median time to progression and median overall survival of 13 and 23.2 months, respectively. In this study, even patients with portal vein thrombus who received boosted-dose TARE had an impressive median time to progression and median overall survival of 10 and 21.5 months, compared to 4.5 and 10 months in patients with portal vein thrombus who received a conventional dose. Overall, there was a low rate (8%) of significant liver injury, which did not vary between the standard and intensified treatment groups.

A single-center, retrospective, propensity score-matched analysis of 178 patients with 235 lesions treated with either segmental TARE (target dose >200 Gy) or segmental TACE (conventional or DEB) was published by Padia et al. in 2017 [47]. Index and complete response rates were 92% and 84%, respectively, following segmental TARE, compared to 74% and 58% following segmental TACE. The cumulative incidence of index tumor progression at 1 and 2 years was 7.7% and 15% for TARE and 30% and 42% for TACE. The median progression-free survival was

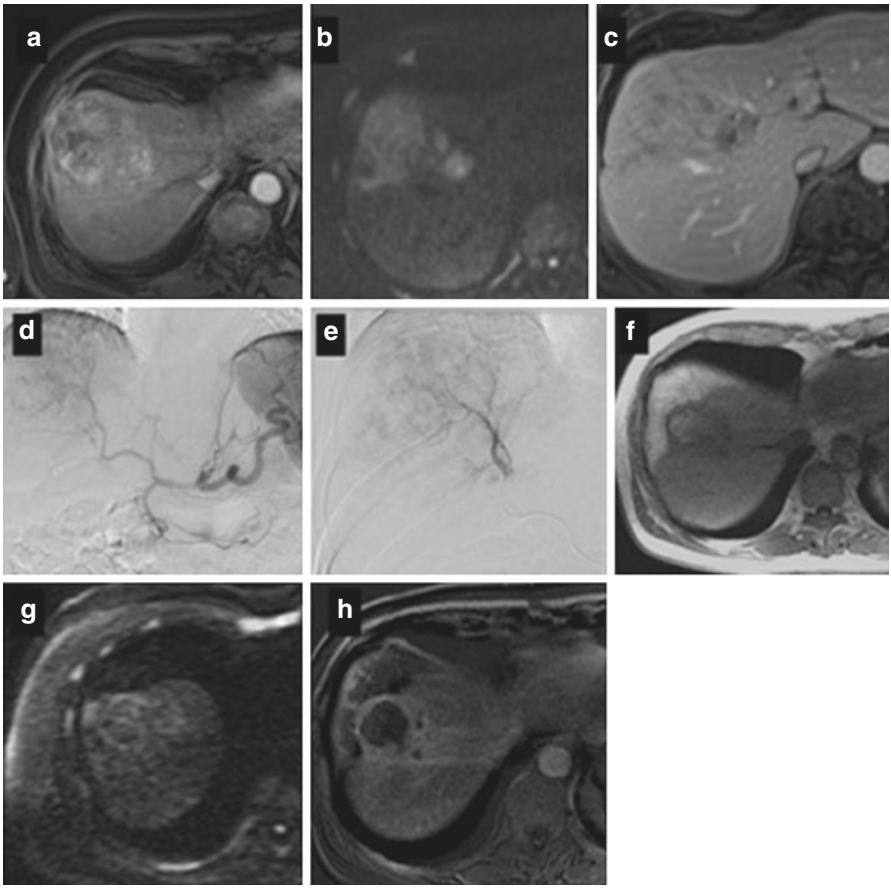

Fig. 6.9 HCV cirrhosis, BCLC C. Radiation segmentectomy. (**a**) Arterial phase fat-saturated T1 MRI demonstrates ~6.5 cm heterogeneously enhancing mass in segment VIII, with surrounding regional perfusional alteration due to associated thrombosis of the right hepatic portal veins. (**b**) Diffuse associated restricted diffusion. (**c**) Venous delay shows thrombus extending centrally into right hepatic portal vein. (**d**, **e**) Digital subtraction angiography shows selection of segment VIII and tumor blush. (**f**) 4 month MRI follow-up. Non-enhanced T1 shows a regressed, ~3 cm treated lesion with central T1 hyperintense signal reflecting hemorrhagic debris and/or coagulative necrosis. (**g**) No convincing diffusion restriction in the treatment field. (**h**) Well-demarcated roughly wedge-shaped region of tissue surrounding the treated lesion exhibits persistent late venous enhancement consistent with fibrotic change. This scarring has resulted in marked retraction of the parenchyma and capsule. No enhancement was appreciated on arterial phase to suggest residual viable tumor in the index lesion or portal veins (not shown), and no new lesions were seen. AFP dropped from >200 to 35 following treatment. Patient tolerated low-dose lenvatinib and became a candidate for transplant

18.5 months following TARE, which was superior to 9 months following TACE. A similar median overall survival of approximately 3 years was achieved in each group.

This was followed in 2018 by another retrospective, propensity score-matched study from Biederman et al. The authors also found radiation segmentectomy

outperformed selective TACE in the treatment of unresectable, solitary lesions measuring 3 cm or less in a cohort of patients who had not undergone prior locoregional therapy. The percentage of complete radiologic response (92% vs 52%) and time to a secondary therapy (812 vs 181 days) greatly favored radiation segmentectomy [52]. Subgroup analysis showed similar response rates to TARE in lesions both with and without vascular invasion. 93% of tumors treated with TARE required only one treatment, while 79% of TACE was successful in a single session. Patients treated with segmental TARE had a recurrence rate of 8% at 1 year, similar to that observed Padia et al., and comparable to resection and ablation. Grade 3 bilirubin and AST toxicities were observed at a low rate of 5.5% and 5.5%, respectively, following radiation segmentectomy. No patients developed severe hepatic failure. The improved tumor response did not translate to a significant difference in overall survival between the two groups, which each had a mean approximately 2.3 years, though it does suggest TARE may be a more ideal downstaging or bridging strategy.

A unique benefit of radiation lobectomy is that it results in delayed, compensatory hypertrophy of the untreated hepatic lobe. Studies have demonstrated enlargement of the untreated liver following radiation lobectomy to volumes similar to those achieved with portal vein embolization. However, this occurs at a much slower pace (up to 6–9 months) than that observed following PVE (several weeks). Hypertrophic effect was enhanced in patients who had portal venous thrombosis of the treated lobe, which could effectively be considered an auto-PVE. Disease progression within the intended liver remnant is a feared complication for patients awaiting surgery following a preoperative PVE. In this regard, TARE should provide better control of potential metastases originating from an index lesion, though in cirrhotic patients the risk of developing metachronous lesions in the untreated lobe may be of greater concern. Overall, radiation lobectomy is well tolerated, and patients are typically able to safely undergo a subsequent resection [53–55]. Radiation lobectomy is not a standard alternative to PVE for early-stage patients, though, in the proper circumstances, it may be used to control more advanced disease and help make otherwise ineligible patients candidates for curative-intent resection or ablation.

A 2016 systematic review and meta-analysis of Western trials compared outcomes following treatment of hepatocellular carcinoma with TARE or TACE [56]. The majority of included patients had early and intermediate-stage BCLC disease. This did not identify any statistically significant difference in overall survival or safety, though trends had favored TARE. Progression-free survival at 1 year following TARE was significantly improved, again highlighting a potential role for more efficient bridging and downstaging. Unfortunately, there was no mention of arterial selectivity employed with either TACE or TARE procedures in this analysis.

One review retrospectively analyzed a cohort of American patients who were bridged or downstaged to transplant between 2006 and 2013 using different therapies selected on the basis of clinical presentation and tumor characteristics. The rate of a complete radiologic response at initial follow-up was 33% for TARE, 25% for TACE, 22% for RFA, and 9% for SBRT. The observed complete pathologic response rate in the explanted liver following transplant was 75% for TARE, 60% for RFA,

41% for TACE, and 29% for SBRT. This evaluation did not remark on arterial selectivity for either TACE or TARE, though the majority of TACE was conventional. Disease-free survival and overall survival were 86% and 79%, respectively, in this cohort at 5 years. 5% of patients had been transplanted despite not yet meeting Milan criteria. There was an 11% rate of recurrence following transplant, nearly half of which manifested as extra-hepatic metastatic disease. The median time to transplant was at least 2 months shorter for patients who underwent SBRT than any other therapy. None of the patients who underwent TARE or RFA died during the course of the study, which had a median follow-up of 41 months after transplant [57] (Fig. 6.10).

Systemic Therapy

Systemic therapy is recommended first-line for BCLC C hepatocellular carcinoma. It is also recommended for BCLC B which is either not amenable or demonstrated refractory to locoregional therapy, and not eligible for a curative treatment approach. Given the growing number of options, at the authors' institution patients receiving locoregional therapy are routinely trialed on adjuvant systemic therapies.

First Line

The first systemic therapy to show efficacy and garner FDA approval for advanced hepatocellular carcinoma was sorafenib. It works by inhibiting serine-threonine kinase activity of RAF1 and BRAF. It also inhibits the receptor tyrosine kinase activity of VEGF receptor (1–3) and PDGFR β. The role of sorafenib in treatment of HCC was evaluated in two randomized phase III trials. In the landmark SHARP trial 602 treatment naïve patients with advanced HCC were randomized between sorafenib 400 mg BD and placebo [58]. In this study, sorafenib showed a significant improvement in overall survival compared to placebo: 10.7 versus 7.9 months. Similar survival benefit over placebo was also observed in the Asia Pacific trial.

Recently, another tyrosine kinase inhibitor, lenvatinib, was FDA approved for the treatment of advanced HCC. This drug targets VEGF receptor (1–3), FGF receptor (1–4), PDGFα receptor, RET, and KIT. It was found to be non-inferior to sorafenib in the phase III randomized REFLECT study [59]. In this study lenvatinib was found to have better progression-free survival (7.3 months versus 3.6 months) and better response rate (18.8 versus 6.5) compared to sorafenib. However, the duration of response was limited to 7.3 months in lenvatinib arm compared to 6.2 months observed in sorafenib arm. Lenvatinib also had modest overall survival benefit compared to sorafenib, 13.6 versus 12.3 months, which was not statistically significant. This study also met its predefined criteria of non-inferiority. Overall, the side effect profile of both sorafenib and lenvatinib were fairly similar in REFLECT. It is also important to note that both of these oral agents were tested in patients with preserved liver functions (Child-Pugh class A) and their effectiveness in patients presenting with higher risk Child-Pugh class B or C cirrhosis is questionable. The toxicity and safety profile of these drugs often limits their use in clinical practice.

Fig. 6.10 NASH cirrhosis, multifocal HCC with a large segment VI and a small segment II lesion. BCLC B. Multimodality downstaging and bridging. (**a**–**c**) Digital subtraction angiography of a 4.7 cm segment VI lesion, treated with cTACE via the cranial (red arrow) and caudal (blue) portions of the arterial supply. (**d**) Cessation of flow within the lesion following injections of chemotherapy oil emulsion and PVA. The segment II lesion is supplied by an accessory left hepatic artery which arises from the left gastric artery, which spasmed when selected with a microcatheter, and treatment was deferred until a later date. (**e**) Dense saturation of segment VI tumor and surrounding parenchyma on post-procedural CT. (**f**) An MRI 6 months later had demonstrated growth of residual tumor at the margin of the segment VI lesion, which is subsequently treated with microwave ablation. The segment II lesion was stable in size, but several new tiny indeterminant nodules were noted. Patient was trialed on systemic chemotherapy during this period, but it was poorly tolerated. Gradual clinical decline from Child-Pugh class A to B occurred in this period as well. (**g**, **h**) One-

Second Line

Patients who fail first-line treatment with lenvatinib or sorafenib can be re-challenged by second-generation tyrosine kinase inhibitors like regorafenib, c-Met inhibitors like cabozantinib, and checkpoint inhibitors like nivolumab, pembrolizumab, and atezolizumab. Regorafenib has anti-angiogenic properties and works by inhibition of VEGFr2-TIE2 tyrosine kinase. In the phase III, RESORCE trial, 573 patients with prior exposure to sorafenib were randomized between regorafenib and placebo [60]. This study demonstrated a significant overall survival benefit of regorafenib over placebo in second-line setting, 10.6 months versus 7.8 months. Common side effects associated with regorafenib were hypertension, hand-foot syndrome fatigue, diarrhea, and dysphonia.

Ramucirumab, another anti-angiogenic agent which targets the VEGFR 2, was recently granted FDA approval for treatment of advanced hepatocellular carcinoma in second-line setting. It was first evaluated against placebo in the REACH trial [61]. In this study, 565 patients with advanced disease and prior exposure to sorafenib were randomized. Patients were treated until disease progression or unacceptable toxicity was noted. Intent to treat analysis revealed a modest overall survival benefit of ramucirumab compared to placebo (9.2 versus 7.6 months) which was not statistically significant. However, in a prespecified subgroup analysis of patients with a baseline alpha-fetoprotein (AFP) level of greater than 400 ng/mL, ramucirumab was found to be superior to placebo (overall survival 7.8 versus 4.2 months). To further evaluate this finding, the phase III REACH 2 study was launched for advanced hepatocellular carcinoma patients with baseline AFP >400 ng/ml and progression following exposure to sorafenib [62]. This study showed a survival benefit of ramucirumab over placebo (8.5 months versus 7.3 months). Common adverse effects associated with ramucirumab include hyponatremia, diarrhea, hypertension, and headache.

Investigators are also evaluating agents that target c-Met pathway. Aberrations of c-Met are found in approximately 50% of patients with advanced hepatocellular carcinoma. Cabozantinib is a novel agent which targets c-Met along with RET, VEGFR 2, AXL 1, and TIE2. In the phase III CELESTIAL trial, 707 patients with advanced hepatocellular carcinoma and a history of prior exposure to at least one systemic therapy were randomized to cabozantinib or placebo [63]. CELESETIAL

month follow-up MRI shows complete treatment response in segment VI, AFP dropped from >1880 to ~220. Patient now within Milan criteria, but segment II lesion continues to grow slowly, along with other indeterminant nodules. Initiated and tolerated sorafenib. (**i**) Repeat segment II cTACE attempt. Celiac digital subtraction angiography demonstrates the accessory left hepatic artery arising from the left gastric. (**j**) Selection of the segment II artery via the left gastric artery approach again results in significant vasospasm. Minimal tumor blush is appreciated, but the segment III branch is well opacified. A more proximal left lobar TACE performed. (**k**) Two-month follow-up CT demonstrates continued slow growth of segment II lesion, now just under 3 cm, and several small indeterminant lesions persist. (**l**) Mild elevation in bilirubin precludes further cTACE, and cryoablation of segment II lesion is performed. Patient does well and is stable for 2 weeks following the cryoablation. Matched and received transplant roughly 13 months from initial diagnosis

trail was a unique trial because it tested cabozantinib in both the second- and third-line setting. In the intent to treat analysis, cabozantinib was found to have significant overall survival benefit (10.2 versus 8 months) compared to placebo. In a subgroup analysis, cabozantinib improved both overall and progression-free survival in the HBV-infected patient but did not improve overall survival in HCV-infected patients. Common side effects associated with cabozantinib include hand-foot skin reaction, hypertension, increased liver function tests, fatigue, and diarrhea.

Immunotherapy

Role of checkpoint inhibitors is now being investigated in patients with advanced hepatocellular carcinoma who progressed after treatment with sorafenib. Inhibition of the PD1/PDL1 axis activates an immune response to the tumor. In September 2017, nivolumab, a recombinant monoclonal immunoglobulin IgG4 antibody specific for PD1, was granted accelerated approval by the FDA for the treatment of hepatocellular carcinoma patients with prior exposure to sorafenib. This approval was granted based on encouraging results of the CheckMate 040 trial [64]. This was a phase 1/2, open-label, non-comparative, dose-escalation, and expansion trial of nivolumab in adults with histologically confirmed advanced hepatocellular carcinoma. 262 patients were found to be eligible for this trial (48 patients in the dose-escalation phase and 214 in the dose-expansion phase). An objective response rate of 20% was observed in patients treated with nivolumab in the dose-expansion phase, while an objective response rate of 15% was noted in patients treated in the dose-escalation phase. Duration of response was calculated to be 17 months. Most common grade 3 toxicities in the dose-escalation phase were increased aspartate aminotransferase (10%), increased alanine aminotransferase (3%), and increased lipase (3%).

The phase III randomized CheckMate 459 trial evaluated nivolumab vs sorafenib in first-line setting for unresectable, advanced hepatocellular carcinoma. This trial did not meet its primary endpoint of significantly improved overall survival with nivolumab (16.5 vs 14.6 months). The objective response rate was 15% for nivolumab and 7% for sorafenib [65].

Pembrolizumab, another anti-PD1 agent, has also received accelerated approval for treatment of patients with advanced hepatocellular carcinoma in the second-line setting based on results of KEYNOTE-224, a phase II non-randomized study [66]. 104 patients were evaluated in this trial; the objective response rate in pembrolizumab arm was 17%. Around 24% of 104 patients experienced grade 3 treatment-related adverse events. Common adverse events were increased AST in (7%) patients, increased ALT in (4%) patients, and fatigue in (4%) patients.

The results of KEYNOTE-240, a randomized, placebo-controlled, phase III confirmatory trial of pembrolizumab vs best supportive care in patients with previously treated advanced hepatocellular carcinoma, were recently presented at ASCO 2019 [67]. In this trial, 413 eligible patients underwent 2:1 randomization; 278 patients received pembrolizumab (200 mg every 3 weeks), and 135 received a placebo. Intention to treat analysis showed modest improvement in overall survival in the pembrolizumab arm compared to placebo, though this did not meet statistical significance. It also failed to show a significant improvement in progression-free

survival with pembrolizumab. Since this trial failed to show the superiority of pembrolizumab over placebo in both primary endpoints, the overall response rate, an anticipated secondary endpoint, was not evaluated formally.

Combination Therapy

The goal of any combined therapeutic strategy is to augment cytotoxicity and achieve a more durable response than the individual component therapies. The expected benefits of a multimodality approach must be weighed against a patient's capacity to tolerate potential cumulative side effects. An effective plan must also account for practical limitations in treatment delivery, including the additional time and resource costs.

TACE-Ablation

In clinical practice, ablation tends to fail at the peripheral margins of lesions measuring greater than 4 cm, while certain TACE preparations may have difficulty penetrating the most central portions of large tumor vasculature. Initially, treatment failure may not be radiologically evident, as microscopic disease can persist below imaging resolution even in cases considered a "complete response." In combination, TACE and ablation not only compensate for the deficiencies of the other therapy but appear to augment their effects (Fig. 6.11). The ischemia which results following TACE is thought to sensitize tumor cells to thermal energy as well as to

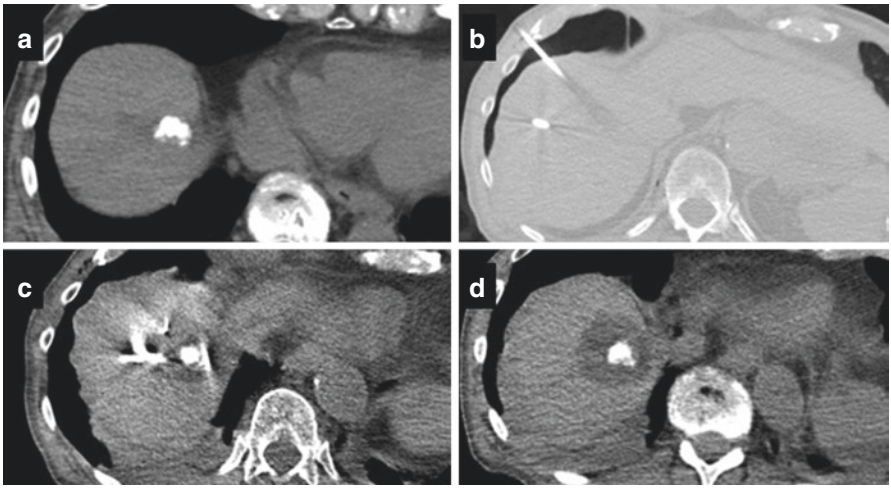

Fig. 6.11 Chronic HCV with solitary 2 cm hepatocellular carcinoma high in the medial liver dome. BCLC A. TACE-cryoablation. Anatomically challenging for resection and in close proximity to the diaphragm. (**a**) The lesion is saturated with ethiodized oil following prior TACE. (**b**) With patient under general anesthesia, a pneumothorax has been intentionally created to displace and protect the lung. (**c**) Cryoablation with multiple overlapping probes. (**d**) Hypodense ring of necrosis demarcates an adequate treatment margin

chemotherapy. Arresting blood flow around the tumor reduces local heat sink and allows for a larger lethal ablation zone [68]. At the authors' institution, conventional TACE is typically performed prior to ablation as the tumor uptake of ethiodized oil also aids in localization for CT guidance.

TACE-RFA

Randomized controlled trials and subsequent meta-analyses have demonstrated the superiority of TACE-RFA to either monotherapy in terms of overall survival, progression-free survival and recurrence [69, 70]. Peng et al. reported a 5-year survival rate of 62% following combination therapy in a cohort of patients which included target lesions measuring up to 7 cm [71].

Given the demonstrable advantage of TACE-RFA in more extensive disease, this combination has also been evaluated and appears to compare favorably to resection for early disease. A meta-analysis performed in Korea evaluated patients with hepatocellular carcinoma within Milan criteria treated with either TACE-RFA or resection. The authors found no significant difference in overall survival at 1, 3, and 5 years nor recurrence-free survival at 5 years [72]. Another retrospective review of patients treated at a Japanese center was notable for its explicit combination of super-selective TACE with RFA. This trial included BCLC 0 patients. In the propensity-matched analysis, the 5-year survival rate following TACE-RFA was an impressive 70% which did not differ significantly from resection [73].

TACE-MWA

The use of TACE-MWA has recently grown in popularity, and early evidence suggests it is similar if not more effective than TACE-RFA. Research continues to define the optimal combination treatment protocol.

One trial randomized a small cohort of patients with solitary, unresectable lesions larger than 4 cm to treatment with cTACE monotherapy, TACE-RFA, and TACE-MWA. The authors found combination therapy was superior to TACE monotherapy for all lesions treated. TACE-MWA was the most efficacious in terms of short-term tumor response (80% complete response rate) with a safety profile similar to TACE-RFA [68].

A 2018 retrospective review by Zhang et al. compared BCLC B patients with fewer than five lesions measuring up to 7 cm treated with either MWA-TACE or cTACE alone. MWA-TACE had 1-, 3-, and 5-year survival rates of 93%, 79%, and 68%, respectively, with a median overall survival of nearly 19 months [74]. Survival rates were significantly improved over cTACE monotherapy, which in this cohort were similar to those described by the large systematic review of TACE conducted by Lencioni et al. [33].

Most recently, Fang et al. retrospectively evaluated a small cohort of patients undergoing cTACE or DEB-TACE prior to MWA. The 1-year survival rate and median overall survival of combination therapy were similar to those found by Zhang et al. [75]. Treated lesions were approximately 3 cm in size. Data trends favored cTACE over DEB-TACE prior to MWA in terms of achieved ablation zone size (67.2 cm^3 ± 51.3 vs 43.5 cm^3 ± 26.9) and overall survival (25 vs 19 months).

However, all differences failed to reach statistical significance. The trend toward a larger ablation zone following cTACE in this group is noteworthy, as it suggests the macrovascular embolization with oil emulsion and particles may be more effective than microscopic beads in either reducing local heat sink, sensitizing tissues to hyperthermia, or both.

Stereotactic Body Radiation Therapy (SBRT)

At the authors' institution, SBRT is typically considered as salvage for patient with hepatocellular carcinoma progressing on conventional therapy or else as part of a clinical trial. High-quality data with long-term clinical outcomes regarding the use of SBRT for hepatocellular carcinoma is limited, particularly in Western populations. Its use as an adjunct modality for patients bridged to transplant is likely to overestimate its individual survival benefit in many of the published small, single-center series.

In the absence of long-term outcomes, much that is written regarding SBRT as a primary therapy emphasizes the response of a single treated lesion as a primary endpoint [76]. This is not an adequate metric in cirrhotic patients, where overall liver function and the development of metachronous lesions outside the treatment field both have an recognized impact on survival and are accounted for in the evaluation of other conventional therapies.

In one study of long-term outcomes following SBRT, Kwon et al. reported a median progression-free interval of 15.4 months and an overall survival of 93% and 59% at 1 and 3 years, respectively [77]. However, two out of every three patients treated with SBRT had experienced local recurrence and had subsequently undergone transplant or received a different locoregional therapy as salvage during the 3-year follow-up period. Nearly 30% of reported tumor recurrence had been in the SBRT treatment field. One patient had died of radiation induced hepatic failure, despite the study population being 90% comprised of patients with Child-Pugh class A cirrhosis and the remainder class B.

Significant hepatotoxicity is of concern when considering SBRT as a primary treatment, given the amount of parenchyma which must be included in the treatment field by design. In one American series, one out of five patients progressed to the next Child-Pugh class following SBRT as a primary therapy [78]. Two sequential trials published in the Journal of Clinical Oncology evaluated American patients who underwent SBRT for intermediate and advanced-stage hepatocellular carcinoma. All patients had Child-Pugh class A cirrhosis. Despite this, 30% had radiation induced liver injury, and as many as seven patients death may have been attributable to therapy [79].

In a cohort of Asian patients treated with SBRT, the incidence of radiation induced liver injury was just under 25%. The authors of this study found that at a Child-Pugh score of only 6, the risk of radiation-induced liver injury rose considerably, and at 8 points the ability to recover following injury significantly declined [80].

Rajyaguru et al. used the National Cancer Database to retrospectively evaluate nearly 4000 American patients with hepatocellular carcinoma. This included patients with TNM stage I or II disease who were treated with either RFA or SBRT as a primary therapy. Patients managed with surgery, alternate locoregional therapy, or any form of chemotherapy were excluded. In a propensity score-weighted and matched analysis, the 5-year overall survival for patients treated primarily with RFA was approximately 30%, significantly greater than 19% for those treated with SBRT. The survival advantage of RFA over SBRT at 1, 3, and 5 years was consistent across all subgroup analysis even when accounting for the severity of liver disease. Overall, the absolute potential survival benefit conferred by primary treatment with RFA over SBRT was calculated to be approximately 10 months [76]. A limitation of this study which likely accounts for the relatively low reported survival rates is the use of TMN staging, which is unconventional in hepatocellular carcinoma literature. TMN Stages I and II are a heterogeneous population who may potentially be BCLC A, B, or C. The authors were unable to reliably differentiate these patient populations, and the indication for selecting either treatment is unclear.

As of 2019, the first prospective randomized trial comparing SBRT and RFA for solitary lesions measuring less than 5 cm is underway.

Future Directions

Curative-Intent Radiation Segmentectomy

Already an effective bridging or downstaging therapy in appropriately selected patients, radiation segmentectomy has the potential to become a standard, minimally invasive curative-intent treatment for early hepatocellular carcinoma.

In an analysis of long-term outcomes at their high-volume TARE center, Lewandowski et al. found that radiation segmentectomy provided response rates, disease control, and survival comparable to resection and ablation in BCLC stage 0-A patients. 90% of treated lesions showed positive radiologic response, of which nearly 60% were a complete response. Median time to disease progression was a full 2.4 years. 72% of patients had no target lesion progression at 5 years. Remarkably, the median overall survival was a 6.7 years. 1-, 3-, and 5-year survival probabilities for the cohort were 98%, 68%, and 57%, respectively. By the time of publication, one patient had complete response at 9 years follow-up and was considered cured [19]. Another retrospective review was conducted by Gabr et al. at the same institution. This included BCLC 0 and A patients with solitary lesions measuring 3 cm or less. Radiation segmentectomy had been performed in instances where curative RFA had been considered but was ultimately deferred. Patients had not received prior locoregional therapy and did not undergo subsequent cross-over therapy. Overall survival rates at 3 and 5 years were 83% and 75%, respectively, following radiation segmentectomy while 60% and 45% after RFA. The median overall survival was just over 4 years following RFA, but had not been reached for the group who underwent radiation segmentectomy during 8 years of follow-up [81].

Biederman et al. also retrospectively reviewed patients treated at their institution, largely BCLC A, with solitary lesions measuring less than 3 cm and no prior locoregional therapy. Patients underwent TACE-MWA or radiation segmentectomy. Similar rates of complete radiologic response (approx. 82%) were seen following both treatment approaches. There were more overall instances of target lesion progression in the ablation group. No significant difference in overall survival was found during follow-up, though the study was not powered to detect a difference. Mean survival following radiation segmentectomy was 31 months [82].

Intra-Procedural Blood Flow Modulation

Balloon occlusion catheters have several recognized endovascular applications outside of the liver. Inflation of a balloon on a microcatheter tip can be used prevent reflux of embolic materials during a forceful injection or may be placed to protect vascular beds distal to the target. When applied appropriately, altered pressure gradients can redirect and encourage flow toward the intended target lesion. This can result in denser deposition of therapeutic agent within the tumor and adjacent microvasculature and potentially enhance the response to a selective TACE or TARE [83, 84].

Investigational Systemic Therapies

In light of the recent FDA approval of several systemic agents, there is a renewed interest in trialing many in an adjuvant capacity. Locoregional therapies may enhance activation of the immune system activation and potentiate the effect of new immuno-modulating agents in particular.

Multiple current studies are exploring the viability of combining TACE with systemic therapy in intermediate stage hepatocellular carcinoma. Most studies evaluating role of combining TACE and tyrosine kinase inhibitors in this setting have been negative. However, encouraging preliminary results of TACTICS trial were recently presented at ASCO GI [86]. This was a multicenter randomized trial which compared TACE plus sorafenib with TACE alone in 156 patients with unresectable HCC. Patients with Child-Pugh class A cirrhosis, a maximum of two previous TACE treatment sessions, and ≤10 lesions with none exceeding 10 cm in size were included in this study. Those with extra-hepatic spread and vascular invasion were excluded. The primary endpoint of progression-free survival was better in the combination therapy arm and was statistically significant at 25.2 months vs 13.5 months (HR 0.59; $P = 0.006$). Overall survival results are pending. The EMERALD 1trial compares TACE in combination with either the checkpoint inhibitor durvalumab as monotherapy or durvalumab plus bevacizumab in patients with localized hepatocellular carcinoma. Another trial known as LEAP 12 is evaluating the safety and efficacy of lenvatinib with pembrolizumab in combination with TACE against TACE monotherapy as palliation in participants with non-metastatic hepatocellular carcinoma.

To date, no systemic therapy has shown a significant long-term benefit in the adjuvant setting following curative-intent treatment, and currently guidelines do not recommend it. The phase III STORM trial, which evaluated sorafenib versus placebo as adjuvant therapy after curative resection or ablation, for example, was negative [85, 87]. Studies have however shown that adjuvant TACE following resection may improve time to recurrence and survival in high-risk patients, such as those

with vascular invasion [72]. Taking these findings into consideration, investigators are now evaluating multiple combination therapies, including TACE with immunotherapy in the adjuvant setting. The combination of atezolizumab and bevacizumab, for example, is being evaluated in the adjuvant setting in IMBRAVE 50 trial. Additionally, the combination of durvalumab with bevacizumab is being evaluated as adjuvant therapy in EMERALD 2. Combination therapy options with different mechanism of actions offers a possibility of a synergistic response and additional advantage of mitigating immune escape mechanisms.

Ablative or Alcohol Chemoembolization (ACE)

ACE is a recently described hybrid treatment which utilizes an emulsion of ethiodized oil and absolute alcohol. A prospective phase I trial of BCLC A-B patients in China found ACE to be highly effective, with median progression-free survival of over 2 years. A higher percentage of patients demonstrated complete imaging tumor response following ACE compared to TACE (100% vs 43%), and more were ultimately bridged to hepatectomy. Median tumor size was approximately 4 cm, but rather impressively, nearly half of the lesions were quite large, measuring 5 to 10 cm. No adverse events were reported in the ACE group. There was less than a 5% rate of intra-tumoral recurrence following ACE by the end of trial follow-up, and only 1 in 4 had any viable tumor demonstrated on pathologic analysis following resection. cTACE had a 74% rate of intra-tumor progression by the end of follow-up, and all had some component of viable tumor in resected samples [88]. Further studies are needed to confirm these results and establish whether they are generalizable to Western populations.

Key Learning Points

1. The incidence of hepatocellular carcinoma in the United States continues to rise, with a substantial proportion of new diagnoses related to metabolic disorders.
2. Long-term outcomes for early hepatocellular carcinoma following curative-intent percutaneous ablation (with or without TACE) and surgical resection are similar. Curative-intent radiation segmentectomy is a promising emerging alternative for appropriate candidates.
3. There is no current standard of care for advanced hepatocellular carcinoma in the United States or the world at large. Several therapeutic strategies have been developed and continue to be refined. Variations of TACE and TARE are commonly utilized. With the approval of several new systemic agents, there is a renewed interest in combining locoregional and systemic therapies to augment tumor response.
4. A multidisciplinary care model for advanced hepatocellular carcinoma is common at American tertiary care centers. When feasible, efforts are directed toward adequate bridging or downstaging with the intent of the patient obtaining a curative liver transplant. The same systemic agents and procedures may also be employed as palliative therapy for those patients who ultimately remain ineligible for transplant.

The ACR LI-RADS criteria are updated and freely available for review at: https://www.acr.org/Clinical-Resources/Reporting-and-Data-Systems/LI-RADS/CT-MRI-LI-RADS-v2018

References

1. Forner A, Reig M, Bruix J. Hepatocellular carcinoma. Lancet. 2018;391:1301–14.
2. Galle PR, Forner A, Llovet JM, Mazzaferro V, Piscaglia F, Raoul J-L, Schirmacher P, Vilgrain V. EASL clinical practice guidelines: management of hepatocellular carcinoma. J Hepatol. 2018;69:182–236.
3. Heimbach JK, Kulik LM, Finn RS, Sirlin CB, Abecassis MM, Roberts LR, Zhu AX, Murad MH, Marrero JA. AASLD guidelines for the treatment of hepatocellular carcinoma: Heimbach et al. Hepatology. 2018;67:358–80.
4. Tang A, Hallouch O, Chernyak V, Kamaya A, Sirlin CB. Epidemiology of hepatocellular carcinoma: target population for surveillance and diagnosis. Abdom Radiol. 2018;43:13–25.
5. Jindal A, Thadi A, Shailubhai K. Hepatocellular carcinoma: etiology and current and future drugs. J Clin Exp Hepatol. 2019;9:221–32.
6. Marrero JA, Kulik LM, Sirlin CB, Zhu AX, Finn RS, Abecassis MM, Roberts LR, Heimbach JK. Diagnosis, staging, and management of hepatocellular carcinoma: 2018 practice guidance by the American Association for the Study of Liver Diseases. Hepatology. 2018;68:723–50.
7. Welzel TM, Graubard BI, Quraishi S, Zeuzem S, Davila JA, El-Serag HB, McGlynn KA. Population-attributable fractions of risk factors for hepatocellular carcinoma in the United States. Am J Gastroenterol. 2013;108:1314–21.
8. Chalasani N, Younossi Z, Lavine JE, Charlton M, Cusi K, Rinella M, Harrison SA, Brunt EM, Sanyal AJ. The diagnosis and management of nonalcoholic fatty liver disease: practice guidance from the American Association for the Study of Liver Diseases: Hepatology, Vol. XX, No. X, 2017. Hepatology. 2018;67:328–57.
9. Kim D, Kim WR, Kim HJ, Therneau TM. Association between noninvasive fibrosis markers and mortality among adults with nonalcoholic fatty liver disease in the United States. Hepatology. 2013;57:1357–65.
10. Perumpail BJ, Khan MA, Yoo ER, Cholankeril G, Kim D, Ahmed A. Clinical epidemiology and disease burden of nonalcoholic fatty liver disease. World J Gastroenterol. 2017;23:8263–76.
11. Dolganiuc A. Alcohol and viral hepatitis: role of lipid rafts. Alcohol Res Curr Rev. 2015;37:299–309.
12. Alferink L, Kiefte-de Jong J, Darwish Murad S. Potential mechanisms underlying the role of coffee in liver health. Semin Liver Dis. 2018;38:193–214.
13. Thorgeirsson SS, Grisham JW. Molecular pathogenesis of human hepatocellular carcinoma. Nat Genet. 2002;31:339–46.
14. Pinyol R, Montal R, Bassaganyas L, et al. Molecular predictors of prevention of recurrence in HCC with sorafenib as adjuvant treatment and prognostic factors in the phase 3 STORM trial. Gut. 2019;68:1065–75.
15. Ren A-H, Zhao P-F, Yang D-W, Du J-B, Wang Z-C, Yang Z-H. Diagnostic performance of MR for hepatocellular carcinoma based on LI-RADS v2018, compared with v2017: LI-RADS v2018 of MRI for diagnosing HCC. J Magn Reson Imaging. 2019;50:746–55.
16. Llovet J, Bruix J. Systematic review of randomized trials for unresectable hepatocellular carcinoma: chemoembolization improves survival. Hepatology. 2003;37:429–42.
17. Zipprich A, Garcia-Tsao G, Rogowski S, Fleig WE, Seufferlein T, Dollinger MM. Prognostic indicators of survival in patients with compensated and decompensated cirrhosis. Liver Int. 2012;32:1407–14.
18. Khalaf N, Ying J, Mittal S, Temple S, Kanwal F, Davila J, El-Serag HB. Natural history of untreated hepatocellular carcinoma in a US cohort and the role of cancer surveillance. Clin Gastroenterol Hepatol. 2017;15:273–281.e1.

19. Lewandowski RJ, Gabr A, Abouchaleh N, et al. Radiation segmentectomy: potential curative therapy for early hepatocellular carcinoma. Radiology. 2018;287:1050–8.
20. Fayek SA, Quintini C, Chavin KD, Marsh CL. The current state of liver transplantation in the United States: perspective from American Society of Transplant Surgeons (ASTS) Scientific Studies Committee and Endorsed by ASTS Council. Am J Transplant. 2016;16:3093–104.
21. Berzigotti A, Reig M, Abraldes JG, Bosch J, Bruix J. Portal hypertension and the outcome of surgery for hepatocellular carcinoma in compensated cirrhosis: a systematic review and meta-analysis. Hepatology. 2015;61:526–36.
22. May B, Madoff D. Portal vein embolization: rationale, technique, and current application. Semin Interv Radiol. 2012;29:081–9.
23. Xu X-L, Liu X-D, Liang M, Luo B-M. Radiofrequency ablation versus hepatic resection for small hepatocellular carcinoma: systematic review of randomized controlled trials with meta-analysis and trial sequential analysis. Radiology. 2018;287:461–72.
24. Huang Y, Shen Q, Bai HX, Wu J, Ma C, Shang Q, Hunt SJ, Karakousis G, Zhang PJ, Zhang Z. Comparison of radiofrequency ablation and hepatic resection for the treatment of hepatocellular carcinoma 2 cm or less. J Vasc Interv Radiol. 2018;29:1218–1225.e2.
25. Mironov O, Jaberi A, Kachura JR. Thermal ablation versus surgical resection for the treatment of stage T1 hepatocellular carcinoma in the surveillance, epidemiology, and end results database population. J Vasc Interv Radiol. 2017;28:325–33.
26. Lee HW, Lee JM, Yoon J-H, Kim YJ, Park J-W, Park S-J, Kim SH, Yi N-J, Suh K-S. A prospective randomized study comparing radiofrequency ablation and hepatic resection for hepatocellular carcinoma. Ann Surg Treat Res. 2018;94:74.
27. Ng KKC, Chok KSH, Chan ACY, Cheung TT, Wong TCL, Fung JYY, Yuen J, Poon RTP, Fan ST, Lo CM. Randomized clinical trial of hepatic resection *versus* radiofrequency ablation for early-stage hepatocellular carcinoma: resection *versus* radiofrequency ablation for early-stage hepatocellular carcinoma. Br J Surg. 2017;104:1775–84.
28. Thamtorawat S, Hicks RM, Yu J, Siripongsakun S, Lin W-C, Raman SS, McWilliams JP, Douek M, Bahrami S, Lu DSK. Preliminary outcome of microwave ablation of hepatocellular carcinoma: breaking the 3-cm barrier? J Vasc Interv Radiol. 2016;27:623–30.
29. Song KD. Percutaneous cryoablation for hepatocellular carcinoma. Clin Mol Hepatol. 2016;22:509–15.
30. Xu J, Noda C, Erickson A, Mokkarala M, Charalel R, Ramaswamy R, Tao Y, Akinwande O. Radiofrequency ablation *vs*. cryoablation for localized hepatocellular carcinoma: a propensity-matched population study. Anticancer Res. 2018;38:6381–6.
31. Chen R, Gan Y, Ge N, Chen Y, Wang Y, Zhang B, Wang Y, Ye S, Ren Z. Transarterial chemoembolization versus radiofrequency ablation for recurrent hepatocellular carcinoma after resection within Barcelona clinic liver Cancer stage 0/a: a retrospective comparative study. J Vasc Interv Radiol. 2016;27:1829–36.
32. Koh PS, Chan ACY, Cheung TT, Chok KSH, Dai WC, Poon RTP, Lo CM. Efficacy of radiofrequency ablation compared with transarterial chemoembolization for the treatment of recurrent hepatocellular carcinoma: a comparative survival analysis. HPB. 2015;1:72–8.
33. Lencioni R, de Baere T, Soulen MC, Rilling WS, Geschwind J-FH. Lipiodol transarterial chemoembolization for hepatocellular carcinoma: a systematic review of efficacy and safety data: Lencioni et al. Hepatology. 2016;64:106–16.
34. Llovet JM, Real MI, Montaña X, et al. Arterial embolisation or chemoembolisation versus symptomatic treatment in patients with unresectable hepatocellular carcinoma: a randomised controlled trial. Lancet. 2002;359:1734–9.
35. Lo C. Randomized controlled trial of transarterial lipiodol chemoembolization for unresectable hepatocellular carcinoma. Hepatology. 2002;35:1164–71.
36. Horikawa M, Miyayama S, Irie T, Kaji T, Arai Y. Development of conventional transarterial chemoembolization for hepatocellular carcinomas in Japan: historical, strategic, and technical review. Am J Roentgenol. 2015;205:764–73.

37. Golfieri R, Cappelli A, Cucchetti A, Piscaglia F, Carpenzano M, Peri E, Ravaioli M, D'Errico-Grigioni A, Pinna AD, Bolondi L. Efficacy of selective transarterial chemoembolization in inducing tumor necrosis in small (<5 cm) hepatocellular carcinomas. Hepatology. 2011;53:1580–9.
38. Kwan SW, Fidelman N, Ma E, Kerlan RK, Yao FY. Imaging predictors of the response to transarterial chemoembolization in patients with hepatocellular carcinoma: a radiological-pathological correlation. Liver Transpl. 2012;18:727–36.
39. Kawaguchi T, Ohkawa K, Imanaka K, Tamai C, Kawada N, Ikezawa K, Uehara H, Itou Y, Nakanishi K, Katayama K. Lipiodol accumulation and Transarterial chemoembolization efficacy for HCC patients. Hepato-Gastroenterology. 2011; https://doi.org/10.5754/hge11258.
40. Kim BK, Kim SU, Kim KA, et al. Complete response at first chemoembolization is still the most robust predictor for favorable outcome in hepatocellular carcinoma. J Hepatol. 2015;62:1304–10.
41. Lammer J, Malagari K, Vogl T, et al. Prospective randomized study of doxorubicin-eluting-bead embolization in the treatment of hepatocellular carcinoma: results of the PRECISION V study. Cardiovasc Intervent Radiol. 2010;33:41–52.
42. Gao S, Yang Z, Zheng Z, Yao J, Deng M, Xie H, Zheng S, Zhou L. Doxorubicin-eluting bead versus conventional TACE for unresectable hepatocellular carcinoma: a meta-analysis. Hepato-Gastroenterology. 2013;60:813–20.
43. Golfieri R, Renzulli M, Cioni R, et al. Randomised controlled trial of doxorubicin-eluting beads vs conventional chemoembolisation for hepatocellular carcinoma. Br J Cancer. 2014;111:255–64.
44. Cammà C, Schepis F, Orlando A, Albanese M, Shahied L, Trevisani F, Andreone P, Craxì A, Cottone M. Transarterial chemoembolization for unresectable hepatocellular carcinoma: meta-analysis of randomized controlled trials. Radiology. 2002;224:47–54.
45. Brown KT, Do RK, Gonen M, et al. Randomized trial of hepatic artery embolization for hepatocellular carcinoma using doxorubicin-eluting microspheres compared with embolization with microspheres alone. J Clin Oncol. 2016;34:2046–53.
46. Tong AKT, Kao YH, Too CW, Chin KFW, Ng DCE, Chow PKH. Yttrium-90 hepatic radioembolization: clinical review and current techniques in interventional radiology and personalized dosimetry. Br J Radiol. 2016;89:20150943.
47. Padia SA, Johnson GE, Horton KJ, et al. Segmental Yttrium-90 radioembolization versus segmental chemoembolization for localized hepatocellular carcinoma: results of a single-center, retrospective, propensity score–matched study. J Vasc Interv Radiol. 2017;28:777–785.e1.
48. Iñarrairaegui M, Thurston KG, Bilbao JI, D'Avola D, Rodriguez M, Arbizu J, Martinez-Cuesta A, Sangro B. Radioembolization with use of Yttrium-90 resin microspheres in patients with hepatocellular carcinoma and portal vein thrombosis. J Vasc Interv Radiol. 2010;21:1205–12.
49. Silva JP, Berger NG, Tsai S, Christians KK, Clarke CN, Mogal H, White S, Rilling W, Gamblin TC. Transarterial chemoembolization in hepatocellular carcinoma with portal vein tumor thrombosis: a systematic review and meta-analysis. HPB. 2017;19:659–66.
50. Mazzaferro V, Sposito C, Bhoori S, et al. Yttrium-90 radioembolization for intermediate-advanced hepatocellular carcinoma: a phase 2 study. Hepatology. 2013;57:1826–37.
51. Garin E, Lenoir L, Edeline J, et al. Boosted selective internal radiation therapy with 90Y-loaded glass microspheres (B-SIRT) for hepatocellular carcinoma patients: a new personalized promising concept. Eur J Nucl Med Mol Imaging. 2013;40:1057–68.
52. Biederman DM, Titano JJ, Korff RA, Fischman AM, Patel RS, Nowakowski FS, Lookstein RA, Kim E. Radiation Segmentectomy versus selective chemoembolization in the treatment of early-stage hepatocellular carcinoma. J Vasc Interv Radiol. 2018;29:30–37.e2.
53. Lewandowski RJ, Donahue L, Chokechanachaisakul A, Kulik L, Mouli S, Caicedo J, Abecassis M, Fryer J, Salem R, Baker T. ^{90}Y radiation lobectomy: outcomes following surgical resection in patients with hepatic tumors and small future liver remnant volumes: liver resection after ^{90}Y radiation lobectomy. J Surg Oncol. 2016;114:99–105.

54. Vouche M, Lewandowski RJ, Atassi R, et al. Radiation lobectomy: time-dependent analysis of future liver remnant volume in unresectable liver cancer as a bridge to resection. J Hepatol. 2013;59:1029–36.
55. Theysohn JM, Ertle J, Müller S, Schlaak JF, Nensa F, Sipilae S, Bockisch A, Lauenstein TC. Hepatic volume changes after lobar selective internal radiation therapy (SIRT) of hepatocellular carcinoma. Clin Radiol. 2014;69:172–8.
56. Facciorusso A, Serviddio G, Muscatiello N. Transarterial radioembolization *vs* chemoembolization for hepatocarcinoma patients: a systematic review and meta-analysis. World J Hepatol. 2016;8:770.
57. Mohamed M, Katz AW, Tejani MA, et al. Comparison of outcomes between SBRT, yttrium-90 radioembolization, transarterial chemoembolization, and radiofrequency ablation as bridge to transplant for hepatocellular carcinoma. Adv Radiat Oncol. 2016;1:35–42.
58. Llovet JM, Ricci S, Mazzaferro V, et al. Sorafenib in advanced hepatocellular carcinoma. N Engl J Med. 2008;359:378–90.
59. Kudo M, Finn RS, Qin S, et al. Lenvatinib versus sorafenib in first-line treatment of patients with unresectable hepatocellular carcinoma: a randomised phase 3 non-inferiority trial. Lancet. 2018;391:1163–73.
60. Bruix J, Qin S, Merle P, et al. Regorafenib for patients with hepatocellular carcinoma who progressed on sorafenib treatment (RESORCE): a randomised, double-blind, placebo-controlled, phase 3 trial. Lancet. 2017;389:56–66.
61. Zhu AX, Park JO, Ryoo B-Y, et al. Ramucirumab versus placebo as second-line treatment in patients with advanced hepatocellular carcinoma following first-line therapy with sorafenib (REACH): a randomised, double-blind, multicentre, phase 3 trial. Lancet Oncol. 2015;16:859–70.
62. Zhu AX, Kang Y-K, Yen C-J, et al. Ramucirumab after sorafenib in patients with advanced hepatocellular carcinoma and increased α-fetoprotein concentrations (REACH-2): a randomised, double-blind, placebo-controlled, phase 3 trial. Lancet Oncol. 2019;20:282–96.
63. Abou-Alfa GK, Meyer T, Cheng A-L, et al. Cabozantinib in patients with advanced and progressing hepatocellular carcinoma. N Engl J Med. 2018;379:54–63.
64. El-Khoueiry AB, Sangro B, Yau T, et al. Nivolumab in patients with advanced hepatocellular carcinoma (CheckMate 040): an open-label, non-comparative, phase 1/2 dose escalation and expansion trial. Lancet. 2017;389:2492–502.
65. Yau T, Park JW, Finn RS, et al. CheckMate 459: a randomized, multi-center phase III study of nivolumab (NIVO) vs sorafenib (SOR) as first-line (1L) treatment in patients (pts) with advanced hepatocellular carcinoma (aHCC). Ann Oncol. 2019;30:mdz394.029.
66. Zhu AX, Finn RS, Edeline J, et al. Pembrolizumab in patients with advanced hepatocellular carcinoma previously treated with sorafenib (KEYNOTE-224): a non-randomised, open-label phase 2 trial. Lancet Oncol. 2018;19:940–52.
67. Finn RS, Ryoo B-Y, Merle P, et al. Results of KEYNOTE-240: phase 3 study of pembrolizumab (Pembro) vs best supportive care (BSC) for second line therapy in advanced hepatocellular carcinoma (HCC). J Clin Oncol. 2019;37:4004.
68. Sheta E, El-Kalla F, El-Gharib M, Kobtan A, Elhendawy M, Abd-Elsalam S, Mansour L, Amer I. Comparison of single-session transarterial chemoembolization combined with microwave ablation or radiofrequency ablation in the treatment of hepatocellular carcinoma: a randomized-controlled study. Eur J Gastroenterol Hepatol. 2016;28:1198–203.
69. Ni J-Y. Meta-analysis of radiofrequency ablation in combination with transarterial chemoembolization for hepatocellular carcinoma. World J Gastroenterol. 2013;19:3872.
70. Cao J, Zhou J, Zhang X, Ding X, Long Q. Meta-analysis on radiofrequency ablation in combination with transarterial chemoembolization for the treatment of hepatocellular carcinoma. J Huazhong Univ Sci Technolog Med Sci. 2014;34:692–700.
71. Peng Z-W, Zhang Y-J, Chen M-S, Xu L, Liang H-H, Lin X-J, Guo R-P, Zhang Y-Q, Lau WY. Radiofrequency ablation with or without transcatheter arterial chemoembolization

in the treatment of hepatocellular carcinoma: a prospective randomized trial. J Clin Oncol. 2013;31:426–32.
72. Wang W, Zhang L, Ni J-Y, Jiang X, Chen D, Chen Y, Sun H, Luo J, Xu L. Radiofrequency ablation combined with transcatheter arterial chemoembolization therapy versus surgical resection for hepatocellular carcinoma within the Milan criteria: a meta-analysis. Korean J Radiol. 2018;19:613.
73. Takuma Y, Takabatake H, Morimoto Y, Toshikuni N, Kayahara T, Makino Y, Yamamoto H. Comparison of combined transcatheter arterial chemoembolization and radiofrequency ablation with surgical resection by using propensity score matching in patients with hepatocellular carcinoma within Milan criteria. Radiology. 2013;269:927–37.
74. Zhang R, Shen L, Zhao L, Guan Z, Chen Q, Wang L. Combined transarterial chemoembolization and microwave ablation versus transarterial chemoembolization in BCLC stage B hepatocellular carcinoma. Diagn Interv Radiol. 2018;24:219–24.
75. Fang A, Morel-Ovalle L, Kao J, Pereira K, Gadani S, Sherwani A, Vaheesan K. 04:21 PM abstract no. 217 retrospective comparison of conventional versus drug-eluting beads transarterial chemoembolization prior to microwave ablation (MWA) in patients with hepatocellular carcinoma (HCC). J Vasc Interv Radiol. 2019;30:S97–8.
76. Rajyaguru DJ, Borgert AJ, Smith AL, Thomes RM, Conway PD, Halfdanarson TR, Truty MJ, Kurup AN, Go RS. Radiofrequency ablation versus stereotactic body radiotherapy for localized hepatocellular carcinoma in nonsurgically managed patients: analysis of the National Cancer Database. J Clin Oncol. 2018;36:600–8.
77. Kwon JH, Bae SH, Kim JY, Choi BO, Jang HS, Jang JW, Choi JY, Yoon SK, Chung KW. Long-term effect of stereotactic body radiation therapy for primary hepatocellular carcinoma ineligible for local ablation therapy or surgical resection. Stereotactic radiotherapy for liver cancer. BMC Cancer. 2010;10:475.
78. Andolino DL, Johnson CS, Maluccio M, Kwo P, Tector AJ, Zook J, Johnstone PAS, Cardenes HR. Stereotactic body radiotherapy for primary hepatocellular carcinoma. Int J Radiat Oncol. 2011;81:e447–53.
79. Bujold A, Massey CA, Kim JJ, et al. Sequential phase I and II trials of stereotactic body radiotherapy for locally advanced hepatocellular carcinoma. J Clin Oncol. 2013;31:1631–9.
80. Jun BG, Kim YD, Cheon GJ, et al. Clinical significance of radiation-induced liver disease after stereotactic body radiation therapy for hepatocellular carcinoma. Korean J Intern Med. 2018;33:1093–102.
81. Gabr A, Ali R, Mora R, Sato K, Desai K, Mouli S, Riaz A, Salem R, Lewandowski R. 3:18 PM abstract no. 83 radiation segmentectomy vs. radiofrequency ablation in early stage hepatocellular carcinoma. J Vasc Interv Radiol. 2018;29:S39–40.
82. Biederman DM, Titano JJ, Bishay VL, Durrani RJ, Dayan E, Tabori N, Patel RS, Nowakowski FS, Fischman AM, Kim E. Radiation segmentectomy versus TACE combined with microwave ablation for unresectable solitary hepatocellular carcinoma up to 3 cm: a propensity score matching study. Radiology. 2017;283:895–905.
83. Hatanaka T, Arai H, Kakizaki S. Balloon-occluded transcatheter arterial chemoembolization for hepatocellular carcinoma. World J Hepatol. 2018;10:485–95.
84. Meek J, Fletcher S, Gauss CH, Bezold S, Borja-Cacho D, Meek M. Temporary balloon occlusion for hepatic arterial flow redistribution during Yttrium-90 radioembolization. J Vasc Interv Radiol. 2019;30:1201–6.
85. Bruix J, Takayama T, Mazzaferro V, et al. STORM: a phase III randomized, double-blind, placebo-controlled trial of adjuvant sorafenib after resection or ablation to prevent recurrence of hepatocellular carcinoma (HCC). J Clin Oncol. 2014;32:4006.
86. Kudo M, Ueshima K, Ikeda M, et al. Randomized, open label, multicenter, phase II trial comparing transarterial chemoembolization (TACE) plus sorafenib with TACE alone in patients with hepatocellular carcinoma (HCC): TACTICS trial. J Clin Oncol. 2018;36:206.

87. Bruix J, Takayama T, Mazzaferro V, et al. Adjuvant sorafenib for hepatocellular carcinoma after resection or ablation (STORM): a phase 3, randomised, double-blind, placebo-controlled trial. Lancet Oncol. 2015;16:1344–54.
88. Yu SCH, Chan SL, Lee KF, et al. Ablative chemoembolization for hepatocellular carcinoma: a prospective phase I case-control comparison with conventional chemoembolization. Radiology. 2018;287:340–8.

Key Reading

Forner A, Reig M, Bruix J. Hepatocellular carcinoma. Lancet. 2018;391:1301–14.
Heimbach JK, Kulik LM, Finn RS, Sirlin CB, Abecassis MM, Roberts LR, Zhu AX, Murad MH, Marrero JA. AASLD guidelines for the treatment of hepatocellular carcinoma. Hepatology. 2018;67:358–80.
Lencioni R, de Baere T, Soulen MC, Rilling WS, Geschwind J-FH. Lipiodol transarterial chemoembolization for hepatocellular carcinoma: a systematic review of efficacy and safety data. Hepatology. 2016;64:106–16.
Lewandowski RJ, Gabr A, Abouchaleh N, et al. Radiation segmentectomy: potential curative therapy for early hepatocellular carcinoma. Radiology. 2018;287:1050–8.
Marrero JA, Kulik LM, Sirlin CB, Zhu AX, Finn RS, Abecassis MM, Roberts LR, Heimbach JK. Diagnosis, staging, and management of hepatocellular carcinoma: 2018 practice guidance by the American Association for the Study of Liver Diseases. Hepatology. 2018;68:723–50.

Chapter 7
Hepatocellular Carcinoma: Eastern Experience

Hyo-Cheol Kim, Jin Woo Choi, and Jin Wook Chung

Epidemiology/Pathophysiology

Hepatocellular carcinoma (HCC) is the second leading cause of cancer death in East Asia and sub-Saharan Africa and the sixth most common in western countries. According to Cancer Today, 80% of HCC cases occur in East Asia and sub-Saharan Africa. Mongolia has the highest age-standardized incidence rates per 100,000 people for liver cancer (93.7), followed by Egypt, the Gambia, and Vietnam. The most common cause of HCC in Korea and Asia is hepatitis B virus (HBV) infection, whereas hepatitis C virus (HCV) infection is the most common cause in Japan and western countries.

In Korea, approximately 15,000 patients are diagnosed as newly developed HCC annually. The number of cases and crude incidence had increased to 16,714 cases and 33.4/100,000 in 2011 and showed a subtle decreasing tendency thereafter [1]. The cause of HBV infection accounts for 70% of HCC, and HCV accounts for approximately 10%. The prevalence of HBV infection ranged from 8 to 10% in 1980s and decreased to 2.9% in 2013 due to the national immunization program. The prevalence of HCV infection based on anti-HCV positivity was 0.7% in 2014. Recent antiviral therapy has shown excellent outcomes of virological response and reduces the risk of HCC. Heavy alcohol consumption accounts for approximately 5% of HCC. Nonalcoholic fatty liver disease (NAFLD) is relatively rare (less than 5%), but HCC cases related with NAFLD is increasing.

In Japan, HCC ranks as the fifth most common cancer, and about 30,000 people died of liver cancer in 2012. Whereas chronic HCV infection accounts for 65% of HCCs, chronic HBV infection accounts for only 15% of HCCs.

H.-C. Kim · J. W. Choi · J. W. Chung (✉)
Department of Radiology, Seoul National University Hospital, Seoul, Republic of Korea
e-mail: chungjw@snu.ac.kr

C. Georgiades, H. S. Kim (eds.), *Image-Guided Interventions in Oncology*,
https://doi.org/10.1007/978-3-030-48767-6_7

In China, liver cancer is the second most common cancer, and about 380,000 people died of liver cancer every year. Whereas chronic HBV infection accounts for 65% of HCCs, chronic HCV infection accounts for only 25% of HCCs.

The key pathologic feature that enables hepatic artery embolotherapy for HCC is dual blood supply of the liver. Although the normal liver parenchyma receives more than 75% of blood from the portal vein, HCC does most blood from the hepatic artery. This facilitates selective ischemic damage of the tumors following embolization of tumor-supplying hepatic artery, while the normal liver cells remain viable.

The arterialization of HCC gradually occurs, as multistep hepatocarcinogenesis processes. Therefore, the blood supply of HCC can vary depending on the differentiation of each tumor. Typical nodular HCC with capsule is almost exclusively supplied by the hepatic artery, while early HCC and peripheral part of advanced HCC can be supplied by both the hepatic artery and portal vein. This is one of the main reasons that HCC shows variable response after hepatic arterial embolotherapy.

Surgery

Hepatic resection is considered as best treatment option for solitary HCC in patients with sufficient hepatic functional reserve. Hepatic resection is commonly performed in patients with Child-Pugh class A with ECOG performance status 0–2. Child-Pugh classification is widely used to preoperatively assess the safety of hepatic resection. However, Child-Pugh classification is insufficient for assessment because many patients belong to Child-Pugh class A despite they have advanced liver cirrhosis. Therefore, the indocyanine green 15-minute retention rate (ICG-R15) is commonly used in Korea and Japan. Major hepatic resection is recommended for patients with ICG-R15 $\leq$10%. Portal hypertension, defined as a hepatic venous pressure gradient $\geq$10 mmHg, has been suggested to evaluate resectability in Western countries. Instead of direct measurement of hepatic venous pressure gradient, esophageal varix and thrombocytopenia <100,000/mm^3 associated with splenomegaly are widely used as clinical indicators of portal hypertension.

The best indication for hepatic resection is generally expected as 1 or 2 small tumors, because larger tumors frequently accompany vascular invasion. However, large HCC without vascular invasion can have favorable results after resection. The results of hepatic resection for HCC have markedly improved due to recent advances in preoperative tests and surgical skills including laparoscopic surgery, and postoperative mortality after HCC resection is less than 1%. The 5-year overall and disease-free survival rate is 46–69.5% and 23–56.3%, respectively.

Liver transplantation is commonly recommended in patients with HCC who meet Milan criteria (single tumor $\leq$5 cm, $\leq$ 3 nodules, and $\leq$3 cm). Overall 5-year survival rate of patients meeting the Milan criteria has been reported up to 78%. Because deceased liver donors are deficient and allocated to patients with end stage of liver cirrhosis (MELD score >30), deceased donor liver transplantation is rarely used as the initial treatment for HCC with compensated liver cirrhosis. Therefore,

living donor liver transplantation is the main type of liver transplantation for patients with HCC in Korea and frequently performed as a salvage option for HCC.

Systemic/Immunotherapy

Systemic therapies include conventional cytotoxic chemotherapeutic agents such as 5-FU and cisplatin, molecularly targeted agent such as sorafenib and lenvatinib, and immune checkpoint inhibitor such as nivolumab.

Sorafenib is a multi-kinase inhibitor that targets vascular endothelial growth factor receptor-2 (VEGFR-2), platelet-derived growth factor receptor (PDGFR), Raf-1, and c-kit. Sorafenib was the first multi-kinase inhibitor approved for the systemic therapy of advanced HCC. The median survival of advanced stage HCC patients treated by sorafenib was significantly longer than that of placebo group in both global randomized controlled trial (RCT) and Asian RCT [2, 3]. Thus, sorafenib had become the standard therapy in BCLC C disease.

Lenvatinib is an oral multi-kinase inhibitor and demonstrated non-inferior overall survival compared with sorafenib in advanced HCC patients. Lenvatinib showed significantly longer progression-free survival than that of sorafenib [4] and can be used as first-line therapy.

Nivolumab is an immune checkpoint inhibitor that disrupts programmed cell death receptor-1 (PD-1) and is a recombinant antibody that can be administered intravenously. While a phase I/II trial of nivolumab demonstrated promising tumor response rate (20%), recent RCT failed to significantly prolong overall survival compared with sorafenib as first-line treatment for advanced HCC.

Adjuvant therapy with cytokine-induced killer cells significantly improved recurrence-free survival and overall survival in HCC patients after curative resection or local ablative therapy [5].

A lot of RCTs regarding various combined therapy (i.e., combined locoregional therapy and systemic therapy) are under investigation, and the systemic therapy may expand its role in management for HCC of intermediate stage as well as of advanced stage in near future.

External Radiation Therapy

The role of external beam radiation therapy (EBRT) for HCC has been limited due to relatively low liver tolerance to radiation. However, modern RT technology such as intensity-modulated radiotherapy (IMRT) and stereotactic body radiotherapy (SBRT) has favorable outcome with acceptable toxicity in selected HCC patients. EBRT should be performed in patients with preserved liver function (Child-Pugh class A or B7). In early-stage HCC, RT may be considered as an alternative therapy when resection or ablative treatment is not possible due to medical or anatomical

reasons such as tumor location near major vessels, and chemoembolization is not effective. In advanced stage HCC, combined treatment of chemoembolization and EBRT is commonly chosen in Korea in HCC patients with portal vein thrombosis or hepatic vein thrombosis. In a recent randomized study for HCC patients with portal vein invasion, combined treatment of chemoembolization and EBRT had a significantly longer overall survival compared with sorafenib alone (55 vs 43 weeks; $P = 0.04$) [6].

Proton beam therapy (PBT) has dosimetric advantages over X-ray RT in patients with HCC, because it has no exit dose along the beam path. Clinical experiences with PBT for HCC are expanding rapidly, even though PBT accompanies high cost and limited availability.

Intra-arterial Therapies (cTACE, DEB-TACE, and Radioembolization)

The majority of HCCs are unresectable at the time of diagnosis due to portal hypertension, poor liver function, multiplicity of tumors, vascular invasion, old age, and insufficient future liver remnant. Transarterial chemoembolization (TACE) is most widely accepted as a primary treatment modality for HCC and can be classified into conventional TACE (cTACE) using Lipiodol and drug-eluting bead TACE (DEB-TACE).

cTACE

Indications

The most common indication of TACE is unresectable multinodular HCCs in patients with reasonably preserved liver function (Child-Pugh class of A or B7) and performance status (Eastern Cooperative Oncology Group [ECOG] 0 or 1). In BCLC staging system, TACE is recommended as first-line therapy for intermediate stage HCC (multinodular, asymptomatic tumors without vascular invasion or extrahepatic spread). Only less than 15% of the patients with HCC initially present with this stage. However, in real clinical situations, TACE is much more frequently performed even in patients with single HCC or HCC with vascular invasion. A recent study using inverse probability weighting showed TACE provided similar long-term survival compared with hepatic resection and radiofrequency ablation (RFA) in patients with small single HCC [7]. Therefore, TACE can be considered as an alternative treatment with curative intent in early-stage HCC which is not eligible for hepatic resection or ablation therapy due to systemic comorbidities or anatomical problems. In HCC patients with vascular invasion, systemic therapy using sorafenib is standard treatment. However, TACE alone or combined treatment of TACE and

EBRT is commonly performed in Asian countries. In patients with Child-Pugh class C disease, best supportive care or liver transplantation (if within Milan criteria) is standard treatment option. When tumor burden is limited, superselective TACE at the segmental or subsegmental hepatic artery can be safely performed in patients with Child-Pugh C disease.

HCC rupture inciting hemodynamic instability can be treated by emergency TACE. Selective embolization for ruptured tumor or tumors at risk of rupture (i.e., nodular HCC with exophytic growth) facilitates safe and effective management of the patients irrespective of their liver function. TACE also plays neoadjuvant roles when it is performed to downstage or to provide a bridge prior to the surgical resection or transplant.

There is no absolute contraindication to TACE. Although decompensated cirrhosis (i.e., Child-Pugh B8 or higher), massive HCC involving both lobes of the liver, and major portal vein invasion are regarded as relative contraindications, TACE can be performed for these cases after adjustment of the chemoembolic agents and the extent of embolization [8]. Other relative contraindications are active gastrointestinal bleeding, refractory ascites, extrahepatic spread, and hepatic encephalopathy.

Procedure

Preparation

Blood sampling for the complete blood cell count, prothrombin time, creatinine levels, and liver function test should be conducted prior to TACE. The baseline tumor marker (e.g., alpha fetoprotein and protein induced by vitamin K absence) measurement is useful to monitor tumor responses after the treatment. In terms of the cross-sectional imaging, the size and segmental location of the tumor, its growth pattern (nodular vs infiltrating), and macroscopic angioinvasion into the hepatic or portal veins should be evaluated. Assessment of the chest and other abdominopelvic organs are also useful to identify metastasis and comorbid diseases. Antiemetics and narcotic analgesics are administered intravenously, and patients with contrast allergies can be managed by preemptive use of oral steroids 1 hour before the procedure. Prophylactic antibiotics are not recommended unless patients have bilioenteric anastomosis, biliary stent, or biliary drainage.

Angiographic Evaluation

Celiac and superior mesenteric arteriographies are conducted to identify the arterial anatomy and patency of the portal vein. Anatomic variations in the celiac trunk and hepatic arteries are frequently encountered, which can be addressed prior to TACE by reviewing arterial phase CT images. The right hepatic artery arising from the superior mesenteric artery and the left hepatic artery arising from the left gastric

artery are the two most frequent hepatic arterial variations [9]. When only the segmental artery of SII is originating from the left gastric artery, the operators often miss the SII segmental artery (Fig. 7.1). For complete angiography, all hepatic arteries should be adequately opacified, and all tumor-feeding arteries should be

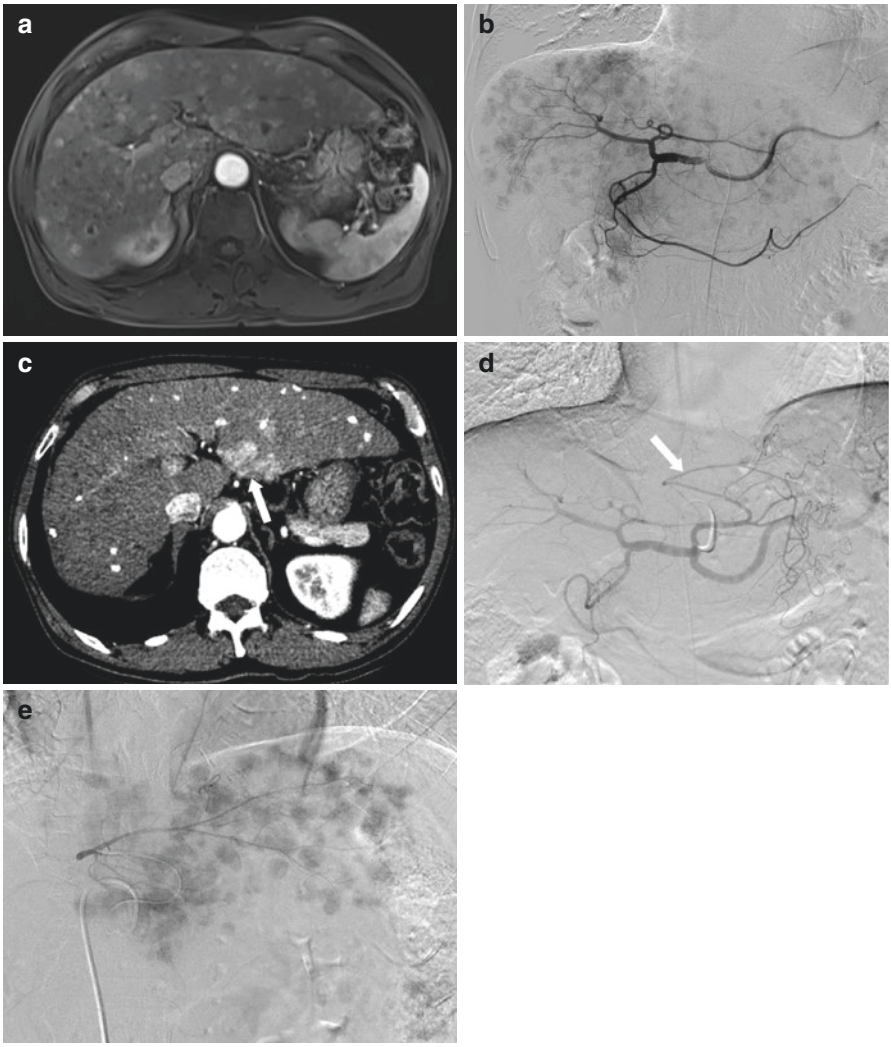

Fig. 7.1 A 66-year-old man has multinodular HCC. (**a**) MRI of hepatic arterial phase shows multiple nodules throughout the whole liver. (**b**) Celiac angiography shows numerous nodular tumor stainings in the both lobes of the liver. Non-selective conventional chemoembolization was performed through the right and left hepatic artery (not shown). (**c**) CT scan 2 months after chemoembolization shows tumor progression in segment II (arrow), whereas tumor burden was decreased in the remaining part of the liver. (**d**) Celiac angiography obtained at the proximal celiac trunk shows the SII segmental artery (arrow) originating from the left gastric artery. (**e**) Selective angiography of SII shows multiple tumor stainings which was not treated at the previous chemoembolization

identified. Selective segmental or subsegmental hepatic arteriograms with multiple oblique angles and magnifications are frequently necessary to identify small tumor-feeding arteries. To avoid non-targeted embolization, it is important to recognize the origin of the cystic artery, the right gastric artery, the hepatic falciform artery, and the accessory left gastric artery originating from the left hepatic artery.

Cone-Beam CT

Recently, cone-beam CT has been routinely used in all TACE procedures, and it reduces the need for selective hepatic angiography in many cases. Cone-beam CT is commonly obtained at the proper or common hepatic artery to reveal the whole hepatic artery anatomy, tumor-feeding arteries, and tumor blush (Fig. 7.2). Undiluted contrast material is commonly administered with a scan delay of 4–6 seconds. It provides information about the patient's vascular anatomy and tumor-feeding arteries, increases the operator's confidence in selecting target artery, and shortens the procedure time by facilitating the catheterization with a help of three-dimensional vascular structure. In addition, confident identification of extrahepatic arteries supplying non-target organs, such as supraduodenal or retroduodenal arteries, right gastric artery, phrenic artery, and falciform artery, is crucial to avoid non-target embolization. It sometimes reveals a small HCC which was obscure on pre-procedural CT/MRI or digital subtraction angiography. When non-enhancing small tumor or unenhanced part within a large tumor is evident on cone-beam CT obtained at the proper hepatic artery, an extrahepatic collateral artery should supply the tumor (Fig. 7.3). To obtain high-quality cone-beam CT images, patients should hold their breath during rotation of C-arm. Thus, sedative agent is seldom used prior to obtaining cone-beam CT images.

Preparation of Lipiodol-Anticancer Drug Emulsion

To date, there is no consensus on optimal chemotherapeutic agent. The most commonly used chemotherapeutic drug is doxorubicin. To make a stable water-in-oil emulsion, the doxorubicin of powder form is dissolved in water-soluble contrast agent and is then mixed with Lipiodol, and volume of Lipiodol must be larger than that of doxorubicin solution. The preferred volume ratio between Lipiodol and doxorubicin solution is 4:1. Prior to injection of Lipiodol emulsion, 0.5–2 mL of 2% lidocaine is injected through the target artery to prevent pain and vasospasm.

Chemoembolization

When injected into the hepatic artery, Lipiodol emulsion is preferentially accumulated in the tumor because of the hemodynamic difference between the tumor and normal liver parenchyma (so-called the siphon effect) and large vessel-seeking

property of oil droplet. Once accumulated in tumor vasculature, Lipiodol is typically retained for a long time because of absence of Kupffer cells in the tumor. In contrast, in the normal liver parenchyma, the Lipiodol accumulates in the terminal portal venules through peribiliary plexus and subsequently passes through sinusoids into the systemic circulation in 2 weeks.

When sufficient amount of Lipiodol emulsion is injected into the tumor-feeding artery, Lipiodol emulsion may fill intratumoral neovasculature and flow into peritumoral portal veins via presinusoidal arterioportal communication or tumoral venous

Fig. 7.2 A 57-year-old man has four nodular HCC. (**a**) CT scan of hepatic arterial phase shows four nodules (arrows) in the both lobes of the liver. (**b**) Celiac angiography shows two tumor stainings (arrows), but the tumor stainings of the remaining two nodules are unclear. (**c**) Volume-rendering image of cone-beam CT obtained at the common hepatic artery shows four tumor stainings (arrows). (**d**) Spot image obtained during superselective chemoembolization shows dense accumulation of iodized oil in the four tumors

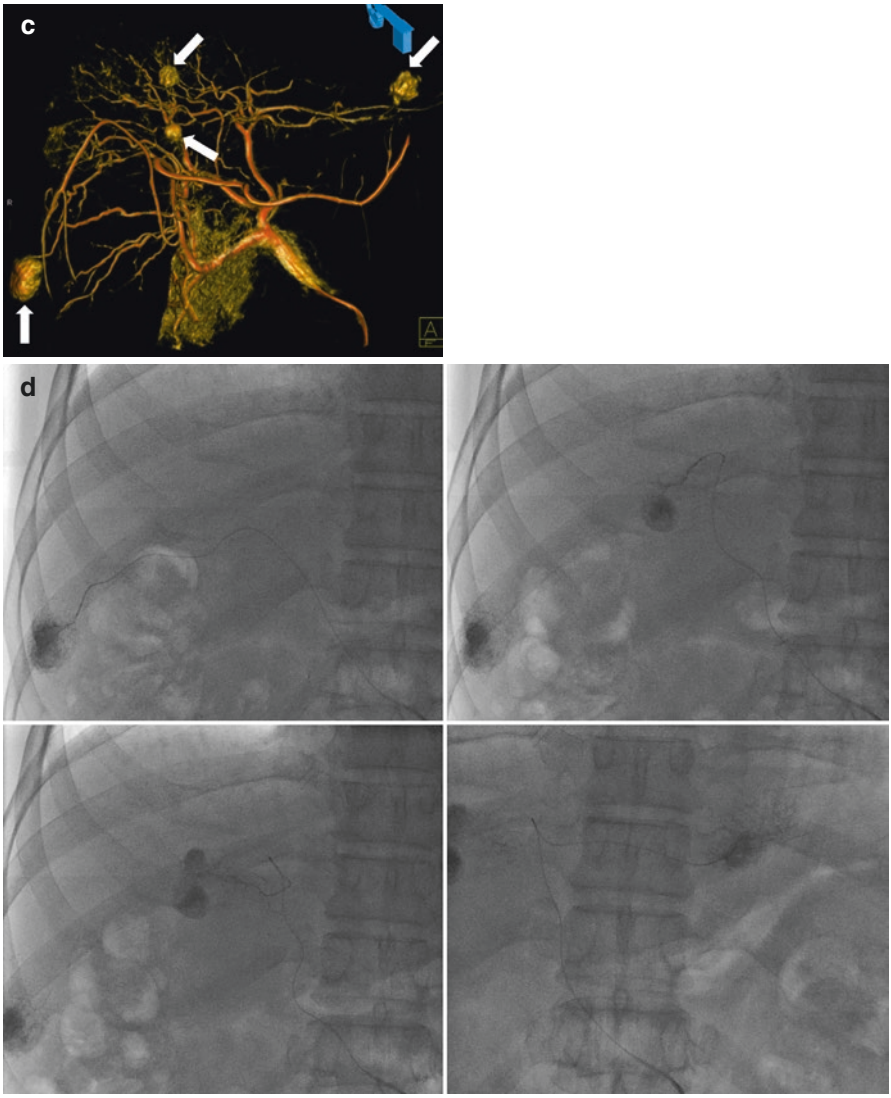

Fig. 7.2 (continued)

drainage. Subsequent embolization of hepatic artery allows dual (arterial and portal) embolization of HCC with high-dose intratumoral delivery of a chemotherapeutic agent. The achievement of this ideal endpoint of Lipiodol chemoembolization is clinically important in treating early stage or extracapsular infiltrative tumors and daughter nodules that are perfused via portal venules.

The amount of Lipiodol emulsion depends on the size and vascularity of the tumor. The usual upper limit in dose of doxorubicin and Lipiodol is 50 mg and

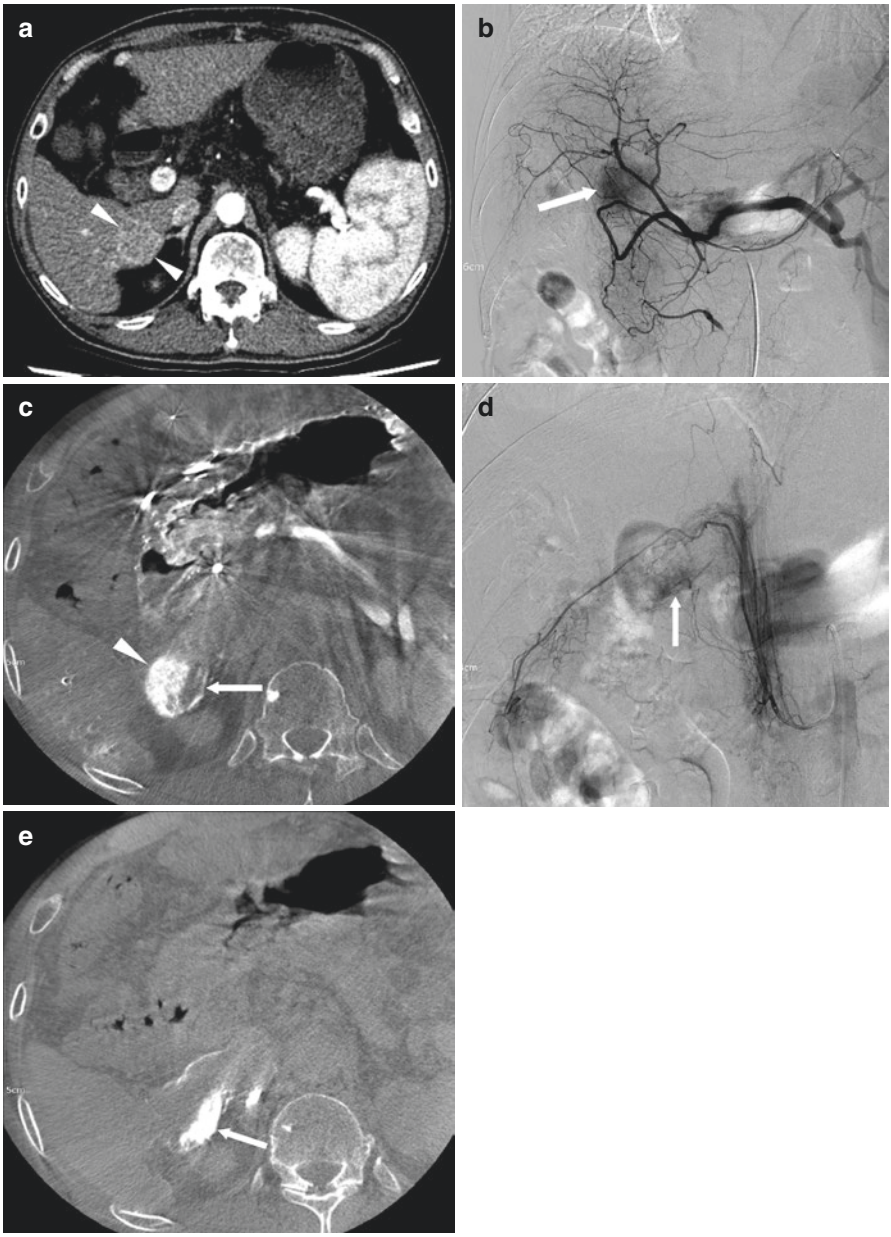

Fig. 7.3 A 66-year-old man has multinodular HCC. (**a**) CT scan of hepatic arterial phase shows a hypervascular tumor (arrowheads) in right lobe of the liver. (**b**) Celiac angiography shows nodular tumor staining (arrow) in the right lobe of the liver. (**c**) Axial image of cone-beam CT obtained at the common hepatic artery shows enhancement of the tumor (arrowhead). Note focal defect (arrow) of tumor enhancement which suggests the presence of extrahepatic collateral artery supplying the tumor. (**d**) Angiography of common trunk of the middle adrenal artery and the renal capsular artery shows suspected tumor staining (arrow). (**e**) Axial image of cone-beam CT obtained at the middle adrenal artery shows enhancement of the tumor (arrow)

10 mL, respectively. For small- or medium-sized tumor, the ideal endpoint of peritumoral portal vein visualization should be attempted. For large tumors (>7 cm), 10 mL of Lipiodol is not enough to saturate intratumoral neovasculature. The larger amount of Lipiodol (at maximum, 20 mL) can be used with special concern about pulmonary shunting. Alternatively, in large hypervascular tumor, main tumor-feeding artery can be embolized with small particulate embolic agents to reduce the amount of Lipiodol emulsion needed, and remaining peripheral tumors can be managed by Lipiodol emulsion.

After infusion of Lipiodol emulsion, tumor-feeding hepatic arteries should be embolized with particulate embolic materials. Hepatic artery embolization induces tumoral ischemic necrosis and increases chemotherapeutic drug dwelling time in the tumor by slowing the rate of efflux from the hepatic circulation. Proximal arterial occlusion should be avoided, because it incites intrahepatic and extrahepatic collateral vessel growth as well as preclude repetitive procedure. Accordingly, the size of embolic materials should be chosen regarding the size of feeding artery, intratumoral vascularity, and the selectivity of catheter positioning. Ideal embolic materials are small enough to reach and occlude the terminal intratumoral arterioles supplying HCC but larger than the size of arteriovenous shunt and peribiliary plexus. The most commonly used embolic material is gelatin sponge particle because it is regarded as a temporary embolic material. However, when gelatin sponge particles are densely packed in the hepatic arteries, they may be permanently occluded. Gelatin sponge particles were used as 1–2 mm cubes which were cut by hand and, by operator's decision, crushed using three-way pumping. Basically, those manually prepared gelatin sponge particles are uneven in size and tend to occlude extratumoral feeding hepatic artery. In addition, they are prone to migrate distally because they are soft and compressible. Therefore, in large hypervascular tumors with dilated intratumoral vessels, delayed completion angiography should be obtained to prevent incomplete treatment due to early recanalization of the embolized vessels. Recently, calibrated gelatin sponge particles of smaller size (150–500 μm in diameter) are available. Polyvinyl alcohol particle and various calibrated microspheres are also used. Small or permanent embolic materials should be used more selectively because the risk of bile duct necrosis or permanent hepatic artery occlusion is definitely higher.

Technical Considerations

The best way to maximize treatment effect and to minimize procedure-related complications is to catheterize every tumor-feeding artery and place a microcatheter as close to the tumor as possible and achieve ideal endpoint of Lipiodol chemoembolization. To preserve liver function, embolization of the hepatic artery supplying nontumorous liver tissue should be avoided by highly selective catheterization. With recent advancement of microcatheter and guidewire technology, a microcatheter of 2.0Fr or smaller in diameter with resilient guidewire facilitates catheterization of subsegmental hepatic artery. Vasospasm may happen during selective catheterization of tumor-feeding arteries. Sometimes, vasospasm precludes

preferential Lipiodol uptake in the tumor due to loss of the siphon effect. If vasospasm is not relieved by waiting, vasodilator such as nitroglycerin can be considered to restore antegrade arterial flow.

In small tumors, the diameter of tumor-feeding artery is equal or thinner than the outer diameter of a microcatheter. In this situation, a microcatheter is wedged into the tumor-feeding artery, and Lipiodol can be forcefully administered by manual injection, not by flow-directed fashion. With this ultraselective technique, dense accumulation of Lipiodol emulsion in the tumor can be achieved even in poorly vascularized tumor [10].

In cases of multiple tumor-supplying arteries, the amount of Lipiodol emulsion in a target artery should be proportioned depending on the tumor volume supplied by each artery. Lipiodol accumulation during TACE should be monitored on fluoroscopy to secure complete embolization. Cone-beam CT imaging can be used to evaluate Lipiodol retention in the tumor. If there is a defect in Lipiodol retention at the peripheral part of the tumor, extrahepatic collateral supply should be considered.

Detection of extrahepatic collaterals supplying the tumors is pivotal to achieve complete treatment. When a tumor is abutting hepatic bare area or suspensory ligaments, or it invades into an adjacent organ, selective arteriogram of possible extrahepatic arteries should be obtained. With thin-section (3 mm or less) multidetector CT scan, those collateral vessels may be identified in pre-procedure CT. Cone-beam CT obtained at the proper hepatic artery is also used to detect the presence of extrahepatic collateral artery supplying the tumor (Fig. 7.3). Common extrahepatic collaterals include the inferior phrenic artery, omental artery, internal mammary artery, colic branch of superior mesenteric artery, adrenal artery, intercostal artery, renal capsular artery, and gastric arteries [11]. When the hepatic artery and extrahepatic collaterals supply the tumor, additional TACE of the extrahepatic collaterals can be tried to increase the therapeutic efficacy. These extrahepatic collaterals can also be used as an access route to the tumors in patients with hepatic artery occlusion. Large tumors are commonly supplied by the extrahepatic collateral arteries at initial TACE, whereas small tumors at the liver surface can be fed by the extrahepatic collateral arteries when the hepatic arteries are attenuated by the multiple previous sessions of TACE.

It is important to evaluate tumor-related arteriovenous shunt for safe procedures. In patients with a prominent arterioportal or arteriovenous shunt, embolization of the shunt by particulate embolic materials or glue is recommended prior to TACE. If not, Lipiodol emulsion may leak into portal vein or hepatic vein and cause liver injury or pulmonary oil embolism. Balloon occlusion of the feeding hepatic artery for arterioportal shunting or balloon occlusion of draining hepatic vein for arteriovenous shunt may be useful. If embolization for massive arterioportal shunt is successful, hepatofugal portal flow may be converted to hepatopetal flow, and performance status and ascites may be improved. If a lot of Lipiodol emulsion is leaked into the hepatic vein, it may cause symptomatic pulmonary oil embolism with severe hypoxemia. Rarely, if there is a hepatofugal arterioportal shunt and portopulmonary venous shunt, Lipiodol emulsion leaked into the portal vein may cause cerebral embolism.

Follow-Up

Narcotic analgesics, chlorpromazine, and acetaminophen can be used as needed. Patients can discharge when activities of daily living are possible without intravenous analgesics. Laboratory studies in terms of the liver function and tumor markers are recommended 2–4 weeks after the procedure. To address the tumor responses, multiphase contrast-enhanced CT or MRI should be conducted every 2–3 months after the procedure. If residual or recurrent tumor is identified on follow-up imaging or tumor markers are elevated, another session of TACE can be considered depending on the patients' liver function. Until now, there is no consensus about the repetition of TACE. From an oncological point of view, chemotherapy should be administered at 3-week intervals in order to fit to cell cycle, but such a strategy would carry the risk of increased side effect and liver damage and unnecessary procedure for patients with good response. Therefore, repeat procedure is generally recommended only when progression of HCC was noted radiographically ("on demand" strategy). It should be considered to discontinue TACE, even if technically feasible, in patients with untreatable progression including failure to achieve objective response in the targeted tumor after at least two treatments, clinical or functional deterioration (ECOG performance status >2 or hepatic decompensation), and development of a contraindication to TACE.

Outcome

Numerous studies have shown that TACE induces a significant tumor necrosis without negative influence on liver function in patients with preserved liver function. The extent of tumor necrosis has been reported to range from 60% to 100%. With introduction of subsegmental TACE using a microcatheter, the tumor necrosis rate was markedly improved. Ultraselective TACE using a 2.0-F microcatheter reported local recurrence rates of 25.6% and 34.7% at 1- and 3-year [10]. The local recurrence was significantly lower when a greater degree of portal vein visualization was demonstrated during TACE.

The survival benefit associated with TACE has been demonstrated by two pivotal randomized controlled trials (RCTs), one from Barcelona [12] and one from Hong Kong [13]. They permitted a positive result in a cumulative meta-analysis which clearly indicated that the 2-year survival of HCC patients treated with TACE is improved compared with conservative management [14]. As a result of these investigations, TACE has become established as the standard of care for patients who meet the criteria for the intermediate stage of the BCLC staging system.

The 4966 patients stratified to TACE recommended by the Japanese guidelines showed that 3-year survival of patients with two or three tumors >3 cm or four or more tumors was 55% and 46% in Child-Pugh class A, respectively, and 30% and 22% in class B, respectively [15]. In an Asian cooperative prospective study from Japan and Korea, the 2-year survival rate of 99 patients with unresectable HCC was

75.0%. The median time to progression was 7.8 months, and the median overall survival period was 3.1 years [16].

At the initial diagnosis of HCC, malignant tumor thrombus in the portal vein is identified in approximately 20–30% in Asia. According to the BCLC system, systemic administration of sorafenib is regarded as the standard of care for these patients. However, in Asian practice, more aggressive treatments such as TACE and EBRT are commonly attempted based on the evidence established in Asian population prior to the era of sorafenib. Once patients have good hepatic function, the risk of liver failure after TACE for HCC with portal vein invasion is acceptably low. A single-center RCT reported that TACE combined with EBRT significantly increased progression-free survival (PFS), overall survival (OS), the objective response rate (OSS), and time to progression (TTP) compared with sorafenib monotherapy in patients with HCC localized in the liver and portal vein invasion [6]. Therefore, even in case of major vascular invasion, the patients with preserved liver function and localized disease should be actively treated with TACE with or without EBRT.

Complications

The complication rate of TACE is reported at approximately 4%. Major complications include liver failure or infarction, liver abscess, biliary necrosis, tumor rupture, cholecystitis, and non-target embolization [17]. Procedure-related mortality is approximately 1%. Known risk factors are main portal vein invasion, compromised hepatic functional reserve, biliary obstruction, previous biliary surgery, excessive use of Lipiodol, and non-selective embolization.

Postembolization syndrome (PES), referring noninfectious fever, pain, nausea, and vomiting, develops in as many as 60–80% of patients. PES is regarded as an expected side effect rather than a complication following hepatic embolotherapy. The etiology of PES has not been fully understood yet. Possible causes of pain are acute ischemia of liver parenchyma, distension of the liver capsule, ischemia of biliary tree, and gallbladder ischemia secondary to inadvertent embolization of the cystic artery. PES is self-limiting and requires only supportive management that includes antiemetics, analgesics, and antipyretics. However, it still remains the major reason for prolonged hospitalization after TACE, particularly in patients with large HCC. Steroids prophylaxis may alleviate postembolization syndrome.

Liver failure is one of the most fatal events that can happen after TACE. Predisposing factors are hyperbilirubinemia, deteriorated baseline liver function, high dose of chemotherapeutic drug, and advanced cirrhosis. Most liver dysfunction that requires hospitalization develops in patients with Child-Pugh class C. Once selectively conducted, in general, TACE do not induce clinically relevant liver dysfunction in patients with Child-Pugh class A and B.

Liver abscess is a rare (0.5% to 2%) but potentially fatal complication of TACE. Portal vein obstruction, metastatic tumors, and biliary abnormalities are associated with the occurrence of liver abscess. In particular, previous bilioenteric bypass surgery and sphincter of Oddi dysfunction for any reason are known as the

most important risk factors for the development of liver abscess. Once occurred, liver abscess can be effectively managed by percutaneous drainage and parenteral antibiotics. In high-risk patients, TACE should be performed selectively with reduced amount of chemoembolic agents and monitored carefully after the procedure.

Because peribiliary capillary plexus can be embolized during TACE, bile duct injury can occur from the ischemic damage. The incidence has been reported between 2% and 12.5%. Bile duct injury can be presented as intrahepatic biloma, focal stricture of the common bile duct, or diffuse dilatation of intrahepatic bile duct within a few months and then be progressed to the obliteration of adjacent portal vein, liver parenchymal atrophy, and liver abscess. Metastatic tumor, noncirrhotic liver, and non-selective embolization are associated with a higher chance of bile duct injury after TACE. The best way to prevent major bile duct injury is to perform TACE selectively at the tumor-feeding arteries. When hilar feeders are selectively treated, special attention should be paid to monitor their perfusion area with the aid of cone-beam CT or angio-CT. Most patients with post-TACE bile duct injury are asymptomatic. However, if biliary infection is suspected, parenteral antibiotics and percutaneous drainage should be applied for the symptomatic patients.

Non-target embolization is a preventable complication by using meticulous angiographic evaluation and appropriate embolization technique. Acute cholecystitis is the most common complication owing to non-target embolization, because the cystic artery is often not sufficiently opacified on hepatic arteriography. The origin of the cystic artery is quite variable, from the segmental hepatic artery to the main trunk of the right hepatic artery. Unintended delivery of chemoembolic materials into the cystic artery can induce prolonged fever, pain, nausea, and vomiting. Although most symptoms are self-limiting, gallbladder perforation, gangrenous cholecystitis, or emphysematous cholecystitis may develop if large amount of chemoembolic materials is infused. The serious complications should be managed by surgical cholecystectomy or percutaneous cholecystostomy.

Skin complications can develop following TACE of extrahepatic collateral vessels, especially the internal mammary artery and intercostal artery. Most patient complains of painful induration and discoloration, but transmural necrosis requiring skin graft is rare. Selective catheterization of tumor-supplying arteries and careful injection of chemoembolic materials can prevent this complication. If exclusion of the cutaneous branches is impossible, bland embolization is highly recommended. When Lipiodol emulsion is infused into the falciform artery, patients may complain of supraumbilical skin rash. Therefore, when the prominent falciform artery is identified on angiography and included in the target embolization territory (e.g., non-selective TACE via the left hepatic artery), it should be embolized using coils or particles prior to the injection of Lipiodol emulsion. Not every falciform artery supplies the skin. If embolization of a falciform artery is not possible due to anatomical difficulties, it is possible to proceed TACE after test injection of chemoembolic materials with careful visual monitoring of epigastric area.

Gastroduodenal ulcer can occur especially when the accessory left gastric arteries from the left hepatic artery or the right gastric artery from the proper or left

hepatic arteries are embolized with chemoembolic materials. In the same line with falciform artery embolization, these gastric arteries should be embolized when non-selective TACE via the left hepatic artery is planned. However, in this case, only coils should be used to prevent far distal embolization that can induce ischemia-induced ulcer.

Infusion of chemoembolic materials through the inferior phrenic artery can result in pulmonary complications, such as pulmonary oil embolism, lung infarction, and pleural effusion. The inferior phrenic artery accompanies an arteriovenous shunt in about half of patients, and an azygoesophageal branch is the most common branch having an arteriovenous shunt. If the catheterization of azygoesophageal branch is possible, bland embolization using PVA particle or gelatin sponge particles should be performed prior to injection of Lipiodol emulsion. Although it is not as clinically significant as the pulmonary complications, diaphragmatic weakness can also occur in about one third of patients as an ischemic complication.

DEB-TACE

Drug-eluting beads (DEBs) are specifically designed microsphere that load a specific chemotherapeutic drug and release the drug locally within the target tissue over an extended period. DEBs can reduce systemic drug toxicity because of sustained controlled release of the drug.

Patient selection of DEB-TACE is basically same as cTACE. Even though cTACE is still a mainstay in Asia, DEB-TACE is commonly chosen in patients with medium-sized (3–7 cm) single or oligonodular HCC.

50–75 mg doxorubicin is loaded into one vial of DEB, and up to two vials are used in one session. For HCCs within the Milan criteria, one vial of DEB is commonly used. For advanced disease, exceeding the Milan criteria, two vials of DEB are often used. In large tumor (>10 cm), the use of two vials of DEB seldom reach near-stasis of tumor-feeding artery. In this situation, two options may be taken; first option is additional embolization using gelatin sponge particles or bland microspheres, and second option is short-term (2–4 weeks interval) repeated DEB-TACE. Non-selective additional embolization using bland microspheres is not generally recommended for residual tumors because of increased risk of biliary complications.

In DEB-TACE, a microcatheter should not be wedged in the target artery, and antegrade flow around the microcatheter should be maintained during injection of DEB. In DEB-TACE, the endpoint of embolization is determined by hepatic arterial flow, not by accumulation of DEB.

The endpoint of embolization is near-stasis of flow in the segmental artery supplying the tumor. If superselective catheterization is possible distal to subsegmental artery, complete stasis of tumor-feeding artery is desirable to achieve complete response without the risk of significant biliary complication. Complete stasis of entire segmental/sectional/lobar hepatic artery may have high incidence of

corresponding biliary injury [18]. After DEB-TACE, completion angiography is mandatory to check the disappearance of tumor blush and the persistence of vascular lake.

Contrast material pooling within the tumor is referred to as a vascular lake and is frequently seen in DEB-TACE (Fig. 7.4). Although the exact cause and hazard of vascular lake is still unknown, a vascular lake located in the liver surface is thought to be a main cause of HCC rupture after DEB-TACE. If a vascular lake is present and tumor margin abuts the liver surface, additional embolization using gelatin sponge particle is recommended to prevent tumor rupture.

Comparison between DEB-TACE and cTACE has been attempted, and controversial results have been published. Meta-analysis showed that there was no significant difference in progression-free survival and overall survival. Recent study which performed DEB-TACE in superselective fashion showed that DEB-TACE shortened progression-free survival than cTACE in small tumor less than 3 cm [19]. So far, in

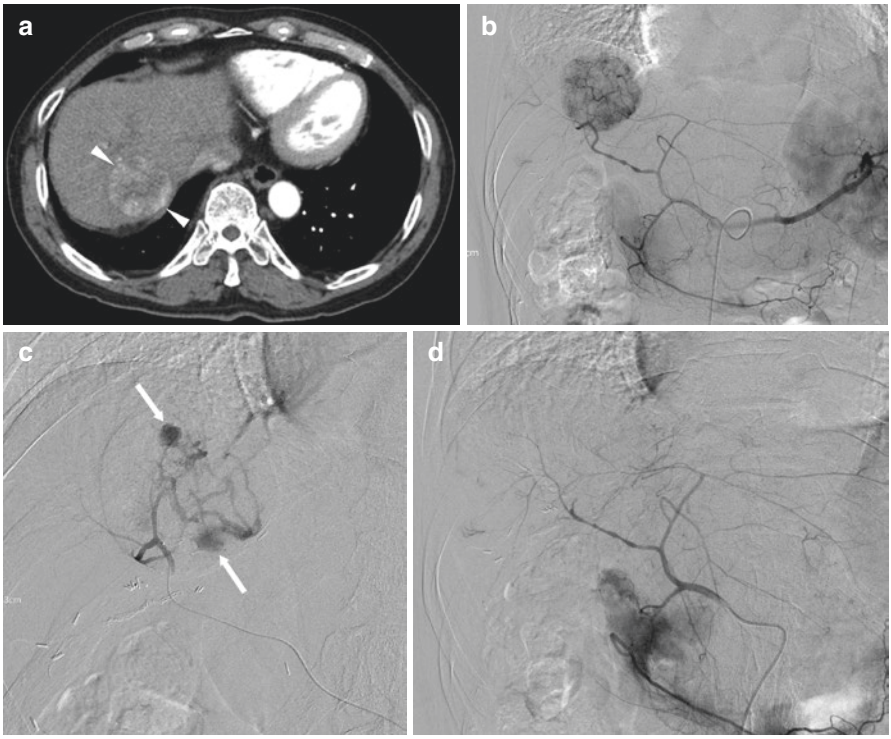

Fig. 7.4 A 72-year-old man has single nodular HCC. (**a**) CT scan of hepatic arterial phase shows a hypervascular tumor (arrowheads) in right lobe of the liver. (**b**) Celiac angiography shows nodular tumor staining in the right lobe of the liver. (**c**) Selective angiography of tumor-feeding artery obtained after embolization using drug-eluting beads shows vascular lakes (arrows) in the tumor staining. Additional embolization using gelatin sponge particles was performed to reach complete stasis of tumor-feeding artery. (**d**) Common hepatic angiography after DEB-TACE shows complete devascularization of the tumor

Asia, there has been no robust evidence favoring use of DEB-TACE over cTACE in terms of efficacy and cost-effectiveness, and cTACE is preferentially selected for small HCCs.

In terms of quality of life, DEB-TACE has less pain, milder postembolization syndrome, and shorter hospitalization than cTACE. A possible explanation for this difference is that the liver parenchyma has no pain sensory nerve, but liver capsule and portal triads sense the pain. Lipiodol emulsion can penetrate deeply into the peribiliary plexus and the liver capsule and irritate those structures.

Radioembolization

Radioembolization, also known as transarterial radioembolization (TARE), selective internal radiation therapy (SIRT), and Y90 therapy, is a transcatheter intra-arterial therapy using radioactive microspheres with yttrium 90 (Y90). The role of TARE in HCC treatments has not been fully established yet. Based on up-to-the-date literatures, TARE provides longer time to progression, higher quality of life, and shorter hospitalization compared with TACE, although the overall survival is comparable between TARE and TACE. In most Asian countries, TARE is performed in limited number of patients, because radioactive microspheres are expensive and not reimbursed by health insurance systems yet.

Indication

Patient selection and indication for TARE are similar with that of TACE. In Asia, economic status and private health insurance are important factors. Relative contraindication includes an ECOG score >2, serum bilirubin >2 mg/dl, Child-Pugh class > B8, excessive tumor burden (more than 70% of liver volume), and severe arterioportal shunt. Absolute contraindication is high lung shunt (>20%) or high lung dose (>30Gy).

Procedure

Planning angiography and ^{99}mTc-MAA nuclear scan is required to determine the radiation dose and to assess lung shunt fraction. Serious complications can develop when radioactive microspheres are infused into non-hepatic arteries such as the cystic artery, accessory left gastric artery, and right gastric artery. Therefore, preemptive coil embolization is usually performed during the planning angiography when the accessory left gastric arteries, right gastric arteries, hepatic falciform arteries, and esophageal branches from the replaced left hepatic artery are included in the target hepatic artery. Because cone-beam CT is very useful to identify the non-hepatic artery originating from the hepatic artery, the use of cone-beam CT is

mandatory in TARE. ^{99}mTc-MAA nuclear scan consists of planar image and SPECT/CT. Although lung shunt fraction is calculated using planar image, SPECT/CT may provide a critical information prior to TARE. SPECT/CT can clearly demonstrate the distribution of MAA on axial image, which can predict the tumor response. When focal high activity outside the liver is noted on SPECT/CT, angiographic image should be reviewed to detect a possible non-hepatic artery.

Standard technique includes delivery of radioactive microspheres into the lobar hepatic artery of target lobe with estimated radiation dose of 120Gy. For resin microspheres, partition model is commonly used with 120 Gy of desired radiation dose to tumor, 70 Gy of liver limiting dose, and 25 Gy of lung limiting dose. For glass microspheres, simple dosimetry is adopted with 120 Gy of perfused tissue volume without consideration of tumor volume.

Intensified radioembolization with selective catheterization at segmental hepatic artery, so called radiation segmentectomy, has become a curative option and feasible alternative of percutaneous ablation and surgical resection in small HCC (<3 cm). Ablative radiation dose up to 1000 Gy can be safely administered into one or two segments and induce complete necrosis of target tissue including tumor and surrounding normal liver, which results in complete atrophy of target segments same as surgical segmentectomy. Even in large tumor (>5 cm), superselective radioembolization with a boosted dose may have favorable tumor response using small caliber microcatheters (Fig. 7.5) [20]. To enhance the outcome of TARE, it is the easiest way to increase the desired radiation dose to the tumor as much as possible. To guarantee the safety of booted TARE, it is important to save normal liver from irradiation as much as possible.

Patients with insufficient future liver remnant (FLR) are contraindicated to surgical resection of HCC. Conventionally, for these patients, portal vein embolization (PVE) is preoperatively used to increase the FLR volume over 40%, which facilitates surgical resection in patients with cirrhosis. However, PVE delays surgical resection 1 or 2 months for FLR growth without controlling the tumor, which may drop out from the surgical lists due to tumor progression. In contrast, radiation lobectomy, lobar infusion of radioactive microspheres, can result in not only the volumetric increase of the untreated lobe but also tumor control. One disadvantage of radiation lobectomy-induced hypertrophy is that it requires longer time to achieve sufficient FLR growth than PVE.

Outcome

Compared to TACE, TARE has similar overall survival but a longer time to progression (TTP) according to the data from the Western countries. So far, clinical experiences with TARE in Asia are limited, and there is no large study with TARE from Asia. TARE also provides better quality of life after the procedure, as it requires shorter hospitalization times, fewer necessitated treatment sessions, and fewer visits to hospital than TACE. Because of the small size of radioactive microspheres, patients complain of only mild postembolization syndrome after the procedure,

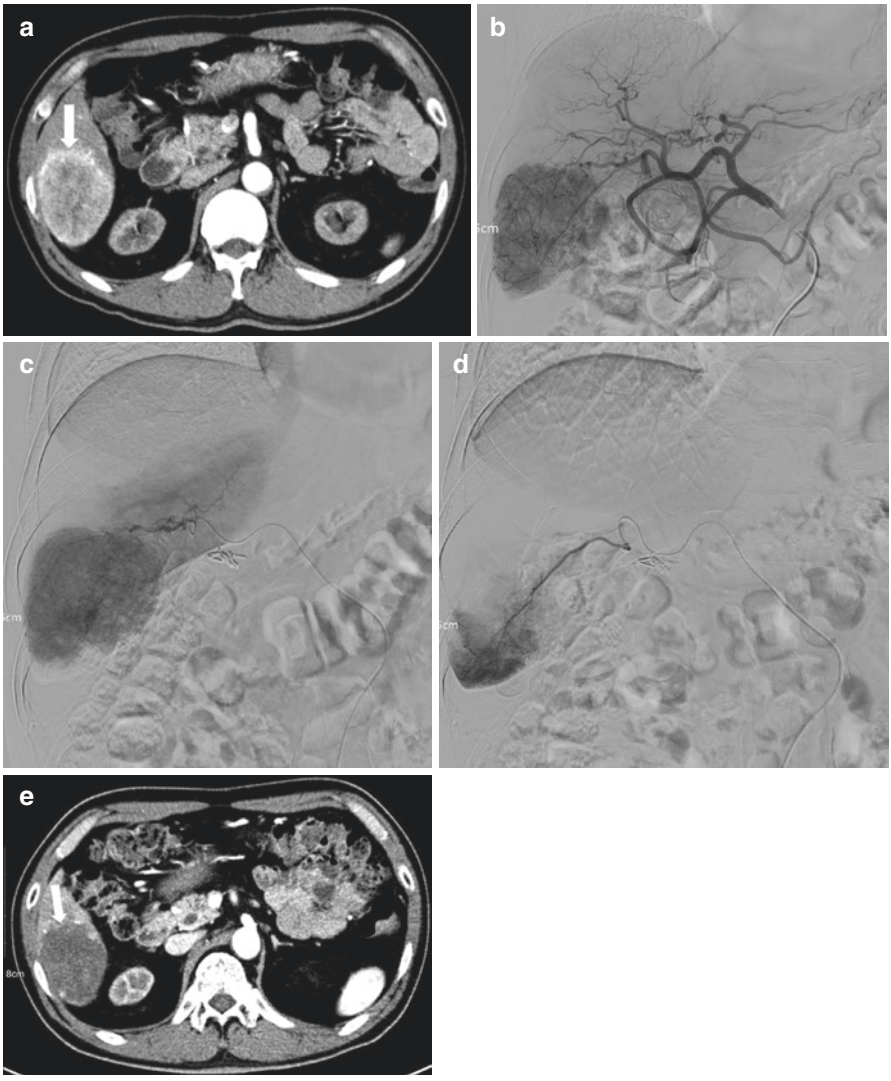

Fig. 7.5 A 49-year-old man has single nodular HCC. (**a**) CT scan of hepatic arterial phase shows a hypervascular tumor (arrow) in right lobe of the liver. (**b**) Common hepatic angiography shows nodular tumor staining in the right lobe of the liver. (**c**) Selective angiography of right posterior hepatic artery shows tumor staining. Radioactive microspheres were injected at this vessel, and radioactivity at administration was 3.82 GBq. (**d**) Selective angiography of tumor-feeding artery branching at the proximal right posterior hepatic artery shows tumor staining. Radioactive microspheres were injected at this vessel, and radioactivity at administration was 0.73 GBq. Total administered activity in this patient was 4.55 GBq, and estimated mean dose was 600 Gy. (**e**) CT scan of hepatic arterial phase obtained 1 month after radioembolization shows complete loss of tumoral enhancement (arrow)

which enables brief hospitalization or even outpatient-based treatment. Thus, TARE is commonly recommended for patients with large tumor burden who can afford it with expensive medical cost, when severe postembolization syndrome is expected if TACE is performed.

Oral sorafenib is considered the standard of care for BCLC C disease such as portal vein invasion. Recent RCTs showed that TARE had similar overall survival and less adverse event compared with sorafenib in patients with portal vein thrombosis. TACE followed by EBRT showed better outcome than TACE alone or sorafenib alone [6]. Thus, further comparative study between TARE vs TACE followed by EBRT is needed in patients with portal vein tumor thrombi.

Complication

Non-target radiation may result in serious complications such as radiation gastrointestinal ulcer and radiation cholecystitis which may need to be managed by surgical treatment. Most of these complications are preventable by comprehensive angiographic evaluation and careful review of cone-beam CT and SPECT/CT. Special caution is needed not to deliver radioactive microspheres into the cystic artery, although the incidence of radiation cholecystitis requiring surgical cholecystectomy is quite low. To prevent radiation cholecystitis, it is the best way to advance the microcatheter distal to the origin of the cystic artery. When a microcatheter cannot be placed distal to the origin of the cystic artery, temporary embolization of the cystic artery using retrievable coil may be considered as a valuable option. Accessory left gastric artery, right gastric artery, and falciform artery should be embolized by coils when left lobe of the liver is supposed to be treated. Embolization of gastroduodenal artery is no longer embolized routinely.

Provided that Y90 dosimetry is properly conducted in patients with acceptable lung shunt, radiation pneumonitis can be prevented. Y90 can be delivered via the right inferior phrenic artery, the most common extrahepatic collateral, with a special caution. Because the right inferior phrenic artery accompanies pulmonary shunting in approximately half of patients, the presence of pulmonary shunt can be detected on angiography and cone-beam CT prior to TARE via the right inferior phrenic artery. The common cause of pulmonary shunting is a prominent azygoesophageal branch of right inferior phrenic artery. Embolization of azygoesophageal branch, if present, with coils, PVA particles, or gelatin sponge particle is needed to prevent radiation pneumonitis. When pleural disease is present, diffuse pulmonary shunt from the inferior phrenic artery is commonly observed. In this situation, bland embolization using PVA particles may induce redistribution of blood supply from the hepatic artery.

The classical manifestation of radiation-induced liver disease includes anicteric ascites, increased alkaline phosphatase levels, and thrombocytopenia. The exact safety dose for the liver is not yet established, and the actual absorbed dose to the nontumorous liver during TARE is hard to be estimated. However, one simple principle to prevent radiation-induced liver disease is to avoid whole liver irradiation in a single treatment or sometimes even in a sequential treatment.

Ablation

Radiofrequency ablation (RFA) is the most widely used ablation technique for HCC. In a patient with a small HCC less than 2 cm in diameter, who is not a potential candidate for liver transplantation, RFA may serve as a first-line therapy alternative to surgical resection. Generally, RFA can be performed in single nodule or oligo nodules (3 or less and less than 3 cm in diameter) with good local tumor control and acceptable complication rates. RFA is less invasive than surgical resection; however, RFA has the higher rate of local tumor progression (LTP) compared to surgical resection. Tumor size and ablation margin are well-known risk factors for the development of LTP after RFA for HCC. Therefore, for achieving complete ablation of HCC, a larger ablation volume has been created by multiple-electrode RFA or combined treatment of TACE and RFA.

The use of multiple electrodes for RFA has the advantage of larger ablation volume and the possibility of the "no-touch" ablation technique. Traditionally, RFA of the HCC has been performed by inserting a single electrode into the central portion of the tumor. Thus, there is a potential risk of tract seeding or peritoneal seeding reported up to 2.8%. In addition, if the electrode is inserted off center into the tumor, the chance of LTP can be increased due to incomplete ablation. The "no-touch" technique indicates that multiple electrodes are inserted into the normal liver along the tumor margin. It can achieve a larger ablation volume with sufficient ablation margin and no risk of track seeding during the RFA procedure. Compared with RFA using single electrode, the "no-touch" ablation using multiple electrodes had lower 5-year cumulative incidence of LTP (7.1% vs 28.7%) [21]. However, due to the multiple electrode insertion and the larger ablation volume, the possibility of major complications such as bleeding would also be increased.

Recently, microwave ablation and cryoablation are getting popularity. The advantage of microwave ablation over RFA is that treatment efficacy is less affected by vessels near the tumor and the ablation size is larger. Cryoablation has the advantage of less procedural pain and monitoring the ablation extent because the ice ball shows a clear margin on guiding image. Moreover, cryoablation can be safely performed the tumor near heart or liver surface without injury to the adjacent organ.

Multimodality Treatment

It has been proposed that TACE might be combined with other local treatments to obtain a synergistic effect on tumor necrosis. Combination with RFA and EBRT has been studied, and better results were reported with the combination treatment than with either of these therapies alone.

TACE eliminates the heat sink effect by blood flow; thus, it induces a larger ablation area by RFA. Combined treatment of TACE and RFA can reduce LTP in patients with medium-sized tumor (3–5 cm). However, in case of small HCC (less than 3 cm), the enhanced therapeutic efficacy from the combined treatment is controversial. Considering the increased medical cost and patient discomfort of additional TACE, it may be reasonable to restrict this combined treatment to medium size tumor.

The combination of TACE and EBRT is commonly used to treat portal vein and inferior vena cava tumor thrombus to enhance the therapeutic effect by TACE.

TACE induces local hypoxia that in turn increases angiogenic factors, such as vascular endothelial growth factor (VEGF). In contrast, sorafenib inhibits the activity of VEGF receptors and other proangiogenic signaling pathways. Therefore, sorafenib administration during and after TACE may counteract hypoxia-induced angiogenesis and potentially reduce tumor recurrence. However, a recent RCT showed that sorafenib combined with cTACE did not improve OS in patients with advanced HCC, compared with sorafenib alone [22].

Unique Treatment Option in the EAST

Hepatic Arterial Infusion Chemotherapy (HAIC)

Compared with systemic chemotherapy, the cytotoxic anticancer drugs are directly infused into the hepatic artery in HAIC. HAIC has the potential to deliver higher local concentrations of drugs to the tumor with reduced systemic reactions. HAIC is widely used for patients with advanced HCC with/without PVTT in Asia, especially in Japan, Korea, and China [23]. The most common regimens are 5-fluorouracil and cisplatin, alone or in combination. Patients undergo catheter placement in the hepatic artery, and chemotherapeutic drugs are continuously infused through a subcutaneously implanted port system. For proper drug distribution throughout the liver, the gastroduodenal artery and right gastric artery are commonly embolized with coils. Whereas HAIC is not recommended as first-line therapy for patients with PVTT in Korean and Chinese guidelines, HAIC is recommended in parallel with hepatectomy, TACE, and molecular targeted therapy for patients with PVTT without extrahepatic metastasis in Japanese guideline. In addition, HAIC is recommended as second-line option in multinodular HCC more than three nodules without vascular invasion in Japanese guideline. In Korean guideline, HAIC might be considered for patients with progressive HCC and portal vein invasion for whom systemic therapies have failed or cannot be used and who still have both good liver function and good performance status.

Transarterial Ethanol Ablation (TEA)

Ethanol can cause endothelial damage and thrombosis when it is infused into the artery, so is commonly used for arteriovenous malformation. Transarterial ethanol ablation (TEA) is a variant of TACE and involves the use of Lipiodol and ethanol mixture. When mixture of Lipiodol and ethanol in a 2:1 ratio is infused into the hepatic artery, long-lasting embolization of both the arterioles and portal venules is highly effective in causing the infarction of the tumor and surrounding tumor border. The ablative effect of ethanol may result in better tumor response and longer progression-free survival when compared with cTACE [24]. Since TEA is performed in limited institutes, particularly in Hong Kong, it is not included in the guideline by the Asian Pacific Association for the Study of the Liver (APASL).

Endovascular Placement of an Iodine-125 Seed

Radioactive seed implantation for the treatment of a various tumors has a long history, especially in prostate tumors. The endovascular implantation of iodine-125 seeds in the PVTT has been tried in many Chinese centers. Iodine-125 has a half-life of 59.4 days, and effective irradiating range is 2 cm. The iodine-125 seeds is prepared in a strand and implanted directly into the PVTT via percutaneous transhepatic approach. Because of limited availability of iodine-125 seed, endovascular implantation of iodine-125 seeds is seldom performed in other countries except China [25].

Key Points

1. Conventional chemoembolization using Lipiodol is a mainstay among intra-arterial therapies in unresectable HCC in the EAST.
2. Superselective catheterization technique is actively applied to guarantee better outcome and safety of chemoembolization and radioembolization.
3. In small HCCs, conventional chemoembolization revealed better local tumor control than DEB-TACE.
4. In general, the indication of intra-arterial therapies in eastern countries is wider than that in western countries. In HCC with major portal vein invasion, conventional chemoembolization combined with external beam radiotherapy revealed survival advantage over sorafenib alone in a randomized controlled trial.
5. Even though there are multiple regional or national practice guidelines for managing HCCs in Asia [26–30], choice of treatment option is still variable depending on the countries, institutes, and medical insurance system as well as tumor stage and liver function.

References

1. Kim BH, Park JW. Epidemiology of liver cancer in South Korea. Clin Mol Hepatol. 2018;24(1):1–9.
2. Llovet JM, Ricci S, Mazzaferro V, Hilgard P, Gane E, Blanc JF, et al. Sorafenib in advanced hepatocellular carcinoma. N Engl J Med. 2008;359(4):378–90.
3. Cheng AL, Kang YK, Chen Z, Tsao CJ, Qin S, Kim JS, et al. Efficacy and safety of sorafenib in patients in the Asia-Pacific region with advanced hepatocellular carcinoma: a phase III randomised, double-blind, placebo-controlled trial. Lancet Oncol. 2009;10(1):25–34.
4. Kudo M, Finn RS, Qin S, Han KH, Ikeda K, Piscaglia F, et al. Lenvatinib versus sorafenib in first-line treatment of patients with unresectable hepatocellular carcinoma: a randomised phase 3 non-inferiority trial. Lancet. 2018;391(10126):1163–73.
5. Lee JH, Lee JH, Lim YS, Yeon JE, Song TJ, Yu SJ, et al. Adjuvant immunotherapy with autologous cytokine-induced killer cells for hepatocellular carcinoma. Gastroenterology. 2015;148(7):1383–91.
6. Yoon SM, Ryoo BY, Lee SJ, Kim JH, Shin JH, An JH, et al. Efficacy and safety of transarterial chemoembolization plus external beam radiotherapy vs sorafenib in hepatocellular carcinoma with macroscopic vascular invasion: a randomized clinical trial. JAMA Oncol. 2018;4(5):661–9.
7. Yang HJ, Lee JH, Lee DH, Yu SJ, Kim YJ, Yoon JH, et al. Small single-nodule hepatocellular carcinoma: comparison of transarterial chemoembolization, radiofrequency ablation, and hepatic resection by using inverse probability weighting. Radiology. 2014;271(3):909–18.
8. Chung GE, Lee JH, Kim HY, Hwang SY, Kim JS, Chung JW, et al. Transarterial chemoembolization can be safely performed in patients with hepatocellular carcinoma invading the main portal vein and may improve the overall survival. Radiology. 2011;258(2):627–34.
9. Song SY, Chung JW, Yin YH, Jae HJ, Kim HC, Jeon UB, et al. Celiac axis and common hepatic artery variations in 5002 patients: systematic analysis with spiral CT and DSA. Radiology. 2010;255(1):278–88.
10. Miyayama S, Matsui O, Yamashiro M, Ryu Y, Kaito K, Ozaki K, et al. Ultraselective transcatheter arterial chemoembolization with a 2-f tip microcatheter for small hepatocellular carcinomas: relationship between local tumor recurrence and visualization of the portal vein with iodized oil. J Vasc Interv Radiol. 2007;18(3):365–76.
11. Kim HC, Chung JW, Lee W, Jae HJ, Park JH. Recognizing extrahepatic collateral vessels that supply hepatocellular carcinoma to avoid complications of transcatheter arterial chemoembolization. Radiographics. 2005;25(Suppl 1):S25–39.
12. Llovet JM, Real MI, Montaña X, Planas R, Coll S, Aponte J, et al. Arterial embolisation or chemoembolisation versus symptomatic treatment in patients with unresectable hepatocellular carcinoma: a randomised controlled trial. Lancet. 2002;359:1734–9.
13. Lo CM, Ngan H, Tso WK, Liu CL, Lam CM, Poon RT, et al. Randomized controlled trial of transarterial lipiodol chemoembolization for unresectable hepatocellular carcinoma. Hepatology. 2002;35:1164–71.
14. Llovet JM, Bruix J. Systematic review of randomized trials for unresectable hepatocellular carcinoma: chemoembolization improves survival. Hepatology. 2003;37(2):429–42.
15. Takayasu K, Arii S, Kudo M, Ichida T, Matsui O, Izumi N, et al. Superselective transarterial chemoembolization for hepatocellular carcinoma. Validation of treatment algorithm proposed by Japanese guidelines. J Hepatol. 2012;56:886–92.
16. Ikeda M, Arai Y, Park SJ, Takeuchi Y, Anai H, Kim JK, et al. Prospective study of transcatheter arterial chemoembolization for unresectable hepatocellular carcinoma: an Asian cooperative study between Japan and Korea. J Vasc Interv Radiol. 2013;24:490–500.
17. Chung JW, Park JH, Han JK, Choi BI, Han MC, Lee HS, et al. Hepatic tumors: predisposing factors for complications of transcatheter oily chemoembolization. Radiology. 1996;198(1):33–40.

18. Lee M, Chung JW, Lee KH, Won JY, Chun HJ, Lee HC, et al. Korean multicenter registry of transcatheter arterial chemoembolization with drug-eluting embolic agents for nodular hepatocellular carcinomas: six-month outcome analysis. J Vasc Interv Radiol. 2017;28(4):502–12.
19. Lee IJ, Lee JH, Lee YB, Kim YJ, Yoon JH, Yin YH, et al. Effectiveness of drug-eluting bead transarterial chemoembolization versus conventional transarterial chemoembolization for small hepatocellular carcinoma in Child-Pugh class A patients. Ther Adv Med Oncol. 2019;11:1758835919866072.
20. Kim HC, Kim YJ, Lee JH, Suh KS, Chung JW. Feasibility of boosted radioembolization for hepatocellular carcinoma larger than 5 cm. J Vasc Interv Radiol. 2019;30(1):1–8.
21. Hocquelet A, Aubé C, Rode A, Cartier V, Sutter O, Manichon AF, et al. Comparison of no-touch multi-bipolar vs. monopolar radiofrequency ablation for small HCC. J Hepatol. 2017;66(1):67–74.
22. Park JW, Kim YJ, Kim DY, Bae SH, Paik SW, Lee YJ, et al. Sorafenib with or without concurrent transarterial chemoembolization in patients with advanced hepatocellular carcinoma: the phase III STAH trial. J Hepatol. 2019;70(4):684–91.
23. Kudo M, Ueshima K, Yokosuka O, Ogasawara S, Obi S, Izumi N, et al. Sorafenib plus low-dose cisplatin and fluorouracil hepatic arterial infusion chemotherapy versus sorafenib alone in patients with advanced hepatocellular carcinoma (SILIUS): a randomised, open label, phase 3 trial. Lancet Gastroenterol Hepatol. 2018;3(6):424–32.
24. Yu SC, Hui JW, Hui EP, Chan SL, Lee KF, Mo F, et al. Unresectable hepatocellular carcinoma: randomized controlled trial of transarterial ethanol ablation versus transcatheter arterial chemoembolization. Radiology. 2014;270(2):607–20.
25. Yang M, Fang Z, Yan Z, Luo J, Liu L, Zhang W, et al. Transarterial chemoembolisation (TACE) combined with endovascular implantation of an iodine-125 seed strand for the treatment of hepatocellular carcinoma with portal vein tumour thrombosis versus TACE alone: a two-arm, randomised clinical trial. J Cancer Res Clin Oncol. 2014;140(2):211–9.
26. Yau T, Tang VY, Yao TJ, Fan ST, Lo CM, Poon RT. Development of Hong Kong Liver Cancer staging system with treatment stratification for patients with hepatocellular carcinoma. Gastroenterology. 2014;146(7):1691–700.e3.
27. Omata M, Cheng AL, Kokudo N, Kudo M, Lee JM, Jia J, et al. Asia-Pacific clinical practice guidelines on the management of hepatocellular carcinoma: a 2017 update. Hepatol Int. 2017;11(4):317–70.
28. Kokudo N, Takemura N, Hasegawa K, Takayama T, Kubo S, Shimada M, et al. Clinical practice guidelines for hepatocellular carcinoma: the Japan Society of Hepatology 2017 (4th JSH-HCC Guidelines) a 2019 update. Hepatol Res. 2019;49(10):1109–13.
29. Zhou J, Sun HC, Wang Z, Cong WM, Wang JH, Zeng M, et al. Guidelines for diagnosis and treatment of primary liver cancer in China (2017 edition). Liver Cancer. 2018;7(3):235–60.
30. Korean Liver Cancer Association; National Cancer Center. 2018 Korean Liver Cancer Association-National Cancer Center Korea practice guidelines for the management of hepatocellular carcinoma. Gut Liver. 2019;13(3):227–99.

Chapter 8
Intrahepatic Cholangiocarcinoma

Sarah B. White and Dilip Maddirela

Introduction

Cholangiocarcinoma (CCA) is the second most common primary liver cancer with a 5-year survival rate of approximately 5% and typical survival times of 5–13 months [1]. Although its incidence and mortality rates have been increasing worldwide at a rate higher than hepatocellular carcinoma (HCC), an escalating concern to the healthcare system in the United States was observed with significant rise in the frequency of CCA-related hospital admissions and associated costs from CCA between 1997 and 2012 [2]. CCA is a male predominant, rare disease, usually diagnosed in the advanced stages, when it is unresectable in patients >70 years and is highly resistant to chemotherapy [3, 4]. Since intrahepatic cholangiocarcinoma (ICC) can remain clinically silent, patients are diagnosed at advanced stages, with few patients meeting eligibility criteria for resectable disease. Survival without treatment is less than a year. Some of the recognized risk factors for CCA include infection with liver flukes, hepatolithiasis, dietary or endogenous nitrosamine compounds, and primary sclerosing cholangitis [5]. Reviews on CCA indicate that perihilar disease represents about 50%, distal disease 40%, and intrahepatic disease less than 10% of CCA cases [6]. A treatment algorithm is presented in Fig. 8.1 [7]. Palliative treatments including systemic therapy alone or in combination with radiation therapy are not curative and have high associated toxicities. Alternatively, image-guided locoregional therapies, such as transarterial chemoembolization (TACE), radiofrequency ablation (RFA), and transarterial radioembolization (TARE), have been

S. B. White (✉)
Department of Radiology, Division of Vascular and Interventional Radiology, Medical College of Wisconsin, Froedtert Memorial Lutheran Hospital, Milwaukee, WI, USA
e-mail: sbwhite@mcw.edu

D. Maddirela
Department of Radiology, Medical College of Wisconsin, Wauwatosa, WI, USA
e-mail: dmaddirela@mcw.edu

C. Georgiades, H. S. Kim (eds.), *Image-Guided Interventions in Oncology*,
https://doi.org/10.1007/978-3-030-48767-6_8

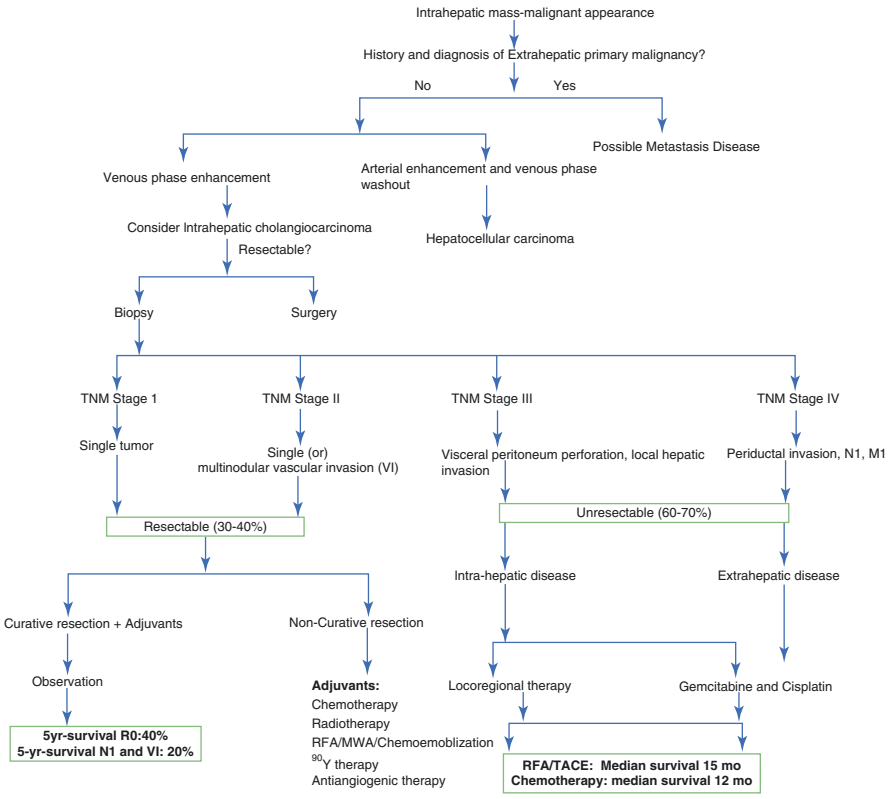

Fig. 8.1 Suggested algorithm for patients with intrahepatic cholangiocarcinoma, partially adopted from Bridgewater et al. [7]. *Abbreviations*: MWA microwave ablation, RFA radiofrequency ablation, TACE transarterial chemoembolization

shown to improve survival in unresectable ICC with minimal associated toxicities [8]. With the advances in treatment techniques and clinical outcomes, recent focus has shifted to maximizing clinical efficacy by using combining IAT with systemic therapy. We will present here the outcomes of conventional TACE (cTACE), drug-eluting bead TACE (DEB-TACE) or TARE providing an overview of the clinical evidence for the use of IAT for unresectable ICC. A summary of clinical trials utilizing different treatment modalities for ICC is seen in Table 8.1.

Treatment Options for Intrahepatic Cholangiocarcinoma

Systemic Therapy

When patients are deemed unresectable or have undergone surgical resection and have recurrence, systemic therapy should be considered. Since 2010, gemcitabine and cisplatin still remain the first-line treatment for advanced ICC, and clinical

Table 8.1 Summary of studies evaluating intra-arterial treatment modalities for intrahepatic cholangiocarcinoma

Treatment modality studied	Authors	No. of patients	Agent utilized	Toxicities	Disease control	Median overall survival (months)
Systemic therapy	Valle et al. ABC-02 [9]	410	Cis + Gem vs. Gem	Decreased liver function: 27% Gem group, 16.7% Cis-Gem group	Tumor control 81.4% Cis plus Gem, 71.8% Gem alone	11.7
	Okusaka et al. [10]	83	Cis + Gem vs. Gem	Neutropenia: 56.1% Gem plus Cis arm, Gem arm 38.1%, thrombocytopenia: 39% Gem plus Cis arm, 7.1% Gem arm, leukopenia: 29.3% Gem plus Cis arm, 19.0% Gem arm	68.3% Gem plus Cis arm, 50.0% Gem arm	11.2
Transarterial chemoembolization	Kim et al. [11]	49	TACE, TACI, Cis	>90 % with Grade 1	55% (Radiologic response)	12 Hypervascular tumors: 15
	Kiefer et al. [12]	62	CAM TACE and PVA	1.6 % Grade 1 pulmonary edema and elevated cardiac enzymes (n = 1), (grade 4), acute renal failure (n = 1),	73% (RECIST)	20
	Gusani et al. [13]	42	TACE regimen with Gem, Cis, and Oxal	Grade 1–2, acute myocardial infarction, hepatic abscess, thrombocytopenia 4% Grade 4	Survival (RECIST) vs. SD 13.1vs. 6.9 PD)	9.1
	Vogl et al. [14]	115	Gem, Cis, mitomycin-C	13% grade 1	PR, 8.7%, SD 57%, PD 33.9% (RECIST)	13
	Yang et al. [15]	26	Gem, Oxal (cTACE in combination with microwave ablation)	Fever 88% mild-to-moderate pain 84.6% thrombocytopenia 11.5%	ECOG 0-2	19.5

(continued)

Table 8.1 (continued)

Treatment modality studied	Authors	No. of patients	Agent utilized	Toxicities	Disease control	Median overall survival (months)
Drug-eluting embolic transarterial chemoembolization	Kuhlmann et al. [16]	26	Irinotecan/DC/LC beads	26% Grade III or IV	66% (RECIST)	iDEB-TACE 11.7 vs. cTACE 5.7 vs. Oxal plus Gem 11.0
	Poggi et al. [17]	20	Oxal-eluting microspheres TACE vs. Oxal and Gem	Pain, nausea, and vomiting, asthenia, elevated AST, ALT	44% (4/9) of patients achieved partial responses and 56% (5/9) stabilization of disease	ChT plus TACE 30 vs. ChT 12.7
^{90}Y-transarterial radioembolization	Al-Adra et al. [18]	298	^{90}Y-microspheres	20–70% Grade 1 19.3% Grade ≥2 7.9% Grade 3 0.9% Grade 4	28% PR, 54% SD	15.5
	Hoffmann et al. [19]	33	Resin ^{90}Y-microspheres	84% abdominal pain	28.3% CA 19-9	22
	Rafi et al. [20]	19	Resin ^{90}Y-microspheres	21% fatigue 32% abdominal pain 5.2% Grade 3	11% PR 13% SD 21% PD	11.5
	Mouli et al. [21]	46	Glass ^{90}Y-microspheres	54% fatigue, 28% transient abdominal pain, 9% Grade 3, 2% gastroduodenal ulcer	WHO imaging: 25% PR, 73% SD; EASL imaging: 73% PR, 27% SD	Solitary lesion 14.6 months vs. multifocal lesions 5.7 months
Comparison of intra-arterial therapies	Hyder et al. [22]	198	DEB, TAE, or ^{90}Y	21% Grade 1	35% (mRECIST)	TACE 13.4. vs. DEB 10.5 TAE 14.3 ^{90}Y11.3

Abbreviations: *RECIST* response evaluation criteria in solid tumors, *mRECIST* modified response evaluation criteria in solid tumors, *ECOG* Eastern Cooperative Oncology Group, *DEB* drug eluting beads, *iDEB* irinotecan-eluting beads, *cTACE* conventional transarterial chemoembolization, *TAE* transarterial embolization, *TACI* transarterial chemo infusion, *^{90}Y* radioembolization, *ChT* chemotherapy, *CAM* cisplatin, adriamycin, and mitomycin, *Gem* gemcitabine, *Cis* cisplatin, *Oxal* oxaloplatin, *PVA* polyvinyl alcohol, *SD* stable disease, *PD* progressive disease, *PR* partial response, *AST* aspartate transaminase, *ALT* alanine aminotransferase

studies were conducted in various centers with this combination. Valle et al. [23] performed a meta-analysis comprised of individual patient data from two prospective, randomized, controlled trials (the United Kingdom ABC-02 phase III study ($n = 410$) and Japanese BT22 randomized phase II study ($n = 84$)) in advanced biliary tract cancer, treated with either gemcitabine alone, or cisplatin plus gemcitabine. The analysis revealed that the use of combination therapy reduced the risk of progression by 36% and risk of the death by 35% compared to gemcitabine alone. The median OS in the combination arms of the two studies were 11.7 and 11.1 months, respectively, indicating the consistency of the treatment effect. The combination of cisplatin and gemcitabine exhibited significant improvement in PFS (HR = 0.64, 95% (CI) 0.53–0.76, $p < 0.001$] and OS (HR = 0.65, 95% CI 0.54–0.78, $p < 0.001$) over gem alone. Patients with a good PS (0–1) benefited more from combination therapy (HR for PFS and OS were 0.61 (95% CI 0.51–0.74) and 0.63 (95% CI 0.53–0.77), $p < 0.001$, respectively). Gem and cis combination therapy improved PS and OS in both intra- and extrahepatic CCA and gall bladder cancer. Although the ampullary group showed the reduced risk of 25% and 30%, the small number of patients in this cohort did not result in these results being statistically significant. Newer studies are now coming out reporting even better response rates with improvement in OS when gem/cis is combined with nab-paclitaxel.

Intra-arterial Directed Therapies

Conventional Transarterial Chemoembolization

Conventional transarterial chemoembolization (TACE) has been used as a successful tool for ICC. Several retrospective and few prospective studies of cTACE revealed a range of survival times; however, neither the technique nor the drugs used in the emulsion were standardized. Therefore, the studies represent a diverse set of patients, with a wide range of outcomes. Burger et al. [24] retrospectively studied cTACE in unresectable ICC. In this study, a total of 17 patients who underwent cTACE from 1995 to 2004 were evaluated. The cTACE regimen consisted of cisplatin, doxorubicin, and mitomycin-C, followed by embolization with polyvinyl alcohol (PVA) or embosphere particles. Of the 17 patients, 15 were Child-Pugh class A, 14 of 17 had an ECOG PS <2. The median OS was found to be 23 months, and 82% of patients tolerated the procedure without side effects. Two patients (12%) with unresectable disease underwent successful resection after cTACE, and one (6%) had a fatal outcome after TACE.

In the largest series, evaluating IAT for ICC, Vogl et al. [14] retrospectively analyzed 115 patients who underwent cTACE. These patients underwent 819 cTACE. The study compared the effectiveness of 4 different drug regimens of chemotherapy (mitomycin-C alone, gemcitabine alone, mitomycin+gemcitabine, and mitomycin+gemcitabine+cisplatin). The clinical outcomes demonstrated a partial response rate of 8.7%, stable disease in 57.4%, and progressive disease in 33.9% of

patients. The mean and median OS was 13 and 20.8 months; survival rates were 52%, 29% and 10% at 1-, 2- and 3 years, respectively, after cTACE treatment. No significant difference was seen among the patients treated with different protocols. Child-Pugh class A patients had statistically significant improvement in OS, while Child-Pugh class B, tumor hypovascularity, and progressive disease were poor prognostic factors for patient's survival.

Another retrospective study evaluated 42 patients with recurrent ICC after hepatic resection [25]. In this patient cohort, cTACE was performed in nine patients with early recurrence. Prognostic factors that significantly affected survival outcomes were identified and included: tumor size of >5 cm (HR, 4.682; 95% CI, 1.092–20.074; $p = 0.022$), cTACE (HR, 0.239; 95% CI, 0.055–1.039; $p = 0.039$), AJCC stage 3 and 4 (HR, 6.370; 95% CI, 2.420–16.770; $p < 0.001$), lymph node metastasis (HR, 3.968; 95% CI, 1.654– 9.521; $p = 0.001$), and CA19-9 >35 kU/L (HR, 2.968; 95% CI, 1.000–8.809; $p = 0.040$). The OS of the patients in the cTACE group demonstrated significantly prolonged survival outcomes (1-year, 88.9%; 3-year, 77.8%; 5-year, 66.7%), compared to the patients not treated with TACE (1-year, 63.6%; 3-year, 30.8%; 5-year, 13.0%). Halappa et al. [26] also retrospectively analyzed early response in a group of 29 patients with unresectable CCA treated with TACE between 2005 and 2010. To assess response, they utilized volumetric apparent diffusion coefficient (ADC) changes. A total of 69 TACE procedures were performed. No additional salvage therapies were given after treatment with TACE. A significant change in the mean volumetric ADC from 1.54×10^{-3} mm^2/s to 1.92×10^{-3}/s ($p < 0.0001$) was seen. A significant increase in mean volumetric ADC and volumetric ADC above threshold level of 1.60×10^{-3}/s ($p < 0.002$) and 60 or greater ($n = 12$; log-rank test, $p < 0.009$) was observed in patients who demonstrated improved survival of 10 months or more. Therefore, changes in ADC measurement could be used to stratify the patients as responders and nonresponders. The results suggest a significant survival of 19 vs 8 months for ≥45% cutoff and 42 vs 17 months for ≥60% cutoff. Though tumor size did not change 1 month after treatment, treatment with TACE improved 25.1% increase in ADC.

Drug-Eluting Bead Therapy

Drug-eluting bead therapy is a minimally invasive procedure, which allows embolization and local release of chemotherapy in unresectable tumors, through intra-arterial delivery of microspheres acting as a drug carrier. Kuhlmann et al. [16] compared DEB-IRI (irinotecan 200 mg; DC/LC Beads, $n = 26$) with cTACE (mitomycin-c 15 mg; gelfoam; $n = 10$) and systemic chemotherapy (gemcitabine and oxaliplatin; $n = 31$) and found that DEBIRI was more effective than cTACE. Seven patients (26.9%) had recevied prior systemic chemotherapy in the DEBIRI group. When compared to cTACE and systemic chemotherapy, the DEBIRI group showed prolonged median OS (DEBIRI 11.7 months, cTACE 5.7 months, gem/ox 11.0 months). On follow-up of patients treated with DEBIRI, 50% had progressive disease, 42% stable disease, and 1 patient had a partial response and underwent

surgical resection. Complications (>grade 3) for DEBIRI included abdominal pain ($n = 7$, 27%), hepatic abscess ($n = 1$, 4%), and pleural empyema due to biliary leakage ($n = 1$, 4%) and one death due to cirrhosis. Post-embolization syndrome was commonly observed in all patients with low-grade fever that lasted up to 2 weeks.

A meta-analysis of 16 studies [27] demonstrated the outcomes following chemotherapy based transarterial therapy in 542 patients with ICC and showed improved tumor response and survival benefit with acceptable toxicities compared with standard chemotherapy. The median OS from the date of diagnosis and initiation of transarterial therapy was 15.7 ± 5.8 months and 13.4 ± 6.7 months, respectively, with an average 1-year survival of 58 ± 14.5%. Based on RECIST criteria, one fourth of the reported subjects showed partial (21.2%) or complete response (1.6%) or stable disease (53.9%) and progressive disease (23.2%). Severe toxicities (National Cancer Institute/WHO grade >3) were reported in 84 subjects and evenly distributed hematological and non-hemotologic complications. Higher severe complication rates were reported in the articles published in 2010 or later compared to 2009 or before, particularly when irinotecan was used in two (30.8% and 30.6%) of three studies as the chemotherapy agent during TACE. Four deaths after TACE (<30 days) were reported with a mortality rate of 0.7%. All the studies observed post-embolization syndrome rates of 16–100%. No standard cTACE or DEB-TACE regimen was used. No significant difference was found in overall 1-year survival for patients treated with DEB vs TACE.

^{90}Y

Radioembolization is a powerful IAT with minimal associated toxicities. Rayar et al. [28] evaluated the combination of intra-arterial ^{90}Y radioembolization and systemic chemotherapy in 45 patients with large unresectable ICC. Of the initial 45 patients, combination therapy resulted in downstaging of 8 (18%) patients to complete resection. The median follow-up was 15.6 months after surgery. Five patients were still alive even at the end of the study period, and one patient was still alive after surgery. Only two patients experienced recurrences. Therefore, chemotherapy with ^{90}Y radioembolization treatment was an effective modality in downstaging initially nonresectable ICCs to resection.

Similarly, downstaging patients into surgical resectability is another application of locoregional therapy. Mouli et al. [21] evaluated 46 patients that underwent ^{90}Y, and 5 (11%) were downstaged to surgery. At follow-up (median 2.5 years), all five patients were alive after surgical resection and were treatment naïve before receiving ^{90}Y treatment. The treatment-related complications include gastroduodenal ulcer ($n = 1$, 2%). The WHO imaging findings suggest a partial response ($n = 11$; 25%), stable disease ($n = 33$; 73%), and progressive disease ($n = 1$; 2%). The survival was varied with multifocal vs solitary (5.7 months vs 14.6 months), infiltrative vs solitary (6.1 months vs 15.6 months), and bilobar vs unilobar disease (10.9 months vs 11.7 months).

Al-Adra et al. [18] systematically reviewed survival and radiological response after radioembolization with ^{90}Y microspheres for unresectable ICC in the salvage

setting. Twelve studies were pooled, 7 prospective, and 5 retrospective and included 298 patients, and the number of patients in each study ranged from 2 to 46. The median follow-up was 10.8 months (range 6–29 months). The data demonstrated that 54% of patients had prior systemic chemotherapy and 33% had prior surgical resection. The mean number of ^{90}Y treatments was 1.5. The median OS was 15.5 months, and the mean OS was 17.7 months. The mean response after ^{90}Y therapy showed partial response in 28% and stable disease in 54% of patients at 3 months. Conversion to resectability was only assessed in 73 patients, and in that cohort 7/73 (10%) were downstaged to resection. The common morbidities following ^{90}Y included fatigue (33%), abdominal pain (28%), and nausea (25%).

In an attempt to assess OS of unresectable ICC, Mosconi et al. [29] carried out a retrospective study between 2010 and 2015 in 23 patients with ICC treated with radioembolization. The analysis shows a median OS of 17.9 months (95% CI:14.3–21.4 months). 17 patients died during the follow-up of 16 months (range: 2–52 months). The cumulative survival rate was 67.9% at 1 year and 20.6% at 2 years. Significantly longer survival was observed with four naïve patients compared to the patients in whom TARE was preceded by other treatments, including surgery (52 vs 16 months, $p = 0.009$). No statistically significant differences in OS were observed according to age, sex, ECOG, PVT, bilobar disease, and number of nodules or metastases at univariate analysis. The radiological response by RECIST did not show statistically significant differences in survival when using both mRECIST and the EASL criteria. ^{90}Y treatment in unresectable or recurrent ICC demonstrated a survival benefit especially in responders at 3 months as defined by mRECIST or the EASL criteria by measuring delayed-phase contrast enhancement and indicated as a safe treatment. Periprocedural adverse events occurred in ten patients with grade 1 or late complications at grade 3.

Due to ethical considerations and longer period to get the results, prospective and randomized trials are always challenging. Recently, White et al. [30] prospectively examined the survival of patients with unresectable, chemotherapy-refractory primary ICC treated with TARE. This study is a single arm; observational study was conducted between December 2013 and February 2017 at ten sites in England. In a total of 61 patients treated with TARE, 91% of patients had ECOG score of 0–1, 92% received prior chemotherapy, and 59% had no extrahepatic disease. Patients had follow-up of 13.9 months (95% CI, 9.6–18.1). At the end of the study, 54% deaths were recorded. The OS was 8.7 months (95% CI, 5.3–12.1), and 37% of patients survived to 12 months. PFS after TARE was 2.8 months and liver-specific PFS was 3.1 months (95% CI, 1.3–4.8). Abdominal pain (grade 1–2) was observed after TARE. A total of 49 adverse events occurred among 30 patients, of which 8% experienced grade $\geq$3.

Recently, a small phase Ib prospective study by Nezami et al. [31] evaluated combining gemcitabine, a potent radiosensitizer, with ^{90}Y in eight patients with unresectable ICC ($n = 5$) or hepatic metastases from pancreatic cancer (PC) ($n = 3$). Patients were initially treated with gemcitabine, followed by ^{90}Y and additional gemcitabine dosing following ^{90}Y. Seven out of 8 patients tolerated dose level 1 at 400 mg/m^2 and dose level 2 at 600 mg/m^2 of gemcitabine regime. The hepatic PFS

for all patients were 8.7 months, but for the ICC patients, it was 20.7 months. Neither treatment-related mortality observed during the first 30 days posttreatment period nor nontarget embolization based on post-^{90}Y bremsstrahlung SPECT/CT scan was observed. Treatment-related toxicities were minor, with all patients experiencing fatigue (n = 8, 100%) and 25% reporting mild abdominal pain.

A large multicenter retrospective study [22] assessed the safety and efficacy of IAT in patients with unresectable ICC in a large cohort of patients treated at five major hepatobiliary centers in the United States. The study examined various intra-arterial therapies (cTACE, 64.7%; DEB, 5.6%; bland embolization (TAE) 6.6% or TARE) with a median number of sessions of two (range 1–8) for ICC. The results indicated that IAT therapy was associated with an ORR in one third of the patients. Adverse events were relatively uncommon, with periprocedural morbidity of 29.8%. About one third of the patients in the study developed some type of complication, and in most cases, the complications were minor (n = 43). However, grade 3–4 complications (renal failure, hepatic failure, and liver abscess) were seen in 16 patients (8.1%). Complete or partial response was seen in 25.5% of patients, stable disease in 61.5% of patients, and 13% had progressive disease. The correlation between the mRECIST and EASL criteria was k = 0.62 for tumor response. The median time from IAT to progression was 1.6 months, 95% CI 1.4–1.9, noted among progressive disease. In this retrospective study, the median overall survival (OS) for all therapies was 13.2 months (cTACE 13.4 months vs DEB 10.5 months vs TAE, 14.3 months vs ^{90}Y, 11.3 months; p = 0.46), suggesting a promising survival period. Univariate analysis demonstrated that higher ECOG status at base line (hazard ratio (HR) 1.5, 95%, confidence interval (CI) 1.08–2.10), major complications (HR 1.76, 95% CI 1.05–2.97), and progressive disease (PD) (HR 2.35, 95% CI 1.44–3.82) predicated a worse overall survival. On multivariate analysis, tumor response was predictive of survival: complete response (CR)/partial response (PR) (HR 0.49, 95% CI 0.30–0.81) and PD (HR 2.45, 95% CI 1.47–4.09), median OS: 6.4 months. This study was limited by its small sample size with mixed population and biased selection of patients. It also had no control group provided for comparison of outcomes.

There is currently an ongoing prospective, multicenter, randomized controlled study, evaluating SIR-Spheres ^{90}Y resin microspheres followed by gem/cis alone vs gem/cis for first-line therapy in patients with ICC (SIRCCA). The primary endpoint of this study is survival at 18 months, with secondary endpoints including liver-specific PFS, PFS at any site, ORR, OS, AEs, and ability of patients to be down-staged to resection and/or ablation. Randomized patients are followed up until the end of the study or death. The results of the trial are anticipated to be forthcoming in 2021 (https://clinicaltrials.gov/ct2/show/NCT02807181 Accessed 28th September, 2019). Figure 8.2 is an illustrative case example where ^{90}Y was combined with systemic chemotherapy and patient had an OS from TARE of 19 months.

In summary, intra-arterial therapy offers a promising strategy for improving outcomes for patients with unresectable ICC. Median OS with systemic therapy alone is reported to be approximately 11 months. When IAT is utilized alone or in combination with systemic therapy, median OS is longer in all reported studies, and the

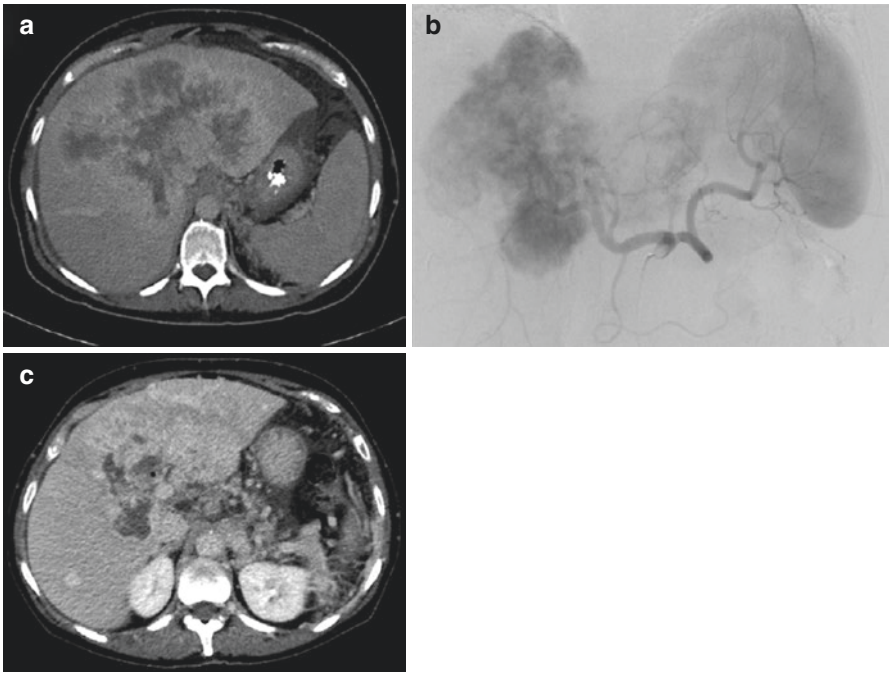

Fig. 8.2 A 63-year-old woman with intrahepatic cholangiocarcinoma, initially presented with abdominal pain and distension. CA-19-9 was 138.8. (**a**) Axial image from a contrast-enhanced CT demonstrated an 18 cm hepatic mass, peritoneal carcinomatosis and associated nodal enlargement. Biopsy revealed cholangiocarcinoma. The patient started on gem/cis, and after 11 months had a good response; however, 7 months after initiating chemotherapy, the patient developed pancytopenia that required multiple transfusions of platelets. The patient, therefore, was referred for radioembolization. (**b**) Digital subtraction angiographic image demonstrates an avidly enhancing ICC. The patient underwent radioembolization. (**c**) Axial image from a contrast-enhanced CT scan of the abdomen performed 18 months after ^{90}Y demonstrates residual disease. The patient died 19 months after TARE. *Abbreviations*: CT computed tomography, ICC intrahepatic cholangiocarcinoma, TARE transarterial radioembolization, ^{90}Y radioembolization

associated toxicities are minor. Additionally, downstaging to surgical resection was reported in 10–18% of patients with IAT. Therefore, integrating IAT into the treatment algorithm for ICC offers prolonged survival without severe impairment of quality of life and can result in curative resection.

Ablation Therapies

Although surgery is only curative treatment for unresectable ICC, its recurrence rate after surgery remains high (~70%), with a 5-year survival ranging from 20% to 40% [32]. Image-guided ablative therapies, radiofrequency ablation (RFA), and microwave ablation (MWA) are increasingly used and have become an acceptable

alternative for surgical treatment in the management of ICC. Ablation is minimally invasive and has low associated morbidity rates [33, 34] and is known for successful clinical outcomes of 80% [35]. Ablation therapies become first-line treatment with small recurrent tumors. The SEER database indicated sixfold ($p = 0.39$) increase in use of ablation therapy, nearly three in five patients undergoing resection in ICC [36]. Patient eligibility includes ablative margins of 0.5–1.0 cm surrounding tumors in unresectable ICC.

The clinical outcomes of RFA are based on small retrospective studies [33, 37–42]. The effectiveness of RFA is reported to be 90% even in the treatment of recurrent ICC with a 5-year survival of 20% after the treatment [40, 41]. In a largest series, 13 patients with 17 primary ICC experienced 88% of technical effectiveness with a tumor size of <5 cm when treated with RFA, but ablation was not effective in tumors >5 cm. Median local progression-free survival and OS periods were 32.2 and 38.5 months, respectively. The survival rates for 1-,3-, and 5 years were 85%, 51%, and 15%, respectively. When the tumors were 1–4 cm size, RFA exhibited higher technical success and median survival of 20 months [38]. Similarly, when the tumor was between 2.5 and 3.2 cm, >80% success rate with recurrence-free survival was reported [43]. However, RFA proved ineffective even in combination treatment with bland transarterial embolization, when lesion was >5 cm [8, 38]. The morbidity associated with RFA is liver abscess, pleural effusion, jaundice, local pain, and formation of biliary strictures.

Recently, Johannes Uhlig et al. retrospectively analyzed the benefit of local ablation in addition to chemotherapy, in patients with primary ICC, identified from National Cancer Database (2003–2015). Of the total 18,343 patients identified, 7462 (41%) received chemotherapy, and patients were 1:1 matched based on their propensity to receive combination therapy. The study included a propensity score-matched cohort comprised of 90 patients in each treatment group with balanced distribution of baseline variables and tumor factors, including tumor stage and grade. The combination treatment was associated with increase in OS compared to chemotherapy alone (HR = 0.6659, 95% CI: 0.4835–0.91; $p = 0.013$). Similarly, higher median OS was observed for patients, treated with ablation and chemotherapy (20.5 months) versus chemotherapy alone (12.5 months). Patients in the combination group had lower tumor stages and experienced fewer [44]. Recent systemic review from seven observational studies (84 patients) on the use of RFA for the treatment of ICC revealed pooled 1-, 3-, and 5-year survival rates of 82% (95% CI, 72–90%), 47% (95% CI, 28–65%), and 24% (95% CI, 11–40%), respectively [45]. Two patients experienced major complications (liver abscess and biliary stricture) and one died due to complications related to a liver abscess.

High-powered microwaves ablation (MWA) offers therapeutic effectiveness for solid malignancies, with higher intra-tumoral temperature, larger ablation volume, and less procedure duration. The survival outcomes with MWA for unresectable ICC includes 1-, 3-, and 5-year OS were 93.5%, 39.6%, and 7.9%, respectively [34]. A recent retrospective study [46] analyzed the survival, recurrence-free survival in 121 patients after hepatectomy and compared it to percutaneous MWA. Though the

estimated 5-year OS after MWA (23%) and surgery (21%) were almost similar, the major complication rates (MWA 3/56; 5.3%; surgery 9/65; 13.8%, $p < 0.001$) were higher after surgery than after MWA ($p < 0.001$). The estimated 3-year recurrence-free survival rates after MWA vs surgery were 33.1% vs 30.6%, respectively. The OS rate predictors for these estimates include tumor number ($p < 0.012$), ALB1 grade ($p = 0.007$) and metastasis ($p = 0.016$) [46]. The risk of local tumor progression was not significantly different for ICCs treated with MWA vs RFA (HF 2.72; 95% CI 0.58–12.84; $p = 0.321$) [47]. Reported complications of MWA include portal vein thrombosis and subscapular bleeding. Therefore, these ablation techniques offer promising benefit/risk balance, in multidisciplinary treatment strategy in unresectable ICC.

Radiation Therapy

Although ablation remains as curative option in unresectable cases and exhibits comparable results to primary resection, ablation is limited by tumor size and location. The role of radiation therapy in ICC is still not clearly outlined. However, with recent advances in dosimetry, patient positioning accuracy, organ motion assessment, and treatment planning, stereotactic body radiation therapy (SBRT) is being utilized to treat unresectable ICC [48]. A recent trial demonstrated [49] that patients undergoing SBRT ($n = 37$) had higher OS, compared with chemoradiation therapy (<5 Gy fraction with concurrent chemotherapy, $n = 61$), (HR = 0.44; 95% CI 0.21–0.91, $p = 0.028$) or TARE ($n = 72$) (HR = 0.42; 95% CI 0.11–0.84, $p = 0.014$) on multivariate analysis. The median OS for patients treated with SBRT or TARE or chemoradiation therapy was 48 months (95% CI 20), 20 months (95% CI 14–24), and 14 months (95% CI 11–20), respectively. A pilot study [50] included 9 patients with primary liver malignancies (8 HCC, 1 ICC), treated SBRT with 16 to 66 Gy in 1–3 fractions and reported ORR of 50% shrinkage, within the follow-up from 1.5 to 38 months. All patients developed fever and nausea.

A phase I study demonstrated that SBRT treatment (from palliative 24 Gy in 6 fractions to highly potent 54 Gy in 6 fractions) in ICC patients ($n = 10$) resulted in a median OS of 11.7 months (95% CI, 9.2–21.6 months) [51]. A recent large retrospective study (34 patients with 42 lesions) exclusively evaluated the efficacy of SBRT (30–40Gy) specifically for unresectable ICC or hilar CCA or positive margin patients with clinical follow-up every 3 months. The median follow-up was 38 months (range 8–71 months). At 4 years, local control was 79%, with a median OS of 17 months; median progression-free survival was 10 months. SBRT was well tolerated with only four grade 3 adverse events (12%) including duodenal ulceration, cholangitis, and liver abscess [52]. Another study indicated a higher duodenal radiation exposure with SBRT with severe duodenal/pyloric ulceration and duodenal stenosis [53]. Therefore, there is a risk of off target radiation to normal tissue near higher-dose areas while treating ICC with SBRT [54].

Combination of Systemic Therapy and Liver-Directed Therapies

Patients with ICC may benefit from surgery in terms of both survival and quality of life but with a higher risk of postoperative morbidity and mortality. The benefits of palliative systemic treatment and adjuvant therapy are meagre and absolutely need to be explored in phase III trials. Growing evidence demonstrate the continued need for research into the effectiveness of multimodal treatment, which will guide the ideal and the most effective treatment combinations for unresectable ICC. Patients with this disease with higher-grade tumor experience limited survival benefits with systemic treatment [36]. Earlier studies strongly suggest that the conversion of inoperable patients to surgery in a sequential treatment planning can be achieved through combination regimens, like cTACE, DEB-TACE, and ^{90}Y-RE with systemic therapies [1]. For example, the highest reported survival for the combination of various chemoinfusion and TACE was 30 months [24]. Due to the rarity of the disease, it is difficult to perform prospective and/or randomized trials. Unfortunately, the current data is limited to retrospective studies, while randomized controlled trials are needed to investigate the efficacy of combined intra-arterial therapies and systemic therapies in the treatment of ICC. To validate further, prospective studies are needed for consistent patient selection criteria, and their outcome measures can provide appropriate quality of data including safety profile [16]. As described earlier, the combination of systemic chemotherapy with another modality for the treatment of unresectable ICC can increase tumor specificity, thus reducing systemic side effects [55]. A significant impovement in the median OS is seen when TACE was combined with systemic therapy, either gemcitabine or oxaliplatin and gemcitabine [17] or in conjunction with RFA [38]. A prospective, phase I trial has determined a highest and maximum tolerable dose of 170Gy from ^{90}Y along with fixed dose of capecitabine in ICC setting [56] but remains unclear whether this combination offers a significant survival advantage. Accumulating evidence suggest that response rates and survival for ICC appear to be more promising if liver-directed therapies are combined with systemic therapies than systemic therapies alone [1, 55], but the conclusive evidence will require large scale prospective randomized studies.

References

1. Zechlinski JJ, Rilling WS. Transarterial therapies for the treatment of intrahepatic cholangiocarcinoma. Semin Interv Radiol. 2013;30(1):21–7.
2. Wadhwa V, Jobanputra Y, Thota PN, Narayanan Menon KV, Parsi MA, Sanaka MR. Healthcare utilization and costs associated with cholangiocarcinoma. Gastroenterol Rep. 2017;5(3):213–8.
3. Banales JM, Cardinale V, Carpino G, Marzioni M, Andersen JB, Invernizzi P, et al. Expert consensus document: cholangiocarcinoma: current knowledge and future perspectives consensus statement from the European Network for the Study of Cholangiocarcinoma (ENS-CCA). Nat Rev Gastroenterol Hepatol. 2016;13(5):261–80.

4. Taylor AC, Maddirela D, White SB. Role of radioembolization for biliary tract and primary liver Cancer. Surg Oncol Clin N Am. 2019;28(4):731–43.
5. Chung YE, Kim MJ, Park YN, Choi JY, Pyo JY, Kim YC, et al. Varying appearances of cholangiocarcinoma: radiologic-pathologic correlation. Radiographics. 2009;29(3):683–700.
6. Razumilava N, Gores GJ. Cholangiocarcinoma. Lancet (London, UK). 2014;383(9935):2168–79.
7. Bridgewater J, Galle PR, Khan SA, Llovet JM, Park JW, Patel T, et al. Guidelines for the diagnosis and management of intrahepatic cholangiocarcinoma. J Hepatol. 2014;60(6):1268–89.
8. Sommer CM, Kauczor HU, Pereira PL. Locoregional therapies of cholangiocarcinoma. Visceral Med. 2016;32(6):414–20.
9. Valle J, Wasan H, Palmer DH, Cunningham D, Anthoney A, Maraveyas A, et al. Cisplatin plus gemcitabine versus gemcitabine for biliary tract cancer. N Engl J Med. 2010;362(14):1273–81.
10. Okusaka T, Nakachi K, Fukutomi A, Mizuno N, Ohkawa S, Funakoshi A, et al. Gemcitabine alone or in combination with cisplatin in patients with biliary tract cancer: a comparative multicentre study in Japan. Br J Cancer. 2010;103(4):469–74.
11. Kim JH, Yoon HK, Sung KB, Ko GY, Gwon DI, Shin JH, et al. Transcatheter arterial chemoembolization or chemoinfusion for unresectable intrahepatic cholangiocarcinoma: clinical efficacy and factors influencing outcomes. Cancer. 2008;113(7):1614–22.
12. Kiefer MV, Albert M, McNally M, Robertson M, Sun W, Fraker D, et al. Chemoembolization of intrahepatic cholangiocarcinoma with cisplatinum, doxorubicin, mitomycin C, ethiodol, and polyvinyl alcohol: a 2-center study. Cancer. 2011;117(7):1498–505.
13. Gusani NJ, Balaa FK, Steel JL, Geller DA, Marsh JW, Zajko AB, et al. Treatment of unresectable cholangiocarcinoma with gemcitabine-based transcatheter arterial chemoembolization (TACE): a single-institution experience. J Gastrointest Surg. 2008;12(1):129–37.
14. Vogl TJ, Naguib NN, Nour-Eldin NE, Bechstein WO, Zeuzem S, Trojan J, et al. Transarterial chemoembolization in the treatment of patients with unresectable cholangiocarcinoma: results and prognostic factors governing treatment success. Int J Cancer. 2012;131(3):733–40.
15. Yang GW, Zhao Q, Qian S, Zhu L, Qu XD, Zhang W, et al. Percutaneous microwave ablation combined with simultaneous transarterial chemoembolization for the treatment of advanced intrahepatic cholangiocarcinoma. Onco Targets Therapy. 2015;8:1245–50.
16. Kuhlmann JB, Euringer W, Spangenberg HC, Breidert M, Blum HE, Harder J, et al. Treatment of unresectable cholangiocarcinoma: conventional transarterial chemoembolization compared with drug eluting bead-transarterial chemoembolization and systemic chemotherapy. Eur J Gastroenterol Hepatol. 2012;24(4):437–43.
17. Poggi G, Amatu A, Montagna B, Quaretti P, Minoia C, Sottani C, et al. OEM-TACE: a new therapeutic approach in unresectable intrahepatic cholangiocarcinoma. Cardiovasc Intervent Radiol. 2009;32(6):1187–92.
18. Al-Adra DP, Gill RS, Axford SJ, Shi X, Kneteman N, Liau SS. Treatment of unresectable intrahepatic cholangiocarcinoma with yttrium-90 radioembolization: a systematic review and pooled analysis. Eur J Surg Oncol. 2015;41(1):120–7.
19. Hoffmann RT, Paprottka PM, Schon A, Bamberg F, Haug A, Durr EM, et al. Transarterial hepatic yttrium-90 radioembolization in patients with unresectable intrahepatic cholangiocarcinoma: factors associated with prolonged survival. Cardiovasc Intervent Radiol. 2012;35(1):105–16.
20. Rafi S, Piduru SM, El-Rayes B, Kauh JS, Kooby DA, Sarmiento JM, et al. Yttrium-90 radioembolization for unresectable standard-chemorefractory intrahepatic cholangiocarcinoma: survival, efficacy, and safety study. Cardiovasc Intervent Radiol. 2013;36(2):440–8.
21. Mouli S, Memon K, Baker T, Benson AB 3rd, Mulcahy MF, Gupta R, et al. Yttrium-90 radioembolization for intrahepatic cholangiocarcinoma: safety, response, and survival analysis. J Vasc Interv Radiol. 2013;24(8):1227–34.
22. Hyder O, Marsh JW, Salem R, Petre EN, Kalva S, Liapi E, et al. Intra-arterial therapy for advanced intrahepatic cholangiocarcinoma: a multi-institutional analysis. Ann Surg Oncol. 2013;20(12):3779–86.
23. Valle JW, Furuse J, Jitlal M, Beare S, Mizuno N, Wasan H, et al. Cisplatin and gemcitabine for advanced biliary tract cancer: a meta-analysis of two randomised trials. Ann Oncol. 2014;25(2):391–8.

24. Burger I, Hong K, Schulick R, Georgiades C, Thuluvath P, Choti M, et al. Transcatheter arterial chemoembolization in unresectable cholangiocarcinoma: initial experience in a single institution. J Vasc Interv Radiol. 2005;16(3):353–61.
25. Jeong S, Zheng B, Wang J, Chi J, Tong Y, Xia L, et al. Transarterial chemoembolization: a favorable postoperative management to improve prognosis of hepatitis B virus-associated intrahepatic cholangiocarcinoma after surgical resection. Int J Biol Sci. 2017;13(10):1234–41.
26. Halappa VG, Bonekamp S, Corona-Villalobos CP, Li Z, Mensa M, Reyes D, et al. Intrahepatic cholangiocarcinoma treated with local-regional therapy: quantitative volumetric apparent diffusion coefficient maps for assessment of tumor response. Radiology. 2012;264(1):285–94.
27. Ray CE Jr, Edwards A, Smith MT, Leong S, Kondo K, Gipson M, et al. Meta-analysis of survival, complications, and imaging response following chemotherapy-based transarterial therapy in patients with unresectable intrahepatic cholangiocarcinoma. J Vasc Interv Radiol. 2013;24(8):1218–26.
28. Rayar M, Sulpice L, Edeline J, Garin E, Levi Sandri GB, Meunier B, et al. Intra-arterial yttrium-90 radioembolization combined with systemic chemotherapy is a promising method for downstaging unresectable huge intrahepatic cholangiocarcinoma to surgical treatment. Ann Surg Oncol. 2015;22(9):3102–8.
29. Mosconi C, Gramenzi A, Ascanio S, Cappelli A, Renzulli M, Pettinato C, et al. Yttrium-90 radioembolization for unresectable/recurrent intrahepatic cholangiocarcinoma: a survival, efficacy and safety study. Br J Cancer. 2016;115(3):297–302.
30. White J, Carolan-Rees G, Dale M, Patrick HE, See TC, Bell JK, et al. Yttrium-90 transarterial radioembolization for chemotherapy-refractory intrahepatic cholangiocarcinoma: A Prospective, Observational Study. J Vasc Interv Radiol. 2019;30(8):1185–92.
31. Nezami N, Camacho JC, Kokabi N, El-Rayes BF, Kim HS. Phase Ib trial of gemcitabine with yttrium-90 in patients with hepatic metastasis of pancreatobiliary origin. J Gastrointest Oncol. 2019;
32. Mavros MN, Economopoulos KP, Alexiou VG, Pawlik TM. Treatment and prognosis for patients with intrahepatic cholangiocarcinoma: systematic review and meta-analysis. JAMA Surg. 2014;149(6):565–74.
33. Zhang SJ, Hu P, Wang N, Shen Q, Sun AX, Kuang M, et al. Thermal ablation versus repeated hepatic resection for recurrent intrahepatic cholangiocarcinoma. Ann Surg Oncol. 2013;20(11):3596–602.
34. Zhang K, Yu J, Yu X, Han Z, Cheng Z, Liu F, et al. Clinical and survival outcomes of percutaneous microwave ablation for intrahepatic cholangiocarcinoma. Int J Hyperth. 2018;34(3):292–7.
35. Shindoh J. Ablative therapies for intrahepatic cholangiocarcinoma. Hepatobiliary Surg Nutr. 2017;6(1):2–6.
36. Amini N, Ejaz A, Spolverato G, Kim Y, Herman JM, Pawlik TM. Temporal trends in liver-directed therapy of patients with intrahepatic cholangiocarcinoma in the United States: a population-based analysis. J Surg Oncol. 2014;110(2):163–70.
37. Chiou YY, Hwang JI, Chou YH, Wang HK, Chiang JH, Chang CY. Percutaneous ultrasound-guided radiofrequency ablation of intrahepatic cholangiocarcinoma. Kaohsiung J Med Sci. 2005;21(7):304–9.
38. Carrafiello G, Lagana D, Cotta E, Mangini M, Fontana F, Bandiera F, et al. Radiofrequency ablation of intrahepatic cholangiocarcinoma: preliminary experience. Cardiovasc Intervent Radiol. 2010;33(4):835–9.
39. Kamphues C, Seehofer D, Eisele RM, Denecke T, Pratschke J, Neumann UP, et al. Recurrent intrahepatic cholangiocarcinoma: single-center experience using repeated hepatectomy and radiofrequency ablation. J Hepatobiliary Pancreat Sci. 2010;17(4):509–15.
40. Kim JH, Won HJ, Shin YM, Kim KA, Kim PN. Radiofrequency ablation for the treatment of primary intrahepatic cholangiocarcinoma. AJR Am J Roentgenol. 2011;196(2):W205–9.
41. Kim JH, Won HJ, Shin YM, Kim PN, Lee SG, Hwang S. Radiofrequency ablation for recurrent intrahepatic cholangiocarcinoma after curative resection. Eur J Radiol. 2011;80(3):e221–5.
42. Xu HX, Wang Y, Lu MD, Liu LN. Percutaneous ultrasound-guided thermal ablation for intrahepatic cholangiocarcinoma. Br J Radiol. 2012;85(1016):1078–84.

43. Giorgio A, Calisti G, Stefano G DE, Farella N, Sarno A DI, Amendola F, et al. Radiofrequency ablation for intrahepatic cholangiocarcinoma: retrospective analysis of a single centre experience. Anticancer Res. 2011;31(12):4575–80.
44. Uhlig J, Sellers C, Stein S, Lacy J, "Kevin" Kim HS. J Clin Oncol. 2018;36(15_suppl):e16150.
45. Han K, Ko HK, Kim KW, Won HJ, Shin YM, Kim PN. Radiofrequency ablation in the treatment of unresectable intrahepatic cholangiocarcinoma: systematic review and meta-analysis. J Vasc Interv Radiol. 2015;26(7):943–8.
46. Xu C, Li L, Xu W, Du C, Yang L, Tong J, et al. Ultrasound-guided percutaneous microwave ablation versus surgical resection for recurrent intrahepatic cholangiocarcinoma: intermediate-term results. Int J Hyperth. 2019;36(1):351–8.
47. Takahashi EA, Kinsman KA, Schmit GD, Atwell TD, Schmitz JJ, Welch BT, et al. Thermal ablation of intrahepatic cholangiocarcinoma: safety, efficacy, and factors affecting local tumor progression. Abdom Radiol (NY). 2018;43(12):3487–92.
48. Venkat PS, Hoffe SE, Frakes JM. Stereotactic body radiation therapy for hepatocellular carcinoma and intrahepatic cholangiocarcinoma. Cancer Control. 2017;24(3):1073274817729259.
49. Sebastian NT, Tan Y, Miller ED, Williams TM, Alexandra DD. Stereotactic body radiation therapy is associated with improved overall survival compared to chemoradiation or radioembolization in the treatment of unresectable intrahepatic cholangiocarcinoma. Clin Transl Radiat Oncol. 2019;19:66–71.
50. Blomgren H, Lax I, Naslund I, Svanstrom R. Stereotactic high dose fraction radiation therapy of extracranial tumors using an accelerator. Clinical experience of the first thirty-one patients. Acta Oncol. 1995;34(6):861–70.
51. Tse RV, Hawkins M, Lockwood G, Kim JJ, Cummings B, Knox J, et al. Phase I study of individualized stereotactic body radiotherapy for hepatocellular carcinoma and intrahepatic cholangiocarcinoma. J Clin Oncol. 2008;26(4):657–64.
52. Mahadevan A, Dagoglu N, Mancias J, Raven K, Khwaja K, Tseng JF, et al. Stereotactic body radiotherapy (SBRT) for intrahepatic and hilar cholangiocarcinoma. J Cancer. 2015;6(11):1099–104.
53. Kopek N, Holt MI, Hansen AT, Hoyer M. Stereotactic body radiotherapy for unresectable cholangiocarcinoma. Radiother Oncol. 2010;94(1):47–52.
54. Sterzing F, Brunner TB, Ernst I, Baus WW, Greve B, Herfarth K, et al. Stereotactic body radiotherapy for liver tumors: principles and practical guidelines of the DEGRO Working Group on Stereotactic Radiotherapy. Strahlenther Onkol. 2014;190(10):872–81.
55. Simo KA, Halpin LE, McBrier NM, Hessey JA, Baker E, Ross S, et al. Multimodality treatment of intrahepatic cholangiocarcinoma: A review. J Surg Oncol. 2016;113(1):62–83.
56. Hickey R, Mulcahy MF, Lewandowski RJ, Gates VL, Vouche M, Habib A, et al. Chemoradiation of hepatic malignancies: prospective, phase 1 study of full-dose capecitabine with escalating doses of yttrium-90 radioembolization. Int J Radiat Oncol Biol Phys. 2014;88(5):1025–31.

Chapter 9
Colorectal Cancer: Liver Metastatic Disease

Ivan Babin, Maha Jarmakani, Louis Fanucci, Farshid Dayyani, and Nadine Abi-Jaoudeh

Introduction

Globally, colorectal cancer (CRC) is the third most commonly diagnosed cancer in males and the second in females, with 1.8 million new cases and almost 861,000 deaths in 2018 according to the World Health Organization. At the time of diagnosis, 20–25% of patients will have stage IV disease (1–4) with metastasis to the liver affecting 40% of patients (1). Additionally, 35–60% of CRC patients will develop liver metastases later in the disease process (2). Prognosis for metastatic CRC (mCRC) is poor, with 5-year survival less than 11%. Liver failure accounts for approximately two-thirds of mCRC-related mortality due to tumor burden replacing normal parenchyma as well as toxicity from chemotherapeutic agents, resulting in functional compromise.

CRC is a multifactorial disease process. Genetic factors, diet and other environmental factors, and inflammatory conditions all play a role in the development of the disease. Although multiple hereditary conditions associated with CRC are known, the majority of cases appear to be sporadic. The progression from a premalignant lesion to invasive adenocarcinoma involves multiple genetic alterations

I. Babin (✉)
Department of Radiology, SUNY Upstate Medical University, Syracuse, NY, USA

M. Jarmakani
Interventional Radiology, Department of Radiological Sciences, OU Medical Center, Oklahoma City, OK, USA

L. Fanucci · N. Abi-Jaoudeh
Department of Radiological Sciences, University of California Irvine Medical Center, Orange, CA, USA

F. Dayyani
Division of Hematology and Oncology, Department of Medicine, University of California Irvine Medical Center, Orange, CA, USA

C. Georgiades, H. S. Kim (eds.), *Image-Guided Interventions in Oncology*,
https://doi.org/10.1007/978-3-030-48767-6_9

including mutation of the APC (adenomatous polyposis gene), KRAS, and p53 tumor suppressor gene. The full discussion is beyond the scope of this chapter.

Management of mCRC is optimized by involving a multidisciplinary team (MDT). A prospective study showed that despite 84% of clinicians being certain of their original plan before MDT discussion, a change was recommended in 36% of cases, 72% of which were major (3).

Role of Surgery

Surgical resection of mCRC provides the best chance at long-term survival and is therefore the treatment of choice when possible. In a surgical case series, 5-year survival rates after resection ranged from 24% to 58%, averaging 40% (5–8). Cancer-related death will affect approximately 1/3 of mCRC patients treated by surgical resection who survive 5 years, while those who survive 10 years are generally considered cured. In an analysis of 612 consecutive patients who underwent resection of liver mCRC and were followed for at least 10 years, 17% (102 patients) survived 10 years with only 1 patient experiencing a disease-specific death (9).

Although previous guidelines for mCRC resection aimed to categorize resectability based on factors such as number of lesions, size, CEA levels, and margins, these systems failed to demonstrate predictive accuracy for long-term survival across institutions. More recent consensus defines resectable mCRC as tumors that can be removed with negative margin (R0) resection, while leaving an adequate liver remnant comprising at least two contiguous segments with preserved function, vascular inflow and outflow, and biliary drainage. Resectability of a mCRC should ideally be determined in an MDT setting (10).

Evaluation of hepatic functional reserve is essential prior to major hepatectomy. CT volumetry is routinely used to calculate future liver remnant (FLR), with post-hepatectomy FLR volumes of 25% for the normal liver and 40% for the compromised liver deemed acceptable. However, it is important to note that FLR volume does not necessarily correlate with liver function, especially since neoadjuvant chemotherapy can affect hepatocyte function (11).

Systemic Therapy

For resectable disease, the European Society for Medical Oncology (ESMO) guidelines recommend that technical and oncological criteria be assessed for resectability (12). The role of perioperative chemotherapy for patients who are resectable and have oncological favorable criteria is unclear. In theory, neoadjuvant chemotherapy has the capacity of shrinking tumor burden, reducing extent of liver resection, and treating micro-metastases. A landmark randomized controlled trial (EORTC intergroup trial 40983) showed perioperative FOLFOX (folinic acid, fluorouracil, and

oxaliplatin; 6 cycles before and 6 cycles after surgery) and showed a modest improvement in 3-year progression-free survival (42.4%), compared with surgery-only control group (33.2%). However, a significant increase in perioperative morbidity was observed (25% vs. 16%) (4). Oxaliplatin was associated with sinusoidal obstruction syndrome in up to 38% patients, and irinotecan was associated with steatosis and steatohepatitis in 9.3% in that trial which were associated with increased postoperative risk. Finally, 7% of patients had disease progression requiring more extensive surgery or rendered them unresectable altogether. The EPOC trial also reported a 5-year OS rate of 51% (95% CI 45–58) with perioperative chemotherapy vs. 48% (95% CI 40–55) with surgery-only group which ESMO deemed unconvincing despite a significant improvement in disease-free survival in the combination group. Moreover, the addition of EGFR inhibitor cetuximab to FOLFOX 12 prior and post-surgery was associated with a significantly worse progression-free survival (14.8 versus 24.2 months). Bevacizumab, an anti-vascular endothelial growth factor (VEGF), only moderately improved resectability rates when added to CAPEOX or FOLFOX in a large randomized trial (8.4 versus 6.1 percent with chemotherapy alone), and overall survival differences did not reach statistical significance (13). Another study showed that bevacizumab plus FOLFIRI in the neoadjuvant setting yielded a response rate of 66.7% in resectable mCRC; whether this translates into any survival benefit remains to be investigated (14). While a meta-analysis including 18 studies also concluded that neoadjuvant treatment, in general, did not offer progression-free survival or overall survival benefit; however, it may be useful in select cases deemed high risk for recurrence (15). In summary, based on currently available data, patients with resectable liver metastases have three options. They could undergo upfront synchronous or staged colectomy and liver resection, followed by adjuvant FOLFOX or CAPEOX. The other option is neoadjuvant FOLFOX or CAPEOX (or FOLFIRI in patients who cannot receive oxaliplatin) for 2–3 months followed by colectomy and liver resection and, finally, upfront colectomy followed by adjuvant FOLFOX or CAPEOX and a stage resection of liver metastases. However, it is important to note that the latter approach should only be considered for patients in whom it would be acceptable to delay systemic control of liver metastases until they have recovered from the upfront colectomy. The overall duration of chemotherapy in completely resected cases should be 6 months (that includes any preoperative chemotherapy).

For unresectable mCRC, societal guidelines still recommend eradication of visible disease if possible, by combining systemic and locoregional and ablative therapies (LAT) in addition to surgery. For initially non-resectable mCRC, neoadjuvant chemotherapy can be used; however the likelihood of downstaging a patient with truly unresectable disease to the point of resectability is only 10 to 15%. Furthermore, longer courses of chemotherapy increase the potential for liver toxicity and postoperative complications. The NCCN guidelines recommend systemic therapy with or without biologic depending on mutations. Reevaluation of conversion to resectable disease should be performed every 2 months. Adjuvant chemotherapy is also recommended for a 6 months total of perioperative chemotherapy. Of note, these recommendations are based on extrapolation of results of the EORTC intergroup trial

40983, which showed perioperative FOLFOX conferred a PFS benefit but did not affect OS. More recent data showed that intensification of the treatment regimen using a triplet chemotherapy and a biologic, i.e., FOLFOXIRI plus bevacizumab, is associated with higher response rates and deeper responses compared to a doublet regimen of FOLFOX or FOLFIRI plus bevacizumab. The TRIBE2 study randomized patients with metastatic colorectal carcinoma to FOLFOXIRI/bevacizumab vs. FOLFOX/bevacizumab and switch to FOLFIRI/bevacizumab at the time of first progression (16). FOLFOXIRI/bevacizumab significantly increased the response rate from 50% to 62%, improved progression-free survival, and at the preliminary analysis showed a consistent overall survival advantage over a sequential doublet chemotherapy approach. Importantly, the authors reported a higher R0 resection rate in the FOLFOXIRI/bevacizumab arm. The German VOLFI trial used a randomized phase II design to evaluate the contribution panitumumab (fully humanized anti-EGFR antibody) added to FOLFOXIRI in patients with RAS wild-type nonresectable metastatic colorectal carcinoma (17). The primary endpoint of overall response rate was met (85.7% vs. 54.5%; $P = 0.0013$). A pre-specified analysis in the cohort of patients deemed potentially resectable after downstaging demonstrated a higher secondary resection rate with FOLFOXIRI/panitumumab vs. FOLFOXIRI alone (60.0% vs. 36.4%). Longer follow-up is needed to better evaluate the long-term outcomes of patients with advanced disease who underwent complete resection of disease after first-line FOLFOXIRI-based regimens. Thus, with more potent systemic treatment options, it appears that in patients who are fit enough for aggressive treatment, more interval curative intent resections might become possible compared to the current estimated rates of 10–15%.

Patients with unresectable disease are generally divided into two categories depending on their functional status and their ability to tolerate intensive therapy for cytoreduction or for an impending threat of organ dysfunction vs. those cannot tolerate intensive therapy with disease control as the goal. The backbone of first-line systemic agents comprises a fluoropyrimidine used in various combination with oxaliplatin or irinotecan with or without biological agents. When possible, a period of discontinuation or maintenance of chemotherapy should be implemented. Second-line therapy and third-line and beyond therapeutic regimens should be offered to patients with good performance status and appropriate organ function. The regimens in the second and third line depend on previous therapies and molecular profile.

The addition of immunotherapy, specifically checkpoint inhibitors, has been integrated in the guidelines per NCCN when microsatellite instability (MSI) high is present as first line for patients who are not appropriate for intensive therapy or as second- or third-line regimens. For poor prognosis patients harboring the BRAF V600E mutation and limited treatment options in second and third line, a chemotherapy-free regimen of encorafenib (BRAF inhibitor), binimetinib (MEK inhibitor), and cetuximab (anti-EGFR) improved response rate and overall survival compared to cetuximab plus irinotecan-based cytotoxic regimens (18). In the small subset of Her-2-amplified colorectal carcinomas (2–3%), treatment strategies of anti-Her-2-targeted agents have shown promising activity (response rates of around 30% in later lines of therapy) and are under active investigation. A comprehensive

review of the systemic therapies is beyond this chapter but can be found at NCCN guidelines for colon cancer and ESMO guidelines (6, 19). Future studies are needed to specifically address the question whether personalized targeted treatments based on tumor profile will lead to higher resectability rates for patients with liver metastatic disease.

Stereotactic Body Radiation Therapy

The limited evidence available on stereotactic body radiation therapy (SBRT) is encouraging as it can achieve high local control rates similar to RFA. Recurrences with SBRT also correlate with tumor size. A systematic review of 18 studies (10 retrospective, 6 prospective, and 2 phase studies) showed pooled 1- and 2-year local control rates of 67% and 59.3% and 1- and 2-year OS 67.2% and 56.5%, respectively. Inclusion criteria was heterogeneous with some studies including only patients with good performance status, less than 3 mCRC, and lesion size <3 cm. Side effects included mild/moderate liver toxicity in 30.7% and severe toxicity in 8.7%.

Definitive validation in large randomized studies is required (20).

Intra-arterial Therapies

Intra-arterial therapies (IAT) for mCRC include transarterial chemoembolization (TACE) with irinotecan agents, hepatic artery infusion (HAI), and transarterial radioembolization (TARE). In all cases, IAT takes advantage of the different pathophysiology of hepatic and tumoral blood supply. While normal hepatocytes are supplied primarily by the portal vein, hepatic primary or hepatic metastases are supplied predominantly by the hepatic arteries. Therefore, therapeutic administration of cytotoxic agents or microspheres during IAT will maximize tumoral exposure to the treatment while minimizing liver toxicity by sparing normal liver parenchyma (19, 21).

Transarterial Radioembolization (TARE)

Selection Criteria and Indication *(Table 9.1)*

Y90 radioembolization involves intra-arterial administration of microspheres (resin or glass) loaded with the B-emitting radioisotope Yttrium-90 (22). Its mechanism of action does not rely on the embolic effect of the microspheres but rather its radioactivity. CRC cells are highly radiosensitive, even in patients with chemotherapy-resistant disease. Y90 can be performed in patients on systemic chemotherapy in an attempt to decrease the disease burden or as a salvage treatment in patients with

Table 9.1 Contraindications to TARE

Contraindications to TARE	
Absolute	Relative
Clinical signs of liver failure on physical exam (i.e., intractable clinical ascites)	Poor hepatic function: Albumin <2.5 g dL^{-1} AST and ALT >5 × ULN ALP >5 × ULN Total bilirubin >2.0 mg dL^{-1}
Significant hepatopulmonary shunt resulting in a per treatment dose of >30 Gy or cumulative dose to the lungs of 50 Gy (2)	
Severe portal hypertension with hepatofugal flow	Bleeding risk Hgb <8.5 g dL^{-1} Platelets <50,000 ul^{-1} INR >2.0
Non-correctable bleeding diathesis	Leukocytes <2500 μl^{-1}
	Prior hepatic external beam radiation therapy

ALP alkaline phosphatase, *ALT* alanine aminotransferase, *AST* aspartate aminotransferase, *INR* international normalized ratio, *ULN* upper limit of normal

chemotherapy-resistant disease. Y90 should not be offered as a first-line therapy; however, it has been proven effective in second- or third-line setting.

Y90 is not a viable option in patients with poor performance status, poor baseline liver function, and extensive multi-organ disease. Weiner et al. concluded that elevated CEA, AST, and neutrophil to lymphocyte ratio (NLR) and increased extrahepatic disease burden were independently associated with worse overall survival following radioembolization.

Survival analysis from the MORE study correlated good performance status, absence of ascites, low tumor-to-liver ratio, limited previous chemotherapy, normal albumin and bilirubin, and low AST and CEA as factors associated with improved overall survival.

Patients with severe peripheral vascular disease or macrovascular toxicities secondary to systemic agents precluding safe catheterization are not candidates. Patients should be off bevacizumab for at least 6 weeks and preferably 8 weeks. Furthermore, unlike TACE, Y90 radioembolization remains an option in the presence of portal vein thrombosis due to limited distal embolic effect of the microspheres. Y90 can also be performed in advanced liver disease where ablative modalities are limited (22). Absolute and relative contraindications are summarized in Table 8.1.

Technique

Pre-procedure multiphase CT or MRI should be reviewed carefully for accurate activity determination which can be performed through one of three methods—the body surface area (BSA) method, Medical Internal Radiation Dose (MIRD), and the partition method (21).

Radioactivity and dosimetry are beyond the scope of this chapter.

Y90 radioembolization is performed in a staged manner. The initial procedure is planning angiography or workup. Its purpose is to delineate hepatic and tumor vascular anatomy, evaluate for extrahepatic arterial supply, and embolize them if appropriate, as well as to calculate the hepatopulmonary shunt fraction.

The procedure is performed under general anesthesia or moderate sedation with radial or femoral arterial puncture and the insertion of a 5 or 6 French vascular sheath. Through the sheath, a 5F catheter, most commonly a C2 or SOS Omni catheter, is used to select the superior mesenteric artery to verify patency of the main portal vein and evaluate for replaced hepatic vasculature (22, 23). Next, the celiac axis is cannulated, and angiography is performed at the celiac axis to map out the hepatic supply and rule out the presence of extrahepatic vessels. A microcatheter/microwire system is inserted coaxially for selective hepatic arteriography, typically, of the common, proper, right, and left hepatic arteries. More selective catheterization is done depending on the findings and the performing physician's discretion. Once the vascular supply to the tumor and flow dynamics are understood, the treatment position of the catheter can be determined, making sure there is complete coverage of the tumor (23).

Of note, it is vitally important to obtain complete opacification of the vessels to ensure that all branches have been opacified. Moreover, diagnostic angiography can be very informative in terms of flow dynamics during the treatment.

Prophylactic embolization of any vessels providing extrahepatic supply distal to the selected injection site should be undertaken in order to protect the patient from non-target embolization. These vessels can include but are not limited to gastric branches, (the right gastric artery RGA), supra-duodenal branches, and esophageal branches. However, if the vessels are proximal to the injection site, embolization depends on several factors including distance of Y90 injection site to vessel origin, volume of microspheres, tumor size, vascular flow (patient with altered flow due to systemic biological agents), possibility of achieving stasis, and reflux during the treatment since these factors were all associated with gastroduodenal ulceration. Most common arteries requiring coil embolization are right gastric artery (RGA), gastroduodenal artery (GDA), phrenic artery, and falciform artery. It is also important to note that routine coil embolization of these vessels could lead to hepatic-intestinal collaterals down the line, potentially limiting the technical ability to perform future radioembolization (22, 23).

The most challenging aspect of treating the GDA is coil migration when coiling near the vessel origin. One technique to combat this is to anchor the coil in a small side branch and advance a support catheter to the origin of the GDA to prevent dislodgement of the microcatheter. Using detachable coils or vascular plugs can also facilitate more precise placement by offering the added ability to retract the coil or plug if it is not placed correctly prior to deployment (23).

The RGA most commonly originates from the proper hepatic artery but can also arise from the GDA, right or left hepatic arteries, and least commonly the common hepatic artery. It can be challenging to cannulate, and therefore it is important to obtain sufficient angiography of the common hepatic artery to delineate its origin.

If it cannot be cannulated at its origin, it can potentially be selected in a retrograde fashion via the left gastric artery through the gastric arcade (22, 23).

Routine coil embolization of the cystic artery is no longer recommended. Theysohn et al. looked at 295 patients, 20 of which had significant Tc 99m MAA accumulation in the gallbladder. For the majority of these, the cystic artery was avoided with altering catheter position. For the rest, temporary occlusion with gelfoam or intentional vasospasm of the cystic artery with a microwire was performed. None of these patients required a cholecystectomy, and only one patient showed clinical signs of cholecystitis (24). Additionally, a weeklong course of prophylactic antibiotics can be considered (23).

Detection of a hepatic falciform artery is more likely on cone beam CT than digital subtraction angiography. With that said, routine embolization of this artery is also not routinely performed. Patients rarely show clinical symptoms, and if there is concern, ice packs can be placed on the anterior abdomen during treatment. If the artery is particularly large and can be cannulated, gelfoam or coil embolization can be considered (22).

Cone beam CT from the selected treatment position of the microcatheter is recommended as it has been shown to increase tumor lesion detection as well as extrahepatic vascular supply (22).

Following prophylactic coil embolization, Technetium 99m macro-aggregated albumin (Tc 99m MAA) is administered from the site of Y90 of administration. In cases of anatomical variants, the Tc 99m MAA can be split into separate injections (22, 23). Following Tc 99m MAA administration, the patient is taken for multiplanar SPECT/CT to calculate the hepatopulmonary shunt fraction.

Recently, certain institutions began offering their patients same day planning angiography and treatments. However, this is not common practice yet. Usually, Y90 delivery is performed within 2 weeks of planning angiography. It is recommended to treat each lobe separately as whole liver single sessions were independently associated with increased liver toxicity and radiation-induced liver disease (REILD). The treatment procedure, like the mapping procedure, begins with diagnostic angiography to ensure continued patency of the portal vein and lack of extrahepatic arterial supply. The catheter is positioned, and the dose is then injected through a closed-circuit delivery system (21).

Risks and Complications

Expected side effects of the treatment include short-term abdominal pain and postembolization syndrome—fever, lethargy, fatigue, decreased appetite, and nausea for up to 10 days following treatment. These side effects are usually minimal and less pronounced than with TACE.

Potential risks of the procedure include radioembolization-induced liver disease (REILD), radiation pneumonitis, non-target radioembolization, lymphopenia, and technical complications related to angiography such as groin hematoma, vessel dissection, and contrast-induced renal failure (22).

Radiation-induced liver disease (REILD) is a syndrome characterized by ascites and jaundice 6–8 weeks post-procedure without disease progression or biliary obstruction. Bilirubin >3 mg/dL, increased PALK/GGT with no change in AST and ALT is typical. Pathological examination reveals sinusoidal obstruction syndrome with veno-occlusive disease in most serious cases. REILD occurs in 4–5.4% of cases with prior chemotherapy especially within 2 months of radioembolization, whole-liver single-session Y90 treatment, small liver volume, advanced age, and limited hepatic reserve as risk factors (19, 20).

Radiation pneumonitis is rare and occurs in less than 1% of cases. Symptoms will appear 1–6 months after Y90 procedures and is categorized by shortness of breath and cough and ventilatory dysfunction with restriction pattern on pulmonary tests as well as bilateral lung infiltrates on computed tomography (CT). Radiation pneumonitis is caused by microspheres circumventing the capillary system and reaching the lung through arteriovenous shunts within the tumor vasculature. A study demonstrated that it can be reduced to 0% with strict adherence to dosimetry adjustment depending on lung shunt fraction including not proceeding if lung shunt fraction is greater than 20% (25, 26).

Non-target radioembolization can potentially cause gastric or duodenal ulcers, esophageal injury, pancreatitis, and skin injury. Radiation cholecystitis occurs 4–6 weeks post Y90 treatment and consists of right upper quadrant pain, tenderness, and fevers. On imaging, the gallbladder wall is thickened with peri-cystic fluid as well as intramural gas. Of note, the described imaging findings are present in asymptomatic patients. Biliary necrosis is very rare but has been described especially in patients with extensive disease. Lymphopenia has been described in up to 25% of cases especially after glass microspheres but is not clinically significant and has not been associated with an increased risk of infection. Physicians should be aware that this may happen and appropriately counsel patients.

Follow-Up

Following treatment, the patient is monitored for toxicities. Follow-up imaging with multiphase CT, MR, or PET-CT should be performed at least 8 weeks post-treatment to avoid the flare phenomena.

Outcomes

Several studies examined the outcomes and adverse events of Y90 in mCRC. The MORE (mCRC Outcomes after RadioEmbolization) study was a retrospective case control registry between 2002 and 2015 that established the prognostic factors for Y90 as well as adverse events (26).

Several clinical trials have studied Y90 in first-line setting including phase I, II, and III. Finally, three phase III multicenter randomized controlled trials, SIRFLOX,

FOXFIRE, and FOXFIRE-Global, were conducted to assess overall survival in chemotherapy-naïve mCRC patients with limited or no extrahepatic disease. Of note, the primary tumor was present in over half the cohort. Thirty-five percent of patients had limited extrahepatic metastasis defined as five or less lung nodules or one single site of extrahepatic disease including lymph nodes. Patients in Y90 group had a reduced dose of systemic therapy, and biologic agent was started 4–6 weeks after Y90. The data reported on over 1100 patients randomized to chemotherapy alone versus systemic chemotherapy plus radioembolization (27).

Although the combined analysis did not demonstrate an improvement in overall survival nor overall progression-free survival, there was statistically significant delayed disease progression in the radioembolization group. An objective response was also observed more frequently in the combination group vs. chemotherapy alone (72.2% vs. 63%, $p = 0.012$) (27). A subgroup analysis demonstrated that patients with right-sided primary tumors had significantly improved overall survival with Y90 group. Normally, right-sided primary tumor is a negative prognostic factor.

Several retrospective studies in the second-line and prospective trials in salvage setting have more positive results (Fig. 9.1). A prospective phase III study on 44

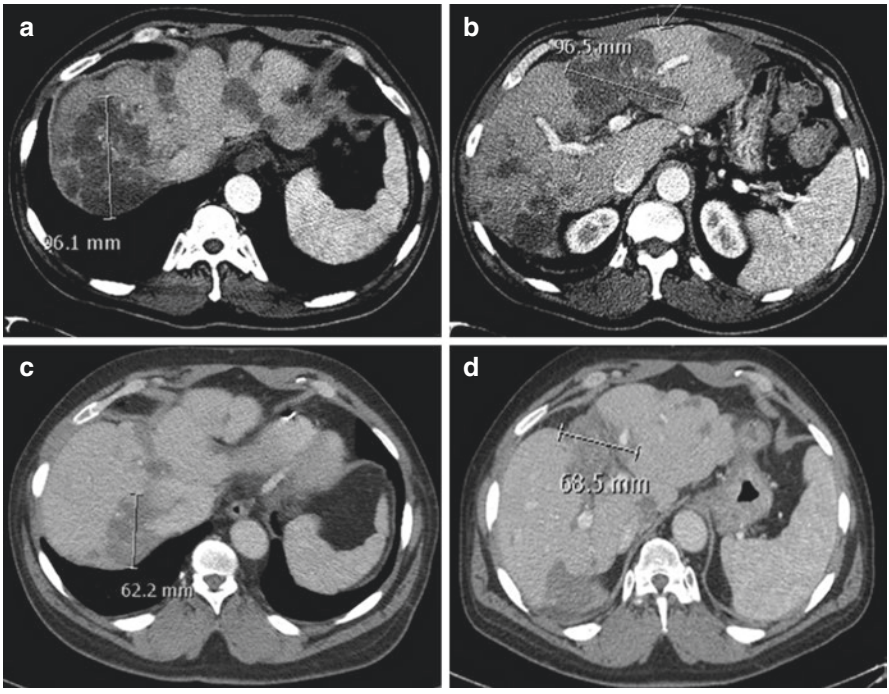

Fig. 9.1 56-year-old male with colorectal metastasis to liver that have failed two lines of chemotherapy. He had liver-dominant disease with large lesions and increasing CEA levels. Patient was referred for radioembolization. He underwent sequential lobar radioembolization with resin. (**a**, **b**) Axial contrast-enhanced CT images showing large hypodense masses consistent with patient's known colorectal metastasis. (**c**, **d**) Axial contrast-enhanced CT images 9 months post-radioembolization showing continued decrease in size of all liver lesions. The patient's CEA decreased to normal levels

patients by Hendlisz demonstrated significant improvement in tumor liver progression and overall tumor progression; however, there was no significant difference in median overall survival, with only a trend towards median overall survival (26, 28).

Transarterial Chemoembolization (TACE)

TACE is a catheter-based locoregional therapy for the treatment of unresectable mCRC which delivers a markedly higher concentration of cytotoxic agents into the liver metastases compared to systemic chemotherapy. The primary indication for TACE is as a second-line treatment after failure of systemic chemotherapy and usually performed with the intent of prolonging survival (19) (Fig. 9.2).

Selection Criteria and Indication (Table 9.2)

TACE is indicated in patients with non-resectable mCRC with a life expectancy >3 months and an adequate performance status (ECOG ≤2). Patient must have adequate liver function. Presence of hepatic encephalopathy or jaundice is an absolute contraindication, as TACE can exacerbate liver dysfunction. Portal vein patency must be carefully assessed. Portal vein thrombosis, once thought to be an absolute contraindication, is now understood as a relative contraindication as TACE can still be performed if hepatopetal collateral flow is present. The presence of a bilioenteric anastomosis, biliary stent, or prior sphincterotomy allows for colonization of the bile ducts with gut bacteria and therefore is high risk for abscess formation following TACE. This can occur despite antibiotic prophylaxis. Severe peripheral vascular disease and other conditions which preclude positioning of the catheter tip selectively are contraindications. Ideal patients will have an adequate performance status with compensated liver function, patent portal vein, and one or few hepatic metastases involving less than 50% of liver volume (29).

Technique

Pre-interventional staging with contrast-enhanced CT or MRI is needed to assess precisely the tumor extent and the arterial anatomy, including anatomical variants. Patency of the portal vein should be confirmed. Prophylactic antibiotics are often routinely administered; however, this is not evidence based.

The procedure begins with radial or femoral arterial puncture and the insertion of a vascular sheath. Through the sheath, a 5F catheter, most commonly a C2 or SOS Omni catheter, is used to select the superior mesenteric artery and to verify patency of the main portal vein as well as to assess for anatomical variants with replaced hepatic vasculature (29, 30).

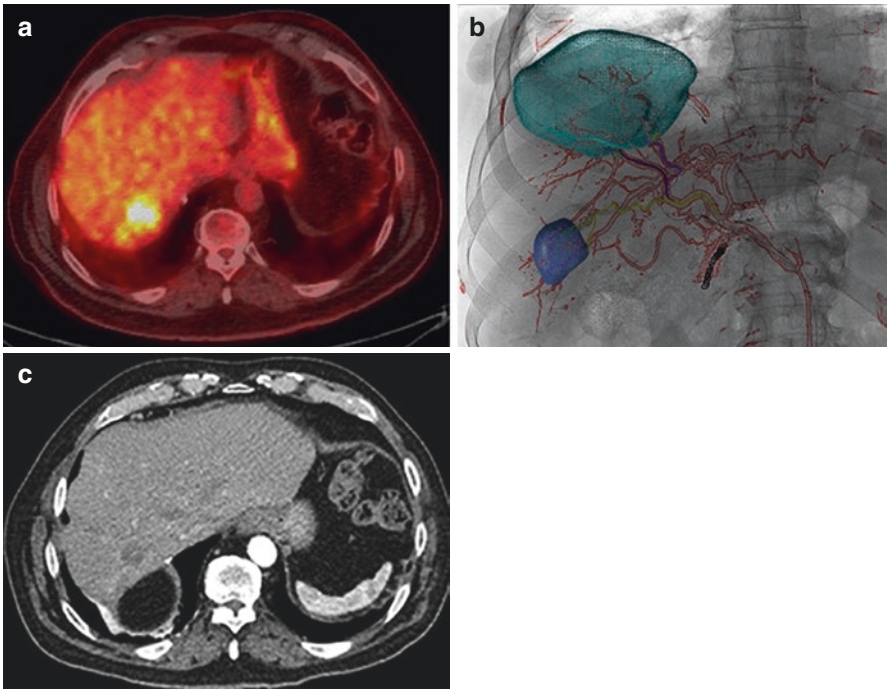

Fig. 9.2 72-year-old male with metastatic colorectal carcinoma with a segment 7 lesion. (**a**) Axial PET-CT scan showing a PET avid lesion. (**b**) Navigation fluoroscopy overlay images during drug-eluting bead chemoembolization where two lesions were segmented (teal and blue). The lesion had grown significantly. (**c**) Contrast-enhanced computed tomography 14 months post-embolization demonstrated that the lesion had shrunk significantly. The patient's CEA also normalized

Table 9.2 Contraindications to TACE

Contraindications to TACE	
Absolute	Relative
Hepatic encephalopathy	Complete main PV thrombosis (TACE can be performed only if hepatopetal collateral flow is present)
Non-correctable bleeding diathesis	Poor hepatic function: Albumin <2.5 g dL^{-1} AST and ALT >5 × ULN ALP >5 × ULN Total bilirubin >2.0 mg dL^{-1}
Severe peripheral vascular disease precluding arterial catheterization	Bleeding risk Hgb <8.5 g dL^{-1} Platelets <50,000 ul^{-1} INR >2.0
Extensive tumor involving the entirety of both lobes of the liver	Leukocytes <2500 μl^{-1}
	Presence of bilioenteric anastomosis, biliary stent, or prior sphincterotomy

ALP alkaline phosphatase, *ALT* alanine aminotransferase, *AST* aspartate aminotransferase, *INR* international normalized ratio, *ULN* upper limit of normal

Next, the celiac axis is cannulated, and angiography is performed to map out the hepatic vascular anatomy and delineate all the tumors and their vascular supply. A microcatheter/microwire system is then inserted coaxially through the 5F catheter and advanced into the segmental or subsegmental arteries supplying the tumors. Ideally, the microcatheter should be advanced in a super-selective manner ensuring complete tumor coverage while sparing normal hepatic parenchyma. Cone beam CT angiography has been demonstrated to be superior in lesion detection, tumor vasculature supply mapping, and assessment of complete tumor coverage (30).

When proper placement of the microcatheter is confirmed, embolization is performed under fluoroscopy until near stasis within the target vasculature is achieved.

A variety of chemotherapeutic and embolic agents are used and in varying combinations. To date, there is no evidence-based treatment standard. Conventional TACE involves the delivery of a mixture of aqueous chemotherapy solution and ethiodized oil in the form of an emulsion, often followed by administration of embolic particles (30).

Embolization with drug-eluting beads (DEB-TACE) is a newer technique which utilizes microspheres loaded with a cytotoxic agent, most commonly irinotecan (DEBIRI) for mCRC. Published regimens include 100 mg of irinotecan loaded on 75–150microns beads (31). After injection of DEBs into the tumor, there is a controlled drug release over several hours or even days, along with the embolic effect of the particles.

The microcatheter can then be repositioned to treat additional lesions. Multiple treatments can be performed as needed.

Risks and Complications

In experienced centers, the overall major and minor complication rates during and after TACE are generally very low. Complication rates vary with embolic material selection, as well as technique and tumor burden. Major complications include hepatic insufficiency or infarction (2%), hepatic abscess (2%), and less frequently biliary necrosis or stricture, cholecystitis, non-target embolization, or renal failure. Hepatic insufficiency is more common with high tumor burden and lobar embolization with stasis.

Post-embolization syndrome is characterized by nausea, vomiting, abdominal pain, and fever. It occurs in the majority of patients after TACE, and many centers will admit patients overnight for observation and symptom management.

Outcomes

A phase III RCT compared DEBIRI vs. FOLFIRI in patients with unresectable mCRC. DEBIRI was associated with a prolonged overall survival, progression-free survival, and improved quality of life compared to systemic chemotherapy (31).

In 2013, a systematic review of five observational trials and one prospective trial recommended DEBIRI in patients not amenable to resection especially if they had failed chemotherapy (32). Unfortunately, that same year, a meta-analysis of chemoembolization vs. no intervention or placebo for liver metastasis with a focus on mCRC concluded that there is not sufficient evidence to recommend TACE outside of clinical trials (33). The NCCN guidelines quote this meta-analysis as the basis for their recommendations (19).

Hepatic Artery Infusion (HAI)

HAI is not widely performed. The NCCN guidelines recommend that "it only be performed at institutions with significant surgical and medical expertise in the oncological aspects of the procedure." HAI involves intra-arterial hepatic port or pump placement and infusion of chemotherapy (19).

Trials have shown improvement in response and progression-free survival with HAI, but overall survival studies are lacking. Data on HAI's role in conversion of non-resectable disease to resectable disease is growing (34).

Of note, a meta-analysis of 90 prospective studies related to intra-arterial therapies for mCRC concluded that TACE, TARE, and HAI were equally effective. For patients who failed one line of chemotherapy, the survival benefit was 21.3 months with TACE, 12.6 months with HAI, and 10.9 months with TARE. However, this was only seen when these therapies were given alone, and this was not maintained when IAT were combined systemic therapies (35). Therefore, the meta-analysis concluded that there was only a marginal benefit in overall survival. The NCCN guidelines consider the role IAT in mCRC as controversial (25).

Ablation

The role of interventional oncology ablative strategies is fast evolving with a multitude of ablative therapies pertaining to the treatment of hepatic metastasis secondary to colorectal cancer. Ablation therapy is a shoebox term that encompasses several ablative techniques. It is suitable to divide the ablative modalities into chemical- and energy-based ablative strategies. Chemical ablation therapy uses substances such as ethanol or acetic acid to induce coagulation necrosis of the tumor. Energy-based ablation includes irreversible electroporation, cryoablation, radiofrequency, and microwave ablation (19).

A review of ablative modalities is beyond the scope of this chapter. Currently in the literature and in practice, heat-based ablation is the most commonly used liver-directed ablative therapy.

Selection Criteria and Indication

Currently, there are no accepted selection criteria for the use of radiofrequency ablation for the treatment of colorectal liver metastasis. However, there have been advocates for the use of clinical score-based proposals and the treatment algorithm for oligometastatic disease. Resection remains the standard of care; however, there is growing data supporting the role of ablation in nonsurgical candidates with oligometastatic disease. Moreover, ablation can also be an adjunct to surgery as long as all sites of disease can be performed to complete treatment (19, 36, 37).

The clinical score-based proposal implements four criteria to facilitate the selection of patients for ablation. These criteria included response to systemic therapy, ≤ 3 colorectal liver metastases, ≤3 cm lesion size, and low CEA level (36). Additionally, authors have endorsed that the indications for ablation of mCRC are in line with the accepted definition of oligometastatic disease. This is defined as patients with <4 metastatic lesions that are <5 cm in greatest diameter, whom are not amenable to surgery, and that have curative intent (38).

Moreover, it is noted that the number of lesions should not be considered for an absolute limiting factor if treatment of all the metastasis can be achieved. In summing up the selection criteria for the use of ablation in the treatment of colorectal liver metastasis, it is generally advocated that the ideal lesions for consistently successful ablation are <3 cm in maximum diameter.

Technique

Ablation is performed under ultrasound, computed tomography, or magnetic resonance imaging depending on lesion visibility, equipment availability, and operator experience. The benefits of ultrasound include real-time control, low cost, and lack of ionizing radiation. Contrast-enhanced ultrasound is helpful in the pretreatment planning, lesion targeting, and ablation assessment. Ablation zone should be assessed with contrast-enhanced imaging.

The procedure can be performed under conscious sedation or general anesthesia depending on patients' comorbidities and lesion location. Prophylactic antibiotic coverage is usually institution dependent except in cases where there has been biliary instrumentation; it is recommended that bowel preparation and full course of antibiotics be administered to avoid abscess formation. A comprehensive lab workup is completed and includes complete blood count, coagulation screen, urea, electrolytes, liver function test, and tumor markers (36–38).

Ablation must include the tumor and ideally 1 cm margin of normal hepatic parenchyma. Use of multiple probes can produce a synergistic effect and ensure complete tumor ablation. Probes should be placed to avoid clefts between ablation zones of each probe. The distance between the probes will vary depending on the

ablation technology used. Primary technical success is achieved when there is ablation of the entire tumor and a satisfactory ablative.

Follow-Up

It is common for patients to remain hospitalized for 24 hours post-treatment. Clinic, laboratory, and imaging follow-up is usually obtained 4 weeks post-treatment to assess tumor response and evaluate for complications. Perilesional nodular rim enhancement is characteristic of residual tumor (36, 39).

Risks and Complications

Rates of major complications of hepatic ablations are extremely low. A systematic review reported that mortality of ablation is 0.16%, while the rate of complications in general was 3.29%. The most common complication include tumor seeding 0.5%, intraperitoneal hemorrhage 0.37%, and liver abscess 0.32%, while ascites, pleural effusions, hepatic infarctions, liver failure, hemothorax, and perforation were all less than 0.25% (40).

Outcomes

The local tumor recurrence after ablation varies depending on tumor size, location, and margin obtained. Indeed, 1 cm margin was associated with no recurrence regardless of ablative technology used as was the use of MWA in tumors located near large vessels (41).

The EORTC-CLOCC trial randomized patients to ablation ± surgery, and chemotherapy vs. chemotherapy alone demonstrated improved progression survival in the combination group (42). A meta-analysis comparing ablation with RFA, MWA, and systemic chemotherapy and partial hepatectomy (PH) for mCRC demonstrated that ablation had PH which was superior to RFA in terms of disease recurrence but not superior to combination of PH and RFA or MWA. RFA had lower complications compared to PH but MWA did not (43). Prospective randomized trials are needed for inclusion of ablation formally in the NCCN and ESMO guidelines (12, 19).

There is growing data for interventional oncology interventions in mCRC; however, prospective randomized data is required for NCCN and ESMO guidelines integration.

References

1. Adam R, de Gramont A, Figueras J, Kokudo N, Kunstlinger F, Loyer E, et al. Managing synchronous liver metastases from colorectal cancer: a multidisciplinary international consensus. Cancer Treat Rev. 2015;41(9):729–41.
2. Chow FC, Chok KS. Colorectal liver metastases: an update on multidisciplinary approach. World J Hepatol. 2019;11(2):150–72.
3. Oxenberg J, Papenfuss W, Esemuede I, Attwood K, Simunovic M, Kuvshinoff B, et al. Multidisciplinary cancer conferences for gastrointestinal malignancies result in measureable treatment changes: a prospective study of 149 consecutive patients. Ann Surg Oncol. 2015;22(5):1533–9.
4. Nordlinger B, Sorbye H, Glimelius B, Poston GJ, Schlag PM, Rougier P, et al. Perioperative chemotherapy with FOLFOX4 and surgery versus surgery alone for resectable liver metastases from colorectal cancer (EORTC Intergroup trial 40983): a randomised controlled trial. Lancet. 2008;371(9617):1007–16.
5. Fernandez FG, Drebin JA, Linehan DC, Dehdashti F, Siegel BA, Strasberg SM. Five-year survival after resection of hepatic metastases from colorectal cancer in patients screened by positron emission tomography with F-18 fluorodeoxyglucose (FDG-PET). Ann Surg. 2004;240(3):438–47; discussion 47–50.
6. Scheele J, Stang R, Altendorf-Hofmann A, Paul M. Resection of colorectal liver metastases. World J Surg. 1995;19(1):59–71.
7. Cummings LC, Payes JD, Cooper GS. Survival after hepatic resection in metastatic colorectal cancer: a population-based study. Cancer. 2007;109(4):718–26.
8. Rees M, Tekkis PP, Welsh FK, O'Rourke T, John TG. Evaluation of long-term survival after hepatic resection for metastatic colorectal cancer: a multifactorial model of 929 patients. Ann Surg. 2008;247(1):125–35.
9. Tomlinson JS, Jarnagin WR, DeMatteo RP, Fong Y, Kornprat P, Gonen M, et al. Actual 10-year survival after resection of colorectal liver metastases defines cure. J Clin Oncol. 2007;25(29):4575–80.
10. Berri RN, Abdalla EK. Curable metastatic colorectal cancer: recommended paradigms. Curr Oncol Rep. 2009;11(3):200–8.
11. Cieslak KP, Runge JH, Heger M, Stoker J, Bennink RJ, van Gulik TM. New perspectives in the assessment of future remnant liver. Dig Surg. 2014;31(4–5):255–68.
12. Van Cutsem E, Cervantes A, Adam R, Sobrero A, Van Krieken JH, Aderka D, et al. ESMO consensus guidelines for the management of patients with metastatic colorectal cancer. Ann Oncol. 2016;27(8):1386–422.
13. Saltz LB, Clarke S, Diaz-Rubio E, Scheithauer W, Figer A, Wong R, et al. Bevacizumab in combination with oxaliplatin-based chemotherapy as first-line therapy in metastatic colorectal cancer: a randomized phase III study. J Clin Oncol. 2008;26(12):2013–9.
14. Nasti G, Piccirillo MC, Izzo F, Ottaiano A, Albino V, Delrio P, et al. Neoadjuvant FOLFIRI+bevacizumab in patients with resectable liver metastases from colorectal cancer: a phase 2 trial. Br J Cancer. 2013;108(8):1566–70.
15. Liu W, Zhou JG, Sun Y, Zhang L, Xing BC. The role of neoadjuvant chemotherapy for resectable colorectal liver metastases: a systematic review and meta-analysis. Oncotarget. 2016;7(24):37277–87.
16. Cremolini C, Antoniotti C, Lonardi S, Rossini D, Morano F, Cordio S, et al. Updated results of TRIBE2, a phase III, randomized strategy study by GONO in the 1st- and 2nd-line treatment of unresectable mCRC. Ann Oncol. 2019;30(Suppl 4):iv154.
17. Geissler M, Tannapfel A, Reinacher-Schick A, Martens U, Ricke J, Riera-Knorrenschield J, et al. Final results of the randomized phase II VOLFI trial (AIO- KRK0109): mFOLFOXIRI + Panitumumab versus FOLFOXIRI as first-line treatment in patients with RAS wild-type metastatic colorectal cancer (mCRC). Ann Oncol. 2019;30(Suppl 4):iv119–iv20.

18. Kopetz S, Grothey A, Yaeger R, Van Cutsem E, Desai J, Yoshino T, et al. Encorafenib, Binimetinib, and Cetuximab in BRAF V600E-Mutated Colorectal Cancer. N Engl J Med. 2019;381(17):1632–43.
19. National Comprehensive Cancer Network. Colon Cancer (Version 1.2019). 2019. https://www.nccn.org/professionals/physician_gls/pdf/colon.pdf.
20. Chang DT, Swaminath A, Kozak M, Weintraub J, Koong AC, Kim J, et al. Stereotactic body radiotherapy for colorectal liver metastases: a pooled analysis. Cancer. 2011;117(17):4060–9.
21. Raval M, Bande D, Pillai AK, Blaszkowsky LS, Ganguli S, Beg MS, et al. Yttrium-90 radioembolization of hepatic metastases from colorectal cancer. Front Oncol. 2014;4:120.
22. Tong AK, Kao YH, Too CW, Chin KF, Ng DC, Chow PK. Yttrium-90 hepatic radioembolization: clinical review and current techniques in interventional radiology and personalized dosimetry. Br J Radiol. 2016;89(1062):20150943.
23. Gaba RC. Planning arteriography for yttrium-90 microsphere radioembolization. Semin Intervent Radiol. 2015;32(4):428–38.
24. Theysohn JM, Muller S, Schlaak JF, Ertle J, Schlosser TW, Bockisch A, et al. Selective internal radiotherapy (SIRT) of hepatic tumors: how to deal with the cystic artery. Cardiovasc Intervent Radiol. 2013;36(4):1015–22.
25. Sangro B, Martinez-Urbistondo D, Bester L, Bilbao JI, Coldwell DM, Flamen P, et al. Prevention and treatment of complications of selective internal radiation therapy: expert guidance and systematic review. Hepatology. 2017;66(3):969–82.
26. Kennedy AS, Ball D, Cohen SJ, Cohn M, Coldwell DM, Drooz A, et al. Multicenter evaluation of the safety and efficacy of radioembolization in patients with unresectable colorectal liver metastases selected as candidates for (90)Y resin microspheres. J Gastrointest Oncol. 2015;6(2):134–42.
27. Wasan HS, Gibbs P, Sharma NK, Taieb J, Heinemann V, Ricke J, et al. First-line selective internal radiotherapy plus chemotherapy versus chemotherapy alone in patients with liver metastases from colorectal cancer (FOXFIRE, SIRFLOX, and FOXFIRE-Global): a combined analysis of three multicentre, randomised, phase 3 trials. Lancet Oncol. 2017;18(9):1159–71.
28. Hendlisz A, Van den Eynde M, Peeters M, Maleux G, Lambert B, Vannoote J, et al. Phase III trial comparing protracted intravenous fluorouracil infusion alone or with yttrium-90 resin microspheres radioembolization for liver-limited metastatic colorectal cancer refractory to standard chemotherapy. J Clin Oncol. 2010;28(23):3687–94.
29. Kritzinger J, Klass D, Ho S, Lim H, Buczkowski A, Yoshida E, et al. Hepatic embolotherapy in interventional oncology: technology, techniques, and applications. Clin Radiol. 2013;68(1):1–15.
30. Kandarpa K, Machan L, editors. Handbook of interventional radiologic procedures. Philadelphia: Lippincott Williams & Wilkins; 2011.
31. Fiorentini G, Aliberti C, Tilli M, Mulazzani L, Graziano F, Giordani P, et al. Intra-arterial infusion of irinotecan-loaded drug-eluting beads (DEBIRI) versus intravenous therapy (FOLFIRI) for hepatic metastases from colorectal cancer: final results of a phase III study. Anticancer Res. 2012;32(4):1387–95.
32. Richardson AJ, Laurence JM, Lam VW. Transarterial chemoembolization with irinotecan beads in the treatment of colorectal liver metastases: systematic review. J Vasc Interv Radiol. 2013;24(8):1209–17.
33. Riemsma RP, Bala MM, Wolff R, Kleijnen J. Transarterial (chemo)embolisation versus no intervention or placebo intervention for liver metastases. Cochrane Database Syst Rev. 2013;4:CD009498.
34. Levi FA, Boige V, Hebbar M, Smith D, Lepere C, Focan C, et al. Conversion to resection of liver metastases from colorectal cancer with hepatic artery infusion of combined chemotherapy and systemic cetuximab in multicenter trial OPTILIV. Ann Oncol. 2016;27(2):267–74.
35. Zacharias AJ, Jayakrishnan TT, Rajeev R, Rilling WS, Thomas JP, George B, et al. Comparative effectiveness of hepatic artery based therapies for unresectable colorectal liver metastases: a meta-analysis. PLoS One. 2015;10(10):e0139940.

36. Mahnken AH, Pereira PL, de Baere T. Interventional oncologic approaches to liver metastases. Radiology. 2013;266(2):407–30.
37. Petre EN, Sofocleous C. Thermal ablation in the management of colorectal cancer patients with oligometastatic liver disease. Visc Med. 2017;33(1):62–8.
38. Tsitskari M, Filippiadis D, Kostantos C, Palialexis K, Zavridis P, Kelekis N, et al. The role of interventional oncology in the treatment of colorectal cancer liver metastases. Ann Gastroenterol. 2019;32(2):147–55.
39. Foltz G. Image-guided percutaneous ablation of hepatic malignancies. Semin Intervent Radiol. 2014;31(2):180–6.
40. Bertot LC, Sato M, Tateishi R, Yoshida H, Koike K. Mortality and complication rates of percutaneous ablative techniques for the treatment of liver tumors: a systematic review. Eur Radiol. 2011;21(12):2584–96.
41. Shady W, Petre EN, Do KG, Gonen M, Yarmohammadi H, Brown KT, et al. Percutaneous microwave versus radiofrequency ablation of colorectal liver metastases: ablation with clear margins (A0) provides the best local tumor control. J Vasc Interv Radiol. 2018;29(2):268–75e1.
42. Ruers T, Van Coevorden F, Punt CJ, Pierie JE, Borel-Rinkes I, Ledermann JA, et al. Local treatment of unresectable colorectal liver metastases: results of a randomized phase II trial. J Natl Cancer Inst. 2017;109(9):djx015.
43. Meijerink MR, Puijk RS, van Tilborg A, Henningsen KH, Fernandez LG, Neyt M, et al. Radiofrequency and microwave ablation compared to systemic chemotherapy and to partial hepatectomy in the treatment of colorectal liver metastases: a systematic review and meta-analysis. Cardiovasc Intervent Radiol. 2018;41(8):1189–204.

Chapter 10
Neuroendocrine Neoplasms

Adam Schwertner, Emily K. Bergsland, Thomas A. Hope, Eric K. Nakakura, Moishir Anwar, Maureen P. Kohi, and Nicholas Fidelman

Epidemiology and Pathophysiology

Neuroendocrine neoplasms (NENs) are epithelial neoplasms with neuroendocrine differentiation, which can arise from a variety of organs throughout the body but most commonly from the gastrointestinal tract, the pancreas, the bronchi, the thyroid, or the neural crest (paraganglioma/pheochromocytoma.) NENs are the second most common GI malignancy after colon cancer with an incidence of 6.98 per 100,000 people per year. For unknown reasons, the incidence of NENs has been rising over the last several decades with incidence rates more than doubling from 1994 to 2009 [1].

Classification of NENs is determined by site or origin, endocrine functionality, and histologic grade. A functional NEN is a tumor, which secretes a substance that results in clinical symptoms such as carcinoid syndrome, Zollinger-Ellison syndrome (gastrinoma), or hypoglycemia (insulinoma). The most commonly secreted

A. Schwertner · M. P. Kohi · N. Fidelman (✉)
Department of Interventional Radiology, University of California San Francisco, San Francisco, CA, USA
e-mail: Nicholas.Fidelman@ucsf.edu

E. K. Bergsland
Department of Medicine – Gastrointestinal Oncology, University of California San Francisco, San Francisco, CA, USA

T. A. Hope
Department of Nuclear Medicine, University of California San Francisco, San Francisco, CA, USA

E. K. Nakakura
Department of Surgery, University of California San Francisco, San Francisco, CA, USA

M. Anwar
Department of Radiation Oncology, University of California San Francisco, San Francisco, CA, USA

C. Georgiades, H. S. Kim (eds.), *Image-Guided Interventions in Oncology*,
https://doi.org/10.1007/978-3-030-48767-6_10

hormones in functional NENs are insulin or gastrin. Vasoactive intestinal peptide (VIP), glucagon, somatostatin, ACTH, serotonin, and parathyroid hormone-related protein hypersecretion occur less commonly. Nonfunctional NENs may secrete a number of substances, which do not result in a hormonal syndrome, and as such, commonly come to medical attention at a more advanced stage.

Pathologically NENs are divided into well-differentiated tumors (WD-NET) and poorly differentiated neuroendocrine carcinoma (NEC). Distinction between WD-NET and NEC is made by examination of tissue morphology. Mitotic count and Ki-67 proliferation index determine tumor grade. Grade 1 NET are characterized by Ki-67 index <3% and mitotic count <2 per 10 high-power fields (HPF). Grade 2 NET possess Ki-67 index 3–20% and 2–20 mitoses per 10 HPF. Grade 3 WD-NET and NEC show Ki-67 index >20% and mitotic count >20 per 10 HPF. NENs are seen in a number of syndromes with predisposition to cancer including multiple endocrine neoplasia (MEN) types 1 and 2, Von Hippel-Lindau syndrome, neurofibromatosis 1, tuberous sclerosis, and hereditary paraganglioma syndrome.

Targeted imaging options for NENs vary for well-differentiated and poorly differentiated tumors. Well-differentiated NENs usually retain the somatostatin receptor and will bind the somatostatin analog octreotide, which can be conjugated to radioactive ^{111}In pentetreotide (OctreoScan) or to ^{68}Ga-DOTATATE or ^{68}Ga DOTATOC. ^{111}In pentetreotide is imaged using single-photon emission computed tomography (SPECT) with a reported sensitivity of approximately 85% for well-differentiated NENs. ^{68}Ga DOTATATE or ^{68}Ga DOTATOC positron emission tomography (PET) is preferred over ^{111}In pentetreotide for imaging well- differentiated NENs due to increased sensitivity at approximately 90% and superior image quality. Targeted somatostatin receptor nuclear imaging can be attempted in poorly differentiated NENs; however, these tumors commonly lose the somatostatin receptors. For less indolent WD-NET and NEC, imaging can be pursued with fluorodeoxyglucose (FDG) PET.

Well-differentiated NENs have a relatively indolent course with a slow growth rate and prognosis varying depending on location of primary tumor, stage at diagnosis, and tumor grade. The liver is a common site for NEN metastasis, and liver metastases are a major determinant in symptomatology and survival. Patients with liver metastases have a worse prognosis when compared to those with localized disease.

In the presence of localized disease, carcinoid neoplasms produce 5-hydroxytryptamine (5-HT), which is taken up and stored in the platelets. Excess 5-HT is metabolized by the liver and lung and transformed into 5-hydroxyindoleacetic acid (5-HIAA). In the presence of liver metastases, vasoactive substances produced by tumors may escape degradation by the liver and are secreted into the systemic circulation, resulting in carcinoid syndrome. Carcinoid syndrome may manifest with cutaneous flushing, diarrhea, and bronchoconstriction. Patients may also develop hemodynamic instability with tachycardia or bradycardia as well as

hypotension or hypertension. Carcinoid syndrome exacerbation with concomitant hemodynamic instability is referred to as carcinoid storm and is a medical emergency.

Nearly 40% of patients exhibiting the carcinoid syndrome will develop carcinoid heart disease with fibrotic endocardial plaques and associated heart valve dysfunction that classically involves the tricuspid and the pulmonic valves. Advanced changes of tricuspid and pulmonic valvular disease have been shown to be associated with poor long-term survival, and carcinoid valvular disease, rather than tumor dissemination, is the cause of death in approximately one-third of these patients. Serotonin is presumed to be the catalyst for the cardiac fibrotic process. Nearly 95% of patients with present with right-sided heart valve disease, characterized by tricuspid insufficiency and pulmonic regurgitation and the subsequent development of right heart failure. Left-sided cardiac disease may be seen in up to 10% of patients, as is commonly associated with angina and coronary vasospasm.

Role of Surgery

Surgical resection plays a key role in the initial management of NENs primarily through the removal of the primary tumor and hepatic metastases. Surgical resection of the primary tumor is vital in NENs arise from the bowel, as removal of the bowel primary is an independent factor for improved survival [2]. Surgical resection of bowel NENs may be curative for patients with localized disease and may decrease the risk of bowel ischemia or bowel obstruction related to primary tumor and regional lymph nodes. Similarly, pancreatic NENs may be resected or enucleated depending on tumor size and location within the pancreas. Surgical resection of bronchial NENs provides symptomatic relief by helping to prevent post-obstruction pneumonia as these tumors commonly obstruct the airways and may also provide a curative option.

The liver is the most common site for gastroenteropancreatic (GEP) NEN metastases, and surgical resection of hepatic metastases should be considered. While hepatic metastectomy provides a survival benefit [3], there are high recurrence rates after liver resection. In a multicenter review from medical centers across the world, recurrence rates after hepatic metastectomy were 94% at 5 years and 99% at 10 years [3]. Recently there has been a trend to decrease the threshold for percent liver metastasis debulking from a 90% to a 70% threshold as there was no significant difference in the 5-year survival rates between the patients for whom 90% and 70% hepatic tumor debulking was achieved [4].

Liver transplantation has been performed to treat metastatic NENs. Studies investigating liver transplantation are limited by small sample size, and more research is needed to investigate survival rates after transplantation. As such, liver transplantation should be considered an experimental option for the treatment of metastatic NENs until more thoroughly studied.

Systemic Therapy

In patients where curative surgical resection is not possible, systemic therapies can be utilized for disease control (typically radiographic stability, not tumor regression) and for symptomatic relief (Fig. 10.1). Somatostatin analogs (SSA), such as octreotide and lanreotide, are the first-line treatment for patients with tumors that express somatostatin receptors on the cell surface. SSA work by binding the somatostatin receptor, which in turn leads to decrease the secretion of a broad range of hormones. Somatostatin analogs have been demonstrated to significantly improve the progression-free survival (PFS) when compared to placebo for patients with WD- NET. PROMID trial showed that depot octreotide use was associated with PFS improvement from 5.9 to 15.6 months when compared to placebo for patients with well-differentiated metastatic midgut NENs [5]. Similarly, CLARINET trial demonstrated that lanreotide was associated with significantly prolonged PFS for patients with grade 1 or 2 metastatic neuroendocrine tumors of gastroenteropancreatic (GEP) origin [6]. Octreotide depot dosing generally begins with 20 mg intramuscular injection monthly and can be titrated up in dose to 60 mg monthly or in frequency to every 2 weeks. Lanreotide dose is fixed at 120 mg monthly. In conjunction with somatostatin analogs, telotristat is a tryptophan hydroxylase inhibitor, which can be used to treat diarrhea related to carcinoid syndrome.

For patients with progressive metastatic disease in the setting of somatostatin analog therapy, everolimus, sunitinib, or radiolabeled somatostatin analogs can be considered. NENs are vascular solid tumors. Everolimus and sunitinib help control tumor growth by targeting angiogenesis and cell proliferation. Everolimus modulates the mammalian target of rapamycin (mTOR) receptor, which mediates signaling in pathways related to cell growth and proliferation. Sunitinib acts by inhibiting receptor tyrosine kinases related to vascular endothelial growth factor. Both agents

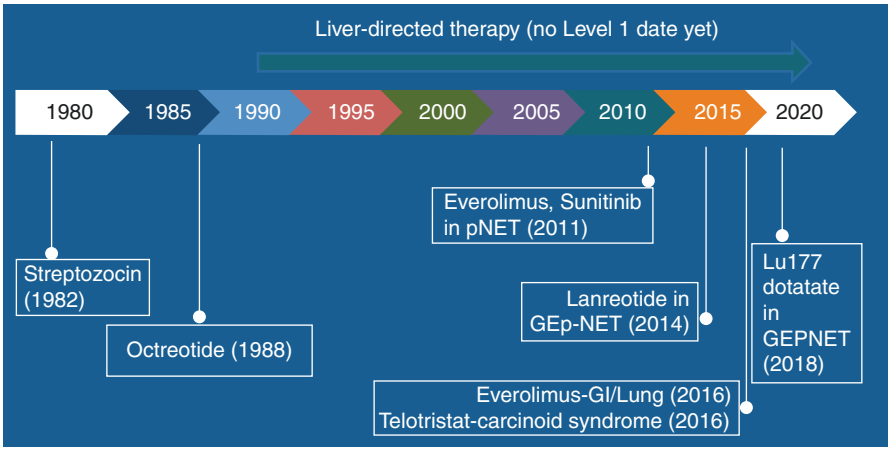

Fig. 10.1 Timeline of FDA approval and availability of systemic therapy agents for WD-NET

tend to have cytostatic effect on tumor growth, not tumor regression. Everolimus has been shown to improve PFS when compared to placebo for patients with progressive pancreatic NET (11 months versus 4.6 months) [7] and for patients with nonfunctional lung and GI NET (11 months versus 3.9 months) [8]. Sunitinib was also demonstrated to improve PFS (versus placebo) for patients with progressive pancreatic NET (11.4 months versus 5.5 months) [9]. Everolimus and sunitinib may be used in conjunction with somatostatin analogs.

Peptide receptor radionuclide therapy (PRRT) is a systemic therapy, in which a radionuclide is bound via a chelator to a somatostatin receptor analog to deliver radiation therapy directly to tumors via somatostatin receptor binding. The two primary compounds used for PRRT are Lutetium-177 DOTATATE and Yttrium-90 DOTATOC. ^{90}Y and ^{177}Lu both generate high-energy electrons via beta decay, which interact with surrounding tissue causing double-stranded DNA breaks leading to cell death. ^{90}Y is generally considered a better choice for larger tumors due to higher energy decay, which results in deeper beta particle penetration in tissue as compared to ^{177}Lu. As demonstrated by NETTER trial, patients with advanced midgut WD-NET who progressed on SSA had significantly longer PFS (>40 months) compared to patients treated with a higher dose of SSA (8.9 months). Significant reduction in tumor bulk (complete or partial response) was observed in 18% of patients [10]. The main risks of PRRT include bone marrow suppression, myelodysplastic syndrome (2.7%), leukemia (0.5%), and renal dysfunction (2%). Clinically significant myelosuppression was seen in fewer than 10% of patients in the ^{177}Lu DOTATATE group in the NETTER trial.

Cytotoxic chemotherapeutic regimens can be considered in patients with progressive and rapidly growing metastatic disease. Treatment regimens used for treatment of WD-NET include capecitabine and temozolomide as well as oxaliplatin-based regimens such as FOLFOX. Capecitabine with temozolomide therapy resulted in a 54% overall response rate based on RECIST criteria in a study of pancreatic NENs [11].

Intra-arterial Therapies

Liver-directed therapies in metastatic NENs are used for a number of indications.

1. Progressive liver metastases (solitary or multiple)
2. Liver metastases that cause bulk symptoms such as pain, nausea, or early satiety
3. Liver metastasis with difficult to control hormonal symptoms and/or elevated urine 24-hour 5-HIAA levels (which may, in turn, increase the risk for carcinoid heart disease)
4. Liver metastases with discordant biologic behavior (liver lesion(s) enlarging out of proportion to other lesions and/or liver lesion(s) with less uptake on SSTR-PET than other lesions)

TACE and TAE

Conventional transarterial chemoembolization (cTACE) is a form of intra-arterial therapy where chemotherapy (commonly doxorubicin, mitomycin C, and cisplatin) is emulsified with ethiodized oil (Lipiodol®) and infused directly into the hepatic artery supplying the hepatic metastases. Ethiodized oil is a viscous, radiopaque liquid derived from poppy seed oil, which slows hepatic arterial blood flow and allows for the delivery of the chemotherapeutic agents. Lipiodol® is thought to be absorbed into the intracellular space of tumor cells where it remains trapped for months to years. Lipiodol® washes out from normal liver tissue after approximately 4 weeks. Hemostasis related to lipiodol and cytotoxicity related to intra-arterially delivered chemotherapy result in tumor ischemia and cell death. Normal hepatocytes typically have enough redundant blood supply from the portal venous system to prevent liver infarction.

Bland transarterial embolization (TAE) without chemotherapy is also a strategy for intra-arterial therapy. NENs are typically hypervascular tumors with blood supply primarily provided by the hepatic artery. Bland embolization causes hepatic arterial stasis, which results in tumoral hypoxia and cell death. There are multiple types of permanent embolic agents, which can be utilized for bland embolization. One type of particles, tris-acryl gelatin microspheres (Embosphere™, Merit Medical, San Jose, CA, USA), are a hydrophilic, non-resorbable acrylic polymer with impregnated porcine gelatin and are manufactured with a range of sphere diameter. Most commonly 40–120 μm, 100–300 μm, or 300–500 μm microspheres are utilized for hepatic artery embolization. Another type of commonly used permanent embolic agent is tightly calibrated hydrogel microspheres (Embozene™, Boston Scientific, Natick, MA, USA). Particle sizes of 40, 75, 100, 250, 400, and 500 μm may be used for TAE. Polyvinyl alcohol particles are an alternative permanent embolic to tris-acryl gelatin microspheres and range in size from 100 to 1100 μm. PVA particles are more heterogenous in shape as compared embolic microspheres with the main drawback of having the tendency to aggregate leading to occlusion of the vessel more proximal than expected. Generally, smaller particles (<100 μm) may be used for smaller and less vascular tumors, whereas large particles (>100 μm) may be safe for larger hypervascular tumors that may contain hepatic artery to hepatic vein shunts.

The efficacy of cTACE and TAE has not been prospectively compared, although a prospective randomized trial (Randomized Embolization Trial for NeuroEndocrine Tumor Metastases to the Liver, RETNET) is currently ongoing (NCT #02724540). Based on retrospective case-control studies, symptomatic, biochemical, imaging improvement, and progression-free survival appear to be similar (Table 10.1). TACE (Fig. 10.2) and TAE (Fig. 10.3) may be used interchangeably for patients with progressive liver-dominant liver metastases, liver metastases that cause bulk symptoms, and patients with difficult to control hormonal symptoms and/or elevated 24-hr urine 5-HIAA levels.

Table 10.1 cTACE and TAE efficacy [12]

	TAE	cTACE
Symptomatic improvement	64–93%	60–95%
Biochemical improvement	50–69%	50–90%
Imaging improvement	32–82%	33–80%
Progression-free survival	18–88 months	18–24 months

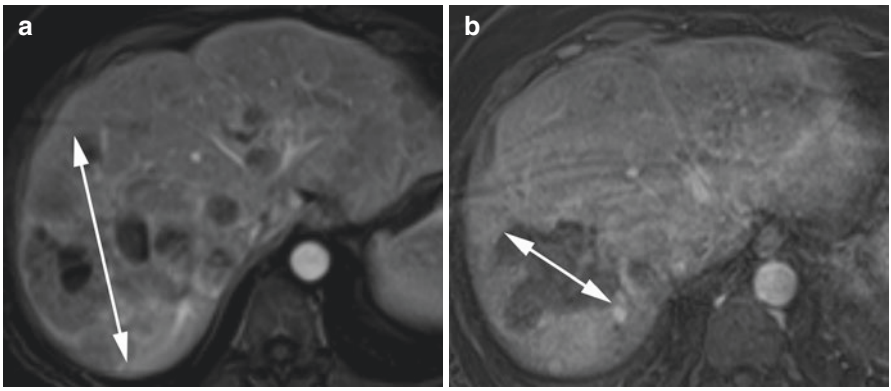

Fig. 10.2 Representative images of abdominal contrast-enhanced MRI obtained prior to (**a**) and 3 months following three transarterial embolizations (**b**) performed for a 64-year-old woman with bulky metastatic grade 1 small bowel NET. Following TAE, there has been interval development of necrosis and decrease in size within the dominant liver lesions (**a** and **b**, arrows)

Incidence and severity of side effects of TACE and TAE are also similar. Post-embolization syndrome is the most common side effect with incidence of nearly 100%. It is characterized by abdominal pain, nausea, vomiting, fever, night sweats, and fatigue. Rare but serious side effects may include biliary strictures, cholangitis, liver abscess, and liver failure. Patients with a history of biliary tract instrumentation (biliary-enteric anastomosis, biliary stents, or percutaneous biliary drains) are at a particularly high risk of serious hepatobiliary infection.

Re-treatment with the same or a different embolotherapy modality is possible for patients with liver-dominant disease. Conventional TACE may be preferred for retreatment after previous embolotherapy, due to the ability of 40 μm chemotherapy in ethiodized oil micelles to penetrate into the tumor vasculature located beyond the truncated or partially obliterated hepatic artery branches.

Drug-eluting bead transarterial chemoembolization (DEB-TACE) is an alternative to conventional TACE that involves delivery of calibrated microspheres loaded with doxorubicin into the tumor feeding arteries. Through ion exchange, doxorubicin is gradually released from the microspheres into the tissue over the course of days to weeks. At its inception, RETNET trial included cTACE, DEB-TACE, and TAE arms. The initial safety review (after the first 30 patients were treated) resulted in closure of the DEB-TACE arm due to an unacceptably high number of severe

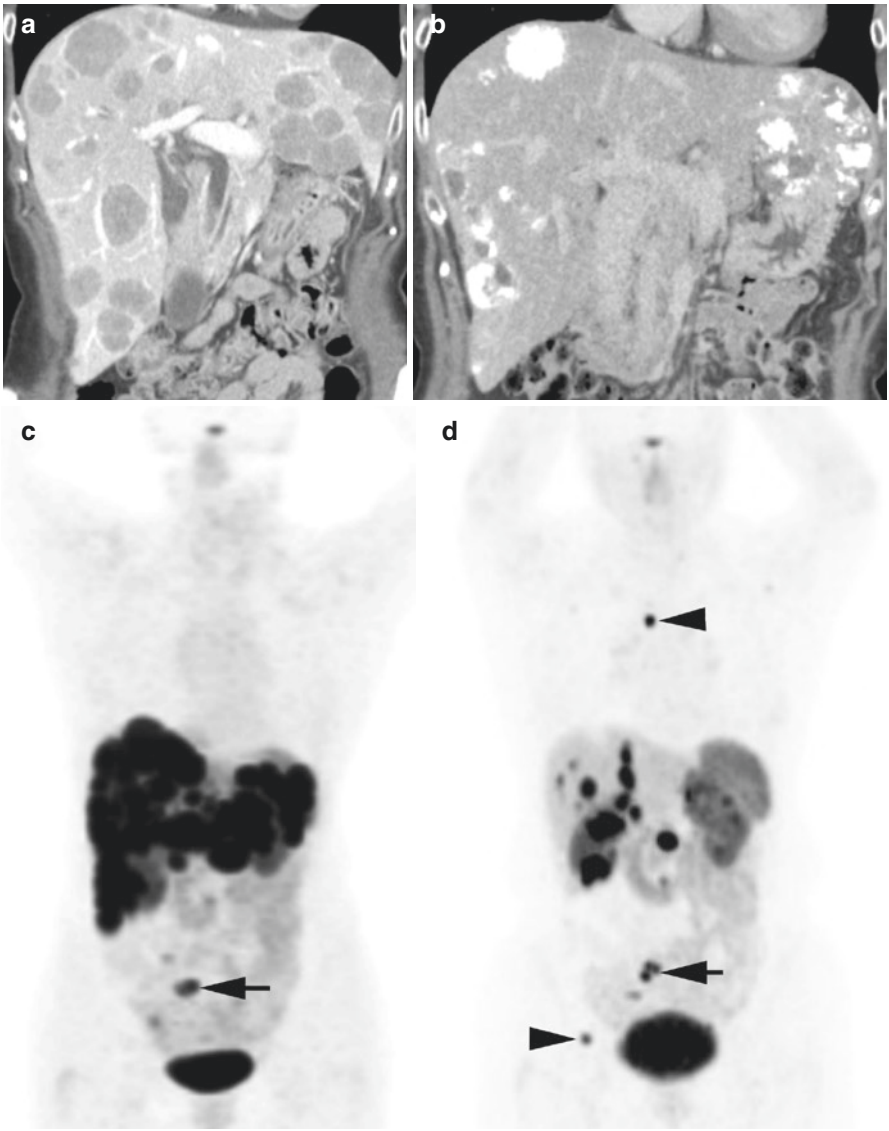

Fig. 10.3 Representative images of abdominal contrast-enhanced coronal CT reformations obtained prior to (**a**) and 3 months (**b**) following 3 TACE sessions performed for a 70-year-old woman with metastatic grade 2 small bowel NET. Following cTACE, multiple bilobar metastases have decreased in size and developed diffuse accumulation of ethiodized oil. SSTR-PET images obtained prior to TACE (**c**) demonstrated diffuse high-intensity radiotracer within the liver and within the ileal primary tumor (arrow). Repeat SSTR-PET obtained 6 months following three TACE sessions (**d**) demonstrated marked reduction of radiotracer uptake within the liver, stable uptake within the primary tumor (arrow), and new metastases in the mediastinum and pelvis (arrowheads). The patient was subsequently treated with PRRT

adverse events, which included hepatobiliary necrosis and biloma in 4 of 10 patients in the DEB-TACE arm [13]. Another study evaluating the use of DEB-TACE for metastatic NENs similarly found a greater than expected incidence of biliary adverse events, with 54% of patients developing bilomas after DEB-TACE [14]. As such, DEB-TACE has generally fallen out of favor as an intra-arterial treatment modality for patient with metastatic NENs.

Radioembolization

Transarterial radioembolization (TARE) with Ytrium-90 is another intra-arterial therapy where ^{90}Y is loaded on microspheres measuring between 20 and 60 μm in diameter. Microspheres lodge within the tumor microvasculature, where ^{90}Y undergoes beta decay, leading to DNA damage and apoptosis. Radiographic response rate to TARE for WD-NET may be as high as 95% (Fig. 10.4). Based on one multicenter retrospective study [15], median overall survival after TARE (48 months) was significantly longer when compared to cTACE (33 months). The role of TARE in the treatment of metastatic NENs is evolving given the recent FDA approval of PRRT in the United States. There is growing concern that combining TARE with PRRT may result in increased hepatic toxicity. Nevertheless, TARE may be used for treatment of tumors that do not express somatostatin receptors and as an alternative to TAE or TACE for patients with a history of biliary tract intervention due to

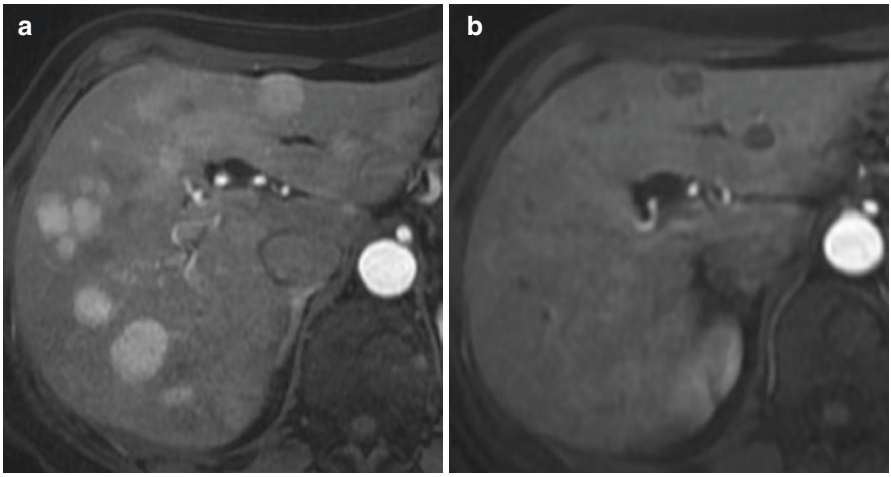

Fig. 10.4 Representative images of abdominal contrast-enhanced MRI obtained prior to (**a**) and 1 month following two sequential lobar 90Y radioembolizations (**b**) performed for a 60-year-old woman with metastatic bilobar grade 2 small bowel NET. Following radioembolization, all of the treated lesions became necrotic, as evidenced by loss of lesion enhancement. Lesions within the right lobe, which were targeted first were no longer apparent on the posttreatment MRI

potentially lower risk of hepatobiliary infection [16]. TARE may also be considered in cases where hepatic lesions are enlarging despite multiple prior lines of therapy including everolimus, capecitabine/temozolomide, and PRRT.

TARE requires a planning angiogram with measurement of pulmonary shunt fraction prior to treatment, whereas TACE and TAE do not require a planning angiogram. If both right and left hepatic lobes are to be treated, the lobar treatments should be spaced out by at least 1 month in order to minimize hepatic toxicity. TARE should not be pursued in patients with underlying liver disease with serum total bilirubin levels above 2 mg/dL. Patients who undergo TARE may be more likely to develop long-term biochemical hepatic toxicity and possibly portal hypertension as compared to TAE or TACE [17].

In summary, conventional TACE and bland TAE should be the first line of intra-arterial treatments for patients with somatostatin receptor avid progressive liver disease with the goal of decreasing tumor volume and controlling hormonal symptoms. The ongoing RETNET trial may provide guidance in the future about whether conventional TACE or TAE is favored for treatment of WD-NETs. Currently available data suggest that conventional TACE and TAE may be equivalent in terms of tumor response rate, symptomatic relief, and side effect severity. There is growing concern that TARE should not be utilized prior to PRRT due to the risk of hepatotoxicity [17]. In a retrospective study evaluating survival outcomes in patients with hepatic WD-NET metastases treated with embolotherapy, factors which predicted improved survival included unimpaired performance status, low tumor grade, and low percent liver replacement by tumor [15]. DEB-TACE has fallen out of favor due to the high incidence of biliary complications. Intra-arterial therapies should be spaced out as much as possible in order to allow hepatic recovery and reduce liver toxicity. When embolotherapy is pursued, largest lesions or liver regions with the largest tumor to normal liver parenchyma ratio should be targeted in order to minimize damage to normal liver tissue. Intra-arterial therapy should be performed on lesions, which are rapidly growing or growing disproportionately relative to other hepatic metastasis. Hepatic lesions which have a low binding affinity for somatostatin receptor (SSTR) PET should be targeted with intra-arterial therapy as these lesions are not likely to respond to PRRT. TARE should be considered for patients with a history of biliary tract intervention or for treatment of hepatic metastases that are not somatostatin receptor avid.

Percutaneous Ablation

Microwave ablation has become the preferred percutaneous treatment modality when treating liver tumors due to superiority at overcoming heat sink effects that can limit efficacy of radiofrequency and cryoablation. Heat sink occurs when energy is deposited into flowing blood within adjacent blood vessels and is carried away from the treatment zone. Heat sink effect may contribute to suboptimal treatment of the target lesions. Microwave ablation has been shown to be non-inferior to

radiofrequency ablation when treating hepatocellular carcinoma. There is a paucity of data regarding survival and recurrence rates when utilizing percutaneous ablation within the liver for NENs. However a meta-analysis of radiofrequency ablation of hepatic metastasis demonstrated that ablation can provide symptomatic relief when performed alone or in combination with surgery [18]. Percutaneous ablation is best utilized in patients with few lesions (less than 10% of hepatic parenchyma replaced by tumor) with individual lesions measuring less than 4 cm in diameter and not amenable to surgical resection.

External Beam Radiation Therapy

Radiation therapy is primarily used for palliation in metastatic neuroendocrine tumors with up to 90% improvement or resolution in symptoms with radiation therapy [19]. Radiation therapy can also be considered in patients who are not surgical candidates for primary tumor resection, particularly in tumors of pancreatic or bronchial origin. Stereotactic body radiation therapy (SBRT) can be used for the treatment of isolated hepatic metastases. External beam radiation therapy to the abdomen may also be helpful for palliation of tumor bulk symptoms, such as pain and gastrointestinal bleeding). Pain related to osseous metastases is an additional common indication for external beam radiation therapy.

Multimodality Treatment

Intra-arterial therapies can be combined with percutaneous ablation for synergistic effects. Data regarding combination intra-arterial therapy and percutaneous ablation for NENs is limited; however, studies within hepatocellular carcinoma literature have demonstrated that TACE with percutaneous ablation significantly improve local tumor response and patient survival rates versus monotherapy for 3–5 cm lesions [20]. When performing multimodality treatment with percutaneous ablation, intra-arterial therapy could be performed first to decrease arterial blood flow to the tumor, allow better tumor visualization during ablation (especially if cTACE is employed), reduce the heat sink effects seen with percutaneous ablation, and to maximize the percutaneous ablation treatment zone.

Timing of Systemic and Liver-Directed Therapy

Somatostatin receptor imaging with SSTR-PET is critical at initial staging and may help monitor disease progression due to high sensitivity and specificity. Additionally, due to the relatively indolent course of growth for the majority of NENs, imaging

studies may need to be compared to remote priors to evaluate for change within slowly growing lesions.

Generally, somatostatin analogues such as octreotide and lanreotide are recognized as first-line systemic therapy for patients with advanced WD-NET that demonstrate somatostatin receptor expression on molecular imaging. Treatment with SSA is typically carried out until symptomatic or radiographic progression. At progression, response may be recaptured by increasing the dose of octreotide and by switching from one SSA to another.

Currently there is no data regarding the specific sequence of regional versus systemic therapy after progression on SSA. Surgical resection should be pursued upfront for patients both with metastases and without. Removal of the primary tumor has been associated with overall survival benefit even in the presence of metastatic disease. Patients with liver-dominant disease may benefit from surgical debulking, if removal of at least 70% of the liver tumor burden is technically feasible, and depending on the extent of underlying comorbidities and liver function. Surgical debulking of liver metastases should be pursued prior to embolotherapy due to scarring and parenchymal damage that may follow embolization, making subsequent surgery more challenging. Alternatively, patients with liver-only or liver-dominant metastases may be treated with embolotherapy or percutaneous ablation if resection is not feasible or at the time of disease recurrence.

Patients should be evaluated for liver-directed therapy at the time of radiographic and/or symptomatic disease progression. Pursuing liver-directed therapy when disease distribution is liver dominant is important. LDT may have a role in the setting of unifocal or diffuse liver disease progression, worsening hormonal symptoms (carcinoid syndrome, hypoglycemia), worsening bulk symptoms (pain, nausea, early satiety), and/or for lesions with discordant biologic behavior, such as faster growing lesions or lesions with less avid uptake on SSTR-PET than other lesions (Fig. 10.5). Of note, number and extent of liver embolization for patients with poorly controlled hormonal symptoms should be tailored to symptomatic improvement. The entire liver disease burden may not have to be treated to achieve adequate symptomatic relief when the lesions are radiographically stable. The generally accepted paradigm for liver-directed therapy for NET involves targeting as little healthy liver parenchyma as possible and to treat as infrequently as possible with the goal of minimizing the long-term risk of liver toxicity.

After progression on SSA, patients with systemic disease distribution may benefit from PRRT, biologic agents (everolimus and/or sunitinib), or chemotherapy. Selection of the systemic treatment depends on the rate of progression, disease bulk, and underlying comorbidities. Chemotherapy may be favored for treatment of faster-growing tumors, especially grade 3 WD- NET. Everolimus, sunitinib, and PRRT may be favored for patients with slow rate of progression. Everolimus may cause hyperglycemia and may not be suitable for patients with diabetes mellitus. Sunitinib may cause cytopenias and hypertension. PRRT may be best suited for patients with diffuse large-volume progression due to bone marrow and renal toxicity that could potentially be spared for patients with low-volume diffuse disease.

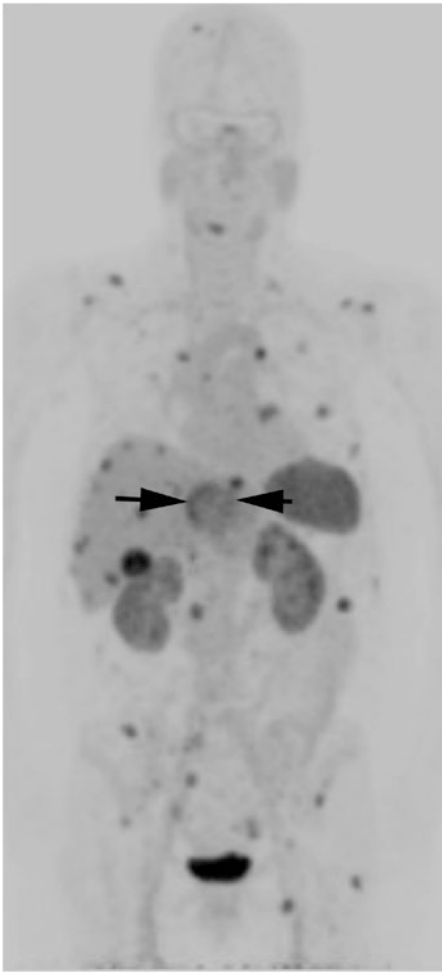

Fig. 10.5 SSTR-PET image of a 63-year-old woman with diffuse metastases from grade 2 small bowel NET demonstrated less avid radiotracer uptake in one of the liver lesions (arrows) than in the other lesions. The patient was treated with cTACE to the lesion with less avid uptake prior to starting PRRT. Following TACE, the patient was treated with four cycles of PRRT

A multidisciplinary approach is critical when treating patients with metastatic NENs due to the variability in clinical symptomatology, rate of progression, disease bulk, and distribution. The multidisciplinary team should include medical oncologists, surgeons, interventional radiologists, theranostics experts, radiologists, radiation oncologists, nutritionists, and survivorship specialists.

Future Trends

Several drugs are in clinical trials dedicated to patients with NENs, including axitinib, cabozantinib, immune checkpoint inhibitors, and chemotherapy combinations. There may be a synergistic effect between local therapy and immunotherapy.

Percutaneous ablation, embolization, and radioembolization cause tissue necrosis and may help expose tumor antigens to the immune system. This synergy is under investigation in an ongoing pilot trial (NCT03457948). Immune checkpoint inhibitor pembrolizumab is being evaluated as monotherapy and in combination with chemotherapy for patients with neuroendocrine carcinoma. Similar to other immune checkpoint inhibitors, pembrolizumab allows the body's immune system to target tumoral cells by blocking the PD-1 receptor. PD-1 is responsible for inhibiting activation of cytotoxic T-lymphocytes. Delivery of PRRT into the hepatic artery is also currently undergoing investigation for treatment of patients with liver-dominant somatostatin receptor avid hepatic metastases with the goal of decreasing renal and bone marrow toxicity of PRRT.

References

1. Hallet J, Law CHL, Cukier M, Saskin R, Liu N, Singh S. Exploring the rising incidence of neuroendocrine tumors: a population-based analysis of epidemiology, metastatic presentation, and outcomes. Cancer. 2015;121(4):589–97.
2. Ahmed A, Turner G, King B, Jones L, Culliford D, McCance D, et al. Midgut neuroendocrine tumours with liver metastases: results of the UKINETS study. Endocr Relat Cancer. 2009;16(3):885–94.
3. Mayo SC, de Jong MC, Pulitano C, Clary BM, Reddy SK, Gamblin TC, et al. Surgical management of hepatic neuroendocrine tumor metastasis: results from an international multi-institutional analysis. Ann Surg Oncol. 2010;17(12):3129–36.
4. Morgan RE, Pommier SJ, Pommier RF. Expanded criteria for debulking of liver metastasis also apply to pancreatic neuroendocrine tumors. Surgery. 2018;163(1):218–25.
5. Rinke A, Müller H-H, Schade-Brittinger C, Klose K-J, Barth P, Wied M, et al. Placebo-controlled, double-blind, prospective, randomized study on the effect of octreotide LAR in the control of tumor growth in patients with metastatic neuroendocrine midgut tumors: a report from the PROMID Study Group. J Clin Oncol Off J Am Soc Clin Oncol. 2009;27(28):4656–63.
6. Caplin ME, Pavel M, Ćwikła JB, Phan AT, Raderer M, Sedláčková E, et al. Lanreotide in metastatic enteropancreatic neuroendocrine tumors. N Engl J Med. 2014;371(3):224–33.
7. Yao JC, Shah MH, Ito T, et al. Everolimus for advanced pancreatic neuroendocrine tumors. N Engl J Med. 2011;364:514–23.
8. Yao JC, Fazio N, Singh S, Buzzoni R, Carnaghi C, Wolin E, et al. Everolimus for the treatment of advanced, non-functional neuroendocrine tumours of the lung or gastrointestinal tract (RADIANT-4): a randomised, placebo-controlled, phase 3 study. Lancet Lond Engl. 2016;387(10022):968–77.
9. Raymond E, Dahan L, Raoul JL, et al. Sunitinib malate for the treatment of pancreatic neuroendocrine tumors. N Engl J Med. 2011;364:501–13.
10. Strosberg J, El-Haddad G, Wolin E, Hendifar A, Yao J, Chasen B, et al. Phase 3 trial of 177Lu-Dotatate for midgut neuroendocrine tumors. N Engl J Med. 2017;376(2):125–35.
11. Cives M, Ghayouri M, Morse B, Brelsford M, Black M, Rizzo A, et al. Analysis of potential response predictors to capecitabine/temozolomide in metastatic pancreatic neuroendocrine tumors. Endocr Relat Cancer. 2016;23(9):759–67.
12. Vogl TJ, Naguib NNN, Zangos S, Eichler K, Hedayati A, Nour-Eldin N-EA. Liver metastases of neuroendocrine carcinomas: interventional treatment via transarterial embolization, chemoembolization and thermal ablation. Eur J Radiol. 2009;72(3):517–28.

13. Soulen M, White S, Fidelman N, Garcia-Monaco R, Wileyto E, Avritscher R, et al. 03:27 PM abstract no. 105 randomized embolization trial for NeuroEndocrine tumors (RETNET): first safety report. J Vasc Interv Radiol. 2019;30(3):S49–50.
14. Bhagat N, Reyes DK, Lin M, Kamel I, Pawlik TM, Frangakis C, et al. Phase II study of chemoembolization with drug-eluting beads in patients with hepatic neuroendocrine metastases: high incidence of biliary injury. Cardiovasc Intervent Radiol. 2013;36(2):449–59.
15. Chen JX, Rose S, White SB, El-Haddad G, Fidelman N, Yarmohammadi H, et al. Embolotherapy for neuroendocrine tumor liver metastases: prognostic factors for hepatic progression-free survival and overall survival. Cardiovasc Intervent Radiol. 2017;40(1):69–80.
16. Devulapalli KK, Fidelman N, Soulen MC, Miller M, Johnson MS, Addo E, et al. 90Y Radioembolization for hepatic malignancy in patients with previous biliary intervention: multicenter analysis of hepatobiliary infections. Radiology. 2018;288(3):774–81.
17. Tomozawa Y, Jahangiri Y, Pathak P, et al. Long-term toxicity after transarterial radioembolization with Yttrium-90 using resin microspheres for neuroendocrine tumor metastases. J Vasc Interv Radiol. 2018;29:858–65.
18. Mohan H, Nicholson P, Winter DC, O'Shea D, O'Toole D, Geoghegan J, et al. Radiofrequency ablation for neuroendocrine liver metastases: a systematic review. J Vasc Interv Radiol. 2015;26(7):935–942.e1.
19. Contessa JN, Griffith KA, Wolff E, Ensminger W, Zalupski M, Lawrence TS, et al. Radiotherapy for pancreatic neuroendocrine tumors. Int J Radiat Oncol Biol Phys. 2009;75(4):1196–200.
20. Katsanos K, Kitrou P, Spiliopoulos S, Maroulis I, Petsas T, Karnabatidis D. Comparative effectiveness of different transarterial embolization therapies alone or in combination with local ablative or adjuvant systemic treatments for unresectable hepatocellular carcinoma: a network meta-analysis of randomized controlled trials. PLOS One [Internet]. 2017;12(9). Available from: https://www.ncbi.nlm.nih.gov/pmc/articles/PMC5608206/.

Chapter 11
Renal Cell Carcinoma

Dimitrios K. Filippiadis, Maria Tsitskari, and Thomas D. Atwell

Introduction

Malignancies of the kidney and renal pelvis are estimated to represent 5% of new cancer cases in the United States in 2019; of these malignancies, renal cell carcinoma (RCC) is the most common cancer of the kidney, representing about 90% of such tumors [1]. The primary histologic subtypes of RCC include clear cell carcinomas in about 88% of patients, papillary carcinomas in about 10% of patients, and chromophobe carcinomas in 2% of patients; when considering prognosis, clear cell histology and high tumor grade have been associated with relatively decreased survival [2]. The incidence of RCC has been increasing over the last several decades. At least in part, this has been attributed to the increased utilization of medical imaging with incidental detection of small renal masses. Such incidental tumors represent more than half of new RCC diagnoses and are typically discovered at a smaller size and stage and in older patients than their symptomatic counterparts [2]. Such trends in RCC prevalence have led to an evolution of tumor management, with a reappraisal of aggressive surgical management for many patients (Fig. 11.1).

Perhaps serendipitously, the maturation of interventional oncology as a clinical specialty has paralleled this migration of RCC toward smaller tumors in older patients. This is reflected by the now accepted role of ablation in the front-line treatment of RCC in select patients. The purpose of this chapter is to detail the role of

D. K. Filippiadis (✉)
2nd Department of Radiology, University General Hospital "ATTIKON", Medical School, National and Kapodistrian University of Athens, Athens, Greece
e-mail: dfilippiadis@med.uoa.gr

M. Tsitskari
2nd Department of Radiology, University General Hospital "ATTIKON", Athens, Greece

T. D. Atwell
Department of Radiology, Mayo Clinic, Rochester, MN, USA

C. Georgiades, H. S. Kim (eds.), *Image-Guided Interventions in Oncology*,
https://doi.org/10.1007/978-3-030-48767-6_11

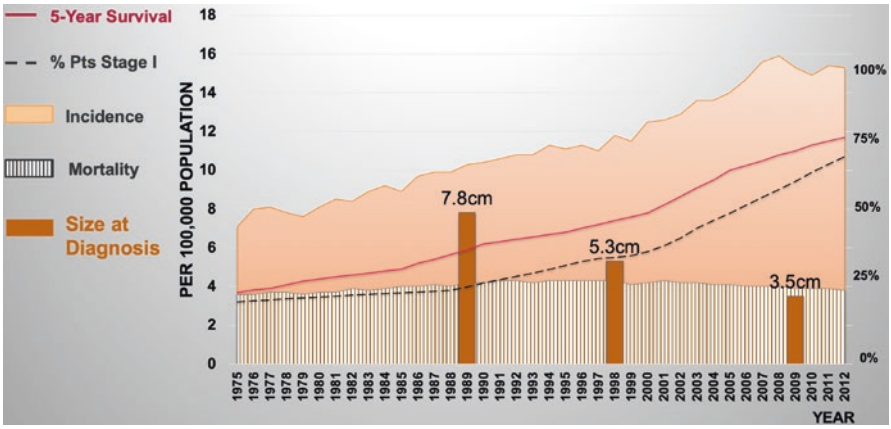

Fig. 11.1 Epidemiology of renal cell carcinoma

the interventional oncologist in the management of RCC, specifically addressing outcomes related to thermal ablation and transarterial embolization.

Percutaneous Ablation

Radiofrequency

Radiofrequency energy is the most widely used and studied percutaneous ablative method with more than 20 years of clinical experience. It produces heat by friction, with the use of an alternating electrical current that causes agitation of the ions of the target tissue. Heating of the target tissue at high temperatures (typically above 55 °C) results in tissue destruction and coagulative necrosis. The first case of renal mass RFA ablation was reported by Zlotta et al. back in 1997. Nowadays, it is widely used in the clinical setting and has been established as an option for the treatment of small RCCs with excellent results. Both exophytic and endophytic tumors can be treated successfully; the ideal candidate is one with a noncentral tumor of 3–4 cm in maximum diameter (Fig. 11.2). Larger tumors can also be treated effectively by overlapping ablations.

The safety and efficacy of RFA for the treatment of small T1 renal cell carcinomas have been extensively reported in the literature; most of these studies report primary success rates of more than 90% and secondary clinical success rates up to 100% after repeated ablation with durable and long-term oncologic outcome [3–5]. Tumor size and position have been shown to be independent predictors of clinical success that may influence local tumor control and recurrence. There is an inverse relationship between tumor size and technical success, with a twofold risk of treatment failure for every 1-cm increase in tumor size above 3.6 cm [3–5]. Centrality of

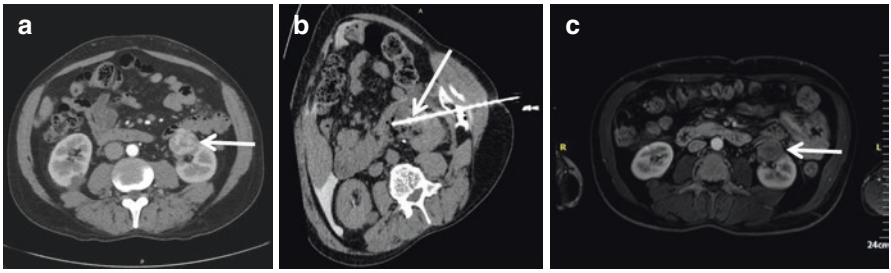

Fig. 11.2 Percutaneous radiofrequency ablation of a 3 cm left renal mass with encroachment on renal sinus fat. (**a**) Computed tomography axial scan depicting the lesion (white arrow); (**b**) Computed tomography axial scan illustrating the electrode (white arrow) inside the lesion; (**c**) MRI post iv Gadolinium illustrates complete necrosis at 1-year follow-up (white arrow)

the tumor, in addition to the size, is another factor limiting the efficacy of RFA, associated with increased local treatment failure and increased risk of collecting system and vascular injury; Gervais et al. reported a 22% of treatment failure in centrally located tumors compared to 0% in exophytic-treated tumors [3].

Cryoablation

Percutaneous cryoablation has slowly established a foundation of oncologic efficacy in managing small renal masses. There are several potential advantages of cryoablation compared to other thermal ablation techniques. Perhaps most importantly is the ability to monitor the ablation margin using CT and MRI. Specifically, the leading edge of the iceball has been shown to correspond to 0 degrees centigrade based on temperature monitoring during CT imaging. And while a precise temperature for complete oncologic treatment has yet to be established, it is known that complete cell destruction in normal renal parenchyma occurs at −19 degrees centigrade. Using 3 mm cryoprobes, −20 degrees centigrade is achieved 3 mm inside outer iceball margin. These measures allow a high level of both predictability and confidence when performing renal ablation.

The ability to use multiple cryoprobes to generate a large ablation zone with real-time monitoring allows the operator to effectively treat much larger tumors than typically managed with heat-based techniques. Specifically, this has allowed the successful treatment of T1b and even T2 RCCs [6]. It is worth mentioning that the treatment of such larger tumors has been associated with increased risk of hemorrhagic complications [7].

A third important attribute of cryoablation compared to heat-based techniques is the potential to propagate lethal temperatures centrally into the kidney to overcome thermal sink effects and with relatively decreased injury to the collecting system (Fig. 11.3). In a study comparing cryoablation and radiofrequency ablation (RFA) in the treatment of small (less than 3 cm) renal masses, cryoablation showed more

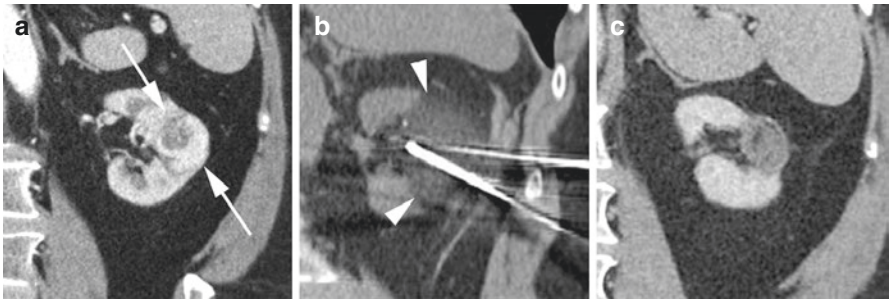

Fig. 11.3 Cryoablation of a 3cm left renal mass with encroachment on renal sinus fat. (**a**) Coronally reconstructed CT with intravenous contrast shows a 3 cm enhancing renal mass (arrows); (**b**) coronally reconstructed CT during cryoablation shows a low density iceball extending well beyond tumor margin, into the renal sinus fat (arrowheads); (**c**) coronally reconstructed CT obtained 54 months following ablation shows successful treatment with no local recurrence

favorable local control in the treatment of tumors encroaching on renal sinus fat compared to RFA [8]. When considering the general oncologic outcomes of cryoablation, the effectiveness of extreme cold in the treatment of renal tumors was initially validated in the surgical theatre.

More recent cryoablation experience has proven the durability of the treatment (Table 11.1). While outcomes are somewhat complicated due to confounding with indeterminate pathology, published experiences exceeding 3 years show progression- free survival in 85–98% of patients. It is well established that small renal cell carcinomas often behave in an indolent fashion, and short-term cancer-specific survival following ablation approaches 100%.

In a study directed to sporadic RCC in 220 patients, Breen et al. described very favorable outcomes at 3 and 5 years following treatment [9]. Progression-free survival following percutaneous cryoablation was 97% and 94%, respectively. In considering T1a and T1b tumors in their series, there was no statistically significant association of size and progression-free survival (for T1a, HR 0.52; p-0.446). These similarly favorable outcomes for both T1a and T1b tumors were found in the Andrews et al. experience, where progression-free survival at 5 years was 93.4% for T1a tumors and 92.7% for T1b tumors [10]. Nevertheless, lesser outcomes in the treatment of larger renal masses have been reported.

In considering the successful treatment of large renal masses, it is important to consider the technical application of lethal ice to the entire tumor, recognizing the isotherms associated with cryoprobe types, synergy of multiple cryoprobes, and monitoring afforded by CT and MRI. As described elsewhere, ice at a temperature of less than −20 degrees is lethal under most circumstances. Thus, it can be implied that tumor progression is often due to failure to treat the tumor completely with adequate thermal margins. In considering this technical challenge, specific adjunctive maneuvers are worth mentioning.

Given inherent encroachment of larger masses on bowel and other critical structures, displacement techniques such as hydrodissection or pneumodissection are

Table 11.1 Contemporary percutaneous cryoablation outcomes

Author	Year	# Patients/ tumors	Mean/ median size	Size details	Mean/median follow-up	RFS (%) all tumor	RFS (%) RCC	MFS (%)	CSS (%)	OS (%)
Andrews et al.	2019	187 pts	–	T1a	6.3 years	95.9% at 5 years	93.4% at 5 years	100% at 5 years	100% at 5 years	77% at 5 years
		52 pts	–	T1b	6.0 years	95% at 5 years	92.7% at 5 years	90% at 5 years	91% at 5 years	56% at 5 years
Aoun et al.	2017	269 tumors	–	T1a	31.8 months	–	98.1%	–	–	–
		67 tumors	–	T1b		–	94.0%	–	–	–
		10 tumors	–	T2		–	80%	–	–	–
Breen et al.	2018	220 tumors	3.3 cm	–	31 months	–	93.9% at 5 years	94.4% at 5 years	–	84.8% at 5 years
Buy et al.	2013	120 tumors	2.6 cm	–	28 months	96.4% at 1 year	–	–	–	96.7% at 1 year
Fraisse et al.	2019	177 patients	2.6 cm	–	63 months	85% at 5 years	–	–	–	–
Georgiades et al.	2014	134 patients	2.8 cm	–	–	–	97.0% at 5 years	–	100%	97.8% at 5 years
Kim et al.	2012	129 tumors	2.7 cm	–	30 months	85% at 3 years	–	–	100%	85% at 3 years

often required to allow extension of the iceball beyond the tumor margin, minimizing harm to adjacent viscera. If there is expectation of ureteral involvement during the ablation, the placement of an externalized ureteral stent to allow retrograde convection relative warming of the ureter during the ablation may have value. Prophylactic selective renal artery embolization of the tumor prior to ablation has been shown to decrease bleeding after cryoablation, allowing the operator the luxury of appropriately aggressive treatment.

Microwave

Microwave radiation applies electromagnetic heating for interacting with biological tissues aiming in coagulative necrosis. During microwave ablation, a continuously switching electric field causes oscillations of molecular dipoles generating frictional heating. All parts of the irradiated tissue are actively, homogeneously, and simultaneously heated with no propagation delay. Comparing microwaves to radiofrequency favors the former in terms of higher temperatures, large, more spherical ablation volumes produced in shorter time period less affected by "heat sink" effect, and any kind of impedance-driven performance; there is no need for grounding pads, and the technique seems to be governed by less intraoperative pain (Fig. 11.4). Similar to other heat-based techniques, microwave ablation when compared to cryoablation is governed by higher complication rates when it comes to centrally located lesions inside the renal pelvis [11]. Recent microwave experience has proven the durability of the treatment (Table 11.2).

Complications

Percutaneous image-guided thermal ablative methods for the treatment of small RCCs have a relatively low complication profile. Generally, main complications can be divided into two categories: hemorrhage-related complications and thermal injury-related complications.

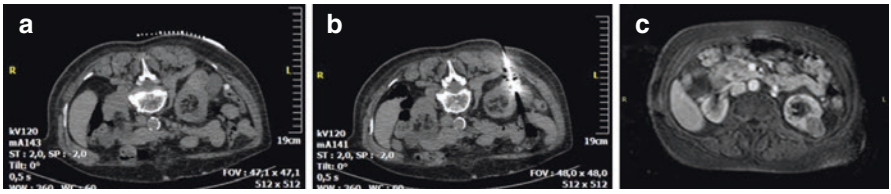

Fig. 11.4 Percutaneous microwave ablation of a 3.8 cm RCC in the left kidney. (**a**) Computed tomography axial scan depicting the lesion (white arrow); (**b**) computed tomography axial scan illustrating the antenna (white arrow) inside the lesion; (**c**) MRI post iv Gadolinium illustrates complete necrosis at 1-year follow-up (white arrow)

Table 11.2 Contemporary percutaneous microwave ablation outcomes

Author	Year	# Patients/ Tumors	Tumor size	Size details	Mean follow-up	PFS (%) RCC	CSS (%)	Complications	OS (%)
Thompson et al.	2018	26/27	2.3 ± 0.8 cm	T1a	20.6 ± 11.6 months	96% at 3 years	94% at 3 years	19.2%	–
Filippiadis et al.	2018	48/48	3.1 cm (range 2.0–4.3 cm)	44/48 T1a 4/48 T1b	3 years	93.75% at 3 years		4%	95.8%aat 3 years
Ierardi et al.	2017	58/58	23.6 ± 9.3		25.7 months		96.5% at 5 years	8.6%	80.6% at 5 years
Wells et al.	2016	29/30	3.1 cm (range 2.3–3.8 cm)	23/30 T1a 7/30 T1b	12 months	–	97% at 1 year	10%	93%% at 1 year
Gao et al.	2016	41/41	3. 6 ± 1.2 (1.9–6.8)	29/41 T1a 12/41 T1b	28 months	81.5 5 at 5 years	–	25%	83.6% at 5 years

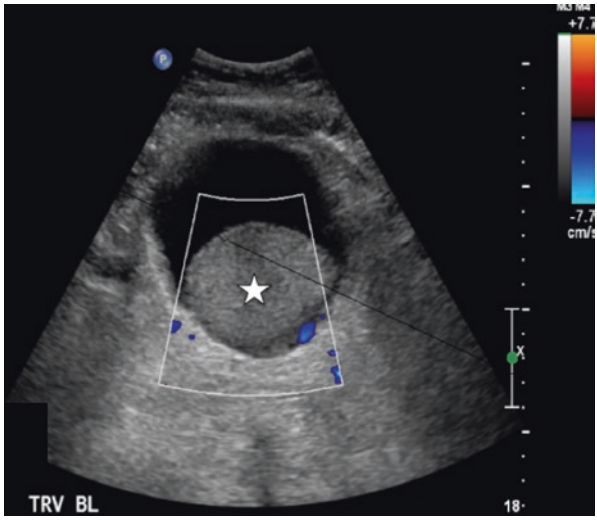

Fig. 11.5 Two hours post cryoablation for RCC patient complained of pelvic pain and inability to void. Pelvic ultrasound revealed a large bladder clot causing bladder outlet obstruction. Continuous irrigation was started. Repeat ultrasound 3 hours later showed complete resolution of the clot

Hemorrhage may manifest as a subcapsular hematoma or retroperitoneal hemorrhage. In the majority of cases, hemorrhage is minor and does not require any further treatment. Massive bleeding has been reported in 1% of cases and can be life- threatening. When conservative management with blood transfusions is not sufficient to control the bleeding, transarterial embolization is required. Hematuria may also occur with a frequency of 0.5–1% especially in centrally located treated tumors. In the majority of cases, it is self-limiting and resolves within 12–24 hours. If persists it may lead to urinary bladder clot formation and outlet obstruction, so prompt recognition and treatment with bladder irrigation are mandatory to prevent obstructive uropathy (Fig. 11.5). Usually CT scan is necessary to exclude thermal damage of the pelvicalyceal system that may additionally require ureteric stent placement.

Thermal injury to the proximal ureter may lead to ureteral stricture or urinoma formation (Fig. 11.6). Continuous pyeloperfusion during ablation, after retrograde ureteral stent placement, can mitigate this risk. Other maneuvers like changes in patient's position, hydro-, and pneumodissection may also be advocated to prevent thermal injury to other critical structures like the small and large bowel, the genitofemoral nerve (Fig. 11.7), and the psoas muscle [12, 13].

Follow-Up

Because of the slow growing characteristics of RCC (doubling time approximately 600 days) long-term follow-up is recommended. An initial 3-month follow-up with contrast-enhanced cross sectional imaging is needed to exclude residual disease (Fig. 11.8). Because local recurrent disease has been reported even up to 5 years, an annual follow-up to 5 years is recommended.

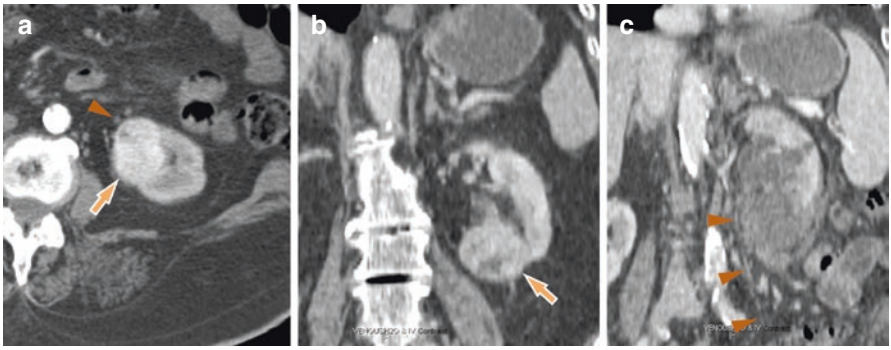

Fig. 11.6 Axial (**a**) and coronal (**b**) CT images showing a 3 cm RCC (arrow). The proximity to the ureter (arrowhead) was not appreciated. The patient returned 2 weeks post-ablation complaining of flank pain. Coronal CT (**c**) showed complete devascularization of the tumor but also hydronephrosis. The ureter was injured near the target lesion (arrowheads) causing stricture and obstruction. A long-term double J was required

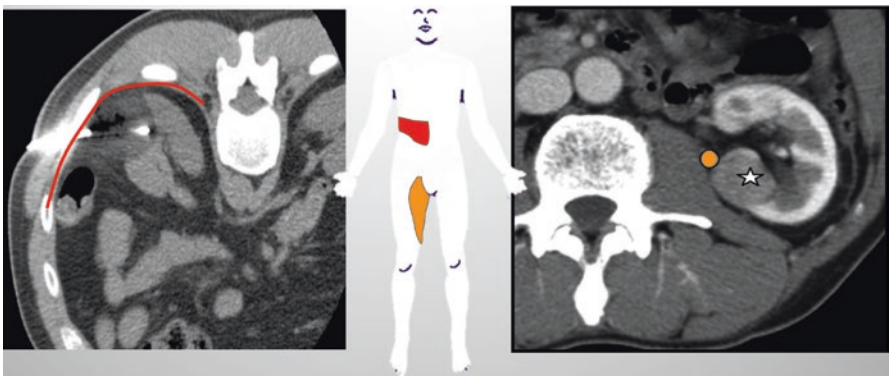

Fig. 11.7 Two common nerves are at risk for injury during renal ablation. The intercostal nerve (red line on image on the left) is a sensory-motor nerve that can be injured during posterior renal ablation. A band-like area of pain and muscle laxity can result. The genitofemoral nerve (brown dot, image on right) is a purely sensory nerve. If injured, it can result in pain in the upper medial thigh area

Comparison to Partial and Radical Nephrectomy

For small, T1a renal masses, current management options include radical nephrectomy (RN), partial nephrectomy (PN), ablation, and surveillance. Currently, partial nephrectomy is the standard of care for active management of small renal masses due to the preservation of renal function and similar oncologic outcomes compared to radical nephrectomy [1]. As the role of thermal ablation expands to the more general patient population, comparison with the surgical standard is needed.

Unfortunately, the quality of comparison studies is limited with primarily retrospective patient studies complicated by selection bias. Ablation has historically

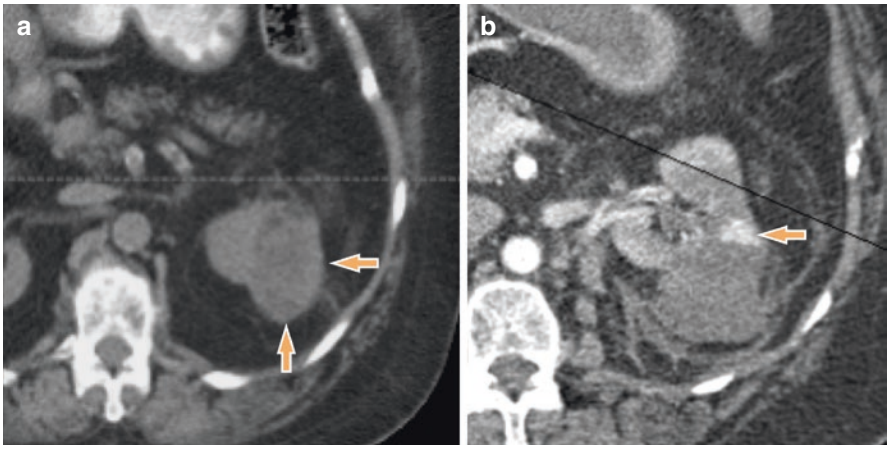

Fig. 11.8 Axial non-contrast CT (**a**) shows a 4 cm left apical RCC (arrows). Three month post-ablation contrast-enhanced CT (**b**) shows a small residual lesion anteriorly (arrow). Repeat ablation resulted in complete response

been reserved for those patients to sick or frail to undergo surgery or with other contraindications to surgery. Such selection is reflected by the frequently demonstrated limited overall survival of patients compared to surgery.

In a very detailed systematic review and meta-analysis funded by the Agency for Healthcare Research and Quality, Pierorazio and colleagues showed that, although disease-free survival was similar, local recurrence-free survival was better following PN (98.9%) compared to ablation (93%) [14]. However, after accounting for ablative re-treatment and secondary efficacy, the outcomes following ablation reached 97–100%, and the difference between PN and ablation was no longer significant.

Another systematic review and meta-analysis published in 2019 by Uhlig et al. included 47 studies with over 24,000 patients [15]. This confirmed that those patients undergoing thermal ablation were older and had more comorbid illness compared with PN. While local tumor progression was higher in those patients treated with thermal ablation, there was no significant difference in cancer-specific mortality.

The best available comparison data currently includes population-based registry studies. While such studies provide information regarding treatment trends and survival, such studies are limited in their ability to specifically track efficacy of focal tumor treatments (e.g., local recurrence). In a Surveillance, Epidemiology, and End Results (SEER) database review published in 2018, Zhou et al. identified 809 patients who underwent thermal ablation and 3783 patients who underwent PN for T1a RCC during 2004–2013 [16]. After propensity matching, the authors found that cancer-specific survival was similar for ablation compared to PN (HR = 1.466; $p = 0.4023$). As anticipated, an overall survival advantage for patients treated with PN compared to ablation was demonstrated (91.0% vs 86.3% at 5 years).

In another review of the SEER database 2002–2011, Xing et al. used propensity matching to compare thermal ablation, surgical resection, and active surveillance in the management of T1a renal masses [17]. In this review, there was no difference in 3-, 5-, and 9-year cancer-specific survival when thermal ablation was compared

with PN, including 9-year cancer-specific survival rates of 96.3% and 96.4% ($p = 0.07$), respectively. Compared to those treated with ablation, patients treated with PN were more likely to experience renal, cardiovascular, and thromboembolic events in the first 30 days ($p < 0.001$) and year ($p < 0.001$) following the procedure.

Talenfeld et al. performed SEER database review to compare percutaneous ablation with both RN and PN in the management of T1a RCC, including patients 66 years of age or older and treated 2006–2011 [18]. Five-year cancer-specific survival was similar between those patients treated with ablation and RN at 96% and 95%, respectively. RCC-specific survival at 5 years was less favorable for those patients treated with ablation (95%) compared to PN (98%). Finally, the authors found that ablation was associated with far fewer complications within 30 days of treatment, with 6% of ablation patients having a non-urologic complication compared to 29% with PN and 30% with RN.

These favorable non-oncologic outcomes were validated in a review of the National Cancer Database. Uhlig et al. showed that thermal ablation was associated with a shorter mean hospital stay and lower unanticipated hospital readmission rates compared to surgery [19]. Thirty- and 90-day postoperative mortality were also lower compared to surgery. While overall survival was higher in the general population for those treated with PN, 5-year overall survival in those patients older than 65 years was comparable for thermal ablation (54%) and nephrectomy (59%).

Patient Selection and Current International Guidelines

Appropriately, in the late 1990s and early/mid-2000s, the relatively novel thermal ablative technique was largely reserved for the treatment of patients with comorbidities or other contraindications to conventional surgery, as detailed in the 2009 American Urological Association guidelines for managing the clinical T1 renal mass. As ablation outcomes have matured, the strengths and limitations of the thermal technique have become apparent, allowing better application to management strategies.

Thermal ablation is primarily reserved for the treatment of small renal masses. In the ablation literature, this was historically considered to be those smaller than 3 cm. This was considered a size threshold for RFA, with expectation of very favorable (97–100%) oncologic outcomes, with lesser outcomes seen for larger tumors. The 3 cm threshold was extended to 4 cm to allow stratification with the TNM classification and urologic guidelines. Favorable outcomes remained using RFA to treat T1a renal masses, although the limitations in treating T1b tumors were evident. Microwave ablation may allow more thorough treatment of larger renal masses, with limited experience showing some success in the ablation of large tumors. As detailed earlier, cryoablation may be used to treat larger renal masses, although published outcomes have been too inconsistent to allow formal incorporation into general treatment guidelines.

Particularly using heat-based ablation techniques, more successful oncologic outcomes have been found in the treatment of exophytic tumors. The thermal sink

effect, created by 37 degree centigrade blood flow, may affect the successful thermal ablation of tumors located centrally in the kidney. Thus, while outcomes with RFA show 98–100% success for exophytic tumors, success drops to 62–82% for centrally located or endophytic tumors. The synergy of ice and relatively limited impact on the urothelium have yielded relatively favorable oncologic outcomes in the treatment of these same central renal masses.

As described earlier, a retrospective comparison of RFA and cryoablation in the treatment of small (≤3 cm) renal masses showed that local tumor progression was more frequently seen following RFA of centrally located masses compared to cryoablation (78% vs 98% at 3 years). This same Mayo group achieved 87% oncologic success at mean 56 months of follow-up in the treatment of 47 completely endophytic renal masses [20]. Microwave ablation may have a role in the treatment of endophytic renal masses. In microwave ablation of 41 RCC adjacent the renal sinus, Gao et al. achieved success in 100% of the T1a and 75% of the T1b tumors [21].

Recognizing these relative strengths and limitations of ablation, several societies have specifically addressed thermal ablation in guidelines specific to managing renal masses:

- A 2014 update to the European Association of Urology guidelines for RCC found that the quality of the available ablation data did not allow any definitive conclusions regarding oncologic outcomes for RFA and cryoablation to be reached [1]. The EAU guidelines specify several indications for thermal ablation: (1) small renal masses in elderly comorbid patients unfit for surgery, (2) patients with a genetic predisposition to develop multiple tumors, and (3) patients with bilateral tumors or with a solitary kidney and high risk of complete loss of renal function following PN.
- The Cardiovascular and Interventional Society of Europe published guidelines regarding the management of small renal masses in 2017 [12]. An overview provided in the document concluded that percutaneous ablation represents an alternative to surgery in the treatment of T1a RCC with excellent technical and functional outcomes. However, the CIRSE guidelines conclude that there remains insufficient evidence to provide a strong recommendation, and until such outcomes are available, ablation is recommended for patients that are not fit or are not willing to undergo surgery.
- The American Urological Association (AUA) updated their guideline for managing localized renal masses suspicious for RCC in 2017 [22]. The AUA guidelines state that physicians should consider thermal ablation as an alternative strategy for managing cT1a renal masses <3 cm in size. Both RFA and cryoablation are thermal ablation options; microwave ablation is considered investigational in these 2017 guidelines. The guidelines also recommend a percutaneous approach over a surgical approach if thermal ablation is performed. In counseling patients, the AUA recommended that patients should be informed of increased likelihood of tumor persistence or local recurrence after primary thermal ablation compared to surgery, although such failures may be amenable to repeat ablation. Finally, a renal mass biopsy should be performed prior to ablation to provide pathologic diagnosis and guide subsequent surveillance.

Transarterial Embolization

Materials and Techniques

The procedure is performed in the angio suite. The patient is placed supine on the angio table. Vascular access is achieved usually through the femoral artery with the use of a five or six French sheath, although radial approach can also be chosen. Initially a preliminary abdominal aortogram is performed as a roadmap to the renal arteries and to assess for any vascular anomalies, such as supernumerary renal arteries. A diagnostic catheter is then used for selective catheterization of the origin of the renal artery. A stable catheter position is required for any embolization. Reverse-curved catheters (Simmons I, SOS Omni) or forward-looking catheters (such as Cobra) can all be effective. A renal aortogram is performed to identify the tumor, assess its vascularity, and depict the course of the feeding vessels.

Then with the use of a microcatheter, the feeding vessels are catheterized in a coaxial manner, and embolization is performed. Different embolic agents may be used; metallic coils, gelfoam, liquid embolics, and particles (Fig. 11.9). There are no adequate data supporting the superiority of any of these agents. Distal embolization of the small vessels and the capillary bed is desired so liquid agents, mainly ethanol, or particles are the most preferred agents, cause they can penetrate deep into the target tissue (Fig. 11.10). Different-sized particles may be used depending on the size of the feeding vessels. Ethanol penetrates deep to the distal arteries resulting in capillary occlusion and has a quite strong ischemic effect. Occlusion balloon catheter delivery system is routinely used when ethanol embolization is performed. Additional proximal large vessel occlusion with coils can also be performed for more efficacious outcome. The goal of embolization is to achieve stasis in the vessel while avoiding reflux into nontarget vessels [23].

Indications

Indications for transarterial embolization of renal cancer include:

- Palliation therapy for advanced stage RCC
- Preoperative embolization before nephrectomy
- Combination of embolization to percutaneous ablation
- Management of nephron-sparing surgery complications

In terms of palliation, transarterial embolization can be proposed for symptomatic management of hematuria/hematoma, paraneoplastic syndrome, pain, and cardiac insufficiency. Preoperative transarterial embolization prior to nephrectomy results in easier surgical removal of the tumor in shorter period of time with reduced blood losses. Superselective embolization leads to minimal loss of viable renal parenchyma and can be safely applied even to patients with solitary kidney. In case

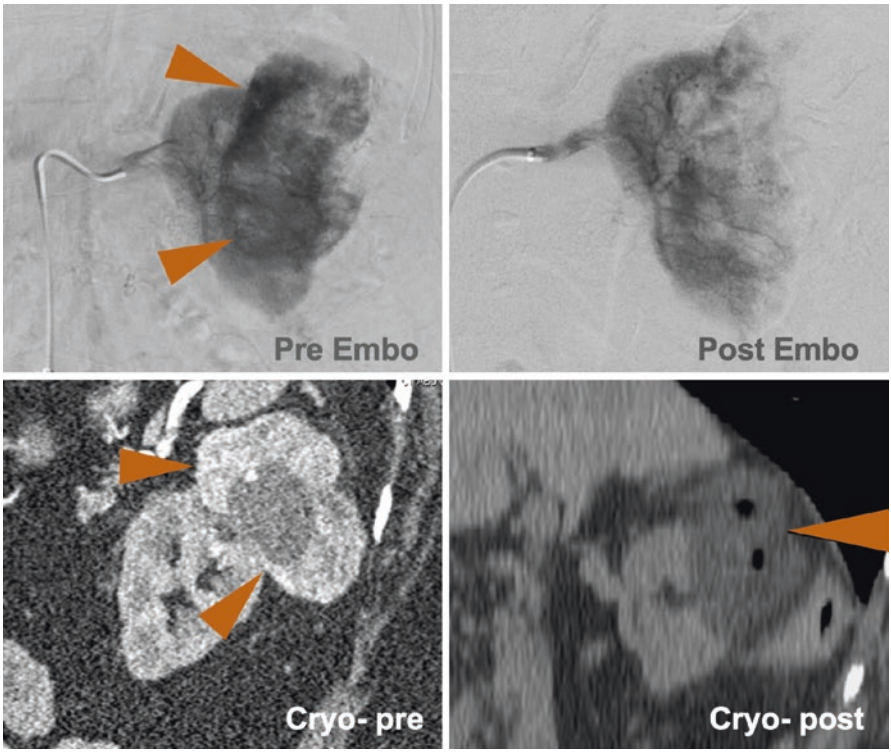

Fig. 11.9 Pre-ablation embolization can mitigate the risk of hemorrhage. The cryo-pre-image shows a large (9 cm) mass (arrowheads) after one session of ablation. The lesions hardly responded (central necrosis) due to hypervascularity. The lesion was then embolized (pre-embo and post-embo images). Repeat ablation (without the heat sink effect) resulted in complete response (Cryo-post)

of tumor recurrence postsurgical treatment, transarterial embolization can be proposed for lesions in complex locations or in patients with solitary kidney. Performing embolization prior to ablation leads to decreased "heat sink" effect and reduced rate of hemorrhagic complications. Nephron-sparing surgical complications account for 0.4–4.9% of cases including arteriovenous fistula, pseudoaneurysm, and active extravasation; all these complications can be easily managed with transarterial embolization.

Immuno-oncology

Scarce literature data support certain immunological benefits in RCC patients undergoing embolization; these benefits are based upon an increase in NK lymphocytes activity which is more profound in the first 24 h post-embolization. Additionally, the immunological system is stimulated by the post-embolization

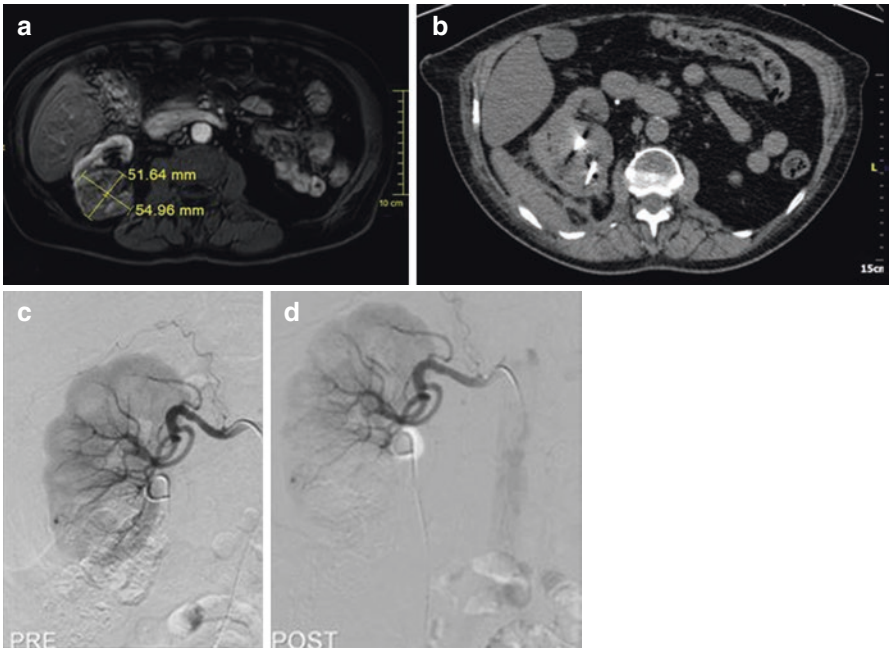

Fig. 11.10 Combined therapy of a 5.9 cm RCC in the right kidney with encroachment on renal sinus fat. (**a**) MRI post iv Gadolinium depicts the mass in the right kidney; (**b**) computed tomography axial scan illustrating two antennas (bipolar microwave ablation) inside the lesion. Immediately post-ablation patient was transferred to the angio suite: (**c**) pre-embolization angiographic image illustrating vascularity at the lesion level; (**d**) post embolization with microparticles there is no vascularity at the lesion level

tumor necrosis resulting an immunotherapy "self-vaccination" most probably due to the production of anticancer antibodies. Furthermore combining ablation with transarterial embolization can positively effect immunomodulatory mechanisms through tumor antigen release, T-regulatory cell promotion, and resultant subversion of the normal immunoregulatory mechanism. However, all these need to be proved in larger cohorts of patients in everyday clinical practice.

Conclusion

Percutaneous ablation of RCC is a safe and efficacious technique for the treatment of T1a renal masses governed by similar efficacy rates when compared to surgical approaches. At the same time, the technique is much less morbid and invasive than surgery governed by lower cost, shorter duration of hospitalization, and lower complication rates. As size grows larger than 4 cm in T1b tumors, addition of transarterial embolization can be suggested in order to enhance percutaneous ablation. Furthermore, transarterial embolization can be proposed as palliative therapy for symptoms management or preoperatively for decreasing blood losses.

References

1. Ljungberg B, et al. EAU guidelines on renal cell carcinoma: 2014 update. Eur Urol. 2015;67(5):913–24.
2. Znaor A, et al. International variations and trends in renal cell carcinoma incidence and mortality. Eur Urol. 2015;67(3):519–30.
3. Gervais DA, McGovern FJ, Arellano RS, McDougal WS, Mueller PR. Radiofrequency ablation of renal cell carcinoma: part 1, indications, results, and role in patient management over a 6-year period and ablation of 100 tumors. AJR. 2005;185:64–71.
4. Psutka SP, Feldman AS, McDougal WS, McGovern FJ, Mueller P, Gervais DA. Long-term oncologic outcomes after radiofrequency ablation for T1 renal cell carcinoma. Eur Urol. 2013;63(3):486–92.
5. Wah TM, Irving HC, Gregory W, Cartledge J, Joyce AD, Selby PJ. Radiofrequency ablation (RFA) of renal cell carcinoma (RCC): experience in 200 tumours. BJU Int. 2014;113:416–28.
6. Atwell TD, et al. Percutaneous cryoablation of stage T1b renal cell carcinoma: technique considerations, safety, and local tumor control. J Vasc Interv Radiol. 2015;26(6):792–9.
7. Atwell TD, et al. Complications following 573 percutaneous renal radiofrequency and cryoablation procedures. J Vasc Interv Radiol. 2012;23(1):48–54.
8. Atwell TD, et al. Percutaneous ablation of renal masses measuring 3.0 cm and smaller: comparative local control and complications after radiofrequency ablation and cryoablation. Am J Roentgenol. 2013;200(2):461–6.
9. Breen DJ, et al. Image-guided cryoablation for sporadic renal cell carcinoma: three- and 5-year outcomes in 220 patients with biopsy-proven renal cell carcinoma. Radiology. 2018;289(2):554–61.
10. Andrews JR, et al. Oncologic outcomes following partial nephrectomy and percutaneous ablation for cT1 renal masses. Eur Urol. 2019;76(2):244–51.
11. Filippiadis D, Mauri G, Marra P, Charalampopoulos G, Gennaro N, De Cobelli F. Percutaneous ablation techniques for renal cell carcinoma: current status and future trends. Int J Hyperth. 2019;36(2):21–30.
12. Krokidis ME, Orsi F, Katsanos K, Helmberger T, Adam A. CIRSE guidelines on percutaneous ablation of small renal cell carcinoma. Cardiovasc Intervent Radiol. 2017;40(2):177–91.
13. Schmit GD, Schenck LA, Thompson RH, Boorjian SA, Kurup AN, Weisbrod AJ, et al. Predicting renal cryoablation complications: new risk score based on tumor size and location and patient history. Radiology. 2014;272(3):903–10.
14. Pierorazio PM, et al. Management of renal masses and localized renal cancer: systematic review and meta-analysis. J Urol. 2016;
15. Uhlig J, et al. Partial nephrectomy versus ablative techniques for small renal masses: a systematic review and network meta-analysis. Eur Radiol. 2019;29(3):1293–307.
16. Zhou M, et al. SEER study of ablation versus partial nephrectomy in cT1A renal cell carcinoma. Future Oncol. 2018;14(17):1711–9.
17. Xing M, et al. Comparative effectiveness of thermal ablation, surgical resection, and active surveillance for T1a renal cell carcinoma: a surveillance, epidemiology, and end results (SEER)-medicare-linked population study. Radiology. 2018;288(1):81–90.
18. Talenfeld AD, et al. Percutaneous ablation versus partial and radical nephrectomy for T1a renal Cancer: a population-based analysis. Ann Intern Med. 2018;169(2):69–77.
19. Uhlig J, et al. Ablation versus resection for stage 1A renal cell carcinoma: national variation in clinical management and selected outcomes. Radiology. 2018;288(3):889–97.
20. Murray CA, et al. Safety and efficacy of percutaneous image-guided cryoablation of completely endophytic renal masses. Urology. 2019;
21. Gao Y, et al. Microwave treatment of renal cell carcinoma adjacent to renal sinus. Eur J Radiol. 2016;85(11):2083–9.
22. Campbell S, Uzzo RG, Allaf ME, et al. Renal mass and localized renal cancer: AUA guideline. J Urol. 2017;198(3):520–9.

23. Gunn AJ, Mullenbach BJ, Poundstone MM, et al. Trans-arterial embolization of renal cell carcinoma prior to percutaneous ablation: technical aspects, institutional experience, and brief review of the literature. Curr Urol. 2018;12(1):43–9.

Recommended Reading List

Georgiades CS, Rodriguez R. Efficacy and safety of percutaneous cryoablation for stage 1A/B renal cell carcinoma: results of a prospective, single-arm, 5-year study. Cardiovasc Intervent Radiol. 2014;37(6):1494–9.

Iannuccilli JD, et al. Effectiveness and safety of computed tomography-guided radiofrequency ablation of renal cancer: a 14-year single institution experience in 203 patients. Eur Radiol. 2016;26(6):1656–64.

Sommer CM, Pallwein-Prettner L, Vollherbst DF, Seidel R, Rieder C, Radeleff BA, Kauczor HU, Wacker F, Richter GM, Bücker A, Rodt T, Massmann A, Pereira PL. Transarterial embolization (TAE) as add-on to percutaneous radiofrequency ablation (RFA) for the treatment of renal tumors: review of the literature, overview of state-of-the-art embolization materials and further perspective of advanced image-guided tumor ablation. Eur J Radiol. 2017;86:143–62.

Wells SA, et al. Percutaneous microwave ablation of T1a and T1b renal cell carcinoma: short-term efficacy and complications with emphasis on tumor complexity and single session treatment. Abdom Radiol (NY). 2016;41(6):1203–11.

Woodrum DA, et al. Role of intraarterial embolization before cryoablation of large renal tumors: a pilot study. J Vasc Interv Radiol. 2010;21(6):930–6.

Chapter 12
Bone Metastatic Disease

Alexios Kelekis and Dimitrios K. Filippiadis

Introduction

Bone metastases most commonly originate from breast, prostate, lung, and kidney cancer as well as lymphoma and multiple myeloma; sequential events including tumor cell seeding and dormancy along with metastatic growth contribute to osseous metastatic disease [1]. Skeletal system is the third most important location for metastatic disease following the lungs and liver with spine being the most common site of osseous metastatic disease due to the presence of red marrow in adult vertebrae and the lack of valves in the communication between the deep thoracic/pelvic veins and the vertebral venous plexuses [2].

The interventional oncology techniques for bone metastatic disease include percutaneous ablation as well as vertebral and osseous augmentation by means of cement injection either solely performed or in combination to various implants. Focusing upon a tailor-based approach, these techniques can be offered either as stand alone or in various combinations (among them and with other therapies as well) aiming in local tumor control (esp. in oligometastatic disease) or in symptoms palliation and tumor decompression.

Percutaneous Ablation

Ablation techniques for percutaneous approaches in interventional oncology include radiofrequency (RFA), microwave ablation (MWA), as well as cryoablation (Fig. 12.1); MR-guided high-intensity-focused ultrasound (HIFU) on the other hand

A. Kelekis (✉) · D. K. Filippiadis
2nd Department of Radiology, University General Hospital "ATTIKON", Medical School, National and Kapodistrian University of Athens, Athens, Greece
e-mail: akelekis@med.uoa.gr; dfilippiadis@med.uoa.gr

C. Georgiades, H. S. Kim (eds.), *Image-Guided Interventions in Oncology*,
https://doi.org/10.1007/978-3-030-48767-6_12

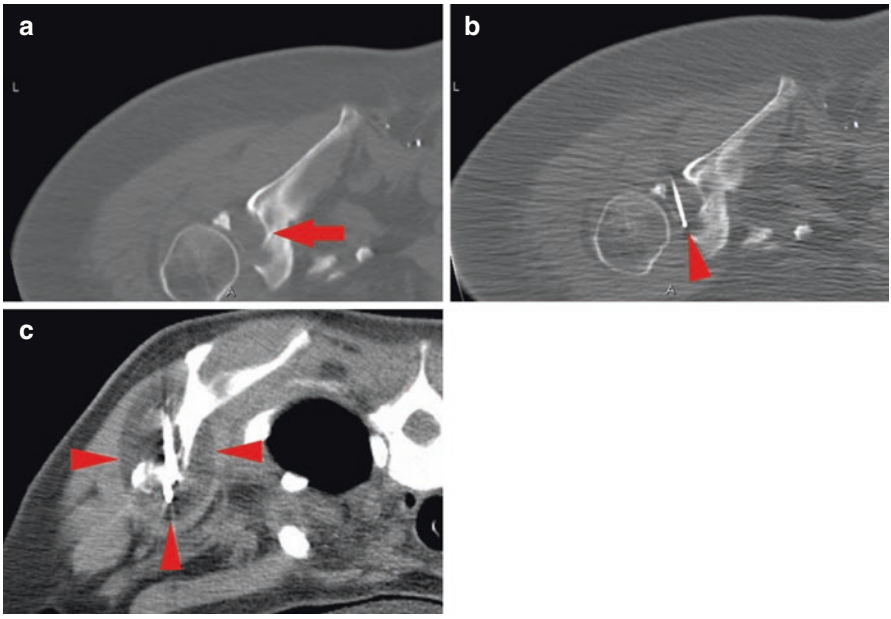

Fig. 12.1 A 52-year-old female with breast cancer metastasis to the right shoulder. Axial CT image (**a**) shows a lytic lesion in the scapula (red arrow). Single microwave probe (red arrowhead) was used to perform an ablation (**b**) which resulted in partial pain response. Repeat cryoablation (**c**) was performed. The ice ball (red arrowheads) is clearly demarcated assuring ablation of the involved periosteum for better analgesia

is a noninvasive imaging-guided method which can be applied in bone metastatic disease. Ablation modalities achieve cytotoxicity by raising target area temperatures above 60 °C (thermal) or below −40 °C (cryo) and may be used to achieve total necrosis of lesions <5 cm, to debulk and reduce the pain associated with larger lesions, and in association with structural support techniques to prevent pathological fractures due to progressive osteolysis and posttreatment osteonecrosis [3].

Pain Palliation

Ablation techniques achieve pain reduction in osseous metastatic disease through ablative necrosis of tumor-periosteum interface (Fig. 12.2), decompression of tumor volume, decrease of nerve-stimulating cytokines (which are released by the tumor), inhibition of osteoclast activity [2], or nerve ablation (Fig. 12.3). According to the National Comprehensive Cancer Network (NCCN) guidelines, ablation for adult cancer pain can be proposed when there is no oncologic emergency (e.g., pathologic fracture or epidural disease) or when the pharmacologic therapy is inadequate and radiation therapy is contraindicated or not desired by the patient [4].

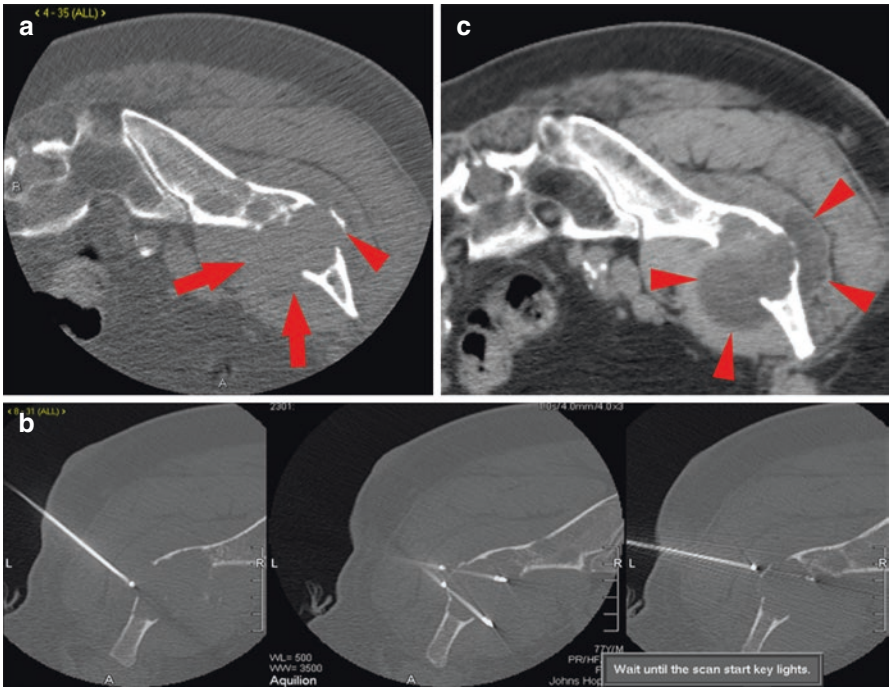

Fig. 12.2 Axial CT (**a**) in a patient with a painful lytic metastatic lung cancer to the right iliac bone (red arrows). The involved, raised periosteum (red arrow head) is noted. Three sequential intra-procedural images (**b**) during cryoablation indicate the location of the four cryoneedles used. Immediate post-procedural CT (**c**) shows a partially thawed ice ball (red arrowheads) that covers the raised periosteum. The patient reported near complete pain resolution on postoperative day #3

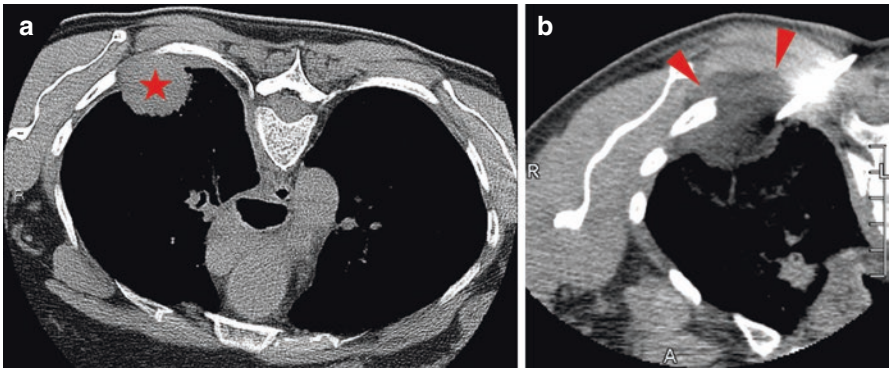

Fig. 12.3 Axial CT (**a**) in a patient with primary lung cancer (asterisk) involving the chest wall and causing severe intractable pain. Percutaneous cryoablation (**b**) shows the ice ball (red arrowheads) encompassing the target mass but also the involved intercostal nerve. Complete pain resolution was reported 2 days postop

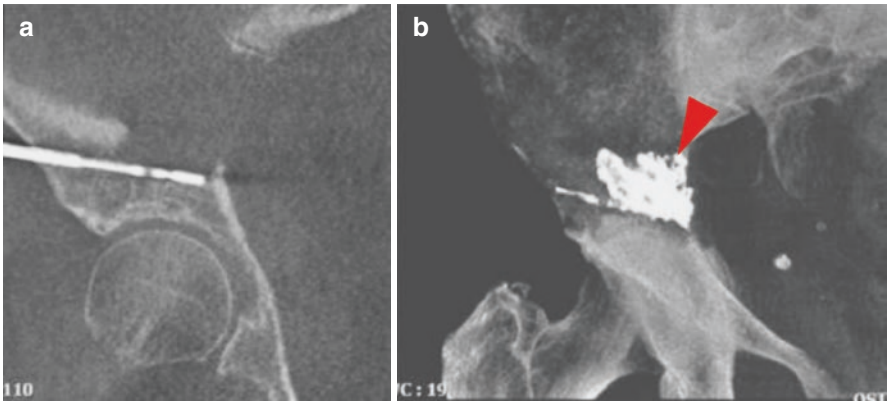

Fig. 12.4 An 82-year-old male patient with a single metastatic sacral lesion from renal cell carcinoma underwent in a single therapeutic session microwave ablation (**a**) followed by cement injection (**b**) for stabilization (acetabular augmentation)

In a multicenter trial published in 2010, Dupuy et al. aimed to assess safety and palliative efficacy of percutaneous ablation by means of radiofrequency, in a total of 55 symptomatic patients with osseous metastatic disease including locations such as the pelvis (n = 22), chest wall (n = 20), spine (n = 8), or extremities (n = 5) [5]. Despite the fact that these patients were pretreated with prior radiotherapy of the painful lesions and had no significant pain reduction or mood improvement, the authors conclude that after percutaneous ablation, there was a statistically significant pain reduction effect at 1 and 3 months of follow-up ($p < 0.0001$) [5].

Hypothesizing that percutaneous ablation and EBRT may act synergistically, Di Staso et al. in two different studies compared pain relief in patients with solitary bone metastases after treatment with percutaneous ablation (RFA or cryoablation) followed by radiotherapy, vs. radiotherapy alone [6, 7]. Patients in the combined therapies group reported significantly higher pain reduction effect that was noted earlier in the follow-up period, lasted longer and was associated with a more significant decrease in analgesics uptake [6, 7]. Adverse events among the combined therapies group did not differ from the complications associated with administering the two therapies individually.

Apart from tumor necrosis and decompression as well as pain palliation, ablation causes bone weakening, resulting in the need for structural support, especially in weight-bearing locations where augmentation techniques should be combined in order to provide consolidation and prevent fractures [8] (Fig. 12.4).

Oligometastatic Disease

Oligometastatic disease can be subjectively defined as the presence of up to 5 distant metastases in ≤2 organs, although the exact number of metastases that should be considered remains debatable [9]. In this setting, ablation can be proposed over

surgery which is technically challenging, morbid, with prolonged recovery, and higher complication rates, thus delaying systemic therapies. Radiation therapy on the other hand is limited by cumulative radiation tolerance of nearby organs and prior application in a specific area [10]. Ablative techniques are minimally invasive, imaging guided which for oligometastatic bone disease can provide effective tumor destruction irrespective of the lesion's histology and can be easily combined in a single session with osseous consolidation techniques [8, 10].

Mc Menomy et al. applied percutaneous cryoablation in 43 oligometastatic (<5 lesions) patients aiming for complete remission; the authors report significant overall survival which is governed by factors including size and number of metastases, length of disease-free interval, treatment adequacy of primary tumor, and presence of multiple metastatic sites [11]. Cazzato et al. applied percutaneous image-guided ablation (radiofrequency and cryoablation) in 46 oligometastatic (<3 lesions) patients with 49 lesions who were followed for a mean of 34 months reporting similar local progression-free survival (LPFS) rates among all the different tumor histologies. Lesion size >2 cm was a predictive factor for local tumor progression [12]. Deschamps et al. performed 152 radiofrequency or cryoablation sessions in 141 oligometastatic (<3 lesions) patients with 193 lesions of variable substrate including thyroid, breast, kidney cancer, and pheochromocytoma; the authors reported that positive prognostic factors for local success included small size (<2 cm), lack of cortical erosion and oligometastatic, and/or metachronous disease [13]. In recent years, the potential of percutaneous ablation has been investigated for complete remission in oligometastatic sarcoma patients [14]. It is evident that progression-free survival is not only related to adequate ablation of the oligometastatic disease but mainly to the type of tumor and its response to systemic therapy.

Osseous Augmentation

Vertebral Augmentation

Vertebral augmentation techniques include percutaneous vertebroplasty and balloon kyphoplasty as well as implant-based technologies (peek cages, stents, jack dilators, etc.) [15–17]. Vertebral augmentation in the setting of metastatic spine disease can be proposed for symptomatic patients with malignant vertebral lesion of varying histologies including among others multiple myeloma, lymphoma, and metastasis [18] (Fig. 12.5).

Contraindications for vertebral augmentation in metastatic spine disease include infection, uncorrectable coagulopathy, asymptomatic or unstable fractures, tumor extension into the vertebral canal, cord compression, or diffuse metastatic disease in the spine [18]. Pain palliation effect of percutaneous vertebroplasty for malignant spine disease ranges among 73–100%, while balloon kyphoplasty when compared to nonoperative management (Cancer Patient Fracture Evaluation study) was proven as effective and safe treatment that significantly reduces pain and improves function compared to conservative therapy [18, 19]. In terms of spine implants, the

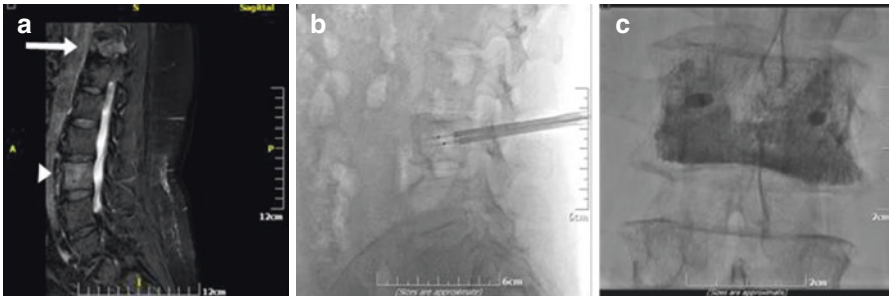

Fig. 12.5 A 59-year-old female breast cancer painful oligometastatic patient with two lesions in T11 (white arrow) and L3 (white arrowhead) vertebral bodies (**a**). The L3 lesion was treated with bipolar RFA (bilateral transpedicular approach) (**b**), followed by cement injection (**c**) (vertebroplasty) for stabilization and additional pain control

PEEK cages have been proven an effective minimally invasive treatment option for patients suffering from severe pain due to osteolytic vertebral metastasis [20]. According to the Cardiovascular Interventional Radiology Society of Europe (CIRSE) guidelines, the suggested threshold for all symptomatic complications post vertebral augmentation techniques performed for malignant indications should be <10%. Reported complications include cement leakage, infection, fracture of ribs, posterior elements or pedicle, bleeding from the puncture site, and allergic reaction [18]. Hirsch and colleagues compared vertebroplasty/kyphoplasty either before or after EBRT reporting that the order of vertebral augmentation and radiotherapy did not impact pain outcomes [21]. New guidelines on vertebral augmentation include system scoring of the risk of pathological fracture (SINS score). Evaluating the risk of spine fracture by scoring can provide an objective criterion for vertebral stabilization [22].

Peripheral Skeleton Augmentation

The most commonly used cement for osseous structural support is poly(methyl methacrylate) (PMMA) (Fig. 12.6). PMMA has been proven weak in tension, strong in compression, and with a low bending modulus of elasticity (lower than that of cortical bone), properties which render the polymer a great supporting material for the spine where cranio-caudal (i.e., axial) forces apply. Where rotational and shearing forces are applied, additional intramedullary instrumentation is required for long-term stabilization [23]. Important factors for choosing PMMA either solely injected or in combination to metallic or PEEK hardware include operator's experience, equipment availability, lesion size, and location as well as cortical involvement [24]. All these techniques are performed under imaging guidance, extensive local sterility (including prophylactic antibiosis), and anesthesiology control (which

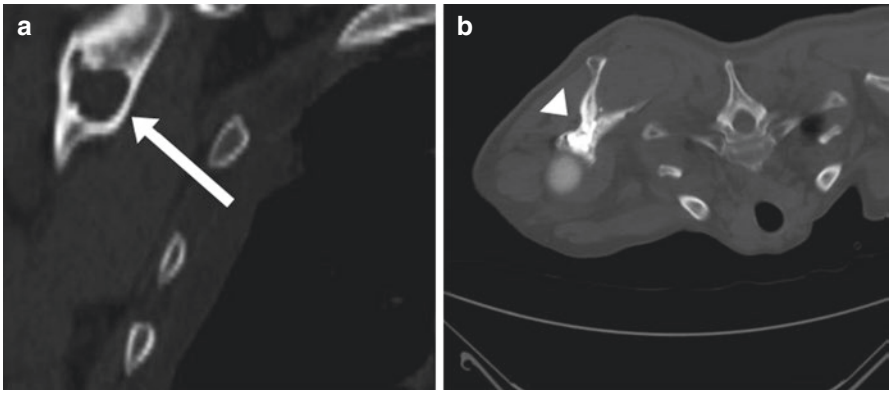

Fig. 12.6 A 58-year-old male sarcoma oligometastatic patient with a solitary painful lytic lesion in the right glenoid. CT scan coronal reconstruction (**a**) showing the lytic lesion in the glenoid (white arrow). Axial post-ablation CT (**b**) shows cement filing of the cavity (white arrowhead), in order to provide the necessary stabilization and prevent future pathologic fractures

depends upon patient and location characteristics as well as operator's preference). Different combinations of PMMA and hardware have been reported in the literature including screws, pins, needles, and peek polymer implants aiming to enhance biomechanical structure and to prevent fracture [23]. These techniques, in metastatic bone disease, are proposed as palliative therapies for cancer patients suffering from pain due to pathological fractures or as preventive treatments providing prophylactic consolidation for patients with impending pathological fractures due to osteolytic metastases. Although surgical, the Mirels classification system can be used for patient selection in case of impending pathological fractures; any lesion with a score >9 is at high risk of pathologic fracture and has to be treated [24]. Apart from treatment failure, other complications include cement leakage, infection, bleeding from the puncture site and allergic reaction.

Trans-arterial Embolization

Transarterial embolization (Fig. 12.7) can be applied in bone metastatic disease preoperatively aiming for reduced blood loss during surgery or as a palliative therapy aiming for tumor growth inhibition and pain reduction [25]. When the lesion is treated to curative intent, embolization provides an additional tool to achieve that goal. Depending upon operator's preference, location, and lesion characteristics, injectates that can be used include onyx, gelfoam, PVA particles, alcohol emulsions, coils, tissue adhesives, and microfibrillar collagen [25]. Post embolization the average pain relief rate ranges up to 89% starting from a few hours to 15 days and lasting for a mean of 8.3 months.

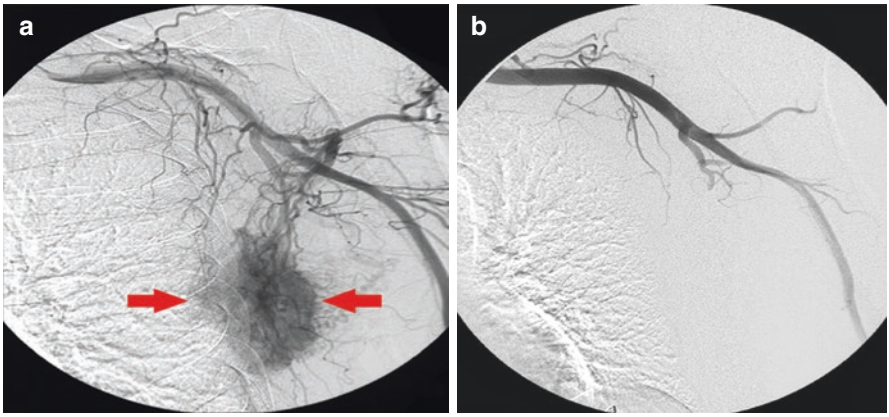

Fig. 12.7 A 57-year-old male patient with metastatic renal cell carcinoma. Digital subtracted angiogram from the left axillary artery (**a**) shows a hypervascular metastatic lesion (red arrows) to the left chest wall. Post-particle embolization angiogram (**b**) shows complete devascularization of the lesion. Embolization can provide pain relief on its own but also augment the volume of subsequent ablation by cutting off the blood supply to the region

Conclusion

Interventional oncology procedures can provide effective and durable solutions in patients with either multi or oligometastatic disease, providing structural support and alleviating painful conditions. The immediate effect of those treatments can hasten systemic therapies, as the latency period compared to other alternatives is shorter. It is important for the treating physician to establish a treatment strategy (palliative or curative) from the start, taking into account not only the local lesion but the type of the tumor and its response to systemic therapy.

References

1. ESMO Guidelines Working Group. Bone health in cancer patients: ESMO clinical practice guidelines. Ann Oncol. 2014;25(Supplement 3):iii124–37.
2. Wallace AN, Robinson CG, Meyer J, Tran ND, Gangi A, Callstrom MR, Chao ST, Van Tine BA, Morris JM, Bruel BM, Long J, Timmerman RD, Buchowski JM, Jennings JW. The metastatic spine disease multidisciplinary working group algorithms. Oncologist. 2015;20(10):1205–15.
3. Filippiadis DK, Tutton S, Mazioti A, et al. Percutaneous image-guided ablation of bone and soft tissue tumours: a review of available techniques and protective measures. Insights Imaging. 2014;5:339–46.
4. National Comprehensive Cancer Network. Adult cancer pain v.2, 2016. Available at: https://www.nccn.org/professionals/physician_gls/f_guidelines.asp. Accessed 21 Nov 2016.
5. Dupuy DE, Liu D, Hartfeil D, et al. Percutaneous radiofrequency ablation of painful osseous metastases. Cancer. 2010;116(4):989–97.

6. Di Staso M, Zugaro L, Gravina GL, Bonfili P, Marampon F, Di Nicola L, Conchiglia A, Ventura L, Franzese P, Gallucci M, Masciocchi C, Tombolini V. A feasibility study of percutaneous radiofrequency ablation followed by radiotherapy in the management of painful osteolytic bone metastases. Eur Radiol. 2011;21(9):2004–10.
7. Di Staso M, Gravina GL, Zugaro L, Bonfili P, Gregori L, Franzese P, Marampon F, Vittorini F, Moro R, Tombolini V, Di Cesare E, Masciocchi C. Treatment of solitary painful osseous metastases with radiotherapy, cryoablation or combined therapy: propensity matching analysis in 175 patients. PLoS One. 2015;10(6):e0129021.
8. Gangi A, Tsoumakidou G, Buy X, Quoix E. Quality improvement guidelines for bone tumour management. Cardiovasc Intervent Radiol. 2010;33(4):706–13.
9. de Souza NM, et al. Strategies and technical challenges for imaging oligometastatic disease. Eur J Cancer. 2017;XX:1–11.
10. Kurup AN, Morris JM, Callstrom MW. Ablation of musculoskeletal metastases. AJR. 2017;209:713–21.
11. Mc Menomy BP, Kurup AN, Johnson GB, et al. Percutaneous cryoablation of musculoskeletal oligometastatic disease for complete remission. JVIR. 2013;24:207.
12. Cazzato RL, Auloge P, De Marini P, et al. Percutaneous image-guided ablation of bone metastases: local tumor control in oligometastatic patients. Int J Hyperth. 2018;35(1):1–7.
13. Deschamps F, Farouil G, Ternes N, et al. Thermal ablation techniques: a curative treatment of bone metastases in selected patients? Eur Radiol. 2014;24(8):1971–80.
14. Vaswani D, Wallace AN, Elswirth PS, et al. Radiographic local tumor control and pain palliation of sarcoma metastases within the musculoskeletal system with percutaneous thermal ablation. CVIR. 2018;41(8):1223–32.
15. Tutton SM, Pflugmacher R, Davidian M, Beall DP, Facchini FR, Garfin SR. KAST study: the kiva system as a vertebral augmentation treatment-a safety and effectiveness trial: a randomized, noninferiority trial comparing the Kiva system with balloon kyphoplasty in treatment of osteoporotic vertebral compression fractures. Spine (Phila Pa 1976). 2015;40(12):865–75.
16. Martín-López JE, Pavón-Gómez MJ, Romero-Tabares A, Molina-López T. Stentoplasty effectiveness and safety for the treatment of osteoporotic vertebral fractures: a systematic review. Orthop Traumatol Surg Res. 2015;101(5):627–32.
17. Li D, Huang Y, Yang H, Chen Q, Sun T, Wu Y, et al. Jack vertebral dilator kyphoplasty for treatment of osteoporotic vertebral compression fractures. Eur J Orthop Surg Traumatol. 2014;24(1):15–21.
18. Tsoumakidou G, Too CW, Koch G, Caudrelier J, Cazzato RL, Garnon J, et al. CIRSE guidelines on percutaneous vertebral augmentation. Cardiovasc Intervent Radiol. 2017;40(3):331–42.
19. Berenson J, Pflugmacher R, Jarzem P, Zonder J, Schechtman K, Tillman JB, Bastian L, Ashraf T, Vrionis F, Cancer Patient Fracture Evaluation (CAFE) Investigators. Balloon kyphoplasty versus non-surgical fracture management for treatment of painful vertebral body compression fractures in patients with cancer: a multicentre, randomised controlled trial. Lancet Oncol. 2011;12(3):225–35.
20. Anselmetti GC, Manca A, Tutton S, Chiara G, Kelekis A, Facchini FR, Russo F, Regge D, Montemurro F. Percutaneous vertebral augmentation assisted by PEEK implant in painful osteolytic vertebral metastasis involving the vertebral wall: experience on 40 patients. Pain Physician. 2013;16:E397–404.
21. Hirsch AE, Jha RM, Yoo AJ, et al. The use of vertebral augmentation and external beam radiation therapy in the multimodal management of malignant vertebral compression fractures. Pain Physician. 2011;14:447–58.
22. Fox S, Spiess M, Hnenny L, Fourney DR. Spinal instability neoplastic score (SINS): reliability among spine fellows and resident physicians in orthopedic surgery and neurosurgery. Global Spine J. 2017;7(8):744–8.
23. Kelekis A, Cornelis F, Tutton S, Filippiadis D. Metastatic osseous pain control: bone ablation and cementoplasty. Semin Intervent Radiol. 2017;34(4):328–36.

24. Mirels H. Metastatic disease in long bones. A proposed scoring system for diagnosing impending pathologic fractures. Clin Orthop Relat Res. 1989;(249):256–64.
25. Rossi G, Mavrogenis AF, Rimondi E, Braccaioli L, Calabro T, Ruggieri P. Selective embolization with N-butyl cyanoacrylate for metastatic bone disease. J Vasc Interv Radiol. 2011;22(4):462–70.

Chapter 13
Breast Cancer

Yolanda C. D. Bryce and Amy R. Deipolyi

Introduction

Breast cancer is the most common cancer in women in both developed and less developed countries [1, 2]. In the USA, 1 in 8 (12%) women develops breast cancer, and 268,600 new cases of invasive breast cancer are expected in 2019 [3]. There are subgroups with higher risk for breast cancer, including those with *BRCA1* and *BRCA2* mutations with a cumulative breast cancer risk to the age of 80 years of 72% and 69%, respectively, and those with less common mutations such as *TP53* and *CHEK2* (Li-Fraumeni syndrome), *PTEN* (Cowden and Bannayan-Riley-Ruvalcaba syndromes), *CDH1* (hereditary diffuse gastric cancer), *STK11* (Peutz-Jeghers syndrome), *PALB2* (interacts with *BRCA2*), and *ATM* (ataxia-telangiectasia) mutations [4]. Other high-risk subgroups include Ashkenazi Jews, with higher risk of BRCA mutations; black women, who carry up to a 39% higher mortality risk from breast cancer largely due to tumor biology; patients with a history of mantle radiation for Hodgkin lymphoma or ≥20 Gray in the first two decades of life or ≥10 Gray by age 30; patients with strong family history of breast cancer without known genetic mutations; patients with a personal history of breast cancer, lobular carcinoma in situ, or atypical hyperplasia; and women with dense breasts [5, 6].

The incidence of invasive breast cancer has increased by 0.4% per year from 2006 to 2015, possibly due to better screening [3, 7–9]. The female breast cancer death rate peaked at 33 per 100,000 in 1989 then dropped to 20 in 100,000 in 2016, a 40% decline [3]. In fact, from 2007 to 2016, the breast cancer death rate has declined by 1.8% per year, possibly due to increase in screening and improvement in therapeutic methods. The 5- and 10-year survival rate for women with invasive breast cancer is 90% and 83%, respectively. With localized stage, the 5-year survival is very favorable at 99% [3].

Y. C. D. Bryce · A. R. Deipolyi (✉)
Department of Radiology, Memorial Sloan Kettering Cancer Center, New York, NY, USA
e-mail: deipolya@mskcc.org

C. Georgiades, H. S. Kim (eds.), *Image-Guided Interventions in Oncology*,
https://doi.org/10.1007/978-3-030-48767-6_13

Nevertheless, despite advances in breast cancer diagnosis and treatment, metastatic breast cancer continues to be a challenge, remaining the second most common cause of cancer death in women. The 5-year survival of metastatic breast cancer is only 27%, and 6–10% of breast cancer patients will initially present as Stage IV disease or have "de novo" metastatic disease [3]. About 20–30% of all breast cancer patients live with metastatic disease, though the exact number is not known [3]. A subset of women with high-risk tumor biology, those with triple-negative breast cancer (TNBC), represent a particular challenge as the tumor does not express estrogen or progesterone receptors or the human epidermal growth factor receptor 2 oncoprotein gene (HER2neu) that allows for tumor-specific therapy. This subset of patients has a very poor prognosis, with a median overall survival of only 1 year [10].

Breast cancer is a heterogeneous disease with variable expression of established prognostic and predictive biomarkers, hormone receptors (estrogen and progesterone), and HER2neu guiding treatment [11]. The National Comprehensive Cancer Network (NCCN) has created guidelines for treatment of breast cancer with recommendations for localized stage, locally advanced disease precluding surgery, and metastatic breast cancer, built on the pillars of surgery (mastectomy or breast conservation therapy), systemic therapy (cytotoxic chemotherapy, endocrine therapy, and/or biologic therapy), and radiation therapy [12]. However, with the evolution of breast cancer care, new approaches to breast cancer therapy by way of interventional oncology have arisen with promising results. We review the role of interventional oncology in the treatment of breast cancer including locoregional percutaneous ablation, treatment of oligometastasis, and liver-directed therapy.

Ablation of Primary Breast Tumors

With the introduction of population-based screening programs, the incidence of smaller primary breast cancer tumors measuring ≤2 cm and of localized stage has increased [3, 5]. Concomitantly, the surgical approach to these localized tumors has evolved. Previously, radical or modified radical mastectomy was the pillar of treatment of breast cancer. Though mastectomy remains standard of care for some patients, breast conservation has emerged as the method of choice in many patients to optimize cosmesis and minimize in-breast recurrence. With the aid of radiation therapy and systemic cytotoxic and hormonal therapy, breast conservation therapy has been widely successful [13]. Moreover, patients with Stage II and Stage III disease who desire conservation but present with a large primary tumor or unfavorable tumor to breast size ratio can be treated with neoadjuvant chemotherapy to become candidates for conversation therapy [14].

Given the evolution of breast cancer care and the success of breast-preserving therapies focused on eradicating tumor and only small amount of surrounding normal tissue, less invasive techniques with better cosmesis have been explored to achieve similar results. Percutaneous ablation is postulated as a viable option for breast conservation, with improved cosmesis, decreased morbidity, and faster

recovery. Percutaneous ablation includes thermal (hyperthermic and hypothermic) and nonthermal mechanisms [15]. The eligibility criteria for percutaneous ablation therapy is evolving. Patients who are not surgical candidates or who refuse surgery after thorough medical counselling can be considered. Other potential candidates are patients that have tumors <2 cm in size, located 0.5–1 cm from the skin surface and possibly also the pectoralis muscle, and no extensive intraductal component [16–18].

Hyperthermic Ablation

Hyperthermic or heat-based ablation includes radiofrequency ablation (RFA), microwave ablation (MWA), laser ablation (LA), and high-intensity focused ultrasound (HIFU). With these modalities, heat energy is transferred to the tumor resulting in coagulative necrosis and cell death [19]. Because of the heat, these modalities carry the risk of skin and pectoralis muscle injury and intraprocedural pain, which can be mitigated by hydrodissection (Fig. 13.1).

In RFA, an electrode placed in a probe is inserted into the tumor with an electrical current applied to the electrode. RFA requires completion of an electrical circuit so grounding pads are needed, which are placed on a large area such as the thigh or back so that the heat is dispersed minimizing skin burns [20]. In a landmark retrospective study involving 386 patients in 10 institutions from June 2003 and June 2009, in which RFA of breast cancer was performed under US guidance, in-breast tumor recurrence-free rates at 5 years were 97% for tumors ≤1 cm, 94% for tumors 1.1–2.0 cm, and 87% for tumors in >2.0 cm. Nine patients had local pain, 15 had skin burns, and 7 had nipple retraction. Patients were followed every 6–12 months for a median of 50 months [21].

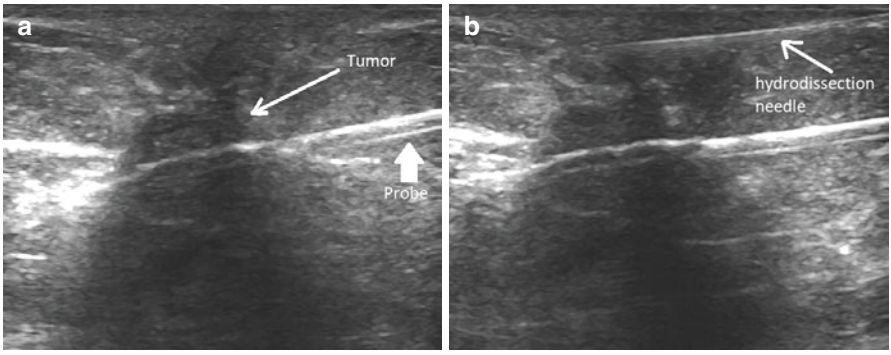

Fig. 13.1 Ultrasound-guided ablation of breast tumor with hydrodissection. (**a**) Ultrasound image depicts the appropriate positioning of the probe within the center of the tumor, placed with ultrasound guidance. (**b**) Ultrasound image depicts a needle placed between the tumor and the skin for hydrodissection (infusion of saline), to avoid burning the skin

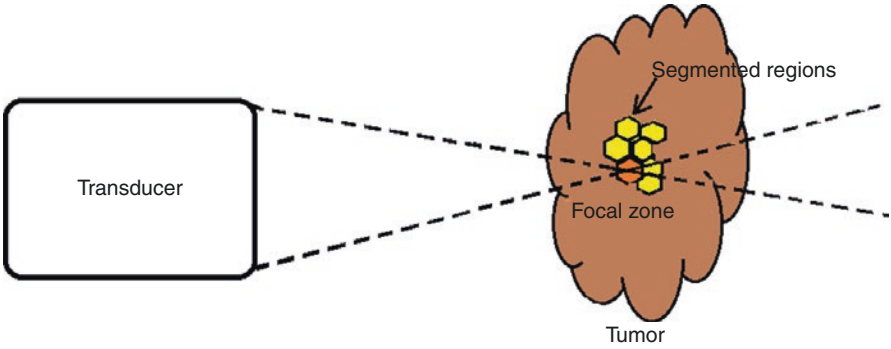

Fig. 13.2 High-frequency focused ultrasound (HIFU). The diagram depicts the piezoelectric energy produced by the transducer used in HIFU to treat tiny focal zones within the tumor, one zone at a time, to assure efficacy of HIFU

Microwave ablation (MWA) uses electromagnetic microwaves applied to a probe to produce heat [22]. The dispersion of heat with microwave ablation is faster and more homogeneous than in RFA, and ablation times are shorter. One or more probes are placed within the tumor, and ablation times range from 2–3 minutes. A few studies have explored microwave ablation in breast cancer with a study by Zhou et al. ablating 12 patients to demonstrate that a predictable spherical size could be achieved with MWA [23].

In LA, there are laser fibers inside a needle which are placed inside the tumor [24], resulting in light energy that heats the tumor [25]. LA has been performed in human patients, with variable outcomes [26].

HIFU is completely noninvasive, using high-intensity piezoelectric energy focused on one small region ($\approx 0.8 \times 0.2 \times 0.2$ mm^2), the focal zone, to cause heat (Fig. 13.2) [27]. The intensity of HIFU is 100–10,000 W/cm^2 compared to <0.1 W/cm^2 for diagnostic ultrasound [28]. The breast tumor is segmented into small focal zones which are treated one at a time. HIFU is performed with either ultrasound or MRI guidance, typically with the patient prone and the breast suspended in a pool of water. HIFU guided by ultrasound is less expensive and allows for real-time visualization of the treated region and detects any movement made by the patient during the treatment. Conversely, MRI guidance has the advantage of optimal anatomical resolution, high sensitivity, and temperature mapping. Phase II and phase III trials in small groups of patients have demonstrated up to 100% ablation rates with low recurrence rates [29, 30].

Hypothermic Ablation

Hypothermic ablation or cryoablation (CA) involves cycles of freezing and thawing facilitated by rapid decompression of argon or nitrogen gas applied to a probe inserted inside the tumor. CA causes cellular damage, death, and necrosis of tissue

by direct cold-induced cellular injury and by indirectly changing the cellular microenvironment and impairing tissue viability [31]. One or more CA probes are placed inside the breast tumor, and typically two freeze/thaw cycles are performed. The number of probes and duration of CA depend on the size of the tumor and the desired ablation margin. The ice ball can injure the skin, though usually not the pectoralis muscle as collagen fibers are less susceptible to the damaging effects from the ice ball [15]. Heat packs and hydrodissection may be utilized to mitigate skin injury (Fig. 13.3). Interestingly, unlike hyperthermic mechanisms, CA creates an ice ball that is analgesic [32].

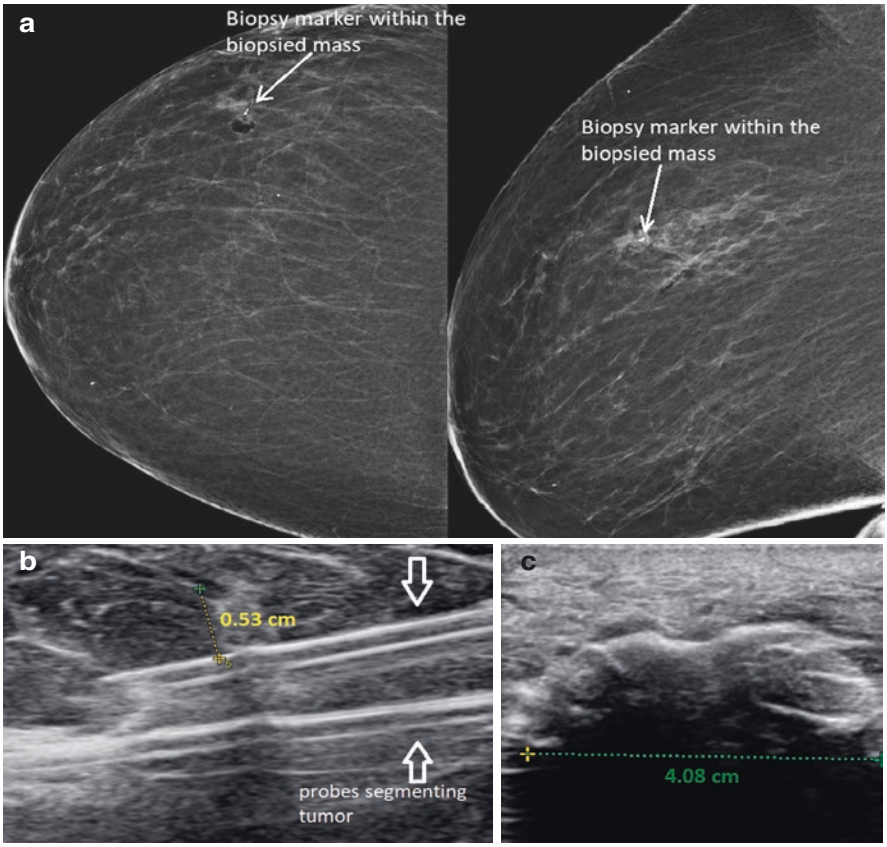

Fig. 13.3 Cryoablation (CA) of a small invasive lobular cancer. (**a**) Post-biopsy mammography demonstrates a localizing biopsy marker in the center of the lesion. (**b**) Ultrasound images demonstrate two probes to span the tumor distance of 1.7 cm. Typically, one probe is placed for each centimeter of tumor. Distance to edge of tumor is 0.53 cm. (**c**) Ultrasound demonstrates the shadowing artifact of an ice ball, measuring about 4 cm. (**d**) Post-ablation mammography shows ablation changes surrounding the tumor region around the localizing biopsy marker. (**e**) Ultrasound images demonstrate post-ablation changes, marked by a zone of heterogeneous echotexture

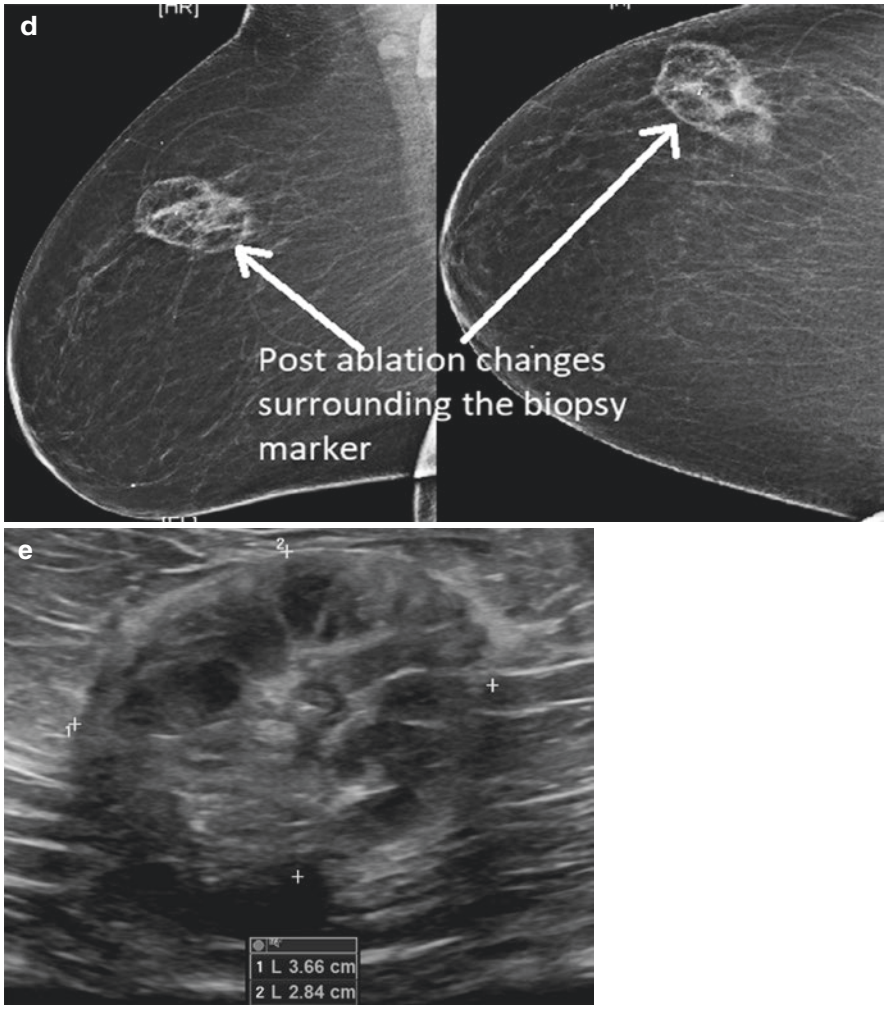

Fig. 13.3 (continued)

CA is a well-established technique to treat breast fibroadenomas, though recent trials have explored its use in breast cancer. The multicenter phase II trial ACOSOG Z-1072 studied the efficacy of CA in invasive breast cancer [33]. Eighty-seven cancers were treated with cryoablation followed by surgery in this study. At the time of surgery, 60 (70.9%) showed no residual cancer, while 27 (31%) had residual DCIS. All patients with tumors less than 1 cm in size treated with cryoablation had no residual invasive cancer on pathologic examination of the specimen. Of note, this trial was performed with primarily single probe placements, which may have led to the suboptimal outcomes. A new trial that expounds on the ACOSOG Z-1072 trial is underway with promising preliminary results.

The possible added benefit of CA of the breast rather than surgical intervention is the potential for positive cryo-immunologic effects, which could theoretically decrease recurrence and metastasis. Necrosis from CA preserves tumor-associated antigens, opposed to other methods of thermal ablation like RFA which cause protein denaturation [34]. Tumor antigens may activate immune response through antigen presentation by dendritic cells to T-cells. Preclinical data in rodents demonstrate that CA increases tumor-specific T-cells and antitumor activity and decreased lymph node metastases compared with surgical resection [35, 36]. Such effects can possibly be potentiated with the administration of agents such as ipilimumab and nivolumab PD-L1 blockers that result in immuno-stimulating properties. The combination of CA and immunotherapy has shown synergistic effect in studies with melanoma, renal cell cancer, and nonsmall cell lung cancer [37]. Research in combining cryoablation with immunotherapy in breast cancer is ongoing [38].

Nonthermal Ablation

Irreversible electroporation (IRE), a type of nonthermal ablation using electric voltages across cell membranes to induce membrane permeabilization [39], has been studied in preclinical models [40, 41]. Though, its clinical utility in the context of primary breast cancer is limited, due to the necessity for general anesthesia and paralysis [42].

Percutaneous Thermal Ablation of Metastatic Disease

Ablation for Oligometastatic Disease

Breast cancer patients are most commonly referred for ablation of metastases in the context of oligometastatic disease or when there are one or two growing lesions and distal metastases are stable or responding to systemic therapy. Oligometastatic disease is defined as five or fewer metastatic tumors. Oligometastatic disease may represent a subtype of metastatic breast cancer with a better prognosis and longer expected survival [43]. No prospective trials have assessed the impact of transarterial and percutaneous locoregional therapies on survival in this group of patients. However, one prospective randomized study showed that local treatment of oligometastatic disease with external radiation is associated with longer progression-free survival, with a trend for longer overall survival [44]. Given that thermal ablation of metastases smaller than 3–5 cm is considered curative in the treatment of hepatocellular carcinoma, with outcomes similar to surgical resection [45], these data together suggest that locoregional therapy with ablation could potentially impact survival. However, the needed trials have not been done.

The most common metastatic breast cancer sites treated with percutaneous ablation are in the liver and the lung. Several retrospective studies have assessed thermal ablation of liver tumors due to metastatic breast cancer [46–48]. Common themes arising from this work include prolonged median overall survival after ablation ranging from 40 to 60 months, improved outcomes after ablation of small (<3 cm) metastases, and that over half of patients will eventually develop new liver lesions. One large retrospective study comparing all patients who underwent surgical resection or thermal ablation for liver metastasis with patients with liver metastasis who did not undergo local resection or ablation showed no survival benefit. However, patients who underwent ablation or resection had prolonged periods without any evidence of metastatic disease [47], which may have delayed a change in systemic therapy or allowed the patient to have a break from systemic treatment. Specifically, more than half of patients were able to refrain from systemic therapy for 2 years, and 15% of patients were free of disease for more than 5 years. The optimal strategies for patient selection are not currently defined, with no biomarkers known to reliably predict outcomes after ablation.

Because breast cancer metastases are typically hypodense and hypoenhancing, similar to ablation zones, and breast cancer tumors are usually FDG-avid [49], PET/CT guidance can be helpful in performing liver ablation when available. Just prior the procedure, 4 mCi of FDG is injected for procedural imaging. Immediately following ablation, an additional 8 mCi FDG is injected for re-imaging and demonstration of eradication of all FDG-avid tumor [50]. The pre-ablation PET images may be overlaid with immediate post-ablation portal venous phase CT images to demonstrate an adequate ablation margin (Fig. 13.4). Prospective randomized studies have not been performed to assess whether PET guidance decreases recurrence rates.

Lung nodules may be treated with radiofrequency, microwave, or cryoablation. Heat-based modalities may render a lower risk of hemorrhagic complications compared with cryoablation [51]. However, when the targeted nodule is near a critical structure, cryoablation may be a safer option [52]. The ablation zone may be estimated by the ground-glass opacity evident immediately following ablation [51] (Fig. 13.5). Pneumothorax is the most common complication, occurring in 10–50% of cases, requiring chest tube placement in 5–30% [53]. Bronchopleural fistula may occur if the needle is placed perpendicular to the pleural surface and may be less likely if the needle is placed in a tangential manner [52].

Palliative Ablation

Finally, thermal ablation may be offered to patients with painful bone metastases in need of palliation. Bone metastasis occurs in 65–75% of patients with metastatic breast cancer [54]. Image-guided cryotherapy, heat-based thermal ablation, and cementoplasty have been demonstrated to be effective and efficient methods to improve bone pain due to metastasis [55]. One prospective multicenter study enrolled patients with painful bone metastases refractory to opioids and external

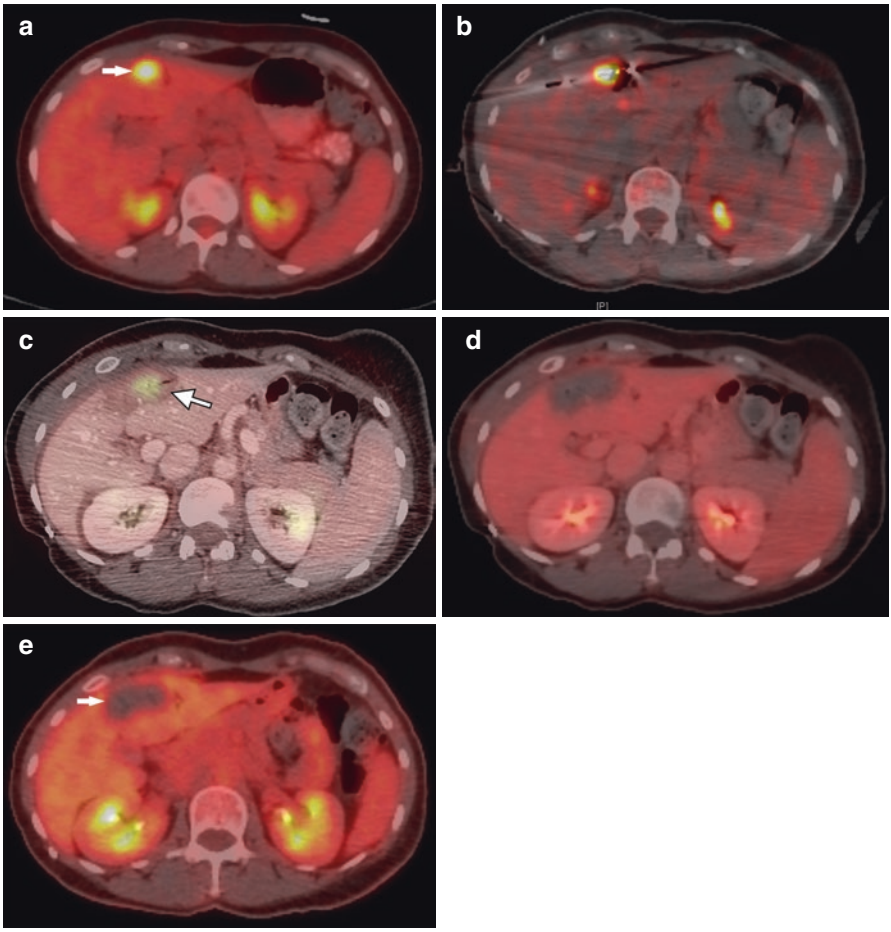

Fig. 13.4 PET-guided ablation. (**a**) PET/CT demonstrates a solitary FDG-avid tumor (ARROW) in segment 4 of a 49-year-old woman with breast cancer. (**b**) Under PET/CT-guidance, a MWA probe is advanced through the lesion. (**c**) Immediate post-ablation venous phase CT image is overlaid on the pre-ablation PET imaging to estimate the ablation margin (arrow). (**d**) After the ablation is complete, an additional 8 mCi of FDG is injected to show the ablation zone. (**e**) Follow-up PET/CT 4 months later shows no residual disease (Arrow)

radiation and showed significant decline in pain scores, though of 32 patients only 1 had breast cancer [56]. Further prospective studies involving larger numbers of women with breast cancer may help future efforts in advocating for these patients to undergo potentially helpful palliative percutaneous procedures.

In summary, thermal ablation may be offered to patients with oligometastatic disease or to patients with one or two sites of growing metastases with stable or decreasing distal sites. Possibly benefits include delaying the need to change systemic therapy, allowing a patient to temporarily cease systemic therapy, and potentially prolonging survival. Patients with painful bone metastases may also benefit

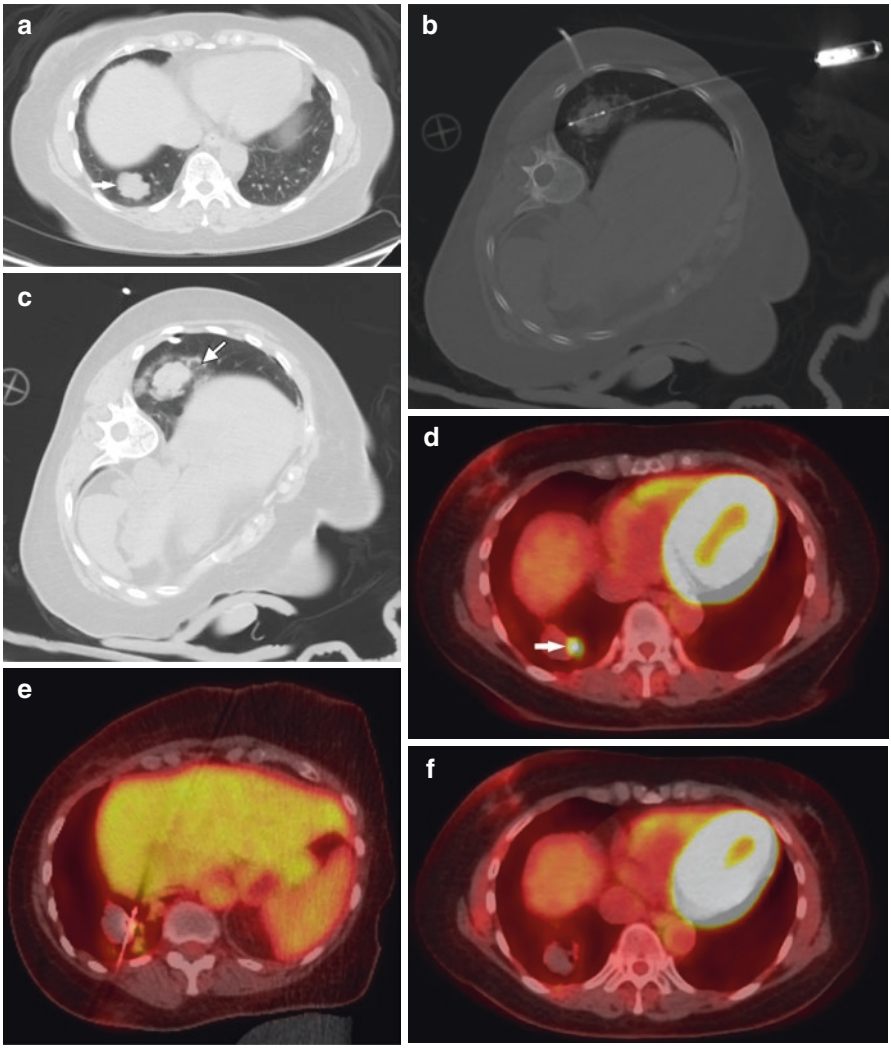

Fig. 13.5 Ablation of a solitary lung mass. (**a**) CT reveals a solitary metastasis (Arrow) at the right lung base of a 52-year-old woman with breast cancer. (**b**) Microwave ablation was performed with repositioning of the needle three times to cover the entire mass. (**c**) Immediate post-ablation intra-procedural CT shows a ground-glass halo around the mass suggestive of the ablation zone (arrow). (**d**) Though the initial post-procedure PET/CT showed no recurrence, a small nodular recurrence (Arrow) developed 5 months after ablation. (**e**) Intra-procedure PET guidance was used to target the small recurrent nodule. (**f**) Follow-up PET/CT imaging 2 months later shows no evidence of residual disease

from percutaneous ablation. Prospective randomized studies have not been performed and would be helpful when advocating for patients who may be candidates for percutaneous ablation.

Transarterial Liver-Directed Therapies

The liver may be the first site of progression in approximately half of patients [57]. Liver-dominant or liver-only progression is a typical referral for liver-directed therapy. For multifocal disease or tumors that are not amenable to thermal ablation due to size or position, transarterial therapies may be considered. These therapies have been applied primarily in a salvage setting after multiple failed lines of systemic therapy.

Both transarterial chemoembolization (TACE) and radioembolization (RE) have been studied in retrospective series for breast cancer [58]. TACE has been performed with various chemotherapies, most commonly, doxorubicin [59–64]. Disease control by RECIST criteria is reported in these studies for roughly 60% of patients, with reported overall survival rates ranging 10–47 months. By comparison, RE has been performed with both resin and glass microspheres [65–72]. Disease control by RECIST criteria is reported in roughly 80% of patients, with reported overall survival rates ranging from 6 to 14 months. Imaging response is associated with longer overall survival in most of these studies. One retrospective single-institution study compared breast cancer patients who underwent either TACE or RE and found that RE was associated with higher imaging response rates, lower complication rates, and a trend for longer survival [73]. No prospective trial has compared the two approaches. However, given the available retrospective data and the finding that RE is associated with better quality of life scores than TACE performed for hepatocellular carcinoma [74], it is reasonable to offer RE before TACE in this population [75].

RE may also be applied to hepatic disease confined to one small portion of the liver, with a plan for a radiation segmentectomy. Radiation segmentectomy has been reported primarily in the context of hepatocellular carcinoma. RE is performed in this setting typically with glass microspheres with the goal of delivering at least 190 Gy to the specific one or two segments involved with tumor [76]. This approach is considered “curative” in the sense that outcomes after radiation segmentectomy for hepatomas are equivalent to other “curative” treatments like ablation [77]. Radiation segmentectomy is not as commonly performed for patients with breast cancer who most commonly present with multifocal liver metastases. Though, when feasible, careful mapping to ascertain all arterial feeders is required to achieve an adequate treatment (Fig. 13.6).

Given that breast cancer is an FDG-avid disease, PET/CT can be helpful in the assessment of treatment response [78] (Fig. 13.7). This has been studied explicitly in RE performed for hepatic metastasis from colorectal cancer, for which objective response by PET/CT better predicts progress-free survival than RECIST criteria [79, 80]. Several retrospective studies have demonstrated that response by PET/CT in breast cancer patients is associated with survival after RE [66, 69]. Hepatotoxicity is a concern in this heavily pretreated population, with grade 3 toxicities occurring in 5–10% of patients [67, 68]. Liver function must be assessed over several months, as RE-induced liver failure can be a relatively late complication occurring

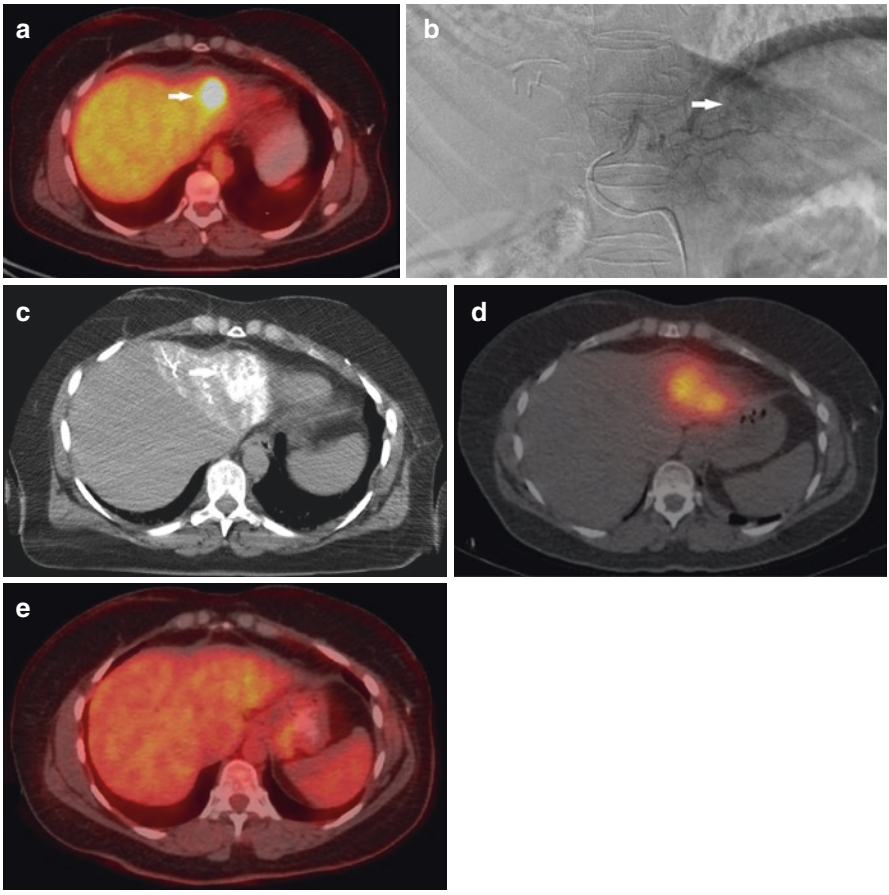

Fig. 13.6 Radiation segmentectomy for isolated liver mass. (**a**) PET/CT shows a solitary 3.5-cm liver metastasis in segment 2/3 adjacent to the heart in a 58-year-old woman with breast cancer. Given its size and location, thermal ablation was considered less safe, and radiation segmentectomy offered. (**b**) Mapping digital subtraction angiography with (**c**) intraprocedural CT angiography shows that the nodule (Arrow) is hypovascular and supplied by both segment 2 and 3 arteries. (**d**) Glass microspheres calculated for the entire left lobe include segment 4 which were administered into the segment 2/3 artery, providing a boosted dose to the tumor. (**e**) Follow-up PET/CT 4 months later shows complete response with no evidence of residual disease

2–6 months after treatment, presenting as new ascites and hyperbilirubinemia [81]. One strategy to prevent hepatoxicity in these frequently heavily pretreated patients is to only treat with a sequential lobar, rather than whole liver plan, and to prolong the time between treatments to assure the safety of the second administration [82]. For high-risk patients (e.g., small liver, borderline elevations in liver function tests), one may consider prophylaxis with 300 mg twice daily ursodeoxycholic acid and 4–8 mg daily methylprednisolone, though this strategy has not been assessed prospectively [81]. Beyond liver failure, nontarget embolization is also a concern, given

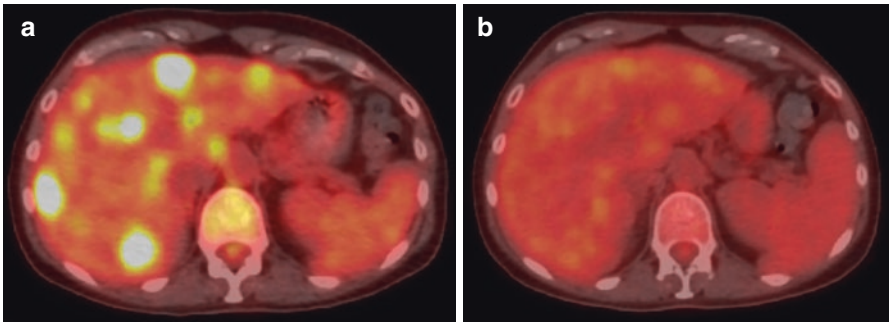

Fig. 13.7 PET/CT imaging pre- and post-radioembolization. (**a**) PET/CT before radioembolization (RE) demonstrates multifocal bilobar disease, which was treated with glass microspheres in a sequential lobar fashion with 1.5 months between treatments. (**b**) Four months after the first lobar administration, there is complete resolution of the FDG-avid lesions indicative of a complete response

the high rates of stasis noted in patients heavily pretreated with a long history of systemic therapy [66].

The potential for locoregional therapy to generate antitumor immune responses has been studied most extensively in the context of external radiation therapy [83]. Abscopal effects, wherein tumors outside a treatment field respond after locoregional therapy due to immune stimulation, have been reported after RE for squamous cell carcinoma and for breast cancer [84, 85]. High-dose "ablative" external radiation may be more effective than lower doses at stimulating antitumor immunity [83]. Theoretically, the higher radiation doses achievable with RE compared with external radiation, and the large quantity of tumor that can be irradiated with transarterial therapies, imply that RE may be even more effective than external radiation in inducing antitumor immunity. However, proof-of-concept studies have not yet been performed.

Conclusions

Breast cancer care has had many advances in recent years. Better screening has led to an increased incidence in localized early stage disease, allowing for continued evolution of locoregional treatments and creating opportunities for minimally invasive and noninvasive treatments. Locoregional therapy for oligometastatic disease may impact survival and outcomes, though prospective studies have not yet been done. Advances in screening and treatment of localized disease have not mitigated the poor prognosis of widely metastatic breast cancer and patients with unfavorable tumor biology. Liver-directed therapy offers a different approach from systemic therapies that may benefit at least a subset of patients for whom liver progression limits survival. Local ablative and transarterial therapies may be one way to

stimulate patients' antitumor immune responses, particularly in combination with immunotherapy. Prospective studies are needed to better demonstrate efficacy, optimize patient selection, and assess the feasibility of combination therapies.

References

1. Bray F, Ferlay J, Soerjomataram I, Siegel RL, Torre LA, Jemal A. Global cancer statistics 2018: GLOBOCAN estimates of incidence and mortality worldwide for 36 cancers in 185 countries. CA Cancer J Clin. 2018;68(6):394–424.
2. Siegel RL, Miller KD, Jemal A. Cancer statistics, 2019. CA Cancer J Clin. 2019;69(1):7–34.
3. American Cancer Society. Cancer facts & figure. 2019. http://www.cancer.org/content/dam/cancer-org/research/cancer-facts-and-statistics/annual-cancer-facts-and-figures/2019/cancer-facts-and-figures-2019.pdf. Accessed 1 Oct 2019.
4. Kuchenbaecker KB, Hopper JL, Barnes DR, Phillips K-A, Mooij TM, Roos-Blom M-J, et al. Risks of breast, ovarian, and contralateral breast cancer for BRCA1 and BRCA2 mutation carriers. JAMA. 2017;317(23):2402–16.
5. DeSantis CE, Ma J, Goding Sauer A, Newman LA, Jemal A. Breast cancer statistics, 2017, racial disparity in mortality by state. CA Cancer J Clin. 2017;67(6):439–48.
6. Monticciolo DL, Newell MS, Moy L, Niell B, Monsees B, Sickles EA. Breast cancer screening in women at higher-than-average risk: recommendations from the ACR. J Am Coll Radiol. 2018;15(3):408–14.
7. Coldman A, Phillips N, Wilson C, Decker K, Chiarelli AM, Brisson J, et al. Pan-Canadian study of mammography screening and mortality from breast cancer. JNCI. 2014;106(11):dju261.
8. Duffy SW, Tabár L, Chen HH, Holmqvist M, Yen MF, Abdsalah S, et al. The impact of organized mammography service screening on breast carcinoma mortality in seven Swedish counties: a collaborative evaluation. Cancer. 2002;95(3):458–69.
9. Tabár L, Vitak B, Chen TH-H, Yen AM-F, Cohen A, Tot T, et al. Swedish two-county trial: impact of mammographic screening on breast cancer mortality during 3 decades. Radiology. 2011;260(3):658–63.
10. Tutt A, Ellis P, Kilburn L, Gilett C, Pinder S, Abraham J, et al. Abstract S3-01: the TNT trial: a randomized phase III trial of carboplatin (C) compared with docetaxel (D) for patients with metastatic or recurrent locally advanced triple negative or BRCA1/2 breast cancer (CRUK/07/012). Cancer Res. 2015;75(9 Supplement):S3–01.
11. Turashvili G, Brogi E. Tumor heterogeneity in breast cancer. Front Med. 2017;4:227.
12. Gradishar WJ, Anderson BO, Balassanian R, Blair SL, Burstein HJ, Cyr A, et al. Breast cancer, version 1.2016. J Natl Compr Canc Netw. 2015;13(12):1475–85.
13. Sakorafas GH. Breast cancer surgery-historical evolution, current status and future perspectives. Acta Oncol. 2001;40(1):5–18.
14. Buchholz TA, Mittendorf EA, Hunt KK. Surgical considerations after neoadjuvant chemotherapy: breast conservation therapy. JNCI Monogr. 2015;2015(51):11–4.
15. Fleming MM, Holbrook AI, Newell MS. Update on image-guided percutaneous ablation of breast cancer. Am J Roentgenol. 2017;208(2):267–74.
16. Fornage BD, Hwang RF. Current status of imaging-guided percutaneous ablation of breast cancer. Am J Roentgenol. 2014;203(2):442–8.
17. Roubidoux MA, Yang W, Stafford RJ. Image-guided ablation in breast cancer treatment. Tech Vasc Interv Radiol. 2014;17(1):49–54.
18. Sabel MS. Nonsurgical ablation of breast cancer: future options for small breast tumors. Surg Oncol Clin. 2014;23(3):593–608.
19. Brace C. Thermal tumor ablation in clinical use. IEEE Pulse. 2011;2(5):28–38.

20. Nguyen T, Hattery E, Khatri VP. Radiofrequency ablation and breast cancer: a review. Gland Surg. 2014;3(2):128.
21. Ito T, Oura S, Nagamine S, Takahashi M, Yamamoto N, Yamamichi N, et al. Radiofrequency ablation of breast cancer: a retrospective study. Clin Breast Cancer. 2018;18(4):e495–500.
22. Simon CJ, Dupuy DE, Mayo-Smith WW. Microwave ablation: principles and applications. Radiographics. 2005;25(suppl_1):S69–83.
23. Zhou W, Jiang Y, Chen L, Ling L, Liang M, Pan H, et al. Image and pathological changes after microwave ablation of breast cancer: a pilot study. Eur J Radiol. 2014;83(10):1771–7.
24. Harms SE. Percutaneous ablation of breast lesions by radiologists and surgeons. Breast Dis. 2001;13:67–76.
25. Van Esser S, Stapper G, Van Diest P, van den Bosch M, Klaessens J, Mali WTM, et al. Ultrasound-guided laser-induced thermal therapy for small palpable invasive breast carcinomas: a feasibility study. Ann Surg Oncol. 2009;16(8):2259.
26. Schwartzberg B, Abdelatif O, Lewin J, Bernard J, Brehm J, Bu-Ali H, et al. Abstract P3-13-03: Multicenter clinical trial of percutaneous laser ablation for early stage primary breast cancer. Results of 49 cases with radiographic and pathological correlation. AACR; 2016.
27. Peek M, Ahmed M, Napoli A, ten Haken B, McWilliams S, Usiskin S, et al. Systematic review of high-intensity focused ultrasound ablation in the treatment of breast cancer. Br J Surg. 2015;102(8):873–82.
28. Zhou Y-F. High intensity focused ultrasound in clinical tumor ablation. World J Clin Oncol. 2011;2(1):8.
29. Wu F, Wang Z-B, Cao Y-D, Chen W, Bai J, Zou J, et al. A randomised clinical trial of high-intensity focused ultrasound ablation for the treatment of patients with localised breast cancer. Br J Cancer. 2003;89(12):2227.
30. Wu F, Wang Z-B, Zhu H, Chen W-Z, Zou J-Z, Bai J, et al. Extracorporeal high intensity focused ultrasound treatment for patients with breast cancer. Breast Cancer Res Treat. 2005;92(1):51–60.
31. Erinjeri JP, Clark TW. Cryoablation: mechanism of action and devices. J Vasc Interv Radiol. 2010;21(8):S187–S91.
32. Tarkowski R, Rzaca M. Cryosurgery in the treatment of women with breast cancer—a review. Gland Surg. 2014;3(2):88.
33. Simmons RM, Ballman KV, Cox C, Carp N, Sabol J, Hwang RF, et al. A phase II trial exploring the success of cryoablation therapy in the treatment of invasive breast carcinoma: results from ACOSOG (Alliance) Z1072. Ann Surg Oncol. 2016;23(8):2438–45.
34. Johnson JP. Immunologic aspects of cryosurgery: potential modulation of immune recognition and effector cell maturation. Clin Dermatol. 1990;8(1):39–47.
35. Misao A, Sakata K, Saji S, Kunieda T. Late appearance of resistance to tumor rechallenge following cryosurgery: a study in an experimental mammary tumor of the rat. Cryobiology. 1981;18(4):386–9.
36. Sabel MS, Arora A, Su G, Chang AE. Adoptive immunotherapy of breast cancer with lymph node cells primed by cryoablation of the primary tumor. Cryobiology. 2006;53(3):360–6.
37. Aarts B, Klompenhouwer E, Rice S, Imani F, Baetens T, Bex A, et al. Cryoablation and immunotherapy: an overview of evidence on its synergy. Insights Imaging. 2019;10(1):53.
38. McArthur HL, Diab A, Page DB, Yuan J, Solomon SB, Sacchini V, et al. A pilot study of preoperative single-dose ipilimumab and/or cryoablation in women with early-stage breast cancer with comprehensive immune profiling. Clin Cancer Res. 2016;22(23):5729–37.
39. Rubinsky B, Onik G, Mikus P. Irreversible electroporation: a new ablation modality—clinical implications. Technol Cancer Res Treat. 2007;6(1):37–48.
40. Al-Sakere B, André F, Bernat C, Connault E, Opolon P, Davalos RV, et al. Tumor ablation with irreversible electroporation. PLoS One. 2007;2(11):e1135.
41. Lee EW, Chen C, Prieto VE, Dry SM, Loh CT, Kee ST. Advanced hepatic ablation technique for creating complete cell death: irreversible electroporation. Radiology. 2010;255(2):426–33.

42. Lee EW, Thai S, Kee ST. Irreversible electroporation: a novel image-guided cancer therapy. Gut Liver. 2010;4(Suppl 1):S99.
43. Di Lascio S, Pagani O. Oligometastatic breast cancer: a shift from palliative to potentially curative treatment? Breast Care (Basel). 2014;9(1):7–14.
44. Palma D, Olson R, Harrow S, Gaede S, Louie A, Haasbeek C, et al. Stereotactic ablative radiation therapy for the comprehensive treatment of oligometastatic tumors (SABR-COMET): results of a randomized trial. Int J Radiat Oncol Biol Phys. 2018;102(3):S3–4.
45. Chen M-S, Li J-Q, Zheng Y, Guo R-P, Liang H-H, Zhang Y-Q, et al. A prospective randomized trial comparing percutaneous local ablative therapy and partial hepatectomy for small hepatocellular carcinoma. Ann Surg. 2006;243(3):321.
46. Meloni MF, Andreano A, Laeseke PF, Livraghi T, Sironi S, Lee FT Jr. Breast cancer liver metastases: US-guided percutaneous radiofrequency ablation--intermediate and long-term survival rates. Radiology. 2009;253(3):861–9.
47. Sadot E, Lee SY, Sofocleous CT, Solomon SB, Gönen M, Kingham TP, et al. Hepatic resection or ablation for isolated breast cancer liver metastasis: a case-control study with comparison to medically treated patients. Ann Surg. 2016;264(1):147.
48. Sofocleous C, Nascimento R, Gonen M, Theodoulou M, Covey A, Brody L, et al. Radiofrequency ablation in the management of liver metastases from breast cancer. Am J Roentgenol. 2007;189(4):883–9.
49. Niikura N, Costelloe CM, Madewell JE, Hayashi N, Yu T-K, Liu J, et al. FDG-PET/CT compared with conventional imaging in the detection of distant metastases of primary breast cancer. Oncologist. 2011;16(8):1111–9.
50. Ryan ER, Sofocleous CT, Schöder H, Carrasquillo JA, Nehmeh S, Larson SM, et al. Split-dose technique for FDG PET/CT–guided percutaneous ablation: a method to facilitate lesion targeting and to provide immediate assessment of treatment effectiveness. Radiology. 2013;268(1):288–95.
51. Sharma A, Abtin F, Shepard J-AO. Image-guided ablative therapies for lung cancer. Radiol Clin. 2012;50(5):975–99.
52. Tafti BA, Genshaft S, Suh R, Abtin F, editors. Lung ablation: indications and techniques. In: Seminars in interventional radiology. New York, NY: Thieme Medical Publishers; 2019.
53. Taslakian B, Muallem N, Moore W. Thermal lung ablation. In: Procedural dictations in image-guided intervention. New York, NY: Springer; 2016. p. 59–64.
54. Kennecke H, Yerushalmi R, Woods R, Cheang MC, Voduc D, Speers CH, et al. Metastatic behavior of breast cancer subtypes. J Clin Oncol. 2010;28(20):3271–7.
55. Filippiadis D, Mavrogenis AF, Mazioti A, Palialexis K, Megaloikonomos PD, Papagelopoulos PJ, et al. Metastatic bone disease from breast cancer: a review of minimally invasive techniques for diagnosis and treatment. Eur J Orthop Surg Traumatol. 2017;27(6):729–36.
56. Goetz MP, Callstrom MR, Charboneau JW, Farrell MA, Maus TP, Welch TJ, et al. Percutaneous image-guided radiofrequency ablation of painful metastases involving bone: a multicenter study. J Clin Oncol. 2004;22(2):300–6.
57. Miles D, Harbeck N, Escudier B, Hurwitz H, Saltz L, Van Cutsem E, et al. Disease course patterns after discontinuation of bevacizumab: pooled analysis of randomized phase III trials. J Clin Oncol. 2011;29(1):83–8.
58. Mouli SK, Gupta R, Sheth N, Gordon AC, Lewandowski RJ, editors. Locoregional therapies for the treatment of hepatic metastases from breast and gynecologic cancers. In: Seminars in interventional radiology. New York, NY: Thieme Medical Publishers; 2018.
59. Cho SW, Kitisin K, Buck D, Steel J, Brufsky A, Gillespie R, et al. Transcatheter arterial chemoembolization is a feasible palliative locoregional therapy for breast cancer liver metastases. Int J Surg Oncol. 2010;2010:251621.
60. Eichler K, Jakobi S, Gruber-Rouh T, Hammerstingl R, Vogl TJ, Zangos S. Transarterial chemoembolisation (TACE) with gemcitabine: phase II study in patients with liver metastases of breast cancer. Eur J Radiol. 2013;82(12):e816–e22.

61. Lin Y-T, Médioni J, Amouyal G, Déan C, Sapoval M, Pellerin O. Doxorubicin-loaded 70–150 μm microspheres for liver-dominant metastatic breast cancer: results and outcomes of a pilot study. Cardiovasc Intervent Radiol. 2017;40(1):81–9.
62. Martin RC, Robbins K, Fages JF, Romero FD, Rustein L, Tomalty D, et al. Optimal outcomes for liver-dominant metastatic breast cancer with transarterial chemoembolization with drug-eluting beads loaded with doxorubicin. Breast Cancer Res Treat. 2012;132(2):753–63.
63. Vogl TJ, Naguib NN, Nour-Eldin N-EA, Mack MG, Zangos S, Abskharon JE, et al. Repeated chemoembolization followed by laser-induced thermotherapy for liver metastasis of breast cancer. Am J Roentgenol. 2011;196(1):W66–72.
64. Vogl TJ, Naguib NN, Nour-Eldin NE, Eichler K, Zangos S, Gruber-Rouh T. Transarterial chemoembolization (TACE) with mitomycin C and gemcitabine for liver metastases in breast cancer. Eur Radiol. 2010;20(1):173–80.
65. Cianni R, Pelle G, Notarianni E, Saltarelli A, Rabuffi P, Bagni O, et al. Radioembolisation with (90)Y-labelled resin microspheres in the treatment of liver metastasis from breast cancer. Eur Radiol. 2013;23(1):182–9.
66. Deipolyi AR, Riedl CC, Bromberg J, Chandarlapaty S, Klebanoff CA, Sofocleous CT, et al. Association of PI3K pathway mutations with early positron-emission tomography/CT imaging response after radioembolization for breast cancer liver metastases: results of a single-center retrospective pilot study. J Vasc Interv Radiol. 2018;29(9):1226–35.
67. Fendler WP, Lechner H, Todica A, Paprottka KJ, Paprottka PM, Jakobs TF, et al. Safety, efficacy, and prognostic factors after radioembolization of hepatic metastases from breast cancer: a large single-center experience in 81 patients. J Nucl Med. 2016;57(4):517–23.
68. Gordon AC, Gradishar WJ, Kaklamani VG, Thuluvath AJ, Ryu RK, Sato KT, et al. Yttrium-90 radioembolization stops progression of targeted breast cancer liver metastases after failed chemotherapy. J Vasc Interv Radiol. 2014;25(10):1523–32, 32.e1–2.
69. Haug AR, Tiega Donfack BP, Trumm C, Zech CJ, Michl M, Laubender RP, et al. 18F-FDG PET/CT predicts survival after radioembolization of hepatic metastases from breast cancer. J Nucl Med. 2012;53(3):371–7.
70. Pieper CC, Meyer C, Wilhelm KE, Block W, Nadal J, Ahmadzadehfar H, et al. Yttrium-90 radioembolization of advanced, unresectable breast cancer liver metastases-a single-center experience. J Vasc Interv Radiol. 2016;27(9):1305–15.
71. Saxena A, Kapoor J, Meteling B, Morris DL, Bester L. Yttrium-90 radioembolization for unresectable, chemoresistant breast cancer liver metastases: a large single-center experience of 40 patients. Ann Surg Oncol. 2014;21(4):1296–303.
72. Saxena A, Meteling B, Kapoor J, Golani S, Danta M, Morris DL, et al. Yttrium-90 radioembolization is a safe and effective treatment for unresectable hepatocellular carcinoma: a single centre experience of 45 consecutive patients. Int J Surg. 2014;12(12):1403–8.
73. Chang J, Charalel R, Noda C, Ramaswamy R, Kim SK, Darcy M, et al. Liver-dominant breast cancer metastasis: a comparative outcomes study of chemoembolization versus radioembolization. Anticancer Res. 2018;38(5):3063–8.
74. Salem R, Gilbertsen M, Butt Z, Memon K, Vouche M, Hickey R, et al. Increased quality of life among hepatocellular carcinoma patients treated with radioembolization, compared with chemoembolization. Clin Gastroenterol Hepatol. 2013;11(10):1358–65.e1.
75. Shamimi-Noori S, Gonsalves CF, Shaw CM, editors. Metastatic liver disease: indications for locoregional therapy and supporting data. In: Seminars in interventional radiology. New York, NY: Thieme Medical Publishers; 2017.
76. Vouche M, Habib A, Ward TJ, Kim E, Kulik L, Ganger D, et al. Unresectable solitary hepatocellular carcinoma not amenable to radiofrequency ablation: multicenter radiology-pathology correlation and survival of radiation segmentectomy. Hepatology. 2014;60(1):192–201.
77. Lewandowski RJ, Gabr A, Abouchaleh N, Ali R, Al Asadi A, Mora RA, et al. Radiation segmentectomy: potential curative therapy for early hepatocellular carcinoma. Radiology. 2018;287(3):1050–8.

78. Riedl CC, Pinker K, Ulaner GA, Ong LT, Baltzer P, Jochelson MS, et al. Comparison of FDG-PET/CT and contrast-enhanced CT for monitoring therapy response in patients with metastatic breast cancer. Eur J Nucl Med Mol Imaging. 2017;44(9):1428–37.
79. Shady W, Kishore S, Gavane S, Do RK, Osborne JR, Ulaner GA, et al. Metabolic tumor volume and total lesion glycolysis on FDG-PET/CT can predict overall survival after (90)Y radioembolization of colorectal liver metastases: a comparison with SUVmax, SUVpeak, and RECIST 1.0. Eur J Radiol. 2016;85(6):1224–31.
80. Shady W, Sotirchos VS, Do RK, Pandit-Taskar N, Carrasquillo JA, Gonen M, et al. Surrogate imaging biomarkers of response of colorectal liver metastases after salvage radioembolization using 90Y-loaded resin microspheres. AJR Am J Roentgenol. 2016;207(3):661–70.
81. Sangro B, Martínez-Urbistondo D, Bester L, Bilbao JI, Coldwell DM, Flamen P, et al. Prevention and treatment of complications of selective internal radiation therapy: expert guidance and systematic review. Hepatology. 2017;66(3):969–82.
82. Seidensticker R, Seidensticker M, Damm R, Mohnike K, Schütte K, Malfertheiner P, et al. Hepatic toxicity after radioembolization of the liver using 90 Y-microspheres: sequential lobar versus whole liver approach. Cardiovasc Intervent Radiol. 2012;35(5):1109–18.
83. Siva S, MacManus MP, Martin RF, Martin OA. Abscopal effects of radiation therapy: a clinical review for the radiobiologist. Cancer Lett. 2015;356(1):82–90.
84. Deipolyi AR, Bromberg JF, Erinjeri JP, Solomon SB, Brody LA, Riedl C. Abscopal effect after radioembolization for metastatic breast cancer in the setting of immunotherapy. J Vasc Interv Radiol. 2018;29(3):432–3.
85. Ghodadra A, Bhatt S, Camacho JC, Kim HS. Abscopal effects and yttrium-90 radioembolization. Cardiovasc Intervent Radiol. 2016;39(7):1076–80.

Chapter 14
Thyroid Cancer

Juan C. Camacho, Eduardo A. Lacayo, and R. Michael Tuttle

Abbreviations

CEUS	Contrast enhanced ultrasound
EA	Ethanol ablation
FNAB	Fine needle aspiration biopsy
MAC	Monitor anesthesia care
MWA	Microwave ablation
PLA	Percutaneous laser ablation
PTC	Papillary thyroid carcinoma
PTMC	Papillary thyroid microcarcinoma
RFA	Radiofrequency ablation
US	Ultrasound

Introduction

The last 20 years has seen a dramatic increase in the diagnosis of thyroid cancer across all developed countries as wide spread use of cross-sectional imaging, neck ultrasonography, and fine needle aspiration has identified small low-risk thyroid cancers that were previously unrecognized. Arising from thyroid follicular cells, papillary thyroid cancers are far and away the most common subtype of thyroid cancers with follicular thyroid cancers and anaplastic thyroid cancers being much

J. C. Camacho (✉) · E. A. Lacayo
Interventional Radiology, Memorial Sloan Kettering Cancer Center, New York, NY, USA
e-mail: camachoj@mskcc.org; lacayoe@mskcc.org

R. M. Tuttle
Endocrinology, Memorial Sloan Kettering Cancer Center, New York, NY, USA
e-mail: tuttlem@mskcc.org

C. Georgiades, H. S. Kim (eds.), *Image-Guided Interventions in Oncology*,
https://doi.org/10.1007/978-3-030-48767-6_14

less common. Medullary thyroid cancer, a neuroendocrine tumor arising from C-cells within the thyroid, is also uncommon and can present as either a sporadic or hereditary form. Primary lymphomas of the thyroid occur but are very uncommon.

Role of Surgery

Since the 1950s, the traditional initial therapies for papillary and follicular thyroid cancers included total thyroidectomy, compartment-oriented resection of clinically involved cervical lymph node chains, and usually radioactive iodine therapy. While this paradigm is still appropriate for large papillary thyroid cancers presenting with disease outside the thyroid, a much more minimalistic management approach has been accepted for low-risk thyroid cancers. These low-risk thyroid cancers can be effectively managed with either active surveillance (observational management) or minimalistic thyroid surgery (thyroid lobectomy without neck dissection). Many studies have now demonstrated that the vast majority of small thyroid cancers (less than 1.5 cm) confined to the thyroid that are followed with observational management remain quiescent demonstrating little or no growth over 5–10 years and a 2–4% risk of developing cervical lymph node metastases. More importantly, studies demonstrate that at the time of disease progression, salvage surgery is nearly 100% effective indicating that an observational management approach can be an effective and safe option for properly selected low-risk papillary thyroid cancers [1].

In papillary thyroid cancers that are not appropriate for observational management, thyroidectomy with or without radioactive iodine is associated with a recurrence rate as low as 1–2% in low-risk patients, 10–15% in intermediate-risk patients, and over 30% in high-risk patients. Disease-specific survival exceeds 98% in low- and intermediate-risk patients but can be as low as 50% in older patients developing radioactive iodine refractory distant metastases. Most recurrences occur in cervical lymph nodes and can be treated with additional surgery and occasionally with radioactive iodine. Distant metastases are present at diagnosis in about 4% of patients with papillary thyroid cancer and are detected years later in an additional 3–4%. In many cases, isolated distant metastases can be effectively treated with localized therapies (external beam irradiation, embolization, ablative therapies, or metastasectomy). Radioactive iodine can also be effective therapy for distant metastases in patients that have radioactive iodine avid disease. Patients with progressive, radioactive-iodine-refractory papillary thyroid cancer that cannot be adequately controlled with localized measures are candidates for systemic therapy which usually involves multikinase inhibitors such as sorafenib or lenvatinib, both approved by the Food and Drug Administration (FDA) for this situation [1].

General Treatment Paradigm

Rather than a one size fits all approach to initial management and follow-up, the American Thyroid Association guidelines recommend a risk adapted management approach. Low-risk patients are considered for observation or thyroid lobectomy, while intermediate-risk patients usually undergo total thyroidectomy and appropriate lymph node dissection. High-risk patients usually demonstrate either gross invasion of major structures in the neck or demonstrate distant metastases and may require additional therapies beyond thyroidectomy and cervical lymph node dissection. Similarly, the approach to follow-up is also risk adapted with neck ultrasonography and serum thyroglobulin (a thyroid specific tumor biomarker) being the keystones of follow-up in low- and intermediate-risk patients. High-risk patients may require additional cross-sectional (computed tomography (CT) or magnetic resonance imaging (MRI)) or functional imaging (radioactive iodine imaging, fluorodeoxyglucose (FDG) positron emission tomography (PET) imaging) depending on the specifics of each case and the response to initial therapy.

Similar to papillary thyroid cancer, the primary treatment modality for medullary thyroid cancer is total thyroidectomy with compartment-oriented resection of involved lymph nodes. Additional therapies such as external beam radiation or chemotherapy are seldom indicated. Both calcitonin and CEA are excellent biomarkers for medullary thyroid cancer and are the primary tools used in follow-up to guide the extent and timing of follow-up imaging. Recently, two multikinase inhibitors were FDA approved for progressive or symptomatic medullary thyroid cancer that is not amenable to localized therapies (cabozantinib and vandetanib). Current trials are evaluating very specific RET inhibitors in medullary thyroid cancer and appear to be showing remarkable results [1].

Anaplastic thyroid cancers are among the most aggressive and lethal solid tumors. Very aggressive multimodality initial therapy is required and usually involves surgical resection if possible, external beam irradiation, and concurrent chemotherapy. Even with aggressive up-front therapy, fewer than 10% of patients survive longer than a year.

Image-Guided Ablation for Papillary Thyroid Cancer

Thermal ablation for thyroid disease began as a minimally invasive option for the management of benign thyroid nodules and now has been incorporated into the American Association of Clinical Endocrinologists, American College of Endocrinology, and Associazione Medici Endocrinologi medical guidelines for the treatment of solid or complex symptomatic or progressively enlarging nodules and/or for nodules causing cosmetic concerns [2]. Although the alternative surgical therapy is a common, well tolerated, and a relatively safe procedure, it does carry risks

including recurrent laryngeal nerve injury (1–2%), permanent hypoparathyroidism (3–4%), and skin numbness overlying the anterior neck (>20%) [3]. Recently, percutaneous thermal ablation has been considered for the treatment of malignant thyroid nodules (particularly in papillary thyroid microcarcinoma (PTMC)) as a new minimally invasive alternative in patients that refuse surveillance or surgical resection. Currently, thermal ablation of thyroid cancers is best done within the context of clinical research projects and is not yet endorsed by major guidelines or considered a standard of care management option in the United States.

Multiple minimally invasive nonsurgical thermal treatment modalities are available including microwave ablation (MWA), radiofrequency ablation (RFA), ethanol ablation (EA), and percutaneous laser ablation (PLA). These modalities have recently demonstrated safety and efficacy in the management of benign thyroid nodules, metastatic cervical lymph nodes from papillary thyroid cancer, and parathyroid adenomas [4–6]. Ethanol ablation has been used for the treatment of predominantly cystic nodules.

Thermal ablation produces irreversible tissue destruction through the application of heat or cold energy. When it comes to thyroid disease, the greatest experience thus far has been with the use of RFA and EA. One recent study has focused on PLA as an alternative in the treatment of micropapillary thyroid cancer due its precise ablation zone and low complication rates. The procedure is performed under monitored anesthesia care (MAC), conscious sedation, or local anesthesia, and it is usually achieved as a single outpatient session.

Indications

Indications for thermal ablation of thyroid malignancy are similar across modalities and include (1) cytologic diagnosis of unifocal PTMC, (2) maximum lesion diameter <10 mm, (3) absence of lymph node metastasis, (4) unwilling to undergo active surveillance, or (5) patients refusing surgery or with medical contraindications for surgery (Table 14.1) [7–9].

Contraindications

Contraindications for thyroid thermal ablation include (1) cytological diagnosis of medullary or anaplastic carcinoma or with aggressive histological phenotype (e.g., tall cell, insular, columnar cell carcinoma), (2) presence of multiple nodules with sonographic features suggestive of malignancy (micro calcification, local invasion, height greater than width, and markedly reduced echogenicity), (3) uncorrectable coagulation disorder, (4) cardiac pacemaker implantation (only if utilizing RFA), (4) extrathyroidal extension/invasion of tracheoesophageal groove, (5) solid lesion with calcification >2 mm, (6) disruption of the thyroid capsule, and (7) contralateral vocal fold paralysis (see Table 14.1) [7–9].

Table 14.1 Indications and contraindications for thyroid cancer ablation

Indications	Contraindications
Cytologic diagnosis of unifocal PTMC	Cytological diagnosis of medullary or anaplastic carcinoma or with aggressive histological phenotype (e.g., tall cell, insular, columnar cell carcinoma)
Maximum lesion diameter < 10 mm	Presence of multiple nodules with sonographic features suggestive of malignancy (micro calcification, local invasion, height greater than width, and markedly reduced echogenicity)[a]
Absence of lymph node metastasis	Uncorrectable coagulation disorder
Unwilling to undergo active surveillance	Cardiac pacemaker implantation (only if utilizing RFA)
Patients with medical contraindications for surgery or refusing surgery	Extra thyroidal extension/invasion tracheoesophageal groove
	Solid lesion with calcifications >2 mm
	Disruption of the thyroid capsule (relative)
	Contralateral vocal fold paralysis

[a]Traditional contraindication for patients undergoing thermal ablation for benign thyroid nodules

Patient Selection

Candidates must have cytologic confirmation of PTMC and ultrasound evaluation of the lesion prior to thermal ablation. Location, size, volume, and vascularization of the thyroid nodule should carefully be assessed. Adequate preparation should include evaluation of the preferred access route and number of applicators needed according to lesion size/volume. Probe trajectory should be as parallel as possible to the long axis of the lesion.

Technique

Anesthesia should be provided based on institutional standard of care for visceral ablations. Thyroid US evaluation is performed at baseline using any commercially available US scanner equipped with a 7.5–13.0 MHz linear transducer. The nodule volume should be calculated with the ellipsoid formula by an experienced sonographer. The procedure should be performed with the patient in the supine position and with neck hyperextension. Before thermal ablation, careful ultrasound (US) evaluation must be performed to evaluate the relationship between the thyroid tumor and surrounding anatomic structures to prevent extrathyroidal injury. If the distance between the tumor and critical structures is <5 mm, hydrodissection must be performed to avoid thermal injury. Hydrodissection can be performed with the local anesthetic used or with normal saline.

Contrast-Enhanced Ultrasound (CEUS)

Once the target lesion is identified, the ultrasound mode is switched to gray-scale harmonic contrast-enhanced ultrasound (CEUS) mode. The focal zone is always placed deeper than the target nodule to avoid microbubble disruption. Intravenous injection of approximately 2.0 ml of sulfur hexafluoride-filled microbubble contrast agent (SonoVue, Bracco, Milan, Italy) is performed through a previously placed 20-gauge intravenous needle in a dorsal hand vein or antecubital fossa. Following SonoVue injection, 10 ml of physiological saline solution are flushed through the intravenous catheter [10] (Fig. 14.1).

Percutaneous Laser Ablation

For PLA, the equipment most commonly used is the EchoLaser EVO (Elesta, Calenzano, Italy) composed of a 1064-nm multisource laser (EchoLaser X4 EVO) with an optimized fiber optic (Orblaze technology), which allows for a spherical, precise ablation zone. After the access point and needle trajectory have been marked, the patient is prepped and draped using sterile technique. Local anesthesia is achieved with 1% lidocaine administered subcutaneously. Standard hydrodissection technique is utilized to create a thermal barrier between the zone of ablation and perithyroidal vital structures (i.e., trachea, recurrent laryngeal nerve, common carotid artery, and esophagus), preventing thermal injury. This is performed by injecting 1–20 ml of physiological saline or lidocaine solution carefully into the superficial cervical tissues surrounding the thyroid capsule (Fig. 14.2) or inside the thyroid to displace the capsule. Then, a 21G guide needle is introduced into the target under real-time US

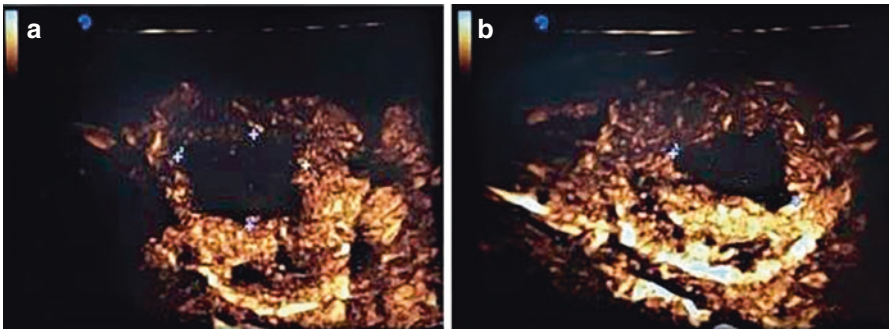

Fig. 14.1 Contrast-enhanced ultrasound examination of the left thyroid lobe (axial **a** and sagittal **b**) 2 hours after laser ablation. The ablated area (previously containing a benign thyroid nodule) is centrally devascularized

guidance. After positioning is confirmed, a 300-micron-flat tip quartz optical fiber is inserted coaxially. The introducer needle is pulled back 5 mm, thus exposing the fiber tip in direct contact with the tumor. Subsequently, the optic fiber is connected to a continuous wave neodymium yttrium-aluminum-garnet (Nd:YAG) laser source at a wave length of 1064 nm [11]. Ablation is performed with a multisource laser with an output power of 3–5 W. Initially the power is set to 5 W for 10 seconds, until the echogenic gas microbubbles at the tip of the fiber are no longer visible on the US image. After that, the power is set at 3 W, and the laser fiber is subsequently pulled back until the entire volume of the nodule is treated. This technique is also known as the "pull-back technique" and has the advantage of reducing the number of direct punctures of the nodule [5]. The energy dose during treatments ranges from 600 to 1800 J per fiber depending on the maximum tumor diameter (Table 14.2).

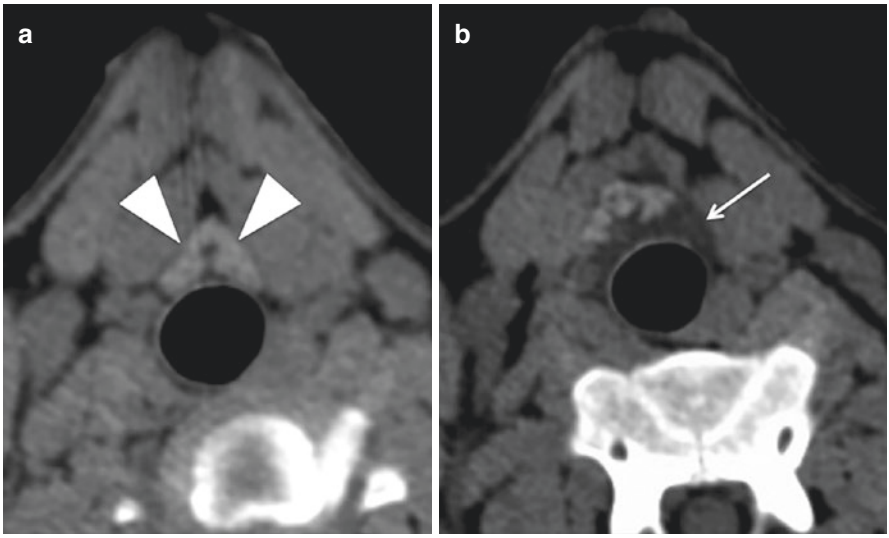

Fig. 14.2 Hydrodissection of the thyroid gland in a swine model. (**a**) Axial CT before hydrodissection shows the target area (arrowheads). The trachea was considered at risk during ablation; thus, sterile water was used (arrow) to push the target lesion away from the trachea (**b**)

Table 14.2 The energy dose range during treatment per fiber depending on the maximum tumor diameter

Maximum tumor diameter	Energy joules) range (power 3 W)	Ablation time
<4 mm	600–800 J	200–267 seconds (3.3–4.5 min)
≥4 to ≤7 mm	1000–1200 J	333–400 seconds (5.6–6.7 min)
>7 to 10 mm	1400–1800 J	467–600 seconds (7.8–10 min)

The ablated area is typically visualized as an enlarging hyperechoic zone due to the gas microbubbles within the coagulated tissue. The objective of treatment in malignant disease is to ablate the whole nodule volume, including an oncologic margin of at least 2–5 mm [5]. The use of CEUS during the ablation is necessary as it identifies areas that require further treatment and allows for continuous evaluation of potential complications. The best estimation of technical success, defined as an ablation zone encompassing the nodule with oncological margins, can be accomplished within 1 week of the procedure.

Identifying critical structures and performing adequate hydrodissection are crucial when considering PLA of locally recurrent thyroid tumors or lymph node metastases. Once a safe ablation zone is identified, the ablation can then be performed with a 3 W fixed protocol and 1200–1800 J [5].

Radiofrequency Ablation

Thermal damage caused by RFA is dependent on both tissue temperature achieved and the duration of heating. Tissue temperatures between 42 and 45 °C cause tissue cells to become more susceptible to damage when exposed to chemotherapy and/or radiation therapy. Irreversible cellular damage occurs when temperatures reach up to 46 °C for 60 min or to 50–52 °C for 4–6 min. Near-immediate tissue coagulation is induced at temperatures between 60 and 100 °C [12]. Thus, achieving and maintaining a temperature of 50–100 °C throughout the target lesion for at least 4–6 minutes is the objective. Tumor tissue that is distant from the electrode will take longer to ablate due to the slow conduction of heat and will require an increase in the ablation time of up to 10–30 minutes to achieve an adequate ablation zone [12].

The patients are placed in the supine position with their necks hyperextended. Two grounding pads are attached to both thighs. After the entry site has been marked, local anesthesia is achieved with 1% lidocaine at the puncture site. RFA can be performed using the transisthmic approach and/or the “moving shot” technique, depending on lesion size and operator preference [13]. An RF generator and an internally cooled 18- or 19-gauge electrode with active 3.8- to 10-mm tips are typically used. Ablation is performed starting at 40 W. If a transient hyperechoic zone did not form at the tip of the electrode within 5–10 s, the power is increased in 5 W increments up to 70 W. When a transient hyperechoic zone appears at the periphery of the nodule, the electrode tip is moved back to prevent thermal injury of normal surrounding tissue. Ablation is terminated when the nodule has changed to a transient hyperechoic zone. During the ablation, both thighs should be checked frequently to prevent skin injury.

Microwave Ablation

The MWA system used includes a generator, a flexible low-loss coaxial cable, and a thyroid-dedicated cooled shaft antenna. The generator is capable of producing 1–100 W of power at 2450 MHz either pulsed or continuous. The shaft antenna is

designed for the thyroid gland with as a 16-gauge needle (3 or 5 mm in length and 1.9 mm in diameter) coated with polytetrafluoroethylene to prevent tissue adhesion. Water circulates through dual channels within the antenna to prevent the shaft from overheating [7]. MWA is faster than RFA and with more predictable ablation margins (Fig. 14.3).

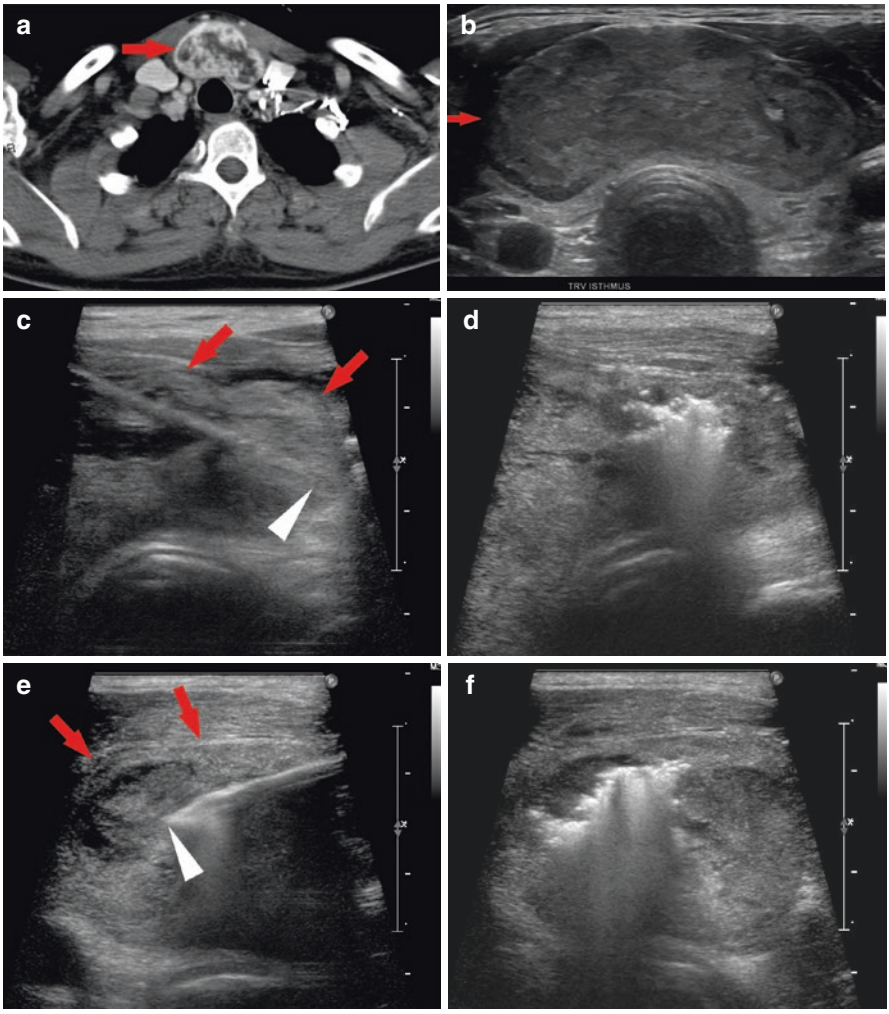

Fig. 14.3 Female with biopsy proven benign thyroid mass and compressive symptoms. The patient was referred for ablation after declining surgery. Axial contrast-enhanced CT (**a**) shows a heterogeneously enhancing mass is the thymic isthmus (red arrow). Intraprocedural ultrasound (**b**) shows the mass before ablation (red arrow). Two overlapping ablations were performed because of the targets size. The MWA probe (white arrowhead) was placed in the left part of the mass (red arrows) (**c**). Ablation resulted in gas formation (**d**) obscuring the left portion of the mass. The procedure was repeated in the right part of the thyroid mass (**e**, **f**) with the same results. (Courtesy of Dr. Kelvin Hong, Johns Hopkins University)

Post-Procedural Complications

Most complications reported are in patients that undergo thermal ablation for benign thyroid nodules, which are usually larger and require larger ablation zones. To date, no major complications have been reported after thermal ablation for PTMC, such as vocal fold paralysis, skin burn, hypocalcemia, hypothyroidism, or critical organ injury (i.e., trachea, esophagus). A few minor complications have been reported in the literature, these include pain, transient hoarseness, and temporary hyperthyroidism. Zhang et al. reported 1% incidence in post-procedural pain that resolved with administration of pain medication, and 4% incidence of transient hoarseness that recovered within 3 hours posttreatment [8]. Yue et al. reported 19% incidence of transient hoarseness that recovered within 3 months. Most patients mentioned a burning sensation and/or pain that was relieved within 12 hrs post-procedure [7]. Zhou et al. reported a 2.8% incidence of hyperthyroidism at 1-month follow-up labs, which recovered without treatment within 2 months [11].

Follow-Up

Immediately after treatment, patients receive NSAIDs and should be observed for at least 1–2 hours in the recovery unit. They should be monitored for complications such as hematoma, voice changes, dysphagia, and tracheal injury. Pain should be managed symptomatically with oral or intravenous analgesics.

Clinical follow-up is US based at 1, 3, and 6 months after treatment and every 6 months thereafter. Focus should be on measuring the size of the ablation zone as well as development of local recurrent lesions within the thyroid and locoregional metastasis to neck lymph nodes [7, 8, 11].

Three and 6-month post-procedural standard thyroid clinical laboratory evaluations (serum TSH, free thyroid hormones, thyroglobulin (Tg), and thyroid antibodies) should also be performed.

Outcomes

PLA

Reported outcomes in patients undergoing thermal ablation for PTMC have shown favorable results. The vast majority of the literature to date has been published in recent years with PLA being the most common modality used. Papini et al. first described PLA for the treatment of PTMC in 2011 with one patient that underwent ablation. The lesion appeared completely ablated based on posttreatment cytological, histological, and imaging findings. No evidence of disease recurrence during a

2-year follow-up period was noted [14]. Valcavi et al. confirmed PLA as a technically feasible option when PLA was performed on the operating room table immediately before thyroidectomy, demonstrating the predicted thermal effects on histopathology [15].

Zhou et al. reported a series of 30 patients with solitary T1N0M0 PTMC treated by PLA. The mean follow-up period was 13.2 months (range 12–24 months). They found that during their last follow-up, 33.3% (10/30 patients) of the ablation zones completely disappeared, and 66.7% (20/30 patients) remained as scar-like areas. There was no evidence of local recurrence at 1, 6, and 12 months by fine needle aspiration biopsy (FNAB) or distant metastasis [16].

Zhang et al. reported the safe and effective use of PLA in 64 patients with solitary PTMC measuring 3–8 mm in maximum diameter. Mean follow-up time was 25.7 months (range 12–42 months) [10]. The average volume of the ablation zone decreased in size from 41 ± 40 mm^3 (range 4–176 mm^3) to 1.8 ± 6.7 mm^3 (range 0–49 mm^3) [10]. Two of the 64 patients had incomplete ablations, confirmed by residual vascularity on post-PLA CEUS and underwent a second PLA procedure. Among the 64 patients, 79.7% (51/64 patients) ablation zones completely disappeared, and in 20.3% (13/64 patients), ablation zones remained as scar-like lesions. There was no evidence of local recurrence on follow-up FNAB, and no regrowth of treated lesions was detected on US during the follow-up period [10].

Zhou et al. reported 1- and 3-year recurrence-free survival rates of 100% and 97.2% after PLA in 36 patients when compared to surgery. Mean follow-up in his study was 49 months, with a recurrence rate of 5.6% (two of 36 treated patients) [11].

MWA/RFA

There are few reports of MWA and RFA for PTMC. Yue et al. reported a series of 21 patients with FNAB-proven PTMC with a mean diameter of 7.3 mm (range 3.7–10 mm). Of the 21 patients, 3 patients underwent thyroidectomy shortly after MWA, and complete necrosis of the tumor was confirmed on final histopathology. Mean volume reduction during follow-up was 90%. Four tumors completely disappeared, and five tumors remained as small scar-like lesions on conventional ultrasound. Ultrasound-guided biopsy was performed 6 months after MWA in five of these patients demonstrating necrosis with inflammatory cells and no viable tumor [7]. During a mean follow-up of 11 months (range 3–22), 1 patient died of acute bleeding from peptic ulcer disease 10 months following the procedure. The remaining patients had no signs of recurrence or distant metastasis on cross-sectional imaging [7].

Zhang et al. reported the experience utilizing RFA on 92 patients with a confirmed histopathologic diagnosis of PTMC. Mean tumor volume was 118.8 mm3 (range 3.4–467.5), and mean follow-up time was 7.8 months (range 3–18 months). Significant decrease in volume of the nodules over the course of follow-up was noted, and no recurrent PTMC or suspicious metastatic lymph nodes were seen [8].

Table 14.3 Clinical outcomes

Author	Papini et al. (2011)	Zhou et al. (2017)	Zhang et al. (2018)	Zhou et al. (2019)[a]	Yue et al. (2014)	Zhang et al. (2016)
Number of patients	1	30	64	36	21	92
Follow-up period	24 m	12–24 m	12–42 m	Mean 49 m	3–22 m	3–18 m
Ablation volume	<10 mm	<10 mm	3–8 mm	<10 mm	3.7–10 mm	3.4–467.5 mm^3
Lesion disappeared on follow-up	1/1 (100%)	10/30 (33.3%)	51/64 (79.7%)	–	4/21 (19%)	–
Scar-like lesion on follow-up	–	20/30 (66.7%)	13/64 (20.3%)	–	5/21 (23.8%)	–
Recurrence	No recurrence	No recurrence	No recurrence	2/36 (5.6%)	No recurrence	No recurrence
Ablation technique	PLA	PLA	PLA	PLA	MWA	RFA

[a]1- and 3-year recurrence-free survival rates were 100% and 97.2%

Recurrent tumors have not been reported during the follow-up periods after MWA or RFA when compared to PLA. This may be due in part to the shorter follow-up period (11 months for MWA and 7.8 months for RFA) compared to PLA (25.7 months). Outcomes are summarized in Table 14.3.

Intra-arterial/Locoregional Therapies in Advanced Disease

While external beam irradiation is the primary treatment modality most often used to treat locoregional disease that is not amenable to surgical resection, tumor embolization has been demonstrated to provide pain relief and local control in the setting of radioactive iodine refractory bone metastases. Furthermore, tumor embolization is routinely used prior to surgical resection of bone metastases as these tumors are very vascular and can cause dramatic blood loss if resected without prior embolization.

Thermal Ablation for Locoregional or Distant Metastases

Thermal ablation has also been used to control thyroid cancer recurrence and locally metastatic lymph nodes in patients with a history of papillary thyroid carcinoma (PTC) post thyroidectomy. Most patients with PTC can be cured during initial treatment, but 20–30% of these patients will present with locoregional recurrence during follow-up [17].

Papini et al. reported treatment with PLA in five patients with eight biopsy-proven metastatic lymph nodes post thyroidectomy. Lymph nodes were subsequently removed 2 weeks after ablation. Mean baseline volume was 0.64 ml (range 0.12–1.9 ml), which decreased to 0.22 ml at 6 months and 0.07 ml at 12-month follow-up. Mean volume reduction was 64.4% at 6 months and 87.7% at 12 months. Four of eight lymph nodes were small hyperechoic areas on 12 months follow- up US. No regrowth of successfully treated lesions was detected. Two of the five patients were found to have another metastatic lymph node on 12-month US examination [18]. Mauri et al. reported the experience of PLA in 15 patients with a total of 24 metachronous nodal metastases. All patients were followed at 6 and 12 months. Local control was achieved in 73% (11/15) and 71% (10/14) of patients at 6 and 12 months follow-up, respectively. On imaging, 83% (20/24) and 80% (16/20) of lymph nodes were found negative at both ^{18}FDG-PET/CT and CEUS at 6 and 12-month follow-up, respectively [19].

Zhou et al. reported results on 21 patients with locoregional recurrence of PTC both at the thyroid bed and in the lateral compartment. A total of 27 lesions measuring <15 mm were included. The average volume reduction rate at final follow-up was 98.9%, with 85.2% (23/27) of lesions having disappeared completely, and 14.8% (4/27) of lesions remaining as scar-like lesions. No regrowth or new suspicious lesions were detected in these patients [9].

Guo et al. recently reported his experience performing PLA on 8 patients with 18 metastatic lymph nodes. Follow-up imaging, lab tests, and clinical evaluations were performed. All patients were found to have complete ablations, defined as the absence of blood flow signals and lack of enhancement on CEUS. The abnormal thyroglobulin levels in these patients went down to normal after treatment. They were found to have a volume reduction rate of 90%. Six of the 18 ablation zones (33.3%) completely disappeared at follow up, and the remaining zones were scar-like areas on imaging. No regrowth of the ablated nodules and no distant metastases were detected [20].

Future Trends

Upregulation of the immune system is a known response to tumor cell death. The dead tumor cells stimulate the immune system leading to the concept that in situ tumor destruction can be used to achieve systemic in vivo vaccination against tumors. It has been shown that tumors can serve as their own antigenic vaccine after ablative therapy, as long as additional signals are provided by immunotherapy [21]. It remains unclear which ablative technique results in the most effective release of tumor antigens, which one upregulates the immune system the most, and which one combines best with immunotherapy for most effective treatment. To date, limited evidence suggests that cryoablation (Fig. 14.4) may have a better post procedure immune response on tumor cells when compared to other modalities. Each ablation technique will generate a unique antigenic fingerprint demonstrated by the difference in desmoplastic response between ablative modalities. The final tumor-directed

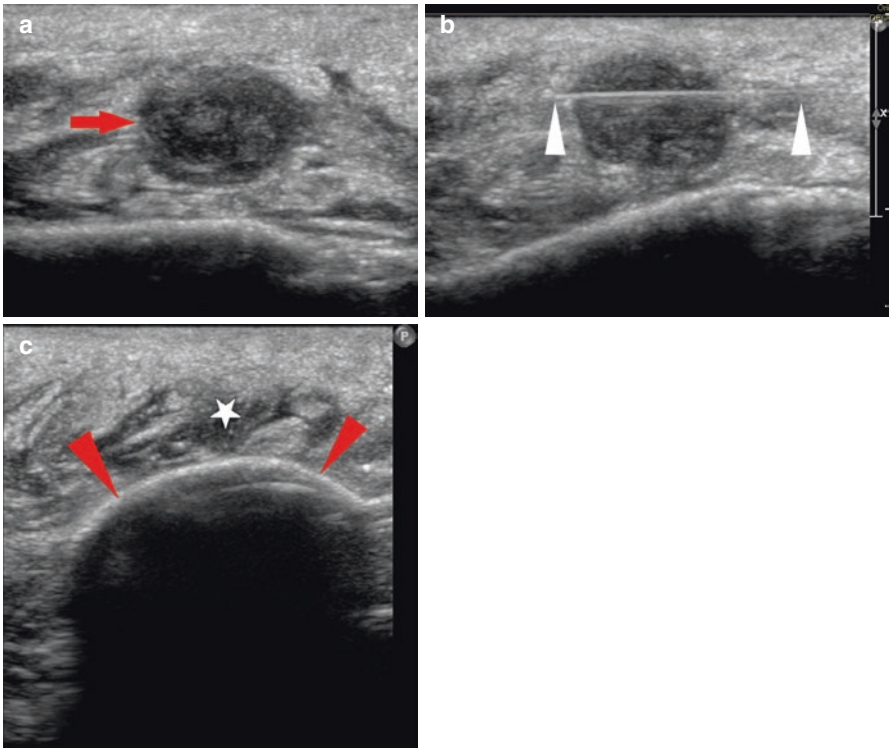

Fig. 14.4 Biopsy proven benign thyroid nodule. Intraprocedural ultrasound (**a**) shows the 1.5 cm nodule (red arrow). The cryoprobe (white arrowheads) is placed along the longitudinal axis of the mass (**b**) with its tip just beyond the target lesion. US exam during cryoablation (**c**) shows the ice ball (red arrows) casting an acoustic shadow beyond it. Saline was injected between the ice ball and skin (white star) to protect the skin from freeze injury. (Courtesy of Dr. Kelvin Hong, Johns Hopkins University)

T-cell repertoire is determined by the unique fingerprint interacting with the existing pre-ablation T-cell pool. Clonal analysis of the final T-cell repertoire following cryoablation has shown that 18% of T cells undergo clonal expansion; this demonstrates remodeling and diversification of the intratumoral T-cell reactivity [21].

Further study is necessary to identify and better understand the unique antigenic fingerprint expressed during thermal ablation to optimize thyroid cancer therapy. Immunotherapy in combination with thermal ablation can provide the next frontier in therapeutic options for these patients.

References

1. Haugen BR, Alexander EK, Bible KC, Doherty GM, Mandel SJ, Nikiforov YE, et al. 2015 American Thyroid Association management guidelines for adult patients with thyroid nodules and differentiated thyroid cancer: the American Thyroid Association guidelines task force on thyroid nodules and differentiated thyroid cancer. Thyroid. 2016;26(1):1–133.

2. Gharib H, Papini E, Garber JR, Duick DS, Harrell RM, Hegedus L, et al. American Association of Clinical Endocrinologists, American College of Endocrinology, and Associazione Medici Endocrinologi medical guidelines for clinical practice for the diagnosis and management of thyroid nodules--2016 update. Endocr Pract. 2016;22(5):622–39.
3. Wang TS, Sosa JA. Thyroid surgery for differentiated thyroid cancer - recent advances and future directions. Nat Rev Endocrinol. 2018;14(11):670–83.
4. Barile A, Quarchioni S, Bruno F, Ierardi AM, Arrigoni F, Giordano AV, et al. Interventional radiology of the thyroid gland: critical review and state of the art. Gland Surg. 2018;7(2):132–46.
5. Mauri G, Gennaro N, Lee MK, Baek JH. Laser and radiofrequency ablations for benign and malignant thyroid tumors. Int J Hyperth. 2019;36(2):13–20.
6. Nixon IJ, Angelos P, Shaha AR, Rinaldo A, Williams MD, Ferlito A. Image-guided chemical and thermal ablations for thyroid disease: review of efficacy and complications. Head Neck. 2018;40(9):2103–15.
7. Yue W, Wang S, Yu S, Wang B. Ultrasound-guided percutaneous microwave ablation of solitary T1N0M0 papillary thyroid microcarcinoma: initial experience. Int J Hyperth. 2014;30(2):150–7.
8. Zhang M, Luo Y, Zhang Y, Tang J. Efficacy and safety of ultrasound-guided radiofrequency ablation for treating low-risk papillary thyroid microcarcinoma: a prospective study. Thyroid. 2016;26(11):1581–7.
9. Zhou W, Zhang L, Zhan W, Jiang S, Zhu Y, Xu S. Percutaneous laser ablation for treatment of locally recurrent papillary thyroid carcinoma <15 mm. Clin Radiol. 2016;71(12):1233–9.
10. Zhang L, Zhou W, Zhan W, Peng Y, Jiang S, Xu S. Percutaneous laser ablation of unifocal papillary thyroid microcarcinoma: utility of conventional ultrasound and contrast-enhanced ultrasound in assessing local therapeutic response. World J Surg. 2018;42(8):2476–84.
11. Zhou W, Ni X, Xu S, Zhang L, Chen Y, Zhan W. Ultrasound-guided laser ablation versus surgery for solitary papillary thyroid microcarcinoma: a retrospective study. Int J Hyperth. 2019;36(1):897–904.
12. Baek JH, Lee JH, Valcavi R, Pacella CM, Rhim H, Na DG. Thermal ablation for benign thyroid nodules: radiofrequency and laser. Korean J Radiol. 2011;12(5):525–40.
13. Jeong WK, Baek JH, Rhim H, Kim YS, Kwak MS, Jeong HJ, et al. Radiofrequency ablation of benign thyroid nodules: safety and imaging follow-up in 236 patients. Eur Radiol. 2008;18(6):1244–50.
14. Papini E, Guglielmi R, Gharib H, Misischi I, Graziano F, Chianelli M, et al. Ultrasound-guided laser ablation of incidental papillary thyroid microcarcinoma: a potential therapeutic approach in patients at surgical risk. Thyroid. 2011;21(8):917–20.
15. Valcavi R, Piana S, Bortolan GS, Lai R, Barbieri V, Negro R. Ultrasound-guided percutaneous laser ablation of papillary thyroid microcarcinoma: a feasibility study on three cases with pathological and immunohistochemical evaluation. Thyroid. 2013;23(12):1578–82.
16. Zhou W, Jiang S, Zhan W, Zhou J, Xu S, Zhang L. Ultrasound-guided percutaneous laser ablation of unifocal T1N0M0 papillary thyroid microcarcinoma: preliminary results. Eur Radiol. 2017;27(7):2934–40.
17. DeGroot LJ, Kaplan EL, McCormick M, Straus FH. Natural history, treatment, and course of papillary thyroid carcinoma. J Clin Endocrinol Metab. 1990;71(2):414–24.
18. Papini E, Bizzarri G, Bianchini A, Valle D, Misischi I, Guglielmi R, et al. Percutaneous ultrasound-guided laser ablation is effective for treating selected nodal metastases in papillary thyroid cancer. J Clin Endocrinol Metab. 2013;98(1):E92–7.
19. Mauri G, Cova L, Tondolo T, Ierace T, Baroli A, Di Mauro E, et al. Percutaneous laser ablation of metastatic lymph nodes in the neck from papillary thyroid carcinoma: preliminary results. J Clin Endocrinol Metab. 2013;98(7):E1203–7.
20. Guo Y, Li Z, Wang S, Liao X, Li C. Single-fiber laser ablation in treating selected metastatic lymph nodes of papillary thyroid carcinoma and benign cold thyroid nodules-preliminary results. Lasers Surg Med. 2019.
21. Erinjeri JP, Fine GC, Adema GJ, Ahmed M, Chapiro J, den Brok M, et al. Immunotherapy and the interventional oncologist: challenges and opportunities-a Society of Interventional Oncology White Paper. Radiology. 2019;292(1):25–34.

Chapter 15
Soft Tissue Sarcoma (STS)

Scott M. Thompson, Brittany L. Siontis, and Matthew R. Callstrom

Abbreviations

CT	Computed tomography
DFSP	Dermatofibrosarcoma protuberans
EAD	Extra-abdominal desmoid
GIST	Gastrointestinal stromal tumor
HIFU	High-intensity focused ultrasound
IRE	Irreversible electroporation
LPS	Liposarcoma
MRI	Magnetic resonance imaging
MWA	Microwave ablation
RFA	Radiofrequency ablation
STS	Soft tissue sarcoma
TACE	Transarterial chemobolization
TAE	Transarterial bland embolization
TARE	Transarterial radioembolization
US	Ultrasound
WHO	World Health Organization

S. M. Thompson (✉) · M. R. Callstrom
Department of Radiology, Mayo Clinic, Rochester, MN, USA
e-mail: Thompson.scott@mayo.edu; Callstrom.Matthew@mayo.edu

B. L. Siontis
Division of Medical Oncology, Mayo Clinic, Rochester, MN, USA
e-mail: Siontis.Brittany@mayo.edu

C. Georgiades, H. S. Kim (eds.), *Image-Guided Interventions in Oncology*,
https://doi.org/10.1007/978-3-030-48767-6_15

Epidemiology and Pathophysiology

Soft tissue sarcomas (STS) are a heterogenous group of malignancies of mesenchymal origin. More than 50 STS histologic subtypes have been identified, and they are categorized according to the 2013 World Health Organization (WHO) classification of soft tissue tumors [1]. STS are rare, comprising less than 1% of new cancer diagnoses annually. The American Cancer Society estimates 1.7 million new cancer diagnoses in 2019, with 12,000 new STS diagnoses [2]. STS occur most commonly in the extremities (28% lower, 12% upper) with liposarcoma (LPS) being the most common histology [3, 4]. Visceral STS account for 22% of STS with gastrointestinal stromal tumor (GIST) representing the most common histologic subtype. Other STS locations include the retroperitoneum (16%), trunk (10%), and head and neck (12%).

Most STS are sporadic and idiopathic; however genetic syndromes such as Li-Fraumeni, retinoblastoma, neurofibromatosis type 1, and familial adenomatous polyposis are associated with increased risk for sarcoma [3, 4]. Additionally, various genetic alterations thought to play a role in the pathophysiology of STS have been identified. Moreover, environmental exposures may contribute to sarcoma development [3, 4]. For example, ionizing radiation as treatment for malignancy may result in development of a radiation-associated sarcoma several years later.

Role of Surgery, Radiation, and Systemic Therapy

Wide surgical resection is the standard of care for treatment of STS. The use of chemotherapy and radiation therapy varies with tumor size, location, histology, and patient characteristics. Despite multimodality therapy, recurrence rates are high. In the setting of oligometastatic disease, particularly with isolated pulmonary metastasis, metastectomy has been shown to improve survival.

Image-Guided Percutaneous Thermal Ablation

Indications

Image-guided thermal ablation offers a therapeutic option for primary and metastatic STS as an adjunct or alternative to other focal therapies, such as surgery or radiation therapy, when those treatments either have failed or have been deemed less appropriate [5, 6].

Technique

Image-guided thermal ablation involves placement of energy device probes percutaneously into the target tumor and subsequently delivering electromagnetic energy (radiofrequency, microwave, ultrasound) or gas (cryoablation) to induce extreme high or low temperatures within the tissue to achieve irreversible cell injury and tumor cell death. Radiofrequency ablation (RFA) and microwave ablation (MWA) both produce heat deposition around the radiofrequency probe or microwave antenna via frictional heating and thermal conduction within the tissue, with the goal of achieving minimum tissue temperature of 50 °C to achieve cell death. Cryoablation most commonly exploits the Joule-Thomson effect of expanding gases to generate extreme low temperatures when pressurized argon gas is allowed to expand within the cryoprobe, with goal temperatures below −20 to −40 °C (Fig. 15.1). High-intensity focused ultrasound (HIFU) delivers focused acoustic energy to noninvasively heat target tissue to temperatures greater than 70 °C. Irreversible electroporation (IRE) is emerging as a predominantly nonthermal-based ablative technology that uses high-voltage, low-energy direct current pulses to induce nanopore formation in cell membranes ultimately resulting in irreversible cell injury and cell death.

All ablative therapies rely on imaging guidance for initial targeting of the tumor, as well as real-time monitoring when possible during the ablation and imaging assessment immediately following ablation. Real-time monitoring allows for avoidance of complications or rapid detection when they do occur. Ultrasound (US), computed tomography (CT), and magnetic resonance imaging (MRI) may be employed for image guidance and monitoring. Cryoablation has a distinct advantage of allowing for real-time imaging of the ice ball whereby the 0 °C margin

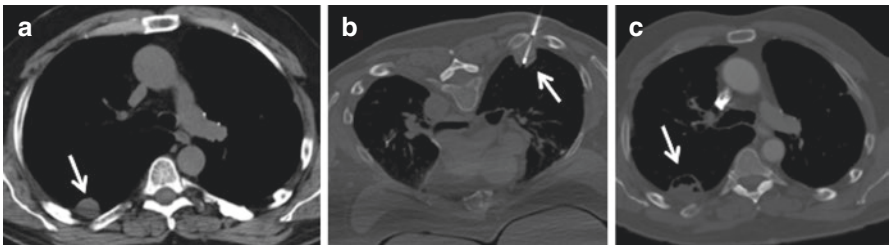

Fig. 15.1 Percutaneous CT-guided cryoablation of pleural-based synovial sarcoma metastasis. A 66-year-old male with history of right foot synovial sarcoma and pulmonary metastasis status post systemic chemotherapy and bilateral pulmonary metastectomy with development of a right pleural-based metastasis. (**a**) Pre-ablation axial non-contrast CT shows the posterior right pleural-based soft tissue metastasis (white arrow). (**b**) CT-guided cryoablation performed with four cryoprobes (white arrow). (**c**) Follow-up CT shows interval decreased size of the pleural-based mass (white arrow)

corresponds to the edge of the hypodensity on CT or hypointensity on MRI. Tumor ablation may be performed under moderate sedation or general anesthesia.

Selection

Potential STS ablation candidates should be reviewed by a multidisciplinary team including oncologists, surgeons, radiation oncologists, and interventional radiologists to determine feasibility of percutaneous image-guided ablation therapy. Many STS may be too large or involve adjacent critical structures to achieve local tumor control without collateral injury using percutaneous ablative therapies. As such, the decision to undertake percutaneous thermal ablation for sarcoma treatment requires a multidisciplinary discussion to set expectations for curative versus palliative intent ablation and consideration of repeat ablation sessions if possible. Once a patient is deemed a candidate for image-guided ablation, imaging studies are carefully reviewed for treatment planning as the primary concern is the local environment and risk of nontarget ablation. Similar to achieving a surgical margin for tumor resection, the interventional radiologist aims to ablate the target tumor plus a margin of normal tissue in order to maximize chance for local tumor control. If a target tumor is too close to critical structures that cannot be protected or moved by various adjunctive methods, then ablation may not be appropriate.

Outcomes: Soft Tissue Sarcoma

Data on thermal ablation of STS are limited, with available reports focused on efficacy of ablation for local control or palliation of recurrent disease no longer amenable to resection (Table 15.1). There is a paucity of long-term follow-up, limiting the ability to fully understand the role of ablation in long-term disease control [5].

The largest study to date utilizing ablation in STS was performed by the French Sarcoma Group [7]. They conducted a multicenter retrospective review of 281 patients with oligometastatic sarcoma defined as having up to five lesions that underwent local therapy. One hundred sixty-four patients underwent surgical resection, radiofrequency ablation, or stereotactic body radiation therapy (SBRT). Median overall survival was 45 months for patients who received local ablative therapy versus 13 months for patients who did not ($p < 0.0001$). Importantly, this overall survival benefit was maintained after repeat local ablative therapy for up to four new oligometastatic relapses.

Desmoid Tumors (Desmoid-Type Fibromatosis)

Desmoid tumors (desmoid-type fibromatosis) are rare, locally aggressive fibroblastic neoplasms without metastatic potential. High local recurrence rates following surgical resection have created a need for less invasive treatment options. Three

Table 15.1 Clinical outcomes for thermal ablation of select soft tissue sarcomas (STS) by tumor histology, ablation device, and/or location

Soft tissue sarcoma	Number of patients	Ablation device	Local control	Pain palliation	Survival
Desmoid tumors (EAD) [8–10]	54	Cryoablation	83–100%	NA	NR
Dermatofibrosarcoma protuberans (DFSP) [11]	19	Cryoablation	100%	NA	PFS 100% at 5+ years
Retroperitoneal sarcoma [12]	39	Cryoablation	72–86%	Decreased pain and morphine-equivalent dose scores at 5- to 25-day post-ablation	PFS (0.5, 1, 2 years) tumors < 10.0 cm 100%, 86%, 21% tumors > 10.0 cm 92%, 40%, 0%
Mixed histologies [13]	36	RFA	33%	NA	OS (1, 3, 5 years) 73%, 39%, 34%
Lung STS metastases					
Mixed histologies [15–19]	200+	RFA MWA Cryoablation	85–100% 98% 76%	NA	OS 1 year: 30–100% 2 years: 70–94% 3 years: 0–85% 5 years: 42%
Liver STS metastases					
Gastrointestinal stromal tumors (GIST) [20–21]	30	RFA	92–100%	NA	PFS (2 years) 75% in patients who continued tyrosine kinase inhibitor therapy post-ablation <30% in patients who discontinued tyrosine kinase inhibitor therapy post-ablation
Mixed histologies [21]	7	RFA	86%	NA	NR

EAD extra-abdominal desmoid tumors, *DFSP* dermatofibrosarcoma protuberans, *GIST* gastrointestinal stromal tumor, *MWA* microwave ablation, *NA* not applicable, *NR* not reported, *OS* overall survival, *PFS* progression-free survival, *RFA* radiofrequency ablation, *STS* soft tissue sarcoma

series have reported on safety and outcomes of percutaneous cryoablation for treatment of extra-abdominal desmoid tumors (EAD). Tremblay et al. performed CT-guided percutaneous cryoablation in 23 patients with EAD over 30 ablation sessions as first-line (61%) or salvage (39%) therapy with curative intent in 52% and palliative intent in 48% [8]. All 30 ablation sessions were technically successful, and there were two major complications, including transient deltoid muscle weakness and transient foot drop. At an average follow-up of 15 months, 90% of patients demonstrated symptomatic improvement with an average reduction in viable tumor volume of 80%. Residual or recurrent disease occurred in four patients (17%) and was successfully treated with repeat cryoablation. Schmitz et al. performed percutaneous cryoablation in 18 patients with 26 EAD who had failed surgery and/or radiation and/or chemotherapy [9]. All 31 ablation sessions were

technically successful with no major complications. At an average follow-up of 16 months, 23 tumors with complete imaging showed volume reduction in 96% of tumors, no residual tumor in 39% of tumors, and tumor progression in only one tumor (4.3%). Similarly, Havez et al. performed percutaneous cryoablation in 13 patients with 17 EAD during 17 ablation sessions. There was one major complication, a transient peroneal nerve injury (6%). At an average follow-up of 11 months, eight patients had residual tumor (47%), but the local tumor progression rate was 0% at 24 months [10]. Taken together, these data suggest that percutaneous cryoablation is a safe and effective treatment option for EAD tumors in patients with unresectable tumors in both the primary and salvage settings with achievement of complete response or stable disease in >90% of patients despite high rates of residual tumor post-ablation.

Dermatofibrosarcoma Protuberans (DFSP)

Dermatofibrosarcoma protuberans (DFSP) is a rare cutaneous STS often treated with wide-local excision. While metastatic disease is rare, there is a high risk of local recurrence.

Xu et al. evaluated percutaneous cryoablation in 19 patients with locally recurrent DFSP [11]. A total of 39 ablation sessions were required to treat all lesions with a median of 2 ablation sessions per patient (range 1–3). There were no major complications and a local control rate of 100%. Progression-free survival was 100% at greater than 5 years of follow-up in all patients. These data suggest that percutaneous cryoablation is safe and may be curative in patients with recurrent DFSP but may require multiple ablation treatments.

Retroperitoneal Sarcomas

Percutaneous cryoablation has been utilized for palliation including local tumor and pain control in retroperitoneal sarcomas. Fan et al. reported retrospective data on 39 patients who underwent percutaneous cryoablation for treatment of retroperitoneal STS including liposarcoma, fibrosarcoma, leiomyosarcoma, and malignant fibrous histiocytoma histologies [12]. Patient reported pain score was significantly decreased from pre-ablation to 25-day post-ablation (7.49 to 5.44; $p < 0.001$). Moreover, there were significant reductions in morphine-equivalent dose (MED) scores from day 5 to day 25 post-ablation (64.2 to 44.2; $p < 0.001$). There were no major complications. Overall objective tumor response rate was 77% and not significantly different for tumors <10 cm (86%) compared with >10 cm (72%; $p = 0.445$). Mean progression-free survival (PFS) was 13 months for all patients. However, 6-month, 1-year, and 2-year PFS was significantly better for patients with tumors <10 cm (100%, 86%, and 21%, respectively) compared to those with tumors

>10 cm (92%, 40%, and 0%; $p = 0.016$). Overall these data suggest that percutaneous cryoablation is safe and effective for pain palliation in patients with recurrent retroperitoneal STS and results in high objective tumor response rates. Nonetheless, palliative rather than curative intent ablation should be considered in patients with tumors >10 cm.

Radiofrequency (RFA) and Microwave (MWA) Ablation

While percutaneous cryoablation is the most common modality utilized in STS, both radiofrequency (RFA) and microwave (MWA) ablation have been reported. Yamakado et al. performed percutaneous RFA in 36 patients with recurrent STS who were not surgical candidates [13]. Major complication rate was less than 1.0%. Local recurrence occurred in 67% of patients with completely ablated tumors, and 1-, 3-, and 5-year overall survival rates were 73%, 39%, and 34%, respectively. Aubry et al. performed MWA in four patients with either primary STS recurrence ($n = 1$) or leiomyosarcoma soft tissue metastases ($n = 3$) [14]. Unfortunately, three of four sarcoma patients developed early residual local recurrence.

STS Percutaneous Ablation Summary

While limited, current data suggest that percutaneous ablation is safe and feasible for STS of various histologic subtypes and in diverse anatomic locations, particularly for symptom control. Local tumor control may be better with percutaneous cryoablation rather than RFA or MWA, but comparative data are lacking. In actuality, many STS may be too large to achieve local tumor control with percutaneous ablative therapies. Although local recurrence rates remain high even in the setting of complete tumor ablation on imaging, repeat palliative ablation may be a therapeutic option that offers lower morbidity than surgical resection. Furthermore, ablation often allows patients to receive systemic therapy sooner than more invasive procedures. Given the paucity of data currently reported, further complicated by a heterogeneous disease and patient population, definitive conclusions regarding long-term efficacy of ablation in STS are limited.

Outcomes: Pulmonary Metastases

Pulmonary metastasis may develop in up to 40% of patients with STS. In oligometastatic disease, pulmonary metastectomy is considered the standard of care with a potential for curative resection and improved overall survival.

Image-guided percutaneous RFA of lung tumors was first reported in 2000 by Dupuy et al. [15]. Subsequently, data have been reported on the safety, local tumor

control, and long-term outcomes of percutaneous thermal ablation or cryoablation of more than 400 pulmonary sarcoma metastases. These data represent more than 200 pediatric and adult patients with diverse sarcoma histologic subtypes. RFA has been the most common modality reported for ablation of pulmonary sarcoma metastases, followed by cryoablation and MWA. Of note, one series reported outcomes of RFA ablation followed by surgical resection in five patients with pulmonary sarcoma metastases and demonstrated complete tumor necrosis at pathologic analysis, thereby providing histologic evidence of complete tumor response [16]. Ablation-related death is very rare occurring only in two patients who underwent treatment for STS pulmonary metastases. Pneumothorax is the most common adverse event, occurring in 10–69% of patients requiring aspiration and/or chest tube placement in 3–59% of cases.

Data on outcomes for specific sarcoma histologies are limited. Yevich and Saumet et al. reported data on ablation of pulmonary osteosarcoma metastasis in 21 pediatric patients [17, 18]. At a median follow-up of 17–24 months, local recurrence was 0%, and 12 patients were in complete remission. Multiple series have reported outcomes for ablation of pulmonary metastases in various STS histologic subtypes with median follow-up ranging from 15 to 50 months and local recurrence rates of 0–15% for RFA, 2% for MWA, and 24% for cryoablation. 1-, 2-, 3-, and 5-year overall survival rates vary widely: 30–100% (1 year), 70–94% (2 years), 0–85% (3 years), and 42% (5 years). Interestingly, Nakamura et al. reported outcomes of RFA for pulmonary STS metastasis in 20 patients and found 1- and 3-year overall survival rates of 89% and 59%, respectively, in patients in whom complete ablation of all lung tumors was achieved [19]. This was significantly better than 1- (30%) and 3-year (0%) survival rates for patients with incomplete ablation of pulmonary metastases ($p = 0.014$).

While limited, existing data suggest that ablation of pulmonary STS metastases is feasible and safe and provides local tumor control. Moreover, complete ablation of all lung tumors has been identified as an important prognostic factor. Nonetheless, the specific effect of percutaneous ablation of pulmonary STS metastases on overall survival is difficult to assess due to the heterogeneity of the disease as well as variability in local and systemic therapies received before and after ablation. Given that aggressive surgical resection is the current standard of care for pulmonary metastases, further studies are needed to determine the comparative effectiveness of ablative modalities with surgical resection as well as the optimal timing of ablation.

Outcomes: Liver Metastases

Image-guided percutaneous thermal ablative therapies have been shown to be safe and effective treatment options of multiple primary and metastatic hepatic tumors. The majority of data on liver ablation is with the treatment of hepatocellular carcinoma (HCC) and colorectal (CRLM) liver metastases. Data on percutaneous thermal ablation for hepatic STS metastases is limited owing to the rarity of the disease and available studies representing various histologic subtypes.

Gastrointestinal Stromal Tumor (GIST)

Gastrointestinal stromal tumor (GIST) is the most common STS and frequently metastasizes to the liver. Imatinib mesylate, a selective tyrosine kinase inhibitor (TKI) targeting c-KIT, is the current standard first-line treatment for metastatic GIST. Hakime et al. reported outcomes of adjuvant RFA after TKI therapy in 17 patients with 27 GIST liver metastases [20]. There were no major complications. At an average follow-up of 49 months, there were no local recurrences. Importantly, 2-year PFS was 75% in patients who continued TKI therapy post-ablation but <30% in patients who discontinued TKI therapy post-ablation. The authors concluded that adjuvant RFA of GIST liver metastases is effective at achieving local tumor control and should be performed once the patient achieves best morphologic response on TKI therapy and that TKI therapy should be continued post-ablation to prevent disease progression remote from the ablation site or at extrahepatic sites. Similarly, Jones et al. reported local control of 92% in 13 patients who underwent RFA for 14 GIST hepatic metastases [21].

Though limited, these data suggest that RFA of hepatic metastases in GIST achieves >90% local control and should be performed once the patient achieves best morphologic response while on TKI therapy and that TKI therapy should be continued post-ablation to prevent systemic disease relapse or progression.

Other Hepatic STS Metastases

Studies on percutaneous ablation of STS hepatic metastasis of other histologic subtypes are rare. Jones et al. reported local control of 86% in seven patients who underwent RFA for leiomyosarcoma ($N = 4$), fibrosarcoma ($N = 1$), synovial sarcoma ($N = 1$), and solitary fibrous tumor ($N = 1$) hepatic metastases [21].

Transcatheter Arterial Embolization for Hepatic Sarcoma Metastasis

Currently available literature includes retrospective series on transarterial therapies including bland embolization (TAE) (Fig. 15.2), chemoembolization (TACE), and yttrium-90 radioembolization (^{90}Y-TARE) for treatment of hepatic STS metastases in approximately 100 patients [22–24] (Table 15.2). All studies were performed in relapsed disease and primarily with palliative intent. Chapiro et al. performed conventional TACE (cTACE) in 30 patients with hepatic STS metastases from leiomyosarcoma ($N = 25$), angiosarcoma ($N = 3$), and fibrosarcoma and chondrosarcoma ($N = 1$ each) [23]. Patients underwent 77 cTACE sessions (average 2.6 cTACE per patient), and there were no major complications. Median OS was 21 months and

Fig. 15.2 Transarterial embolization (TAE) of hepatic synovial sarcoma metastases. A 39-year-old female with history of left leg synovial sarcoma status postsurgery, chemotherapy, and radiation with development of extensive hepatic and pulmonary metastases and tumor-related hypoglycemia. (**a**) Pre-ablation coronal contrast-enhanced CT shows multiple enhancing hepatic metastases (white arrow). (**b**) Selective proper hepatic angiogram shows multiple hypervascular liver masses (white arrow), treated with three-stage bland embolization. (**c**) Follow-up coronal contrast-enhanced CT shows interval decreased size and enhancement of the hepatic masses

Table 15.2 Clinical outcomes for transcatheter arterial embolization for hepatic soft tissue sarcoma (STS) metastases

Embolization method	Number of patients	Embolization sessions	Objective response	Survival
cTACE [23]	30	77	NR	OS 21 months PFS 6 months
^{90}Y-TARE [24]	39	NR	36%	OS 30 months
TAE, cTACE and ^{90}Y-TARE [25]	18 elective 10 emergency (rupture)	25 TAE 24 cTACE 13 ^{90}Y-TARE	61% elective 20% emergency	Elective OS 27 months PFS 14 months

cTACE conventional transarterial chemoembolization, *NR* not reported, *OS* overall survival, *PFS* progression-free survival, *TAE* transarterial bland embolization, *^{90}Y-TARE* yttrium-90 transarterial radioembolization

PFS 6 months. The authors found enhancement-based tumor response by imaging predicted improved overall survival (hazard ratio 0.3, $p = 0.006$).

Miller et al. [22] performed ^{90}Y-TARE in 39 patients with hepatic STS metastases from 14 STS subtypes with leiomyosarcoma the most common (51%). There were three major complications including liver abscess, gastric ulceration, and pneumonitis (8%). Objective response rate was 36% with the majority of patients achieving disease control (77%). Median overall survival was 30 months. There was a significant increase in OS in patients with disease control (44 months) compared to those with progressive disease (7.5 months) at 3 months ($p < 0.0001$).

Finally, Pierce et al. performed TAE, TACE, or ^{90}Y-TARE in 28 patients with hepatic STS metastases, 18 of which were treated on an elective basis and 10 of which were performed on an emergent basis to control acute hemorrhage from GIST ($N = 3$) or angiosarcoma ($N = 7$) rupture [24]. Patients underwent 25 TAE sessions (average 2 per patient), 24 TACE sessions (average 3 per patient), and 13 ^{90}Y-TARE sessions (average 1 per patient) with only 1 major complication. The overall objective response rate was 61% in the elective treatment group and 20% in

the emergency-treated group. For electively treated patients, median OS was 27 months and PFS 14 months, with no significant difference by treatment modality ($p = 0.43$). Conversely, median OS was 19 days in patients with ruptured angiosarcoma ($N = 7$) and 611 days in patients with ruptured GIST ($N = 3$). Taken together, existing data suggest that liver-directed embolization may provide a safe and effective palliative or salvage therapy option in patients with hepatic STS metastases treated in the elective setting. There is currently no evidence to suggest superiority of one embolization modality over another in the treatment of hepatic STS metastases.

Multimodality Treatment and Future Trends

Given the complexity and rarity of STS, multidisciplinary management for the treatment of STS is critical. A multimodality combined treatment approach is often necessary in these patients with various combinations of systemic therapy combined with percutaneous ablation, radiation, and/or surgery to various lesions in the metastatic setting depending on location and tumor type throughout the disease course. The sequencing and timing of various multimodal therapies require an individualized approach and multidisciplinary decision-making.

Currently, there are no data to support the routine clinical use of immunooncologic therapies in the treatment of STS [25, 26]. There are several ongoing early stage clinical trials evaluating combination immunotherapy and radiation therapy in localized extremity STS. Emerging preclinical evidence suggests potential complex mechanistic and synergistic effects of combining immunooncologic therapies with percutaneous thermal ablation in various solid tumors [27, 28]. Nonetheless, a better understanding of the complex and heterogeneous immune tumor microenvironment of STS will be needed in order to develop rational combinations such as immunotherapy with percutaneous ablative techniques.

Key Points

- Given the complexity and rarity of soft tissue sarcomas (STS), multidisciplinary management for the treatment of STS is critical.
- The sequencing and timing of various multimodal therapies for STS including systemic or locoregional therapies, surgery, and/or radiation require an individualized approach and multidisciplinary decision-making.
- Percutaneous image-guided thermal ablative therapies are a minimally invasive, safe, and repeatable treatment option for STS involving the soft tissue, liver, and lung and provide an adjunct or alternative to other local therapies where local tumor control or palliation is desired.
- Liver-directed transarterial embolization including bland embolization (TAE), chemoembolization (TACE), or radioembolization (TARE) may provide a safe and effective palliative or salvage therapy option in patients with hepatic STS metastases treated in the elective setting.

References

1. Fletcher CD. The evolving classification of soft tissue tumours - an update based on the new 2013 WHO classification. Histopathology. 2014;64(1):2–11.
2. Siegel RL, Miller KD, Jemal A. Cancer statistics, 2019. CA Cancer J Clin. 2019;69(1):7–34.
3. Burningham Z, Hashibe M, Spector L, Schiffman JD. The epidemiology of sarcoma. Clin Sarcoma Res. 2012;2(1):14.
4. Hui JY. Epidemiology and etiology of sarcomas. Surg Clin North Am. 2016;96(5):901–14.
5. Thompson SM, Schmitz JJ, Schmit GD, Callstrom MR, Kurup AN. Image-guided thermal ablative therapies in the treatment of sarcoma. Curr Treat Options in Oncol. 2017;18(4):25.
6. de Baere T, Tselikas L, Gravel G, Hakime A, Deschamps F, Honoré C, et al. Interventional radiology: role in the treatment of sarcomas. Eur J Cancer. 2018;94:148–55.
7. Falk AT, Moureau-Zabotto L, Ouali M, Penel N, Italiano A, Bay JO, et al. Effect on survival of local ablative treatment of metastases from sarcomas: a study of the French sarcoma group. Clin Oncol (R Coll Radiol). 2015;27(1):48–55.
8. Redifer Tremblay K, Lea WB, Neilson JC, King DM, Tutton SM. Percutaneous cryoablation for the treatment of extra-abdominal desmoid tumors. J Surg Oncol. 2019;120(3):366–75.
9. Schmitz JJ, Schmit GD, Atwell TD, Callstrom MR, Kurup AN, Weisbrod AJ, et al. Percutaneous cryoablation of extraabdominal desmoid tumors: a 10-year experience. AJR Am J Roentgenol. 2016;207(1):190–5.
10. Havez M, Lippa N, Al-Ammari S, Kind M, Stoeckle E, Italiano A, et al. Percutaneous image-guided cryoablation in inoperable extra-abdominal desmoid tumors: a study of tolerability and efficacy. Cardiovasc Intervent Radiol. 2014;37(6):1500–6.
11. Xu J, Li J, Zhou X, Zeng J, Yao F, Wang Y, et al. Cryotherapy for local recurrent dermatofibrosarcoma protuberans: experience in 19 patients. Cryobiology. 2014;68(1):134–8.
12. Fan W-Z, Niu L-Z, Wang Y, Yao X-H, Zhang Y-Q, Tan G-S, et al. Initial experience: alleviation of pain with percutaneous CT-guided cryoablation for recurrent retroperitoneal soft-tissue sarcoma. J Vasc Interv Radiol. 2016;27(12):1798–805.
13. Yamakado K, Matsumine A, Nakamura T, Nakatsuka A, Takaki H, Matsubara T, et al. Radiofrequency ablation for the treatment of recurrent bone and soft-tissue sarcomas in non-surgical candidates. Int J Clin Oncol. 2014;19(5):955–62.
14. Aubry S, Dubut J, Nueffer J-P, Chaigneau L, Vidal C, Kastler B. Prospective 1-year follow-up pilot study of CT-guided microwave ablation in the treatment of bone and soft-tissue malignant tumours. Eur Radiol. 2017;27(4):1477–85.
15. Dupuy DE, Zagoria RJ, Akerley W, Mayo-Smith WW, Kavanagh PV, Safran H. Percutaneous radiofrequency ablation of malignancies in the lung. AJR Am J Roentgenol. 2000;174(1):57–9.
16. Jaskolka JD, Kachura JR, Hwang DM, Tsao MS, Waddell TK, Asch MR, et al. Pathologic assessment of radiofrequency ablation of pulmonary metastases. J Vasc Interv Radiol. 2010;21(11):1689–96.
17. Yevich S, Gaspar N, Tselikas L, Brugieres L, Pacquement H, Schleiermacher G, et al. Percutaneous computed tomography-guided thermal ablation of pulmonary osteosarcoma metastases in children. Ann Surg Oncol. 2016;23(4):1380–6.
18. Saumet L, Deschamps F, Marec-Berard P, Gaspar N, Corradini N, Petit P, et al. Radiofrequency ablation of metastases from osteosarcoma in patients under 25 years: the SCFE experience. Pediatr Hematol Oncol. 2015;32(1):41–9.
19. Nakamura T, Matsumine A, Yamakado K, Matsubara T, Takaki H, Nakatsuka A, et al. Lung radiofrequency ablation in patients with pulmonary metastases from musculoskeletal sarcomas [corrected]. Cancer. 2009;115(16):3774–81.
20. Hakime A, Le Cesne A, Deschamps F, Farouil G, Boudabous S, Auperin A, et al. A role for adjuvant RFA in managing hepatic metastases from gastrointestinal stromal tumors (GIST) after treatment with targeted systemic therapy using kinase inhibitors. Cardiovasc Intervent Radiol. 2014;37(1):132–9.

21. Jones RL, McCall J, Adam A, O'Donnell D, Ashley S, Al-Muderis O, et al. Radiofrequency ablation is a feasible therapeutic option in the multi modality management of sarcoma. Eur J Surg Oncol. 2010;36(5):477–82.
22. Miller MD, Sze DY, Padia SA, Lewandowski RJ, Salem R, Mpofu P, et al. Response and overall survival for Yttrium-90 Radioembolization of hepatic sarcoma: a multicenter retrospective study. J Vasc Interv Radiol. 2018;29(6):867–73.
23. Chapiro J, Duran R, Lin M, Mungo B, Schlachter T, Schernthaner R, et al. Transarterial chemoembolization in soft-tissue sarcoma metastases to the liver - the use of imaging biomarkers as predictors of patient survival. Eur J Radiol. 2015;84(3):424–30.
24. Pierce DB, Johnson GE, Monroe E, Loggers ET, Jones RL, Pollack SM, et al. Safety and efficacy outcomes of embolization in hepatic sarcomas. AJR Am J Roentgenol. 2018;210(1):175–82.
25. Lee A, Huang P, DeMatteo RP, Pollack SM. Immunotherapy for soft tissue sarcoma: tomorrow is only a day away. Am Soc Clin Oncol Educ Book. 2016;35:281–90.
26. Nathenson MJ, Conley AP, Sausville E. Immunotherapy: a new (and old) approach to treatment of soft tissue and bone sarcomas. Oncologist. 2018;23(1):71–83.
27. Slovak R, Ludwig JM, Gettinger SN, Herbst RS, Kim HS. Immuno-thermal ablations - boosting the anticancer immune response. J Immunother Cancer. 2017;5(1):78.
28. Minami Y, Nishida N, Kudo M. Radiofrequency ablation of liver metastasis: potential impact on immune checkpoint inhibitor therapy. Eur Radiol. 2019;29(9):5045–51.

Chapter 16
The Role of Interventional Oncology in the Treatment of Metastatic Melanoma

Amgad M. Moussa, DaeHee Kim, and Joseph P. Erinjeri

Introduction

All melanomas develop from a single cell of origin, the melanocyte. Most melanocytes reside in the basal layer of the epidermis of the skin, but they are also seen in the uveal tract of the eye, the oral and sinonasal mucosa, and the vulva. Melanomas have thus been broadly divided into cutaneous and non-cutaneous melanomas, with non-cutaneous melanomas subdivided into ocular and mucosal melanomas according to the site of origin. However, this classification is considered oversimplified as some melanomas that arise from the eye behave more like cutaneous melanomas than non-cutaneous melanomas, such as conjunctival and adnexal melanomas [1].

Although ocular melanoma accounts for approximately 3–5% of all melanoma cases reported in the United States, it is the most common primary intraocular malignancy in adults [2]. Around 80% of ocular melanomas arise from the uveal tract and are often referred to as uveal melanomas in order to differentiate them from conjunctival and adnexal melanomas which behave differently and are thus managed differently [1].

Unlike the incidence of cutaneous melanoma which has increased greatly over the past 40 years, the incidence of uveal melanoma has been stable [2, 3]. At a reported age-adjusted incidence of 5.1 per million, around 1500 cases of uveal melanoma are diagnosed in the United States each year [1, 2]. Male patients showed a significantly higher age-adjusted incidence of 5.8 per million compared to 4.4 per million for female patients. Between 92% and 98% of cases of uveal melanoma are reported in Caucasians, and when combined with a median reported age of 60–62 years at diagnosis, the typical uveal melanoma patient is often an elderly, Caucasian male.

A. M. Moussa · D. Kim · J. P. Erinjeri (✉)
Interventional Radiology Service, Memorial Sloan Kettering Cancer Center, New York, NY, USA
e-mail: moussaa@mskcc.org; kimd1@mskcc.org; erinjerj@mskcc.org

C. Georgiades, H. S. Kim (eds.), *Image-Guided Interventions in Oncology*,
https://doi.org/10.1007/978-3-030-48767-6_16

The reported 5-year relative survival rate for uveal melanoma patients is 81.6–83.5% [2]. Survival is greatly affected by the presence or absence of metastatic disease, specifically to the liver. The reported 4-year relative survival rate for metastatic uveal melanoma patients is 22%. Patients rarely present initially with metastatic disease, but metastases develop in 25% of patients over the next 5 years and most commonly affect the liver [1]. Isolated liver metastases are seen in up to 60% of patients with metastatic disease, and liver metastases are seen in up to 91% of patients at time of death.

Studies in the 1980s and 1990s identified the impact of liver involvement on survival of uveal melanoma patients, reporting that median overall survival of patients who develop metastases to the liver first was 5–7 months compared to a median overall survival of 18 months in patients who first develop metastases elsewhere. More recent studies have identified that involvement of non-liver organs as a site of first metastases and history of surgery or intrahepatic chemotherapy correlated with prolonged overall survival, confirming the impact of liver involvement on survival [1].

The propensity of uveal melanoma to metastasize to the liver and the effect of liver involvement on survival have identified treatment of liver metastases as an integral part in prolonging survival of uveal melanoma patients. Improved survival has been reported in patients with liver metastases who undergo surgical resection, with reported survival rates 3.7-fold higher than patients who do not undergo surgical resection. A smaller number of metastatic lesions and a more comprehensive surgical resection (with microscopically clean histological margins) were both associated with improved survival. However, less than 10% of patients are candidates for surgical resection mostly because metastases are seen involving both lobes of the liver prior to surgery or, sometimes, in the operating room [4]. Therefore, other minimally invasive treatment modalities have been developed to control progression of disease in the liver in patients who are not surgical candidates.

Drawing on the experience gained from treating other tumors in the liver (e.g., hepatocellular carcinoma, colorectal cancer liver metastases), percutaneous image-guided thermal ablation has been studied in patients with a small number of hepatic metastases and high surgical morbidity, and trans-arterial treatments have been studied in patients with multiple, bilobar hepatic metastases. Several, small retrospective studies looking at the role of different image-guided thermal ablation modalities in these patients have shown that it may be useful in selected groups of patients, specifically patients who are considered high risk for surgery. In patients with multiple, bilobar hepatic metastases, the use of a growing armamentarium of trans-arterial treatments has provided significant benefit in selected groups of patients, yet the lack of studies comparing these intra-arterial treatments has left much to be studied.

In patients with widely metastatic melanoma, the developments in the field of immunotherapy over the last decade have provided notable benefit. Several randomized, controlled trials comparing different immunotherapeutic agents in varying combinations have shown improved progression-free survival and overall survival in this patient population [5]. All these advancements in the management of melanoma patients have helped shift this disease from an inevitably deadly pathway to a potentially manageable one.

Pathology

The pathological evolution of cutaneous melanoma is believed to begin as a patch of atypical melanocytes that spreads radially across the skin, also known as the "radial growth phase" followed after a variable period of time by a "vertical growth phase" in which growth is mainly up above the skin or invading deeper into the skin. However, vertical growth can occur without an evident radial growth phase in a pattern of melanoma called "nodular melanoma." The vertical growth phase, characterized by increased thickness and invasion, is the phase associated with the increased risk of metastasis and death. At a molecular level, cutaneous melanoma is believed to develop through mutations in BRAF, NRAS, and KIT genes which influence the mitogen-activated protein kinase (MAPK) signaling pathway.

The pathological evolution of uveal melanoma shares some characteristics with that of cutaneous melanoma but shows several significant differences. Most uveal melanomas arise from melanocytes residing in the choroid and exhibit similar growth patterns to those seen in cutaneous melanoma, vertical growth preceded by a varying period of radial growth. On a molecular level, uveal melanoma is also believed to occur through activation of the MAPK signaling pathway, but mutations in BRAF, NRAS, or KIT are rarely seen. The mechanism instead was recently discovered to be through mutations in GNAQ/GNA11, which was emphasized by studies showing the presence of this mutation in 83% of uveal melanoma patients and 96% of metastatic uveal melanoma patients. Another mutation that has been implicated in the progression of uveal melanoma is inactivation of the BRCA-1 associated protein (BAP1) which is seen in 84% of metastatic tumors. These molecular mutations translate to changes on a chromosomal level, which have been associated with prognosis, as is the case in monosomy of chromosome 3 which is associated with metastasis and mortality [6].

The correlation between molecular characteristics, genetic characteristics, and their clinical implications emphasizes the importance of pathological evaluation of uveal melanoma tissue, either from the primary tumor or suspected metastases through biopsy rather than relying on imaging or clinical data to establish a diagnosis. Establishing a tissue diagnosis in patients with nonmetastatic melanoma is important as it allows stratification of their prognosis and likelihood to develop metastasis in the future according to the class of gene expression of the tumor (class 1 tumors are unlikely to metastasize, while class 2 tumors are more likely to metastasize). This is valuable as patients rarely present initially with metastatic disease, and knowing that a patient is at increased risk of metastases due to the class of the tumor may be useful in the future to actively attempt to prevent or delay it. It is also valuable in establishing diagnosis in patients with atypical presentations, specifically patients with amelanotic melanomas [1]. Tissue acquisition in metastatic uveal melanoma patients is important to establish diagnosis, as some of these patients present with liver lesions years after treatment of their primary tumor, and important in advancing our understanding of this patient population that suffers the most from this disease.

Imaging

Uveal melanoma patients rarely have metastatic disease at the time of initial diagnosis, but up to 50% of patients will eventually develop metastases. Metastases are diagnosed on average 3 years after diagnosis of the primary tumor, with a cumulative metastatic rate of 34% at 10 years. Metastases have even been identified in a case report up to 42 years after diagnosis of the primary tumor.

The metachronous nature of uveal melanoma metastases, as well as the large impact their presence has on the prognosis of the patient, dictates that surveillance for the development of metastases is an integral part of the management of these patients. However, the frequency, type, and even benefits of surveillance have been debated, mainly because no studies have documented improved survival with early detection of uveal melanoma metastases. Surveillance programs are highly variable, with different institutions utilizing different modalities at differing time intervals. Centers with high experience in uveal melanoma tailor surveillance programs to patients according to their tumor histology and genetic profile, with patients who harbor tumors with class 2 genetic profile receiving more frequent surveillance, as they have an increased risk of metastasis.

Uveal melanoma metastasizes mainly through a hematogenous route, with the liver being the most common site of metastases and the site associated with a worse prognosis. Other sites of metastases include the lungs, bones, subcutaneous tissue, and, rarely, lymph nodes. The large number of possible locations of metastatic disease has made positron emission tomography-computed tomography (PET-CT) a very attractive option for surveillance in this patient population, as it is able to detect lesions almost anywhere in the body. That along with the ^{18}F-fluorodeoxyglucose (^{18}FDG) avidity of melanoma metastases makes it very useful in the initial staging of patients [1]. However, the routine use of PET-CT in surveillance is very expensive and carries a high radiation dose to the patient. In addition, PET-CT has been shown to be inferior to magnetic resonance imaging (MRI) in detection of small lesions in the liver. Therefore, in most centers, PET-CT is used in initial staging and as a problem-solving tool in later surveillance.

Surveillance for liver lesions was done using ultrasonography in the past, owing to its wide availability, low cost, and lack of radiation exposure. With the increased availability of computer tomography (CT) and MRI, most centers in the United States have shifted to them for routine surveillance [1]. MRI is the modality of choice for detection of melanoma metastases to the liver. MRI has proven superiority over PET-CT in detection of liver lesions and was found to be as sensitive and more specific than CT, without the radiation exposure. The superiority of MRI over PET-CT is attributed to the high background activity of liver tissue on PET-CT, which can make detection of small lesions difficult. The superior specificity of MRI over CT in characterization of melanoma metastases in the liver is explained by the large variety of MRI sequences that are used, some of which can show almost pathognomonic findings, such as the high signal of melanoma lesions on T1-weighted imaging due to the presence of melanin. With the use of

hepatocyte-avid contrast agents, which are contrast agents that are taken up by normal liver parenchyma, even small lesions can be visualized against the enhancing liver parenchyma.

Treatment

Pre-immunotherapy Era

As previously mentioned, one of the debates surrounding surveillance for detection of melanoma metastases was that early detection of metastases did not affect the poor outcome of this patient population. This held true in the pre-immunotherapy era, in which the chemotherapeutic treatment options offered to metastatic melanoma patients did not improve overall survival. Dacarbazine and temozolomide, two chemotherapeutic agents that are used for the treatment of metastatic cutaneous melanoma, were used in metastatic uveal melanoma patients but showed no improvement in overall survival with significant toxicities [1]. Interferon alfa-2a, another adjuvant drug used in cutaneous melanoma, was studied as an adjuvant drug in uveal melanoma patients and showed no influence on survival. A recently published phase II study investigating the combination of dacarbazine and interferon alfa-2a as adjuvant therapy for patients with class 2 gene expression showed no significant difference in 5-year overall survival when results were adjusted for differences in age, tumor size, and initial treatment.

Fotemustine is another chemotherapeutic agent that was studied in patients with metastatic uveal melanoma. Owing to its use in metastatic cutaneous melanoma patients, its short half-life, and its high first-pass liver extraction ratio with consequent high concentrations within the liver, it was initially studied as an intra-arterial infusion into the hepatic artery for patients with liver metastases and shown to have a 40% response rate. These positive results instigated a phase III randomized study comparing intra-arterial and intravenous fotemustine, which showed similar median overall survival of around 14 months, with improved response rate and progression-free survival in the intra-arterial arm.

Post-immunotherapy Era

As our understanding of the relationship between the immune system and malignancy grew over the past few decades, a potential role for immune modulation in management of malignancy became evident. The discovery of immune checkpoint pathways which regulate activation of T-cells, specifically cytotoxic T-lymphocyte-associated antigen 4 (CTLA-4) and programmed death 1 (PD1) and how tumor cells evade the immune system by utilizing these pathways, has led to the development

of checkpoint inhibitors. Checkpoint inhibitors act by inhibiting the regulation of T-cells, resulting in increased activation and proliferation of T-cells and a stronger immune response against tumor cells that has been proven in preclinical studies [7]. Checkpoint inhibition is achieved through the use of monoclonal antibodies designed to bind to CTLA-4 or PD1 and prevent their activation, which leads to increased immune stimulation [8].

In 2010, ipilimumab, an anti-CTLA-4 monoclonal antibody, was shown to significantly improve overall survival in patients with metastatic melanoma [5]. This signaled the start of the immunotherapy era, with the development of other checkpoint inhibitors closely following, such as nivolumab, an anti-PD1 monoclonal antibody, which also showed improved overall survival. The combined use of ipilimumab and nivolumab was also investigated and showed improved overall survival compared to monotherapy. Pembrolizumab, a newer anti-PD1 monoclonal antibody, showed less toxicity and adverse events in patients with metastatic melanoma compared to ipilimumab, which sometimes prevented continuation of treatment in some patients.

These advancements in the use of checkpoint inhibitors were studied in patients with metastatic non-ocular melanoma, with ocular melanoma an exclusion criterion [5, 9]. Small-scale studies investigated the role of checkpoint inhibitors in metastatic uveal melanoma and showed less impressive results. A multicenter retrospective analysis studying the use of ipilimumab in 39 patients with metastatic uveal melanoma showed a response rate of 5.1% and a median overall survival of 9.6 months. A multicenter phase II trial investigating the safety and efficacy of ipilimumab in patients with metastatic uveal melanoma reported a median overall survival of 6.8 months and a median progression-free survival of 2.8 months, with serious treatment-related adverse effects seen in 36% of patients. Ongoing phase II trials are investigating the safety and efficacy of combination ipilimumab and nivolumab (NCT01585194) and pembrolizumab (NCT02359851) in patients with metastatic uveal melanoma, with results expected in late 2019. Overall, while the use of checkpoint inhibitors in metastatic uveal melanoma patients has failed to show statistically significant improved overall survival, some patients have shown response and improved disease control, which warrants further investigation by larger prospective trials [10].

Another interesting advancement in the treatment of metastatic uveal melanoma is the use of MAPK inhibitors, such as selumetinib, which has produced promising preliminary outcomes [1]. A randomized, phase II trial comparing selumetinib to chemotherapy showed improved progression-free survival in the selumetinib arm yet with no statistically significant difference in median overall survival. The rate of treatment-related adverse events was very high (97% of patients) with 37% of patients requiring dose reduction. While a phase III trial investigating the efficacy of selumetinib plus dacarbazine compared to placebo plus dacarbazine failed to show improved progression-free survival in the selumetinib group, other trials are ongoing to study the best dose and the side effects of selumetinib (NCT02768766), and MAPK inhibitors are expected to play a role in the metastatic uveal melanoma population.

IO in the Treatment of Melanoma Metastases

Image-Guided Biopsy

The role of interventional oncology in management of metastatic melanoma patients often begins with image-guided biopsy of a lesion suspicious for being metastatic in a patient with history of melanoma, most often in the liver. Biopsy not only confirms the diagnosis of metastatic melanoma but also allows analysis of the molecular and genetic characteristics of the tumor and allows enrollment in clinical trials in tertiary care centers, most of which require tissue diagnosis for enrollment. The imaging modality used to guide the biopsy relies on the location and adequate visualization of the lesion, with MRI-guided and PET-CT-guided biopsies saved for lesions that are not adequately visualized by ultrasound or CT.

Image-Guided Thermal Ablation

Owing to the impact of liver involvement on prognosis in patients with metastatic uveal melanoma, combined with the small percentage of patients who can undergo surgical resection of liver metastases, liver-directed therapies have emerged to address this population of patients. Image-guided thermal ablation has been studied in melanoma patients with oligometastatic disease involving the liver and who are not candidates for surgical resection or as an adjuvant to or following surgical resection to spare hepatic parenchyma, with promising results [11, 12]

Radiofrequency ablation (RFA) and microwave ablation (MWA) achieve controlled heating (through different methods) at the tip of an applicator that is placed within the lesion under image guidance, which leads to coagulation necrosis of a pre-calculated volume of tissue surrounding the applicator. Cryoablation (CRYO), on the other hand, achieves a rapid drop in the temperature at the tip of the applicator, which leads to formation of extracellular and intracellular crystals and immediate cell death. Similar to image-guided biopsy, the choice of imaging modality used in guidance of ablation applicator placement relies on the location and adequate visualization of the lesion.

A retrospective study looking at 66 patients with melanoma metastases, 44 of which are to the liver, who underwent RFA or CRYO reported a 5-year overall survival of 30% and a median overall survival of 45.2 months, which are comparable with surgical resection yet in a relatively sicker population [13]. Another study looking at the role of RFA in management of recurrent liver lesions following surgical resection in patients with metastatic uveal melanoma showed a 5-year overall survival of 70% and a 10-year survival of 35%. The improved overall survival can be attributed to the healthier population, as these patients could tolerate surgical resection, as well as the repeated treatment [12].

Trans-arterial Therapies

Patients who have multiple bilobar liver metastases are candidates for trans-arterial treatments, as the metastases recruit blood supply preferentially from the arterial system rather than the portal vein [14]. A growing variety of treatments can be delivered to the hepatic arterial system, with encouraging results. These include delivery of chemotherapy in hepatic artery infusion (HAI) and percutaneous hepatic perfusion (PHP), chemotherapy followed by embolic material in trans-arterial chemoembolization (TACE), embolic material in trans-arterial embolization (TAE) (Fig. 16.1), immunotherapy in trans-arterial immunoembolization (TAIE), and radioactive particles in trans-arterial radioembolization (TARE). The technique for all percutaneous trans-arterial treatments is similar, with arterial access achieved using the Seldinger technique, followed by navigation of catheters and microcatheters under fluoroscopic imaging, and using contrast injections into the hepatic arterial system, where the treatment can be delivered (Fig. 16.2). Super-selective catheterization of hepatic artery branches supplying the target lesions, typically using microcatheters, is done to allow delivery of the full dose of treatment to the target lesion and to prevent nontarget embolization, which can have catastrophic implications in some cases [15].

TACE has shown its ability to induce response in patients with uveal melanoma liver metastases since the 1980s (Fig. 16.3). A retrospective study comparing TACE to intra-arterial chemotherapy and systemic therapy showed that TACE was able to induce a response in 36% of patients. While TACE showed no significant difference in overall survival, patients who responded to TACE survived significantly longer (median overall survival 14.5 months) than patients who did not respond (median

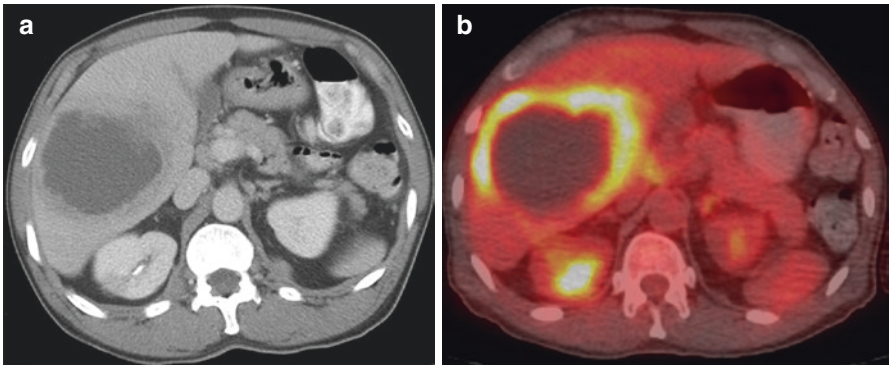

Fig. 16.1 Portal venous phase (**a**) computed tomography shows a large hypodense melanoma metastasis involving the right lobe of the liver with an enhancing rim. Positron emission tomography (**b**) shows the enhancing rim to be metabolically active. Due to continuously downtrending hematocrit concerning for intra-tumoral bleeding, the patient was referred for trans-arterial embolization

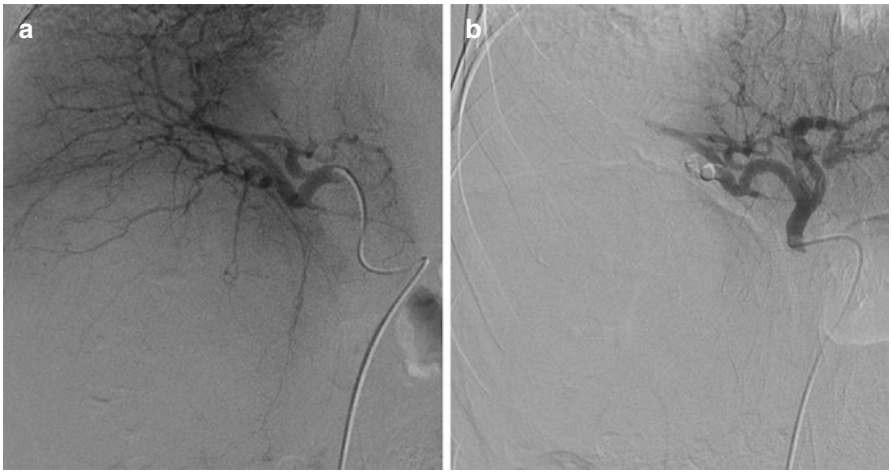

Fig. 16.2 Digital subtraction angiography of the right hepatic artery prior to bland embolization (**a**) and the proper hepatic artery post-bland embolization (**b**) of the right hepatic artery

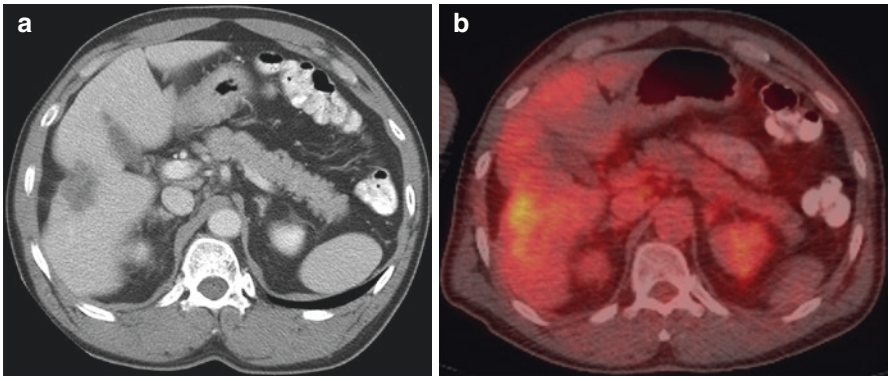

Fig. 16.3 Portal venous phase (**a**) computed tomography and positron emission tomography (**b**) 1 year following trans-arterial embolization show marked reduction in size and metabolic activity of the liver melanoma metastasis

overall survival 5 months) and patients who received systemic therapy (median overall survival 5 months) [16].

A variety of chemotherapeutic agents have been used in TACE, such as melphalan and dacarbazine. In conventional TACE, the chemotherapeutic drug is mixed with Lipiodol and air to form an emulsion which can be visualized under fluoroscopy and is preferentially trapped in tumor microvasculature compared to normal liver parenchyma, followed by embolization with an embolic agent. In drug-eluting bead TACE or DEB-TACE, the chemotherapeutic drug is ionically bound to

drug-eluting microspheres, which gradually release the chemotherapeutic drug and have an inherent embolic effect, and mixed with nonionic contrast. A phase II clinical study assessing the safety and efficacy of DEB-TACE in patients with liver metastases from uveal melanoma reported objective response in all ten patients who underwent the procedure, with three patients showing a major response, defined as metastases reduction of 90% by modified RECIST criteria [17].

More recent studies investigating the effect of conventional TACE in patients with liver metastases from uveal melanoma reported median overall survival of 11.5 months in all patients, with median overall survival of 14.5 months in responders and 10 months in nonresponders [18]. Encouraging results were also seen with DEB-TACE, with reported median overall survival of 15.5 months [19].

TAIE, which is infusion of granulocyte-macrophage colony-stimulating factor (GM-CSF) followed by embolization of the hepatic artery, is believed to attract and stimulate antigen-presenting cells within the liver metastases, leading to a local inflammatory response that eliminates tumor cells and a systemic immune response that suppresses the growth of metastases elsewhere, in addition to the ischemic effect of the embolization. A double-blind phase II clinical trial comparing TAIE with bland embolization reported median overall survival of 21.5 months with TAIE and 17.2 months with bland embolization, both of which are considerably higher than reported with TACE. The TAIE arm also showed a stronger inflammatory response with longer time to extrahepatic progression [20]. Results for TAIE and bland embolization from this study are very promising and highlight the importance of the ischemic component in trans-arterial treatments.

TARE, which is infusion of microspheres loaded with yttrium-90 (^{90}Y), a pure β-emitter, into the hepatic artery, is also known as selective internal radiation therapy, because it applies high radiation doses to the liver tumors with minimal radiation to the surrounding liver tissue. It is a two-step angiographic procedure, the first step of which is infusion of technetium-99-labelled macroaggregated albumin to assess the lung shunt fraction, which will determine the dose of ^{90}Y used in the second step of the procedure, if any. Additionally, during the first step, the arterial anatomy of the liver is outlined, and branches that may lead to nontarget delivery of ^{90}Y are embolized. During the second step of the procedure, the ^{90}Y dose (calculated according to the tumor burden and lung shunt fraction) is delivered to the tumor [21].

TARE is currently employed as salvage therapy, with studies showing improved overall survival with TARE compared to best supportive care. A retrospective study comparing TARE to best supportive care in patients with liver metastases from melanoma refractory to systemic therapy showed a significant difference in median overall survival time between the TARE group (19.9 months) and the best supportive care group (4.8 months), with self-limiting adverse events reported in the TARE group [21]. Another retrospective study assessing the safety and efficacy of TARE in uveal melanoma patients with liver metastases who have failed TAIE or TACE reported a median overall survival of 14.7 months in patients who responded following TARE compared to a median overall survival of 4.9 months in patients who did not respond. They also reported that pretreatment tumor burden <25% was significantly related to longer overall survival and progression-free survival compared to a pretreatment tumor burden >25%. These results led to the initiation of a single

institution, phase II trial investigating the safety and efficacy of TARE in patients with uveal melanoma liver metastases who have not received prior liver-directed treatment and patients who have progressed following TAIE. Reported median overall survival was 19.1 months in the treatment-naïve group compared to 18.9 months in the post-TAIE group, which is promising regarding the role TARE can play in management of patients with uveal melanoma liver metastases not only as salvage therapy but as a first-line therapy [22].

Following the promising results of surgical intra-arterial fotemustine in patients with ocular melanoma liver metastases in the 1990s, similar, less invasive procedures were developed with the same concept. The concept of percutaneous hepatic perfusion (PHP) is to administer high doses of chemotherapy through a catheter placed in the hepatic artery and "capture" the chemotherapy from the hepatic veins using a double-balloon system placed at the level of the confluence of the hepatic veins and inferior vena cava and funnel it outside the body through filters that remove the chemotherapy, before returning the blood to the systemic vasculature through a third catheter placed in a systemic vein. The results of PHP have been variable, with a randomized, controlled, phase III trial comparing it to best available care reporting no significant difference in median overall survival between PHP (10.6 months) and best available care (10.0 months) [23]. On the other hand, a retrospective study assessing the safety and efficacy of PHP in patients with uveal melanoma liver metastases reported median overall survival of 27.4 months [24]. Further prospective studies are needed to accurately assess its role in this patient population.

Future Directions

With all the ongoing progress in our understanding of the molecular and genetic characteristics of melanoma, as well as the continuous development of different treatment modalities and approaches, the need for a multidisciplinary approach toward management of these patients is now greater than ever. There are numerous ongoing developments in each of the fields of treatment of metastatic melanoma. The discovery of the overexpression of c-Kit and c-Met in uveal melanoma, which are growth factor receptors for hepatocyte growth factor, and the consequent development of sunitinib, a c-Kit inhibitor, add to our understanding of the pathology of this disease. Multikinase inhibitors, such as sorafenib and cabozantinib, are currently being studied in phase II trials to assess safety and efficacy.

The role of combination therapies is likely to expand in the near future. One of the exciting fields of combination therapy is the interaction between thermal ablation and immunomodulation. Distant tumor regression has been seen following thermal ablation, also known as the "abscopal effect," with accumulating evidence that this occurs through an antitumor immune response. Thermal ablation is believed to induce the antitumor immune response through the release of tumor antigens and "danger signals" (such as heat-shock proteins) from the ablated tumor. However, this immune response is regulated by cytokines [25], such as interleukin-6 (IL-6)

and IL-10, as well as CTLA-4 and PD1. The combination of thermal ablation and checkpoint inhibitors (anti-CTLA-4 and anti-PD1) may potentially strengthen the antitumor immune response and has been shown to improve survival in a mouse melanoma model. A phase 1b/2 trial assessing the safety and efficacy of combination of RFA and ipilimumab in patients with uveal melanoma liver metastases showed a median overall survival of 13.6 months. Other trials are underway to investigate the different combinations of thermal ablation and checkpoint inhibitors that would achieve the highest antitumor response.

Another combination therapy under study in patients with uveal melanoma liver metastases is TARE and sorafenib with a completed phase I clinical trial (NCT01893099), with results pending. Sorafenib is a multikinase inhibitor with antiangiogenic effects, and combination of sorafenib with TARE is hypothesized to cause more normalized angiogenesis within the tumor, with improved delivery of oxygen into the tumor and consequently, increased sensitivity to radiation.

Conclusion

Metastatic melanoma remains a disease with relatively poor long-term survival. Advances over the past years in our understanding of the molecular and genetic makeup of melanoma, along with ongoing developments in the field of immunotherapy, hold the key to turning this deadly disease into a potentially treatable one. Interventional oncology plays an important role in the diagnosis and management of melanoma patients. With continuously improving techniques and innovations, interventional oncologists will continue to be essential members of the care team of melanoma patients.

References

1. Chattopadhyay C, Kim DW, Gombos DS, Oba J. Uveal melanoma: from diagnosis to treatment and the science in between. Cancer. 2016;122:2299–312. https://doi.org/10.1002/cncr.29727.
2. Singh AD, Turell ME, Topham AK. Uveal melanoma: trends in incidence, treatment, and survival. Ophthalmology. 2011;118(9):1881–5. https://doi.org/10.1016/j.ophtha.2011.01.040.
3. Siegel RL, Miller KD, Jemal A. Cancer statistics, 2018. CA Cancer J Clin. 2018;68(1):7–30. https://doi.org/10.3322/caac.21442.
4. Hsueh EC, Essner R, Foshag LJ, Ye X, Wang H, Morton DL. Prolonged survival after complete resection of metastases from intraocular melanoma. Cancer. 2004;100:122–9. https://doi.org/10.1002/cncr.11872.
5. Hodi FS, O'day SJ, McDermott DF, et al. Improved survival with ipilimumab in patients with metastatic melanoma. N Engl J Med. 2010;363(8):711–23.
6. Prescher G, Bornfeld N, Hirche H, Horsthemke B, Jockel K, Becher R. Prognostic implications of monosomy 3 in uveal melanoma. Lancet. 1996;347:1222–5.
7. Leach DR, Krummel MF, Allison JP. Enhancement of antitumor immunity by CTLA-4 blockade. Science (80-). 1996;271:1734–6.

8. Pardoll DM. The blockade of immune checkpoints in cancer immunotherapy. Nat Rev Cancer. 2012;12(4):252–64. https://doi.org/10.1038/nrc3239.
9. Larkin J, Chiarion-Sileni V, Gonalez R, et al. Combined nivolumab and ipilimumab or monotherapy in untreated melanoma. N Engl J Med. 2015;373(1):23–34. https://doi.org/10.1056/NEJMoa1504030.
10. Luke JJ, Callahan MK, Postow MA, et al. Clinical activity of ipilimumab for metastatic uveal melanoma: a retrospective review of the Dana-Farber Cancer Institute, Massachusetts General Hospital, Memorial Sloan-Kettering Cancer Center and University Hospital of Lausanne experience. Cancer. 2014;119(20):3687–95. https://doi.org/10.1002/cncr.28282.Clinical.
11. Servois V, Bouhadiba T, Dureau S, et al. Iterative treatment with surgery and radiofrequency ablation of uveal melanoma liver metastasis: retrospective analysis of a series of very long-term survivors. Eur J Surg Oncol. 2019;45:1717–22. https://doi.org/10.1016/j.ejso.2019.06.036.
12. Mariani P, Almubarak MM, Kollen M, Wagner M. Radiofrequency ablation and surgical resection of liver metastases from uveal melanoma. Eur J Surg Oncol. 2016;42:706–12. https://doi.org/10.1016/j.ejso.2016.02.019.
13. White ML, Atwell TD, Kurup AN, et al. Recurrence and survival outcomes after percutaneous thermal ablation of oligometastatic melanoma. Mayo Clin Proc. 2016;91(3):288–96. https://doi.org/10.1016/j.mayocp.2015.10.025.
14. Lodh S, Maher R, Guminski A. Intra-arterial infusion and chemo-embolization for melanoma liver metastases. J Surg Oncol. 2014;109:376–82. https://doi.org/10.1002/jso.23551.
15. Sato T. Locoregional management of hepatic metastasis from primary uveal melanoma. Semin Oncol. 2010;37(2):127–38. https://doi.org/10.1053/j.seminoncol.2010.03.014.
16. Bedikian AY, Legha SS, Mavligit G, et al. Treatment of uveal melanoma metastatic to the liver: a review of the M. D Anderson Cancer Center Experience and Prognostic Factors. Cancer. 1995;76:1665–70.
17. Fiorentini G, Aliberti C, Del Conte A, et al. Intra-arterial hepatic chemoembolization (TACE) of liver metastases from ocular melanoma with slow-release irinotecan-eluting beads. Early results of a phase II clinical study. In Vivo. 2009;23:131–8.
18. Huppert PE, Fierlbeck G, Pereira P, et al. Transarterial chemoembolization of liver metastases in patients with uveal melanoma. Eur J Radiol. 2010;74:e38–44. https://doi.org/10.1016/j.ejrad.2009.03.064.
19. Valpione S, Aliberti C, Parrozzani R, et al. A retrospective analysis of 141 patients with liver metastases from uveal melanoma: a two-cohort study comparing transarterial chemoembolization with CPT-11 charged microbeads and historical treatments. Melanoma Res. 2015;25:164–8. https://doi.org/10.1097/CMR.0000000000000129.
20. Valsecchi ME, Terai M, Eschelman DJ, et al. Double-blinded, randomized phase II study using embolization with or without granulocyte – macrophage colony-stimulating factor in uveal melanoma with hepatic metastases. J Vasc Interv Radiol. 2015;26:523–32. https://doi.org/10.1016/j.jvir.2014.11.037.
21. Xing M, Prajapati HJ, Dhanasekaran R, et al. Selective internal Yttrium-90 radioembolization therapy (90 Y-SIRT) versus best supportive care in patients with unresectable metastatic melanoma to the liver refractory to systemic therapy. Safety and Efficacy Cohort Study. Am J Clin Oncol. 2017;40:27–34. https://doi.org/10.1097/COC.0000000000000109.
22. Gonsalves CF, Eschelman DJ, Adamo RD, Rani Anne P, Orloff MM, Sato T. Radioembolization for treatment of uveal melanoma hepatic metastasis: results of a phase II, single institution, prospective trial. J Clin Oncol. 2018;36(15_suppl):9535.
23. Hughes MS, Zager J, Faries M, et al. Results of a randomized controlled multicenter phase III trial of percutaneous hepatic perfusion compared with best available care for patients with melanoma liver metastases. Ann Surg Oncol. 2016;23:1309–19. https://doi.org/10.1245/s10434-015-4968-3.
24. Artzner C, Mossakowski O, Hefferman G, et al. Chemosaturation with percutaneous hepatic perfusion of melphalan for liver- dominant metastatic uveal melanoma: a single center experience. Cancer Imaging. 2019;19(31):1–8.
25. Erinjeri JP, Thomas CT, Samoilia A, et al. Image-guided thermal ablation of tumors increases the plasma level of interleukin-6 and interleukin-10. J Vasc Interv Radiol. 2013;24(8):1105–12.

Chapter 17
Pancreatic Cancer

Ronald S. Arellano and Ryan Nipp

Epidemiology and Pathophysiology

Pancreatic cancer is highly lethal, and surgery remains the only potentially curative approach. Pancreatic cancer is the third leading cause of cancer death in the United States, and estimates suggest it will emerge as the second leading cause of cancer death by 2030 [1]. In 2017, over 50,000 new diagnoses of pancreatic cancer were expected in the United States, and projections expect over 40,000 deaths will be attributed to pancreatic cancer each year [2]. Incidence rates for this cancer increased at a rate of 1.2% per year between 2000 and 2012, and death rates increased by 0.4% [3]. Pancreatic cancer represents a particularly aggressive and lethal malignancy, with approximately 93% of pancreatic cancer patients dying within 5 years of diagnosis [3, 4]. Historically, 5-year survival rates for patients with pancreatic adenocarcinoma were below 6%, and those with metastatic disease had approximately 3–6-month median life expectancy [5–7]. Metastatic pancreatic cancer is incurable, but for patients with disease localized to the pancreas, surgical resection represents a potentially curative option. Unfortunately, many patients with pancreatic cancer present with initially unresectable disease, and thus oncologists frequently employ preoperative treatment to try to shrink the tumor and improve resectability [8, 9].

R. S. Arellano (✉)
Department of Radiology, Massachusetts General Hospital, Harvard Medical School, Boston, MA, USA
e-mail: rarellano@mgh.harvard.edu

R. Nipp
Department of Hematology/Oncology, Massachusetts General Hosptial, Harvard Medical School, Boston, MA, USA

C. Georgiades, H. S. Kim (eds.), *Image-Guided Interventions in Oncology*,
https://doi.org/10.1007/978-3-030-48767-6_17

Role of Surgery

Pancreatic cancer remains highly lethal despite incremental gains with the use of multi-agent chemotherapy in the metastatic setting. Surgery remains the best opportunity for cure, but historically only 15–20% of patients with pancreatic cancer present with upfront, resectable disease. Recently, the combination regimens of FOLFIRINOX [10] and gemcitabine/nab-paclitaxel [11] have demonstrated encouraging results for patients with metastatic disease and also for patients with locally advanced and potentially resectable disease [12]. In the metastatic setting, median survival has been pushed out to beyond 11 months, and we are now seeing approximately 10% of patients alive at 2 years [10, 11, 13]. Several institutions have now published data about their ability to convert locally advanced or borderline resectable disease to resectable by using FOLFIRINOX [8, 12, 14, 15].

A Paradigm Shift Is Occurring in the Management of Potentially Resectable Pancreatic Cancer

Recent advances in combination chemotherapy regimens for pancreatic cancer have led to innovative strategies using these agents as preoperative therapy for patients with upfront unresectable disease [8–11, 14, 15]. Oncologists frequently introduce these therapies preoperatively to help convert locally advanced or borderline resectable disease to resectable and ensure a more successful operation. However, although surgery represents the only potentially curative approach for patients with pancreatic cancer, studies historically demonstrated 5-year survival rates of only 10–20% for patients with resected disease [13, 16–19].

Future Directions

Based on promising clinical results in other cancer types, the use of immunotherapy has been tested in pancreatic adenocarcinoma. Results to date are limited, but efforts remain to understand how best to harness the improved outcomes seen with immunotherapy in other malignancies. In addition, preliminary data of resected pancreatic adenocarcinoma from patients on angiotensin system inhibitors suggest enhanced T-cell activation and antigen presentation pathways, with analysis of mouse model tumors treated with an angiotensin receptor blocker (ARB) revealing suppression of tumor-associated macrophages [20, 21]. Collectively, these data underscore the potential for ARBs to modulate the immune microenvironment toward a permissive environment for immunotherapy. Future work will also continue to investigate how best to target available treatment options to patients most likely to benefit. For example, future studies will seek to demonstrate predictive biomarkers that will help guide clinicians and patients toward choosing a

gemcitabine versus a 5FU-based regimen. Moreover, the addition of other agents to known therapies will continue to emerge. For example, a regimen such a gemcitabine plus Abraxane in combination with cisplatin will have data in the coming years. Furthermore, studies of circulating tumor DNA (ctDNA) and circulating tumor cells will help identify patients with recurrent/progressive disease earlier while also helping identify patients for whom novel treatment paradigms may prove beneficial. Importantly, ongoing work is critically needed to investigate how best to provide supportive care to patients with pancreatic cancer. In the metastatic setting, understanding the role of palliative care and symptom monitoring interventions are urgently needed [22]. For patients with potentially resectable pancreatic cancer, additional research should seek to determine how best to help with the complex shared decision-making for these patients while also helping to support these patients along their journey of neoadjuvant treatment.

Patients receiving neoadjuvant therapy often experience numerous side effects, including nausea, vomiting, diarrhea, fatigue, fever, neuropathy, and loss of appetite [8, 10, 11]. Frequently, patients require hospital admissions to help address uncontrolled symptoms related to their cancer and side effects related to the treatment [8, 23]. A prior study demonstrated that nearly one-third of patients receiving combination chemotherapy for locally advanced pancreatic cancer required hospital admissions while receiving treatment. In addition, when patients complete their preoperative therapy and are able to undergo resection, the surgical operation is fraught with postoperative morbidity and occasional mortality [17, 24, 25]. Therefore, it is critically important that patients understand the risks and benefits when considering preoperative treatment for pancreatic cancer.

Another area of need within the field of pancreatic cancer includes the opportunity to help patients develop accurate understanding of their prognosis. Despite patients' general preference for accurate information regarding their prognosis, data suggest that the majority of patients misunderstand the curability of their cancer [26–28]. Patients often report a more optimistic assessment of their prognosis than their oncologist [29]. Importantly, research suggests that patient-clinician communication about prognosis does not take away patients' hope but rather enables patients to make informed treatment decisions and prepare for the future [28]. Thus, improving patient-clinician communication about prognosis and treatment options should be a priority for enhancing the quality of cancer care and improving informed treatment decision-making [30–35].

Pain Management for Patients with Pancreatic Carcinoma

Pain management represents one of the most challenging aspects of treating pancreatic carcinoma and often requires chronic high-dose narcotics [36, 37]. Because of the high risk of dependency and adverse effects of chronic narcotic use, an alternative approach to pain control is by neurolysis of the celiac ganglion. Pain from upper abdominal visceral organs, including the pancreas, is relayed via visceral afferent fibers through the splanchnic nerves and celiac plexus [38]. The celiac ganglion is

located deep in the retroperitoneum and typically overlies the anterolateral abdominal aorta, near the origins of the celiac plexus and superior mesenteric artery [38]. Tumor infiltration and/or desmoplastic reaction from pancreatic carcinoma often leads to an increased in nociceptive impulses to the celiac ganglion, resulting in excruciating pain. Kappis first described neurolysis of the celiac ganglion as a means of controlling upper abdominal visceral pain [39]. Anesthesiologists or interventional radiologists use imaging guidance to target the celiac ganglion for neurolysis. Because of the superior anatomic resolution offered by computed tomography (CT) versus fluoroscopic guidance of ultrasound, celiac neurolysis is often performed with CT guidance.

Computed Tomography-Guided Celiac Ganglion Neurolysis

Patient Selection

Pain associated with abdominal malignancies may be multifactorial; thus careful patient selection and elucidation of pain sources are essential in order to maximize the potential benefit of celiac neurolysis. While pain associated with pancreatic cancer is often the result of perineural or duodenal invasion, somatic pain from musculoskeletal involvement of tumor can contribute to the overall pain profile and will not be alleviated by neurolysis of celiac ganglion. Careful review of cross-sectional imaging and detailed patient history will help to identify patients who will receive maximum benefit from the neurolysis procedure.

Patient Preparation

Preliminary evaluation included patient education and discussion of the goals of care associated with neurolysis. Many patients who qualify for celiac ganglion neurolysis are on chronic opioid usage; thus an important goal of the procedure is to reduce the opioid usage with reduction of opioid-related side effects. Once appropriate patients are identified, imaging review and assessment of coagulation profile is necessary. A thorough neurological exam is essential in order to establish a baseline level of pain and to assess for post-procedure complications. Patients should be fasting for 8–10 hours prior to the procedure, and any correctable coagulopathies should be addressed prior to the procedure. Neurolysis can be performed with intravenous procedural sedation, monitored anesthesia care, or general anesthesia. Continuous hemodynamic monitoring is essential throughout the procedure.

Patient Positioning

Various approaches can be utilized to target the celiac ganglion, depending on patient body habitus, patients' overall condition, and the best percutaneous access to the ganglion. The most commonly used positions are prone, lateral decubitus, or supine.

Prone The prone position is the most commonly used approach, as it facilitates access to the celiac ganglion from a posterior approach. This allows a transcrural trajectory to target the para-aortic soft tissues at the level of the celiac axis (Fig. 17.1). When tumor infiltration precludes a transcrural approach, the prone position allows a retrocrural trajectory that targets neurolysis of preganglionic splanchnic nerves in the retrocrural space.

Lateral Decubitus When patients are unable to lie prone, a lateral decubitus position can be used for either retrocrural or antecrural approaches to the celiac ganglion. Because the independent lung is often more inflated than the dependent lung, this position may increase the risk of procedure-related pneumothorax.

Supine When either the lateral decubitus or supine position is not feasible, an anterior approach with the patient in the supine position is possible. This approach often necessitates a transhepatic or transgastric approach, which is usually of no clinical consequence.

Targeting

Antecrural The antecrural approach targets the soft tissue anterior to the diaphragmatic crura and the abdominal aorta in which the celiac ganglia reside. Injection of neurolytic agent in this space is most effective in achieving pain relief.

Retrocrural When the antecrural space is replaced by tumor, a retrocrural injection of neurolytic agent can be used to achieve splanchnic nerve block. In this targeting approach, the neurolytic agent spreads along the retroaortic space and treats the splanchnic nerves.

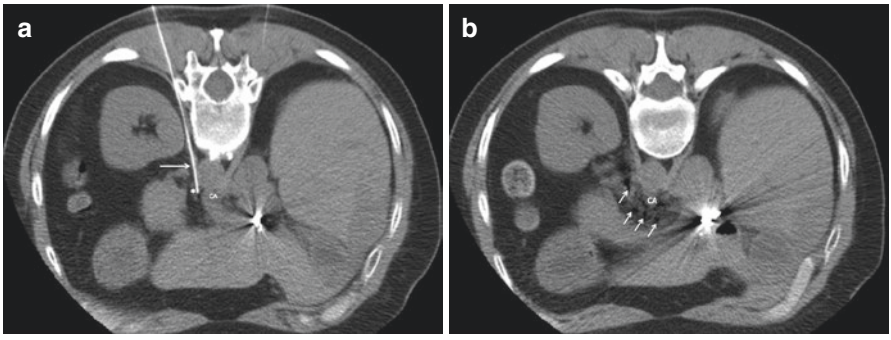

Fig. 17.1 (**a**) Axial unenhanced CT scan of the abdomen with the patient in the prone position. White arrow indicates 22-gauge needle on the celiac ganglion (white asterisk) via an antecrural approach. CA indicates origin of the celiac axis. (**b**) Axial unenhanced CT scan of the abdomen with the patient in the prone position. White arrows indicate distribution of ethanol in the retroperitoneal space. CA indicates origin of the celiac axis

Neurolytic agents Absolute alcohol is the most common neurolytic agent used for neurolysis. It acts by causing immediate precipitation of lipoproteins and mucoproteins of the neural elements. When an antecrural approach is used, approximately 20 ml of 95–100% absolute ethanol is injected on either side of the aorta at the level of celiac ganglion. When a retrocrural approach is chosen, the confined space limits the amount of neurolytic agent to approximately 5–10 ml. Phenol is an alternative agent that has been used to achieve celiac neurolysis. At a concentration of 3–20%, phenol acts as a protein coagulant and causes necrosis of neural elements. The data are limited comparing the effectiveness of ethanol versus phenol, but ethanol is considered to be more effective than phenol and is thus more commonly used [40].

Recovery Post-procedure care involves overnight observation for treatment response and potential complications. Hypotension may be encountered in the immediately post-procedure; therefore, patients should adhere to strict bed rest for a minimum of 12 hours post-procedure. Hemodynamic monitoring should continue in the post-procedure observation period for up to 24 hours. If necessary, acute hypotension can be treated with fluid replacement and medications if needed. A neurological examination should be performed immediately after the procedure to assess the changes in lower extremity function, especially when a retrocrural approach is used. Subjective evaluation of pain relief and changes in opioid requirement should be assessed the following day and compared with pre-procedure baseline to assess effectiveness.

Follow-up Follow-up care is carried out by the interventional team in collaboration with anesthesia, oncology services for inpatients. Outpatients typically follow up with pain control specialists for ongoing management of pain control if needed.

Complications Overall, celiac plexus neurolysis is a safe procedure with major complications occurring in fewer than 2% of patients. Most patients experience some transient back pain, especially when ethanol is used, that is likely the result of the neurolytic effect of the ethanol on sensory fibers within the ganglion. Orthostatic hypotension may result from diminished sympathetic tone that in turn leads to vasodilation [36, 40]. Transient self-limiting diarrhea can occur in up to 44% of patients who undergo celiac plexus neurolysis [36]. Neurologic complications are extremely rare and can include anal and bladder dysfunction. Inadvertent injection of neurolytic agent into or near the spinal artery can result in ischemia and subsequent lower extremity paralysis. With CT guidance, these complications are uncommon.

Outcomes Reported clinical efficacy of celiac plexus neurolysis is up to 90% of patients with upper abdominal malignancy [36]. With regard to patients with pancreatic cancer, celiac plexus neurolysis can eliminate pain in 10–20% when used without other therapies and up to 80–90% when combined with other therapies [41]. Even for patients who achieve partial relief, the major benefit of celiac plexus neurolysis is an overall reduction in opioid requirements and its associated adverse effects.

Locoregional Therapy for Pancreatic Carcinoma

Irreversible Electroporation

Irreversible electroporation (IRE) is an emerging nonthermal ablative technology with potential application in treating pancreatic carcinoma [42, 43]. With IRE cell death is achieved by subjecting tumor cell to high-voltage electrical pulses. The high electrical pulses result in permanent disruption of the phospholipid bilayer of the cellular membrane, resulting in multiple nanometer size pores. As a result, the normal homeostasis that exists between extracellular and intracellular environments is disrupted, ultimately leading to cell death by apoptosis. Because of its nonthermal mechanism of action, IRE may have a role in local control of pancreatic carcinoma. Early experiments in animals suggested that IRE achieves significant tissue destruction while maintaining vessel patency [44, 45]. In a retrospective analysis of 221 patients with 325 tumors, including 69 with pancreatic carcinoma, Scheffer et al. found that when IRE was combined with surgical resection of pancreatic carcinoma, overall survival was extended to 20 months from 13 months. In three patients, significant complications of bile leak and portal vein thrombosis were identified, despite early reports that suggested IRE preserved vasculature [46]. In contrast, Manson enrolled 24 patients in a prospective study in which ultrasound-guided percutaneous IRE was used as first-line therapy. The results showed that overall survival was 13.3 months in the IRE group compared to 9.9 months in patients identified through a registry. Because the overall survival between the two groups was not significant, the authors advocated against the use of IRE as first-line therapy. More recently, Flak et al. reported on a series of 33 patients with locally advanced pancreatic cancer who underwent 44 open IRE procedures. These authors found that the 30-day mortality was only 5% and the median overall survival was 10.7 months from the initial IRE procedure and 18.5 months from the time of diagnosis [47]. Despite a growing body of literature, more level I and II evidence are necessary to help define the potential role of IRE in the management of pancreatic carcinoma.

Transarterial Chemoembolization (TACE)

Pancreatic Adenocarcinoma Data regarding the use of transarterial chemoembolization for treatment of locally advanced pancreatic carcinoma is limited. Early studies proposed that locoregional delivery of chemotherapy should result in high concentrations of cytotoxic agents directly to tumors [48]. They studied 22 patients divided into 2 groups. Group A consisted of 12 patients who were treated with transarterial delivery of epirubicin, folic acid, and f-fluorouracil. Group B consisted of ten patients treated with transarterial delivery of mitoxantrone, 5-fluorouracil, and folic acid. For these two cohorts, Group A showed 33.3% 1-year survival rate, compared to 20% 1-year survival rate for Group B. A more recent study evaluated the

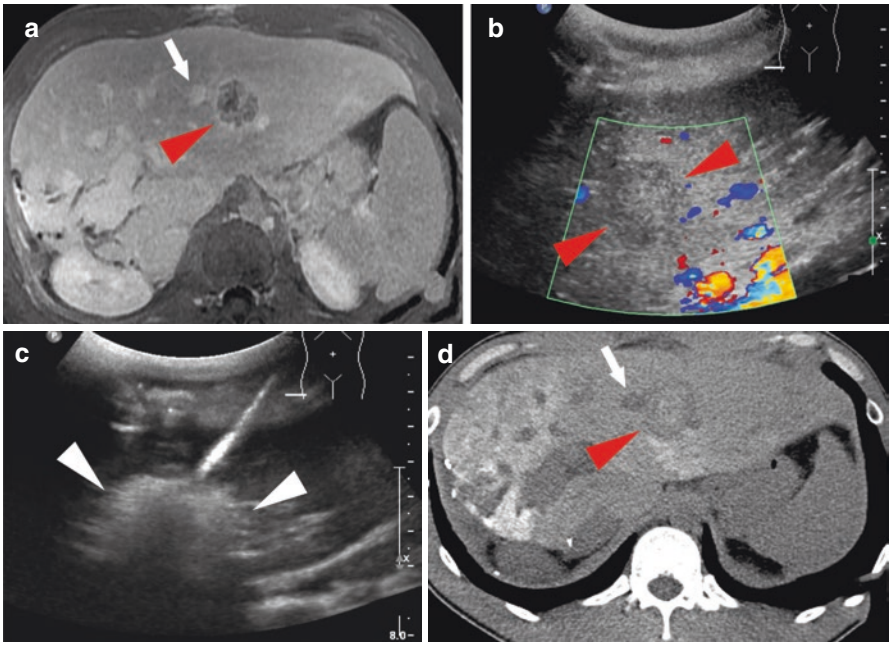

Fig. 17.2 72-year-old female with metastatic pancreatic adenocarcinoma s/p Whipple. Despite systemic chemotherapy, the single hepatic lesion grew, and a multidisciplinary team opted for percutaneous ablation. Contrast-enhanced MR image (**a**) shows the lesion (red arrowhead) in the left lobe near a portal vein branch (white arrow). Ultrasound examination (**b**) shows the same lesion (red arrowheads). Toward the end of microwave ablation (**c**), the lesion is completely obscured by gas (white arrowheads) as a result of tissue heating. Post-ablation non-contrast CT (**d**) shows the ablation zone (red arrowhead) covering the entire lesion and now extending to the portal vein branch (white arrow). Studies confirm excellent imaging responses for pancreatic metastatic lesions to the liver smaller than 3 cm; however we lack high-level studies as to any survival benefit

safety and efficacy of locoregional therapy for metastatic pancreatic adenocarcinoma. This study included 20 patients with hepatic metastatic pancreatic adenocarcinoma that were treated with thermal ablation (Fig. 17.2), chemoembolization (Fig. 17.3), or radioembolization. While the authors report a median overall survival of 25 months from the time of diagnosis, there were only three patients who underwent transarterial chemoembolization [49]. Thus, the clinical impact of TACE to treat metastatic pancreatic adenocarcinoma is limited. Sun et al. evaluated 27 patients with liver metastases from pancreatic cancer treated with TACE and found that the median survival time was 13.6 months and that the 1-, 3-, and 5-year survival rates were 70.4%, 22.2%, and 11.1%, respectively [50]. To date, there are no strong levels 1 or II data that advocate the use of TACE as primary treatment for locally advanced pancreatic carcinoma.

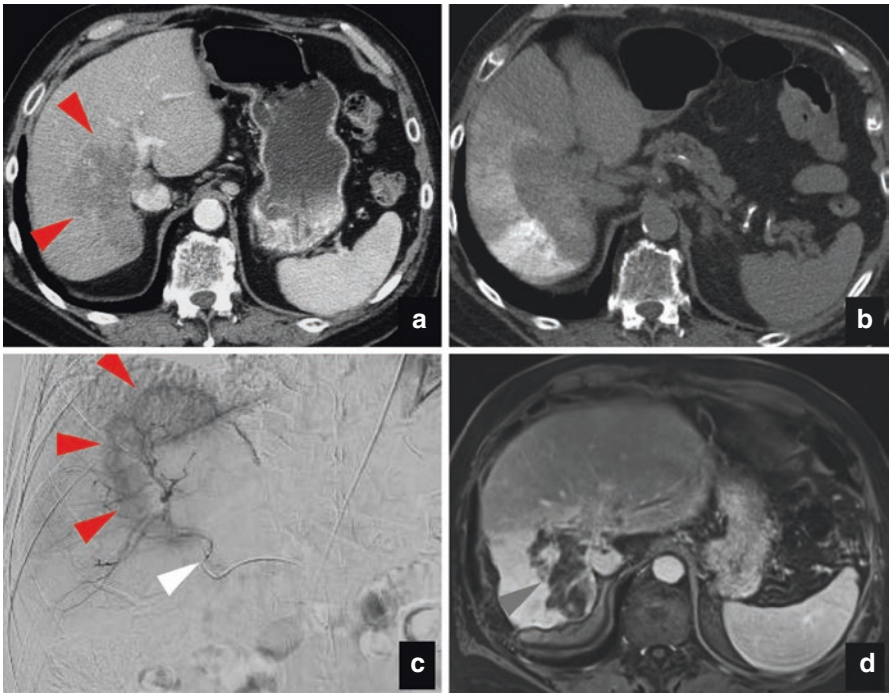

Fig. 17.3 62-year-old male with liver metastatic pancreatic adenocarcinoma. Axial contrast-enhanced CT (**a**) shows an infiltrating lesion in the right posterior liver lobe (red arrowheads). Post-chemoembolization CT (**b**) shows Lipiodol distribution peripheral to the lesion. Unlike in hepatocellular carcinoma where Lipiodol shows selective uptake by tumors, in pancreatic adenocarcinomas, Lipiodol distribution is preferentially seen in the tumors' periphery. This is despite the fact that during chemoembolization (**c**) with a superselective microcatheter (white arrowhead), the target lesion appears hypervascular (red arrowheads). Eighteen-month follow-up with contrast-enhanced MRI (**d**) shows complete devascularization of the slightly smaller lesion (red arrowhead). As with ablation, despite the encouraging imaging responses, high-level studies on oncologic outcomes after intra-arterial therapies are lacking

Radioembolization Emerging data suggests a possible role of radioembolization for treatment of liver metastases from pancreatic adenocarcinoma. Kim et al. reported on a series of 33 patients with hepatic metastases treated with yttrium-90 microspheres and showed post-treatment imaging findings consistent with partial response in 42%, stable disease in 37%, and progressive disease in 21%. Importantly, radioembolization produced only grade 3 or less toxicities up to 12 weeks post-procedure and a survival benefit of up to 20.8 months [51]. As with transarterial chemoembolization, additional clinical trials are necessary to further evaluate the efficacy and clinical outcomes of radioembolization for metastatic pancreatic adenocarcinoma.

References

1. Rahib L, Smith BD, Aizenberg R, Rosenzweig AB, Fleshman JM, Matrisian LM. Projecting cancer incidence and deaths to 2030: the unexpected burden of thyroid, liver, and pancreas cancers in the United States. Cancer Res. 2014;74:2913–21.
2. Siegel RL, Miller KD, Jemal A. Cancer statistics, 2017. CA Cancer J Clin. 2017;67:7–30.
3. American Cancer Society. Cancer facts & figures 2016. Atlanta: American Cancer Society; 2016.
4. Jemal A, Siegel R, Xu J, Ward E. Cancer statistics, 2010. CA Cancer J Clin. 2010;60:277–300.
5. Jemal A, Siegel R, Ward E, et al. Cancer statistics, 2006. CA Cancer J Clin. 2006;56:106–30.
6. Hawes RH, Xiong Q, Waxman I, Chang KJ, Evans DB, Abbruzzese JL. A multispecialty approach to the diagnosis and management of pancreatic cancer. Am J Gastroenterol. 2000;95:17–31.
7. Sultana A, Smith CT, Cunningham D, Starling N, Neoptolemos JP, Ghaneh P. Meta-analyses of chemotherapy for locally advanced and metastatic pancreatic cancer. J Clin Oncol Off J Am Soc Clin Oncol. 2007;25:2607–15.
8. Faris JE, Blaszkowsky LS, McDermott S, et al. FOLFIRINOX in locally advanced pancreatic cancer: the Massachusetts General Hospital Cancer Center experience. Oncologist. 2013;18:543–8.
9. Ferrone CR, Marchegiani G, Hong TS, et al. Radiological and surgical implications of neoadjuvant treatment with FOLFIRINOX for locally advanced and borderline resectable pancreatic cancer. Ann Surg. 2015;261:12–7.
10. Conroy T, Desseigne F, Ychou M, et al. FOLFIRINOX versus gemcitabine for metastatic pancreatic cancer. N Engl J Med. 2011;364:1817–25.
11. Von Hoff DD, Ervin T, Arena FP, et al. Increased survival in pancreatic cancer with nab-paclitaxel plus gemcitabine. N Engl J Med. 2013;369:1691–703.
12. Murphy JE, Wo JY, Ryan DP, et al. Total neoadjuvant therapy with FOLFIRINOX in combination with losartan followed by chemoradiotherapy for locally advanced pancreatic cancer: a phase 2 clinical trial. JAMA Oncol. 2019;5:1020–7.
13. Ryan DP, Hong TS, Bardeesy N. Pancreatic adenocarcinoma. N Engl J Med. 2014;371:2140–1.
14. Boone BA, Steve J, Krasinskas AM, et al. Outcomes with FOLFIRINOX for borderline resectable and locally unresectable pancreatic cancer. J Surg Oncol. 2013;108:236–41.
15. Hosein PJ, Macintyre J, Kawamura C, et al. A retrospective study of neoadjuvant FOLFIRINOX in unresectable or borderline-resectable locally advanced pancreatic adenocarcinoma. BMC Cancer. 2012;12:199.
16. Geer RJ, Brennan MF. Prognostic indicators for survival after resection of pancreatic adenocarcinoma. Am J Surg. 1993;165:68–72; discussion −3.
17. Trede M, Schwall G, Saeger HD. Survival after pancreatoduodenectomy. 118 consecutive resections without an operative mortality. Ann Surg. 1990;211:447–58.
18. Yeo CJ, Cameron JL, Sohn TA, et al. Six hundred fifty consecutive pancreaticoduodenectomies in the 1990s: pathology, complications, and outcomes. Ann Surg. 1997;226:248–57; discussion 57–60.
19. Perysinakis I, Avlonitis S, Georgiadou D, Tsipras H, Margaris I. Five-year actual survival after pancreatoduodenectomy for pancreatic head cancer. ANZ J Surg. 2015;85:183–6.
20. Cortez-Retamozo V, Engblom C, Pittet MJ. Remote control of macrophage production by cancer. Onco Targets Ther. 2013;2:e24183.
21. Cortez-Retamozo V, Etzrodt M, Newton A, et al. Angiotensin II drives the production of tumor-promoting macrophages. Immunity. 2013;38:296–308.
22. Temel JS, Greer JA, El-Jawahri A, et al. Effects of early integrated palliative care in patients with lung and GI cancer: a randomized clinical trial. J Clin Oncol Off J Am Soc Clin Oncol. 2017;35:834–41.
23. Smyth EN, Bapat B, Ball DE, Andre T, Kaye JA. Metastatic pancreatic adenocarcinoma treatment patterns, health care resource use, and outcomes in France and the United Kingdom between 2009 and 2012: a retrospective study. Clin Ther. 2015;37:1301–16.

24. Dias-Santos D, Ferrone CR, Zheng H, Lillemoe KD, Fernandez-Del CC. The Charlson age comorbidity index predicts early mortality after surgery for pancreatic cancer. Surgery. 2015;157:881–7.
25. Barugola G, Falconi M, Bettini R, et al. The determinant factors of recurrence following resection for ductal pancreatic cancer. JOP. 2007;8:132–40.
26. Greer JA, Pirl WF, Jackson VA, et al. Perceptions of health status and survival in patients with metastatic lung cancer. J Pain Symptom Manag. 2014;48:548–57.
27. Weeks JC, Catalano PJ, Cronin A, et al. Patients' expectations about effects of chemotherapy for advanced cancer. N Engl J Med. 2012;367:1616–25.
28. Epstein AS, Prigerson HG, O'Reilly EM, Maciejewski PK. Discussions of life expectancy and changes in illness understanding in patients with advanced cancer. J Clin Oncol Off J Am Soc Clin Oncol. 2016;34:2398–403.
29. Gramling R, Fiscella K, Xing G, et al. Determinants of patient-oncologist prognostic discordance in advanced cancer. JAMA Oncol. 2016;2(11):1421–6.
30. Steinhauser KE, Christakis NA, Clipp EC, et al. Preparing for the end of life: preferences of patients, families, physicians, and other care providers. J Pain Symptom Manag. 2001;22:727–37.
31. Steinhauser KE, Christakis NA, Clipp EC, McNeilly M, McIntyre L, Tulsky JA. Factors considered important at the end of life by patients, family, physicians, and other care providers. JAMA. 2000;284:2476–82.
32. Steinhauser KE, Clipp EC, McNeilly M, Christakis NA, McIntyre LM, Tulsky JA. In search of a good death: observations of patients, families, and providers. Ann Intern Med. 2000;132:825–32.
33. Lundquist G, Rasmussen BH, Axelsson B. Information of imminent death or not: does it make a difference? J Clin Oncol Off J Am Soc Clin Oncol. 2011;29:3927–31.
34. Smith TJ, Dow LA, Virago E, Khatcheressian J, Lyckholm LJ, Matsuyama R. Giving honest information to patients with advanced cancer maintains hope. Oncology. 2010;24:521–5.
35. Zhang B, Wright AA, Huskamp HA, et al. Health care costs in the last week of life: associations with end-of-life conversations. Arch Intern Med. 2009;169:480–8.
36. Eisenberg E, Carr DB, Chalmer TC. Neurolytic celiac plexus block for treatment of cancer pain: a meta-analysis. Anesth Analg. 1995;80:290–5.
37. Kaugman M, Singh G, Das S, Concha-Parra R, et al. Efficacy of endoscopic ultrasound guided celiac plexus block and celiac plexus neurolysis for managing abdominal pain associated with chronic pancreatitis and pancreatic cancer. J Clin Gastroenterol. 2010;44:127–34.
38. Loukas M, Klaasen A, Merbs W, Tubbs RS, Gielecki J, Zurada A. A review of the thoracic splanchnic nerves and celiac ganglia. Clin Anat. 2010;23(5):512–22.
39. Fujita Y, Sari A. Max Kappis and the celiac plexus block. Anesthesiology. 1997;86:508.
40. Wang PJ, Shang MY, Qian Z, Shao CW, Wang JH, Zhao XH. CT-guided percutaneous neurolytic celiac plexus block technique. Abdom Imaging. 2006;31(6):710–8.
41. Sachev AH, Gress FG. Celiac plexus block and neurolysis: a review. Gastrointest Endosc Clin N Am. 2018;28(4):579–86.
42. Silk M, Tahour D, Srimathveeravalli G, Solomon SB, Thornton RH. The state of irreversible electroporation in interventional oncology. Semin Intervent Radiol. 2004;31:111–7.
43. Scheffer HJ, Nielsen K, de Jong MC, et al. Irreversible electroporation for nonthermal tumor ablation in the clinical setting: a systematic review of safety and efficacy. J Vasc Interv Radiol. 2014;25:997–1011.
44. Charpentier KP, Wolf F, Noble L, Winn B, Resnick M, Dupuy DE. Irreversible electroporation of the pancreas in swine: a pilot study. HPB (Oxford). 2010;12:348–51.
45. Bower M, Sherwood L, Li Y, Martin R. Irreversible electroporation of the pancreas: definitive local therapy without systemic effects. J Surg Oncol. 2011;104:22–8.
46. Narayanan G, Bhatia S, Echenique A, Suthar R, Barbery K, Yrizarry J. Vessel patency post irreversible electroporation. Cardiovasc Intervent Radiol. 2014;37:1523–9.
47. Flak RV, Stender MT, Jensen TM, Andersen KL, et al. Treatment of locally advanced pancreatic cancer with irreversible electroporation; A Danish single center study of safety and feasibility. Scand J Gastroenterol. 2019;54(2):252–8.

48. Meyer F, Grote R, Lippert H, Ridwelski K. Marginal effects of regional intra-arterial chemotherapy as an alternative treatment option in advanced pancreatic carcinoma. Langenbeck's Arch Surg. 2004 Feb.;389:32–9.
49. Bailey RE, Srapanemi PK, Core J, Vidal LLC, LeGout J, et al. Safety and efficacy of locoregional therapy for metastatic pancreatic ductal adenocarcinoma to the liver: a single-center experience. J Gastrointest Oncol. 2019;10:688–94.
50. Sun JH, Zhou TY, Zhang YL, Zhou GH, et al. Efficacy of transcatheter arterial chemoembolization for liver metastases arising from pancreatic cancer. Oncotarget. 2017;8:39746–55.
51. Kim AY, Frantz S, Bower J, Akhter N. Radioembolization with Yttrium-90 microspheres for the treatment of LIver metastases of pancreatic adenocarcinoma: a multicenter analysis. J Vasc Interv Radiol. 2019;30:298–304.

Chapter 18
Image-Guided Biopsy/Liquid Biopsy

Rene Roberts, Bilal A. Siddiqui, Sumit K. Subudhi, and Rahul A. Sheth

Background

Cancer treatment relies on the direct acquisition of tumor tissue, most commonly via image-guided percutaneous biopsy, in order to establish diagnosis, stage, and tumor histology [2, 34]. In the personalized medicine era, biopsies provide key insight into specific molecular alterations in the tumor that can influence treatment decisions, a point highlighted by the Food and Drug Administration (FDA) mandate that targeted therapies be accompanied by relevant companion diagnostic tests [21]. These biopsies also provide valuable information regarding the tumor microenvironment, such as nonmalignant stromal elements and infiltrating immune cells, offering a window into the biology of the cancer. Indeed, the deployment of longitudinal tumor biopsies at multiple time points permits the treating oncologist to observe the changes in disease biology that occur in response to treatment and can shed light into the mechanisms of resistance.

The role of molecular profiling in tissue samples is well established in clinical oncology. For example, in the 1970s, estrogen receptor (ER) expression in breast cancer tissue was linked to the efficacy of antiestrogen-based therapies. Since that time, immunohistochemistry (IHC) of ER is now standard in breast cancer and helps guide the selection of hormonal therapies for patients. In addition to analysis of protein expression, investigation of somatic genetic alterations to determine therapy is now a routine in certain cancers, such as *EGFR*, *ALK*, and *ROS1* in non-small cell lung cancer. In such cases, longitudinal tissue biopsies can identify the

R. Roberts · R. A. Sheth (✉)
Interventional Radiology, MD Anderson Cancer Center, Houston, TX, USA
e-mail: rasheth@mdanderson.org

B. A. Siddiqui · S. K. Subudhi
Genitourinary Medical Oncology, MD Anderson Cancer Center, Houston, TX, USA

C. Georgiades, H. S. Kim (eds.), *Image-Guided Interventions in Oncology*,
https://doi.org/10.1007/978-3-030-48767-6_18

emergence of resistance mutations in response to targeted therapy, such as the canonical T790M gatekeeper mutation in *EGFR*.

More recently, advances in cancer immunotherapy have highlighted the importance of obtaining tumor tissue for analysis. Immune checkpoint therapy (ICT), including monoclonal antibodies against the surface proteins PD-1, PD-L1, or CTLA-4, blocks inhibitory immune checkpoints, thereby stimulating host cytotoxic T cell responses against tumors. Multiple ICT agents have been approved for the treatment various solid tumors, including melanoma and lung cancer, and have demonstrated a survival benefit for a subset of patients [3]. A major challenge of ICT is identifying which patients will respond to therapy. Tissue expression of PD-1 and/or PD-L1 is often used to stratify patients for ICT. In metastatic non-small cell lung cancer, for example, the tumor proportion score (TPS) is the percentage of viable tumor cells showing partial or complete membrane staining of PD-L1 and is used to predict potential response to pembrolizumab, an anti-PD-1 monoclonal antibody. In locally advanced or metastatic, cisplatin-ineligible, bladder cancer, a combined positive score (CPS), which captures PD-L1 expression on both tumor and immune cells, is used to select patients for pembrolizumab. Despite its routine use, tissue expression of PD-L1 is an imperfect biomarker, as certain patients with low PD-L1 expression may benefit from ICT, and conversely, some patients with high expression may not. A range of biomarkers are emerging to capture the dynamics of the immune response, mechanisms of resistance, and changes in the tumor microenvironment, including assessment of tumor infiltrating lymphocytes (TILs) and other cell populations, gene expression profiling (e.g., interferon-γ signatures), and tumor mutational burden. For those biomarkers that require preservation of the tumor and stromal architecture, direct tissue sampling by core biopsy is essential.

Finally, the growing use of immune checkpoint therapy has also revealed the problem of immune-related adverse events (irAEs), in which the stimulation of the body's immune system can lead to inflammation of a diverse array of normal tissue. These events can range from mild skin involvement (e.g., dermatitis) to fulminant neuromuscular and cardiac irAEs (e.g., myositis, myasthenia gravis, and/or myocarditis), which can be fatal. Biopsy of the relevant tissues is commonly performed to establish the diagnosis and is being employed in the research setting to understand the molecular mechanisms of these irAEs, with an ultimate goal of selectively targeting immunotoxicity while preserving antitumor immunity. In addition to autoimmune toxicity, traditional oncologic therapies, including chemotherapy and targeted therapy, are associated with adverse effects, including organ dysfunction and infection. Image-guided biopsies can be used to obtain tissue to help establish the cause of organ dysfunction (e.g., for hepatic cirrhosis or renal failure) and can be used to obtain samples for culture in cases of suspected infection.

As image-guided percutaneous biopsy continues to grow in importance, advances in imaging, needle design, and techniques have improved their yield and safety. A comprehensive understanding of the available devices and tools, the most appropriate imaging modality for guidance, and the biopsy technique most likely to yield

high-quality tissue is essential to ensure safe and adequate tissue sampling of the targeted site.

Indications and Contraindications

Percutaneous image-guided biopsy has become an integral part of the diagnostic workup of cancer patients. Accurate pathologic diagnosis is essential to establish a treatment plan. Molecular profiling of malignancies and identification of tumor markers are essential in the era of targeted drug therapy and personalized cancer medicine, leading to increasing demand for more robust tissue acquisition [4].

Percutaneous image-guided biopsies are also increasingly being used to obtain tissue for molecular biomarker analysis in patients participating in clinical trials. Biopsies at multiple time points may be used to determine trial eligibility, study the tumor microenvironment, and determine drug-to-target activation or mechanism of resistance [41]. Image-guided biopsies are used not only at the time of initial diagnosis but also at multiple points during management, to evaluate response to treatment, assess for residual or recurrent disease, and guide next-line therapy. In addition to its role with cancer patients, percutaneous image-guided biopsies can be used to obtain tissue from nonmalignant tissue to help establish the cause of organ dysfunction in patients with parenchymal diseases, such as in patients with liver cirrhosis, renal failure, or renal transplant rejection [45]. Percutaneous image-guided biopsy can also be used to obtain samples for microbiology analysis in cases of suspected infection [45].

There are no absolute contraindications for percutaneous image-guided biopsy, but relative contraindications include uncorrectable coagulopathy, severely compromised cardiopulmonary function or hemodynamic instability, lack of a safe approach to the target lesion, patient uncooperative or unable to tolerate positioning for the procedure, patient refusal, and pregnant patient when imaging guidance involves ionizing radiation [12].

Preprocedure Care

Prior to the procedure, a patient should undergo a thorough evaluation in order to determine if they are proper candidate for safe and successful tissue sampling. A clinical evaluation includes a detailed history and physical examination and laboratory investigations. Assessment for comorbidities such as obesity, sleep apnea, cardiac disease, and respiratory compromise is required, as these factors may affect the patient's ability to tolerate sedation or the desired positioning on the procedural table. In addition, a preprocedure clinic visit is helpful for patient education and discussions on the benefits and potential risks of the procedure. It can be beneficial

to review the imaging with the patient so that he or she has an accurate understanding of the procedural plan; this facilitates discussions on lesion size, proximity to vital organs, and relation to neurovascular structures. In addition, discussion with the medical care team provides value in assuring an adequate specimen, appropriate specimen handling, and optimal target selection [35, 36].

Routine preprocedural labs include a complete blood count, serum chemistries, and coagulation profile. Societal guidelines recommend a platelet count above 50,000/ul and an international normalized ratio (INR) less than 1.5 [28]. Depending on the relative bleeding risks and lesion location, exceptions to these thresholds are made on a case-by-case basis. Anticoagulation medication such as heparin and enoxaparin should be withheld prior to the procedure. Antiplatelet medications should also be held if possible, though again, exceptions can be made based on the relative risks of drug cessation versus the risks or periprocedural bleeding.

Procedure

Image Guidance and Selection

A wide array of modalities can be considered for image guidance during percutaneous biopsy, including ultrasonography (US), fluoroscopy, computed tomography (CT), CT fluoroscopy, magnetic resonance imaging (MRI), and positron computed tomography/computed tomography (PET/CT). Several factors affect the choice of the imaging modality, including imaging characteristics of the lesion, size and location of the lesion, physician preference, and equipment availability and cost.

Ultrasonography

US is a highly versatile imaging modality that can be used for guiding percutaneous biopsies in many different areas of the body. It is used to take biopsies not only of superficial lesions (such as breast and thyroid abnormalities, superficial soft tissue musculoskeletal masses, and superficial lymph nodes in the neck, axilla, and inguinal regions) but also for relatively deep lesions such as liver and kidney lesions, lesions involving the pancreas and spleen, bowel wall lesions, large retroperitoneal and mesenteric lesions, and occasionally pleural masses and peripheral pulmonary or mediastinal lesions in contact with the chest wall. The real-time imaging capability of US allows for continuous visualization of the needle tip as it is advanced from the skin to the target site. Additional advantages of US include relatively universal availability, portability, decreased cost, lack of ionizing radiation, multiplanar imaging allowing needle paths in virtually any plane, and flexibility with the patient

positioning [32]. Color-flow Doppler imaging can be used to identify and avoid major blood vessels in the vicinity of the target site and in the needle path [23]. Limitations to the use of ultrasound are based on ultrasound waves inability to penetrate bone and air, and hence US is not useful for visualizing and guiding needle biopsies of lesions that are located deep in the bone, aerated lung, or gas-filled bowel loops [9]. Tissue attenuation of the ultrasound beam will also limit the use of ultrasonography for deeper lesions and larger patient size.

Fluoroscopy

Although highly utilized in the past, with the development of cross-sectional imaging, the use of fluoroscopy as an image guidance modality for percutaneous biopsy has decreased. Fluoroscopy is principally used for guiding endoluminal brush or forceps biopsies of tumors or strictures of the bile duct and ureters after opacification with contrast material [17, 42] and for guiding transvenous liver or kidney biopsies [24]. Fluoroscopic guidance also plays a role in biopsy of bone lesions, especially those without a significant soft tissue component. Fluoroscopy can also be used for guiding the biopsy of pulmonary lesions; it is especially useful during biopsy of lower lobe lung lesions that move with breathing.

A fluoroscopy unit with the capability to perform frontal, oblique, and lateral angle imaging is preferred for biopsy guidance. Under fluoroscopic guidance, biopsies are typically performed under the frontal plane, while oblique and lateral projections are used to verify the position and the depth of the needle. Alternatively, the C-arm can be angled parallel to the ideal needle path, allowing a "down-the-barrel" view of the needle as it is advanced toward the target lesion.

C-arm cone beam CT (CBCT) is now more readily available in modern angiography suites. CBCT creates a three-dimensional (3D) volumetric imaging data set from multiple two-dimensional (2D) fluoroscopic projection images that are obtained in a circular trajectory (approximately 200 degrees) around the patient. Reconstructed images can be displayed in any desired plane, a useful tool that enhances the capabilities of fluoroscopic guided interventions by substantially improving needle positioning and lesion targeting [38].

The main advantage of fluoroscopic guidance is real-time visualization during needle insertion and tissue sampling. This is particularly useful when attempting to biopsy lesions that translate significantly with respiratory motion, such as lesions of the lower lobes of the lungs.

The main disadvantages of fluoroscopy include the use of ionizing radiation, limited soft tissue contrast resolution, and lack of visualization of the surrounding structures during needle advancement. Moreover, when compared to conventional CT, CBCT image quality is generally inferior, particularly when targeting a deeply seated structure within the abdomen [38].

Computed Tomography

CT guidance is a mainstay for percutaneous biopsies. As demand for CT-guided interventions has increased, the technology has evolved from both a hardware and software perspective to accommodate the needs of interventional radiologists. Ultrafast imaging and near-real-time 3D and multiplanar image reconstruction allow better procedure planning. Artifact suppression techniques improve target visualization by minimalizing needle artifacts. Wide-bore gantry openings up to 85 cm provide better patient access for the interventional radiologist during the procedure. In addition, modern interventional CT units have been constructed to achieve the requisite image quality while diminishing the dose of ionizing radiation to the patient [9].

During CT-guided biopsies, intermittent imaging is performed after each needle advancement or manipulation. This allows confirmation of the needle insertion along the desired path. CT-guided biopsies are typically performed in true axial planes. The operator, therefore, must be conscious with regard to the craniocaudal angulation of the needle, as this dimension is not captured on a single axial image. The craniocaudal extent can be detected on sequential CT images, and the needle can be adjusted accordingly. Alternatively, CT gantries do allow a small degree of craniocaudal angulation, which can be useful to image in a plane parallel to the planned needle path [43].

A key feature of CT guidance is high-spatial and high-contrast resolution. This offers several advantages: (a) visualization of the adjacent vital structures, allowing safe planning of the biopsy needle path; (b) accurate needle tip localization; (c) target lesion characterization, facilitating sample from viable portions of the lesion and avoiding areas of necrosis or cystic degeneration; and (d) application of image guidance for biopsying virtually any part of the body, including small abdominal and intrathoracic masses that cannot be visualized by US or fluoroscopy. Another advantage to the use of CT guidance is the relatively shorter learning curve compared to ultrasound-guided biopsies [9].

Limitations of CT imaging guidance include lack of real-time imaging and the use of ionizing radiation. In addition, attenuation differences between normal tissue and lesions may be insufficient to differentiate on the non-contrast CT images, making visualization of the lesion difficult and can result in off-target sampling.

Computed Tomography Fluoroscopy

CT fluoroscopy is an effort to combine the main advantages of CT and fluoroscopy: the high-spatial and high-contrast resolution of CT with the real-time imaging of fluoroscopy. CT fluoroscopy images are displayed in near real-time on a monitor inside the procedure room to provide almost instantaneous feedback to the radiologist.

CT fluoroscopy is commonly used for targeting mobile lesions, such as pulmonary nodules in the lower lobes that translate significantly with respiratory motion. With its near-real-time imaging capability, CT fluoroscopy allows the operator to time the needle insertion with the patient's respiratory movements while avoiding interposed structures like the ribs. High technical success rates, shorter procedure times, and fewer needle punctures have been reported in several studies investigating the use of CT fluoroscopy guidance when biopsying pulmonary lesions [16]. CT fluoroscopy also can be a useful tool for biopsying liver lesions, particularly masses close to the diaphragm, as well as abdominopelvic lesions with difficult access that require precise needle advancement [31].

The main disadvantage to CT fluoroscopy is higher radiation exposure not only to the patient but in particular to the interventional radiologist compared to conventional CT-guided interventions [16]. This can be reduced by using needle-holder or forceps to increase the distance between the CT beam and the operator's hands [16]. Up to 98% reduction in the hand dose have been reported [16]. Alternatively, intermittent use of CT fluoroscopy between incremental needle advancements can be performed. In addition, sterile lead gloves and lead eyewear can be worn to reduce radiation exposure.

Magnetic Resonance Imaging

MRI is a valuable "problem-solving" modality for biopsy image guidance. It offers better soft tissue contrast than CT or US, and this plays an important role in biopsying lesions that cannot be visualized by other imaging modalities. Examples include bone and soft tissue lesions and liver lesions. MRI can also characterize areas of necrosis within a tumor, providing useful information to select the ideal location within the tumor to maximize tissue sample quality [29]. Also, exquisite delineation of the vascular anatomy without the use of intravenous contrast medium is useful in minimizing the risk of hemorrhage.

In addition, MR images can be acquired at any obliquity, and thus imaging planes truly parallel or orthogonal to the biopsy trajectory can be readily obtained. This can be very helpful when sampling lesions in difficult locations, such as tumors in the dome of the liver [29] or head and neck lesions. While metal needles can cause susceptibility artifacts, the use of pulse sequences that minimize this artifact can provide better identification of target lesions than do CT images degraded by beam hardening artifacts. Lack of ionizing radiation makes the MRI a highly desirable image guidance modality in the pediatric and obstetric patient population. The development of ultrafast imaging sequences makes the MRI a practically real-time imaging modality. Also, new open-configuration MRI systems provide a more comfortable experience for claustrophobic patients.

Major limitations of using MRI as an image guidance modality in interventional procedures include the availability and cost of the MRI units compared to ultrasound and CT. MRI-compatible patient monitors and biopsy equipment are also

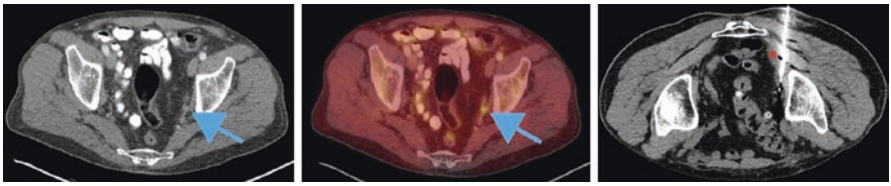

Fig. 18.1 A small pelvic lymph node was identified on a conventional contrast-enhanced CT in a patient with prostate cancer (left). Despite the lymph node's small size, the lesion was found to be radiotracer-avid on a fluciclovine PET scan (middle). Targeted biopsy was performed (right), confirming the presence of metastatic disease

required. MRI-compatible titanium needles are reported to have a lower quality than their stainless-steel counterparts [44].

Positron Emission Tomography/Computed Tomography

Functional imaging with PET using 2-fluorodeoxyglucose (FDG) as well as other new radiotracers including fluciclovine, gallium-68 dotatate, and gallium-68 PSMA is an invaluable tool for cancer patients [30] (Fig. 18.1). Reviewing FDG-PET data prior to a biopsy can not only help identify the location of a tumor within the body but also determine where viable tissue resides within a particular lesion. Some institutions have demonstrated the possibility of FDG-PET/CT-guided interventions, taking the functional advantage of the PET data and the anatomical advantage of CT in the same setting [30].

Navigation Techniques and Guidance Systems

Navigation techniques and guidance systems that bring preprocedure imaging into the procedure room are commonly employed in a variety of surgical specialties, including neurosurgery, orthopedics, and otolaryngology. They are also expanding the boundaries of minimally invasive procedures such as bronchoscopy. Navigation technologies provide multiple advantages over conventional image guidance approaches. Rather than relying on intermittent visualization of a biopsy needle during a CT-guided intervention, a proceduralist using navigation technology can view a tracked needle in real time and in three dimensions. Furthermore, multiple imaging modalities can be coregistered to provide real-time overlays; in this manner, for example, functional images from the preprocedure diagnostic scan (e.g., PET data) can be superimposed upon the procedural anatomic images (e.g., CT) to improve target visualization [20].

Device-tracking navigation systems function by registering imaging data with fixed points in real space. By recognizing fiducials attached to superficial anatomic landmarks on the patient's skin, navigation systems transform actual patient information to imaging coordinates that can be viewed in three dimensions and in real time. Navigation technologies commonly use either optical or electromagnetic tracking (e.g., PercuNav Image Fusion and Instrument Navigation, from Philips Healthcare, Cleveland, Ohio, and Veran Medical Technologies Inc., from St. Louis, Missouri) to perform image registration. With current technology, electromagnetic sensors can be miniaturized to fit within needles as small as 22 gauge and certainly applicable to percutaneous biopsy procedures [39]. Clinical trials have demonstrated a high level of accuracy with electromagnetic-based navigation systems used in both US and CT-guided biopsies [20].

Moreover, once a patient's anatomy in real space has been mapped to imaging space, then theoretically any available imaging studies can be coregistered to provide multimodality image fusion. For example, if the target lesion was best identified on a preprocedure PET study, these data can be superimposed upon the intraprocedural images in real time and with a high level of anatomic accuracy.

Techniques

Percutaneous Biopsy Techniques

Fine Needle Aspiration Biopsy

The goal of a fine needle aspiration is to acquire individual cells for cytologic analysis. The needles used for this procedure are high-gauge, non-coring needles. Once the needle is positioned within the target lesion, rapid, short excursions of the needle are performed to obtain the aspirate. This motion can be performed while creating negative pressure using a syringe applied to the hub. The syringe is disconnected from the hub prior to removing the needle from the tissue to avoid blood filling the syringe or aspiration of the cells into the syringe.

Some operators prefer to avoid using a syringe attached to the needle with negative pressure applied to the plunger to minimize the blood or background clot in the sample. Several studies have reported that adequate samples can be obtained without the need of the syringe's negative pressure [14]. Without a syringe, sampling depends on capillary motion of cells into the small needle. There is some evidence to suggest that negative pressure aspiration results in a more cellular aspirate without significantly increased bleeding compared to capillary sampling [14]. Alternatively, self-aspirating FNA needles are also available; these needles apply minimal suction through an internal diaphragm, eliminating the need to have the syringe at the needle hub [26].

Core Needle Biopsy

The goal of core needle biopsy is to obtain tissue for histological analysis. The needles used for this procedure are low-gauge, cutting needles. Cutting needles can be subdivided into end-cutting and side-cutting needles. Side-cutting needles are the more commonly used core biopsy system. When performing the biopsy, the inner stylet is advanced into the target lesion, followed by forward movement of the outer cannula-trapping tissue in the stylet tray [22].

Single Needle Technique

The single needle biopsy technique is the most conceptually straightforward biopsy method. In this technique, a single biopsy needle is advanced into the target lesion, and after a single sample is obtained, the needle is withdrawn. The limitation of this approach is that a single sample may not provide adequate tissue for analysis. Particularly in the contemporary era of molecular assays, multiple samples are usually required; thus, with a single needle technique, multiple needle passes must be performed. Every single pass necessitates imaging guidance from the skin entry site down to the level of the target lesion. This consequently adds procedure time and increases the radiation dose if CT or fluoroscopy is used as the imaging guidance modality. In addition, the risk of complications and patient discomfort increases each time the operator inserts the needle [11]. Single needle technique is usually reserved for very superficial lesions sampled under US guidance (e.g., cervical lymph nodes or thyroid nodules).

Tandem Needle Technique

In the tandem needle technique, a small-caliber needle is advanced down to the level of the target lesion under image guidance. Following this, without imaging guidance, multiple needles are inserted alongside and parallel to the initially placed needle. The major limitation of this technique is the inability to control the needle tip for additional needles. Also, this technique requires multiple skin punctures. On the other hand, it shortens the procedure time and minimizes the ionizing radiation exposure if CT or fluoroscopy is used [11].

Coaxial Needle Technique

The coaxial needle technique is the most commonly performed method of percutaneous tissue sampling. A hollow-bore introducer needle with a sharp stylet is advanced incrementally under image guidance into or adjacent to the target lesion. Subsequently, the stylet is removed, and the biopsy needles (either aspiration or cutting needles) are inserted in a coaxial manner through the introducer needle and into

the lesion. The introducer needle must have a larger caliber than the biopsy needle (e.g., a 17-gauge introducer needle is needed to obtain 18-gauge core biopsy samples). This technique allows multiple tissue samples to be acquired without increasing the risk of complications and without causing extra discomfort to the patient [9].

One drawback of this technique is that each successive sample is acquired from essentially the same location as the one before it. This results in not only progressively lower-quality tissue samples with each additional pass, but also potentially an inaccurate reflection of tumoral heterogeneity. That is, since only one area of a tumor is sampled, the possible variability in tumoral tissue across the whole lesion is not represented. This can have substantial implications, particularly for patients on molecularly targeted therapies, for whom specific mutational patterns are being investigated. Because a tumor's mutational status is not homogenous within a single lesion, this biopsy technique can potentially yield misleading results.

Several strategies have been developed to avoid this potential shortcoming. One solution is an introducer needle with a side hole near its tip through which a 25-gauge aspiration needle can exit [19]. Rotational movement of the guide needle with successive sampling allows access to different portions of the lesion. However, cutting needles cannot be introduced through this guide needle.

An alternative strategy is to apply a gentle curve on the aspiration needle prior to its placement into the introducer needle [10]. Side-cutting core biopsy needles can be shaped in a similar manner, allowing sampling of different portions of the tumor [33]. However, care must be taken when advancing or removing curved needles within the introducer needle. Increased resistance is felt while advancing the needle in the cannula until the tip exits from its end. The position of the tip of the guiding cannula may change with the excessive pressure that may be needed to overcome this resistance. Similarly, during removal of a curved tip biopsy needle, the tip of the guided needle may be changed. The interventional radiologist should fix the introducer needle in position during removal of the biopsy needle; otherwise, the curved-tip biopsy needle may pull back the guide needle during its withdrawal.

Finally, another alternative strategy is redirecting the introducer needle. Torqueing the needle in different directions will redirect the tip of the needle, allowing sampling from different portions of the lesion. However, the stiffness of the needle, depth of the lesion, and the nature of the intervening tissue are important factors contributing to the success of this strategy.

Many coaxial biopsy introducer sets come with both sharp- and blunt-tipped stylets. The blunt stylet is particularly useful when navigating the introducer needle beyond bowel loops or vascular structures to reach the target lesion; this commonly occurs when approaching deep abdominal lesions such as lymph nodes at the root of the mesentery [5]. The sharp introducer is used to gain access into the abdominal cavity. Subsequently, the sharp introducer is exchanged for the blunt-tipped stylet. The needle is then advanced incrementally, bluntly dissecting without cutting its way down to the target. This technique avoids the injury of the adjacent bowel or vasculature [5].

A modified coaxial needle technique has been created with the development of the vanSonnenberg needle. A 23-gauge needle with a removable hub is advanced

into the lesion. After adequate positioning of the needle, the hub is detached, and a 19-gauge needle is advanced over the 23-gauge needle, which is then removed. The 19-gauge needle is used as a guiding cannula, through which aspiration or cutting needles are inserted in a coaxial fashion [40].

Transvenous Biopsy Technique

The transvenous hepatic biopsy technique was developed for nontargeted sampling of liver parenchyma in high-risk patients, including those with ascites or uncorrectable coagulopathy [8]. Using a transjugular approach, access is obtained via the right jugular vein. The multipurpose 5-Fr catheter and a soft wire are used to select the right hepatic vein. The soft wire is exchanged for a stiff wire, over which a 9-Fr sheath is advanced to the level of the hepatic vein. This provides stable access into the hepatic vein.

Next, a 7-Fr metal cannula is advanced into the right hepatic vein. A 60-cm side-cutting, semiautomatic biopsy needle is introduced coaxially through the stiff cannula, which is then rotated anteriorly to obtain tissue samples. Multiple samples can be obtained using this technique. Caution should be taken, as the stiff cannula can move with the respiratory movements and disengage from the hepatic vein. We recommend exerting gentle forward pressure on the stiff cannula to avoid its displacement into the inferior vena cava (IVC). Although the right jugular vein is preferred, a left jugular vein approach can also be used. In addition, some authors have described a femoral approach to the hepatic veins when neck vein access is not available [37].

The right hepatic vein is the most common site from which to perform transvenous liver sampling, as typically there is abundant liver parenchyma anterior to this vein. The left and middle hepatic veins are alternative options. Regardless of which vein is selected, it is imperative that the interventionalist be aware of which vein has been selected and adjust the metal cannula in the appropriate direction to minimize the risk of capsular penetration.

Transvenous sampling of the renal parenchyma can be performed in a similar manner. The transjugular renal biopsy set is similar to the transjugular liver biopsy set, with some modifications. A 5-Fr selective catheter is used to select the right renal vein, as this vein is preferable due to the more favorable angle offering for easier selection. A subcortical vein in the lower pole is then selected. Contrast injection is used to confirm adequate positioning of the catheter. The needle is then introduced, and the stiff cannula is directed laterally and posteriorly. Multiple samples (up to five) can be obtained [24].

Endoluminal Biopsy Technique

Endoluminal lesions affecting the bile ducts or ureters can be biopsied by flexible forceps or brush biopsy devices [17, 42]. After traversing the lesion using a guidewire, an introducer sheath is advanced just beyond the stricture. A 5-Fr catheter

containing the unexposed biopsy brush is then advanced in a coaxial fashion through the sheath. The sheath is then pulled back after adequate positioning of the biopsy device within the housing catheter at the target site. The 5-Fr catheter is then retracted to expose the brush. Multiple to-and-fro movements at the target site are performed to abrade the epithelium of the target stricture and trap cells within the bristles of the brush. The brush is then pulled back inside the housing catheter, and the whole set is removed as one unit, while the sheath maintains access. The brush can be used to prepare touch preps or rinsed in saline for cytological evaluation.

Differences Between Fine Needle Aspirate and Core Biopsy

Percutaneous needle biopsy (PNB) is a minimally invasive technique used to obtain sample tissue or cells for diagnosis. The two basic techniques for sample acquisition include fine needle aspiration (FNA) and core biopsy (CB). FNA by convention utilizes a needle with a diameter of 22 gauge or higher, which is inserted into a region of interest to extract cells for cytologic evaluation. In some instances, a larger needle (21-gauge or 18-gauge) is used, such as for endobronchial ultrasound-guided transbronchial needle aspiration or endoscopic ultrasound-guided FNA (EUS-FNA). CB is the use of a needle with a diameter of 20-gauge or lower that is inserted into a region of interest to extract a tissue sample for histologic evaluation or molecular/genetic profiling.

FNA and CNB each have their own advantages and disadvantages as summarized in Tables 18.1 and 18.2. The interventional radiologist should be familiar with the specimen handling and institution protocols as this can impact the method of acquisition (FNA vs CB) and ultimately the yield of the biospecimen. Sampling

Table 18.1 Indications for percutaneous biopsy

Establish the benign or malignant nature of a lesion
Obtain samples for microbiologic analysis in patients with known or suspected infections
Stage patients with known or suspected malignancy when local spread or distant metastasis is suspected
Determine the nature and extent of diffuse parenchymal diseases (e.g., hepatic cirrhosis, renal transplant rejection, glomerulonephritis)
Obtain tissue for biomarker, protein, or genotype analysis to subsequently guide therapy
Determine the primary cell of origin in a patient with metastatic disease and an unknown primary tumor

Table 18.2 Relative contraindications for percutaneous biopsy

Significant coagulopathy that cannot be adequately corrected
Severely compromised cardiopulmonary function or hemodynamic instability
Lack of a safe pathway to the lesion
Inability of the patient to cooperate with the positioning required for the procedure
Patient refusal of biopsy
Pregnant patient when imaging guidance involves ionizing radiation

requirements may vary depending on the indication for biopsy; however, performing both FNA and CB of the same lesion has been shown to increase yield over FNA alone for both benign and malignant lesions, with core biopsies providing more tissue for immunohistochemical testing [12]. On-site immediate assessment of sampling adequacy by cytopathology may improve diagnostic yield [12], although this practice may not be standard or feasible at every institution. For fibrotic or densely sclerotic lesions, FNA is often unable to acquire samples, and a core biopsy is required (Fig. 18.2).

On the other hand, given that an FNA requires higher gauge needles and does not remove a macroscopic volume of tissue, FNA is often preferred over core biopsy in higher-risk locations (Fig. 18.3).

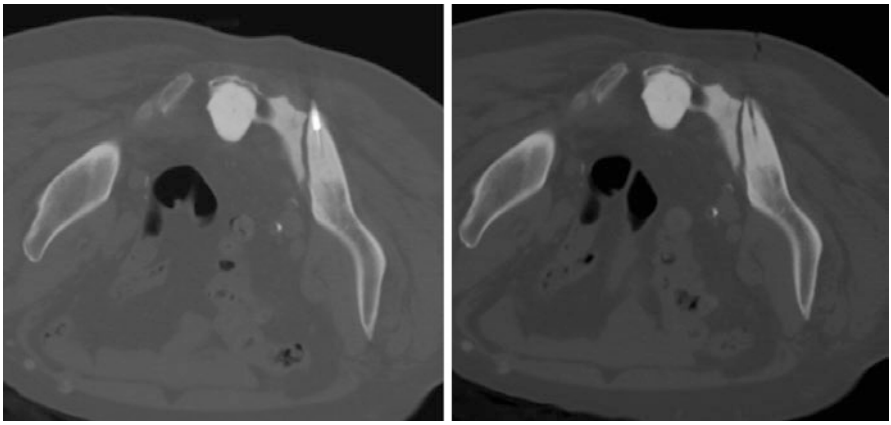

Fig. 18.2 Core biopsy of a sclerotic bone metastasis from prostate cancer. Preprocedure (left) imaging demonstrates multiple sclerotic metastases in the pelvis. Given the density of these lesions, FNA would be unable to acquire samples, and a core biopsy is required. Postprocedure imaging (right) reveals the deficit in the lesion from which the core tissue was acquired

Fig. 18.3 For a patient with a lesion in the retropharyngeal space, FNA alone (blue arrow shows FNA needle trajectory) was preferred over core biopsy for safety considerations

Good Practice to Optimize Outcomes

Postprocedure Management

After the procedure, patients should be observed in a monitored care unit where recovery from sedation can be documented, post-biopsy adverse events can be assessed, and vital signs can be continuously monitored. For transthoracic biopsies, postprocedure care should involve imaging assessment for pneumothorax. While practices vary across institutions, at the minimum this requires observation and imaging with chest radiographs to evaluate for pneumothorax.

Complications

Complications following percutaneous biopsy can be generally divided into general and organ specific. General complications include bleeding, infection, damage to surrounding structures (e.g., nerves and vessels), as well as organ injury [18]. In general, clinically significant bleeding is infrequent; however, the risk of bleeding increases with increasing needle caliber, use of cutting needles, and vascularity of the organ or lesion biopsied [12]. Infection as a result of biopsy is rarely seen. Injury may occur to the target or adjacent intervening organ along the pathway of the needle, although less than 2% of patient with this type of injury require further intervention [12].

Organ-specific complications are unique to the particular organ being biopsied. For example, pneumothorax is associated with lung or mediastinal biopsy. Other examples of organ-specific complications are hemoptysis after pulmonary biopsy and hematuria after renal biopsy (Fig. 18.4).

Several maneuvers and devices have been investigated as adjunctive steps to reduce postprocedure complication rates. Examples include using blood patches,

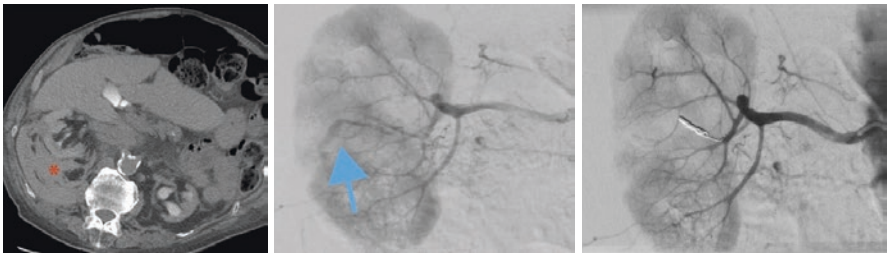

Fig. 18.4 A renal biopsy was performed in a patient to under ultrasound guidance. The patient developed symptomatic hypotension within 30 minutes of the biopsy. CT scan revealed a large perinephric hematoma (left, asterisk). Immediate angiography demonstrated evidence of acute hemorrhage (middle, arrow). The culprit artery was successfully embolized with microcoils (right)

gelatin sponge, and self-expanding plugs [12] to reduce pneumothorax and/or chest tube rates following lung biopsies.

According to the Society of Interventional Radiology (SIR) quality improvement guidelines for percutaneous needle biopsy, complications should be categorized as either minor or major [12]. Minor complications include those that do not have any consequences, with or without nominal therapy. Major complications include those that require therapy and hospital admission and/or cause permanent adverse effects or death.

Outcome and Results

Patient selection, procedure technique, patient monitoring, and postprocedure management all contribute to the outcome of the procedure. Several variables affect the biopsy success rate, including the size of the lesion, the organ to be biopsies, the nature of the lesion (benign versus malignant), the number of samples, the availability and experience of the cytopathologist, the availability of imaging modalities used for guidance, and the skill and experience of the interventionalist. The overall technical success rate of percutaneous needle biopsy is high (approximately 70–90%) [12]. The technical success rate reported for sampling thoracic/pulmonary lesions is 77–96% [12]. A technical success rate of up to 93% has been reported for sampling musculoskeletal lesions [12].

More important than the technical success rate, however, is the diagnostic yield of the tissue sample. The acquired tissue sample must be able to address the clinical question that motivated the biopsy. Obtaining an appropriate tissue sample can be a challenging task for the interventional radiologist, especially with small, deep-seated lesions. It is imperative for the radiologist to be familiar with the most up-to-date sampling techniques and imaging modalities as well as communicating expectations to the treatment team. As biopsies become integral in clinical trial needs for personalized cancer medicine, the importance for the diagnostic yield and high-quality of the tissue sample is paramount.

Liquid Biopsy

While percutaneous image-guided biopsies are used to obtain samples for cytologic or histologic analysis by invasive means, “liquid biopsies” provide the opportunity to characterize tumor in a noninvasive fashion through sampling blood or other bodily fluids. While the use of blood-based protein biomarkers (e.g., prostate-specific antigen [PSA] and cancer antigen 125 [CA-125]) and DNA biomarkers (e.g., PCR testing for BCR-ABL transcripts in chronic myeloid leukemia) is established in routine oncologic care for disease monitoring, liquid biopsy techniques are continuing to expand, including DNA-based assays such as circulating tumor DNA

(ctDNA), cellular techniques such as circulating tumor cells (CTCs), and extracellular structures such as exosomes [13].

The advantages of liquid biopsy with ctDNA over percutaneous image-guided biopsy include the ability to sample tumor heterogeneity, as liquid biopsies contain DNA fragments that are released from the entire tumor and include metastatic sites. Additional advantages include noninvasive methodology, ease of obtaining serial samples, lower risk, lower cost, and less pain [32]. In addition, it has been proposed as a tool to monitor response and resistance to therapy, as well as to direct targeted therapy, for example, by monitoring the development of defined resistance mutations such as EGFR T790M in adenocarcinoma of the lung [15]. Liquid biopsy has also been shown to provide information regarding tumor burden in patients with lung, breast, colon, skin, and prostate cancers [27]. Circulating tumor cells (CTCs), on the other hand, benefit from the preservation of cellular structures, which permits evaluation of cell surface markers and assessment of nuclear or cytoplasmic localization of proteins.

Disadvantages of liquid biopsy using either ctDNA or CTCs include variations in levels among patients, which may compromise the sensitivity, accuracy, and reliability of the tests [25]. The level of ctDNA or CTC depends on a variety of factors, such as the cancer stage, tumor vascularization, tumor burden, metastatic potential of cancerous cells, and apoptosis rate [6, 7]. Variations that occur in ctDNA or CTC levels with disease burden and stage suggest that some patients suffering from the early-stage disease will not have sufficient material to facilitate accurate testing [27]. Cost remains a barrier to widespread adoption of these liquid biopsy techniques, and validation in prospective clinical studies remains essential for their development and integration into routine clinical practice [1].

Exosomes represent a novel frontier of liquid biopsies. Exosomes are extracellular vesicles secreted by nearly all mammalian cells through the fusion of bodies with plasma membrane (Kim et al., Molecular & Cellular Toxicology 2018). Exosomes serve to protect molecular components such as microRNAs and proteins from enzymatic degradation, allowing for interrogation of disease biology.

As liquid biopsy techniques continue to develop, there is high potential for integration into routine clinical practice, although prospective clinical studies are warranted for validation of these approaches as clinical biomarkers. For now, liquid biopsies remain a valuable adjunct to percutaneous image-guided biopsy but will not replace them. Indeed, as new technologies emerge, interventional radiology will continue to play a role in obtaining liquid biopsies, such as through selective acquisition via tumor draining veins.

Summary

Percutaneous image-guided biopsies have long been a vital diagnostic tool, predominantly used for the initial diagnosis, staging, and surveillance of cancer. In the era of personalized cancer medicine, the importance of image-guided biopsies will

continue to increase. A comprehensive understanding of recent advancements in imaging guidance modalities, technical considerations, and best practices for biopsy technique all increase the likelihood of a safe and effective biopsy.

References

1. Ameth B. Updates on the types and usage of liquid biopsies in the clinical setting: a systematic review. BMC Cancer. 2018;18:527.
2. Basik M, Aguilar-Mahecha A, Rousseau C, et al. Biopsies: next generation biospecimens for tailoring therapy. Nat Rev Clin Oncol. 2013;10:437–50.
3. Chen PL, Roh W, Reuben A, et al. Analysis of immune signatures in longitudinal tumor samples yields insight into biomarkers of response and mechanisms of resistance to immune checkpoint blockade. Cancer Discov. 2016;6(8):827–37.
4. Clark DP. Seize the opportunity: underutilization of fine needle aspiration biopsy to inform targeted cancer therapy decisions. Cancer. 2009;117(5):289–97.
5. de Bazelaire C, Farges C, Mathieu O, et al. Blunt-tip coaxial introducer: a revisited tool for difficult CT-guided biopsy in the chest and abdomen. Am J Roentgenol. 2009;193(2):W144–8.
6. Diaz LA, Bardelli A. Liquid biopsies: genotyping circulating tumor DNA. J Clin Oncol Off J Am Soc Oncol. 2014;32(6):579–86.
7. Diehl F, Schmidt K, Choti MA, Romans K, Goodman S, Li M, et al. Circulating mutant DNA to assess tumor dynamics. Nat Med. 2008;14(9):985–90.
8. Gamble P, Colapinto RF, Stronell RD, Colman JC, Blendis L. Transjugular liver biopsy: a review of 461 biopsies. Radiology. 1985;157(3):589–93.
9. Gupta S. Role of image-guided percutaneous needle biopsy in cancer staging. Semin Roentgenol. 2006;41(2):78–90.
10. Gupta S, Ahrar K, Morello FA Jr, Wallace MJ, Madoff DC, Hicks ME. Using a coaxial needle with a curved inner needle for CT-guided fine needle aspiration biopsy. Am J Roentgenol. 2002;179(1):109–12.
11. Gupta S, Madoff DC. Image-guided percutaneous needle biopsy in cancer diagnosis and staging. Tech Vasc Interv Radiol. 2007;10(2):88–101.
12. Gupta S, Wallace MJ, Cardella JF, et al. Quality improvement guidelines for percutaneous needle biopsy. J Vasc Interv Radiol. 2010;21(7):969–75.
13. Heizter E, Perakis S, Geigi J, Speicher MR. The potential of liquid biopsies for the early detection of cancer. NPJ Precis Oncol. 2017;1:36.
14. Hopper KD, Grenko RT, Fisher AI, Tenhave TR. Capillary versus aspiration biopsy: effect of needle size and length on the cytopathological specimen quality. Cardiovasc Intervent Radiol. 1996;19(5):341–4.
15. Ilie M, Hofman V, Long E, et al. Current challenges for detection of circulating tumor cells and cell-free circulating nucleic acids, and their characterization in non-small cell lung carcinoma patients. What is the best blood substrate for personalized medicine? Ann Trans Med. 2014;2(11):107.
16. Irie T, Kajitani M, Yoshioka H, et al. CT fluoroscopy for lung nodule biopsy: a new device for needle placement and a phantom study. J Vasc Interv Radiol. 2000;11(3):359–64.
17. Jung GS, Huh JD, Lee SU, Han BH, Chang HK, Cho YD. Bile duct: analysis of percutaneous transluminal forceps biopsy in 130 patients suspected of having malignant biliary obstruction. Radiology. 2002;224(3):725–30.
18. Kim KW, Kim MJ, Kim HC, et al. Value of “patent track” sign on Doppler sonography after percutaneous liver biopsy in detection of postbiopsy bleeding: a prospective study in 352 patients. Am J Roentgenol. 2007;189(1):109–16.

19. Kopecky KK, Broderick LS, Davidson DD, Burney BT. Side-exiting coaxial needle for aspiration biopsy. Am J Roentgenol. 1996;167(3):661–2.
20. Krucker J, Xu S, Glossop N, et al. Electromagnetic tracking for thermal ablation and biopsy guidance: clinical evaluation of spatial accuracy. J Vasc Interv Radiol. 2007;18(9):1141–50.
21. Lee JM, Han JJ, Altwerger G, Kohn EC. Proteomics and biomarkers in clinical trials for drug development. J Proteome. 2011;74(2):3632–41.
22. Littlewood ER, Gilmore IT, Murray-Lyon IM, Stephens KR, Paradinas FJ. Comparison of the Trucut and Surecut liver biopsy needles. J Clin Pathol. 1982;35(7):761–3.
23. Longo JM, Bilbao JI, Barettino MD, et al. Percutaneous vascular and nonvascular puncture under US guidance: role of color Doppler imaging. Radiographics. 1994;14(5):959–72.
24. Mira S, Gyamlani G, Swaminathan S, et al. Safety and diagnostic yield of transjugular renal biopsy. J Vasc Interv Radiol. 2008;19(4):546–51.
25. Molina-Vila MA, Mayo-de-las-Casas C, Gimenez-Capitan A, Jordana-Ariza N, Garzon M, Balada A, et al. Liquid biopsy in non-small cell lung cancer. Front Med. 2016;3:69.
26. Monsein LH, Kelsey CA, Williams WL, Olson NJ. Fine needle biopsy without syringe aspiration. Cardiovasc Intervent Radiol. 1993;16(1):11–3.
27. Newman AM, Bratman SV, To J, Wynne JF, Eclov NC, Modlin LA, et al. An ultrasensitive method for quantitating circulating tumor DNA with broad patient coverage. Nat Med. 2014;20(5):548–54.
28. Patel IJ, Davidson JC, Nikolic B, et al. Consensus guidelines for periprocedural management of coagulation status and hemostasis risk in percutaneous image-guided interventions. J Vasc Interv Radiol. 2012;23(6):727–36.
29. Schmidt AJ, Kee ST, Sze DY, et al. Diagnostic yield of MR-guided liver biopsies compared with CT- and US-guided liver biopsies. J Vasc Interv Radiol. 1999;10(10):1323–9.
30. Schwartz DL, Ford E, Rajendran J, et al. FDG-PET/CT imaging for preradiotherapy staging of head and neck squamous cell carcinoma. Int J Radiat Oncol Biol Phys. 2005;61(1):129–36.
31. Schweiger GD, Yip VY, Brown BP. CT fluoroscopic guidance for percutaneous needle placement into abdominopelvic lesions with difficult access routes. Abdom Imaging. 2000;25(6):633–7.
32. Sheafor DH, Paulson EK, Simmons CM, Delong DM, Nelson RC. Abdominal percutaneous interventional procedures: comparison of CT and US guidance. Radiology. 1998;207(3):705–10.
33. Singh AK, Leeman J, Shankar S, Ferrucci JT. Core biopsy with curved needle technique. Am J Roentgenol. 2008;191(6):1745–50.
34. Tam AL, Lim HJ, Wistuba II, Tamrazi A, Kuo MD, Ziv E, et al. Image-guided biopsy in the era of personalized cancer care: proceedings from the Society of Interventional Radiology Research Consensus Panel. J Vasc Interv Radiol. 2016;27(1):8–19.
35. Taslakian B, Georges Sebaaly M, Al-Kutoubi A. Patient evaluation and preparation in vascular and interventional radiology: what every interventional radiologist should know (part 1: patient assessment and laboratory tests). Cardiovasc Intervent Radiol. 2016;39(3):325–33.
36. Taslakian B, Sebaaly MG, Al-Kutoubi A. Patient evaluation and preparation in vascular and interventional radiology: what every interventional radiologist should know (part 2: patient preparation and medications). Cardiovasc Intervent Radiol. 2016;39(4):489–99.
37. Teare JP, Watkinson AF, Erb SR, et al. Transfemoral liver biopsy by forceps: a review of 104 consecutive procedures. Cardiovasc Intervent Radiol. 1994;17(5):252–7.
38. Wallace MJ, Kuo MD, Glaiberman C, et al. Three-dimensional C-arm cone-beam CT: applications in the interventional radiology suite. J Vasc Interv Radiol. 2009;20(7 Suppl):S523–37.
39. Wood BJ, Locklin JK, Viswanathan A, et al. Technologies for guidance of radiofrequency ablation in the multimodality interventional suite of the future. J Vasc Interv Radiol. 2007;18(1 Pt 1):9–24.
40. van Sonnenberg E, Lin AS, Casola G, Nakamoto SK, Wing VW, Cubberly DA. Removable hub needle system for coaxial biopsy of small and difficult lesions. Radiology. 1984;152(1):226.

41. Vieillard MH, Boutry N, Chastanet P, Duquesnoy B, Cotten A, Cortet B. Contribution of percutaneous biopsy to the definite diagnosis in patients with suspected bone tumor. Joint Bone Spine. 2005;72(1):53–60.
42. Xing GS, Geng JC, Han XW, Dai JH, Wu CY. Endobiliary brush cytology during percutaneous transhepatic cholangiodrainage in patients with obstructive jaundice. Hepatobiliary Pancreat Dis Int. 2005;4(1):98–103.
43. Yueh N, Halvorsen RA Jr, Letourneau JG, Crass JR. Gantry tilt technique for CT-guided biopsy and drainage. J Comput Assist Tomogr. 1989;13(1):182–4.
44. Zango S, Eichler K, Wetter A, et al. MR-guided biopsies of lesions in the retroperitoneal space: technique and results. Eur Radiol. 2006;16(2):307–12.
45. ACR. ACR–SIR–SPR practice parameter for the performance of image-guided percutaneous needle biopsy (PNB). Available from:www.acr.org/~/media/ACR/Documents/PGTS/guidelines/PNB.pdf.

Chapter 19
Tumor Profiling

Etay Ziv

Overview

Tumor profiling—the molecular characterization of an individual patient's tumor—is a rapidly evolving field in cancer medicine. It is the focus of major research efforts backed by industry, academic institutions, and governments and is increasingly at the center of clinical cancer care. A major goal of tumor profiling is to identify biomarkers that can guide clinical decisions tailored to the patient. These biomarkers make up a growing list of tools in the development of precision oncology. Spurred in part by advances in biotechnology and decreasing costs of genomic sequencing and in part by a number of successful examples of targeted therapy, tumor profiling has gained broad acceptance [1].

Conceptually the main goal for tumor profiling is to define subsets of patients into clinically meaningful categories. There are several current uses of tumor profiling in clinical oncology. Profiling can resolve diagnostic dilemmas as in the case of distinguishing between a new primary versus a metastasis or establishing the primary site of disease in tumors of undetermined primary site. Profiling can give prognostic information about aggressiveness of the disease or likelihood of recurrence. Profiling can be used to predict response in a subset of patients and therefore be used to select patients which should or should not get a targeted treatment. Finally, profiling can be used to identify mechanisms of resistance to an ongoing treatment. Most of the success stories have been in the field of medical oncology. There are some examples in surgical oncology and radiation oncology of using biomarkers to define subsets of patients requiring adjuvant therapy or patients at high risk of recurrence. But efforts to develop profiling in interventional oncology (IO) have been more limited. In this chapter, we review some of the ongoing efforts to employ tumor profiling to improve outcomes in IO and discuss some of the potential applications in IO.

E. Ziv (✉)
Department of Radiology, Memorial Sloan Kettering Cancer Center, New York, NY, USA
e-mail: zive@mskcc.org

C. Georgiades, H. S. Kim (eds.), *Image-Guided Interventions in Oncology*,
https://doi.org/10.1007/978-3-030-48767-6_19

Assays

Initial efforts in molecular profiling of tumors were focused on single oncogenic driver genes. An early example is in chronic myeloid leukemia with the discovery of the Bcr-Abl gene fusion that results in a constitutively active BCR/ABL tyrosine kinase and that is exquisitely sensitive to an inhibitor of the kinase [2]. In lung cancer, tumors with mutations in the epidermal growth factor receptor (Egfr) gene were responsive to EGFR inhibitors [3]. As the number of actionable targets expanded and sequencing costs decreased, multi-gene assays were developed. Much of the current clinical effort has focused on alterations in tumor DNA. This is likely in part historical as the earliest successes of biomarkers in precision oncology were identified in patients with genetic alterations; and in part technical, as DNA is a more stable molecule and easier to recover from tissue samples. More recently, tumor profiling is expanding to other molecular changes in the tumor (mRNA, proteins, metabolites) as well as the tumor microenvironment, the host, tumor histopathology, and even broader, radiomic features of the tumor and host. As clinical oncology reaches an asymptote of identified subsets of actionable gene mutations, multimodal profiling (combining information about mutations and mRNA or protein expression, or even imaging features) is also likely to play a larger role.

Utility of Tumor Profiling in IO

There are several important areas where tumor profiling may make significant impacts in IO. First, IO encompasses multiple tumoricidal modalities, including ischemia-based trans-arterial embolization (TAE) or chemoembolization (TACE), radiation-based trans-arterial radio-embolization (TARE) and heat-based microwave ablation, radiofrequency ablation, and cryoablation. It is likely that some tumors may have developed different resistant mechanisms for each of these stressors and therefore have different capacities to survive these stressors (e.g., degree of ischemia-resistance versus radiation-resistance may be different in different tumors). Second, defining mechanisms of resistance to a stressor can also establish appropriate adjuvants that can be used to overcome the resistance mechanism. Third, treatment-sensitive signaling pathways may be histology agnostic so that rather than treating tumors of a particular histology, IO therapies can be used on any tumor with the appropriate "treatment-sensitive" profile. This approach is analogous to basket trials in medical oncology where a therapy is targeted to a biomarker, independent of the tumor of origin [4].

In the next sections, we review some of the ongoing efforts to incorporate tumor profiling in IO. We organize this section by histology rather than by treatment modality.

Hepatocellular Carcinoma Hepatocellular carcinoma (HCC) is a heterogeneous disease defined by multiple molecular subclasses [5, 6]. Multiple attempts to establish a molecular classification for HCC have been proposed. Based on transcriptome

data, Boyault et al. defined six subgroups (G1-G6) [6]. Genomic studies revealed several common driver pathways including Wnt/B-catenin, telomere maintenance, oxidative stress, and PI3K/AKT/mTOR [5]. From these studies two broad classes of HCCs have emerged, proliferative and non-proliferative, which correspond to aggressive and nonaggressive tumors, respectively [7]. Despite these efforts, there are no predictive biomarkers in HCC that can be used to guide treatment.

HCC Profiling and IO There have been several efforts to correlate HCC molecular subclasses with outcomes in IO, although these have mostly been limited to very small cohorts. Gaba et al. correlated tumor response to TACE with mRNA expression using a microarray panel of 60 genes associated with chemotherapy-sensitivity, hypoxia, mitosis, and inflammation [8]. Tumors with complete response showed increase in genes associated with chemotherapy-sensitivity and mitosis compared with tumors with partial response. In another small study including both HCC and non-HCC tumors, mutations related to Wnt/B-catenin activation were predictive of better response to TAE [9]. Gade et al. showed that HCC cells survive ischemia by undergoing autophagy, suggesting that targeting autophagy in conjunction with TAE may improve outcomes [10]. Known prognostic biomarkers of HCC, such as AFP, have also been established as relevant to TAE/TACE, but there are no known *predictive* biomarkers that can guide treatment [11, 12].

Colorectal Cancer Established predictive biomarkers in colorectal cancer (CRC) are routinely performed. Presence of RAS/RAF pathway mutations is used to select out patients who should not get anti-EGFR-targeted monoclonal antibodies as they are insensitive to these treatments. Mutations in PI3K/AKT pathway may also demonstrate similar resistance [13]. Microsatellite instability (MSI) testing is used as a prognostic and predictive biomarkers as patients with MSI-H have better prognosis but at the same time can have worse outcomes if treated with 5-fluorouracil or capecitabine [14]. MSI testing is also used to identify patients with Lynch syndrome.

CRC Profiling and IO Several groups have associated outcomes after TARE of CRC liver metastases. Lahti et al. demonstrated that KRAS status was an independent prognostic factor for survival after TARE [15]. In a follow-up paper with a smaller cohort, they combined mutation status with histopathologic grade to define three distinct cohorts of patients with different prognosis after TARE. In another small cohort, patients with mutations in PI3K pathway genes demonstrated longer time to hepatic progression after TARE [16]. Finally, despite the lack of survival benefit of TARE in conjunction with first-line chemotherapy, a post hoc analysis identified a subgroup of patients with right-sided primary colon tumors which did show significant benefit to combination of chemotherapy and TARE [17]. This finding is intriguing and merits further exploration as there are now well-established clinical, pathological, and molecular differences between left- and right-sided colon tumors [18]. Shady et al. demonstrated that KRAS mutation status was associated with worse outcomes after radiofrequency ablation of CRC liver metastases [19]. The difference in outcome between KRAS mutant and wild-type tumors decreased if the ablation margin was greater than 5 mm.

Lung Cancer In lung cancer, tumor profiling is critical to establish treatment. The majority of lung adenocarcinomas can be sub-classified based on an oncogenic driver mutation, and many of these have approved targeted therapies in the setting of metastatic disease [20]. Moreover, expression of PD-1/PD-L1 in tumors is associated with response to PD-1 blocking antibodies [21].

Lung Cancer Profiling and IO Percutaneous ablation for lung cancer is an option for non-surgical patients in the primary [22]. In a small cohort of patients with lung adenocarcinoma, KRAS mutation was associated with shorter time to local recurrence [23]. In another small cohort, EGFR mutation status was not associated with outcome after ablation [24]. For stage 1a lung adenocarcinoma, perhaps the most important biomarker predicting recurrence is the presence of micro-papillary histology subtype, as has been reported after surgery [25], stereotactic beam radiation therapy [26], and ablation [27]. The relevance of this biomarker for IO is twofold. First, presence of this subtype suggests the need for adjuvant therapy in conjunction with percutaneous ablation, as is currently being explored in surgery [28]. Second, in the absence of this subtype, the local recurrence rates are extremely low after ablation [27], suggesting that for this group, there is equipoise between the different local therapy modalities.

Neuroendocrine Tumor Neuroendocrine tumors (NETs) represent a heterogeneous group of tumors. Several recent papers have reported on the mutational landscape of NETs. Pancreatic NETs have high rates of mutations in the tumor suppressor gene, MEN1, the chromatin remodeling complex genes DAXX/ATRX, genes in the mTOR pathway, and germline mutations in DNA damage repair genes [29, 30]. Interestingly, the MEN1/DAXX/ATRX mutated pancreatic NETs appear to represent a distinct subgroup that arise from alpha cells [31]. The clinical significance of this subgroup is unclear. For example, DAXX/ATRX mutations have been associated with both improved and worse outcomes [30, 32]. Genomic studies of small bowel NETs and lung carcinoids showed distinct mutational landscapes compared with each other and pancreatic NETs [33, 34].

NET Profiling and IO Ki67 is a well-established prognostic variable for NETs that remains relevant to IO [35]. Recently, well-differentiated G3 NETs have been described as a distinct entity from poorly differentiated neuroendocrine carcinomas, and this distinction can be differentiated by the lack of p53 or Rb loss [36]. In a small cohort, the presence of DAXX mutation was associated with shorter time to progression after embolization [37]. Interestingly, a subset of patients with DAXX mutant tumors that have been treated with alkylating agents demonstrate exceptional response [38].

Gaps in Knowledge

Despite the growing number of correlative reports in the IO literature, there is a stark dearth of predictive biomarkers to guide treatment. At the same time, within IO there are multiple examples of treatment strategies which are largely guided by

institutional and operator preference and where clinical guidelines are sorely needed. These areas are precisely where predictive biomarkers can be used to further the field. Here we list a few of these common themes in IO.

Defining Aggressiveness in Early-Stage Cancers There are several instances of early stage cancers (e.g., renal, lung, hcc, breast) that are currently treated by surgery but are also in some settings appropriate for percutaneous ablation. Renal cell carcinomas (RCC) are perhaps the best example of primary tumors treated by thermal ablation with long-term cancer-specific survival equivalent to resection (partial nephrectomy) [39]. Currently percutaneous ablation is predominantly in the setting of smaller cortical tumors in high surgical risk patients or compromised renal function or bilateral tumors [40]. Tumor profiling in this context can be used to better delineate subsets of patients with low recurrence risk profiles and that are best suited for percutaneous ablation. In RCC, for example, several gene signatures have been proposed to predict recurrence-free survival [41, 42]. Similarly, identifying and validating low aggressive signatures in the setting of primary lung, primary hcc, and primary breast tumors can help establish subsets of patients that can be treated with thermal ablation rather than undergoing invasive surgery. For these low-aggressive tumors, percutaneous ablation is an attractive option due to low morbidity, low cost, shorter hospital stay, and high organ preservation.

Modality-Specific Signatures We have previously alluded to the hypothesis that there may be some molecular signatures that determine sensitivity or resistance to particular stressors and that are histology-agnostic. There are multiple examples of this in the radiation oncology literature, seeking to define radiation-resistant or sensitive mutation signatures [43], and such signatures may have predictive relevance to TARE. By analogy, it may be possible to identify tumor-agnostic ischemia-resistant or ischemia-sensitive molecular signatures for prediction of response to TAE/TACE [9]. For example, the HCC escape mechanism of quiescence and autophagy in the setting of ischemia may also be relevant to embolization of non-HCC tumors [10]. In the case of ablation, Thompson et al. have demonstrated that AKT signaling mediates HCC survival after heat stress [44]. PI3K/AKT pathway dysregulation is commonly seen in other tumors and may also play a role in heat-stress resistance in non-HCC tumors. Given the complexity of variables at play in the tumor stress response, including epigenetic factors, tumor microenvironment, and the host immune system, it is possible that such tumor-agnostic signatures would rely on multi-modal –omic approaches including transcriptomic, proteomic, and radiomic features.

Oligo-progression Despite the numerous success stories of precision medicine in oncology, all patients develop resistance to these therapies and progress during the course of their treatment. Once resistance is widespread, treatment generally reverts to standard chemotherapy. Not uncommonly, however, progression on targeted therapies starts at localized sites. Local therapy including ablation in this oligo-progression setting has demonstrated some promising results in preliminary studies [45, 46]. By analogy, solitary immune-cold regions may be relevant targets for local

therapy in the immunotherapy context. An inherent difficulty with this strategy is that in practice it is quite difficult to discriminate true oligo-progression from full-fledged progression. While there may be only one or two sites of progression visible at the time of imaging, multiple microscopic sites of resistance may already exist. Tumor profiling is likely to play an important role in defining this important subset of patients. In fact, some preliminary work in lung cancer may already shed some light on distinguishing features. For example, a subset of EGFR mutant non-small cell lung cancers that have developed TKI resistance can transform into small cell—a more aggressive lung cancer. Recent data suggests that this subset of EGFR-mutant tumors demonstrate concurrent Rb loss and p53 alterations [47]. Defining subsets of patients with true oligo-progression and therefore appropriate candidates for local therapy is a necessary step to establish this strategy in clinical practice. Ongoing efforts to identify signatures of true oligo-metastasis are also under way.

Temporal and Spatial Heterogeneity In the past 5–10 years, there is growing awareness of the vast molecular diversity within tumors, between and within different tumor sites and over time. When present, oncogenic driver mutations tend to exist ubiquitously in a tumor. But beyond these few drivers, multiple subclones exist. This molecular heterogeneity is a major limiting factor in determining robust, clinically relevant molecular signatures. Principles and tools borrowed from the theory of evolution are helping to shed light on how subclones evolve over time and space. From a data mining perspective, this heterogeneity makes the task of identifying biomarkers more challenging—specifically in IO, where typical datasets are in the tens. To overcome this, profiling efforts may need to include serial biopsies over time and space, global features including circulating tumor markers and radiomic features. Moreover, multi-institutional efforts will be needed to develop more robust predictors.

Conclusion

Tumor profiling is now an established tool in medical oncology, and a developing tool in surgical and radiation oncology. In the IO literature, correlative studies between tumor profiling and IO outcomes are beginning to emerge. The underlying assumption driving biomarker development is that more robust, clinically relevant categorization of tumors can be identified via tumor profiling. To this end, profiling is critical to the advancement of IO through the identification of appropriate subsets of patients.

References

1. FDA FACT SHEET: CDRH'S approach to tumor profiling next generation sequencing tests. 2017; https://www.fda.gov/media/109050/download. Accessed 3 Oct 2019.
2. Druker BJ, Talpaz M, Resta DJ, et al. Efficacy and safety of a specific inhibitor of the BCR-ABL tyrosine kinase in chronic myeloid leukemia. N Engl J Med. 2001;344(14):1031–7.

3. Lynch TJ, Bell DW, Sordella R, et al. Activating mutations in the epidermal growth factor receptor underlying responsiveness of non-small-cell lung cancer to gefitinib. N Engl J Med. 2004;350(21):2129–39.
4. Qin BD, Jiao XD, Liu K, et al. Basket trials for intractable cancer. Front Oncol. 2019;9:229.
5. Zucman-Rossi J, Villanueva A, Nault JC, Llovet JM. Genetic landscape and biomarkers of hepatocellular carcinoma. Gastroenterology. 2015;149(5):1226–1239.e1224.
6. Boyault S, Rickman DS, de Reynies A, et al. Transcriptome classification of HCC is related to gene alterations and to new therapeutic targets. Hepatology. 2007;45(1):42–52.
7. Desert R, Rohart F, Canal F, et al. Human hepatocellular carcinomas with a periportal phenotype have the lowest potential for early recurrence after curative resection. Hepatology. 2017;66(5):1502–18.
8. Gaba RC, Groth JV, Parvinian A, Guzman G, Casadaban LC. Gene expression in hepatocellular carcinoma: pilot study of potential transarterial chemoembolization response biomarkers. J Vasc Interv Radiol. 2015;26(5):723–32.
9. Ziv E, Yarmohammadi H, Boas FE, et al. Gene signature associated with upregulation of the Wnt/beta-catenin signaling pathway predicts tumor response to transarterial embolization. J Vasc Intervntional Radiol. 2017;28(3):349–355.e341.
10. Gade TPF, Tucker E, Nakazawa MS, et al. Ischemia induces quiescence and autophagy dependence in hepatocellular carcinoma. Radiology. 2017;283(3):702–10.
11. Riaz A, Ryu RK, Kulik LM, et al. Alpha-fetoprotein response after locoregional therapy for hepatocellular carcinoma: oncologic marker of radiologic response, progression, and survival. J Clin Oncol. 2009;27(34):5734–42.
12. Wang Y, Chen Y, Ge N, et al. Prognostic significance of alpha-fetoprotein status in the outcome of hepatocellular carcinoma after treatment of transarterial chemoembolization. Ann Surg Oncol. 2012;19(11):3540–6.
13. Vacante M, Borzi AM, Basile F, Biondi A. Biomarkers in colorectal cancer: current clinical utility and future perspectives. World J Clin Cases. 2018;6(15):869–81.
14. El-Deiry WS, Goldberg RM, Lenz HJ, et al. The current state of molecular testing in the treatment of patients with solid tumors, 2019. CA Cancer J Clin. 2019;69(4):305–43.
15. Lahti SJ, Xing M, Zhang D, Lee JJ, Magnetta MJ, Kim HS. KRAS status as an independent prognostic factor for survival after Yttrium-90 radioembolization therapy for Unresectable colorectal cancer liver metastases. J Vasc Interv Radiol. 2015;26(8):1102–11.
16. Ziv E, Bergen M, Yarmohammadi H, et al. PI3K pathway mutations are associated with longer time to local progression after radioembolization of colorectal liver metastases. Oncotarget. 2017;8(14):23529–38.
17. Wasan HS, Gibbs P, Sharma NK, et al. First-line selective internal radiotherapy plus chemotherapy versus chemotherapy alone in patients with liver metastases from colorectal cancer (FOXFIRE, SIRFLOX, and FOXFIRE-Global): a combined analysis of three multicentre, randomised, phase 3 trials. Lancet Oncol. 2017;18(9):1159–71.
18. Lee MS, Menter DG, Kopetz S. Right versus left colon cancer biology: integrating the consensus molecular subtypes. J Natl Comper Cancer Netw. 2017;15(3):411–9.
19. Shady W, Petre EN, Vakiani E, et al. Kras mutation is a marker of worse oncologic outcomes after percutaneous radiofrequency ablation of colorectal liver metastases. Oncotarget. 2017;8(39):66117–27.
20. Kris MG, Johnson BE, Berry LD, et al. Using multiplexed assays of oncogenic drivers in lung cancers to select targeted drugs. JAMA. 2014;311(19):1998–2006.
21. Garon EB, Rizvi NA, Hui R, et al. Pembrolizumab for the treatment of non-small-cell lung cancer. N Engl J Med. 2015;372(21):2018–28.
22. Dupuy DE, Fernando HC, Hillman S, et al. Radiofrequency ablation of stage IA non-small cell lung cancer in medically inoperable patients: results from the American College of Surgeons Oncology Group Z4033 (Alliance) trial. Cancer. 2015;121(19):3491–8.
23. Ziv E, Erinjeri JP, Yarmohammadi H, et al. Lung adenocarcinoma: predictive value of KRAS mutation status in assessing local recurrence in patients undergoing image-guided ablation. Radiology. 2016;282:251.

24. Wei Z, Ye X, Yang X, et al. Advanced non small cell lung cancer: response to microwave ablation and EGFR status. Eur Radiol. 2017;27(4):1685–94.
25. Nitadori J, Bograd AJ, Kadota K, et al. Impact of micropapillary histologic subtype in selecting limited resection vs lobectomy for lung adenocarcinoma of 2cm or smaller. J Natl Cancer Inst. 2013;105(16):1212–20.
26. Leeman JE, Rimner A, Montecalvo J, et al. Histologic subtype in core lung biopsies of early-stage lung adenocarcinoma is a prognostic factor for treatment response and failure patterns after stereotactic body radiation therapy. 2016(1879-355X (Electronic)).
27. Gao S, Stein S, Petre EN, et al. Micropapillary and/or solid histologic subtype based on pre-treatment biopsy predicts local recurrence after thermal ablation of lung adenocarcinoma. Cardiovasc Intervent Radiol. 2018;41(2):253–9.
28. Ma M, She Y, Ren Y, et al. Micropapillary or solid pattern predicts recurrence free survival benefit from adjuvant chemotherapy in patients with stage IB lung adenocarcinoma. J Thorac Dis. 2018;10(9):5384–93.
29. Scarpa A, Chang DK, Nones K, et al. Whole-genome landscape of pancreatic neuroendocrine tumours. Nature. 2017;543(7643):65–71.
30. Jiao Y, Shi C, Edil BH, et al. DAXX/ATRX, MEN1, and mTOR pathway genes are frequently altered in pancreatic neuroendocrine tumors. Science (New York, NY). 2011;331(6021):1199–203.
31. Chan CS, Laddha SV, Lewis PW, et al. ATRX, DAXX or MEN1 mutant pancreatic neuroendocrine tumors are a distinct alpha-cell signature subgroup. Nat Commun. 2018;9(1):4158.
32. Marinoni I, Kurrer AS, Vassella E, et al. Loss of DAXX and ATRX are associated with chromosome instability and reduced survival of patients with pancreatic neuroendocrine tumors. Gastroenterology. 2014;146(2):453–460.e455.
33. Banck MS, Kanwar R, Kulkarni AA, et al. The genomic landscape of small intestine neuroendocrine tumors. J Clin Invest. 2013;123(6):2502–8.
34. Laddha SV, da Silva EM, Robzyk K, et al. Integrative genomic characterization identifies molecular subtypes of lung carcinoids. Cancer Res. 2019;79(17):4339–47.
35. Chen JX, Rose S, White SB, et al. Embolotherapy for neuroendocrine tumor liver metastases: prognostic factors for hepatic progression-free survival and overall survival. Cardiovasc Intervent Radiol. 2017;40(1):69–80.
36. Tang LH, Untch BR, Reidy DL, et al. Well-differentiated neuroendocrine tumors with a morphologically apparent high-grade component: a pathway distinct from poorly differentiated neuroendocrine carcinomas. Clin Cancer Res. 2016;22(4):1011–7.
37. Ziv E, Rice SL, Filtes J, et al. DAXX mutation status of embolization-treated neuroendocrine tumors predicts shorter time to hepatic progression. J Vasc Interv Radiol. 2018;29(11):1519–26.
38. Wu Y, Reidy-Lagunes D, Bielska A, Kelly V, Raj N. Outcomes after cessation of therapy with alkylating agents (AA) for pancreatic neuroendocrine tumors (panNETs). Paper presented at: 2019 Gastrointestinal Cancers Symposium 2019; San Francisco.
39. MacLennan S, Imamura M, Lapitan MC, et al. Systematic review of oncological outcomes following surgical management of localised renal cancer. Eur Urol. 2012;61(5):972–93.
40. Escudier B, Porta C, Schmidinger M, et al. Renal cell carcinoma: ESMO clinical practice guidelines for diagnosis, treatment and follow-up. Ann Oncol. 2016;27(suppl 5):v58–68.
41. Rini B, Goddard A, Knezevic D, et al. A 16-gene assay to predict recurrence after surgery in localised renal cell carcinoma: development and validation studies. Lancet Oncol. 2015;16(6):676–85.
42. Brooks SA, Brannon AR, Parker JS, et al. ClearCode34: a prognostic risk predictor for localized clear cell renal cell carcinoma. Eur Urol. 2014;66(1):77–84.
43. Yard BD, Adams DJ, Chie EK, et al. A genetic basis for the variation in the vulnerability of cancer to DNA damage. Nat Commun. 2016;7:11428.
44. Thompson SM, Callstrom MR, Jondal DE, et al. Heat stress-induced PI3K/mTORC2-dependent AKT signaling is a central mediator of hepatocellular carcinoma survival to thermal ablation induced heat stress. PLoS One. 2016;11(9):e0162634.

45. Yu HA, Sima CS, Huang J, et al. Local therapy with continued EGFR tyrosine kinase inhibitor therapy as a treatment strategy in EGFR-mutant advanced lung cancers that have developed acquired resistance to EGFR tyrosine kinase inhibitors. J Thorac Oncol. 2013;8(3):346–51.
46. Weickhardt AJ, Scheier B, Burke JM, et al. Local ablative therapy of oligoprogressive disease prolongs disease control by tyrosine kinase inhibitors in oncogene-addicted non-small-cell lung cancer. J Thorac Oncol. 2012;7(12):1807–14.
47. Offin M, Chan JM, Tenet M, et al. Concurrent RB1 and TP53 alterations define a subset of EGFR-mutant lung cancers at risk for histologic transformation and inferior clinical outcomes. J Thorac Oncol. 2019;14(10):1784–93.

Chapter 20
Imaging Findings Following Locoregional Cancer Therapies

Jeeban Paul Das, Ines Nikolovski, and Darragh F. Halpenny

Locoregional therapies (LRTs) administered by interventional radiologists (IR) have been proposed as potential alternatives to surgery for certain patients with select primary and metastatic malignancies, most commonly hepatic, renal, and pulmonary neoplasms [1–3]. Currently available IR-guided LRTs include energy-based ablation techniques such as radiofrequency ablation (RFA), microwave ablation (MWA), cryoablation, and irreversible electroporation (IRE). For primary and secondary liver cancers, catheter-guided endovascular therapies utilizing oil emulsion, bland or chemotherapeutic embolic material, or beta-particle emitting microspheres may also be employed [1, 2, 4]. In addition to cryoablation and IRE, select cases of localized clinically significant prostate cancers (csPCA) can also be treated with high-frequency ultrasound (HIFU), focal laser ablation (FLA), and photodynamic therapy (PDT) [5–7].

Imaging at the time of treatment and during follow-up plays a vital role in assessing treatment response and identifying recurrent disease. Response assessment has traditionally been based on serial size-based tumor measurements. However increasing recognition of the complex imaging appearances that may be encountered after embolization and ablation has placed a growing emphasis on assessment of contrast enhancement patterns, tumor morphology, and tumor metabolic activity, when assessing lesion response [8–10].

This review will provide a detailed discussion of (i) the expected post-treatment imaging findings after LRT in pulmonary, renal, hepatic, and prostatic malignancy and (ii) the imaging findings of local tumor recurrence.

J. P. Das (✉) · I. Nikolovski · D. F. Halpenny
Department of Radiology, Memorial Sloan Kettering Cancer Center, New York, NY, USA
e-mail: dasj@mskcc.org

C. Georgiades, H. S. Kim (eds.), *Image-Guided Interventions in Oncology*,
https://doi.org/10.1007/978-3-030-48767-6_20

Pulmonary Tumor Ablation

Introduction

Curative surgical resection is considered the optimal treatment strategy for early-stage lung malignancy [11]; however locally ablative therapies including stereotactic body radiation therapy (SBRT) and minimally invasive energy-based therapies have been proposed as alternatives to surgery for certain primary lung cancers and in patients with oligometastatic disease.

Currently, no consensus imaging protocol or timing schedule following ablative treatment of lung malignancies has been established, and practice for imaging follow-up can vary across institutions [12–16]. The Society for Interventional Radiology (SIR) suggests that an initial post-ablation imaging study be performed within 3 months; this scan can act as a post-ablation "new baseline" study to which subsequent studies can be compared, with subsequent surveillance studies performed every 3–4 months [17]. Follow-up imaging is predominantly with computed tomography (CT) and positron emission tomography (PET)/CT [18, 19]. Recognition of anticipated and unexpected cross-sectional imaging findings is crucial in differentiating successful treatment from disease progression.

Expected Post-treatment Imaging Appearance

RFA and MWA

Immediately following RFA and MWA, an increase in size of the treated lesion is observed, in part due to congestion and hemorrhage within the tumor and adjacent ablated lung, resulting in the formation of a halo of ground-glass opacification (GGO) surrounding the treated lesion in most cases. This halo represents cellular necrosis and delineates the ablation margin between viable benign tissue and nonviable ablated malignant tissue [20–22]. Circumferential GGO extending >/=5 mm beyond the tumor margin or demonstrating a ratio of post-treatment GGO to pre-treatment tumor area of 4 or more has been demonstrated to predict successful ablation rates of 96–100% at 4–22 months [13, 22] (Fig. 20.1a–c). Intratumoral gas locules and a hyperdense electrode tract may be seen on immediate post-ablation imaging [23]. Obstructive pneumonitis can occur in lung adjacent to the treated tumor within the first week after ablation as a result of vascular obliteration caused by heat ablation [24–26].

Within the first week, the ablation zone can enlarge further as a result of peritumoral hemorrhage, inflammation, and consolidation [27]. At 1–2 months, the ablation zone should decrease in size compared with the immediate post-treatment appearance but still remain bigger than the original tumor. Gradual involution of the GGO is also observed [24] (Fig. 20.1d, e). On CT with intravenous contrast, the

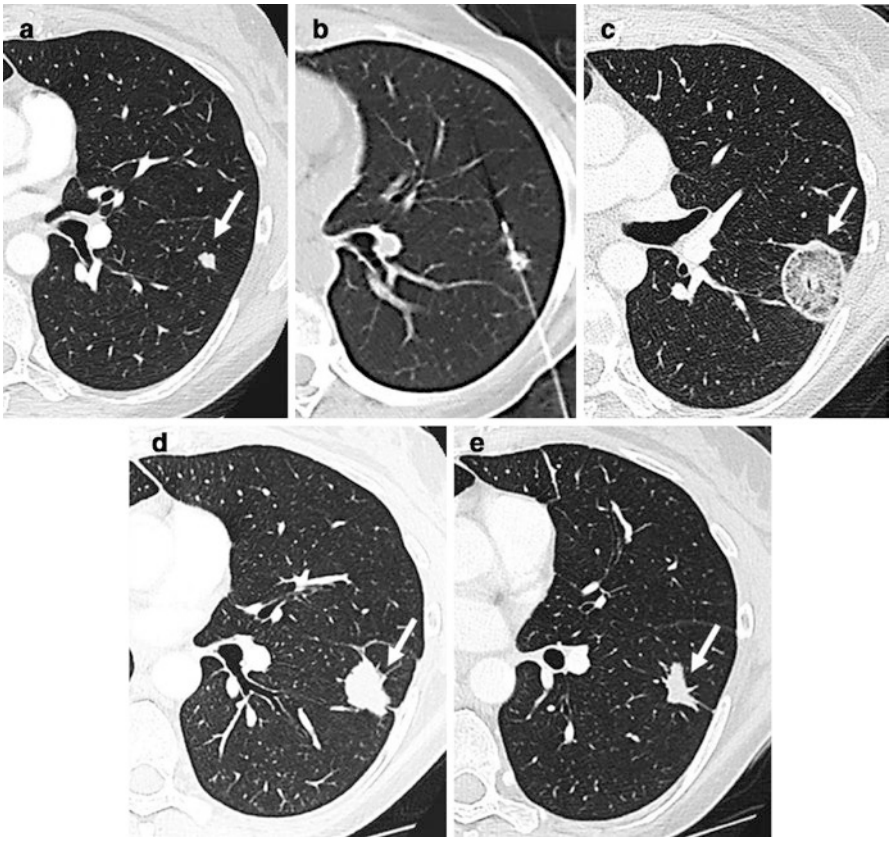

Fig. 20.1 Development of sequential lung changes following RFA on CT. A pre-ablation CT (**a**) shows a biopsy-proven non-small cell lung cancer in the left upper lobe (arrow). CT performed during percutaneous ablation (**b**) and 1 month after treatment (**c**) showing circumferential GGO surrounding the tumor (arrow). At 2-month post-ablation follow-up CT (**d**), the GGO involutes and the ablation zone decreases in size (arrow). CT at 6 months (**e**) shows a further decrease in size of the ablated tumor (arrow)

treated tumor shows central hypoenhancement with a thin rim of peri-ablational enhancement (<5 mm), representing a hyperemic response of normal lung parenchyma to thermal insult, lasting up to 6 months [28].

Gas locules can appear within the ablation zone and represent necrosis, usually resolving by 1 year [26]. Frank cavitation frequently develops within the treated tumor and may be thick-walled, occurring more commonly in lesions closely approximated to segmental bronchi, and may be a marker of successful treatment. Pleural thickening and pleural-parenchymal tags adjacent to the treated tumor can also develop [23, 26].

By month 6, the size of the ablation zone should be the same size or smaller than the tumor prior to ablation. Intratumoral cavities should contract further with

development of parenchymal scarring and minimal architectural distortion of the surrounding normal lung. After 6 months, the ablation zone demonstrates further involution of the cavitation without appreciable changes in size or enhancement pattern [20] (Fig. 20.2).

On PET/CT, a ring-shaped area of increased 18-fluorine (18F)-fluorodeoxyglucose (FDG) uptake can be seen immediately (Fig. 20.3) and, for up to 2 months, representing post-ablation inflammatory change. This inflammatory uptake can potentially mask residual malignant tissue and can limit evaluation for viable disease in the immediate post-ablation period. Maximum FDG uptake typically occurs at 2 weeks post RFA. At approximately 2 months post-ablation, uptake in the ablation zone should return to normal mediastinal blood pool [28, 29]. At 1–4 months, expected benign patterns of FDG uptake in the ablated tumor include peri-ablational/rim uptake and heterogeneous non-mass-like uptake in the ablation zone [19]. Expected ancillary findings post-ablation of pulmonary neoplasms include

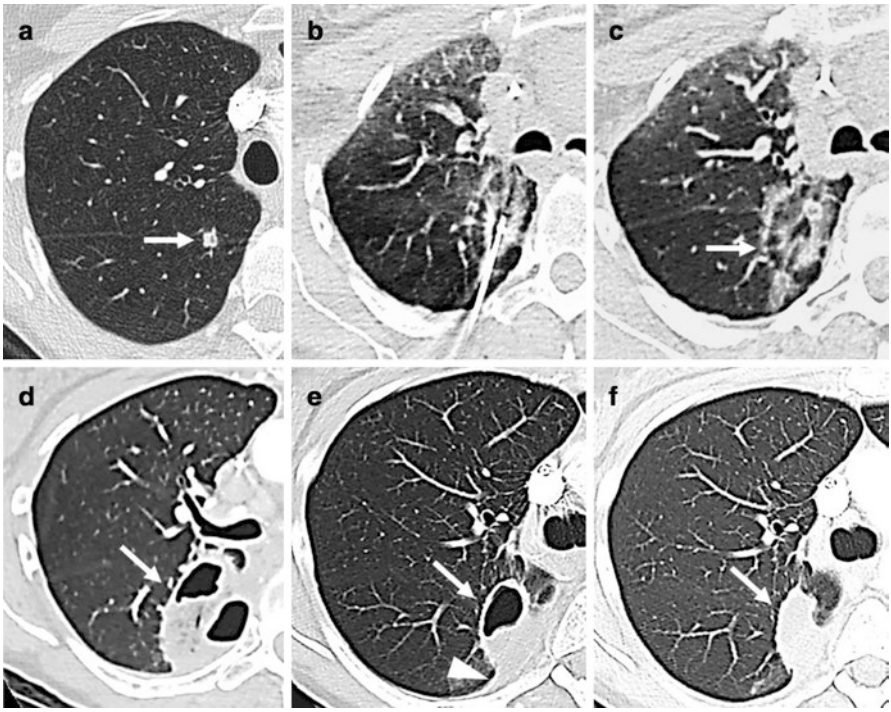

Fig. 20.2 Development of sequential lung changes following RFA on axial CT. A pre-ablation CT (**a**) showing a right upper lobe adenocarcinoma (arrow) CT performed during percutaneous ablation (**b**) and immediately post-ablation (**c**) showing surrounding GGO (arrow) with subsequent development of cavitation (arrow) at 1 month after treatment (**d**) and pleural thickening (arrowhead) at 3 months (**e**). Axial CT at 9 months (**f**) shows resolution of cavitation and decreased ablation zone (arrow)

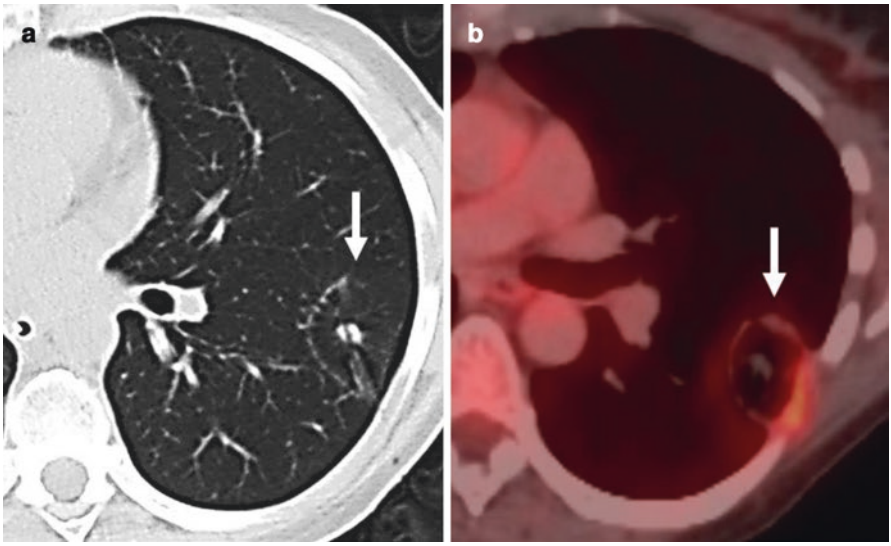

Fig. 20.3 Axial CT (**a**) and fused FDG-PET/CT (**b**) performed 3 days post RFA showing a thin halo of faint ground-glass change demonstrating a rim of increased FDG uptake, representing inflammatory change (arrow)

enlargement and increased FDG uptake in one or more thoracic lymph nodes, occurring in ~ two thirds of cases at 1-month follow-up with decrease in both size and FDG avidity seen by 6 and 12 months, respectively [30, 31].

Cryoablation

Involution of the cryoablation zone tends to occur earlier and more rapidly, when compared to both RFA and MWA [32]. During cryoablation, a well-defined ovoid hypoattenuating ice ball can be visualized, ideally with a circumferential margin >/= 5 mm to ensure complete devitalization of tumor (Fig. 20.6a–c). Higher attenuation may also be seen within the ice ball on subsequent freeze-thaw cycles, consistent with blood products. On completion of the final thaw, the ablation zone is larger than the treated tumor and is surrounded by ground-glass consolidation, the sequelae of ischemia and hemorrhage. Unlike RFA, cryoablation more frequently results in an asymmetric region of GGO, in the dorsal area of the ablation zone [32, 33].

Within the first 24 hours, most ablation zones appear atelectatic/consolidative, demonstrating a wedge or irregular shape, surrounded by a more high-density area [32, 33]. At 1 week, the majority of cryoablated tumors demonstrate a nodular pattern with 80% showing no further enlargement on surveillance imaging with gradual resolution of the peripheral consolidation as peri-ablational edema improves [32, 33].

At 1 month post-ablation, almost all treated tumors remain unchanged or decrease in size compared to immediate post-treatment appearance [33]. Persistent mild enhancement within the ablation zone can be seen in a minority of cases, but typically resolves by 4 weeks [32, 33]. Between 1-month and 6-month follow-up, treated tumor can appear well-defined, or as a "stripe pattern" demonstrating a flat/linear dense appearance, without nodularity [33]. Cavitation following cryoablation occurs frequently, seen in 35–53% of ablation zones with most cases disappearing by 6–12 months [33–35].

As with RFA/MWA PET/CT cannot reliably differentiate post-treatment inflammatory response from tumor within the first 1–2 weeks following cryoablation as residual tumor is impossible to distinguish from post-ablation inflammatory change [32, 33]. FDG uptake patterns on PET-CT imaging at initial follow-up and at 2 months can demonstrate a wide variety of nonspecific uptake patterns, most commonly a diffuse or heterogeneous pattern of low-grade uptake (~80%) [36].

Imaging Findings Suspicious for Pulmonary Recurrence

Recurrence on CT

On immediate post-ablation imaging, failure to develop a complete, circumferential GGO has been associated with recurrent tumor on surveillance imaging. Of note, the point of interface between normal lung parenchyma and tumor where there is no GGO margin is the most likely location of recurrence on surveillance imaging [12, 21, 22].

Compared to the immediate post-ablation scan, the post-treatment opacity should gradually decrease in size on follow-up, and this pattern of gradual reduction in size within the first 6 months is important to establish. Sequential increase in size, or mass-like change in the contour of the lesion after this time period, should be considered suspicious for recurrent tumor (Figs. 20.5e–g and 20.6d–f) [12]. New satellite nodularity immediately adjacent to the treatment opacity or nodular interruption of the expected electrode array tracts can also suggest seeding by viable tumor cells [28] (Fig. 20.4). On CT with intravenous contrast, increasing enhancement within the ablation zone of >/=15 Hounsfield units (HU) or enhancement greater than baseline, peripheral nodular enhancement, or new or increasing solid enhancing component in the ablation zone is suspicious for viable tumor [28].

Recurrent tumor is most commonly seen within the ablation zone but can develop in a regional lymph node or may recur as a distant metastasis. Enlarged reactive lymph nodes can be seen on surveillance CT imaging post-ablation, potentially confounding the evaluation for locoregional nodal recurrence [31, 37].

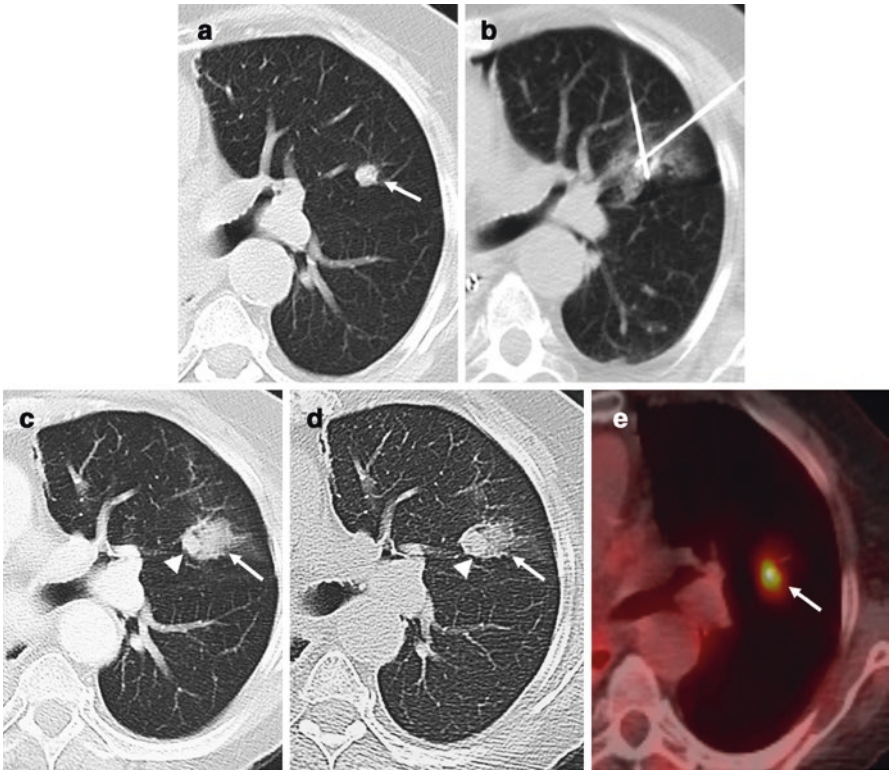

Fig. 20.4 Recurrence following microwave ablation (MWA) on axial CT. A pre-ablation CT (**a**) shows a biopsy-proven left upper lobe non-small cell lung cancer (arrow). Axial CT performed during percutaneous MWA (**b**) demonstrating a rim of GGO surrounding MWA probes, incompletely enveloping the tumor. Axial CT at 6 months (**c**) shows more confluent GGO (arrow) with a solid nodular component (arrowhead). Axial CT at 9 months (**d**) shows a further increase in nodule size, demonstrating FDG avidity on axial PET/CT (**e**) suspicious for viable tumor

Recurrence PET/CT

After the initial post-ablation period (approximately 2 months), PET-CT may be useful in detecting recurrence [29, 38]. After 2 months, persistent or new uptake of FDG, reduced uptake <60% compared to index, and the development of nodular FDG avidity at the site of the original tumor have been associated with tumor recurrence on PET/CT (Figs. 20.5 and 20.6d–g) [29, 32, 33, 38]. A pattern of rim uptake with superimposed focal uptake in the ablation zone is also suggestive of local tumor recurrence [19]. In addition to evaluation of FDG uptake post-ablation, a pre-ablation maximum standardized uptake value (SUV) of less than 8 has been found to be a predictor of improved disease-free survival [19].

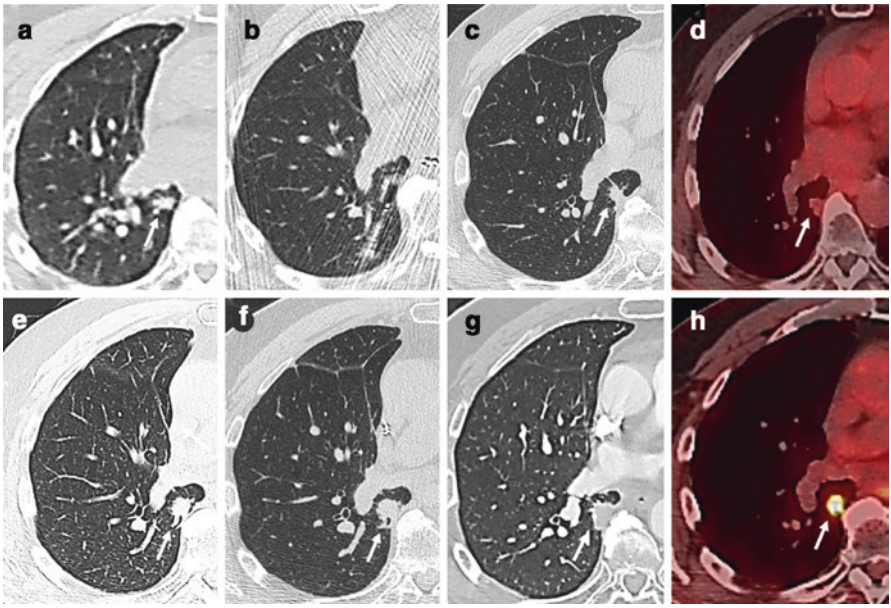

Fig. 20.5 Recurrence following RFA on axial CT. A pre-ablation CT (**a**) shows a right lower lobe tumor (arrow). Axial CT performed during percutaneous RFA (**b**). Axial CT at 3 months post RFA (**c**) shows treated tumor (arrow), non-FDG avid on axial PET/CT (**d**). Sequential axial CT imaging at 6 months (**e**), 9 months (**f**), and 11 months (**g**) shows a gradual increase in nodule size (arrows) demonstrating FDG avidity (arrow). On axial PET/CT at 12 months post RFA, (**h**) suspicious for viable tumor

Locoregional Treatment of Liver Tumors

Introduction

Treatment of primary hepatocellular carcinoma (HCC) and liver metastases has evolved over recent decades, with several locoregional therapies (LRTs) growing in popularity for select patients as part of potentially curative or palliative strategies [1, 39, 40]. Many variables can impact the imaging appearance of treated hepatic malignancies following local ablative or transarterial therapies, including the type(s) of treatment, the additive effects and timing of prior treatments, differences in individual perfusional physiology, and the presence of background liver cirrhosis or steatosis [41]. Therefore, a wide range of post-treatment liver findings may be observed.

When interpreting liver findings following LRT, radiologists should adhere to the consensus unified terminology and standardized reporting criteria for hepatic malignancies [2, 4]. For patients with HCC, the American College of Radiology (ACR) Liver Imaging Reporting and Data System (LI-RADS) version 2018 treatment response (LR-TR) algorithm is used to categorize response categories for treated liver observations, ascribing a LR-TR status of "equivocal," "viable," "nonviable," or, in the setting of poor image quality, "nonevaluable," all of which reflect the perceived probability of tumor viability following LRT [42].

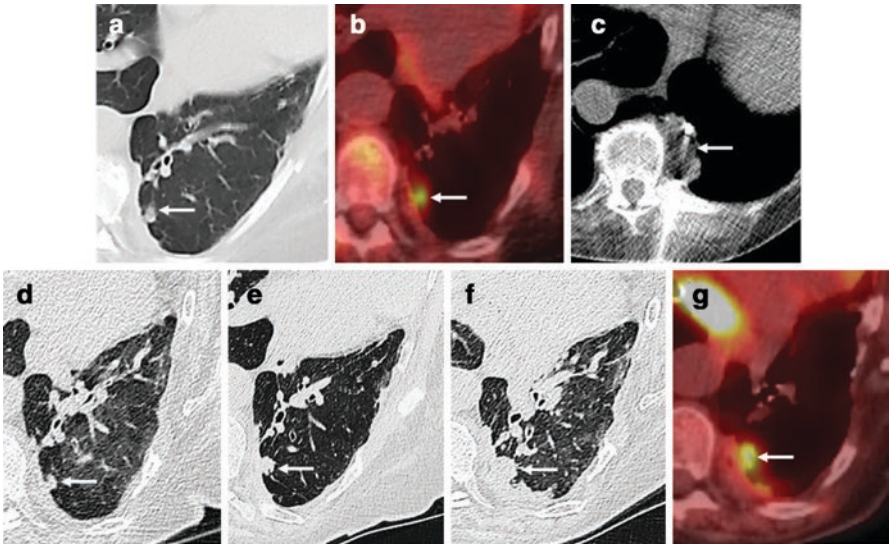

Fig. 20.6 Recurrence following cryoablation. Stage T1a NSCLC (arrow) on axial pre-ablation CT (**a**) demonstrating FDG avidity (arrow) on axial PET/CT (**b**). Axial CT performed during cryoablation (**c**) demonstrated a hypodense "ice ball" (arrow) completely enveloping neoplasm. Follow-up axial CT imaging at 4 months (**d**), 9 months (**e**), and 12 months (**f**) shows a gradual increase in the size of the ablated tumor (arrows). Axial PET/CT at 12 months following cryoablation (**g**) demonstrating intense FDG uptake (arrow) suspicious for recurrent viable tumor

Imaging protocols may differ across institutions depending on the availability of cross-sectional modalities. Following energy ablation, some authors recommend performing contrast-enhanced CT or MRI within 24 hours of ablation [43, 44], while others consider first follow-up imaging at 1–2 weeks post-procedure as adequate [45]. Further surveillance imaging can be performed at 1 month and 4 months post-treatment and can then be approached on an individual basis, often performed every 3–6 months [46–48]. Patients awaiting liver transplant may undergo imaging at 3-month intervals until they receive a liver graft, whereas those treated for secondary hepatic malignancies are often imaged at the discretion of the referring physician [49]. After intra-arterial therapies, follow-up CT or MR imaging at the authors' institution is usually performed using a similar timeline as for ablative therapies, at 1 month and then every 3 months [43, 50].

Intra-arterial Therapies

Expected Findings After Transarterial Chemoembolization (TACE)

Imaging appearances differ following conventional (Lipiodol-based) transarterial chemoembolization (cTACE) versus bland or drug-eluting bead (DEB) TACE. Immediately following cTACE a CT without intravenous contrast is performed to ensure successful delivery of oily emulsion to the target tumor(s).

Successfully treated lesions (HCC or metastases) typically appear markedly hyperdense. Areas of reduced uptake may represent suboptimally treated tumor, or foci of preexisting necrosis [47]. In general, the greater the accumulation of ethiodized oil within the tumor, the greater the degree of future necrosis and therapeutic success [50]. Evaluation with contrast-enhanced (CE) CT is limited in these early stages as the high attenuation coefficient of Lipiodol can obscure the enhancement of residual viable tumor [51] (Fig. 20.7).

Within 1 week of cTACE for primary HCC, MRI may be superior to CT for evaluating residual viable tumor as T1 enhancement characteristics are not significantly affected by the presence of Lipiodol. Signal intensity becomes higher on T1-weighted imaging (T1WI) in the treated tumor and decreases in most cases on T2-weighted imaging (T2WI) with development of a T2 hypointense rim immediately following TACE [52–54].

Immediate or early imaging with CT following bland or DEB-TACE typically does not clearly delineate the treated tumor as the beads are non-radio-opaque. However, retention of embolic beads may be seen in larger lesions in ~75% of cases within the first 12 hours [50, 52]. In addition, tumor viability may be evaluable on CT following bland or DEB-TACE due to the lack of artifact from Lipiodol.

Initial surveillance imaging at 1–2 months following TACE for HCC or metastases assesses for intratumoral necrosis, with gas foci seen in some cases [55, 56]. At 1-month surveillance imaging post-TACE, the median diameter of treated lesions can slightly decrease [57]. In addition, increased T1 and variable T2 signal in the treated lesion may be seen, due to the presence of blood products. Over time, the treated tumor may appear more homogenously T2 hypointense. For HCC treated with TACE, dynamic contrast-enhanced (DCE) MRI demonstrating a non-enhancing

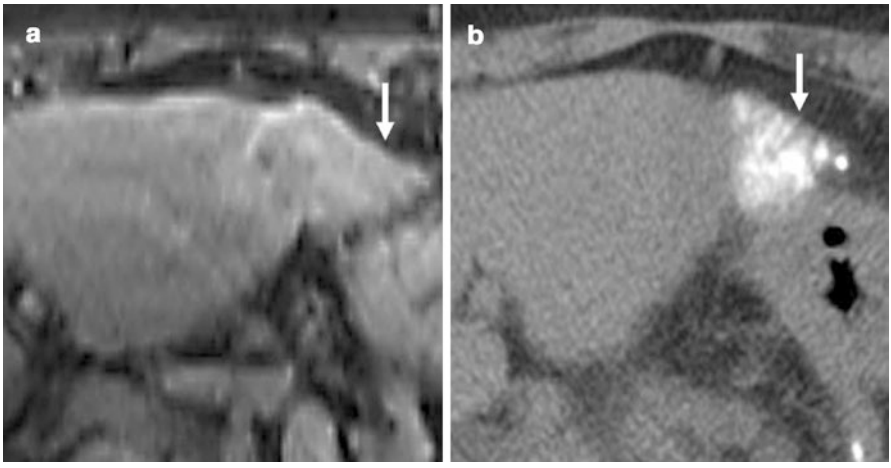

Fig. 20.7 Axial arterial phase T1-weighted gadolinium-enhanced MRI (**a**) demonstrating HCC (arrow). Axial non-contrast CT post cTACE (**b**) showing hyperdense material (Lipiodol) accumulated in the treated tumor

tumor surrounded by thin rim enhancement also usually indicates necrosis and treatment success [50, 52, 58, 59] (Fig. 20.8). In the months following TACE for HCC or hepatic metastases, regional parenchymal enhancement surrounding the tumor (reflecting post-treatment perfusional alterations due to inflammation) and rim enhancement (due to the presence of granulation tissue) may be present and can persist for years [41].

Using diffusion-weighted MR imaging (DWI), an increase in the apparent diffusion coefficient (ADC) of treated hepatic metastases can be seen as a result of cellular necrosis increasing membranous permeability, correlating with successful treatment response [60]. A significantly higher mean ADC increase can be seen in responders to TACE compared to nonresponders in patients with both HCC and liver metastases [57, 61].

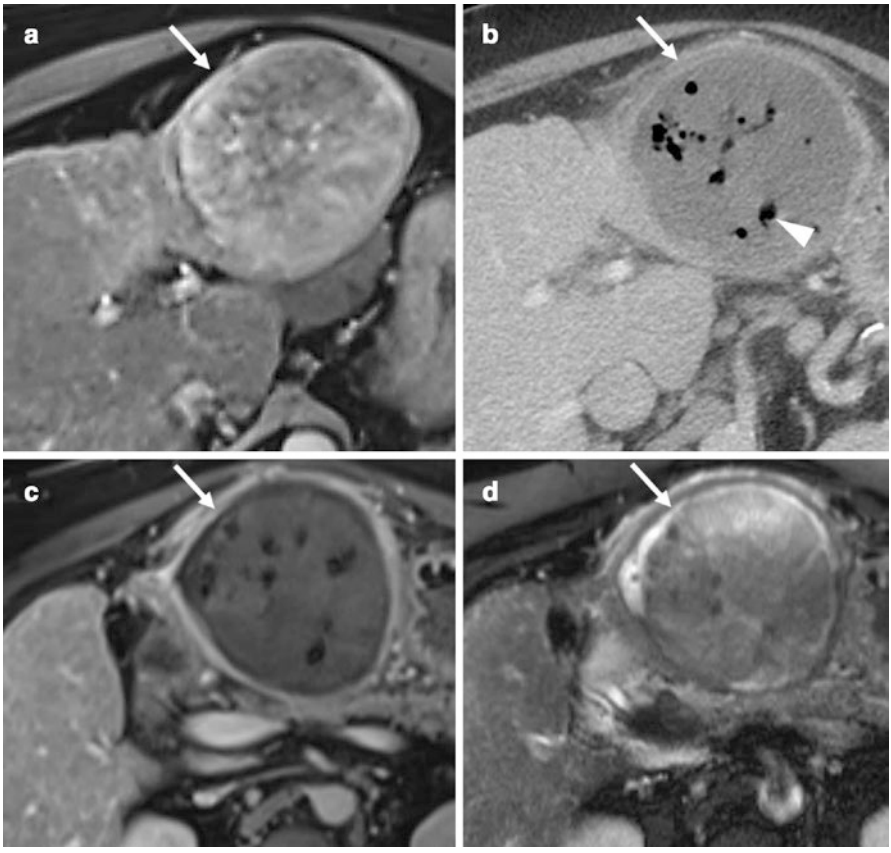

Fig. 20.8 Axial arterial phase T1-weighted gadolinium-enhanced MRI (**a**) demonstrating HCC (arrow). Axial portal venous phase CT (**b**), gadolinium-enhanced MRI (**c**) and T2-weighted (**d**) images 2 months post bland TACE, showing a hypoenhancing treated tumor (arrows) demonstrating heterogeneous T2 signal and containing foci of gas (arrowhead), consistent with necrosis and treatment response

Expected Findings After Radioembolization

Unlike TACE, both primary hepatic tumors and metastases treated with transarterial radioembolization (TARE) may demonstrate an immediate increase in size as a result of edema and hemorrhage, persisting for up to 1 month post-treatment. Therefore, assessment of tumor response to TARE by size criteria alone can result in underestimation of treatment effect [47, 62–66]. Transient geographical perfusional changes in normal adjacent liver parenchyma can appear as ill-defined and wedge-shaped hypo- or hyperdense regions, demonstrating variable enhancement (related to non-selective post-radiation change), but usually resolve by 6 months [66, 67] (Fig. 20.9).

In the first 6 months post TARE for HCC, volume reduction, architectural distortion, and capsular retraction can develop in the treated lobe (or segment), as well as compensatory enlargement of the contralateral lobe [68]. Small (<5 mm) arterially enhancing nodules within primary HCC treated with TARE can persist even following confirmation of complete histologic necrosis, but typically regress at 5–6 months [63, 69]. For HCC treated with TARE, assessing response based on tumor necrosis (indicated by lack of intratumoral enhancement) can demonstrate a more accurate and earlier indication of response rate, compared to using size alone [62, 63]. Within the first 6 months, perivascular low attenuation and thin (<5 mm) peritumoral rim enhancement may also be seen in ~33%, persisting for up to 6 months, related to reactive hyperemia [63, 70].

On MRI, HCC may demonstrate perivascular and peritumoral high T2 signal, representing edema, persisting for up to 6 months after TARE [66]. In addition, the mean ADC can increase (by up to almost 20%) within the first month, preceding an anatomic size change at 3 months [71–73].

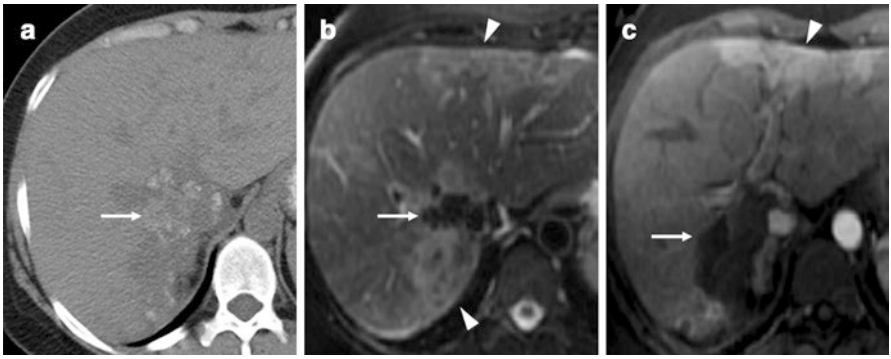

Fig. 20.9 Axial CT without intravenous contrast (**a**) showing a calcified, hypoenhancing hepatic metastasis (arrow). Axial T2 fat saturation (**b**) and arterial phase MRI (**c**) performed 2 months post transarterial radioembolization show ill-defined geographic signal abnormality in the liver periphery (arrowheads) with probably unchanged size of treated lesion (arrows), allowing for comparison across different modalities

For patients with hypovascular hepatic metastases (where contrast-enhanced imaging provides limited value), PET/CT may demonstrate resolution of lesion hypermetabolism earlier than a reduction in size, as measured on CT or MRI [40, 74].

Energy-Based Ablation

Expected Findings Following Microwave Ablation (MWA) and Radiofrequency Ablation (RFA)

Within the first 24 hours following heat-based ablation (with microwave or radiofrequency energy), the ablation zone is typically 0.5–1 cm larger than the targeted tumor (to ensure a satisfactory ablation margin). Morphologically, the ablation zone can be round, oval, or trapezoidal depending on the type and number of electrodes used [43, 44, 46, 75]. The ablation zone can appear heterogeneously hyperdense on non-enhanced CT (representing blood products) but should become less dense and more homogenous over time [49]. Foci of gas can also appear in the treated tumor immediately following ablation, typically resolving within 3 months [46, 76, 77] (Fig. 20.10). Central rounded or linear hyperattenuating foci can be seen within the ablation zone (representing relatively greater cellular disruption along the path of the electrode compared with adjacent parenchyma) and can persist for up to 7 months [43].

A thin peripheral rim of enhancement can surround the ablation zone in up to ~80% of cases, representing hyperemic injury of normal peritumoral parenchyma,

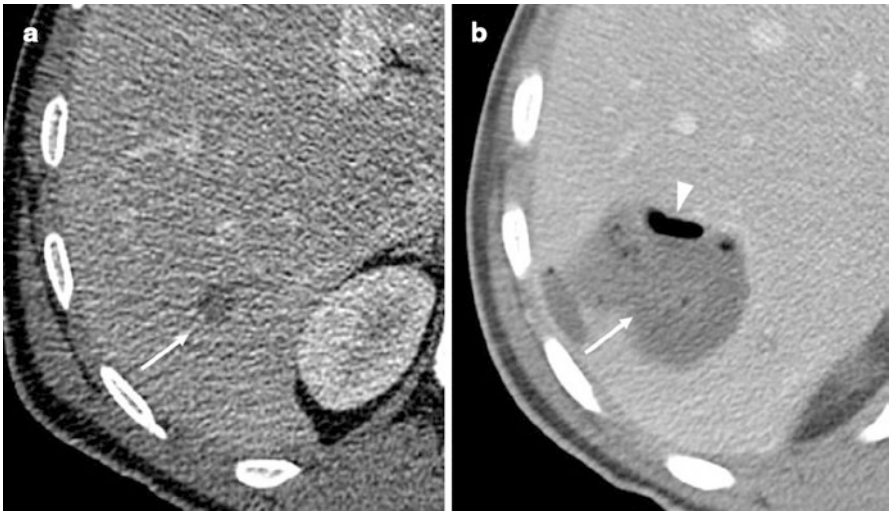

Fig. 20.10 Axial portal venous phase contrast-enhanced CT (**a**) demonstrating a hypovascular metastasis (colorectal) (arrow). Axial portal venous phase contrast-enhanced CT (**b**) at 2 months (**b**) post RFA showing an enlarged hypodensity at the site of treated tumor (arrow) containing an intratumoral gas locule (arrowhead), consistent with necrosis

persisting for up to 1 month [43, 76, 78]. Wedge-shaped or geographic regional hyperenhancement can be seen in up to 25% of treated tumors immediately following RFA, representing a transient arterioportal shunt, usually resolving at 1 month [76].

At 1-month follow-up, the ablation zone typically contracts by ~20% compared to immediate post-treatment imaging [45, 76]. At 2 months, on unenhanced CT images, the treated areas may demonstrate low or heterogeneous attenuation and contain hyperattenuating foci without appreciable enhancement, in most cases. At 4 months, the ablation zone may have decreased in size by ~50%, compared to immediate post-treatment imaging [43, 50]. At 6–12 months, the volume of treated tumor can decrease by up to 90% compared to immediate post-treatment with fibrosis and non-enhancing scar forming [49, 79] (Fig. 20.11).

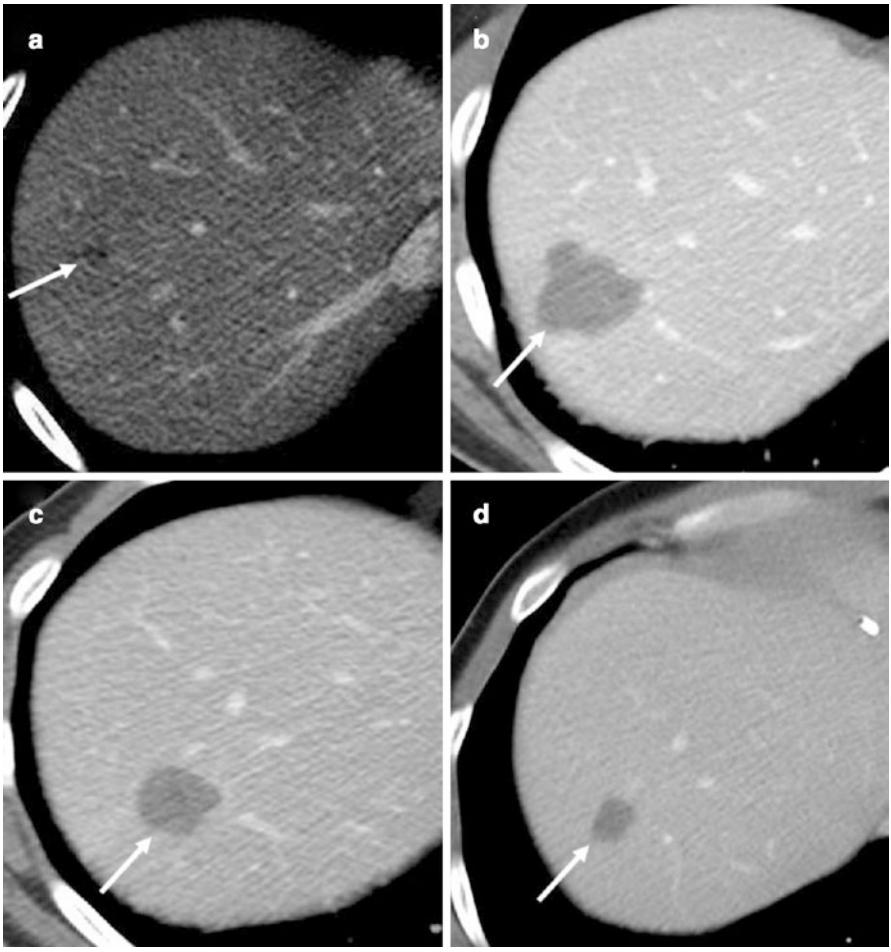

Fig. 20.11 Axial portal venous phase contrast-enhanced CT (**a**) demonstrating a hypovascular colorectal metastasis (arrow). Axial portal venous phase contrast-enhanced CTs at 3 months post RFA (**b**) showing an enlarged hypodensity at the site of treated tumor (arrow), progressively decreasing in size at 5 months post RFA (**c**) and 8 months post RFA (**d**)

Immediately following heat-based ablation, heterogeneously increased T1 and T2 signal can be observed within the ablation zone on MRI, consistent with blood products and coagulative necrosis. A thin uniform rim of high T2 signal and peripheral enhancement surrounding the ablation zone can be seen, secondary to peritumoral edema and thermal injury of adjacent tissue and may persist for ~6 months. A thin, linear ablation tract, mildly hyperintense on T2-weighted imaging, may be also seen [43, 50].

Within the first month post-heat-based ablation for HCC, the ablation zone may demonstrate decreased T2 signal with absence of enhancement suggesting satisfactory treatment response [50] At 2–6 months, the ablation zone tends to become more iso- to hypointense on T1WI. On T2WI, the ablation zone may demonstrate a further decrease in signal. On gadolinium-enhanced imaging, rim enhancement surrounding the ablation cavity may be seen within the first 6 months post-ablation, before progressively decreasing [43, 78, 80].

On PET/CT, smooth, symmetric uptake of FDG in the periphery of the ablation zone is a normal, expected finding following heat-based ablation for hepatic metastases, usually seen within 3 days of treatment and persisting for up to 6 months post-ablation [81, 82].

Expected Findings Following Cryoablation

During and immediately following cryoablation, the ice ball can appear as hypodense on CT. Within 24 hours of cryoablation, a hypoenhancing ablation zone is seen on MRI [83, 84]. At 1–3 months, the margin of the ablation cavity may be surrounded by a T1 and T2 hypointense fibrous capsule demonstrating prominent enhancement on delayed phase imaging [84, 85]. The cryoablation zone involutes more rapidly over time when compared to RFA, with a mean decrease of 56% in cross-sectional area at 2–4 months [84]. After long-term follow-up complete involution of the ablation zone can be seen [83, 86].

Expected Findings Following Irreversible Electroporation (IRE)

On CT, in the immediate 48 hours post-IRE, the ablation zone can increase in size, and subsequently contracts; however the ablated target lesion remains visible within the ablation zone in the majority of patients for a median of 12 weeks [87].

On MRI immediately following IRE, the ablation zone appears homogenously T2 hyperintense. At 24 hours post-IRE, the ablation zone demonstrates a decreased, predominantly intermediately hypointense signal, with a rim of high T2 signal. On gadolinium-enhanced imaging, marginal arterial rim enhancement is observed. The enhancing, T2 hyperintense rim resolves in most (95% of) patients within 3 months [87, 88]. Following IRE for HCC in patients with liver cirrhosis, the T2 hyperintense and peripheral arterial rim enhancement may persist for a longer period (up to 4 months) and may be explained by the decreased healing capacity of cirrhotic liver parenchyma [89].

Residual or Recurrent Tumor Following Locoregional Therapy (LRT)

Residual or Recurrent HCC Following LRT

Recurrent or residual HCC following conventional TACE may be difficult to assess with CT within the first 1–2 months as high attenuation from Lipiodol artifact can mask enhancement of any underlying viable tumor [56]. On later (>3 months) surveillance imaging, enhancement suspicious for viable tumor may be more readily identified as artifact diminishes.

Following bland embolization or DEB-TACE, residual or recurrent HCC may demonstrate nodular, mass-like, or thick irregular tissue along the treated lesion on CT or MRI, in addition to any of the following features of arterial phase hyperenhancement (APHE), washout appearance, or enhancement similar to the pretreatment lesion, in order for a liver observation of LR-TR viable to be ascribed, according to LI-RADS version 2018 [41, 51] (Fig. 20.12).

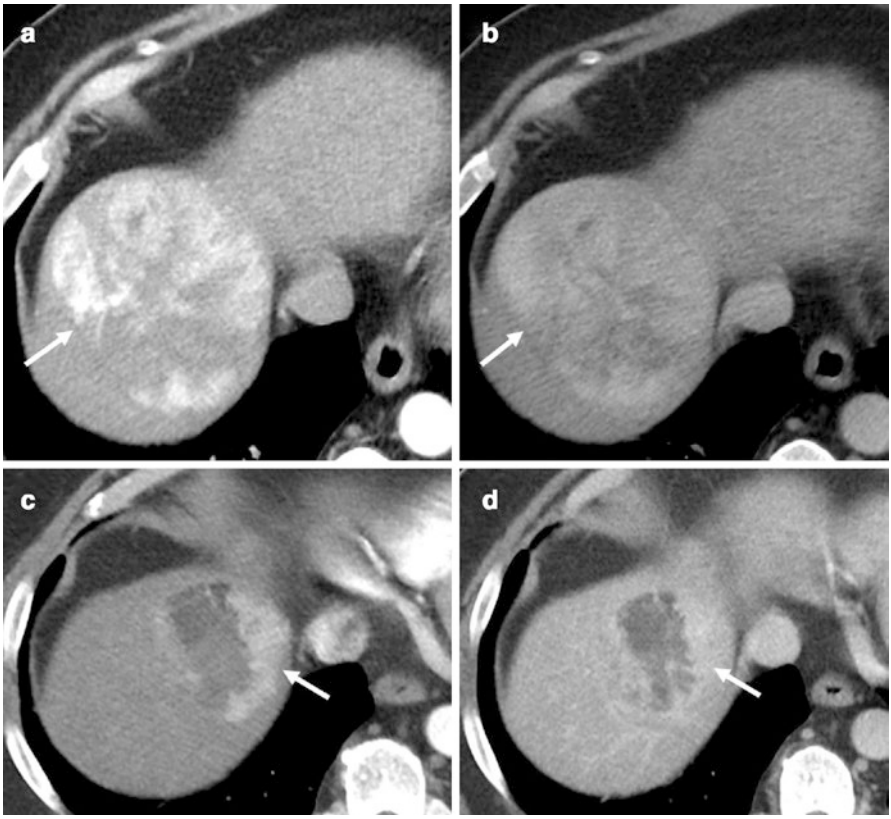

Fig. 20.12 Axial arterial phase (**a**) and portal venous phase (**b**) contrast-enhanced CTs demonstrating HCC (arrow). Repeat axial arterial (**c**) and portal venous (**d**) phase CT imaging at 1 month post bland TACE showing a thick nodular asymmetric rind of arterial phase hyperenhancement showing washout on portal venous phase imaging (arrows) consistent with residual tumor

Following TARE for HCC, intralesional APHE and washout can persist for up to 6 months but should decrease over time. However, gradually enlarging enhancing peripheral nodules (usually >5 mm) in diameter are suspicious for incompletely treated viable tumor in watershed areas (between two vascular distributions) resulting from irregular distribution of radioembolic microspheres inside treated lesions [63].

MRI with DWI may be helpful in equivocal cases of treatment response for HCC treated with TACE as unchanged (or decreased) ADC signal following treatment can be as a result of suboptimal treatment response [61].

Following thermal ablation for HCC, multiplanar evaluation of ablation zone tumor margins (using coronal and sagittal plane reconstructions) has been shown to improve the sensitivity of detecting viable tumor following thermal ablation, mitigating the potentially limiting effects of partial volume averaging on interpretation of axial plane images at the periphery of the ablation zone [90].

Residual or Recurrent Hypovascular Metastatic Disease Following LRT

In cases of hypovascular metastases treated with TACE, assessing for enhancement is a less reliable method for detecting tumor recurrence. However morphological changes in the ablation zone that suggest recurrence (such as new or increased mural nodularity or thickening) may be seen, with or without associated subtle changes in enhancement [41, 45]. Following TARE of hypovascular metastases, PET/CT and MRI with DWI have been utilized to try to help in the assessment of residual/recurrent disease, given the potential lack of tumoral enhancement [40, 91].

Following thermal ablation of hypovascular metastases, morphological changes in the ablation zone, such as nodular disruption of the smooth margin at the interface of the ablation zone with surrounding normal hepatic parenchyma, may be an indicator of recurrent disease [49, 77, 79, 92] (Fig. 20.13). Additionally, if the ablation zone does not decrease in size as expected, or gradually increases over time, hypovascular recurrent or residual tumor should be considered [43] (Fig. 20.14). Notably, if an ablation zone abuts a blood vessel >3 mm in diameter, residual disease or incomplete ablation may preferentially occur in this area due to "heat sink" effect. Therefore, on follow-up imaging, it is important to closely evaluate any areas adjacent to a prominent or large vessel [93].

Evaluating Residual or Recurrent Tumor Following LRT: Problem-Solving with MRI and PET/CT

MRI may be more sensitive than CT in detecting local regrowth for both primary HCC and liver metastases following thermal ablation at 4 months or sooner, based on the added value of T2WI. Residual or recurrent tumor can be focal, eccentric, or nodular and demonstrate moderately high T2 signal (less intense than cyst fluid) compared with the T2 hypointense ablation zone [78]. DWI can show restriction in residual or recurrent disease following thermal ablation (particularly if the pretreatment tumor demonstrated restricted diffusion), possibly helping in cases of

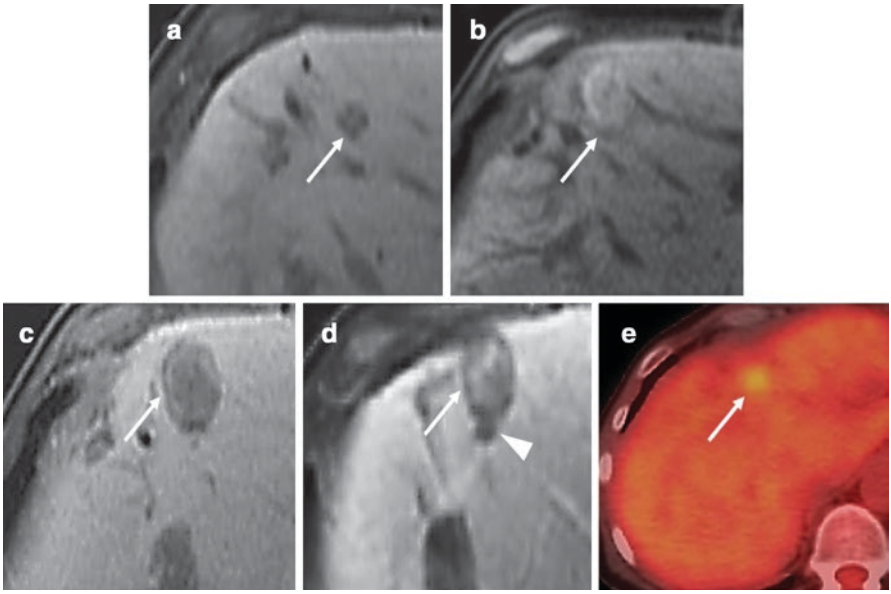

Fig. 20.13 Axial non-contrast T1-weighted MRI showing colorectal metastasis (arrow) pre RFA (**a**). Axial non-contrast T1-weighted MRI immediately post RFA (**b**) showing increased signal consistent with coagulative necrosis/blood products in the ablation zone. Surveillance T1-weighted MRI at 4 months (**c**) showing decreased T1 signal in the ablation zone, consistent with evolving post-treatment change. Axial T1-weighted post-contrast MRI at 6 months (**d**) demonstrating a new nodule along margin of ablation zone (arrowhead) suspicious for recurrent tumor. On PET/CT (**e**) the nodule demonstrates increased FDG avidity (arrow), further increasing suspicion for recurrent disease

equivocal T2 signal abnormality or enhancement [78]; however, limitations of DWI include poor spatial resolution and poor specificity [94]. On DCE-MRI, subtraction imaging can help distinguish the intrinsic T1 signal of blood products from enhancing viable tumor in the ablation zone [49, 86].

PET/CT can be useful in assessing recurrent tumor in patients with hypovascular tumors following thermal ablation. Although inflammatory uptake in the ablation zone can be seen up to 6 months post-treatment, gradually increasing uptake in the peripheral ablation zone in the first 6 months or new uptake in the ablation zone after 6 months should raise the suspicion of viable tumor [81, 82, 95] (Figs. 20.13 and 20.14).

Ablation of Renal Tumors

Introduction

Locoregional therapy for small renal cell cancers (RCC) is increasingly being considered as a suitable alternative to partial nephrectomy in select patients with T1a disease (defined as tumors limited to the kidney, size equal to or smaller than 4 cm),

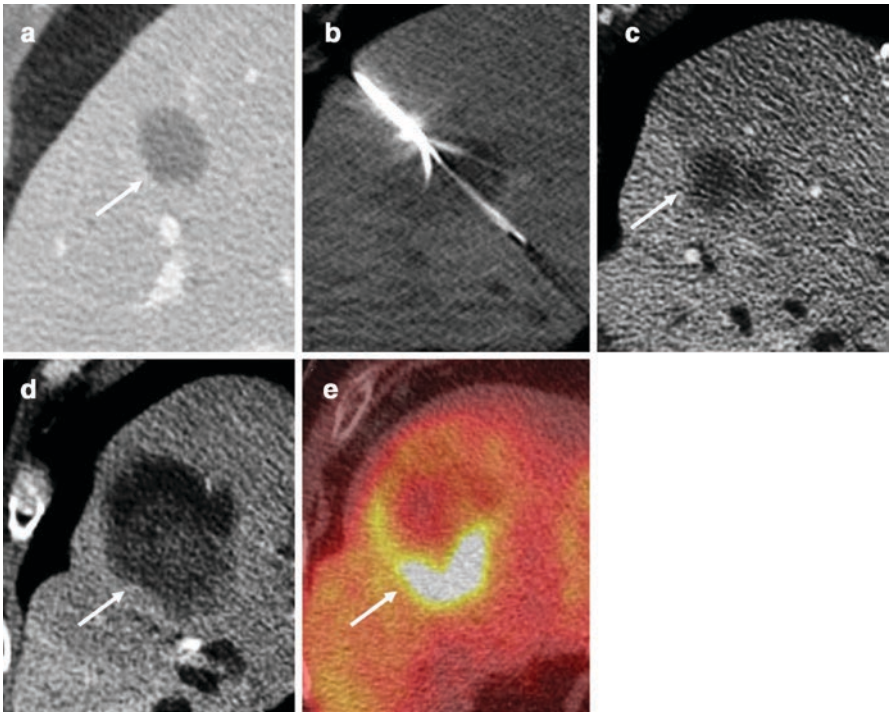

Fig. 20.14 Axial CT with contrast acquired in the portal venous phase (**a**) showing a hypoenhancing metastasis (arrow) which was subsequently treated with microwave ablation (**b**). Follow-up CT at 2 months (**c**) showing treated metastasis (arrow). Subsequent CT with contrast at 6 months (**d**) showing a markedly enlarged ablation zone demonstrating ill-defined soft tissue within the periphery of the treated lesion (arrow) suspicious for recurrent tumor. Axial FDG PET/CT at 6 months (**e**) showing intense FDG uptake (arrow) along the margin of the ablation zone consistent with recurrent tumor

particularly in patients with medical comorbidities, potentially unsuitable for more invasive surgical interventions [96, 97]. Currently, no consensus guidelines on timing of surveillance imaging post thermal ablation exist, but several timetables have been proposed, typically consisting of several cross-sectional imaging studies in the first year with subsequent imaging performed every 6 to 12 months for up to 5 years [96, 98, 99]. It is preferable that the choice of imaging modality for follow-up is consistent over the course of surveillance with CT or MRI. The Society of Abdominal Radiology post-ablation protocol comprises non-enhanced and nephrographic (90 seconds) phases of CT with optional delayed phase (7 minutes), while some authors advocate an additional corticomedullary phase (30 seconds) for both CT and MRI [100, 101].

Expected Post-treatment Imaging Appearance Following Radiofrequency Ablation

Computed Tomography

During RFA, the ablated renal tumor may appear slightly hypodense, followed by development of perinephric fat stranding and thickening of the pararenal fascia, which can be seen for up to 4 weeks post-ablation. A small perinephric or subcapsular hematoma can develop and may be associated with self-limiting contrast extravasation following administration of intravenous contrast [102]. In addition, small locules of gas may form within the treated tumor and surrounding tissue as charring and vaporization of tumor and normal renal tissue occur at high temperatures [103].

Immediately following RFA, successfully treated tumors can increase in size, in part due to hemorrhage, demonstrating higher attenuation compared with background renal parenchyma on CT without intravenous (IV) contrast [104]. Following IV contrast administration, an enhancing penumbra can define the zone between devitalized and viable tissue along the periphery of the ablation zone [105].

Within the first 3 months post RFA, granulation tissue demonstrating low-level enhancement within the ablation zone can be seen (usually </=10 Hounsfield units [HU]) and should not be mistaken for recurrent tumor. On subsequent contrast-enhanced CT performed between 3 and 6 months, decreasing enhancement is typically observed within the ablation zone [106]. The shape of the ablation zone can vary, and can be cylindrical or spherical, depending on the ablation system used and whether overlapping ablations were required [92]. On surveillance imaging up to 6 months post-ablation, some ablated tumors remain stable in size, while others may decrease in size by up to 30% [107–110].

On subsequent (>6 month) surveillance CT imaging, on unenhanced CT, a hyperattenuating central area represents the ablated tumor. Following the administration of IV contrast treated tumor appears as non-enhancing or minimally enhancing (<10 HU) soft tissue surrounded by a thick rind of fat and a thin rim of peripherally enhancing fibrous tissue demonstrating a “bulls-eye” or “halo” appearance, often associated with atrophy of adjacent renal parenchyma, seen in up to 75% of treated lesions, especially when the lesion is peripheral or exophytic [102]. For more centrally located or endophytic lesions, the interposition of fat between devitalized tumor and normal surrounding renal parenchyma may occur over time. In addition, fat can be seen interspersed between the central zone and the surrounding normal parenchyma as the ablated tumor contracts over time [103, 111].

Magnetic Resonance Imaging

Immediately following RFA, the ablated tumor typically demonstrates increased T1 and decreased T2 signal on MRI as a result of coagulative necrosis [108, 112]. Within the first month post RFA, follow-up MRI can demonstrate heterogeneous

and persistently increased T1 signal abnormality within the ablation zone due to the presence of accumulated blood products. On T2-weighted imaging (T2WI), the ablation zone can show variable signal intensity due to evolving necrosis. Heterogeneously decreased T2 signal with small internal foci of increased T2 signal may be seen [102, 103, 108, 109] Fig. 20.15a–d. On post-contrast imaging with gadolinium, benign marginal enhancement of the ablation zone can be visualized immediately following treatment, lasting for up to 3 months on follow-up MRI [103, 113]. Thermal injury insufficient to cause cell death in the tissues surrounding the ablation zone results in this reactive hyperemia in the parenchyma adjacent to the ablation zone [102].

On subsequent MR imaging at 2–6 months, the treated tumor should appear non-enhancing and demonstrate more homogenously decreased T2 signal. On in-phase and opposed-phase imaging, a well-defined rim of low signal delineating the ablation zone margin can be seen [103, 108, 109]. A thin T1 and T2 hypointense halo surrounding the ablation zone may also be encountered [102] (Fig. 20.15e, f)

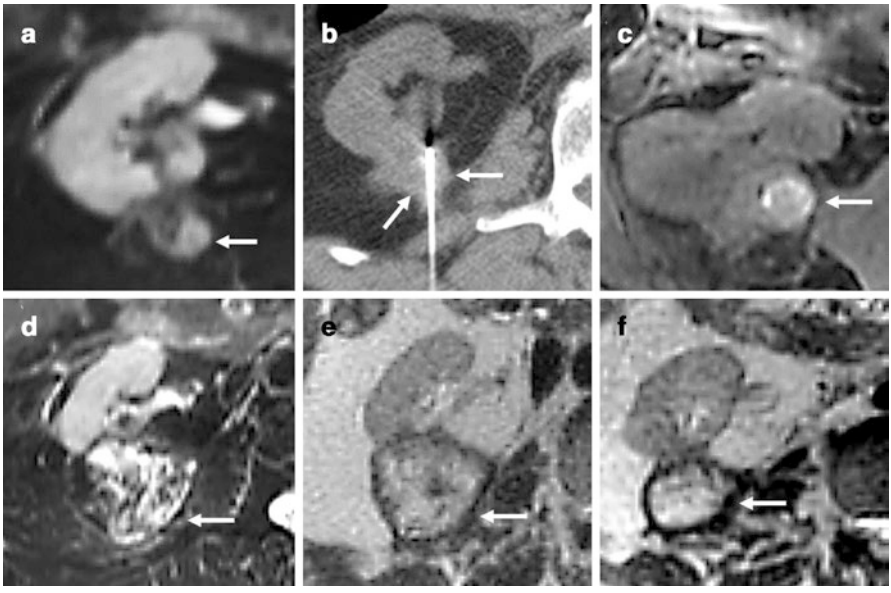

Fig. 20.15 Expected imaging findings following RFA. A pre-ablation nephrographic phase MRI (**a**) shows an exophytic renal cortical tumor (arrow). Axial intraprocedural CT without intravenous contrast (**b**) shows the RFA probe within neoplasm (arrow). MRI performed 1 week following RFA (**c**) demonstrates increased T1 signal within the treated lesion due to coagulative necrosis and hemorrhage (arrow). Heterogeneously increased T2 signal within the ablation zone (arrow) is seen at 1 month (**d**), gradually decreasing in size and developing an increasingly conspicuous T2 hypointense rim (arrow) at 4 (**e**) and 6 months (F) of follow-up

Expected Post-treatment Imaging Appearance Following Cryoablation

Computed Tomography

The CT appearance of renal tumors treated with cryoablation differs slightly compared to those treated with RFA. During cryoablation, a well-defined area of low attenuation surrounding the cryoprobe is seen on non-IV contrast-enhanced CT as the tumor is frozen (i.e., an "ice ball"), allowing for intraprocedural sculpting of a satisfactory ablation zone (extending at least 0.5 cm beyond the tumor margin) and is more conspicuous than the changes that occur during RFA [102, 114]. On immediate non-enhanced CT (following multiple freeze-thaw cycles and removal of the cryoprobe) and on follow-up imaging, the well-demarcated low-attenuation region persists and commonly contains hemorrhage, more marked than with RFA [102].

On CT with intravenous contrast, a thin curvilinear rim of enhancing tissue representing the margin of the ablation zone is more commonly seen following cryoablation than RFA [115, 116]. The ablation zone can show low-level (<10 HU) homogenous enhancement, similar to the imaging appearance following successful RFA [117, 118]. In the long-term follow-up of cryoablated tumors, up to 20% of treated lesions can demonstrate residual enhancement for a few months post-ablation and should not be interpreted as residual tumor, but should be evaluated on follow-up to ensure resolution [119, 120] (Fig. 20.16a–e).

Regression in size of renal tumors treated with cryoablation occurs to a greater degree compared to RFA [114, 116, 121]. One study showed that median size decrease was almost 75% at 36 months of follow-up. If the ablated tumor failed to follow the evolution pattern of size, locally persistent or recurrent cancer was suspected [122]. Rarely, regions of fat necrosis have been described to develop in the ablation zone on surveillance imaging, sometimes mimicking recurrent tumor and requiring biopsy to definitively exclude a malignant process [123]. On long-term follow-up, dystrophic calcifications can develop in necrotic, degenerated tissue within the ablation zone following RFA [107] and may also occur following cryoablation (Fig. 20.16f).

Magnetic Resonance Imaging

During cryoablation under MR guidance, the ice ball surrounding the cryoprobe appears as a well-defined signal void on T1WI and T2WI [103, 117, 118] (Fig. 20.17). Immediately post cryoablation, variable signal intensity on both T1WI and T2WI imaging can be seen. Hemorrhage may be observed in the treatment zone, appearing iso- or hyperintense to background parenchyma on T1WI. The ice ball can increase in size at day one post cryoablation, with gradual contraction of the ablated tumor usually beginning at 3 months post-procedure [116, 121, 124].

At 1–3 months following cryoablation, the ablation zone can demonstrate decreased signal intensity on T1WI relative to adjacent renal tissue. On T2WI, the ablation zone appears predominantly T2 hypointense with a rim of increased T2

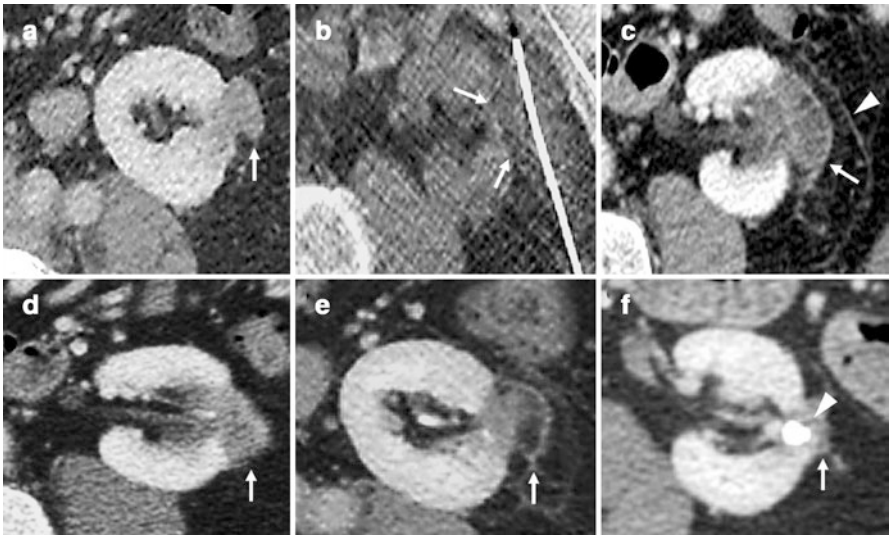

Fig. 20.16 Expected evolution of CT imaging findings following cryoablation. A pre-ablation axial CT with contrast (nephrographic phase) (**a**) shows an exophytic renal mass (arrow). Axial intraprocedural CT without intravenous contrast (**b**) shows the cryoprobe and hypoattenuating "ice ball" within the neoplasm (arrow). Axial nephrographic CT performed 2 weeks following cryoablation (**c**) shows a hypoenhancing ablated tumor (arrow) containing mildly enhancing granulation tissue, as well as thickening of Gerota's fascia (arrowhead). Sequential axial CT images show a decrease in size of the treated tumor in comparison to 2-week post-ablation images (**d**, arrow) with a halo delineating the ablation zone (**e**, arrow). Axial CT with contrast at 2 years post-ablation (**f**) demonstrates parenchymal atrophy at the site of treated tumor (arrow) and dystrophic calcification within the ablation zone (arrowhead)

signal seen along the periphery of the treatment zone [124, 125]. On post-gadolinium-enhanced MR imaging, benign peri-ablational enhancement is common, similar to the patterns described on CT [103, 116, 119, 120]. On diffusion-weighted imaging (DWI), increased signal (with corresponding low value on apparent diffusion coefficient images) can be seen up to 3 months following cryoablation and can diminish over time, appearing hypointense on the 2-year post-treatment follow-up MRI [122]. On long-term follow-up following cryoablation, most treated tumors undergo marked involution over time. In one series, almost one third of ablated tumors were undetectable 24 months post cryoablation [121] (Fig. 20.18).

Imaging Findings Suspicious for Recurrent Tumor

Residual or recurrent tumor is seen in up to 5–11% of cases on follow-up imaging but may be challenging to detect on surveillance due to slow growth. Most cases are identified in the first 12 months after treatment (range 1–68 months) [100, 102, 114, 116, 126]. The two features that are most suggestive of recurrence on post-contrast imaging are an enlarging ablation zone and new nodular enhancement, with most

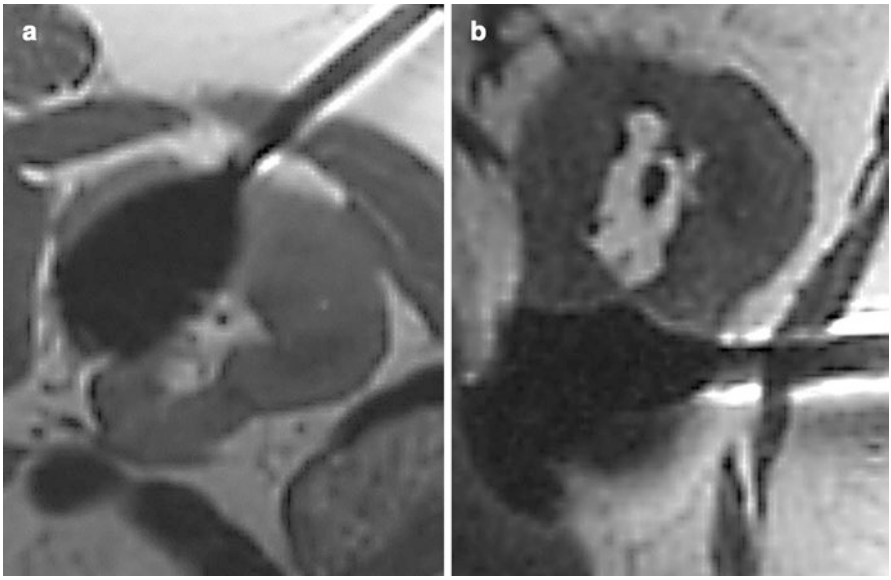

Fig. 20.17 Intraprocedural axial (**a**) and coronal (**b**) T1-weighted imaging during cryoablation demonstrating the "ice ball" surrounding the cryoprobe appearing as a well-defined signal void

(65%) cases of recurrent or residual tumor located in the periphery of the ablation zone, along the deep margin [100]. In addition, an increase in the degree of enhancement within the ablated tumor of greater than 20 HU on surveillance imaging after 6–12 months should be considered suspicious for possible recurrent tumor [101, 106, 107] (Fig. 20.19).

Unlike benign peri-ablational enhancement that can appear as concentric and symmetric with smooth inner margins, residual viable tumor demonstrates more focal, irregular, and nodular morphology and enhancement and typically increases in size over time [14, 102, 126] (Fig. 20.20). Of note, although visible on several phases of enhancement, it has been postulated that recurrence following thermal ablation may be most conspicuous on the corticomedullary phase of imaging (30 seconds) depending on initial tumor histology [100]. Although the presence of enhancement and nodularity are very useful radiological signs for detecting recurrence, biopsy of the ablated zone performed 6 months post-treatment has shown that almost 50% of patients with biopsy-proven residual tumor did not have any detectable enhancement on CT or MRI performed at the time of biopsy. Of note, in the same series, all tumor recurrences following cryoablation demonstrated contrast enhancement [127].

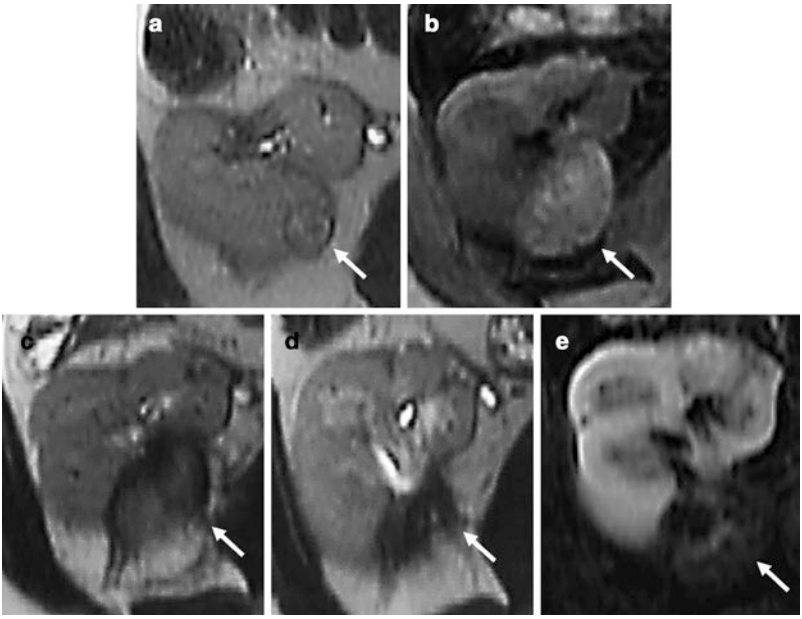

Fig. 20.18 Normal evolution of MR imaging findings following cryoablation. Axial T2-weighted imaging (**a**) shows an exophytic cortical neoplasm (arrow). Axial T2-weighted imaging with fat saturation at 5 days post cryoablation (**b**) showing a heterogeneously high T2 signal ablation zone (arrow). Axial T2-weighted imaging at 3 months (**c**) shows decreased signal intensity and contraction of the treated tumor. Further decrease in size and hypointense T2 signal of treated tumor (arrow) is seen at 6-month follow-up on axial T2WI. (**d**) Axial contrast-enhanced T1WI with subtraction (**e**) demonstrates no suspicious enhancement within the ablated tumor (arrow)

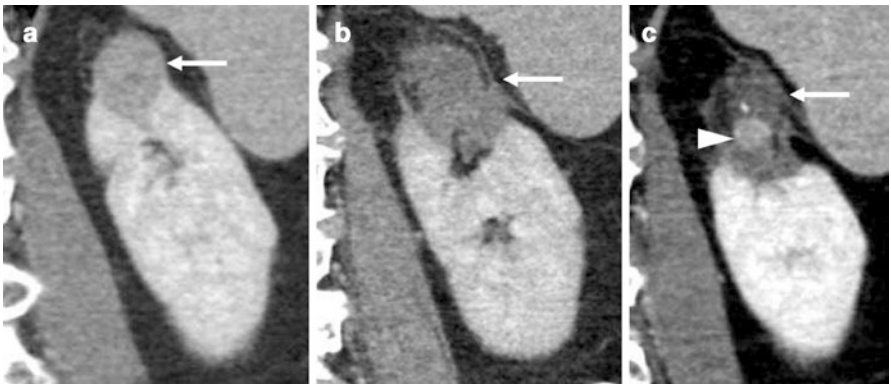

Fig. 20.19 Findings of tumor recurrence following cryoablation. Pre-ablation coronal nephrographic phase CT image (**a**) demonstrating a partially exophytic tumor arising from the upper pole of the left kidney (arrow). Post-ablation coronal nephrographic phase CT at 6 months (**b**) shows a hypoenhancing ablation zone (arrow). Follow-up CT with intravenous contrast at 6 months (**c**) shows a further decrease in the ablation zone but now demonstrating a new enhancing nodule (arrowhead) consistent with recurrent tumor

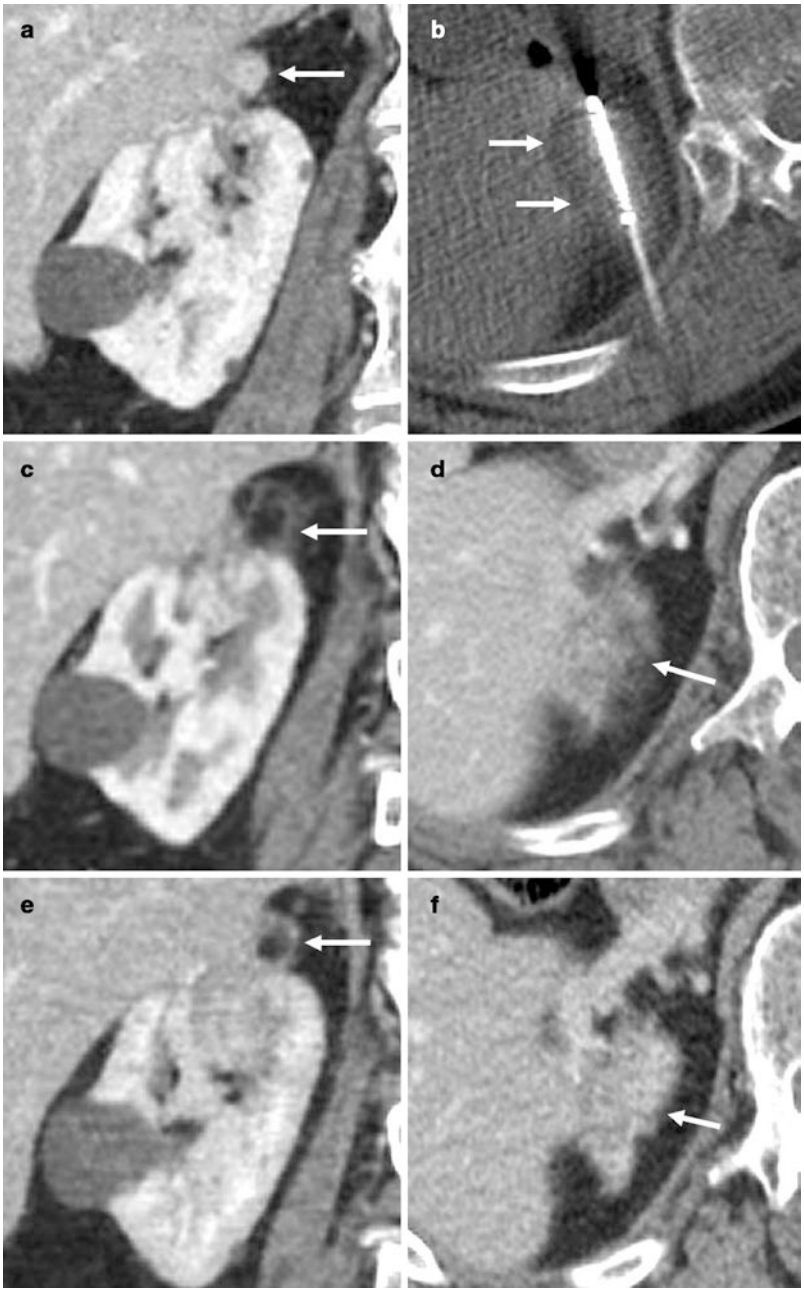

Fig. 20.20 Findings of tumor recurrence following cryoablation. Pre-ablation coronal nephrographic phase CT image (**a**) following partial upper pole nephrectomy demonstrating a biopsy-proven recurrence in the surgical bed (arrow). Axial CT without intravenous contrast (**b**) showing intraprocedural "ice ball" (arrows) enveloping the tumor. Post-ablation coronal (**c**) and axial (**d**) nephrographic phase CT at 4 months shows an ill-defined ablation zone (arrow) with more nodular soft tissue. Follow-up axial (**e**) and (**f**) CT imaging with intravenous contrast at 12 months shows increased nodular and enhancing soft tissue involving the ablation zone (arrows) consistent with recurrent tumor

On MRI, benign post-ablation change should demonstrate hypointense signal on T2WI. New or increased regions of high T2 signal within the ablation defect should raise the suspicion of tumor recurrence [101], particularly in combination with new or increased nodular enhancement on post-contrast sequences. Post-contrast T1 subtraction imaging is a requisite sequence for surveilling ablated tumors with MRI to depict subtle enhancement seen in the context of recurrent tumor that may be less conspicuous without subtraction techniques due to background T1 hyperintense signal from blood products and coagulative necrosis in the ablation zone [103] (Fig. 20.19e). DWI can be useful in the context of any contraindications to the safe administration of gadolinium or iodinated-based contrast media, as foci of residual tumor may demonstrate restricted diffusion [102].

Imaging Post-prostate Cancer Ablation

Introduction

Minimally invasive ablative therapies are growing in acceptance for the treatment of localized clinically significant prostate cancer (PCa). Unlike radical treatment options (such as prostatectomy and external beam radiation), locoregional therapies can potentially eradicate tumor while increasing the likelihood of preserving urinary continence and sexual function [5, 128]. Recent improvements in multiparametric magnetic resonance imaging (mpMRI) have improved the accuracy for detecting and localizing index lesions suitable for percutaneous ablative management [25]. Traditional clinical and biochemical means of post-treatment surveillance can be inadequate following local treatments for PCa, as serum prostate-specific antigen (PSA) can remain unchanged following local therapy. Therefore, knowledge of the pertinent imaging features of viable and treated tumor is crucial for radiologists interpreting post-ablation imaging [5, 129, 130]. When focal prostatic therapy is being considered, mpMRI should be utilized for patient selection, treatment planning, and post-treatment follow-up [6]. The ideal surveillance algorithm after focal prostate therapy remains undefined. Some authors propose mpMRI at 3–6 months and further imaging annually for up to 5 years [131, 132]. In our institution, the post-ablative MRI protocol includes large field-of-view axial T1WI; axial, coronal, and sagittal T2WI with a small field of view; axial DWI (with multiple *b* values ranging from 0 to 1500 sec/mm^2); and DCE T1WI after intravenous injection of gadolinium chelate (0.1 mmol/per kg) at 2 mL/sec.

Expected Post-treatment Imaging Appearance

High-Frequency Ultrasound (HIFU)

HIFU applies ultrasound energy waves that are absorbed by targeted tissues and rapidly converted into heat, achieving temperatures from 70 to 100 degrees Celsius causing instantaneous coagulative necrosis and cell death [133, 134]. Following

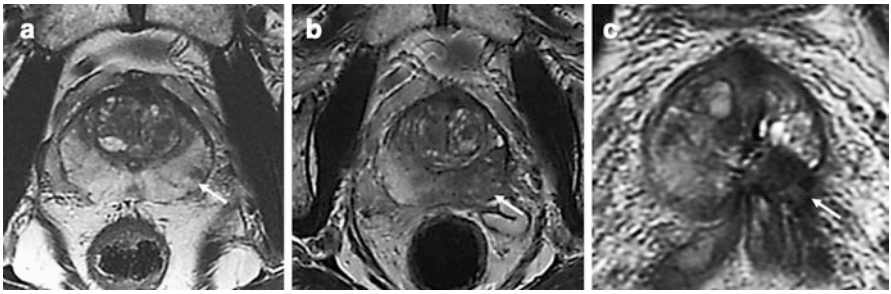

Fig. 20.21 Evolution of changes in the prostate on T2WI following HIFU. Axial pre-ablation MRI (**a**) shows a biopsy-proven prostate cancer in the left posterior mid-gland peripheral zone (arrow). Axial MRI performed 1 month post-ablation (**b**) showing heterogeneous hypointense T2 signal in the left gland with relative loss of normal zonal anatomy and minimal volume loss (arrow). At 6 months post-ablation, axial MRI (**c**) demonstrates increased asymmetric volume loss and increased T2 low signal in the ablation zone (arrow)

HIFU, a consistent series of expected post-ablation changes are typically seen on mpMRI [135–137]. Within the first 5 days, the prostatic volume can increase due to transient post-procedural edema. On T1-weighted imaging (T1WI), the target area can demonstrate slightly increased signal, related to interstitial hemorrhage. On T2-weighted imaging (T2WI), the central component of the target area is usually ill-defined and T2 hypointense. On post-gadolinium-enhanced T1WI, the treated area is non-enhancing and surrounded by a rim of peripheral enhancement [137].

At 1–5 months post-treatment, a decrease in prostatic volume is usually seen. On T1WI, the prostate gland typically demonstrates predominantly low signal with some foci of intermediate to high signal. On T2WI, heterogeneous signal is seen within the gland. Following administration of intravenous contrast, a central non-enhancing cavity (representing necrosed tissue) is seen (and can extend extra-prostatically), surrounded by a rind of enhancing benign viable prostatic tissue [137].

At 5–6 months, the ablated prostatic tissue typically decreases in volume (by up to 70% from initial post-treatment study). On T2WI, the residual prostatic tissue demonstrates predominantly low signal intensity and a poorly defined margin with some regions of intermediate to high signal [135, 137] (Fig. 20.21).

Cryoablation

Cryoablation utilizes extremely low temperatures (−40 °C) to cause cell membrane disruption resulting in coagulative necrosis and has demonstrated effective short-term biochemical disease-free results in the treatment of PCa [138–141]. The American Urological Associations' Best Practice Statement declared cryoablation a possible therapeutic option for organ-confined PCa or in cases where radiation therapy has failed [142].

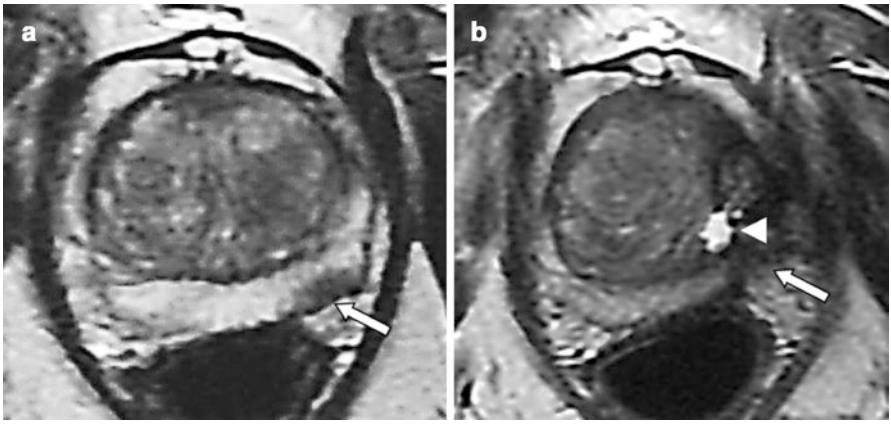

Fig. 20.22 Evolving changes in the prostate gland on MRI following cryoablation. Pre-ablation axial T2WI (**a**) shows a biopsy-proven Gleason 6 prostate cancer (arrow). Axial T2 imaging at 6 months (**b**) demonstrates low T2 signal and volume loss of at the site of the ablated malignancy (arrow) with a hyperintense focus consistent with necrosis (arrowhead)

During prostatic cryoablation, a signal void (representing the frozen prostatic tissue) is noted on all conventional MRI sequences, clearly delineating frozen and nonfrozen regions [142]. Immediately following ablation, the treated prostate demonstrates homogenous non-enhancement, [143] with loss of normal zonal anatomy and thickening of the prostatic capsule [144]. At 1–3 weeks post cryoablation, the prostatic volume may increase [143, 144].

At 3-month follow-up, prostatic volume can decrease by as much as 33% from the original pre-treatment volume [145]. On T2WI reticular regions of intraprostatic high signal consistent with edema can be seen as well as heterogeneous enhancement and predominantly increased T2 signal consistent with hypothermic injury. Foci of non-enhancing high T2 signal are also noted consistent with cryonecrotic prostatic tissue [145] (Fig. 20.22).

Photodynamic Therapy (PDT)

Photodynamic therapy (PDT) is a nonthermal cancer treatment that involves the administration of a photosensitizing agent followed by light exposure in the target tissue stimulating the production of reactive oxygen species causing cell death and inducing necrosis.

There are limited data regarding the imaging appearance following PDT. At 1 week, T1 post-contrast images demonstrate intraprostatic necrosis (defined as a region of non-enhancement) involving up to 80% of the gland, with a similar number demonstrating irregularity of the treatment margin. On T2WI, heterogeneous low signal intensity can be seen within the prostate [7]. At 4 weeks, increased signal intensity on a non-enhanced T1 sequence is often seen up to 44%, suggesting

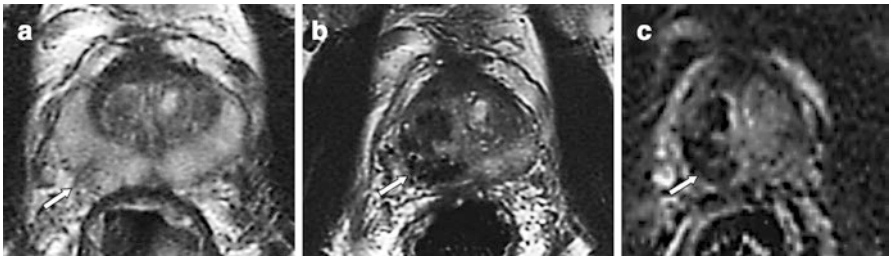

Fig. 20.23 Evolution of changes in the prostate on MRI following PDT. Axial pre-ablation T2WI (**a**) shows a biopsy-proven Gleason 6 prostate cancer in the right posterior mid-gland peripheral zone (arrow). Axial T2WI performed 6 months post-ablation (**b**) showing loss of normal zonal anatomy and ill-defined heterogeneously T2 hypointense signal in the right gland with volume loss (arrow). Axial contrast-enhanced T1 subtraction imaging performed at 8 months post-ablation (**c**) demonstrates a non-enhancing cavity (arrow) in the treated right prostate gland

hemorrhagic necrosis [7]. At 6-month follow-up, a non-enhancing intraprostatic cavity may be visualized. Most treated areas appeared ill-defined and contracted with a minority demonstrating mild enhancement on DCE T1WI [7] (Fig. 20.23).

Irreversible Electroporation (IRE)

Irreversible electroporation (IRE) is an ablative therapy that induces cell death by delivering high-voltage electrical pulses to the cell membrane. Needle electrodes are placed in (or around) a targeted tissue volume and deliver direct electrical current to create a permanently porous cell membrane disrupting cellular homoeostasis resulting in cell death. The feasibility and safety for the treatment of localized pCA have been demonstrated [146, 147].

At 4 weeks post-IRE, the prostate volume on MRI is typically similar to baseline pre-treatment volume. On T2WI, moderately increased signal intensity is seen within the ablation zone consistent with edema. On post-contrast T1WI, the ablation zone demonstrates an absence of contrast enhancement. At 6- and 12-month surveillance MRI post-IRE, prostate deformations and decreased definition of the ablation zone are demonstrated. Involution of the ablation zone is also observed, resulting in a decrease in overall prostate volume of prostate gland volume (mean reduction 28%) compared with baseline MRI [147] (Fig. 20.24).

Laser Ablative Therapy

Focal ablation of the prostate utilizing lasers can be achieved with laser interstitial thermal therapy (LITT) or focal laser ablation (FLA). LITT involves thermal destruction of prostatic tissue by using a neodymium-doped yttrium aluminum garnet (Nd-YAG) laser delivered by an interstitial fiber [148]. FLA is achieved by vaporization of the prostatic tissue with minimal damage to surrounding tissue and

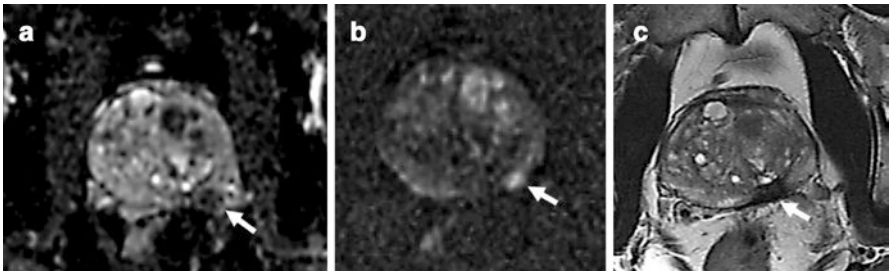

Fig. 20.24 Imaging findings on MRI following IRE. Pre-ablation ADC map (**a**) and B-1000 diffusion-weighted images (**b**) demonstrate a biopsy-proven localized Gleason 7 (4 + 3) prostate cancer in the peripheral zone (arrow). Axial T2WI at 6 months following IRE (**c**) showing focal deformity and volume loss at the site of treated prostatic malignancy (arrow)

is considered a safe and feasible treatment option for clinically low-risk prostate cancer [149]. FLA can be guided by real-time MRI temperature imaging to create a predictable and reproducible ablation zone [150].

Immediately post-FLA, dynamic contrast-enhanced T1WI shows a hypovascular defect in the ablation zone [150]. Focal deformity at the site of ablation is noted [151] with a gradual reduction in size (of up to 80%) of the ablation zone over the first 12 months post-ablation [151, 152]. At 3 months post-FLA, the ablation defect appears as a T2 hypointense band-like, or ill-defined, region of signal, dark on ADC maps [150]. At 12 months, a region of fibrotic change and scarring is typically seen on T2WI and ADC maps and appears as a non-enhancing focus on DCE images [150] (Fig. 20.25a).

Imaging Findings Suspicious for Recurrence

The optimal imaging strategy to best identify recurrence following local treatment of prostatic malignancy remains unclear, with conflicting opinions and study results.

Some reports have suggested that mpMRI demonstrates a very high sensitivity (94–97%) in detecting local recurrence on surveillance imaging following ablative treatments, while other authors suggest the use of simultaneous FDG-positron emission tomography (with MRI) optimizes detection of recurrent tumor [136, 153].

Evaluation for residual tumor using mpMRI may be limited for 3–6 months [150, 152] following local prostatic therapy as a result of (a) the potentially microscopic size of viable tumor foci and (b) the post-ablative enhancement pattern of residual malignancy, which may be indistinguishable from the post-contrast enhancement of inflammatory change surrounding treated tumor [136, 153, 154].

After 6 months post-FLA, T2WI can demonstrate residual or recurrent tumor as a mass-like region of intermediate to low signal intensity demonstrating marked diffusion restriction on DWI with focal early enhancement on DCE in up to 66%. These findings suggest that recurrence at the ablation zone has imaging

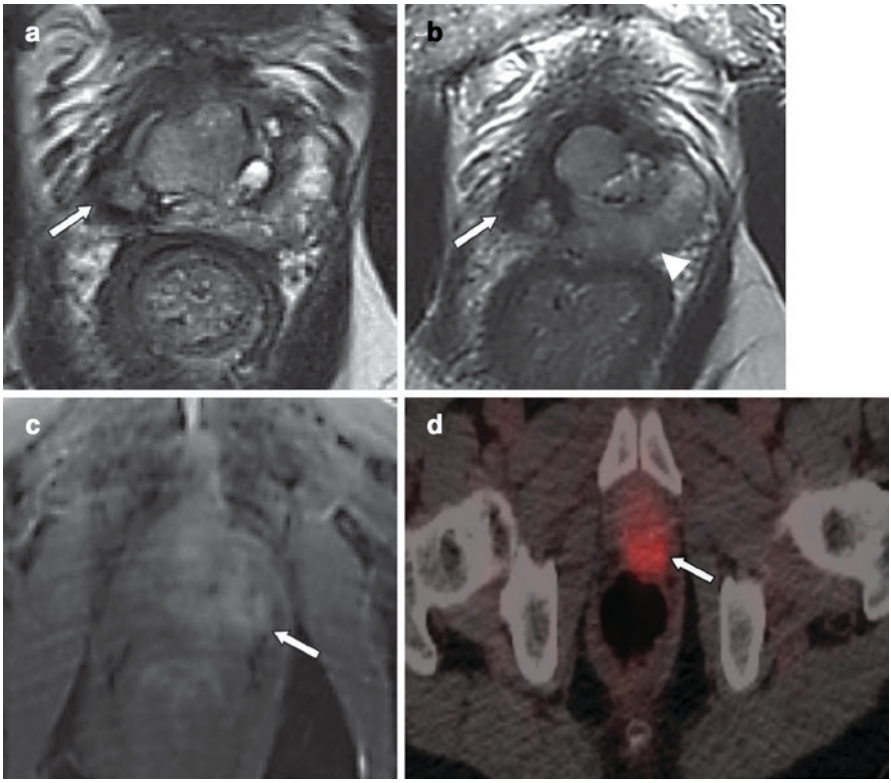

Fig. 20.25 Imaging findings following laser ablation of a right prostate cancer with recurrence in the contralateral gland. Axial T2-weighted MRI performed 12 months following FLA (**a**) demonstrating loss of zonal anatomy and volume loss in the treated right gland with hypointense fibrotic change (arrow). Axial T2 weighted at 15 months post-ablation (**b**) demonstrating further scarring of the treated gland (arrow) with new ill-defined low T2 signal in the left posterior peripheral zone (arrowhead), demonstrating focal early arterial enhancement on contrast enhanced T1WI (**c**) (arrow), suspicious for viable malignancy on axial gadolinium-enhanced imaging (**d**). Axial image from 68Ga-PSMA PET/CT shows focal PSMA uptake in the left prostate gland (arrow), consistent with recurrent tumor

characteristics similar to treatment-naïve prostate cancer on mpMRI [150, 152]. Interestingly, some authors have concluded that qualitative findings suspicious for recurrent cancer may be apparent only at 12-month mpMRI exam. However, others report excellent diagnostic accuracy of mpMRI for residual or recurrent tumor at both 6 and 12 months following ablation [150, 152].

There are variable data available regarding the optimal combination of MRI sequences for detecting recurrence following local therapy. Some authors suggest that combining T2-weighted and DCE imaging provided the best sensitivity for guiding biopsy toward areas containing potentially viable tumor following local therapy [136]. For predicting recurrence following local prostatic treatment, others have reported increased specificity for detecting viable tumor by combining T2WI

and diffusion-weighted imaging (DWI) [155]. However, other retrospective series of suspected PCa recurrences post-ablative treatment have reported that the sensitivity of T2WI and DWI for detecting PCa recurrence was not improved by DCE, nor did DCE improve the performance of the readers with different/lesser experience [153].

Gallium-68 (68 Ga) prostate-specific membrane antigen (PSMA) positron emission tomography (PET) imaging has demonstrated some utility in the assessment of patients with PCa. In a small series assessing its use following local prostate ablation, 68Ga-PSMA PET/MRI detected viable tumor in 60% of patients with recurrent disease not detected on mpMRI suggesting that 68Ga-PSMA-11 PET/MR is more sensitive than mpMRI. Of note, up to 10% of PCa cases do not express PSMA, so in this small proportion of patients, PSMA PET/MRI may be of limited use [130] (Fig. 20.25b–d).

Acknowledgment The authors would like to acknowledge the help of Dr. Richard K. Do in the preparation of the manuscript.

References

1. Bruix J, Sherman M, Llovet JM, Beaugrand M, Lencioni R, Burroughs AK, Christensen E, Pagliaro L, Colombo M, Rodés J, Bismuth H, Bolondi L, Shouval D. Clinical management of hepatocellular carcinoma. Conclusions of the barcelona-2000 EASL conference. European Association for the Study of the Liver. J Hepatol. 2001;35(3):421–30. https://doi.org/10.1016/s0168-8278(01)00130-1.
2. Ahmed M. Image-guided tumor ablation: standardization of terminology and reporting criteria-a 10-year update. Radiology. 2014;273:241–60. https://doi.org/10.1148/radiol.14132958.
3. Kashima M, Yamakado K, Takaki H, Kodama H, Yamada T, Uraki J, Nakatsuka A. Complications after 1000 lung radiofrequency ablation sessions in 420 patients: a single center's experiences. Am J Roentgenol. 2011;197:576–80. https://doi.org/10.2214/AJR.11.6408.
4. Gaba RC, Lewandowski RJ, Hickey R, Baerlocher MO, Cohen EI, Dariushnia SR, D'Othée BJ, Padia SA, Salem R, Wang DS, Nikolic B, Brown DB. Transcatheter therapy for hepatic malignancy: standardization of terminology and reporting criteria. J Vasc Interv Radiol. 2016;27:457–73. https://doi.org/10.1016/j.jvir.2015.12.752.
5. Vargas HA, Wassberg C, Akin O, Hricak H. MR imaging of treated prostate cancer. Radiology. 2012;262:26–42. https://doi.org/10.1148/radiol.11101996.
6. Scheltema MJ, Tay KJ, Postema AW, de Bruin DM, Feller J, Futterer JJ, George AK, Gupta RT, Kahmann F, Kastner C, Laguna MP, Natarajan S, Rais-Bahrami S, Rastinehad AR, de Reijke TM, Salomon G, Stone N, van Velthoven R, Villani R, Villers A, Walz J, Polascik TJ, de la Rosette JJMCH. Utilization of multiparametric prostate magnetic resonance imaging in clinical practice and focal therapy: report from a Delphi consensus project. World J Urol. 2017;35:695–701. https://doi.org/10.1007/s00345-016-1932-1.
7. Haider MA, Davidson SRH, Kale AV, Weersink RA, Evans AJ, Toi A, Gertner MR, Bogaards A, Wilson BC, Chin JL, Elhilali M, Trachtenberg J. Prostate gland: MR imaging appearance after vascular targeted photodynamic therapy with palladium-bacteriopheophorbide. Radiology. 2007;244:196–204. https://doi.org/10.1148/radiol.2441060398.
8. Rosen MA. Use of modified RECIST criteria to improve response assessment in targeted therapies: challenges and opportunities. Cancer Biol Ther. 2010;9:20.

9. Therasse P, Arbuck SG, Eisenhauer EA, Wanders J, Kaplan RS, Rubinstein L, Verweij J, Glabbeke M Van, Van Oosterom AT, Christian MC, Gwyther SG. New guidelines to evaluate the response to treatment in solid tumors. European Organization for Research and Treatment of Cancer, National Cancer Institute of the United States, National Cancer Institute of Canada. J Natl Cancer Inst. 2000;92(3):205-216. https://doi.org/10.1093/jnci/92.3.205.
10. Wahl RL, Jacene H, Kasamon Y, Lodge MA. From RECIST to PERCIST: evolving considerations for PET response criteria in solid tumors. J Nucl Med. 2009;50
11. Cerfolio RJ, Bryant AS. Survival of patients with true pathologic stage I non-small cell lung Cancer. Ann Thorac Surg. 2009;88:917–23. https://doi.org/10.1016/j.athoracsur.2009.05.040.
12. Smith SL, Jennings PE. Lung radiofrequency and microwave ablation: a review of indications, techniques and post-procedural imaging appearances. Br J Radiol. 2015;88 https://doi.org/10.1259/bjr.20140598.
13. Lee JM, Jin GY, Goldberg SN, Lee YC, Chung GH, Han YM, Lee SY, Kim CS. Percutaneous radiofrequency ablation for inoperable non-small cell lung cancer and metastases: preliminary report. Radiology. 2004;230:125–34. https://doi.org/10.1148/radiol.2301020934.
14. Goldberg SN, Grassi CJ, Cardella JF, Charboneau JW, Dodd GD, Dupuy DE, Gervais DA, Gillams AR, Kane RA, Lee FT, Livraghi T, McGahan J, Phillips DA, Rhim H, Silverman SG, Solbiati L, Vogl TJ, Wood BJ, Vedantham S, Sacks D. Image-guided tumor ablation: standardization of terminology and reporting criteria. J Vasc Interv Radiol. 2009;20:S377–90. https://doi.org/10.1016/j.jvir.2009.04.011.
15. Suh RD, Wallace AB, Sheehan RE, Heinze SB, Goldin JG. Unresectable pulmonary malignancies: CT-guided percutaneous radiofrequency ablation – preliminary results. Radiology. 2003;229:821–9. https://doi.org/10.1148/radiol.2293021756.
16. Swensen SJ, Viggiano RW, Midthun DE, Müller NL, Sherrick A, Yamashita K, Naidich DP, Patz EF, Hartman TE, Muhm JR, Weaver AL. Lung nodule enhancement at CT: multicenter study. Radiology. 2000;214:73–80. https://doi.org/10.1148/radiology.214.1.r00ja1473.
17. Rose SC, Dupuy DE, Gervais DA, Millward SF, Brown DB, Cardella JF, Wallace MJ. Research reporting standards for percutaneous thermal ablation of lung neoplasms. J Vasc Interv Radiol. 2009;20:S474–85. https://doi.org/10.1016/j.jvir.2009.01.016.
18. Okuma T, Okamura T, Matsuoka T, Yamamoto A, Oyama Y, Toyoshima M, Koyama K, Inoue K, Nakamura K, Inoue Y. Fluorine-18-fluorodeoxyglucose positron emission tomography for assessment of patients with unresectable recurrent or metastatic lung cancers after CT-guided radiofrequency ablation: preliminary results. Ann Nucl Med. 2006;20:115–21. https://doi.org/10.1007/BF02985623.
19. Singnurkar A, Solomon SB, Gönen M, Larson SM, Schöder H. 18F-FDG PET/CT for the prediction and detection of local recurrence after radiofrequency ablation of malignant lung lesions. J Nucl Med. 2010;51:1833–40. https://doi.org/10.2967/jnumed.110.076778.
20. Yasui K, Kanazawa S, Sano Y, Fujiwara T, Kagawa S, Mimura H, Dendo S, Mukai T, Fujiwara H, Iguchi T, Hyodo T, Shimizu N, Tanaka N, Hiraki Y. Thoracic tumors treated with CT-guided radiofrequency ablation: initial experience. Radiology. 2004;231:850–7. https://doi.org/10.1148/radiol.2313030347.
21. Anderson EM, Lees WR, Gillams AR. Early indicators of treatment success after percutaneous radiofrequency of pulmonary tumors. Cardiovasc Intervent Radiol. 2009;32:478–83. https://doi.org/10.1007/s00270-008-9482-6.
22. De Baère T, Palussière J, Aupérin A, Hakime A, Abdel-Rehim M, Kind M, Dromain C, Ravaud A, Tebboune N, Boige V, Malka D, Lafont C, Ducreux M. Midterm local efficacy and survival after radiofrequency ablation of lung tumors with minimum follow-up of 1 year: prospective evaluation. Radiology. 2006;240:587–96. https://doi.org/10.1148/radiol.2402050807.
23. Gadaleta C, Mattioli V, Colucci G, Cramarossa A, Lorusso V, Canniello E, Timurian A, Ranieri G, Fiorentini G, De Lena M, Catino A. Radiofrequency ablation of 40 lung neoplasms: preliminary results. Am J Roentgenol. 2004;183:361–8. https://doi.org/10.2214/ajr.183.2.1830361.

24. Steinke K, Sewell PE, Dupuy D, Lencioni R, Helmberger T, Kee ST, Jacob AL, Glenn DW, King J, Morris DL. Pulmonary radiofrequency ablation – an international study survey. Anticancer Res. 2004;24:339–43.
25. Johnson DC, Raman SS, Mirak SA, Kwan L, Bajgiran AM, Hsu W, Maehara CK, Ahuja P, Faiena I, Pooli A, Salmasi A, Sisk A, Felker ER, Lu DSK, Reiter RE. Detection of individual prostate cancer foci via multiparametric magnetic resonance imaging. Eur Urol. 2019;75:712–20. https://doi.org/10.1016/j.eururo.2018.11.031.
26. Bojarski JD, Dupuy DE, Mayo-Smith WW. CT imaging findings of pulmonary neoplasms after treatment with radiofrequency ablation: results in 32 tumors. Am J Roentgenol. 2005;185:466–71. https://doi.org/10.2214/ajr.185.2.01850466.
27. Vogl TJ, Naguib NNN, Gruber-Rouh T, Koitka K, Lehnert T, Nour-Eldin NEA. Microwave ablation therapy: clinical utility in treatment of pulmonary metastases. Radiology. 2011;261:643–51. https://doi.org/10.1148/radiol.11101643.
28. Abtin FG, Eradat J, Gutierrez AJ, Lee C, Fishbein MC, Suh RD. Radiofrequency ablation of lung tumors: imaging features of the postablation zone. Radiographics. 2012;32:947–69. https://doi.org/10.1148/rg.324105181.
29. Yoo DC, Dupuy DE, Hillman SL, Fernando HC, Rilling WS, Shepard JAO, Siegel BA. Radiofrequency ablation of medically inoperable stage IA non-small cell lung cancer: are early posttreatment PET findings predictive of treatment outcome? Am J Roentgenol. 2011;197:334–40. https://doi.org/10.2214/AJR.10.6108.
30. Wolf FJ, Grand DJ, Machan JT, DiPetrillo TA, Mayo-Smith WW, Dupuy DE. Microwave ablation of lung malignancies: effectiveness, CT findings, and safety in 50 patients. Radiology. 2008;247:871–9. https://doi.org/10.1148/radiol.2473070996.
31. Sharma A, Digumarthy SR, Kalra MK, Lanuti M, Shepard JAO. Reversible locoregional lymph node enlargement after radiofrequency ablation of lung tumors. Am J Roentgenol. 2010;194:1250–6. https://doi.org/10.2214/AJR.09.3206.
32. Chheang S, Abtin F, Guteirrez A, Genshaft S, Suh R. Imaging features following thermal ablation of lung malignancies. Semin Intervent Radiol. 2013;30:157–68. https://doi.org/10.1055/s-0033-1342957.
33. Ito N, Nakatsuka S, Inoue M, Yashiro H, Oguro S, Izumi Y, Kawamura M, Nomori H, Kuribayashi S. Computed tomographic appearance of lung tumors treated with percutaneous cryoablation. J Vasc Interv Radiol. 2012;23:1043–52. https://doi.org/10.1016/j.jvir.2012.04.033.
34. Wang H, Littrup PJ, Duan Y, Zhang Y, Feng H, Nie Z. Thoracic masses treated with percutaneous cryotherapy: initial experience with more than 200 procedures. Radiology. 2005;235:289–98. https://doi.org/10.1148/radiol.2351030747.
35. Chaudhry A, Grechushkin V, Hoshmand M, Kim CW, Pena A, Huston B, Chaya Y, Bilfinger T, Moore W. Characteristic CT findings after percutaneous cryoablation treatment of malignant lung nodules. Med (United States). 2015;94:e1672. https://doi.org/10.1097/MD.0000000000001672.
36. Logiurato B, Matthews R, Safaie E, Moore W, Bilfinger T, Relan N, Franceschi D. 18 F-FDG PET-CT: predicting recurrence in patients following percutaneous cryoablation treatment for stage i primary non-small-cell lung cancer. Nucl Med Commun. 2015;36:908–13. https://doi.org/10.1097/MNM.0000000000000344.
37. Beland MD, Wasser EJ, Mayo-Smith WW, Dupuye DE. Primary non-small cell lung cancer: review of frequency, location, and time of recurrence after radiofrequency ablation. Radiology. 2010;254:301–7. https://doi.org/10.1148/radiol.00000090174.
38. Herrera LJ, Fernando HC, Perry Y, Gooding WE, Buenaventura PO, Christie NA, Luketich JD, Whyte R, Mitchell J, Benfield JR, Blum M. Radiofrequency ablation of pulmonary malignant tumors in nonsurgical candidates. J Thorac Cardiovasc Surg. 2003;125:929–37. https://doi.org/10.1067/mtc.2003.18.
39. Lencioni R, Cioni D, Bartolozzi C. Percutaneous radiofrequency thermal ablation of liver malignancies: techniques, indications, imaging findings, and clinical results. Abdom Imaging. 2001;26:345–60. https://doi.org/10.1007/s002610000194.

40. Lewandowski RJ, Memon K, Mulcahy MF, Hickey R, Marshall K, Williams M, Salzig K, Gates VL, Atassi B, Vouche M, Atassi R, Desai K, Hohlastos E, Sato K, Habib A, Kircher S, Newman SB, Nimeiri H, Benson AB, Salem R. Twelve-year experience of radioembolization for colorectal hepatic metastases in 214 patients: survival by era and chemotherapy. Eur J Nucl Med Mol Imaging. 2014;41:1861–9. https://doi.org/10.1007/s00259-014-2799-2.
41. Voizard N, Cerny M, Assad A, Billiard JS, Olivié D, Perreault P, Kielar A, Do RKG, Yokoo T, Sirlin CB, Tang A. Assessment of hepatocellular carcinoma treatment response with LI-RADS: a pictorial review. Insights Imaging. 2019;10:121.
42. Chernyak V, Fowler KJ, Kamaya A, Kielar AZ, Elsayes KM, Bashir MR, Kono Y, Do RK, Mitchell DG, Singal AG, Tang A, Sirlin CB. Liver imaging reporting and data system (LI-RADS) version 2018: imaging of hepatocellular carcinoma in at-risk patients. Radiology. 2018;289:816–30. https://doi.org/10.1148/radiol.2018181494.
43. Kim YS, Rhim H, Lim HK. Imaging after radiofrequency ablation of hepatic tumors. Semin Ultrasound CT MRI. 2009;30:49–66. https://doi.org/10.1053/j.sult.2008.12.004.
44. Sofocleous CT, Sideras P, Petre EN. How we do it – a practical approach to hepatic metastases ablation techniques. Tech Vasc Interv Radiol. 2013;16:219–29. https://doi.org/10.1053/j.tvir.2013.08.005.
45. Rhim H. Essential techniques for successful radio-frequency thermal ablation of malignant hepatic tumors. Radiographics. 2001;21:S17–39.
46. Lee SR, Kilcoyne A, Kambadakone A, Arellano R. Interventional oncology: pictorial review of post-ablation imaging of liver and renal tumors. Abdom Radiol. 2016;41:677–705. https://doi.org/10.1007/s00261-016-0665-3.
47. Adam SZ, Miller FH. Imaging of the liver following interventional therapy for hepatic neoplasms. Radiol Clin N Am. 2015;53:1061–76. https://doi.org/10.1016/j.rcl.2015.05.009.
48. Boas FE, Do B, Louie JD, Kothary N, Hwang GL, Kuo WT, Hovsepian DM, Kantrowitz M, Sze DY. Optimal imaging surveillance schedules after liver-directed therapy for hepatocellular carcinoma. J Vasc Interv Radiol. 2015;26:69–73. https://doi.org/10.1016/j.jvir.2014.09.013.
49. Sainani NI, Gervais DA, Mueller PR, Arellano RS. Imaging after percutaneous radiofrequency ablation of hepatic tumors: part 2, abnormal findings. Am J Roentgenol. 2013;200:194–204.
50. Brennan IM, Ahmed M. Imaging features following transarterial chemoembolization and radiofrequency ablation of hepatocellular carcinoma. Semin Ultrasound CT MRI. 2013;34:336–51. https://doi.org/10.1053/j.sult.2013.04.004.
51. Kwan SW, Fidelman N, Ma E, Kerlan RK, Yao FY. Imaging predictors of the response to transarterial chemoembolization in patients with hepatocellular carcinoma: a radiological-pathological correlation. Liver Transplant. 2012;18:727–36. https://doi.org/10.1002/lt.23413.
52. Sahin H, Harman M, Cinar C, Bozkaya H, Parildar M, Elmas N. Evaluation of treatment response of chemoembolization in hepatocellular carcinoma with diffusion-weighted imaging on 3.0-T MR imaging. J Vasc Interv Radiol. 2012;23:241–7. https://doi.org/10.1016/j.jvir.2011.08.030.
53. Yoshioka H, Nakagawa K, Shindou H, Ono Y, Kawakami A, Mabuchi N, Arita S, Fujii K, Hamada T, Ishida O, Miyakoshi K, Uta T. MR imaging of the liver before and after transcatheter hepatic chemo-embolization for hepatocellular carcinoma. Acta Radiol. 1990;31(1):63–67.
54. Hunt SJ, Yu W, Weintraub J, Prince MR, Kothary N. Radiologic monitoring of hepatocellular carcinoma tumor viability after transhepatic arterial chemoembolization: estimating the accuracy of contrast-enhanced cross-sectional imaging with histopathologic correlation. J Vasc Interv Radiol. 2009;20:30–8. https://doi.org/10.1016/j.jvir.2008.09.034.
55. Bisseret D, Ronot M, Abdel-Rehim M, Sibert A, Bouattour M, Castera L, Belghiti J, Vilgrain V. Intratumoral gas in hepatocellular carcinoma following transarterial chemoembolization: associated factors and clinical impact. J Vasc Interv Radiol. 2013;24:1623–31. https://doi.org/10.1016/j.jvir.2013.07.021.
56. Kloeckner R, Otto G, Biesterfeld S, Oberholzer K, Dueber C, Pitton MB. MDCT versus MRI assessment of tumor response after transarterial chemoembolization for the treatment of hepatocellular carcinoma. Cardiovasc Intervent Radiol. 2010;33:532–40. https://doi.org/10.1007/s00270-009-9728-y.

57. Li Z, Bonekamp S, Halappa VG, Corona-Villalobos CP, Pawlik T, Bhagat N, Reyes D, Lai H, Geschwind JF, Kamel IR. Islet cell liver metastases: assessment of volumetric early response with functional MR imaging after transarterial chemoembolization. Radiology. 2012;264:97–109. https://doi.org/10.1148/radiol.12112161.
58. Kubota K, Hisa N, Nishikawa T, Fujiwara Y, Murata Y, Itoh S, Yoshida D, Yoshida S. Evaluation of hepatocellular carcinoma after treatment with transcatheter arterial chemoembolization: comparison of lipiodol-CT, power doppler sonography, and dynamic MRI. Abdom Imaging. 2001;26:184–90. https://doi.org/10.1007/s002610000139.
59. Bonekamp S, Jolepalem P, Lazo M, Gulsun MA, Kiraly AP, Kamel IR. Hepatocellular carcinoma: response to TACE assessed with semiautomated volumetric and functional analysis of diffusion-weighted and contrast-enhanced MR imaging data. Radiology. 2011;260:752–61. https://doi.org/10.1148/radiol.11102330.
60. Liapi E, Geschwind JF, Vossen JA, Buijs M, Georgiades CS, Bluemke DA, Kamel IR. Functional MRI evaluation of tumor response in patients with neuroendocrine hepatic metastasis treated with transcatheter arterial chemoembolization. Am J Roentgenol. 2008;190:67–73. https://doi.org/10.2214/AJR.07.2550.
61. Mannelli L, Kim S, Hajdu CH, Babb JS, Clark TWI, Taouli B. Assessment of tumor necrosis of hepatocellular carcinoma after chemoembolization: diffusion-weighted and contrast-enhanced MRI with histopathologic correlation of the explanted liver. Am J Roentgenol. 2009;193:1044–52. https://doi.org/10.2214/AJR.08.1461.
62. Salem R, Thurston KG. Radioembolization with 90yttrium microspheres: a state-of-the-art brachytherapy treatment for primary and secondary liver malignancies – part 1: technical and methodologic considerations. J Vasc Interv Radiol. 2006;17:1251–78. https://doi.org/10.1097/01.RVI.0000233785.75257.9A.
63. Keppke AL, Salem R, Reddy D, Huang J, Jin J, Larson AC, Miller FH. Imaging of hepatocellular carcinoma after treatment with yttrium-90 microspheres. Am J Roentgenol. 2007;188:768–75. https://doi.org/10.2214/AJR.06.0706.
64. Bester L, Hobbins PG, Wang SC, Salem R. Imaging characteristics following 90yttrium microsphere treatment for unresectable liver cancer. J Med Imaging Radiat Oncol. 2011;55:111–8. https://doi.org/10.1111/j.1754-9485.2011.02241.x.
65. Wong CY, Salem R, Raman S, Gates VL, Dworkin HJ. Evaluating 90Y-glass microsphere treatment response of unresectable colorectal liver metastases by [18F]FDG pet: a comparison with CT or MRI. Eur J Nucl Med. 2002;29:815–20. https://doi.org/10.1007/s00259-002-0787-4.
66. Ibrahim SM, Nikolaidis P, Miller FH, Lewandowski RJ, Ryu RK, Sato KT, Senthilnathan S, Riaz A, Kulik L, Mulcahy MF, Omary RA, Salem R. Radiologic findings following Y90 radioembolization for primary liver malignancies. Abdom Imaging. 2009;34:566–81.
67. Singh P, Anil G. Yttrium-90 radioembolization of liver tumors: what do the images tell us? Cancer Imaging. 2014;13:645–57. https://doi.org/10.1102/1470-7330.2013.0057.
68. Theysohn JM, Ertle J, Müller S, Schlaak JF, Nensa F, Sipilae S, Bockisch A, Lauenstein TC. Hepatic volume changes after lobar selective internal radiation therapy (SIRT) of hepatocellular carcinoma. Clin Radiol. 2014;69:172–8. https://doi.org/10.1016/j.crad.2013.09.009.
69. Riaz A, Lewandowski RJ, Kulik L, Ryu RK, Mulcahy MF, Baker T, Gates V, Nayar R, Wang E, Miller FH, Sato KT, Omary RA, Abecassis M, Salem R. Radiologic-pathologic correlation of hepatocellular carcinoma treated with chemoembolization. Cardiovasc Intervent Radiol. 2010;33:1143–52. https://doi.org/10.1007/s00270-009-9766-5.
70. Atassi B, Bangash AK, Bahrani A, Pizzi G, Lewandowski RJ, Ryu RK, Sato KT, Gates VL, Mulcahy MF, Kulik L, Miller F, Yaghmai V, Murthy R, Larson A, Omary RA, Salem R. Multimodality imaging following 90Y radioembolization: a comprehensive review and pictorial essay. Radiographics. 2008;28:81–99. https://doi.org/10.1148/rg.281065721.
71. Young S, Taylor AJ, Sanghvi T. Post locoregional therapy treatment imaging in hepatocellular carcinoma patients: a literature-based review. J Clin Transl Hepatol. 2018;6:1–9. https://doi.org/10.14218/jcth.2017.00059.

72. Rhee TK, Naik NK, Deng J, Atassi B, Mulcahy MF, Kulik LM, Ryu RK, Miller FH, Larson AC, Salem R, Omary RA. Tumor response after yttrium-90 radioembolization for hepatocellular carcinoma: comparison of diffusion-weighted functional MR imaging with anatomic MR imaging. J Vasc Interv Radiol. 2008;19:1180–6. https://doi.org/10.1016/j.jvir.2008.05.002.
73. Deng J, Miller FH, Rhee TK, Sato KT, Mulcahy MF, Kulik LM, Salem R, Omary RA, Larson AC. Diffusion-weighted MR imaging for determination of hepatocellular carcinoma response to yttrium-90 radioembolization. J Vasc Interv Radiol. 2006;17:1195–200. https://doi.org/10.1097/01.RVI.0000227234.81718.EB.
74. Miller FH, Keppke AL, Reddy D, Huang J, Jin J, Mulcahy MF, Salem R. Response of liver metastases after treatment with yttrium-90 microspheres: role of size, necrosis, and PET. Am J Roentgenol. 2007;188:776–83.
75. Nakazawa T, Kokubu S, Shibuya A, Ono K, Watanabe M, Hidaka H, Tsuchihashi T, Saigenji K. Radiofrequency ablation of hepatocellular carcinoma: correlation between local tumor progression after ablation and ablative margin. Am J Roentgenol. 2007;188:480–8. https://doi.org/10.2214/AJR.05.2079.
76. Lim HK, Choi D, Lee WJ, Kim SH, Lee SJ, Jang HJ, Lee JH, Lim JH, Choo IW. Hepatocellular carcinoma treated with percutaneous radio-frequency ablation: evaluation with follow-up multiphase helical CT. Radiology. 2001;221:447–54. https://doi.org/10.1148/radiol.2212010446.
77. Oei T, VanSonnenberg E, Shankar S, Morrison PR, Tuncali K, Silverman SG. Radiofrequency ablation of liver tumors: a new cause of benign portal venous gas. Radiology. 2005;237:709–17. https://doi.org/10.1148/radiol.2372041295.
78. Dromain C, De Baere T, Elias D, Kuoch V, Ducreux M, Boige V, Petrow P, Roche A, Sigal R. Hepatic tumors treated with percutaneous radio-frequency ablation: CT and MR imaging follow-up. Radiology. 2002;223:255–62. https://doi.org/10.1148/radiol.2231010780.
79. Park MH, Hyunchul R, Kim YS, Dongil C, Hyo KL, Won JL. Spectrum of CT findings after radio-frequency ablation of hepatic tumors. Radiographics. 2008;28:379–90. https://doi.org/10.1148/rg.282075038.
80. Sainani NI, Gervais DA, Mueller PR, Arellano RS. Imaging after percutaneous radiofrequency ablation of hepatic tumors: part 1, normal findings. Am J Roentgenol. 2013;200:184–93.
81. Vogt FM, Antoch G, Veit P, Freudenberg LS, Blechschmid N, Diersch O, Bockisch A, Barkhausen J, Kuehl H. Morphologic and functional changes in nontumorous liver tissue after radiofrequency ablation in an in vivo model: comparison of 18F-FDG PET/CT, MRI, ultrasound, and CT. J Nucl Med. 2007;48:1836–44. https://doi.org/10.2967/jnumed.107.042846.
82. Nielsen K, Van Tilborg AAJM, Scheffer HJ, Meijerink MR, De Lange-De Klerk ESM, Meijer S, Comans EFI, Van Den Tol MP. PET-CT after radiofrequency ablation of colorectal liver metastases: suggestions for timing and image interpretation. Eur J Radiol. 2013;82:2169–75. https://doi.org/10.1016/j.ejrad.2013.08.024.
83. Shyn PB, Mauri G, Alencar RO, Tatli S, Shah SH, Morrison PR, Catalano PJ, Silverman SG. Percutaneous imaging-guided cryoablation of liver tumors: predicting local progression on 24-hour MRI. Am J Roentgenol. 2014;203:W181. https://doi.org/10.2214/AJR.13.10747.
84. Shyn PB, Oliva MR, Shah SH, Tatli S, Catalano PJ, Silverman SG. MRI contrast enhancement of malignant liver tumours following successful cryoablation. Eur Radiol. 2012;22:398–403. https://doi.org/10.1007/s00330-011-2254-8.
85. Glazer DI, Tatli S, Shyn PB, Vangel MG, Tuncali K, Silverman SG. Percutaneous image-guided cryoablation of hepatic tumors: single-center experience with intermediate to long-term outcomes. Am J Roentgenol. 2017;209:1381–9. https://doi.org/10.2214/AJR.16.17582.
86. Chen C, Xu LC, Wang Y, Wang YH, Li GD, Huang HZ, Wang B, Li WT, He XH. Assessment of the cryoablation margin using MRI–CT fusion imaging in hepatic malignancies. Clin Radiol. 2019;74:652.e21–8. https://doi.org/10.1016/j.crad.2019.03.021.
87. Barabasch A, Distelmaier M, Heil P, Krämer NA, Kuhl CK, Bruners P. Magnetic resonance imaging findings after percutaneous irreversible electroporation of liver metastases: a systematic longitudinal study. Investig Radiol. 2017;52:23–9.
88. Faroja M, Ahmed M, Appelbaum L, Ben-David E, Moussa M, Sosna J, Nissenbaum I, Goldberg BSN. Irreversible electroporation ablation: is all the damage nonthermal? Radiology. 2013;266:462. https://doi.org/10.1148/radiol.12120609/-/DC1.

89. Padia SA, Johnson GE, Yeung RS, Park JO, Hippe DS, Kogut MJ. Irreversible electroporation in patients with hepatocellular carcinoma: immediate versus delayed findings at mr imaging. Radiology. 2016;278:285–94. https://doi.org/10.1148/radiol.2015150031.
90. Motoyama T, Ogasawara S, Chiba T, Higashide T, Yokota H, Kanogawa N, Suzuki E, Ooka Y, Tawada A, Irie R, Ochi S, Masuda Y, Uno T, Yokosuka O. Coronal reformatted CT images contribute to the precise evaluation of the radiofrequency ablative margin for hepatocellular carcinoma. Abdom Imaging. 2014;39:262–8. https://doi.org/10.1007/s00261-013-0054-0.
91. Schmeel FC, Simon B, Sabet A, Luetkens JA, Träber F, Schmeel LC, Ezziddin S, Schild HH, Hadizadeh DR. Diffusion-weighted magnetic resonance imaging predicts survival in patients with liver-predominant metastatic colorectal cancer shortly after selective internal radiation therapy. Eur Radiol. 2017;27:966–75. https://doi.org/10.1007/s00330-016-4430-3.
92. Dodd GD, Frank MS, Aribandi M, Chopra S, Chintapalli KN. Radiofrequency thermal ablation. Am J Roentgenol. 2001;177:777–82. https://doi.org/10.2214/ajr.177.4.1770777.
93. Lu DS, Raman SS, Vodopich DJ, Wang M, Sayre J, Lassman C. Effect of vessel size on creation of hepatic radiofrequency lesions in pigs: assessment of the "heat sink" effect. AJR Am J Roentgenol. 2002;178(1):47–51. https://doi.org/10.2214/ajr.178.1.1780047.
94. Vandecaveye V, De Keyzer F, Nuyts S, Deraedt K, Dirix P, Hamaekers P, Vander Poorten V, Delaere P, Hermans R. Detection of head and neck squamous cell carcinoma with diffusion weighted MRI after (chemo)radiotherapy: correlation between radiologic and histopathologic findings. Int J Radiat Oncol Biol Phys. 2007;67:960–71. https://doi.org/10.1016/j.ijrobp.2006.09.020.
95. McLoney ED, Isaacson AJ, Keating P. The role of PET imaging before, during, and after percutaneous hepatic and pulmonary tumor ablation. Semin Intervent Radiol. 2014;31:187–92. https://doi.org/10.1055/s-0034-1373793.
96. Salas N, Ramanathan R, Dummett S, Leveillee RJ. Results of radiofrequency kidney tumor ablation: renal function preservation and oncologic efficacy. World J Urol. 2010;28:583–91. https://doi.org/10.1007/s00345-010-0562-2.
97. Davenport MS, Chandarana H, Curci NE, Doshi A, Kaffenberger SD, Pedrosa I, Remer EM, Schieda N, Shinagare AB, Smith AD, Wang ZJ, Wells SA, Silverman SG. Society of Abdominal Radiology disease-focused panel on renal cell carcinoma: update on past, current, and future goals. Abdom Radiol. 2018;43:2213–20. https://doi.org/10.1007/s00261-018-1663-4.
98. Casalino DD, Remer EM, Bishoff JT, Coursey CA, Dighe M, Harvin HJ, Heilbrun ME, Majd M, Nikolaidis P, Preminger GM, Raman SS, Sheth S, Vikram R, Weinfeld RM. ACR appropriateness criteria post-treatment follow-up of renal cell carcinoma. J Am Coll Radiol. 2014;11:443–9. https://doi.org/10.1016/j.jacr.2014.01.023.
99. Zagoria RJ, Pettus JA, Rogers M, Werle DM, Childs D, Leyendecker JR. Long-term outcomes after percutaneous radiofrequency ablation for renal cell carcinoma. Urology. 2011;77:1393–7. https://doi.org/10.1016/j.urology.2010.12.077.
100. Eiken PW, Atwell TD, Kurup AN, Boorjian SA, Thompson RH, Schmit GD. Imaging following renal ablation: what can we learn from recurrent tumors? Abdom Radiol. 2018;43:2750–5. https://doi.org/10.1007/s00261-018-1541-0.
101. Lum MA, Shah SB, Durack JC, Nikolovski I. Imaging of small renal masses before and after thermal ablation. Radiographics. 2019;39:2134–45. https://doi.org/10.1148/rg.2019190083.
102. Iannuccilli JD, Grand DJ, Dupuy DE, Mayo-Smith WW. Percutaneous ablation for small renal masses-imaging follow-up. Semin Intervent Radiol. 2014;31:50–63. https://doi.org/10.1055/s-0033-1363843.
103. Dyer RB, Zagoria RJ. CT and MR imaging after imaging-guided thermal ablation of renal neoplasms. Radiographics. 2007;27:325–40.
104. Patel U, Sokhi H. Imaging in the follow-up of renal cell carcinoma. Am J Roentgenol. 2012;198:1266–76. https://doi.org/10.2214/AJR.11.8381.
105. Rutherford EE, Cast JEI, Breen DJ. Immediate and long-term CT appearances following radiofrequency ablation of renal tumours. Clin Radiol. 2008;63:220–30. https://doi.org/10.1016/j.crad.2007.07.002.

106. Javadi S, Ahrar JU, Ninan E, Gupta S, Matin SF, Ahrar K. Characterization of contrast enhancement in the ablation zone immediately after radiofrequency ablation of renal tumors. J Vasc Interv Radiol. 2010;21:690–5. https://doi.org/10.1016/j.jvir.2009.12.400.
107. Gervais DA, McGovern FJ, Arellano RS, Scott McDougal W, Mueller PR. Renal cell carcinoma: clinical experience and technical success with radio-frequency ablation of 42 tumors. Radiology. 2003;226:417–24. https://doi.org/10.1148/radiol.2262012062.
108. Merkle EM, Nour SG, Lewin JS. MR imaging follow-up after percutaneous radiofrequency ablation of renal cell carcinoma: findings in 18 patients during first 6 months. Radiology. 2005;235:1065–71. https://doi.org/10.1148/radiol.2353040871.
109. Kawamoto S, Solomon SB, Bluemke DA, Fishman EK. Computed tomography and magnetic resonance imaging appearance of renal neoplasms after radiofrequency ablation and cryoablation. Semin Ultrasound CT MRI. 2009;30:67–77. https://doi.org/10.1053/j.sult.2008.12.005.
110. Ganguli S, Brennan DD, Faintuch S, Rayan ME, Goldberg SN. Immediate renal tumor involution after radiofrequency thermal ablation. J Vasc Interv Radiol. 2008;19:412–8. https://doi.org/10.1016/j.jvir.2007.10.024.
111. Matsumoto ED, Watumull L, Johnson DB, Ogan K, Taylor GD, Josephs S, Cadeddu JA. The radiographic evolution of radio frequency ablated renal tumors. J Urol. 2004;172:45–8. https://doi.org/10.1097/01.ju.0000132124.01060.0c.
112. Davenport MS, Caoili EM, Cohan RH, Ellis JH, Higgins EJ, Willatt J, Fox GA. MRI and CT characteristics of successfully ablated renal masses: imaging surveillance after radiofrequency ablation. Am J Roentgenol. 2009;192:1571–8. https://doi.org/10.2214/AJR.08.1303.
113. Svatek RS, Sims R, Anderson JK, Abdel-Aziz K, Cadeddu JA. Magnetic resonance imaging characteristics of renal tumors after radiofrequency ablation. Urology. 2006;67:508–12. https://doi.org/10.1016/j.urology.2005.09.046.
114. Aoun HD, Littrup PJ, Jaber M, Memon F, Adam B, Krycia M, Prus M, Heath E, Pontes E. Percutaneous cryoablation of renal tumors: is it time for a new paradigm shift? J Vasc Interv Radiol. 2017;28:1363–70. https://doi.org/10.1016/j.jvir.2017.07.013.
115. Beemster P, Phoa S, Wijkstra H, De La Rosette J, Laguna P. Follow-up of renal masses after cryosurgery using computed tomography; enhancement patterns and cryolesion size. BJU Int. 2008;101:1237–42. https://doi.org/10.1111/j.1464-410X.2007.07437.x.
116. Gill IS, Remer EM, Hasan WA, Strzempkowski B, Spaliviero M, Steinberg AP, Kaouk JH, Desai MM, Novick AC. Renal cryoablation: outcome at 3 years. J Urol. 2005;173:1903–7. https://doi.org/10.1097/01.ju.0000158154.28845.c9.
117. Gupta A, Allaf ME, Kavoussi LR, Jarrett TW, Chan DYS, Su LM, Solomon SB. Computerized tomography guided percutaneous renal cryoablation with the patient under conscious sedation: initial clinical experience. J Urol. 2006;175:447–53. https://doi.org/10.1016/S0022-5347(05)00247-8.
118. Miki K, Shimomura T, Yamada H, Kishimoto K, Ohishi Y, Harada J, Egawa S. Percutaneous cryoablation of renal cell carcinoma guided by horizontal open magnetic resonance imaging. Int J Urol. 2006;13:880–4. https://doi.org/10.1111/j.1442-2042.2006.01432.x.
119. Stein AJ, Mayes JM, Mouraviev V, Chen VH, Nelson RC, Polascik TJ. Persistent contrast enhancement several months after laparoscopic cryoablation of the small renal mass may not indicate recurrent tumor. J Endourol. 2008;22:2433–9. https://doi.org/10.1089/end.2008.0261.
120. Allen BC, Remer EM. Percutaneous cryoablation of renal tumors: patient selection, technique, and postprocedural imaging. Radiographics. 2010;30:887–900. https://doi.org/10.1148/rg.304095134.
121. Hegarty NJ, Gill IS, Desai MM, Remer EM, O'Malley CM, Kaouk JH. Probe-ablative nephron-sparing surgery: cryoablation versus radiofrequency ablation. Urology. 2006;68:7–13. https://doi.org/10.1016/j.urology.2005.12.049.
122. Lee HJ, Chung HJ, Wang HK, Shen SH, Chang YH, Chen CK, Chou HP, Chiou YY. Evolutionary magnetic resonance appearance of renal cell carcinoma after percutaneous cryoablation. Br J Radiol. 2016;89(1065):20160151. https://doi.org/10.1259/bjr.20160151.

123. Durack JC, Richioud B, Lyon J, Solomon SB. Late emergence of contrast-enhancing fat necrosis mimicking tumor seeding after renal cryoablation. J Vasc Interv Radiol. 2014;25:133–7. https://doi.org/10.1016/j.jvir.2013.07.006.
124. Remer EM, Weinberg EJ, Oto A, O'Malley CM, Gill IS. MR imaging of the kidneys after laparoscopic cryoablation. Am J Roentgenol. 2000;174:635–40. https://doi.org/10.2214/ajr.174.3.1740635.
125. Bolte SL, Ankem MK, Moon TD, Hedican SP, Lee FT, Sadowski EA, Nakada SY. Magnetic resonance imaging findings after laparoscopic renal cryoablation. Urology. 2006;67:485–9. https://doi.org/10.1016/j.urology.2005.09.015.
126. Matin SF, Ahrar K, Cadeddu JA, Gervais DA, McGovern FJ, Zagoria RA, Uzzo RG, Haaga J, Resnick MI, Kaouk J, Gill IS. Residual and recurrent disease following renal energy ablative therapy: a multi-institutional study. J Urol. 2006;176:1973–7. https://doi.org/10.1016/j.juro.2006.07.016.
127. Weight CJ, Kaouk JH, Hegarty NJ, Remer EM, O'Malley CM, Lane BR, Gill IS, Novick AC. Correlation of radiographic imaging and histopathology following cryoablation and radio frequency ablation for renal tumors. J Urol. 2008;179:1277–83. https://doi.org/10.1016/j.juro.2007.11.075.
128. Klotz L, Zhang L, Lam A, Nam R, Mamedov A, Loblaw A. Clinical results of long-term follow-up of a large, active surveillance cohort with localized prostate cancer. J Clin Oncol. 2010;28:126–31. https://doi.org/10.1200/JCO.2009.24.2180.
129. Rosenkrantz AB, Scionti SM, Mendrinos S, Taneja SS. Role of MRI in minimally invasive focal ablative therapy for prostate cancer. Am J Roentgenol. 2011;197:90–6. https://doi.org/10.2214/AJR.10.5946.
130. Burger IA, Müller J, Donati OF, Ferraro DA, Messerli M, Kranzbühler B, ter Voert EEGW, Muehlematter UJ, Rupp NJ, Mortezavi A, Eberli D. 68Ga-PSMA-11 PET/MR detects local recurrence occult on mpMRI in prostate cancer patients after HIFU. J Nucl Med. 2019;60:1118–23. https://doi.org/10.2967/jnumed.118.221564.
131. Muller BG, van den Bos W, Brausi M, Fütterer JJ, Ghai S, Pinto PA, Popeneciu IV, de Reijke TM, Robertson C, de la Rosette JJMCH, Scionti S, Turkbey B, Wijkstra H, Ukimura O, Polascik TJ. Follow-up modalities in focal therapy for prostate cancer: results from a Delphi consensus project. World J Urol. 2015;33:1503–9. https://doi.org/10.1007/s00345-014-1475-2.
132. Tay KJ, Amin MB, Ghai S, Jimenez RE, Kench JG, Klotz L, Montironi R, Muto S, Rastinehad AR, Turkbey B, Villers A, Polascik TJ. Surveillance after prostate focal therapy. World J Urol. 2019;37:397–407. https://doi.org/10.1007/s00345-018-2363-y.
133. ter Haar G. Therapeutic applications of ultrasound. Prog Biophys Mol Biol. 2007;93:111–29. https://doi.org/10.1016/j.pbiomolbio.2006.07.005.
134. ter Haar G, Coussios C. High intensity focused ultrasound: physical principles and devices. Int J Hyperth. 2007;23:89–104. https://doi.org/10.1080/02656730601186138.
135. Kirkham APS, Emberton M, Hoh IM, Illing RO, Freeman AA, Allen C. MR imaging of prostate after treatment with high-intensity focused ultrasound. Radiology. 2008;246:833–44. https://doi.org/10.1148/radiol.2463062080.
136. Rouvière O, Girouin N, Glas L, Ben Cheikh A, Gelet A, Mège-Lechevallier F, Rabilloud M, Chapelon JY, Lyonnet D. Prostate cancer transrectal HIFU ablation: detection of local recurrences using T2-weighted and dynamic contrast-enhanced MRI. Eur Radiol. 2010;20:48–55. https://doi.org/10.1007/s00330-009-1520-5.
137. Rouvière O, Lyonnet D, Raudrant A, Colin-Pangaud C, Chapelon JY, Bouvier R, Dubernard JM, Gelet A. MRI appearance of prostate following transrectal HIFU ablation of localized cancer. Eur Urol. 2001;40:265–74. https://doi.org/10.1159/000049786.
138. Gage AA, Baust J. Mechanisms of tissue injury in cryosurgery. Cryobiology. 1998;37:171–86. https://doi.org/10.1006/cryo.1998.2115.
139. Larson TR, Rrobertson DW, Corica A, Bostwick DG. In vivo interstitial temperature mapping of the human prostate during cryosurgery with correlation to histopathologic outcomes. Urology. 2000;55:547–52. https://doi.org/10.1016/S0090-4295(99)00590-7.

140. Cohen JK, Miller RJ, Ahmed S, Lotz MJ, Baust J. Ten-year biochemical disease control for patients with prostate cancer treated with cryosurgery as primary therapy. Urology. 2008;71:515–8. https://doi.org/10.1016/j.urology.2007.09.059.
141. Babaian RJ, Donnelly B, Bahn D, Baust JG, Dineen M, Ellis D, Katz A, Pisters L, Rukstalis D, Shinohara K, Thrasher JB. Best practice statement on cryosurgery for the treatment of localized prostate cancer. J Urol. 2008;180:1993–2004. https://doi.org/10.1016/j.juro.2008.07.108.
142. Gangi A, Tsoumakidou G, Abdelli O, Buy X, De Mathelin M, Jacqmin D, Lang H. Percutaneous MR-guided cryoablation of prostate cancer: initial experience. Eur Radiol. 2012;22:1829–35. https://doi.org/10.1007/s00330-012-2411-8.
143. Donnelly SE, Donnelly BJ, Saliken JC, Raber EL, Vellet AD. Prostate cancer: gadolinium-enhanced MR imaging at 3 weeks compared with needle biopsy at 6 months after cryoablation. Radiology. 2004;232:830–3. https://doi.org/10.1148/radiol.2323030841.
144. Parivar F, Hricak H, Shinohara K, Kurhanewicz J, Vigneron DB, Nelson SJ, Carroll PR. Detection of locally recurrent prostate cancer after cryosurgery: evaluation by transrectal ultrasound, magnetic resonance imaging, and three-dimensional proton magnetic resonance spectroscopy. Urology. 1996;48:594–9. https://doi.org/10.1016/S0090-4295(96)00250-6.
145. Vellet AD, Saliken J, Donnelly B, Raber E, McLaughlin RF, Wiseman D, Ali-Ridha NH. Prostatic cryosurgery: use of MR imaging in evaluation of success and technical modifications. Radiology. 1997;203:653–9. https://doi.org/10.1148/radiology.203.3.9169684.
146. Ting F, Tran M, Böhm M, Siriwardana A, Van Leeuwen PJ, Haynes AM, Delprado W, Shnier R, Stricker PD. Focal irreversible electroporation for prostate cancer: functional outcomes and short-term oncological control. Prostate Cancer Prostatic Dis. 2016;19:46–52. https://doi.org/10.1038/pcan.2015.47.
147. Scheltema MJ, Postema AW, de Bruin DM, Buijs M, Engelbrecht MR, Laguna MP, Wijkstra H, de Reijke TM, de la Rosette JJMCH. Irreversible electroporation for the treatment of localized prostate cancer: a summary of imaging findings and treatment feedback. Diagnostic Interv Radiol. 2017;23:365–70. https://doi.org/10.5152/dir.2017.16608.
148. Viswanath S, Toth R, Rusu M, Sperling D, Lepor H, Futterer J, Madabhushi A. Quantitative evaluation of treatment related changes on multi-parametric MRI after laser interstitial thermal therapy of prostate cancer. Med imaging 2013 image-guided Proced robot Interv model. Proc SPIE Int Soc Opt Eng. 2013;8671:86711F. https://doi.org/10.1117/12.2008037.
149. Oto A, Sethi I, Gregory Karczmar M, McNichols R, Ivancevic MK, Stadler WM, Watson S, Eggener S. Section of hematology/oncology. Dept Med. 2013;267 https://doi.org/10.1148/radiol.12121652/-/DC1.
150. Wenger H, Yousuf A, Oto A, Eggener S. Laser ablation as focal therapy for prostate cancer. Curr Opin Urol. 2014;24:236–40. https://doi.org/10.1097/MOU.0000000000000044.
151. Toth R, Sperling D, Madabhushi A. Quantifying post-laser ablation prostate therapy changes on MRI via a domain-specific biomechanical model: preliminary findings. PLoS One. 2016;11:1–17. https://doi.org/10.1371/journal.pone.0150016.
152. Felker ER, Raman SS, Lu DSK, Tuttle M, Margolis DJ, FF ElKhoury, Sayre J, Marks LS. Utility of Multiparametric MRI for Predicting Residual Clinically Significant Prostate Cancer After Focal Laser Ablation. AJR Am J Roentgenol. 2019;213(6):1253–8. https://doi.org/10.2214/AJR.19.21637.
153. Lotte R, Lafourcade A, Mozer P, Conort P, Barret E, Comperat E, Ezziane M, de Guibert PHJ, Tavolaro S, Belin L, Boudghene F, Lucidarme O, Renard-Penna R. Multiparametric MRI for suspected recurrent prostate cancer after HIFU: is DCE still needed? Eur Radiol. 2018;28:3760–9. https://doi.org/10.1007/s00330-018-5352-z.
154. Anzai Y, Lufkin RB, Farahani K, Hirschowitz S, Castro DJ. MR imaging—histopathologic correlation of thermal injuries induced with interstitial Nd: YAG laser irradiation in the chronic model. J Magn Reson Imaging. 1992;2:671–8. https://doi.org/10.1002/jmri.1880020611.
155. Kim CK, Byung KP, Hyun ML, Sam SK, Kim EJ. MRI techniques for prediction of local tumor progression after high-intensity focused ultrasonic ablation of prostate cancer. Am J Roentgenol. 2008;190:1180–6. https://doi.org/10.2214/AJR.07.2924.

Chapter 21
Immune Modulation in Interventional Oncology

Johannes Maximilian Ludwig, Michael Cecchini, and Hyun S. Kim

Abbreviations

CD	Cluster of differentiation
CTLA-4	Cytotoxic T-lymphocyte-associated protein 4
DAMPs	Damage-associated molecular patterns
DC	Dendritic cells
HCC	Hepatocellular carcinoma
HGF	Hepatocyte growth factor
HLA-DR	Human leukocyte antigen-DR isotype
IFN-γ	Interferon gamma
IL	Interleukin

J. M. Ludwig
Section of Interventional Radiology, Department of Radiology and Biomedical Imaging, Yale School of Medicine, New Haven, CT, USA

Department of Diagnostic and Interventional Radiology and Neuroradiology, University Hospital Essen, University of Duisburg-Essen, Essen, Germany
e-mail: johannes.ludwig@yale.edu

M. Cecchini
Section of Medical Oncology, Department of Internal Medicine, Yale School of Medicine, New Haven, CT, USA

Yale Cancer Center, Yale School of Medicine, New Haven, CT, USA

H. S. Kim (✉)
Section of Interventional Radiology and Section of Medical Oncology, Yale Cancer Center, Yale School of Medicine, New Haven, CT, USA
e-mail: kevin.kim@yale.edu

C. Georgiades, H. S. Kim (eds.), *Image-Guided Interventions in Oncology*,
https://doi.org/10.1007/978-3-030-48767-6_21

IO	Interventional oncology
LRT	Locoregional therapies
MDSC	Myeloid-derived suppressor cells
MWA	Microwave ablation
NF-κβ	Nuclear factor kappa-light-chain-enhancer of activated B cells
NK	Natural killer cells
OI	Oncoimmunology
PD-L1	Programmed death-ligand 1
RFA	Radiofrequency ablation
SIRT	Selective intraarterial radioembolization
TAA	Tumor-associated antigen
TACE	Transarterial chemoembolization
TGF-β	Transforming growth factor beta
TIM-3	T-cell immunoglobulin and mucin domain-3
TLR	Toll-like receptor
TME	Tumor microenvironment
TNF-α	Tumor necrosis factor alpha
T_{regs}	T regulatory cells
VEGF	Vascular endothelial growth factor

Immune System in Cancer: A Janus-Faced Role

Discovering immune cells in tumors has raised fundamental questions regarding the interaction of tumor and immune cells. It is a well-accepted hallmark that chronic inflammation plays a pivotal role during carcinogenesis in at least 25% of all cancers as it leads to genomic instability, epigenetic modification, cancer proliferation, angiogenesis, activation of anti-apoptotic signaling pathways, and cancer metastasis [1, 2]. Thus, one may think that immunosuppression is critical to prevent cancer. Indeed, long-term use of nonsteroidal anti-inflammatory drugs has been reported to lower cancer risk [3]. Conversely, immunosuppression in patients suffering from AIDS-related immunodeficiency or therapeutic immunosuppression for the treatment of rheumatologic diseases and after organ transplantation is linked to increased cancer risk [4–6]. Moreover, acute inflammation can be utilized for the cancer treatment of, e.g., squamous cell cancer of the bladder, where an attenuated *Mycobacterium bovis* strain is instilled into the bladder [7]. The interplay of cancer and the immune system is highly complex, with no simple and straightforward answer to the exact role of the immune system in cancer. There is a myriad of different interactions between adaptive and innate immune cells with cancer cells within the tumor microenvironment (TME). Their interactions play a crucial role, which in some cases leads to the promotion of cancer progression and, in others, successful eradication by the immune system.

With the potential for cancer cells to evolve every day, it borders on a miracle that not all of us develop and die from cancer. The evolution of cancer development occurs in three steps (Fig. 21.1).

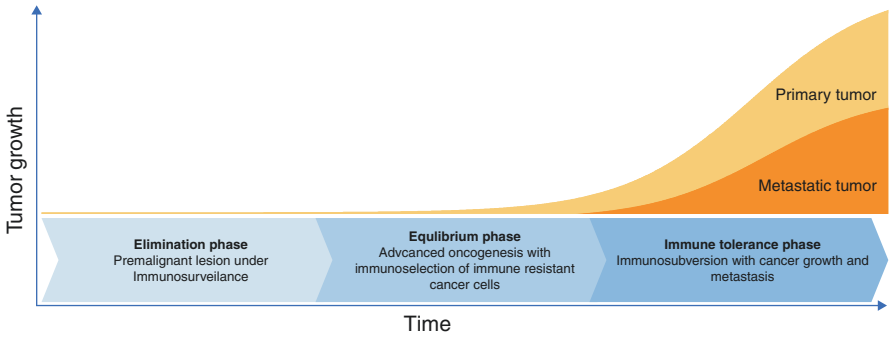

Fig. 21.1 Immunoediting during the evolution of cancer: Premalignant cells are eliminated, selecting less immunogenic cell clones, which then grow to a clinically evident tumor building up immune tolerance

- *Elimination phase*: Early in the course of tumor development, tumor-specific antigens are recognized, and secretion of Th-1 cytokines (IFN-γ, IL-2, IL-12) promotes maturation of dendritic cells priming $CD8^+$ T-cells against tumor antigens, and activation of natural killer (NK) cells occurs. Subsequent tumoricidal immune response is then carried out by NK and $CD8^+$ T-cells by exocytosis of perforins and granzymes [1, 8], which then ideally eliminates all potential cancer cells.
- *Equilibrium phase*: Considering that tumors usually consist of cells with varying expression profiles and mutations, it is likely that some tumor cells are less immunogenetic and thus successfully evade the first elimination phase. These cells continue to grow unaffected by the immune system leading to the selection of lesser immunogenic cancer cells.
- *Immune tolerance phase*: Cancer cells subverse the immune system, grow, and become clinically evident. It must be noted, though, that the immune system and cancer cells still interact and, dependent on the intratumoral immune cells, the prognosis is known to be impacted substantially. For example, high infiltration rates of macrophages, neutrophils, and $CD4^+$ T-regulatory cells (T_{regs}) are associated with a poor prognosis, whereas infiltration with $CD8^+$ T-cells and NK cells correlates with a better prognosis [1].

Stimulating the Immune System by Locoregional Therapies: The Abscopal Effect

Interventional oncologists have a vast array of locoregional antitumor therapies available such as radioembolization, chemoembolization, thermal ablation, irreversible electroporation, and high-intensity focused ultrasound. Although the techniques and mechanisms of tumor damage vary greatly, they all share the characteristic feature of leaving damaged tumor tissue in situ compared to surgical resection [9].

In rare cases, tumor regression of non-treated tumor lesions has been observed after LRT (Fig. 21.2). This phenomenon is acknowledged as the abscopal effect ("ab," away from; "scopus," target) introduced by H.R. Mole in 1953 after observing tumor regression of a non-treated distant tumor after applying ionizing irradiation to the target lesion [10]. The underlying mechanisms remained unclear for around half a century until 2004, where it has been postulated that the immune system drives the off-target antitumor effects [11]. Discovering that in situ remaining tumor tissue with tumor-derived antigens can activate a systemic antitumor immune response, the concept of an in vivo vaccination against tumors was born. Unfortunately, the abscopal effect with relevant clinical tumor regression is a scarce and infrequently observed element following LRT alone. Much research has been pursued to broaden the understanding of immune modulation in cancer by LRTs, which created a rationale for the combination with immunotherapies aiming at synergistic immunostimulatory effects to improve treatment outcomes.

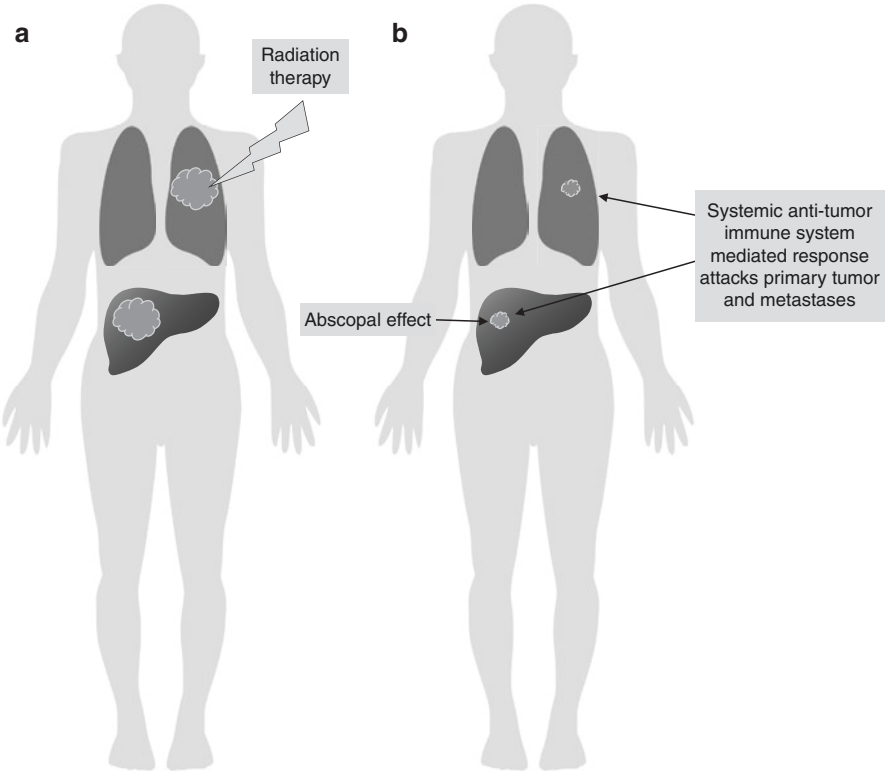

Fig. 21.2 Abscopal effect: Radiation treatment of lung metastases (**a**) leads to a systemic antitumor immune response targeting primary tumor and metastases with tumor shrinkage or even complete eradication (**b**)

Ablation

Most research regarding the immune-stimulating effect of IO techniques has been described for ablation with the majority performed in animal models. Although the mechanisms of cell death and the expression patterns of cytokines vary between IO techniques, the general pathway of how to ignite an antitumor immune response is substantially overlapping. Thus, the antitumor immunostimulatory pathway is outlined based on ablation (Fig. 21.3).

How Ablation Induces an Antitumor Immune Response: The Mechanism

1. Reducing immune tolerance by reducing immunosuppressive factors: The tumor strategy to evade the immune system is based on avoiding recognition (presenting fewer antigens on cell surface, e.g., by major histocompatibility complex (MHC) loss), becoming resistant to death stimuli (NK receptors↓, resistance to T-cell death stimuli TNF-α and IFN-γ), and to create an immunosuppressive TME. An immunosuppressive TME is achieved by complex interactions of a myriad of suppressive factors (IL-10, TGF-β, prostaglandin E2, VEGF), increased expression of immune checkpoint inhibitors (e.g., CTLA-4, PD-L1), and secretion of chemokines to achieve chemotaxis of "cancer-friendly" immune cells (tumor-associated macrophages (TAMs), T_{regs}, myeloid-derived suppressor cells (MDSCs)). By destroying tumor mass, ablation disrupts this immunosuppressive network taking off the brake of the antitumor immune response [1, 12, 13].
2. Increased availability of tumor-specific antigens and inflammation: As ablation causes necrotic cell death, the release and availability of tumor-specific antigens are significantly increased, thus raising immunogenicity as an in situ vaccine. Subsequent drainage of antigens to the nearby lymph node can stimulate immature dendritic cells (DCs) to prime naïve T-cells (Fig. 21.3).
3. Activating antigen-presenting cells: Damaged and necrotic tumor tissue also releases a variety of damage-associated molecular patterns (DAMPs) such as heat shock proteins (HSPs), high mobility group protein B1 (HMGB1), DNA, and more. These DAMPs are phagocytized by DCs, which leads to activation, maturation, and the expression of co-stimulatory molecules (e.g., CD80/86) via the NF-κβ pathway necessary for the activation of antitumor $CD8^+$ T-cells [14, 15]. This step is crucial as dysfunctional, insufficient, or lack of DC activation will not result in the activation of naïve T-cells and thus abrogate the initiation of the adaptive immune response. To potentially overcome this issue, several strategies have been developed on how to improve the DC function. For example, in a preclinical study with the B16OVA mouse melanoma model, topical treatment with the TLR7 agonist imiquimod (induction of CD80/86) in combination with

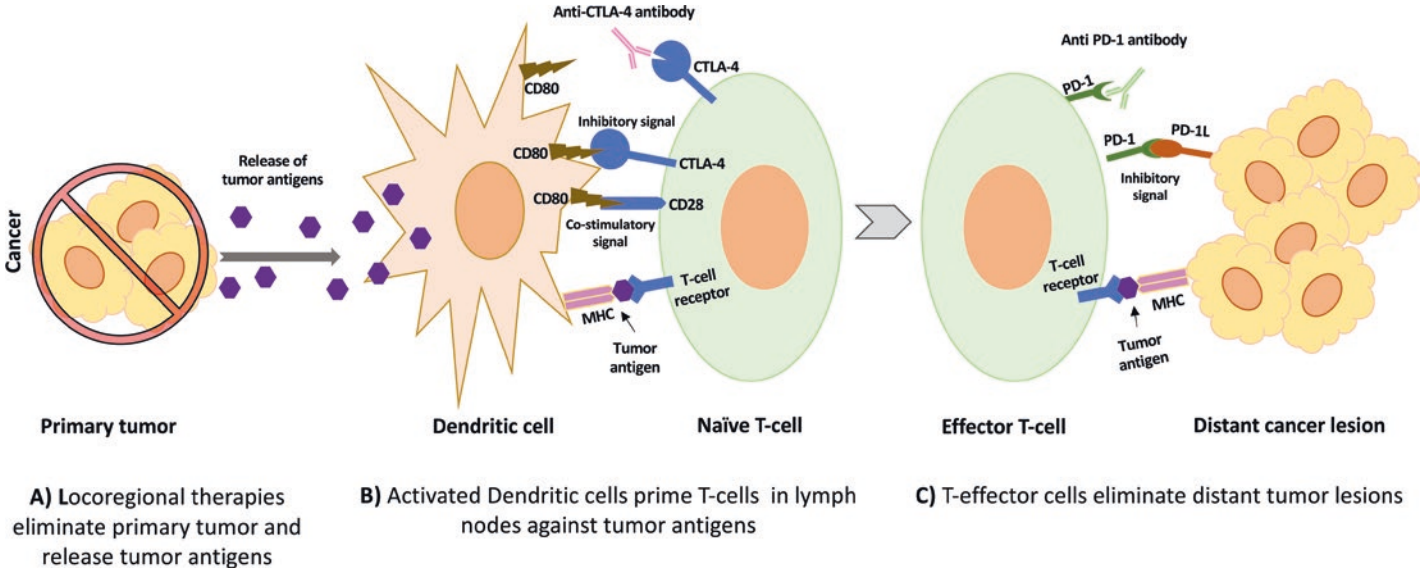

Fig. 21.3 Immunostimulation of interventional oncology (IO) techniques and synergistic effects in combination with immune checkpoint inhibitors – boosting the antitumor immune response: (**a**) IO modalities increase the availability of tumor antigens, promote inflammation, and decrease immunosuppressive factors. (**b**) Priming of naïve T-cells against tumor antigens is promoted by the increased availability of tumor antigens, activation of dendritic cells, and blocking CTLA-4 which increases the likelihood of T-cell priming. (**c**) Anti-PD-1 blocks T-effector cell inhibition by tumor cells, thus promoting cancer cell elimination

cryotherapy resulted in significant protection against tumor rechallenge (90% protection) compared to mice which were only treated with cryoablation (30% protection) [16]. In the same mouse model, TLR9 activation with a peritumoral injection of CpG oligodeoxynucleotides (IFN-α-mediated DC recruitment) in combination with cryoablation showed complete protection against tumor outgrowth after tumor rechallenge [17]. Thus, TLR4 and TLR7 agonist may be a useful additive strategy to improve treatment outcome.

4. Priming of naïve $CD8^+$ T-cells against tumor antigens: In the locoregional lymph node, activated DCs present tumor antigens to naïve T-cells, which ideally results in T-cell activation, clonal expansion, infiltration of viable tumor tissue, and cancer cell killing.

Positive immunostimulatory effects have been for as hepatocellular carcinoma (HCC) and colorectal carcinoma liver metastases where treatment with RFA demonstrated increased numbers and an elevated cytotoxic activity (100-fold) of antitumoral $CD8^+$ T-cells in the peripheral blood four weeks after RFA [18]. Furthermore, immunogenic antitumor findings were reported in patients with high-risk prostate cancer where antitumor cytotoxic T-cell stimulation resulted in increased levels of TNF-alpha and IFN-gamma as well as in increased cytolytic activity of T-cells against cancer cells [19]. In another study of 69 patients with HCC, an increase of T-cells specifically primed against tumor-associated antigens (TAA; 11 were tested) was observed in 62.3% of patients after RFA. The number of TAA-specific T-cells inversely correlated with the number of tumor-suppressive MDSCs and with HCC recurrence. However, at the time of 24 weeks post ablation, TAA-specific T-cells have decreased [20]. Overall, despite the immune activation of tumor ablation, the observed effects are short-lived and do not often translate into a prolonged and robust antitumor immune response.

Tumorigenic Effects of Ablation Modalities

LRT only with its anticancer immune activation, unfortunately, only rarely results in a substantial abscopal treatment effect (Fig. 21.3.). Moreover, ablation does not always successfully activate the immune system against cancer and even has the capability to achieve the opposite effect and promote immune tolerance, tumor growth, and metastases. Several factors have been identified to promote immunosuppression by clonal deletion and anergy of T-cells: Apoptosis leads to immune tolerance as this results in uptake of cellular debris without causing inflammation and liberating DAMPs. Thus, the lack of stimulating DAMPs and the inhibitory effect of phagocytized apoptotic cell bodies will prevent maturation of DCs, leading to clonal deletion and anergy [12, 14, 21]. Additionally, increased tumor ablation can increase levels of interleukin-6 (IL-6), hypoxia-inducible factor-1α (HIF-1α), hepatocyte growth factor (HGF), and its receptor c-MET which not only are meant to support physiological regeneration of tissue after damage but also are known to

have tumorigenic effects [22–24]. Also, the upregulation of the expression of the immune checkpoint PD-L1 has been observed which provides the rationale for combination with immune checkpoint inhibitors, which will be outlined below [25, 26].

The potential tumorigenic impact of LRT should not be underestimated. In one example, 580 patients with HCC smaller than 3 cm were either resected or ablated (RFA). Here, an increased rate of new distant intrahepatic lesions (62.7% vs. 36.6% within 5 years) and a shorter disease-free survival (31.7% vs. 61.1%) was observed for patients treated with RFA compared to surgery [27]. Moreover, in another example, 63 patients with multifocal hereditary renal cell carcinoma, RFA of one lesion resulted in four times the accelerated growth rate of the untreated lesions [28].

How to Ablate Best to Stimulate an Anticancer Immune Response?

Regarding the immunostimulatory effects, two main factors appear to be critical: ablation modality and ablation protocol. Based on the limited data available, there is a significant biological variance of study models (species, tumor location, tumor biology, age, time point, size etc.) as well as technical differences (ablation method, device settings, ablation zone etc.), thus not allowing for a definite conclusion yet on "how to ablate best" to induce the best possible anticancer immune reaction.

Regarding the ablation modality, data suggests cryoablation as one of the most promising candidates as, e.g., the induction of an inflammatory response is higher than for RFA and laser-induced therapy [29]. Moreover, the availability of well-persevered and for the immune system visible antigens is greater for cryoablation compared to heat denaturated antigens by, e.g., RFA.

In terms of the ablation protocol, Velez et al. investigated the tumoricidal effect of MWA and RFA of healthy liver tissue on tumor growth in a rat breast cancer model [24]. Three ablation protocols were applied: MWA at 5 W for 2 min. (low power, long duration), MWA at 20 W for 15 sec. (high power, short duration), and RFA (70 °C, 5 min). Low-energy MWA and RFA both had significantly increased tumor size at day 7 (MWA, 16.3 mm ± 1.1; RFA, 16.3 mm ± 0.9; mean with standard deviation) compared to the high MWA (14.6 mm ± 0.9, $p < 0.05$) and sham procedure (13.6 mm ± 1.3, $p < 0.01$) groups. For the high MWA group, local periablational immune cell infiltration and expression of pro-tumorigenic factors (VEGF; HGF, IL-6) were lower. The authors conclude that higher power and shorter ablation time (of healthy liver tissue) may mitigate the pro-tumorigenic effect when tumor tissue is ablated. However, drawing a conclusion for the ablation of tumor lesions is limited as the effect of higher energy regarding the in situ vaccine immunogenicity of an ablated tumor can only be speculated. In a breast cancer mouse model, Sabel et al. investigated the immunogenic response following to rapid (~30 sec) vs. slow (several minutes) freezing of subcutaneous tumors (8–12 mm). Compared to surgical excision, mice had an increased rate of tumor-specific T-cells in the tumor-draining lymph node after 7 days, a lower rate of lung metastases, and more prolonged survival. Divergent tumor behavior was seen in the low freeze group,

where an increased rate of T_{reg} cells and a higher rate of metastases were observed [30]. Although transferability to humans and clinical routine is limited, a quicker cooling process may be beneficial.

Immunostimulatory Modulation by Arterial Embolization Techniques

Investigations on the immune modulation of transarterial chemoembolization (TACE) in patients with HCC revealed that, before treatment, the ratio of $CD4^+$/$CD8^+$ peripheral T-lymphocytes was lower, and the levels of $CD4^+CD25^+$ T_{reg} cells of all $CD4^+$ cells were elevated compared to healthy volunteers which can be interpreted as a suppressed systemic immune function frequently observed in cancer patients. Following TACE, ratios of $CD4^+/CD8^+$ T lymphocytes increased, and the fraction of $CD4^+CD25^+$ T_{reg} cells of all $CD4^+$ cells decreased, demonstrating the ability to improve the immune function [31, 32]. Following bland embolization of primary and metastatic liver tumors, different effects were observed: T_{reg} cells were similarly found to be reduced, but also the number of $T_{helper1}$ cells, which usually enhance antitumor immune response by secreting IFN-γ and activating cytotoxic antitumor T-cells, was found to be reduced. It may be speculated that post embolization, increased IL-6 levels inhibited differentiation of $T_{helper1}$ cells from naïve T-cells [33]. Another study investigated the alterations of cytokines following TACE of HCC lesions and concluded that there is no uniform pattern of inflammation as they are influenced by liver function and HCC stage. In patients with tumors >5 cm, early IL-6 levels were significantly higher, and post-TACE hepatitis occurred more often which indicates a more considerable hepatic trauma whose subsequent repair signals can thrive tumor growth. Also, 2 months after TACE, $T_{helper2}$ cytokines (Il-4, IL-5, IL-10) were increased suggesting a suppressive environment limiting antitumor response [34]. In summary, embolization with and without additive drugs causes complex alterations of the immune system with pro- and antitumorigenic effects further influenced by several non-treatment-associated modulators. As tissue damage with the induced repair cascade has a pro-tumorigenic effect, it may be speculated that a more selective TACE may be beneficial in this regard.

Immunostimulatory Modulation by Selective Intraarterial Radioembolization (SIRT)

The ionizing radiation of SIRT is mainly used to induce tumor cell death through DNA damage. As external beam radiation therapy is a well-known inducer of immunogenic cell death, recent research focused on the anti-cancer immune stimulatory potential of SIRT [35].

In a study with 41 HCC patients who underwent surgical resection for HCC with or without prior SIRT a higher expression of granzyme B containing $CD8^+$ T-cells and NK cells in tissue after radioembolization was observed, which furthermore positively correlated with a sustained therapeutic response. Also, increased expression of the negative immune checkpoint TIM-3 (T-cell immunoglobulin and mucin domain-3) was observed [36], which has also has been reported in patients developing resistance to anti-PD-1 immunotherapy [37]. On the other hand, it has to be noted that following SIRT, peripheral lymphopenia is induced, affecting all lymphocyte subsets as well as reduced activation of monocytes and memory T-cells [38]. Further research is warranted regarding the stimulation and suppression of immune cells and how that affects the immunological antitumor immune response. Additionally, considering the discovery that hypofractionated external beam radiation maximizes the antitumor immune effect, similar studies regarding the immunostimulatory effects in varying radiation doses of SIRT still lack and are highly warranted [39].

Combination of LRTs with Further Immunostimulatory Therapies to Maximize Treatment Effects

The idea to harness the power of the immune system to combat cancer has existed for decades. Several approaches have demonstrated promising treatment benefits in animal models and humans by activating the innate and/or adaptive immune system. The immune checkpoint inhibitors are widely acknowledged as the most significant breakthrough immunotherapies and are currently approved for numerous cancers.

Functioning of Immune Checkpoint Inhibitors

Immune checkpoints are crucial regulators of the immune system to prevent autoimmunity by promoting self-tolerance. The currently available immune checkpoint inhibitors block inhibitory pathways to skew the balance toward an immune stimulation against presented antigens. The blockade of the immune co-inhibitory receptors CTLA-4 (cytotoxic T-lymphocyte antigen 4), PD-1 (programmed death 1), and PD-L1 (programmed death-ligand 1) using monoclonal antibodies has been the most promising (Fig. 21.3). Anti CTLA-4 blocks the interaction between the CD80/86 and CTLA-4 during the tumor-antigen presentation of dendritic cells to naïve T-cells. Blocking an inhibitory cell-cell interaction signal for T-cell priming increases the likelihood that naïve T-cells will undergo clonal expansion and differentiation to effector antigen-specific T-cells [40, 41]. Once T-cells are activated and migrate into the tumor, interaction between the PD-L1 on the tumor cell surface with the PD-1 receptor of the $CD8^+$ T-effector cells can block antitumor cytotoxicity. Thus, blocking the interaction by PD-1 or PD-L1 targeting antibodies promotes

immune cell-mediated tumor elimination [42, 43]. It has to be noted that CTLA-4 and PD-1/PD-L1 are expressed on many more cells with a diversity of functions, which are still not fully understood.

Durable responses and long-term survival benefit have been demonstrated in many cancer types with favorable toxicity profiles compared to conventional chemotherapy leading to FDA approval of several immune checkpoint inhibitors (anti-CTLA-4, anti-PD-1, and anti-PD-L1) for many cancer types such as melanoma, renal cell carcinoma and non-small cell lung cancer, triple-negative breast cancer, Merkel cell carcinoma, liver cancer, head and neck cancer, and bladder cancer [44].

Immunotherapy for HCC

The liver is exposed to a great variety of antigens, such as gut-derived microbes and toxins. Thus, immune tolerance is crucial to prevent an aberrant immune response, and the environment is generally considered immunosuppressive. Furthermore, HCC mostly occurs in the setting of a chronic viral infection associated with increased expression of inhibitory checkpoint molecules, increased immune inhibitory cytokines, inhibitory alterations of dendritic cell function, and increased numbers of T_{regs}. Moreover, the constant exposure to antigens of T-cells also lead to overexpression of inhibitory immune checkpoint molecules, causing energy depletion and exhaustion of T-cells. All these factors help primary but also secondary liver cancer to more easily evade the immune system and promote tumor growth compared to extrahepatic tumor locations [45]. Modifying the immune system toward an anticancer immune reaction is therefore a promising but also a challenging approach for effective cancer therapy. Here, in general, the key is not only to increase the number and functionality (IFN-γ, perforins, granzymes↑) of T-cells primed against tumor antigens but also to create an environment (e.g., glucose and pH↑/non-acidotic to counteract depletion and exhaustion) where they can exert their maximum activity [45, 46].

Nivolumab is a human IgG4 recombinant monoclonal antibody specifically binding to PD-1. In the single-arm Checkmate-040 trial (phase I/II), all patients received nivolumab 3 mg/kg every 2 weeks, and an objective response rate (ORR) of 20% with a median response duration of 9.9 months could be achieved. The 6- and 9-month survival rates were 83% and 74%, respectively, as the median was not reached. Patients in the escalation group (0.1 mg/kg to 10 mg/kg nivolumab every 2 weeks) had an ORR of 15% and a median response duration of 17 months. The median overall survival (OS) was 28.6 months in sorafenib-naïve patients and 15 months in patients with prior sorafenib therapy [45, 46]. The results led to the FDA approval as second-line treatment after sorafenib. Similar to nivolumab, pembrolizumab is a human immunoglobulin IgG4 antibody that binds to PD-1 and achieves comparable response rates in HCC of approximately 17% [47]. However, in patients intolerant or refractory to sorafenib, in the placebo-controlled phase III trial KEYNOTE-240, pembrolizumab demonstrated an improved OS (HR: 0.78;

one-sided $p = 0.0238$) and PFS (HR: 0.78; one-sided $p = 0.0209$). Yet, as differences did not meet significance per prespecified statistical plan, the study was considered negative [48, 49].

Rationale for Combining LRTs with Immune Checkpoint Inhibitors

Combining locoregional with immunotherapies may be a promising approach due to several factors. (1) As previously described, the antitumor immune response induced by locoregional modalities is usually too weak to elicit an antitumor immune response but may be able to augment overall immune response to immunotherapies. (2) Larger and matured tumors in the immune escape phase breaking through the immune inhibitory TME by immunotherapeutics may result in lesser treatment effects [50]. As LRTs bear the potential to disrupt the immunosuppressive environment, treatment response may increase by reducing primary treatment resistance to immunotherapeutics. (3) In the case of tumor progression, LRT can be utilized to eliminate or control these resistant lesions as well as to potentially reinduce response to immunotherapy. The interplay of LRT and immune checkpoint inhibitors (anti-CTLA-4 and anti-PD-1) to augment priming of T-cells against tumor antigens is outlined in Fig. 21.3.

First Experiences in Combining LRT with Immune Checkpoint Inhibitors in Humans

To date, only limited data has been published on the treatment combination Especially data on the effectiveness of the treatment combination in human studies is greatly lacking. However, with many studies underway, we will soon better understand the actual benefits of this combination. Initial experience in a study of 26 patients with HCC treated with nivolumab within 90 days after SIRT proved to be safe, causing limited treatment-related side effects. Delayed grades 3/4 hepatobiliary toxicities were seen in two patients in the setting of disease progression and one occurrence of pneumonitis in a patient with 30% lung shunt fraction which resolved under steroid therapy. The median OS from the first radioembolization session was 16.5 months and the median PFS was 5.7 months [51].

In a separate study, tremelimumab (anti-CTLA-4) was followed by subtotal microwave ablation of biliary tract tumor [52]. Safety analysis was notable for 15% of patients that had severe study-related adverse events (lymphopenia, neutropenia, and hypotension), although no toxicity-related deaths were observed. Tumor response was achieved in 12.5%, and a disease control rate of 50% was observed. Immune

monitoring of peripheral cells revealed an increase of (HLA-DR positive) $CD8^+$ T-cells and an expanded T-cell repertoire for various antigens, which did not reach statistical significance ($p = 0.057$). Interestingly there was no increase for individual CTLA-4, TIM3, PD-1, and PD-L1, positive CD8 T-cells [52]. Additionally, further studies are underway, which will likely shed more light on this matter: NCT03237572, NCT02303366, NCT03099564, NCT03033446, NCT03143270, and NCT03572582.

Timing of LRT and Immunotherapy

One study in a mouse breast cancer model investigated the treatment effect of immunotherapy (CpG + anti-PD-1) with and without magnetic resonance-guided focused ultrasound ablation. In mice with high tumor burden (three orthotopic tumors with successive ablation of two), ablation after immune priming resulted in the survival of 60% compared to 25% when only treated with immunotherapy. In contrast, starting immunotherapy directly after ablation, the abscopal effect quickly diminished, and no complete response could be observed [53]. Overall, these findings suggest initial treatment with immune checkpoint inhibitors may be important when combining these therapies with LRT. Early use of immune checkpoint inhibitors is based on the hypothesis that immunostimulation by immunotherapies may take time to induce an immune reaction and that the immunostimulatory effects of LRTs are rather short-lived which may not allow for a simultaneous immune stimulation. The optimal treatment sequence however warrants further investigations as well as on the effect of combination with repetitive LRTs.

Concluding Remarks

Aside from physical tumor elimination, LRTs can modulate the immune system by inducing an antitumor immune response, which in rare cases alone, can result in eliminating distant tumor lesions. Several studies have demonstrated the potential of combining LRTs with immunotherapies to boost the overall antitumor immune response with better outcomes than for each treatment alone. However, structured protocols and treatment approaches need to be elaborated to achieve the best synergistic effects possible.

Aside from boosting the immune response, IO modalities can be utilized supplementary to immunotherapy in cases with one or a limited number of progressing lesions in otherwise stable disease to maintain overall tumor control. Additionally, in patients becoming treatment-resistant to immunotherapies, future studies are highly warranted to evaluate if LRTs with its immunomodulating properties can help to overcome treatment resistance by reinducing treatment response.

Key Points

- Locoregional therapies can modulate the immune system and induce an antitumor immune response which in rare cases can result in regression of distant, non-treated tumor lesions (abscopal effect).
- The combination of locoregional therapies and immunotherapies can act synergistically to boost the overall systemic antitumor immune response and thus improve the treatment outcome.
- Novel interventional oncological treatment concepts may have the potential to sensitize immunological "cold" tumors to immunostimulatory therapies with the ultimate aim of improving patient outcomes.

References

1. Gonzalez H, Hagerling C, Werb Z. Roles of the immune system in cancer: from tumor initiation to metastatic progression. Genes Dev. 2018;32(19–20):1267–84.
2. Hanahan D, Weinberg RA. Hallmarks of cancer: the next generation. Cell. 2011;144(5):646–74.
3. Thun MJ, Henley SJ, Patrono C. Nonsteroidal anti-inflammatory drugs as anticancer agents: mechanistic, pharmacologic, and clinical issues. J Natl Cancer Inst. 2002;94(4):252–66.
4. Frisch M, Biggar RJ, Engels EA, Goedert JJ, Group AI-CMRS. Association of cancer with AIDS-related immunosuppression in adults. JAMA. 2001;285(13):1736–45.
5. Kempen JH, Gangaputra S, Daniel E, Levy-Clarke GA, Nussenblatt RB, Rosenbaum JT, et al. Long-term risk of malignancy among patients treated with immunosuppressive agents for ocular inflammation: a critical assessment of the evidence. Am J Ophthalmol. 2008;146(6):802–12.. e1
6. Grulich AE, van Leeuwen MT, Falster MO, Vajdic CM. Incidence of cancers in people with HIV/AIDS compared with immunosuppressed transplant recipients: a meta-analysis. Lancet. 2007;370(9581):59–67.
7. Shalapour S, Karin M. Immunity, inflammation, and cancer: an eternal fight between good and evil. J Clin Invest. 2015;125(9):3347–55.
8. Teng MW, Galon J, Fridman WH, Smyth MJ. From mice to humans: developments in cancer immunoediting. J Clin Invest. 2015;125(9):3338–46.
9. den Brok MH, Sutmuller RP, van der Voort R, Bennink EJ, Figdor CG, Ruers TJ, et al. In situ tumor ablation creates an antigen source for the generation of antitumor immunity. Cancer Res. 2004;64(11):4024–9.
10. Mole RH. Whole body irradiation; radiobiology or medicine? Br J Radiol. 1953;26(305):234–41.
11. Demaria S, Ng B, Devitt ML, Babb JS, Kawashima N, Liebes L, et al. Ionizing radiation inhibition of distant untreated tumors (abscopal effect) is immune mediated. Int J Radiat Oncol Biol Phys. 2004;58(3):862–70.
12. Chu KF, Dupuy DE. Thermal ablation of tumours: biological mechanisms and advances in therapy. Nat Rev Cancer. 2014;14(3):199–208.
13. Chang X, Lu X, Guo J, Teng GJ. Interventional therapy combined with immune checkpoint inhibitors: emerging opportunities for cancer treatment in the era of immunotherapy. Cancer Treat Rev. 2019;74:49–60.
14. Slovak R, Ludwig JM, Gettinger SN, Herbst RS, Kim HS. Immuno-thermal ablations – boosting the anticancer immune response. J Immunother Cancer. 2017;5(1):78.
15. Basu S, Binder RJ, Suto R, Anderson KM, Srivastava PK. Necrotic but not apoptotic cell death releases heat shock proteins, which deliver a partial maturation signal to dendritic cells and activate the NF-kappa B pathway. Int Immunol. 2000;12(11):1539–46.

16. Redondo P, del Olmo J, Lopez-Diaz de Cerio A, Inoges S, Marquina M, Melero I, et al. Imiquimod enhances the systemic immunity attained by local cryosurgery destruction of melanoma lesions. J Invest Dermatol. 2007;127(7):1673–80.
17. den Brok MH, Sutmuller RP, Nierkens S, Bennink EJ, Toonen LW, Figdor CG, et al. Synergy between in situ cryoablation and TLR9 stimulation results in a highly effective in vivo dendritic cell vaccine. Cancer Res. 2006;66(14):7285–92.
18. Hansler J, Wissniowski TT, Schuppan D, Witte A, Bernatik T, Hahn EG, et al. Activation and dramatically increased cytolytic activity of tumor specific T lymphocytes after radio-frequency ablation in patients with hepatocellular carcinoma and colorectal liver metastases. World J Gastroenterol. 2006;12(23):3716–21.
19. Si T, Guo Z, Hao X. Immunologic response to primary cryoablation of high-risk prostate cancer. Cryobiology. 2008;57(1):66–71.
20. Mizukoshi E, Yamashita T, Arai K, Sunagozaka H, Ueda T, Arihara F, et al. Enhancement of tumor-associated antigen-specific T cell responses by radiofrequency ablation of hepatocellular carcinoma. Hepatology. 2013;57(4):1448–57.
21. Wu F. Heat-based tumor ablation: role of the immune response. Adv Exp Med Biol. 2016;880:131–53.
22. Rozenblum N, Zeira E, Scaiewicz V, Bulvik B, Gourevitch S, Yotvat H, et al. Oncogenesis: an "off-target" effect of radiofrequency ablation. Radiology. 2015;276(2):426–32.
23. Ahmed M, Kumar G, Moussa M, Wang Y, Rozenblum N, Galun E, et al. Hepatic radiofrequency ablation-induced stimulation of distant tumor growth is suppressed by c-met inhibition. Radiology. 2016;279(1):103–17.
24. Velez E, Goldberg SN, Kumar G, Wang Y, Gourevitch S, Sosna J, et al. Hepatic thermal ablation: effect of device and heating parameters on local tissue reactions and distant tumor growth. Radiology. 2016;281(3):782–92.
25. Balan M, Mier y Teran E, Waaga-Gasser AM, Gasser M, Choueiri TK, Freeman G, et al. Novel roles of c-Met in the survival of renal cancer cells through the regulation of HO-1 and PD-L1 expression. J Biol Chem. 2015;290(13):8110–20.
26. Chen MF, Chen PT, Chen WC, Lu MS, Lin PY, Lee KD. The role of PD-L1 in the radiation response and prognosis for esophageal squamous cell carcinoma related to IL-6 and T-cell immunosuppression. Oncotarget. 2016;7(7):7913–24.
27. Kang TW, Lim HK, Lee MW, Kim YS, Rhim H, Lee WJ, et al. Aggressive Intrasegmental recurrence of hepatocellular carcinoma after radiofrequency ablation: risk factors and clinical significance. Radiology. 2015;276(1):274–85.
28. Erinjeri JP, Fine GC, Adema GJ, Ahmed M, Chapiro J, den Brok M, et al. Immunotherapy and the interventional oncologist: challenges and opportunities-a society of interventional oncology white paper. Radiology. 2019;292(1):25–34.
29. Jansen MC, van Hillegersberg R, Schoots IG, Levi M, Beek JF, Crezee H, et al. Cryoablation induces greater inflammatory and coagulative responses than radiofrequency ablation or laser induced thermotherapy in a rat liver model. Surgery. 2010;147(5):686–95.
30. Sabel MS, Su G, Griffith KA, Chang AE. Rate of freeze alters the immunologic response after cryoablation of breast cancer. Ann Surg Oncol. 2010;17(4):1187–93.
31. Horiguchi S, Petersson M, Nakazawa T, Kanda M, Zea AH, Ochoa AC, et al. Primary chemically induced tumors induce profound immunosuppression concomitant with apoptosis and alterations in signal transduction in T cells and NK cells. Cancer Res. 1999;59(12):2950–6.
32. Liao J, Xiao J, Zhou Y, Liu Z, Wang C. Effect of transcatheter arterial chemoembolization on cellular immune function and regulatory T cells in patients with hepatocellular carcinoma. Mol Med Rep. 2015;12(4):6065–71.
33. Takaki H, Imai N, Contessa TT, Srimathveeravalli G, Covey AM, Getrajdman GI, et al. Peripheral blood regulatory T-cell and type 1 helper T-cell population decrease after hepatic artery embolization. J Vasc Interv Radiol. 2016;27(10):1561–8.
34. Kim MJ, Jang JW, Oh BS, Kwon JH, Chung KW, Jung HS, et al. Change in inflammatory cytokine profiles after transarterial chemotherapy in patients with hepatocellular carcinoma. Cytokine. 2013;64(2):516–22.

35. Ross GM. Induction of cell death by radiotherapy. Endocr Relat Cancer. 1999;6(1):41–4.
36. Chew V, Lee YH, Pan L, Nasir NJM, Lim CJ, Chua C, et al. Immune activation underlies a sustained clinical response to Yttrium-90 radioembolisation in hepatocellular carcinoma. Gut. 2019;68(2):335–46.
37. He Y, Cao J, Zhao C, Li X, Zhou C, Hirsch FR. TIM-3, a promising target for cancer immunotherapy. Onco Targets Ther. 2018;11:7005–9.
38. Domouchtsidou A, Barsegian V, Mueller SP, Best J, Ertle J, Bedreli S, et al. Impaired lymphocyte function in patients with hepatic malignancies after selective internal radiotherapy. Cancer Immunol Immunother. 2018;67(5):843–53.
39. Dewan MZ, Galloway AE, Kawashima N, Dewyngaert JK, Babb JS, Formenti SC, et al. Fractionated but not single-dose radiotherapy induces an immune-mediated abscopal effect when combined with anti-CTLA-4 antibody. Clin Cancer Res. 2009;15(17):5379–88.
40. Tarhini AA, Kirkwood JM. Tremelimumab (CP-675,206): a fully human anticytotoxic T lymphocyte-associated antigen 4 monoclonal antibody for treatment of patients with advanced cancers. Expert Opin Biol Ther. 2008;8(10):1583–93.
41. Singh PP, Sharma PK, Krishnan G, Lockhart AC. Immune checkpoints and immunotherapy for colorectal cancer. Gastroenterol Rep (Oxf). 2015;3(4):289–97.
42. Postow MA, Callahan MK, Wolchok JD. Immune checkpoint blockade in cancer therapy. J Clin Oncol. 2015;33(17):1974–82.
43. Waterhouse P, Penninger JM, Timms E, Wakeham A, Shahinian A, Lee KP, et al. Lymphoproliferative disorders with early lethality in mice deficient in Ctla-4. Science. 1995;270(5238):985–8.
44. Institute CR. Immunotherapy – timeline of progress 2019. Available from: https://www.cancerresearch.org/immunotherapy/timeline-of-progress.
45. Xu W, Liu K, Chen M, Sun JY, McCaughan GW, Lu XJ, et al. Immunotherapy for hepatocellular carcinoma: recent advances and future perspectives. Ther Adv Med Oncol. 2019;11:1758835919862692.
46. El-Khoueiry AB, Sangro B, Yau T, Crocenzi TS, Kudo M, Hsu C, et al. Nivolumab in patients with advanced hepatocellular carcinoma (CheckMate 040): an open-label, non-comparative, phase 1/2 dose escalation and expansion trial. Lancet. 2017;389(10088):2492–502.
47. Zhu AX, Finn RS, Edeline J, Cattan S, Ogasawara S, Palmer D, et al. Pembrolizumab in patients with advanced hepatocellular carcinoma previously treated with sorafenib (KEYNOTE-224): a non-randomised, open-label phase 2 trial. Lancet Oncol. 2018;19(7):940–52.
48. Kudo M. Immune checkpoint blockade in hepatocellular carcinoma: 2017 update. Liver Cancer. 2016;6(1):1–12.
49. Kudo M. Targeted and immune therapies for hepatocellular carcinoma: predictions for 2019 and beyond. World J Gastroenterol. 2019;25(7):789–807.
50. Kim K, Skora AD, Li Z, Liu Q, Tam AJ, Blosser RL, et al. Eradication of metastatic mouse cancers resistant to immune checkpoint blockade by suppression of myeloid-derived cells. Proc Natl Acad Sci U S A. 2014;111(32):11774–9.
51. Zhan C, Ruohoniemi D, Shanbhogue KP, Wei J, Welling TH, Gu P, et al. Safety of combined yttrium-90 radioembolization and immune checkpoint inhibitor immunotherapy for hepatocellular carcinoma. J Vasc Interv Radiol. 2020;31:25.
52. Xie C, Duffy AG, Mabry-Hrones D, Wood B, Levy E, Krishnasamy V, et al. Tremelimumab in combination with microwave ablation in patients with refractory biliary tract cancer. Hepatology. 2019;69(5):2048–60.
53. Silvestrini MT, Ingham ES, Mahakian LM, Kheirolomoom A, Liu Y, Fite BZ, et al. Priming is key to effective incorporation of image-guided thermal ablation into immunotherapy protocols. JCI Insight. 2017;2(6):e90521.

Suggested Reading

Aarts BM, Klompenhouwer EG, Rice SL, Imani F, Baetens T, Bex A, et al. Cryoablation and immunotherapy: an overview of evidence on its synergy. Insights Imaging. 2019;10(1):53.

Erinjeri JP, Fine GC, Adema GJ, Ahmed M, Chapiro J, den Brok M, et al. Immunotherapy and the interventional oncologist: challenges and opportunities-a Society of Interventional Oncology White Paper. Radiology. 2019;292(1):25–34.

Hickey RM, Kulik LM, Nimeiri H, Kalyan A, Kircher S, Desai K, et al. Immuno-oncology and its opportunities for interventional radiologists: immune checkpoint inhibition and potential synergies with interventional oncology procedures. J Vasc Interv Radiol. 2017;28(11):1487–94.

Slovak R, Ludwig JM, Gettinger SN, Herbst RS, Kim HS. Immuno-thermal ablations – boosting the anticancer immune response. J Immunother Cancer. 2017;5(1):78.

Wu F. Heat-based tumor ablation: role of the immune response. Adv Exp Med Biol. 2016;880:131–53.

Index

C. Georgiades, H. S. Kim (eds.), *Image-Guided Interventions in Oncology*,
https://doi.org/10.1007/978-3-030-48767-6